SOIL REHABILITATION IN THE MUNICIPALITY OF LAVRION
ΑΠΟΚΑΤΑΣΤΑΣΗ ΕΔΑΦΟΥΣ ΣΤΟ ΔΗΜΟ ΛΑΥΡΙΟΥ

LIFE Programme Contract No.: 93/GR/A14/GR/4576

Volume 1
Τόμος 1

Explanatory text
Ερμηνευτικό κείμενο

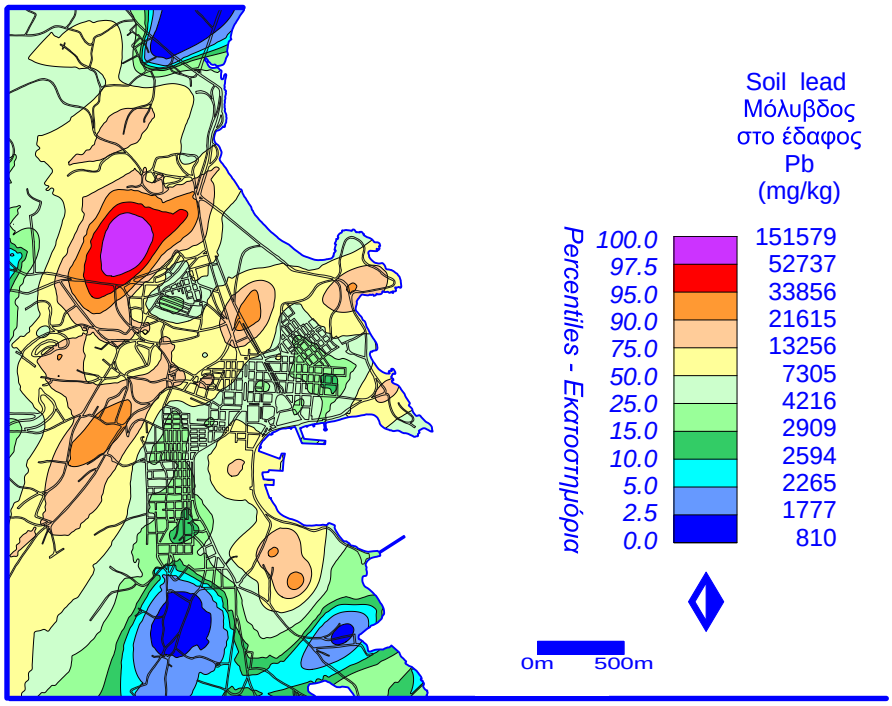

GEOCHEMICAL ATLAS OF THE LAVRION URBAN AREA FOR ENVIRONMENTAL PROTECTION AND PLANNING

ΓΕΩΧΗΜΙΚΟΣ ΑΤΛΑΣ ΤΗΣ ΑΣΤΙΚΗΣ ΠΕΡΙΟΧΗΣ ΤΟΥ ΛΑΥΡΙΟΥ ΓΙΑ ΠΕΡΙΒΑΛΛΟΝΤΙΚΗ ΠΡΟΣΤΑΣΙΑ ΚΑΙ ΣΧΕΔΙΑΣΜΟ

Institute of Geology and Mineral Exploration, Athena, Hellas
Ινστιτούτο Γεωλογικών και Μεταλλευτικών Ερευνών, Αθήνα, Ελλάδα

It is recommended that reference to this report should be made in the following way:

Demetriades, A. (Editor), 1999. *Geochemical Atlas of the Lavrion Urban Area for Environmental Protection and Planning, Volume 1, Explanatory text*. Project “Soil rehabilitation in the Municipality of Lavrion”, EU LIFE programme contract No. 93/GR/A14/GR/4576. Institute of Geology and Mineral Exploration, Athens, Hellas, Open File Report E8272, 365 pp.

Η αναφορά σ’ αυτή την έκθεση προτείνεται να γίνεται με τον παρακάτω τρόπο:

Δημητριάδης, Α. (Συντάκτης), 1999. *Γεωχημικός Άτλας της Αστικής Περιοχής του Λαυρίου για Περιβαλλοντική Προστασία και Σχεδιασμό, Τόμος 1: Ερμηνευτικό κείμενο*. Έργο «Αποκατάσταση Εδάφους στο Δήμο Λαυρίου», EU LIFE Πρόγραμμα, Αρ. συμβολαίου 93/GR/A14/GR/4576. Ινστιτούτο Γεωλογικών και Μεταλλευτικών Ερευνών, Αθήνα, Ελλάδα, Αρ. Έκθεσης Ε8272, 365 σελ.

Reference to Chapters of this report should be made in the following way:
Η αναφορά σε Κεφάλαια αυτής της έκθεσης προτείνεται να γίνεται με τον παρακάτω τρόπο:

Demetriades, A. and Vergou-Vichou, K., 1999. *General Introduction: Regional Geology, Mineralisation, Mining & Metallurgical Activities, Environmental Impact, Regional Soil Geochemistry and Contamination Index Maps*. Chapter 1 In: A. Demetriades (Editor), Geochemical Atlas of the Lavrion Urban Area for Environmental Protection and Planning, Volume 1, Explanatory text. Project “Soil rehabilitation in the Municipality of Lavrion”, EU LIFE programme contract No. 93/GR/A14/GR/4576. Institute of Geology and Mineral Exploration, Athens, Hellas, Open File Report E8272, 1−13.

SOIL REHABILITATION IN THE MUNICIPALITY OF LAVRION
ΑΠΟΚΑΤΑΣΤΑΣΗ ΕΔΑΦΟΥΣ ΣΤΟ ΔΗΜΟ ΛΑΥΡΙΟΥ

LIFE Programme Contract No.: 93/GR/A14/GR/4576

Volume 1
Τόμος 1

GEOCHEMICAL ATLAS OF THE LAVRION URBAN AREA FOR ENVIRONMENTAL PROTECTION AND PLANNING

EXPLANATORY TEXT

Edited by

Alecos Demetriades

ΓΕΩΧΗΜΙΚΟΣ ΑΤΛΑΣ ΤΗΣ ΑΣΤΙΚΗΣ ΠΕΡΙΟΧΗΣ ΤΟΥ ΛΑΥΡΙΟΥ ΓΙΑ ΠΕΡΙΒΑΛΛΟΝΤΙΚΗ ΠΡΟΣΤΑΣΙΑ ΚΑΙ ΣΧΕΔΙΑΣΜΟ

ΕΡΜΗΝΕΥΤΙΚΟ ΚΕΙΜΕΝΟ

Σύνταξη από

Αλέξανδρο Δημητριάδη

It is recommended that reference to all or part of this report should be made in one of the following ways:

Demetriades, A. (editor), 1999. Geochemical atlas of the Lavrion urban area for environmental protection and planning: Explanatory text. Inst. Geol. Mineral. Explor., Athens, Open File Report., Vol. 1, 365 pp.

Tristán, E., Demetriades, A., Ramsey, M.H., Rosenbaum, M.S., Thornton, I., Vassiliades, E., Vergou-Vichou, K. and Kazantzis, G., 1999. Spatially resolved hazard and exposure assessments. In: A. Demetriades (editor), Geochemical atlas of the Lavrion urban area for environmental protection and planning: Explanatory text. Inst. Geol. Mineral Explor., Athens, Open File Report, Vol. 1, Chapter 11: 311-349.

Η βιβλιογραφική αναφορά σε όλο ή τμήμα αυτής της έκθεσης μπορεί να γίνεται με έναν από τους παρακάτω τρόπους:

Δημητριάδης, Αλ. (συντάκτης), 1999. Γεωχημικός άτλας της αστικής περιοχής του Λαυρίου για περιβαλλοντική προστασία και σχεδιασμό: Ερμηνευτικό κείμενο. Αδημοσίευτη έκθεση, Ι.Γ.Μ.Ε., Αθήνα, Τόμος 1, 365 σελ.

Tristán, E., Δημητριάδης, Αλ. Ramsey, M.H., Rosenbaum, M.S., Thornton, I., Βασιλειάδης, Ε., Βέργου-Βήχου, Αικ. και Καζάντζης, Γ., 1999. Χωρική εκτίμηση της επικινδυνότητας και έκθεσης. Στο: Αλ. Δημητριάδης (συντάκτης), Γεωχημικός άτλας της αστικής περιοχής του Λαυρίου για περιβαλλοντική προστασία και σχεδιασμό: Ερμηνευτικό κείμενο. Αδημοσίευτη έκθεση, Ι.Γ.Μ.Ε., Αθήνα, Τόμος 1, Κεφάλαιο 11: 311-349.

I.G.M.E. - Ι.Γ.Μ.Ε.
Athens, December 1999
Αθήνα, Δεκέμβριος 1999

Blank back page
Λευκή οπίσθια σελίδα

In Memoriam

Nicos Demetriades

(1980-1997)

Nicos Demetriades was born in Athens on the 5th May 1980 and passed away on the 25th May 1997 at the age of seventeen. He was a very sensitive child, who cared about the people around him. In fact, he had radiant goodness, which was recognised by the sensitive and cultivated persons of his circle. Everybody was his friend, and always stood by them, but more importantly he helped those in need and encouraged the weak. All his friends sought his advice. His words had wisdom and weight, and for his friends they were law. He was a charismatic child and a first grade pupil. He had an inclination and exceptional performance in architecture, music, synthesis, athletics and the theatre. The roles he played in the musicals of the Municipality of Zografou Music School will never be forgotten. The well-known Greek actor Nikos Tsoyias, after the performance of the musical play "Dream Car" congratulated him. He told him " ..... *you were not playing the drunk, you were actually drunk. In my lifetime I only saw two people playing the drunk so well, Orestis Makris, and you*." He played the saxophone, guitar, piano, tampouras, *etc.* With respect to architecture he had an unbelievable 3-D vision, and his drawings and constructions were extraordinary for his age.

Unfortunately, at the age of fifteen he contracted one of the terminal forms of cancer, and was forced to be away from school for long periods. One of his teachers described his absence as "… *the light has gone away from the classroom*". During our long stay in the Philippines, where he was being treated for his illness, we had the chance to discuss my work at Lavrion and the Global Geochemical Baselines project. After my detailed explanations, and when he realised how serious were the health related problems on the local population and, children especially, he said to me "*father something must be done to improve the quality of life of these children, for it is not right for them to live in such a degraded environment. Your work must be devoted to the children of Lavrion*". Considerable effort has, therefore, been put to make his wish a reality. As Nicos was a unique person and a perfectionist, as a tribute to his short, but full and righteous life, this work is unique, and as perfect as was humanly possible. The technical problems encountered during the compilation of this report, and its completion at end of the present millennium is not a chance happening. It emphasises that the children of Lavrion have the right to live in a healthier environment at the start of the new millennium. The present volumes contain all the information required by even the most demanding scientist, technocrat and politician to make his/her own thorough assessment of the health related environmental problems, and to acknowledge the need for the investment to improve the quality of life of children in Lavrion.

This report is dedicated to the Lavrion children for a better quality of life, and to the memory of Nicos Demetriades, whose wish is partly fulfilled by this manner. The full realisation of his wish, for a better quality of life for the children of Lavrion, is now in the hands of decision-makers.

Στη Μνήμη

Νίκου Δημητριάδη

(1980-1997)

Ο Νίκος Δημητριάδης γεννήθηκε στην Αθήνα στις 5 Μαίου 1980 και κοιμήθηκε στις 25 Μαϊου 1997 σε ηλικία δεκαεπτά ετών. Ήταν ένα πολύ ευαίσθητο παιδί, που ενδιαφερόταν πολύ για τους συνανθρώπους του. Είχε πραγματικά μία ακτινοβόλο καλωσύνη, η οποία αναγνωριζόταν από ευαίσθητα και καλλιεργημένα άτομα του περιβάλλοντός του. Όλοι ήσαν φίλοι του και τους συμπαραστεκόταν πάντα, ιδιαίτερα σε όσους είχαν περισσότερο ανάγκη. Οι φίλοι του ζητούσαν τη συμβουλή του. Τα λόγια του είχαν σοφία και βαρύτητα και για τους φίλους του ήσαν νόμος. Ήταν χαρισματικός και άριστος μαθητής. Είχε κλίση και εξαιρετικές επιδόσεις στην αρχιτεκτονική, τη μουσική, τη σύνθεση, τον αθλητισμό και το θέατρο. Οι ρόλοι που υποδύθηκε στα μιούζικαλ του Δημοτικού Ωδείου Ζωγράφου θα μείνουν αξέχαστοι. Ο διάσημος ηθοποιός Νίκος Τζόγιας, μετά την παράσταση του μουσικού θεατρικού έργου «Το Αμάξι του Ονείρου», τον συνεχάρη και του είπε «… *δεν έπαιζες το μεθυσμένο, αλλά ήσουν μεθυσμένος. Μέχρι στιγμής μόνο δύο ηθοποιοί κατόρθωσαν να υποδυθούν το ρόλο του μεθυσμένου τέλεια, ο Ορέστης Μακρής και εσύ*». Έπαιζε σαξόφωνο, κιθάρα, πιάνο, ταμπουρά και άλλα όργανα. Όσον αφορά την αρχιτεκτονική, είχε μία απίστευτη συναίσθηση του τρισδιάστατου χώρου και τα σχέδια, καθώς και οι αρχιτεκτονικές κατασκευές του, ήσαν εξαιρετικές για την ηλικία του.

Δυστυχώς, στην ηλικία των δεκαπέντε ετών ασθένησε από μία θανατηφόρο μορφή καρκίνου, που τον ανάγκασε να μείνει μακριά από το σχολείο για μακρές χρονικές περιόδους. Μία από τις καθηγήτριές του περιέγραψε την απουσία του ως εξής: «… *το φως έφυγε από την τάξη*». Κατά τη μακρά παραμονή μας στις Φιλιππίνες, όπου γινόταν προσπάθεια θεραπείας της ασθένειάς του, είχαμε την ευκαιρία να μιλήσουμε για την εργασία μου στο Λαύριο και το έργο της Παγκόσμιας Γεωχημικής Χαρτογράφησης. Μετά από τις λεπτομερείς εξηγήσεις μου και όταν συνειδητοποίησε πόσο σοβαρά είναι τα προβλήματα σχετικά με την υγεία του τοπικού πληθυσμού και, ιδιαίτερα των παιδιών, μου είπε «*πατέρα πρέπει να γίνει κάτι για να καλυτερεύσει η ποιότητα ζωής αυτών των παιδιών, γιατί δεν είναι σωστό να ζουν σε τόσο υποβαθμισμένη περιοχή. Η εργασία σου πρέπει να αφιερωθεί στα παιδιά του Λαυρίου*». Γι' αυτό το λόγο έγινε μεγάλη προσπάθεια να γίνει η επιθυμία του πραγματικότητα. Όπως ο Νίκος ήταν ένα μοναδικό παιδί και τελειομανής, ως φόρος τιμής για τη σύντομη, αλλά γεμάτη και ενάρετη ζωή του, αυτή η εργασία είναι μοναδική και όσο τέλεια μπορούσε να γίνει μέσα στα ανθρώπινα πλαίσια. Οι τεχνικές δυσκολίες που αντιμετωπίσθηκαν κατά τη σύνταξη αυτής της έκθεσης και η ολοκλήρωσή της στο τέλος αυτής της χιλιετίας δεν είναι τυχαία. Προβάλλει το δικαίωμα των παιδιών του Λαυρίου να ζήσουν σε ένα υγιέστερο και ποιοτικά καλύτερο περιβάλλον στην αρχή της νέας χιλιετίας. Οι παρόντες τόμοι περιέχουν όλη την αναγκαία πληροφόρηση, ακόμη και για τον πιο απαιτητικό επιστήμονα, τεχνοκράτη και πολιτικό για να κάνει τη δική του λεπτομερή εκτίμηση των περιβαλλοντικών προβλημάτων που επιδρούν στην ανθρώπινη υγεία και να αναγνωρίσει την αναγκαιότητα της επένδυσης για την καλυτέρευση της ποιότητας ζωής των παιδιών του Λαυρίου.

Η έκθεση αυτή αφιερώνεται στα παιδιά του Λαυρίου για καλύτερη ποιότητα ζωής και στη μνήμη του Νίκου Δημητριάδη, του οποίου η επιθυμία εκπληρώνεται μερικώς με αυτόν τον τρόπο. Η πλήρης εκπλήρωση της επιθυμίας του, για καλύτερη ποιότητα ζωής των παιδιών του Λαυρίου, επαφίεται πλέον στα χέρια των αρμοδίων.

In Memoriam

Antonios Kontopoulos

(1944-1998)

Antonios Kontopoulos was born in Chania (Crete) on the 31st August 1944 and passed away on the 26th April 1998 at the age of fifty-three. The news about his sudden departure was a great shock to his family, but also to friends, colleagues, collaborators and students from Greece and all over the World.

He studied at the Department of Mining and Metallurgical Engineering of the National Technical University of Athens (NTUA), and continued his studies with a scholarship at the McMaster University in Canada, where he completed his Ph.D. in 1971 on Metallurgy and Technology of Materials.

Upon his return to Greece he started a multi-faceted activity, which included teaching, basic research at NTUA and close co-operation with the metallurgical industry. He served as Adviser to Fimisco and METVA, where he later had undertaken the position of Deputy-Chairman and Managing Director. In his academic career he served as Chairman of the Department of Mining and Metallurgical Engineering (1986-1988), Director of the Metallurgy and Technology of Materials Sector (1986-1990), member of the Senate (1986-1988) and Director of the Laboratory of Metallurgy since 1984.

During the last decade he was involved in teaching and research in subjects concerned with Environmental Protection, Development and Simulation of Metallurgical Processes. As a result of this great effort, with significant research achievements, was his election as member to the New York Academy of Science, and the honorary position of Visiting Professor of the Henry Krumb Chair in the Department of Earth and Environmental Engineering at the University of Columbia in New York, the most significant university post in Mining and Environmental Engineering of USA.

One of his last research ideas he discussed with Professor Constantinos Panagopoulos. It concerned, the use of the Dwight-Lloyd blast roasting kiln in the French company's factory in Lavrion for pelletising metallurgical wastes from LARCO S.A. This is a legacy that he leaves for further research to his colleagues and collaborators at NTUA.

Professor Antonios Kontopoulos was one of the principal compilers of the present project. We all remember vividly his forward suggestions and, especially his proposal for "*the development of an integrated environmental management scheme for the Lavrion area*". After five years of hard work, the scientists that remained in the project until the end, can say that an enormous amount of scientific research has been carried out, and a few innovative approaches had made possible his suggestion. We submit to the Councillors of the Municipality of Lavrion a work of six informative volumes, which are worthy of the scientific perfectionism of Professor Antonios Kontopoulos, as well as a proposed "environmental management scheme". This is the legacy left by Antonios Kontopoulos to the people of Lavrion for a better quality of life. A legacy that rests on the shoulders of the Municipality of Lavrion Councillors for making it a reality.

Στη Μνήμη

Αντώνιου Κοντόπουλου

(1944-1998)

Ο Αντώνιος Κοντόπουλος γεννήθηκε στα Χανιά Κρήτης στις 31 Αυγούστου και απεβίωσε στις 26 Απριλίου 1998 σε ηλικία πενηντατριών ετών. Η είδηση για τον αναπάντεχο θάνατό του προκάλεσε μεγάλη θλίψη στην οικογένειά του, αλλά και στους φίλους, συναδέλφους, συνεργάτες και φοιτητές από την Ελλάδα και από όλο τον κόσμο.

Σπούδασε στο Τμήμα Μηχανικών Μεταλλείων-Μεταλλουργών Μηχανικών του Εθνικού Μετσόβιου Πολυτεχνείου (ΕΜΠ) και στη συνέχεια με υποτροφία στο Πανεπιστήμιο McMaster του Καναδά, όπου ολοκλήρωσε το 1971 τη Διδακτορική του Διατριβή στη Μεταλλουργία και Τεχνολογία Υλικών.

Επιστρέφοντας στην Ελλάδα ξεκίνησε μία πολύπλευρη δραστηριότητα, που περιελάμβανε διδασκαλία, βασική έρευνα στο ΕΜΠ και στενή συνεργασία με τη μεταλλευτική βιομηχανία. Υπηρέτησε ως Σύμβουλος της Fimisco και της ΜΕΤΒΑ και αργότερα ανέλαβε καθήκοντα Αντιπροέδρου και Δ/ντος Συμβούλου της ΜΕΤΒΑ. Στην ακαδημαϊκή του καριέρα διετέλεσε Πρόεδρος του Τμήματος Μηχανικών Μεταλλείων-Μεταλλουργών Μηχανικών (1986-1988), Δ/ντής του Τομέα Μεταλλουργίας και Τεχνολογίας Υλικών (1988-1990), μέλος της Συγκλήτου (1986-1988) και Δ/ντής του Εργαστηρίου Μεταλλουργίας από το 1984.

Την τελευταία δεκαετία ασχολήθηκε με τη διδασκαλία και την έρευνα στα θέματα της Προστασίας Περιβάλλοντος, στην Ανάπτυξη και Προσομοίωση Μεταλλουργικών Διεργασιών. Ως αποτέλεσμα αυτής της μεγάλης προσπάθειας, με σημαντικά ερευνητικά επιτεύγματα, ήταν η εκλογή του ως μέλος της Ακαδημίας Επιστημών της Νέας Υόρκης και η τιμητική θέση του επισκέπτη καθηγητή στην έδρα Henry Krumb του Τμήματος της Γήϊνης και Περιβαλλοντικής Μηχανικής του Πανεπιστημίου της Κολούμπια της Νέας Υόρκης, την πιο σημαντική πανεπιστημιακή έδρα στη Μεταλλευτική και Περιβαλλοντική Τεχνολογία στις ΗΠΑ.

Μία από τις τελευταίες ερευνητικές του ιδέες συζήτησε με τον καθηγητή Κωνσταντίνο Παναγόπουλο στην τελευταία τους συνάντηση και η οποία αφορούσε τη χρησιμοποίηση της καμίνου Dwight-Lloyd, στο εργοστάσιο της Γαλλικής Εταιρείας στο Λαύριο, για τη δημιουργία συσφαιρωμάτων των μεταλλευτικών απορριμμάτων της ΛΑΡΚΟ. Μία παρακαταθήκη, που αφήνει για περισσότερη διερεύνηση στους συναδέλφους και συνεργάτες του στο ΕΜΠ.

Ο καθηγητής Αντώνιος Κοντόπουλος ήταν ένας από τους κύριους συντελεστές του παρόντος έργου. Όλοι θυμόμαστε ζωντανά τις προωθημένες εισηγήσεις του και ειδικά την πρότασή του για την «*ανάπτυξη ενός ολοκληρωμένου σχεδίου περιβαλλοντικής διαχείρισης για την πόλη του Λαυρίου*». Μετά από πέντε χρόνια σκληρής δουλειάς, οι επιστήμονες, που παρέμειναν στο έργο μέχρι το τέλος, μπορούν να πουν ότι έχει διεξαχθεί ένα μεγάλο ποσοστό επιστημονικής έρευνας και ορισμένες καινοτόμες προσεγγίσεις κατέστησαν δυνατή την πραγματοποίηση των προτάσεών του. Παραδίδουμε στους Δημοτικούς Συμβούλους του Δήμου Λαυρεωτικής ένα εξάτομο πληροφοριακό υλικό, αντάξιο της επιστημονικής αρτιότητας του καθηγητή Αντώνιου Κοντόπουλου, καθώς και ένα προτεινόμενο «σχέδιο περιβαλλοντικής διαχείρισης». Αυτό είναι το κληροδότημα που αφήνει ο Αντώνιος Κοντόπουλος στους κατοίκους του Λαυρίου για καλύτερη ποιότητα ζωής. Ένα κληροδότημα που εναποτίθεται στους ώμους των Δημοτικών Συμβούλων του Λαυρίου να το κάνουν πραγματικότητα.

CONTENTS - ΠΕΡΙΕΧΟΜΕΝΑ	Page

CHAPTER	Tables	Figures	CHAPTER	Tables	Figures	CHAPTER	Tables	Figures	Pages
1	6	2	3	13	11	8	8	6	
2	4	-	4	4	2	9	-	-	
2A	-	-	5	1	30	10	2	-	
2B	5	1	6	8	25	11	18	8	
2C	-	3	7	6	6	12	-	-	
						Total	75	94	365 + xxxvi

Blank back page
Λευκή οπίσθια σελίδα

FOREWORD

The six volumes you have in your hands are the result of five years painstaking work, following the approval of the project proposal by the EU LIFE Programme of Directorate DG-XI of the European Commission. The project was carried out during a sensitive period, with respect to environmental issues, at the aftermath of the 1992 Rio de Janeiro United Nations Earth Summit conference on *"Environment and Development"*. The ten principles of the Rio declaration on environment and development must undoubtedly form the basis for sustainable development of our human-centred environment. Other milestones published during the life of the present project were:

- "*Europe's Environment: The Dobříš Assessment*" (1995) and *"Europe's Environment: The Second Assessment*" (1998) published by the European Environmental Agency;
- "*Risk Assessment for Contaminated Sites in Europe, Volume 1: Scientific Basis*" (1998) *& "Volume 2: Policy Frameworks*" (1999), which constitute the final report of the "Concerted Action on Risk Assessment for Contaminated Sites in the European Union" ("CARACAS").

Essentially, these reports are the European contribution to sustainable development, and finally

- "*A Global Geochemical Database: for environmental and resource management*" (final report of United Nations IGCP Project 259 "International Geochemical Mapping", 1995).

All these reports have a common aim, which is the sustainable long-term management of environmental issues.

The second volume of the "CARACAS" project places an unprecedented *"stress factor"* on the present project, for in the report about Greece it is stated that "*research on contaminated land in Lavrion is related to development of a methodology for the environmental characterisation of the site …* " (Isaakidis *et al.* in Ferguson and Kasamas, 1999, p.81). The Lavrion project was indeed a challenge and, in the opinion of scientists acquainted with project results, the approach used for characterisation of contamination and the subsequent risk assessment are innovative.

The report begins, by giving a taste of the present environmental conditions at Lavrion, with the Contamination Index Maps and the distribution of lead in natural and anthropogenic materials and child blood. Then it goes back in history to the bare rock surface, on which the original soil covered developed. To begin with, the geochemistry of parent rocks, which depicts the natural levels of elements at the archetype state is studied. Subsequently, human intervention follows with the

ΠΡΟΛΟΓΟΣ

Οι έξι τόμοι που έχετε μπροστά σας είναι αποτέλεσμα πέντε χρόνων σκληρής εργασίας, μετά την έγκριση της πρότασης του έργου από το Πρόγραμμα LIFE της XI Διεύθυνσης της Ευρωπαϊκής Επιτροπής. Το έργο εκτελέστηκε σε μία ευαίσθητη περίοδο, όσον αφορά τα περιβαλλοντικά θέματα, μετά τη Διάσκεψη Κορυφής των Ηνωμένων Εθνών με θέμα *«Προστασία του Περιβάλλοντος και Ανάπτυξη»*, που έγινε στο Ρίο ντε Ιανέϊρο το 1992. Οι δέκα αρχές της Διάσκεψης του Ρίο για το περιβάλλον και την ανάπτυξη πρέπει αναμφισβήτητα να αποτελούν τη βάση της αειφόρου ανάπτυξης του ανθρωποκεντρικού περιβάλλοντος. Άλλα ορόσημα που δημοσιεύτηκαν κατά τη διάρκεια του παρόντος έργου ήταν:

- «*Το Ευρωπαϊκό Περιβάλλον: Η Εκτίμηση Dobříš*» (1995) και «*Το Ευρωπαϊκό Περιβάλλον: Η Δεύτερη Εκτίμηση*» (1998), που εκδόθηκαν από την Ευρωπαϊκή Υπηρεσία Περιβάλλοντος,
- «*Εκτίμηση της επικινδυνότητας για ρυπασμένες περιοχές στην Ευρώπη, Τόμος 1: Επιστημονικές Βάσεις*» (1998) & «*Τόμος 2: Πολιτική Οργάνωση*» (1999), που αποτελούν την τελική έκθεση της «Συντονιστικής Δράσης Εκτίμησης της Επικινδυνότητας των Ρυπασμένων Περιοχών» ("CARACAS") στην Ευρωπαϊκή Ένωση.

Ουσιαστικά, οι εκθέσεις αυτές είναι η Ευρωπαϊκή συνεισφορά στην αειφόρο ανάπτυξη, και τέλος

- «*Η Παγκόσμια Γεωχημική Βάση Δεδομένων: για διαχείριση του περιβάλλοντος και πόρων*» (τελική έκθεση του έργου των Ηνωμένων Εθνών IGCP 259 «Διεθνής Γεωχημική Χαρτογράφηση», 1995).

Όλες αυτές οι εκθέσεις έχουν ένα κοινό στόχο, που είναι η μακροχρόνια αειφόρος διαχείριση των περιβαλλοντικών θεμάτων.

Ο δεύτερος τόμος του έργου "CARACAS" θέτει έναν πρωτοφανή *«παράγοντα πίεσης»* στο παρόν έργο, αφού στην έκθεση για την Ελλάδα αναφέρεται ότι «*η έρευνα του ρυπασμένου εδάφους στο Λαύριο σχετίζεται με την ανάπτυξη μεθοδολογίας για τον περιβαλλοντικό χαρακτηρισμό της περιοχής* ….» (Isaakidis *et al.* in Ferguson and Kasamas, 1999, p.81). Το έργο του Λαυρίου ήταν πραγματικά πρόκληση και, κατά την μαρτυρία επιστημόνων που γνωρίζουν τα αποτελέσματα του έργου, η προσέγγιση που χρησιμοποιήθηκε για τον χαρακτηρισμό της ρύπανσης και την επακόλουθο εκτίμηση του κινδύνου είναι καινοτόμος.

Η έκθεση αρχίζει με την περιγραφή της παρούσας κατάστασης του περιβάλλοντος στο Λαύριο, με τους χάρτες του Δείκτη Ρύπανσης και της κατανομής του μολύβδου σε φυσικά και ανθρωπογενούς προέλευσης υλικά, καθώς και στο αίμα των παιδιών. Μετά ανατρέχει στη γεωλογική ιστορία της περιοχής κατά τη διάρκεια της δημιουργίας του αρχικού εδάφους από τα μητρικά πετρώματα. Στην αρχή εξετάζεται η γεωχημεία των μητρικών πετρωμάτων, που υποδηλώνει τα φυσικά επίπεδα των χημικών στοιχείων στην αρχική κατάσταση. Στη συνέχεια ακολουθεί η επέμβαση του ανθρώπου με την εκμετάλλευση των ορυκτών πόρων της ευρύτερης περιοχής του Λαυρίου και της Λαυρεωτικής χερσονήσου, η οποία είχε σοβαρή επίπτωση στο χημισμό του εδάφους. Η πρώτη

exploitation of the mineral resources of the greater Lavrion area and the Lavreotiki peninsula, which had severe effects on the chemistry of soil. According to the classical Greek historian Xenophon, the first mining and smelting activities began early in history, certainly before 3500 BC and, hence, the first wastes generated. The destruction of the Lavreotiki peninsula's landscape was, however, more methodical from 3500 BC onwards with a peak between the 6th and 4th centuries BC. Antiquarian mining and smelting activities, although considerable in area extent and intensity, cannot be compared with the damage caused by recent exploitation, which began in 1865 and ended in 1989.

The enormous amount and expanse of metallurgical wastes in the Lavrion urban area contributed, together with other factors (aerial, fluvial, *etc.*), in the contamination of soil by lead, zinc, arsenic, antimony, cadmium, copper, mercury, *etc.* The geochemical investigation of the soil cover revealed the intensity and extent of the contamination problem. House dust is also severely contaminated. Use of a sequential extraction method has given information about the geochemical behaviour, leachability and bioavailability of elements in soil and house dust. These parameters are significant in the assessment of the effects of environmental contamination.

Exposure to local environmental pressures is indicated by high lead concentrations in child blood. This parameter, together with the geological, geochemical, metallurgical processing wastes and land use variables, were used in the risk assessment and subsequent environmental management scheme for the Lavrion urban area. The methods used are described in detail. It is hoped, therefore, that these techniques will be applied for the characterisation of other contaminated areas, and at some stage, in the not too distant future, they may be refined and incorporated in a standardised methodology for contaminated land assessment.

Alecos Demetriades
Editor

δραστηριότητα εξόρυξης και εκκαμίνευσης άρχισε, σύμφωνα με τον κλασσικό ιστορικό Ξενοφώντα, πριν το 3500 π.Χ., με αποτέλεσμα να δημιουργηθούν τα πρώτα απορρίμματα. Η επέμβαση του ανθρώπου στο ανάγλυφο της Λαυρεωτικής άρχισε, όμως, συστηματικά από το 3500 π.Χ. παρουσιάζοντας έξαρση μεταξύ του 6ου και 4ου αιώνα π.Χ. Αν και οι αρχαίες εργασίες της εξόρυξης και εκκαμίνευσης ήσαν σημαντικότερες σε έκταση και ένταση, δεν μπορούν σε καμμία περίπτωση να συγκριθούν με τις καταστροφικές συνέπειες της νεώτερης εκμετάλλευσης, που άρχισε το 1865 και τελείωσε το 1989.

Η μεγάλη ποσότητα και εξάπλωση των μεταλλουργικών απορριμμάτων στην αστική περιοχή του Λαυρίου συνετέλεσαν, μαζί με άλλους παράγοντες (άνεμο, υδάτινα ρεύματα κ.ά.), στη ρύπανση του εδαφικού καλύμματος από μόλυβδο, ψευδάργυρο, αρσενικό, αντιμόνιο, κάδμιο, χαλκό, υδράργυρο, κ.ά. Η γεωχημική έρευνα του εδαφικού καλύμματος αποκάλυψε την έκταση και την ένταση του προβλήματος της ρύπανσης. Η σκόνη των σπιτιών είναι επίσης έντονα επιβαρυμένη. Η εφαρμογή μεθόδου διαδοχικών εκχυλίσεων παρείχε πληροφορίες για τη γεωχημική συμπεριφορά, την εκχυλισιμότητα και τη βιοδιαθεσιμότητα των στοιχείων στο έδαφος και τη σκόνη των σπιτιών. Αυτές οι παράμετροι είναι μεγάλης σημασίας για την εκτίμηση των επιπτώσεων της περιβαλλοντικής ρύπανσης.

Οι επιπτώσεις της έκθεσης του πληθυσμού στις τοπικές περιβαλλοντικές συνθήκες διαπιστώνονται από τις υψηλές συγκεντρώσεις μολύβδου στο αίμα των παιδιών. Αυτή η παράμετρος, σε συνδυασμό με τις άλλες μεταβλητές, της γεωλογίας, της γεωχημείας του εδάφους, των μεταλλουργικών απορριμμάτων και των χρήσεων γης, χρησιμοποιήθηκαν για την εκτίμηση της επικινδυνότητας και τη μετέπειτα διαμόρφωση του σχεδίου περιβαλλοντικής διαχείρισης της αστικής περιοχής του Λαυρίου. Όλες οι μέθοδοι που εφαρμόσθηκαν περιγράφονται με λεπτομέρεια. Συνεπώς, θέλουμε να ελπίζουμε ότι οι τεχνικές αυτές θα εφαρμοστούν για το χαρακτηρισμό άλλων ρυπασμένων περιοχών και σε κάποιο στάδιο, όχι στο πολύ μακρινό μέλλον, θα βελτιωθούν και θα συμπεριληφθούν σε μία τυποποιημένη μεθοδολογία για την εκτίμηση ρυπασμένων περιοχών.

Αλέξανδρος Δημητριάδης
Συντάκτης

PREFACE

Project results, under the responsibility of the IGME Division of Geochemistry, are presented in five volumes, *i.e.*, 1, 1A, 1B, 2 and 4. This subdivision was necessary, because of the vast quantity of results to be reported. The ***"Geochemical Atlas of the Lavrion Urban Area for Environmental Protection and Planning"*** comprises four volumes:

1. *Explanatory text,*
1A. *Tables and Figures,*
1B. *Appendix Reports, and*
2. *Geochemical Atlas* (colour maps).

Volumes 1 and 2 are subdivided into 12 Chapters with the same headings. Volume 1 contains the explanatory text to the maps, which are in Volume 2. Tables and Figures that could not be included in Volume 1 are presented in Volume 1A. Finally, preliminary project results and other reports, on particle characterisation, core-drilling and analytical results of ground water geochemistry, are presented in Volume 1B. The following summary concerns the results reported in these four volumes.

Volume 3 *"Environmental characterisation of Lavrion site – Development of remediation techniques"* comprises the work carried out by the National Technical University of Athens on rehabilitation techniques, and Volume 4 the *"Environmental Management Plan for the Rehabilitation of Soil in the Lavrion Urban Area"*. These two stand alone volumes are not summarised below.

This study has shown that for an effective risk assessment of toxic element contamination of soil it is important to have information about:

- the lithology,
- the geographical distribution of wastes, and all possible emission sources,
- land use categories,
- the geochemical distribution of elements in soil and house dust,
- the spatial distribution of pH,
- extractability and bioavailability of elements,
- uptake by plants,
- intake by humans, and
- ground water geochemistry.

The above information can be used in a multi-criteria evaluation to determine hazard and exposure, and to prioritise areas for rehabilitation.

Alecos Demetriades, Editor

ΕΙΣΑΓΩΓΗ

Τα αποτελέσματα του έργου υπό την ευθύνη της Διεύθυνσης Γεωχημείας του ΙΓΜΕ, παρουσιάζονται σε πέντε τόμους, δηλ., 1, 1Α, 1Β, 2 και 4. Αυτή η υποδιαίρεση ήταν αναγκαία λόγω του μεγάλου όγκου των δεδομένων. Ο ***«Γεωχημικός Άτλας της Αστικής Περιοχής του Λαυρίου για Περιβαλλοντική Προστασία και Σχεδιασμό»*** περιλαμβάνει τέσσερις τόμους:

1. *Ερμηνευτικό κείμενο,*
1Α. *Πίνακες και Σχήματα,*
1Β. *Εκθέσεις Παραρτήματος, και*
2. *Γεωχημικός Άτλας* (έγχρωμοι χάρτες).

Οι Τόμοι 1 και 2 υποδιαιρούνται σε 12 Κεφάλαια με τους ίδιους τίτλους. Ο Τόμος 1 περιέχει το ερμηνευτικό κείμενο των χαρτών, που είναι στον Τόμο 2. Οι Πίνακες και τα Σχήματα, που δεν μπορούσαν να συμπεριληφθούν στον Τόμο 1 παρουσιάζονται στον Τόμο 1Α. Τέλος, τα προκαταρκτικά αποτελέσματα του έργου και οι επί μέρους εκθέσεις, για το χαρακτηρισμό σωματιδίων, τις γεωτρήσεις πυρηνοληψίας και τα αναλυτικά αποτελέσματα της γεωχημείας των υπόγειων νερών, παρουσιάζονται στον Τόμο 1Β. Η παρακάτω περίληψη αφορά τα αποτελέσματα που αναφέρονται σ' αυτούς τους τέσσερις τόμους.

Ο Τόμος 3 *«Περιβαλλοντικός χαρακτηρισμός περιοχής Λαυρίου – Ανάπτυξη τεχνικών αποκατάστασης»* περιέχει την εργασία που εκτελέστηκε από το Εθνικό Μετσόβιο Πολυτεχνείο της Αθήνας για τις τεχνικές αποκατάστασης και ο Τόμος 4 το *«Περιβαλλοντικό Σχέδιο Διαχείρισης για την Αποκατάσταση του Εδάφους στην Αστική Περιοχή του Λαυρίου»*. Αυτοί οι δύο αυτόνομοι τόμοι δεν αναφέρονται παρακάτω.

Η μελέτη αυτή έδειξε ότι μία αποτελεσματική εκτίμηση της επικινδυνότητας της ρύπανσης του εδάφους από τοξικά στοιχεία είναι σημαντικό να έχει πληροφόρηση για:

- τη λιθολογία,
- τη γεωγραφική κατανομή των απορριμμάτων και όλες τις πιθανές πηγές εκπομπών,
- τις κατηγορίες χρήσης γης,
- τη γεωχημική κατανομή των στοιχείων στο έδαφος και τη σκόνη σπιτιών,
- τη χωρική κατανομή του pH,
- την εκχυλισιμότητα και βιοδιαθεσιμότητα των στοιχείων,
- την προσρόφηση από τα φυτά,
- την πρόσληψη από τους ανθρώπους, και
- τη γεωχημεία του υπόγειου νερού.

Η παραπάνω πληροφόρηση μπορεί να χρησιμοποιηθεί για την με πολλαπλά κριτήρια εκτίμηση της επικινδυνότητας και της έκθεσης, καθώς και για την ιεράρχηση των περιοχών για αποκατάσταση.

Αλέξανδρος Δημητριάδης, Συντάκτης

Blank back page
Λευκή οπίσθια σελίδα

SUMMARY OF CHAPTERS — ΠΕΡΙΛΗΨΗ ΤΩΝ ΚΕΦΑΛΑΙΩΝ

VOLUME 1 : EXPLANATORY TEXT
VOLUME 1A: TABLES AND FIGURES
VOLUME 2 : ATLAS

ΤΟΜΟΣ 1 : ΕΡΜΗΝΕΥΤΙΚΟ ΚΕΙΜΕΝΟ
ΤΟΜΟΣ 1Α: ΠΙΝΑΚΕΣ ΚΑΙ ΣΧΗΜΑΤΑ
ΤΟΜΟΣ 2 : ΑΤΛΑΣ

Lavrion is an industrial town situated 55 km to the south-east of Athens. Mining and metallurgical activities in the area from ca. 3500 BC to 1989 AD, are responsible for the multi-source and multi-element contamination of surface soil. A number of cross-sectional epidemiological studies in the 1980's have shown that children and adults in Lavrion have high blood-lead and urine-arsenic contents. These results, in combination with those of the first urban geochemical study in Lavrion, carried out by the Division of Geochemistry of the Institute of Geology and Mineral Exploration (IGME), have given the impetus for this particular research project.

Το Λαύριο είναι μία βιομηχανική πόλη που βρίσκεται 55 χλμ. νοτιοανατολικά της Αθήνας. Οι μεταλλευτικές και μεταλλουργικές δραστηριότητες στην περιοχή από περίπου το 3500 π.Χ. μέχρι το 1989 μ.Χ. ευθύνονται για την πολυστοιχειακή ρύπανση του εδάφους από πολλαπλές εστίες. Οι επιδημιολογικές μελέτες, που πραγματοποιήθηκαν τη δεκαετία του 1980, έδειξαν ότι τα παιδιά και οι ενήλικες στο Λαύριο παρουσιάζουν υψηλές συγκεντρώσεις μολύβδου στο αίμα και αρσενικού στα ούρα. Αυτά τα αποτελέσματα σε συνδυασμό με εκείνα της πρώτης αστικής γεωχημικής έρευνας στο Λαύριο, που έγινε από τη Διεύθυνση Γεωχημείας του Ινστιτούτου Γεωλογικών και Μεταλλευτικών Ερευνών (ΙΓΜΕ), έδωσαν το έναυσμα για το συγκεγκριμένο ερευνητικό έργο.

The principal objectives of the project were:

- **to assess soil contamination,**
- **to apply, on a demonstration scale, appropriate techniques for the rehabilitation of the heavily contaminated industrial area of Lavrion, and**
- **to develop an integrated environmental management scheme for the Lavrion urban area.**

Οι κυριότεροι στόχοι του έργου ήσαν:

- **η εκτίμηση της ρύπανσης του εδάφους,**
- **η εφαρμογή, σε κλίμακα επίδειξης, κατάλληλων τεχνικών για την αποκατάσταση της έντονα ρυπασμένης βιομηχανικής περιοχής του Λαυρίου και**
- **η ανάπτυξη ενός ολοκληρωμένου σχεδίου περιβαλλοντικής διαχείρισης για την αστική περιοχή του Λαυρίου.**

Project objectives, under the responsibility of the IGME Division of Geochemistry and/or in collaboration with the other partners [National Technical University of Athens (NTUA), Municipality of Lavreotiki & PRISMA], as defined in the approved proposal were:

- **to evaluate in detail the current status of the greater Lavrion urban area, focusing mainly on soil contamination,**
- **to identify and map the main pollution sources in the area,**
- **to produce environmental impact maps, and a video film showing all the methods applied,**
- **to carry out a cost-benefit analysis of the rehabilitation methods,**
- **to develop an integrated environmental management scheme for the greater Lavrion urban area, and**
- **to inform Lavrion residents about project results.**

Οι στόχοι του έργου, πού εντάσσονται στην ευθύνη της Διεύθυνσης Γεωχημείας του ΙΓΜΕ ή/και σε συνεργασία με τους άλλους εταίρους [Εθνικό Μετσόβιο Πολυτεχνείο (ΕΜΠ), Δήμος Λαυρεωτικής και εταιρεία PRISMA], όπως καθορίζονται από την εγκεκριμένη πρόταση ήσαν:

- **η λεπτομερής εκτίμηση της υπάρχουσας κατάστασης στην ευρύτερη αστική περιοχή του Λαυρίου, εστιάζοντας κυρίως στη ρύπανση του εδάφους,**
- **ο καθορισμός και η χαρτογράφηση των κυριοτέρων πηγών ρύπανσης στην περιοχή,**
- **η κατασκευή χαρτών περιβαλλοντικών επιπτώσεων, καθώς και βιντεοταινίας των μεθόδων που εφαρμόστηκαν,**
- **η πραγματοποίηση ανάλυσης κόστους-οφέλους των τεχνικών αποκατάστασης,**
- **η ανάπτυξη ενός ολοκληρωμένου σχεδίου περιβαλλοντικής διαχείρισης της ευρύτερης αστικής περιοχής του Λαυρίου και**
- **η ενημέρωση του πληθυσμού του Λαυρίου για τα αποτελέσματα του έργου.**

Chapter 1. General introduction: Regional geology, Mineralisation, Mining & metallurgical activities, Environmental impact, Regional soil geochemistry and Contamination index maps (Volumes 1 & 2)

The Lavreotiki peninsula is made up from alternate marble and schist units, which are intruded by a granodiorite batholith with dykes of granitic porphyry. The rich base metal mineralisation, at the contact of marble and schist, comprising argentiferous galena, sphalerite and pyrite, was responsible for the intensive mining and metallurgical activities from antiquarian to recent times, and the subsequent contamination of the environment. Regional soil geochemical maps of Lavreotiki peninsula (~170 km^2) showed the extent and intensity of contamination.

Metallurgical processing activities in Lavrion from 1865 to 1989 produced a vast quantity of toxic wastes, which are distributed haphazardly all over the urban area. The two Contamination Index maps of As, Be, Ba, Cd, Cr, Cu, Ni, Pb, V and Zn using (a) statutory limits and (b) the "Lavrion Soil Action Levels" show the extent and intensity of contamination. It is concluded, that the whole Lavrion urban area (7.24 km^2) is seriously contaminated by toxic elements.

Κεφάλαιο 1: Γενική εισαγωγή: Γενική γεωλογία, Μεταλλοφορία, Μεταλλευτικές & μεταλλουργικές δραστηριότητες, Περιβαλλοντικές επιπτώσεις, Καθολική εδαφογεωχημεία και Χάρτες δείκτη ρύπανσης (Τόμοι 1 & 2)

Η Λαυρεωτική χερσόνησος δομείται από εναλλαγές ενοτήτων μαρμάρου και σχιστολίθου, στις οποίες διείσδυσε βαθόλιθος γρανοδιορίτη με φλέβες γρανιτικού πορφύρη. Η πλούσια μεταλλοφορία βασικών μετάλλων, που απαντάται στην επαφή μαρμάρου και σχιστολίθου και αποτελείται από αργυρούχο γαληνίτη, σφαλερίτη και πυρίτη, ευθύνεται για την εντατική μεταλλευτική και μεταλλουργική δραστηριότητα από την αρχαιότητα μέχρι πρόσφατα, καθώς και την επακόλουθη ρύπανση του περιβάλλοντος. Η καθολική εδαφογεωχημική χαρτογράφηση της Λαυρεωτικής χερσονήσου (~170 km^2) καθόρισε την έκταση και ένταση της ρύπανσης.

Οι μεταλλουργικές εργασίες στο Λαύριο από το 1865 έως το 1989 δημιούργησαν ένα μεγάλο όγκο τοξικών απορριμμάτων, τα οποία είναι άτακτα κατανεμημένα σε όλη την έκταση της αστικής περιοχής. Οι δύο χάρτες του Δείκτη Ρύπανσης As, Be, Ba, Cd, Cr, Cu, Ni, Pb, V και Zn βάσει (α) των νομοθετημένων ορίων και (β) των «Ορίων Λήψης Μέτρων του Λαυρίου» απεικονίζουν την έκταση και ένταση της ρύπανσης. Συμπεραίνεται ότι, ολόκληρη η έκταση (7.24 km^2) της αστικής περιοχής του Λαυρίου είναι σοβαρά ρυπασμένη από τοξικά στοιχεία.

Chapter 2. General thematic maps of the Lavrion urban area: Digital topography, Lithology, Metallurgical processing residues & contaminated soil, Soil and house dust pH (Volumes 1 & 2)

Different thematic maps, compiled at a scale of 1:5000, are described:

- digital topographical map,
- lithological map (6 units),
- map of metallurgical processing wastes and contaminated overburden (11 categories),
- land use map (30 categories),
- distribution of pH in overburden, and
- distribution of pH in house dust.

Κεφάλαιο 2. Γενικοί θεματικοί χάρτες της αστικής περιοχής του Λαυρίου: Ψηφιακή τοπογραφία, Λιθολογία, Μεταλλουργικά απορρίμματα & ρυπασμένο έδαφος, pH εδάφους και σκόνης σπιτιών (Τόμοι 1 & 2)

Περιγράφονται διάφοροι θεματικοί χάρτες, που εκπονήθηκαν σε κλίμακα 1:5000:

- ψηφιακός τοπογραφικός χάρτης,
- λιθολογικός χάρτης (6 ενότητες),
- χάρτης μεταλλουργικών απορριμμάτων και ρυπασμένου εδαφικού καλύμματος (11 κατηγορίες),
- χάρτης χρήσης γης (30 κατηγορίες),
- κατανομή του pH στο εδαφικό κάλυμμα και
- κατανομή του pH στη σκόνη σπιτιών.

Chapter 2A. Sampling and sample preparation
Chapter 2B. Analytical methods
Chapter 2C. Analytical and sampling variance (Volumes 1, 1A & 2)

Sampling, sample preparation, analytical methods and quality control procedures are described.
The following sample types were collected:

- rock (n=140),
- metallurgical processing residues (n=62),
- overburden including residual soil (n=224),
- house-dust (n=127),
- metallurgical processing wastes and residual soil for particle-size analysis (n=21),
- ground water (n=15),
- metallurgical wastes for particle characterisation (n=31, *i.e.*, 21 contamination source, 4 soil, 5 house dust & 1 slag samples), and
- overburden from drill-hole core and vertical profiles (n=165).

Further, the biomedical samples (n=235) collected during the last cross-sectional epidemiological study in March 1988, and soil samples for an agronomy study (n=583) were utilised.

Strict quality control procedures were employed, and the integrity of the analytical data examined before proceeding to their statistical and geostatistical processing for the production of geochemical distribution maps. Tables of analytical and sampling variance are presented in Appendix 1A of Volume 1A.

An innovation is the presentation on geochemical maps of quality control parameters in the form of a pie chart for each element, *i.e.*,

- apportionment of sampling, analytical and geochemical variance, and
- lower detection and analytical precision equation for the estimation of precision at the 95th confidence level for any concentration.

Hence, the reader is able to verify the reliability of the geochemical distribution maps.

Κεφάλαιο 2Α. Δειγματοληψία και προετοιμασία των δειγμάτων για ανάλυση
Κεφάλαιο 2Β. Αναλυτικές μέθοδοι
Κεφάλαιο 2C. Αναλυτική και δειγματοληπτική διασπορά (Τόμοι 1, 1Α & 2)

Περιγράφονται οι μέθοδοι δειγματοληψίας, ανάλυσης και ποιοτικού ελέγχου.
Συλλέχθηκαν οι παρακάτω τύποι δειγμάτων:

- πέτρωμα (n=140),
- μεταλλουργικά απορρίμματα (n=62),
- εδαφικό κάλυμμα συμπεριλαμβανομένου και του υπολειμματικού εδάφους (n=224),
- σκόνη σπιτιών (n=127),
- μεταλλουργικά απορρίμματα και υπολειμματικό έδαφος για κοκκομετρική ανάλυση (n=21),
- υπόγειο νερό (n=15),
- μεταλλουργικά απορρίμματα για χαρακτηρισμό σωματιδίων (n=31, δηλ., 21 δείγματα από πηγές ρύπανσης, 4 κηπευτικού εδάφους, 5 σκόνης σπιτιών & 1 σκουριάς), και
- εδαφικό κάλυμμα από γεωτρήσεις πυρηνοληψίας και κάθετες τομές (n=165).

Επιπρόσθετα χρησιμοποιήθηκαν τα βιοϊατρικά δείγματα (n=235), που συλλέχθηκαν κατά την τελευταία επιδημιολογική έρευνα, η οποία έγινε τον Μάρτιο 1988, καθώς και τα δείγματα εδάφους (n=583) της μελέτης φυτοκάλυψης.

Χρησιμοποιήθηκαν αυστηρές διαδικασίες ποιοτικού ελέγχου και ελέγχθηκε η πιστότητα των αναλυτικών αποτελεσμάτων πρίν τη στατιστική και γεωστατιστική τους επεξεργασία για την κατασκευή των γεωχημικών χαρτών κατανομής. Οι πίνακες της αναλυτικής και δειγματοληπτικής διασποράς παρουσιάζονται στο Παράρτημα 1Α του Τόμου 1Α.

Μία καινοτομία είναι η παρουσίαση στους γεωχημικούς χάρτες των ποιοτικών παραμέτρων υπό μορφήν πίτας για κάθε στοιχείο, δηλ.:

- διαχωρισμός της δειγματοληπτικής, αναλυτικής και γεωχημικής διασποράς και
- το χαμηλότερο όριο ανίχνευσης και η εξίσωση της αναλυτικής επαναληψιμότητας για τον υπολογισμό της επαναληψιμότητας στο 95ο επίπεδο εμπιστοσύνης για οποιαδήποτε συγκέντρωση.

Με αυτό τον τρόπο ο μελετητής μπορεί να διαπιστώσει την αξιοπιστία των γεωχημικών χαρτών κατανομής.

Chapter 2D. Data processing: Statistical and geostatistical methods and geochemical map production (Volumes 1 & 2)

The statistical and geostatistical methods used for the production of geochemical maps are described. Use of geostatistics is recommended for environmental studies, because this method has been specifically developed for the study of regionalised (spatial) variables. Since, the parameters used in the interpolation of point geochemical data into a grid (unsampled area) are obtained from the spatial distribution of the data set itself, geostatistics is considered to be, therefore, an "*exact interpolator*".

An innovation is the presentation, on geochemical maps, of the variogram surface and the modelled variogram parameters, which indicate the spatial structural characteristics of the elements studied and, therefore, the validity of interpolation and their geochemical distribution.

Κεφάλαιο 2D. Επεξεργασία δεδομένων: Στατιστικές και γεωστατιστικές μέθοδοι και εκπόνηση γεωχημικών χαρτών (Τόμοι 1 & 2)

Περιγράφονται οι στατιστικές και γεωστατιστικές μέθοδοι που χρησιμοποιήθηκαν για την κατασκευή-σχεδίαση των γεωχημικών χαρτών. Για περιβαλλοντικές μελέτες προτείνεται η χρήση της γεωστατιστικής, δεδομένου ότι η μέθοδος αυτή έχει αναπτυχθεί ειδικά για τη μελέτη των χωρικών μεταβλητών. Επειδή, οι παράμετροι, που χρησιμοποιούνται για την παρεμβολή σημειακών γεωχημικών δεδομένων σε κάνναβο (μη δειγματισθείσα περιοχή), προέρχονται από τη χωρική κατανομή των ίδιων των δεδομένων, η γεωστατιστική παρέχει τη δυνατότητα της «*ακριβούς παρεμβολής*».

Μία καινοτομία είναι η παρουσίαση στους γεωχημικούς χάρτες της επιφάνειας του βαριογράμματος και των παραμέτρων προσομοίωσης, οι οποίες δείχνουν τα χωρικά δομικά χαρακτηριστικά των υπό μελέτη στοιχείων και συνεπώς την πιστότητα της παρεμβολής και της γεωχημικής κατανομής.

Chapter 3. Distribution of lead in the Lavrion urban environment (Volumes 1 & 2)

Cross sectional epidemiological studies in the 1980's have studied lead (Pb) and its effects on the local population and, especially, children. Lead has also been extensively studied all over the world, because of its known adverse health related effects. Hence, in this chapter are discussed all the results concerning lead, *i.e.*, its distribution in

- rocks,
- metallurgical processing wastes,
- different grain-size fractions of metallurgical wastes and residual soil,
- overburden (total Pb and five-step sequential extraction),
- house dust (total Pb and five-step sequential extraction), and
- child-blood.

Lead distribution in rocks depicts the natural conditions on which the first natural residual soil developed in Lavrion. Its concentrations vary from <1 to 1,850 ppm Pb, with a mean of 76.9 ppm and a median of 22 ppm. Then the distribution of Pb in metallurgical processing wastes is studied, *i.e.*,

Κεφάλαιο 3. Κατανομή του μολύβδου στην αστική περιοχή του Λαυρίου (Τόμοι 1 & 2)

Οι επιδημιολογικές μελέτες της δεκαετίας του 1980 μελέτησαν το μόλυβδο (Pb) και τις επιδράσεις του στον τοπικό πληθυσμό και ειδικά στα παιδιά. Ο μόλυβδος έχει μελετηθεί εκτενώς σε όλο τον κόσμο, λόγω των γνωστών δυσμενών επιπτώσεών του στην υγεία. Γι' αυτό το λόγο στο κεφάλαιο αυτό περιγράφονται όλα τα αποτελέσματα που αφορούν το μόλυβδο, δηλ., την κατανομή του στα:

- πετρώματα,
- μεταλλουργικά απορρίμματα
- διάφορα κοκκομετρικά κλάσματα των μεταλλουργικών απορριμμάτων και του υπολειμματικού εδάφους,
- δείγματα εδαφικού καλύμματος (ολικός Pb και στα πέντε στάδια των διαδοχικών εκχυλίσεων),
- δείγματα σκόνης σπιτιών (ολικός Pb και στα πέντε στάδια των διαδοχικών εκχυλίσεων) και
- δείγματα αίματος των παιδιών.

Η κατανομή του μολύβδου στα πετρώματα υποδηλεί τις φυσικές συνθήκες, όπου αναπτύχθηκε το πρώτο φυσικό υπολειμματικό έδαφος στο Λαύριο. Οι συγκεντρώσεις του μολύβδου κυμαίνονται από <1 έως 1.850 ppm, με μέση τιμή 76.9 ppm και διάμεση 22 ppm. Ακολουθεί η μελέτη της κατανομής του Pb στα μεταλλουργικά απορρίμματα και συγκεκριμένα:

(a) slag varies from 5,000 to 51,200 ppm Pb (mean 16,495 & median 11,800 ppm),
(b) flotation residues varies from 18,500 to 28,100 ppm Pb (mean 24,535 & median 24,950 ppm, and
(c) pyritiferous tailings from 9,800 to 85,200 ppm Pb (mean 47,042 & median 45,400 ppm).

Finally, the distribution of total Pb in overburden and house dust is presented. Total Pb contents in overburden vary from 810 to 151,579 ppm (mean 11,578 & median 7,305 ppm), and in house dust from 488 to 18,617 ppm Pb (mean 4,006 & median 3,091 ppm). These results show clearly that contamination of overburden in Lavrion, including residual soil, was caused by the metallurgical processing activities, and especially the metallurgical wastes, which cover approximately 25% of the 7.235 km^2 studied. Lead levels greatly exceed the statutory threshold level of 500 ppm Pb for residential soil.

The sequential extraction results on overburden and house dust have given interesting information on Pb contents that could be available for intake by humans and uptake by plants. The detrimental adverse effects are observed in child blood, which contains Pb concentrations from 5.98 to 60.49 μg/100 ml (mean 19.43 & median 17.83 μg/100 ml). An astounding 95% of children in Lavrion have blood-Pb levels exceeding the level of concern, 10 μg Pb/100 ml. The results are not, therefore, very encouraging for the local people. It is concluded, that exposure risk on the animal and human population in Lavrion is greater than hitherto anticipated, and rehabilitation of the surface environment is considered to be an urgent task.

(α) στις σκουριές από 5.000 έως 51.200 ppm Pb (μέσος 24.535 & διάμεσος 24.950 ppm),
(β) στα απορρίμματα επίπλευσης από 18.500 έως 28.100 ppm Pb (μέσος 24.535 & διάμεσος 24.950 ppm), και
(γ) στα πυριτούχα απορρίμματα από 9.800 έως 85.200 ppm Pb (μέσος 47.042 & διάμεσος 45.400 ppm).

Τέλος, παρουσιάζεται η κατανομή του ολικού Pb στο εδαφικό κάλυμμα και στη σκόνη σπιτιών. Οι ολικές συγκεντρώσεις του Pb στο εδαφικό κάλυμμα κυμαίνονται από 810 έως 151.579 ppm (μέσος 11.578 & διάμεσος 7.305 ppm) και στη σκόνη σπιτιών από 488 έως 18.617 ppm Pb (μέσος 4.006 & διάμεσος 3.091 ppm). Αυτά τα αποτελέσματα δείχνουν ξεκάθαρα ότι η ρύπανση του εδαφικού καλύμματος στο Λαύριο, συμπεριλαμβανομένου και του υπολειμματικού εδάφους, προξενήθηκε από τις μεταλλουργικές εργασίες και ιδιαίτερα τα μεταλλουργικά απορρίμματα, τα οποία καλύπτουν περίπου το 25% των 7.235 km^2 που μελετήθηκαν. Τα επίπεδα του μολύβδου υπερβαίνουν κατά πολύ το νομοθετημένο όριο των 500 ppm Pb για το αστικό έδαφος.

Τα αποτελέσματα των διαδοχικών εκχυλίσεων στα δείγματα του εδαφικού καλύμματος και της σκόνης σπιτιών έδωσαν ενδιαφέρουσες πληροφορίες για τις συγκεντρώσεις του Pb που μπορεί να είναι διαθέσιμες για πρόσληψη από τους ανθρώπους και τα φυτά. Οι δυσμενείς συνέπειες παρατηρούνται στο αίμα των παιδιών, το οποίο περιέχει συγκεντρώσεις Pb από 5,98 έως 60,49 μg/100 ml (μέσος 19,43 & διάμεσος 17,83 μg/100 ml). Ένα εξαιρετικά υψηλό ποσοστό, της τάξεως των 95% των παιδιών του Λαυρίου, παρουσιάζει επίπεδα Pb στο αίμα που υπερβαίνουν το όριο εγρήγορσης των 10 μg Pb/100 ml. Συνεπώς, τα αποτελέσματα δεν είναι καθόλου ενθαρρυντικά για τον τοπικό πληθυσμό. Συμπεραίνεται ότι ο κίνδυνος έκθεσης του ανθρώπου και του ζωϊκού πληθυσμού του Λαυρίου είναι μεγαλύτερος απ' ότι αρχικά είχε θεωρηθεί και η αποκατάσταση του επιφανειακού περιβάλλοντος θεωρείται επείγουσα εργασία.

Chapter 4. Geochemistry of parent rocks (Volumes 1, 1A & 2)

The only valid cheap method to obtain background geochemical data in an environment with extreme contamination as Lavrion is rock geochemistry. Background geochemical data are given for 30 elements (Ag, Al, As, B, Ba, Be, Bi, Ca, Cd, Co, Cr, Cu, Fe, Hg, K, La, Li, Mn, Mo, Ni, P, Pb, S, Sb, Sn, Sr, Ti, U, V, Zn), and the spatial distribution is

Κεφάλαιο 4. Γεωχημεία των μητρικών πετρωμάτων (Τόμοι 1, 1Α & 2)

Η μόνη φθηνή και έγκυρη μέθοδος, για τον καθορισμό των γενικών γεωχημικών συγκεντρώσεων των στοιχείων σε ένα περιβάλλον με έντονη ρύπανση, όπως το Λαύριο, είναι η γεωχημεία των μητρικών πετρωμάτων. Γενικά γεωχημικά δεδομένα δίνονται για 30 στοιχεία (Ag, Al, As, B, Ba, Be, Bi, Ca, Cd, Co, Cr, Cu, Fe, Hg, K, La, Li, Mn,

plotted for eighteen. Lavrion rocks, in comparison with global average element concentrations of the upper continental crust, are enriched in

As>Sb>Cd>Ag>Hg>Ni>Ca>Pb>Zn>
P>Mn>Cr>Co>Cu>Ba>S>U,

and depleted in

Fe>Mo>Li> Sr>La>Ti>Al>V>K>B.

Because of the high geochemical background of rocks, which is due to mineralisation, normal residual soil in Lavrion would have had toxic element concentrations, above stipulated statutory trigger levels. Since, abnormal element contents in the first residual soil would have been largely restricted over geochemically anomalous rocks, the potential hazardous area would have covered, depending on the toxic element, from 10% to 50% of the urban area of Lavrion.

R-mode factor and cluster analyses were able to define subtle associations among the elements.

Mo, Ni, P, Pb, S, Sb, Sn, Sr, Ti, U, V, Zn), αλλά σχεδιάστηκε η χωρική κατανομή δεκαοκτώ εξ αυτών. Τα πετρώματα του Λαυρίου, σε σύγκριση με τις παγκόσμιες μέσες συγκεντρώσεις των στοιχείων του ανωτέρου ηπειρωτικού φλοιού της γης, παρουσιάζονται εμπλουτισμένα σε:

As>Sb>Cd>Ag>Hg>Ni>Ca>Pb>Zn>
P>Mn>Cr>Co>Cu>Ba>S>U,

και με μειωμένες συγκεντρώσεις σε:

Fe>Mo>Li> Sr>La>Ti>Al>V>K>B.

Λόγω των υψηλών γενικά γεωχημικών τιμών των πετρωμάτων, που οφείλονται στη μεταλλοφορία, ήταν αναμενόμενο το κανονικό υπολειμματικό έδαφος στο Λαύριο να παρουσιάζει τοξικές συγκεντρώσεις, που να υπερβαίνουν τα νομοθετημένα όρια. Δεδομένου, ότι οι ασυνήθιστες συγκεντρώσεις των στοιχείων στο πρώτο υπολειμματικό έδαφος θα ήταν περιορισμένες κυρίως στην περιοχή που αναπτύσσεται πάνω στα από γεωχημικής πλευράς ανώμαλα πετρώματα, η δυνητικά επικίνδυνη περιοχή θα κάλυπτε, ανάλογα με το τοξικό στοιχείο, το 10% έως 50%, της αστικής περιοχής του Λαυρίου.

Η ανάλυση παραγόντων και ομάδων διασαφήνισε τους λεπτούς συσχετισμούς μεταξύ των στοιχείων.

Chapter 5. Chemistry of metallurgical processing wastes (Volumes 1 & 2)

Metallurgical processing wastes cover about 25% of the area studied (7.235 km^2), and their chemistry is, therefore, important. For this purpose the distribution of thirty elements (Ag, Al, As, B, Ba, Be, Bi, Ca, Cd, Co, Cr, Cu, Fe, Hg, K, La, Li, Mn, Mo, Ni, P, Pb, S, Sb, Sn, Sr, Ti, U, V, Zn) is presented.

It is concluded that metallurgical processing wastes have high toxic element contents (Pb, Zn, As, Sb, Cd, Cu, Hg, Be), and their transportation by aerial, fluvial and anthropogenic means has resulted in the contamination of residual and alluvial soil of the Lavrion urban area.

Κεφάλαιο 5. Χημεία των μεταλλουργικών απορριμμάτων (Τόμοι 1 & 2)

Τα μεταλλουργικά απορρίμματα καλύπτουν περίπου το 25% της περιοχής (7,235 km^2) που μελετήθηκε και, συνεπώς, η χημεία τους παίζει σημαντικό ρόλο. Για το λόγο αυτό παρουσιάζεται σε χάρτες η κατανομή τριάντα στοιχείων (Ag, Al, As, B, Ba, Be, Bi, Ca, Cd, Co, Cr, Cu, Fe, Hg, K, La, Li, Mn, Mo, Ni, P, Pb, S, Sb, Sn, Sr, Ti, U, V, Zn).

Συμπεραίνεται ότι τα μεταλλουργικά απορρίμματα έχουν υψηλές συγκεντρώσεις τοξικών στοιχείων (Pb, Zn, As, Sb, Cd, Cu, Hg, Be), και η μεταφορά τους μέσω του αέρα, ποτάμιων συστημάτων και λόγω ανθρώπινων ενεργειών έχει ως συνέπεια τη ρύπανση του υπολειμματικού και αλλουβιακού εδάφους της αστικής περιοχής του Λαυρίου.

Chapter 6. Geochemistry of overburden (Volumes 1 & 2)

The distribution of twenty-four elements (Ag, Al, As, Ba, Be, Ca, Cd, Co, Cr, Cu, Fe, Hg, K, La, Li, Mn, Mo, Ni, P, Pb, Sr, Ti, V, Zn) in overburden is studied. The results are compared against the mean or median values of Lavrion rocks, normal global soil, and for toxic elements against their statutory trigger or guide levels. The ratio of element

Κεφάλαιο 6. Γεωχημεία του επιφανειακού καλύμματος (Τόμοι 1 & 2)

Μελετήθηκε η κατανομή εικοσιτεσσάρων στοιχείων (Ag, Al, As, Ba, Be, Ca, Cd, Co, Cr, Cu, Fe, Hg, K, La, Li, Mn, Mo, Ni, P, Pb, Sr, Ti, V, Zn) στο εδαφικό κάλυμμα. Τα αποτελέσματα συγκρίνονται με τις μέσες ή διάμεσες τιμές στα πετρώματα του Λαυρίου, τις κανονικές παγκόσμιες τιμές στο έδαφος και, όσον αφορά τα τοξικά

contents in Lavrion overburden/soil to

- global soil mean/median values depicts that the former is contaminated with respect to Pb>As>Zn>Ag>Cd> Sb>Cu>Hg>Ca>Cr> Ni> Mn>P>Mo>Co>Sr>Ba>Fe>V, and
- statutory levels indicates that the former is contaminated with regards to As>Zn>Pb>Cd> Ag>Sb>V>Cr.

The percentage proportion of the Lavrion urban area with potentially hazardous element concentrations to human health is:

- 100% for As, Pb, Cd and Zn,
- 90 to 99% for Ag, V and Sb,
- 45 to 68.8% for Cu and Mo, and
- 13.8 to 33% for Ba, Ni and Cr.

Whereas the percentage proportion of the area with phytotoxic levels is:

- 100% for As, Pb and Zn,
- >90 to 99% for Ag, Cd and Sb,
- >75 to 90% for Ba, Cu, Cr and Ni, and
- >19 to 31% for Mn and V.

It is concluded that the multi-element contamination of the Lavrion overburden/soil is extremely high, and presents an unacceptable risk on the quality of life of the local population, and is also potentially hazardous to plants and animals. Hence, it is highly urgent to rehabilitate the whole area by suitable remediation techniques.

στοιχεία, με τα νομοθετημένα όρια. Ο λόγος των συγκεντρώσεων των στοιχείων στο εδαφικό κάλυμμα του Λαυρίου σε σχέση:

- με τις παγκόσμιες μέσες/διάμεσες τιμές υποδηλώνει ότι το προηγούμενο είναι ρυπασμένο στα στοιχεία Pb>As>Zn>Ag>Cd> Sb>Cu>Hg> Ca>Cr> Ni> Mn>P>Mo>Co>Sr>Ba>Fe>V και
- με τα νομοθετημένα όρια δείχνει ότι είναι ρυπασμένο όσον αφορά τα στοιχεία As>Zn>Pb>Cd> Ag>Sb>V>Cr.

Η εκατοστιαία αναλογία της έκτασης της αστικής περιοχής του Λαυρίου με δυνητικά επικίνδυνες συγκεντρώσεις των στοιχείων για την ανθρώπινη υγεία είναι:

- 100% για As, Pb, Cd και Zn,
- 90 έως 99% για Ag, V και Sb,
- 45 έως 68,8% για Cu και Mo, και
- 13,8 έως 33% για Ba, Ni και Cr.

Ενώ η εκατοστιαία αναλογία της έκτασης του Λαυρίου με φυτοτοξικά επίπεδα είναι:

- 100% για As, Pb και Zn,
- >90 έως 99% για Ag, Cd και Sb,
- >75 έως 90% για Ba, Cu, Cr και Ni, και
- >19 έως 31% για Mn και V.

Συμπεραίνεται ότι, η πολυστοιχειακή ρύπανση του εδαφικού καλύμματος του Λαυρίου είναι πολύ υψηλή, παρουσιάζει μη-αποδεκτό κίνδυνο για την ποιότητα ζωής του τοπικού πληθυσμού και είναι δυνητικά επικίνδυνη για τα φυτά και τα ζώα. Συνεπώς, κρίνεται άκρως επείγουσα η αποκατάσταση όλης της περιοχής με κατάλληλες μεθοδολογίες.

Chapter 6A. Distribution of EDTA extractable elements in overburden (Volumes 1 & 2)

Cold EDTA extractable Cd, Pb and Zn contents in soil are assumed to provide information about probable plant-available levels. Hence, inferences can be made on the selection of suitable plants for growing on soil with different contamination levels. As it has been shown, however, by the detailed studies, planting of vegetation alone is not the answer to the hazardous surface environmental conditions that exist in the Lavrion urban area. Consequently, this line of action was not pursued further.

Κεφάλαιο 6Α. Κατανομή των με EDTA εκχυλιζόμενων στοιχείων στο εδαφικό κάλυμμα (Τόμοι 1 & 2)

Οι συγκεντρώσεις, που προέρχονται από την εν ψυχρώ εκχύλιση των στοιχείων Cd, Pb και Zn με EDTA, θεωρείται ότι παρέχουν πληροφόρηση για τις πιθανές διαθέσιμες συγκεντρώσεις των στοιχείων αυτών στο έδαφος. Ως εκ τούτου, μπορούν να εξαχθούν συμπεράσματα όσον αφορά την επιλογή κατάλληλων φυτών για ανάπτυξη σε εδάφη με διαφορετικά επίπεδα ρύπανσης. Όπως έχει αποδειχθεί όμως, από τις λεπτομερείς μελέτες που έγιναν, η φυτοκάλυψη από μόνη της δεν μπορεί να δώσει απάντηση για την επικινδυνότητα της κατάστασης στο επιφανειακό περιβάλλον της αστικής περιοχής του Λαυρίου. Συνεπώς, αυτή η μεθοδολογία δεν ακολουθήθηκε περαιτέρω.

Chapter 7. Partitioning of the operationally defined phases in overburden – Sequential extraction results (Volumes 1, 1A & 2)

Κεφάλαιο 7. Διαχωρισμός των ορυκτοχημικών φάσεων των στοιχείων στα δείγματα επιφανειακού καλύμματος – Αποτελέσματα των αναλύσεων με τη μεθοδολογία των διαδοχικών εκχυλίσεων (Τόμοι 1, 1A & 2)

Chapter 8. Partitioning of the operationally defined phases in house dust – Sequential extraction results (Volumes 1, 1A &2)

Κεφάλαιο 8. Διαχωρισμός των ορυκτοχημικών φάσεων των στοιχείων στα δείγματα σκόνης σπιτιών – Αποτελέσματα των αναλύσεων με τη μεθοδολογία των διαδοχικών εκχυλίσεων (Τόμοι 1, 1A & 2)

A five-step sequential extraction method was applied on samples of overburden (n=224) and house dust (n=127) in order to study element concentrations in the "operationally" defined phases and their potential availability to plants, animals and humans, *i.e.*,

- exchangeable phase (adsorbed fraction),
- carbonate phase (carbonate and specifically adsorbed fraction),
- reducible phase (Fe-Mn oxide fraction),
- oxidisable phase (organic/sulphide fraction), and
- residual phase (silicate/refractory minerals fraction).

On each of the five extractant solutions twenty-two elements were determined by ICP-AES, *i.e.*, Ag, Al, Ba, Be, Ca, Cd, Co, Cr, Cu, Fe, K, La, Li, Mn, Mo, Ni, P, Pb, Sr, Ti, V and Zn. The results of the five phases are presented pictorially at each sampling site as coloured five-bar plots.

To our knowledge this is the first study to analyse routinely such a large number of overburden/soil and house dust samples by a five-step sequential extraction method, and to present the multi-element results geographically. Thus, enabling comparison of element contents in the five fractions within and between samples.

Interpretation of such a large number of variables required a good knowledge of lithology, mineralisation, rock alteration, chemistry and mineralogy of the different types of metallurgical processing wastes, and land uses. Otherwise, due to the unusual primary and secondary mineral phases present in the Lavrion overburden and house dust samples, sequential extraction results would have been difficult to interpret.

Problems encountered, due to the non-selectivity and specificity of reagents, used in the sequential extraction method, were overcome by the determination of a large number of elements on each of the extractant solutions. Inter-element relationships in each step were studied by means of boxplots, linear correlation coefficients, R-mode cluster and

Εφαρμόστηκε μέθοδος διαδοχικών εκχυλίσεων πέντε φάσεων στα δείγματα εδαφικού καλύμματος (n=224) και σκόνης σπιτιών (n=127), με στόχο τη μελέτη των συγκεντρώσεων των στοιχείων στις διάφορες φάσεις και τη δυνητική διαθεσιμότητά τους στα φυτά, ζώα και ανθρώπους, δηλ.:

- ανταλλάξιμη φάση (προσροφημένο κλάσμα),
- ανθρακική φάση (ανθρακικά και προσροφημένο κλάσμα με μηχανισμούς «ειδικής» προσρόφησης).
- αναγώγιμη φάση (κλάσμα συνδεδεμένο με οξείδια Fe & Mn),
- οξειδώσιμη φάση (κλάσμα συνδεδεμένο με οργανικά και θειούχες ενώσεις) και
- υπολειμματική φάση (κλάσμα στο πλέγμα πυριτικών και πυρίμαχων ορυκτών).

Σε κάθε ένα από τα πέντε εκχυλιστικά διαλύματα προσδιορίστηκαν εικοσιδύο στοιχεία με ICP-AES, δηλ. Ag, Al, Ba, Be, Ca, Cd, Co, Cr, Cu, Fe, K, La, Li, Mn, Mo, Ni, P, Pb, Sr, Ti, V and Zn. Τα αποτελέσματα των πέντε φάσεων απεικονίζονται σε κάθε θέση δειγματοληψίας με έγχρωμα ιστογράμματα πέντε ράβδων.

Σύμφωνα με τη βιβλιογραφία αυτή είναι η πρώτη μελέτη στα πλαίσια της οποίας αναλύθηκε τόσος μεγάλος αριθμός δειγμάτων εδαφικού καλύμματος και σκόνης σπιτιών με τη μέθοδο των διαδοχικών εκχυλίσεων (πέντε φάσεις) και παρουσιάστηκαν σε χάρτη τα πολυστοιχειακά αποτελέσματα. Με αυτόν τον τρόπο δίνεται η δυνατότητα σύγκρισης των συγκεντρώσεων των στοιχείων στα πέντε κλάσματα, τόσο στο κάθε δείγμα ξεχωριστά, όσο και μεταξύ των δειγμάτων.

Η ερμηνεία ενός τόσο μεγάλου αριθμού μεταβλητών απαιτούσε πολύ καλή γνώση της λιθολογίας, της μεταλλοφορίας, της εξαλλοίωσης των πετρωμάτων, χημείας και ορυκτολογίας των διαφορετικών τύπων μεταλλουργικών απορριμμάτων και των χρήσεων γης. Διαφορετικά, λόγω των ασυνήθιστων πρωτογενών και δευτερογενών ορυκτών που απαντώνται στα δείγματα του επιφανειακού καλύμματος και σκόνης σπιτιών, η ερμηνεία των αποτελεσμάτων των διαδοχικών

factor analyses.

Readily available overburden/soil element contents to plants, their bioavailable concentrations in house dust and biological effects on humans are discussed. The very low pH of gastric fluids (1-3), means that a greater proportion of element contents, present in overburden and house dust, can be made available for absorption by the human body, *i.e.*, even oxidisable element contents could be available. Consequently, it is not surprising that children, and adults alike, have high blood-Pb concentrations and high urine-As excretions.

Recommendations are also made about heavy metal detoxification.

It is concluded that, despite the limitations of sequential extraction methods, the multi-element (>40) determination on each of the extractant solution, in conjunction with pH measurements and total organic content, can provide significant information about geochemical dispersion processes in the surficial environment, leachability, mobility and bioavailability of elements in soil and sediments.

εκχυλίσεων θα ήταν δύσκολη.

Προβλήματα που δημιουργήθηκαν, λόγω της μη απόλυτης επιλεκτικότητας και εξειδίκευσης των αντιδραστηρίων που χρησιμοποιήθηκαν στη μέθοδο διαδοχικών εκχυλίσεων, αντιμετωπίσθηκαν με τον προσδιορισμό μεγάλου αριθμού στοιχείων σε κάθε εκχυλιστικό διάλυμα. Η σχέση μεταξύ των στοιχείων μελετήθηκε με κυψελοειδή διαγράμματα, συντελεστές γραμμικής συσχέτισης, ομαδική και παραγοντική ανάλυση.

Στο κείμενο εξετάζονται οι εύκολα προσλήψιμες συγκεντρώσεις για τα φυτά στο εδαφικό κάλυμμα, οι βιοδιαθέσιμες συγκεντρώσεις στη σκόνη σπιτιών και οι βιολογικές επιδράσεις τους στους ανθρώπους. Το πολύ χαμηλό pH των γαστρικών υγρών (1-3) σημαίνει ότι ένα μεγαλύτερο ποσοστό των συγκεντρώσεων, από αυτόν των ανταλλάξιμων μορφών, των στοιχείων στο έδαφος και στη σκόνη σπιτιών μπορεί να γίνει διαθέσιμο για απορρόφηση από τον ανθρώπινο οργανισμό, δηλ., ακόμη και οι συγκεντρώσεις της οξειδώσιμης φάσης μπορεί να είναι διαθέσιμες. Συνεπώς, δεν είναι παράξενο ότι τα παιδιά, καθώς και οι ενήλικοι, παρουσιάζουν υψηλές συγκεντρώσεις Pb στο αίμα τους και αυξημένες εκκρίσεις As στα ούρα.

Γίνονται επίσης προτάσεις για την αποτοξίνωση από βαρέα μέταλλα.

Συμπεραίνεται ότι, παρ' όλους τους περιορισμούς που υφίστανται για τα αποτελέσματα των μεθόδων διαδοχικών εκχυλίσεων, ο πολυστοιχειακός (>40) προσδιορισμός σε κάθε ένα από τα εκχυλιστικά διαλύματα, σε συνδυασμό με μετρήσεις pH και ολικής οργανικής ύλης, μπορούν να δώσουν σημαντική πληροφόρηση για τις γεωχημικές διεργασίες διασποράς στο επιφανειακό περιβάλλον, την εκχυλισιμότητα, κινητικότητα και βιοδιαθεσιμότητα των στοιχείων στο έδαφος και τα ιζήματα.

Chapter 9. Distribution of elements in different grain-size fractions of the metallurgical wastes and residual soil (Volumes 1 & 2)

The distribution of As, Cd, Hg, Pb, Sb and Zn is studied in five different grain-size fractions of metallurgical wastes (n=15) and residual soil (n=8). Their distribution is studied by means of boxplots and presented as coloured five-bar plots at each sampling site in order to study within and between sample variability. The highest element concentrations are found in the fine-grain sand (<0.125 +0.063 mm) and silt size (<0.063 mm) fractions,

Κεφάλαιο 9. Κατανομή των στοιχείων σε διαφορετικά κοκκομετρικά κλάσματα στα μεταλλουργικά απορρίμματα και το υπολειμματικό έδαφος (Τόμοι 1 & 2)

Μελετήθηκε η κατανομή του As, Cd, Hg, Pb, Sb και Zn σε πέντε διαφορετικά κοκκομετρικά κλάσματα σε δείγματα των μεταλλουργικών απορριμμάτων (n=15) και υπολειμματικού εδάφους (n=8). Η κατανομή τους παρουσιάζεται με κυψελοειδή διαγράμματα και έγχρωμα σχεδιαγράμματα με πέντε ράβδους σε κάθε θέση δειγματοληψίας για τη μελέτη της μεταβλητότητας εντός και μεταξύ των δειγμάτων.

which make up to 35% of the total sample weight.

Οι υψηλότερες συγκεντρώσεις των στοιχείων βρίσκονται στα κλάσματα της λεπτόκοκκης άμμου (<0.125 +0.063 mm) και ιλύος (<0.063 mm), τα οποία αποτελούν μέχρι και 35% του ολικού βάρους του δείγματος.

Chapter 10. Geochemistry of ground water: A preliminary assessment
(Volumes 1, 1B & 2)

Κεφάλαιο 10. Γεωχημεία των υπογείων νερών: Προκαταρκτική μελέτη
(Τόμοι 1, 1Β & 2)

Ground water resources in Lavrion were used until 30th April 1984 for the potable water supply of the town. After this date, the town was linked to the Athens conurbation water supply network, and ground water is only used for irrigation purposes. This preliminary study collected ground water from fifteen wells and drill-holes.

The concentrations of calcium, magnesium, manganese, nitrate, ammonium, and sulphate locally in ground water exceed their corresponding WHO maximum admissible limits. High concentrations of sodium and chloride in some wells indicate seawater infiltration. Potassium is generally high in agricultural areas, suggesting contamination from fertilisers and seawater intrusion. Lead, zinc, cadmium and copper contents are below their respective maximum admissible limits. The levels of lead, zinc and cadmium in ground water are, however, above normal in the area covered by the flotation residues, suggesting that downward leaching of these elements has started.

It is recommended that ground water chemistry be monitored continuously, and should not be used for drinking and cooking purposes. Although it is highly recommended that all agricultural activities in Lavrion be terminated immediately, in case ground water is used for irrigation purposes, its chemical properties must comply with stipulated legislative guidelines.

Οι υπόγειοι υδάτινοι πόροι του Λαυρίου εχρησιμοποιούντο μέχρι τις 30 Απριλίου 1984 για την ύδρευση της πόλης. Μετά από αυτή την ημερομηνία η πόλη του Λαυρίου υδρεύεται μέσω του συστήματος ύδρευσης της Αθήνας και το υπόγειο νερό χρησιμοποιείται μόνο για αρδευτικούς σκοπούς. Σ' αυτή την προκαταρκτική μελέτη δειγματίσθηκαν δεκαπέντε πηγάδια και γεωτρήσεις.

Οι συγκεντρώσεις ασβεστίου, μαγνησίου, μαγγανίου, αμμωνίου, νιτρικών και θειϊκών αλάτων υπερβαίνουν τοπικά τα μέγιστα αποδεκτά όρια. Οι υψηλές συγκεντρώσεις νατρίου και χλωριόντων σε μερικά πηγάδια δείχνουν τη διείσδυση του θαλασσινού νερού. Οι συγκεντρώσεις του καλίου είναι γενικά υψηλές στις αγροτικές περιοχές, υποδηλώνοντας ρύπανση από λιπάσματα και διείσδυση θαλασσινού νερού.

Οι συγκεντρώσεις του μολύβδου, ψευδαργύρου, καδμίου και χαλκού στο υπόγειο νερό είναι κάτω από τα αντίστοιχα μέγιστα αποδεκτά όρια της Παγκόσμιας Οργάνωσης Υγείας. Όμως, τα επίπεδα του μολύβδου, ψευδαργύρου και καδμίου στο υπόγειο νερό είναι υπεράνω των κανονικών ορίων στην περιοχή που καλύπτεται από τα απορρίμματα επίπλευσης (σαβούρα), γεγονός που υποδηλώνει ότι η κατείσδυση αυτών των στοιχείων έχει ήδη αρχίσει.

Προτείνεται η συνεχής παρακολούθηση της χημείας του υπόγειου νερού, καθώς και η μη χρησιμοποίησή του για πόση και μαγείρευμα. Αν και συνιστάται ο άμεσος τερματισμός όλων των αγροτικών δραστηριοτήτων στο Λαύριο, στην περίπτωση που το υπόγειο νερό χρησιμοποιείται για άρδευση, η χημική του σύσταση πρέπει να βρίσκεται εντός των πλαισίων, που καθορίζεται από τις αναφερόμενες νομοθετημένες οδηγίες.

Chapter 11. Spatially resolved hazard and exposure assessments (Volumes 1, 1A & 2)

Spatially Resolved Hazard Assessment (SRHA) and Spatially Resolved Exposure Assessment (SREA) are methodologies that have been devised for assessing child exposure to soil containing environmental pollutants. These are based on either a quantitative or a semi-quantitative approach. The feasibility of such methodologies has been demonstrated in a study assessing child exposure to lead (Pb) accessible in soil.

Using a quantitative approach, both measured and kriged concentrations of Pb in soil were compared with an "established" statutory threshold value. The probabilistic approach gives a refined classification of contaminated land, since it takes into consideration the uncertainty in both the actual measurement and estimated kriged values of lead.

Two exposure assessment models, the "*Integrated Exposure Uptake BioKinetic*" model (IEUBK) and "*Human Exposure from Soil Pollutants*" (HESP), were used as the basis of the quantitative SREA methodologies. The significant correlation, between child blood-Pb predictions, using the IEUBK model, and measured concentrations, provides a partial validation of the method, because it allows for the uncertainty in the measurements, and the lack of some site-specific measurements.

The semi-quantitative applications of SRHA and SREA incorporate both qualitative information (*e.g.*, land use and dustiness of waste) and quantitative information (*e.g.*, distance from wastes and distance from industry). The significant correlation, between the results of these assessments and the measured child blood-Pb levels, confirms the robust nature of this approach.

Successful application of these multi-criteria evaluation methodologies could reduce the cost of assessment, and allow areas to be prioritised for further investigation, remediation or risk management.

Κεφάλαιο 11. Εκτίμηση του χωρικού καθορισμού της επικινδυνότητας και έκθεσης (Τόμοι 1, 1A & 2)

Η Εκτίμηση του Χωρικού Καθορισμού της Επικινδυνότητας (SRHA) και η Εκτίμηση του Χωρικού Καθορισμού της Έκθεσης (SREA) είναι μεθοδολογίες, οι οποίες δημιουργήθηκαν για την εκτίμηση της έκθεσης των παιδιών στο έδαφος, που περιέχει περιβαλλοντικούς ρύπους. Αυτές οι μεθοδολογίες βασίζονται, είτε σε ποσοτικές, είτε σε ημιποσοτικές προσεγγίσεις. Η καταλληλότητα αυτών των μεθοδολογιών αποδείχθηκε από τη μελέτη εκτίμησης της έκθεσης των παιδιών στο βιοδιαθέσιμο μόλυβδο (Pb) του εδάφους.

Χρησιμοποιώντας την ποσοτική προσέγγιση, αμφότερες οι πραγματικές και οι παρεμβαλλόμενες συγκεντρώσεις «kriging» του Pb στο έδαφος συγκρίθηκαν με τα νομοθετημένα όρια. Η προσέγγιση πιθανότητας δίνει μία πιο λεπτομερή ταξινόμηση του ρυπασμένου εδάφους, λόγω του ότι λαμβάνει υπ' όψη την αβεβαιότητα σε αμφότερες τις πραγματικές και εκτιμώμενες «kriged» συγκεντρώσεις του μολύβδου.

Χρησιμοποιήθηκαν δύο μοντέλα ως βάση των μεθοδολογιών της ποσοτικής Εκτίμησης του Χωρικού Καθορισμού της Έκθεσης (SREA), η «*Ολοκληρωμένη Βιοκινητική Προσομοίωση Έκθεσης-Λήψης*» (IEUBK) και η «*Προσομοίωση της Ανθρώπινης Έκθεσης σε Ρύπους του Εδάφους*» (HESP). Η σημαντική συσχέτιση μεταξύ των εκτιμωμένων συγκεντρώσεων του Pb στο αίμα των παιδιών χρησιμοποιώντας το μοντέλο IEUBK και των μετρηθεισών συγκεντρώσεων, παρέχει μερική πιστοποίηση για την αξιοπιστία της μεθόδου, δεδομένου ότι λαμβάνει υπ' όψη την αβεβαιότητα στις μετρήσεις, καθώς και τη μη ύπαρξη μερικών μετρήσεων στη θέση δειγματοληψίας.

Οι ημιποσοτικές εφαρμογές των μεθοδολογιών SRHA και SREA συμπεριλαμβάνουν ποιοτική πληροφόρηση (π.χ., χρήση γης και βαθμός κονιορτοποίησης των απορριμμάτων) και ποσοτική πληροφόρηση (π.χ., απόσταση από τα απορρίμματα και από τη βιομηχανία). Η σημαντική συσχέτιση μεταξύ αυτών των εκτιμήσεων και του μετρηθέντος επιπέδου Pb στο αίμα των παιδιών πιστοποιεί τη δυναμική φύση αυτής της προσέγγισης.

Η επιτυχής εφαρμογή αυτών των μεθοδολογιών αξιολόγησης με πολλαπλά κριτήρια μπορεί να μειώσει το κόστος της εκτίμησης, καθώς και να επιτρέψει την ιεράρχιση περιοχών για πιο λεπτομερή μελέτη, αποκατάσταση ή διαχείριση της επικινδυνότητάς τους.

Chapter 12. Environmental management and planning (Volumes 1 & 2)

Six maps are presented, which are related to environmental management and planning in Lavrion, *i.e.*,

- Location of demonstration scale rehabilitation techniques (refer to Volume 3),
- Distribution of cost index of the rehabilitation techniques (refer to Volume 4),
- Distribution of benefit index for the rehabilitation of contaminated land (refer to Volume 4),
- Distribution of cost/benefit index for the rehabilitation of the Lavrion urban area (refer to Volume 4),
- Property characterisation map, and
- Map of urban control zones.

With these maps the geochemical atlas of the Lavrion urban area for environmental protection and planning is completed.

Κεφάλαιο 12. Περιβαλλοντική διαχείριση και σχεδιασμός (Τόμοι 1 & 2)

Παρουσιάζονται έξι χάρτες, οι οποίοι αναφέρονται στη διαχείριση του περιβάλλοντος και το σχεδιασμό στο Λαύριο, δηλ.

- Θέσεις των τεχνικών αποκατάστασης που εφαρμόστηκαν σε κλίμακα επίδειξης (βλ. Τόμο 3),
- Κατανομή του Δείκτη Κόστους των μεθόδων αποκατάστασης (βλ. Τόμο 4),
- Κατανομή του Δείκτη Οφέλους των μεθόδων αποκατάστασης (βλ. Τόμο 4),
- Κατανομή του Δείκτη Κόστους/Οφέλους των μεθόδων αποκατάστασης (βλ. Τόμο 4),
- Χάρτης χαρακτηρισμού ιδιοκτησιών και
- Χάρτης ζωνών οικιστικού ελέγχου.

Με αυτούς τους χάρτες ολοκληρώνεται ο γεωχημικός άτλας της αστικής περιοχής του Λαυρίου για περιβαλλοντική προστασία και σχεδιασμό.

VOLUME 1B: APPENDIX REPORTS

ΤΟΜΟΣ 1Β: ΕΚΘΕΣΕΙΣ ΠΑΡΑΡΤΗΜΑΤΟΣ

1. Multi-element geochemical desk study of garden soil in Lavrion

This multi-element preliminary soil geochemical desk study has given information about element levels and, therefore, assisted in the selection of elements to be determined in the individual particle characterisation and subsequent detailed environmental studies. Lavrion garden soil results were compared to normal uncontaminated soil and an enrichmement/depletion index calculated (elements arranged in a decreasing order of concentrations), *i.e.*,

Cd>Pb>Zn>As>Ag>Sb>W>S>Cu>Bi>Ca>Mn>Ni>
B>P>Ce>Mo>U>Hg>Cr>Mg>Sn>Fe>Sr>Ba>Rb>Co.

Cluster and factor analyses were able to distinguish elements related to smelting activities and to lithology. It was concluded that smelting of polymetalllic sulphide ore, and the wastes generated, were responsible for the complex multi-element contamination.

1. Πολυστοιχειακή γεωχημική μελέτη προϋπαρχόντων δειγμάτων κηπευτικού εδάφους στο Λαύριο

Η προκαταρκτική πολυστοιχειακή εδαφογεωχημική μελέτη των προϋπαρχόντων δειγμάτων κηπευτικού εδάφους έδωσε πληροφόρηση για τα επίπεδα των χημικών στοιχείων. Οι πληροφορίες αυτές βοήθησαν στην επιλογή των στοιχείων για τη μελέτη του χαρακτηρισμού σωματιδίων και τις μετέπειτα λεπτομερείς περιβαλλοντικές μελέτες. Τα αποτελέσματα της ανάλυσης των δειγμάτων του κηπευτικού εδάφους του Λαυρίου συγκρίθηκαν με τα επίπεδα των μη ρυπασμένων εδαφών και υπολογίστηκε ο δείκτης εμπλουτισμού/ανεπάρκειας (τα στοιχεία είναι σε φθίνουσα σειρά συγκέντρωσης), δηλ.,

Cd>Pb>Zn>As>Ag>Sb>W>S>Cu>Bi>Ca>Mn>Ni>
B>P>Ce>Mo>U>Hg>Cr>Mg>Sn>Fe>Sr>Ba>Rb>Co.

Με την ομαδική και την παραγοντική ανάλυση κατέστη δυνατή η αναγνώριση στοιχείων που σχετίζονται με τη μεταλλουργική δραστηριότητα και τη λιθολογία. Συμπεραίνεται, ότι η μεταλλουργική επεξεργασία των πολυμεταλλικών θειούχων μεταλλευμάτων και τα απορρίμματα που προέκυψαν ευθύνονται για την πολυσύνθετη πολυστοιχειακή ρύπανση.

2. Individual particle analysis of metallurgical wastes, overburden and house-hold dust from the town of Lavrion, Greece	**2. Χαρακτηρισμός σωματιδίων των μεταλλουργικών απορριμμάτων, του επιφανειακού καλύμματος και της σκόνης σπιτιών από την πόλη του Λαυρίου, Ελλάδα**
Computer controlled scanning electron microscopy with X-ray analysis provides a high resolution characterisation technique for individual particle characterisation. The method was first calibrated using samples from metallurgical processing wastes (source samples). Subsequently, a small number of overburden/soil and house dust samples were analysed to investigate the potential of this scheme for source apportionment. The method has been shown to be capable of identifying different contamination source particles in overburden/soil and house dust samples. It is concluded that a detailed study could provide information on particle size and elemental composition, information which will be invaluable in setting up priorities for exposure reduction and, ultimately, cost-effective remediation.	Το σαρωτικό ηλεκτρονικό μικροσκόπιο με ανάλυση ακτίνων-Χ, ελεγχόμενο από υπολογιστή, παρέχει μία υψηλής ευκρίνειας τεχνική για το χαρακτηρισμό σωματιδίων. Η μέθοδος βαθμονομήθηκε χρησιμοποιώντας τα δείγματα από τα μεταλλουργικά απορρίμματα (δείγματα πηγής). Στη συνέχεια, ένας μικρός αριθμός δειγμάτων εδαφικού καλύμματος και σκόνης σπιτιών αναλύθηκε με στόχο τη διερεύνηση της δυνατότητας διαχωρισμού των πηγών ρύπανσης. Αποδείχθηκε ότι η μέθοδος μπορεί να διαχωρίσει τα σωματίδια, ανάλογα με τις πηγές ρύπανσης από τις οποίες προέρχονται, στα δείγματα εδαφικού καλύμματος και σκόνης σπιτιών. Συμπεραίνεται, ότι μία λεπτομερής μελέτη μπορεί να δώσει πληροφόρηση για το μέγεθος των κόκκων και τη στοιχειακή τους σύσταση, η οποία θα είναι χρήσιμη στον καθορισμό προτεραιοτήτων για τη μείωση της έκθεσης και τελικά για την αποτελεσματική και ως προς το κόστος αποκατάσταση.
3. An introduction to the technique of individual particle analysis (IPA) using computer controlled scanning electron microscopy (CCSEM)	**3. Εισαγωγή στην τεχνική της ανάλυσης μοναδιαίων (ατομικών) σωματιδίων χρησιμοποιώντας το ηλεκτρονικό μικροσκόπιο σάρωσης ελεγχόμενο από υπολογιστή.**
The technique of individual particle analysis, using computer controlled scanning electron microscopy, is described. The classification scheme developed for the Lavrion samples is also given.	Περιγράφεται η τεχνική της μοναδιαίας (ατομικής) ανάλυσης σωματιδίων, χρησιμοποιώντας το ηλεκτρονικό μικροσκόπιο σάρωσης ελεγχόμενο από υπολογιστή. Αναφέρεται επίσης το σχέδιο ταξινόμησης, που αναπτύχθηκε για τα δείγματα του Λαυρίου.
4. Subsurface geochemistry of the Lavrion urban area: Drill-hole and vertical profile results	**4. Γεωχημεία του υπεδάφους στην αστική περιοχή του Λαυρίου: Αποτελέσματα γεωτρήσεων και κάθετων τομών.**
Twenty-two drill-holes and two vertical profiles were used in the study of the subsurface distribution of elements. It is stressed that drill-holes and vertical profiles, in such an area as Lavrion with extremely variable contamination, provide information about the site only. Results have shown that contamination is not restricted to the metallurgical wastes, but extends into the subsurface overburden, and in some cases reaches bedrock. Depending, therefore, on drill-hole site, the thickness of contaminated overburden, including metallurgical wastes, varies from as little as 0.37 m, a residual soil background area, to 14.60 m, a site situated on the flotation residues.	Για τη μελέτη της κατανομής των στοιχείων στο υπέδαφος έγιναν εικοσιδύο γεωτρήσεις και δύο κάθετες τομές. Επισημαίνεται, ότι οι γεωτρήσεις και οι κάθετες τομές σε μία περιοχή, όπως το Λαύριο, με πολύ μεγάλη μεταβλητότητα της ρύπανσης, παρέχουν πληροφόρηση μόνο για τη θέση δειγματοληψίας. Τα αποτελέσματα έδειξαν ότι η ρύπανση δεν περιορίζεται μόνο στα μεταλλουργικά απορρίμματα, αλλά εκτείνεται στο υπέδαφος και σε μερικές περιπτώσεις φθάνει μέχρι το μητρικό πέτρωμα. Ανάλογα με τη θέση της γεώτρησης, το πάχος της ρύπανσης του εδαφικού καλύμματος, συμπεριλαμβανομένων και των μεταλλουργικών απορριμμάτων, κυμαίνεται

Levels of toxic elements in fluvial sediments, derived from the erosion of mining wastes outside the study area, are significantly lower than overburden in the Lavrion urban area, which is partly affected and/or derived from the metallurgical processing activities.

Mobility of contaminants, due to the generation of acid drainage, is considerable in the areas with pyritiferous wastes, and especially the pyrite tailings on the beach between Komobil and Kiprianos. Some, downward leaching of contaminants was noted even in areas with an alkaline pH and high carbonate contents.

It is concluded that the drill-holes and vertical profiles have provided valuable information about the subsurface geochemistry in the Lavrion urban area, and the potential contamination problems of ground water resources.

από 0,37 m, σε μία θέση με υπολειμματικό έδαφος με τιμές «background», έως 14,60 m, σε θέση που βρίσκεται στην περιοχή με τις αποθέσεις απορριμμάτων εμπλουτισμού (σαβούρα).

Τα επίπεδα των τοξικών στοιχείων στα ποτάμια ιζήματα, που προέρχονται από τη διάβρωση των μεταλλευτικών απορριμμάτων εκτός της περιοχής μελέτης, είναι σημαντικά πιο χαμηλά από αυτά του εδαφικού καλύμματος της αστικής περιοχής του Λαυρίου, το οποίο επηρεάζεται ή/και προέρχεται από τα μεταλλουργικά απορρίμματα.

Η κινητικότητα των ρυπαντών, η οποία οφείλεται στη δημιουργία όξινης απορροής, είναι σημαντική σε περιοχές με πυριτούχα απορρίμματα και κυρίως στα απορρίμματα πυρίτη στην παραλία της Κομομπίλ-Κυπριανού. Παρατηρήθηκε μερική κατείσδυση των ρυπαντών ακόμη και σε περιοχές με αλκαλικό pH και υψηλές συγκεντρώσεις ανθρακικών.

Συμπεραίνεται, ότι οι γεωτρήσεις και οι κάθετες τομές έδωσαν αξιόλογη πληροφόρηση για τη γεωχημεία του υπεδάφους της αστικής περιοχής του Λαυρίου και για τα πιθανά προβλήματα ρύπανσης του υπόγειου νερού.

5. Geochemistry of ground water, Lavrion

Geochemical results of ground water samples are tabulated together with admissible limits, certain useful indices and ionic ratios, pie diagrams and histograms (for more details refer to the summary of Chapter 10).

5. Γεωχημεία του υπόγειου νερού, Λαύριον

Τα αποτελέσματα της γεωχημείας των δειγμάτων του υπόγειου νερού παρουσιάζονται σε πίνακες με τα αποδεκτά τους όρια, μερικούς χρήσιμους δείκτες και ιοντικούς λόγους, διαγράμματα και ιστογράμματα (για περισσότερες πληροφορίες αποτανθείτε στην περίληψη του Κεφαλαίου 10).

CONCLUSIONS AND RECOMMENDATIONS

"The transition to sustainable development requires among other things an adequate supply of environmental information. State of environment reports can help in the assessment of alternative policy options, improve political accountability and meet the public right to know" (Stanners and Bourdeau, 1995, p.2). This report satisfies the above premise, but also the fifth conclusion reached by the Dobříš Castle conference of European Environmental Ministers (June 1991), but for application at the scale of a town by the Councillors of the Municipality of Lavreotiki the report should

ΣΥΜΠΕΡΑΣΜΑΤΑ ΚΑΙ ΠΡΟΤΑΣΕΙΣ

«Η μετάβαση στην αειφόρο ανάπτυξη απαιτεί μεταξύ των άλλων μία ικανοποιητική παροχή περιβαλλοντικής πληροφόρησης. Αναλυτικές εκθέσεις για το περιβάλλον μπορούν να βοηθήσουν στην εκτίμηση εναλλακτικών στρατηγικών, να βελτιώσουν την πολιτική αξιοπιστία και να ικανοποιήσουν το δικαίωμα των πολιτών να γνωρίζουν» (Stanners and Bourdeau, 1995, σελ.2). Η μελέτη αυτή ικανοποιεί την παραπάνω απαίτηση, καθώς επίσης και το πέμπτο συμπέρασμα που προέκυψε κατά τη συνάντηση των Ευρωπαίων Υπουργών Περιβάλλοντος στο Κάστρο Dobříš (Ιούνιο 1991), αλλά για να εφαρμοστεί στην κλίμακα μίας πόλης, από τους Δημοτικούς Συμβούλους η έκθεση πρέπει

- be used as a "… **basis for the effective implementation of environmental policies and strategies**", and
- serve "… **as a useful tool to inform the public and raise awareness about environmental problems**".

The most significant practical and geoenvironmental scientific conclusions of this multi-sampling media and multi-element environmental study of the Lavrion urban area are summarised below together with recommendations. For more detailed conclusions and recommendations the interested reader should consult individual chapters.

(a) The following practical conclusions and recommendations are for the Councillors of the Municipality of Lavreotiki:

1. Intensive metallurgical activities, emissions and the dumps of metallurgical processing wastes are responsible for the contamination of surface and sub-surface overburden.
2. Redistribution of metallurgical wastes by aerial, fluvial and anthropogenic processes resulted in the contamination of even the remotest parts of the Lavrion urban area.
3. The interior home environment is extremely contaminated as has been shown by the high levels of toxic elements (As, Cd, Pb, Zn) in house dust.
4. Cross-sectional epidemiological studies have shown that children and adults alike have high blood-lead and urine-arsenic contents, which have been related to a number of adverse health effects.
5. The enormous amount of metallurgical processing wastes and contaminated soil are responsible for the high blood-lead and urine-arsenic contents of the Lavrion population.
6. Human exposure to environmental contaminants must be reduced to acceptable levels. The rehabilitation of the greater Lavrion urban area environment is considered, therefore, an urgent task, otherwise alternate actions must be seriously examined, such as resettling the population in a better and healthier environment.
7. Local people must be informed about the adverse health effects, which are related to the extremely high environmental contamination, and suggestions made for their temporary protection.
8. All agricultural activities must stop, for edible plants have high toxic element concentrations.

- να χρησιμοποιηθεί ως «… **βάση για την αποτελεσματική εφαρμογή της περιβαλλοντικής πολιτικής και στρατηγικής**», και
- να λειτουργήσει «… **ως ένα χρήσιμο εργαλείο για την πληροφόρηση του κοινού και την ευαισθητοποίησή του σε περιβαλλοντικά προβλήματα**».

Παρακάτω συνοψίζονται τα πιο σημαντικά πρακτικά και γεωπεριβαλλοντικά επιστημονικά συμπεράσματα και προτάσεις αυτής της πολυστοιχειακής περιβαλλοντικής μελέτης της αστικής περιοχής του Λαυρίου. Για πιο λεπτομερή συμπεράσματα και προτάσεις ο αναγνώστης πρέπει να ανατρέχει στα αντίστοιχα κεφάλαια.

(α) Τα παρακάτω πρακτικά συμπεράσματα και προτάσεις απευθύνονται στους Δημοτικούς Συμβούλους του Δήμου Λαυρεωτικής:

1. Οι εντατικές μεταλλουργικές δραστηριότητες, οι εκπομπές και οι σωροί των μεταλλουργικών απορριμμάτων ευθύνονται για τη ρύπανση του επιφανειακού και υπο-επιφανειακού εδαφικού καλύμματος.
2. Η ανακατανομή των μεταλλουργικών απορριμμάτων μέσω αέριων, ποτάμιων και ανθρωπογενών διεργασιών ευθύνονται για τη ρύπανση ακόμη και των πιο απομακρυσμένων σημείων της αστικής περιοχής του Λαυρίου.
3. Το εσωτερικό περιβάλλον των σπιτιών είναι έντονα ρυπασμένο, όπως δείχνουν οι υψηλές συγκεντρώσεις των τοξικών στοιχείων (As, Cd, Pb, Zn) στη σκόνη σπιτιών.
4. Οι επιδημιολογικές έρευνες έδειξαν ότι τα παιδιά και οι ενήλικες έχουν υψηλές συγκεντρώσεις μολύβδου στο αίμα και αρσενικού στα ούρα, οι οποίες συσχετίζονται με μία σειρά αρνητικών επιπτώσεων στην υγεία.
5. Ο τεράστιος όγκος των μεταλλουργικών απορριμμάτων και το ρυπασμένο έδαφος ευθύνονται για τις υψηλές συγκεντρώσεις μολύβδου στο αίμα και αρσενικού στα ούρα του πληθυσμού του Λαυρίου.
6. Η έκθεση του πληθυσμού στους περιβαλλοντικούς ρύπους πρέπει να μειωθεί σε αποδεκτά όρια. Κατά συνέπεια, η αποκατάσταση της ευρύτερης αστικής περιοχής του Λαυρίου θεωρείται επείγουσα δράση, διαφορετικά πρέπει να εξεταστούν σοβαρά εναλλακτικές λύσεις, όπως η εγκατάσταση του πληθυσμού σε καλύτερο και πιο υγιές περιβάλλον.
7. Ο τοπικός πληθυσμός πρέπει να ενημερωθεί για τις αρνητικές επιπτώσεις στην υγεία του, οι οποίες οφείλονται στην πολύ ισχυρή περι-

9. The Municipality of Lavreotiki must ensure that the beneficiation/flotation residues, because of their high toxic element contents, are no longer used as sand in the construction industry, and must not be transported outside Lavrion.
10. The Muncipality of Lavreotiki must ensure that non-ferrous slag (lumpy and pelletised) and sand-blast wastes, because of their high toxic element contents, are no longer used in the construction industry, and are not transported outside Lavrion. It is stressed that although the mechanical properties of non-ferrous slag may be considered satisfactory for construction purposes, this material is chemically reactive, it is not inert, for it releases toxic elements in the environment, and could cause serious deterioration to concrete and other structures.
11. The Municipality of Lavreotiki must monitor the geochemistry of ground water, and if used for agricultural purposes, it must safeguard that its chemical parameters do not exceed recommended limits. It is noted that the proposal is that all agricultural activities must be stopped immediately.
12. The Municipality of Lavreotiki, in collaboration with the Lavrion Medical Centre and the Ministry of Health, must monitor the health of children and adults alike.
13. Any new housing estate plans in the Lavrion area and Lavreotiki peninsula must take seriously into account the problem of contaminated land, and its effects on the quality of life of the population.
14. The Municipality of Lavreotiki and State Authorities are legally bound to inform, future land and house buyers and industrialists, the problems of contamination, which are responsible for adverse health effects. Otherwise, in the future they may face legal actions against them, and compensations paid to interested parties.

βαλλοντική ρύπανση, καθώς και να του γίνουν υποδείξεις για την προσωρινή προστασία του.

8. Όλες οι αγροτικές δραστηριότητες πρέπει να σταματήσουν, διότι όλα τα εδώδιμα φυτά έχουν υψηλές συγκεντρώσεις τοξικών στοιχείων.
9. Ο Δήμος Λαυρεωτικής πρέπει να διασφαλίσει τη μη χρησιμοποίηση των απορριμμάτων εμπλουτισμού (σαβούρα), ως άμμο στην οικοδομική βιομηχανία, καθώς και τη μη μεταφορά τους εκτός της πόλης του Λαυρίου, λόγω της υψηλής περιεκτικότητάς τους σε τοξικά στοιχεία.
10. Ο Δήμος Λαυρεωτικής πρέπει να διασφαλίσει τη μη χρησιμοποίηση των μη-σιδηρούχων σκουριών (πλινθώματα και συσφαιρώματα) και των απορριμμάτων αμμοβολής στην κατασκευαστική βιομηχανία, καθώς και τη μη μεταφορά τους εκτός του Λαυρίου, λόγω των υψηλών συγκεντρώσεων τοξικών στοιχείων που περιέχουν. Επισημαίνεται ότι, παρ' όλο που οι μηχανικές ιδιότητες των μη-σιδηρούχων σκουριών θεωρούνται ικανοποιητικές για κατασκευαστικούς σκοπούς, το υλικό αυτό είναι χημικά ενεργό, δεδομένου ότι αποδευσμεύει τοξικά στοιχεία στο περιβάλλον και μπορεί να δημιουργήσει σοβαρή φθορά στο μπετόν και άλλες κατασκευές.
11. Ο Δήμος Λαυρεωτικής πρέπει να ελέγχει τη γεωχημική ποιότητα του υπόγειου νερού και, εφ' όσον αυτό χρησιμοποιείται για αγροτικούς σκοπούς, να διασφαλίζει ότι οι χημικές παράμετροι αυτού δεν υπερβαίνουν τα συνιστώμενα όρια. Επισημαίνεται, ότι η πρόταση είναι να σταματήσουν άμεσα όλες οι αγροτικές δραστηριότητες.
12. Ο Δήμος Λαυρεωτικής, σε συνεργασία με το Κέντρο Υγείας Λαυρίου και το Υπουργείο Υγείας, πρέπει να παρακολουθούν την υγεία των παιδιών και των ενηλίκων.
13. Κάθε νέος οικιστικός σχεδιασμός στο Λαύριο και τη Λαυρεωτική χερσόνησο πρέπει να λαμβάνει σοβαρά υπ' όψη το πρόβλημα του ρυπασμένου εδάφους και τις επιπτώσεις του στην ποιότητα ζωής του πληθυσμού.
14. Ο Δήμος Λαυρεωτικής και οι Κρατικοί Φορείς δεσμεύονται νομικά να ενημερώνουν μελλοντικούς αγοραστές γης και οικιών, καθώς και βιομηχάνους, για τα προβλήματα ρύπανσης, τα οποία επιφέρουν αρνητικές επιπτώσεις στην υγεία. Διαφορετικά, είναι δυνατόν να αντιμετωπίσουν μελλοντικά δικαστικές διεκδικήσεις και την καταβολή αποζημιώσεων στους ενδιαφερομένους.

(b) Geoenvironmental scientific conclusions and recommendations related to environmental impact assessment of contaminated land.

For an effective appraisal of environmental contamination at a site the following conclusions and recommendations, which resulted from this work, should be taken into account:

1. Desk study: collection and evaluation of all available data.
2. An orientation soil survey should be carried out to establish contamination levels of toxic elements. It is stressed that a large number of major and trace elements should be determined, during this phase, in order to decide on the elements to be determined in the detailed study.
3. Detailed mapping of contamination sources should be carried out, and their chemical and mineralogical properties determined.
4. Detailed multi-element soil geochemical survey, with field observations and photographs;
5. Based on the results of the soil geochemical survey, suitable sites should be selected to study the distribution of elements in the subsurface environment, either by drilling or vertical soil profiles. One of the aims of this work is to determine local natural background element variation in order to correctly evaluate anthropenic contamination.
6. Detailed land use mapping is important for both multi-criteria evaluation of risk, but also for land rehabilitation, depending on the end-user principle (management).
7. Based on the results of the soil geochemical survey, and the maps of land use and contamination sources, an optimum sampling plan must be devised to collect house dust, human tissues, and plants.
8. In agricultural areas, ground water must be sampled and analysed for inorganic and organic contaminants.
9. Soil, house dust, plant and human tissue samples, apart from the determination of toxic elements, should be analysed for as many elements as is practically possible, because they will aid interpretation of results.
10. Sequential extraction methods provide significant information about the mobilitiy, leachability and bioavailability of elements;
11. pH and total organic matter should be determined on soil and house dust samples.

(β) Γεωπεριβαλλοντικά επιστημονικά συμπεράσματα και προτάσεις για την εκτίμηση των περιβαλλοντικών επιπτώσεων της ρυπασμένης γης.

Για αποτελεσματική αξιολόγηση της περιβαλλοντικής ρύπανσης σε μία περιοχή τα παρακάτω συμπεράσματα και προτάσεις, που προέκυψαν απ' αυτή την εργασία, πρέπει να λαμβάνονται υπ' όψη:

1. Μελέτη γραφείου: συλλογή και αξιολόγηση όλων των υπαρχουσών πληροφοριών.
2. Διεξαγωγή προσανατολιστικής εδαφογεωχημικής μελέτης με στόχο τον καθορισμό των επιπέδων ρύπανσης των τοξικών χημικών στοιχείων. Επισημαίνεται ότι είναι απαραίτητο να προσδιοριστεί μεγάλος αριθμός μακρο- και ιχνο-στοιχείων, σ' αυτή τη φάση, προκειμένου να καθοριστούν τα στοιχεία που θα προσδιοριστούν κατά τη λεπτομερή έρευνα.
3. Λεπτομερής χαρτογράφηση των πηγών ρύπανσης και προσδιορισμός της χημικής και ορυκτολογικής τους σύστασης.
4. Λεπτομερής πολυστοιχειακή εδαφογεωχημική μελέτη, με παρατηρήσεις υπαίθρου και φωτογραφίες.
5. Βάσει των αποτελεσμάτων της εδαφογεωχημικής έρευνας, πρέπει να επιλεγούν κατάλληλες θέσεις για τη μελέτη της κατανομής των χημικών στοιχείων στο υπέδαφος, είτε με γεωτρήσεις είτε με κάθετες εδαφοτομές. Ένας από τους στόχους αυτής της εργασίας είναι ο καθορισμός της φυσικής διακύμανσης των στοιχείων για την ορθή εκτίμηση της ανθρωπογενούς ρύπανσης.
6. Η λεπτομερής χαρτογράφηση της χρήσης γης είναι σημαντική για την με πολλαπλά κριτήρια εκτίμηση της επικινδυνότητας, καθώς επίσης και για την αποκατάσταση της γης, βάσει της τελικής της χρήσης (διαχείριση).
7. Βάσει των αποτελεσμάτων της εδαφογεωχημικής έρευνας, των χαρτών χρήσης γης και των πηγών ρύπανσης, πρέπει να προγραμματιστεί ένα βέλτιστο σχέδιο δειγματοληψίας σκόνης σπιτιών, ανθρώπινων ιστών και φυτών.
8. Σε αγροτικές περιοχές, πρέπει να δειγματίζεται το επιφανειακό και υπόγειο νερό και να προσδιορίζονται ανόργανοι και οργανικοί ρυπαντές.

12. Strict quality control procedures must be used during sampling, sample preparation and analysis, and quality control parameters presented on the distribution maps for the verification of the quality of results;
13. Geostatistics is considered to be the optimum method for the treatment of spatial data and map plotting of element distribution, and should be used in all environmental studies. Geostatistics should also be used in planning the detailed sampling network to reduce sampling errors. In this case, the geostatistical parameters of the sampling network should be extracted from the results of the orientation soil geochemical survey.
14. Factor and cluster analyses should be used for the determination of subtle associations among the elements/determinants;
15. Good knowledge of the area is required for a full interpretation of data;
16. Risk assessment should be based on multi-criteria evaluation techniques, and
17. All spatial parameters should be presented on maps for contamination is a geographical problem.

9. Τα δείγματα εδάφους, σκόνης σπιτιών, φυτών και ανθρώπινων ιστών, εκτός από τον προσδιορισμό των τοξικών στοιχείων, πρέπει να αναλύονται για όσο το δυνατόν περισσότερα στοιχεία, δεδομένου ότι θα βοηθήσουν στην καλύτερη ερμηνεία των αποτελεσμάτων.
10. Οι μέθοδοι των διαδοχικών εκχυλίσεων παρέχουν σημαντική πληροφόρηση για την κινητικότητα, εκχυλισιμότητα και βιοδιαθεσιμότητα των στοιχείων.
11. Το pH και η ολική οργανική ύλη πρέπει να προσδιορίζεται στα δείγματα εδάφους και της σκόνης σπιτιών.
12. Πρέπει να χρησιμοποιούνται αυστηροί έλεγχοι κατά τη δειγματοληψία, προπαρασκευή και ανάλυση των δειγμάτων και οι ποιοτικές παράμετροι να παρουσιάζονται στους χάρτες κατανομής για την πιστοποίηση της ποιότητας των αποτελεσμάτων.
13. Η γεωστατιστική θεωρείται η βέλτιστη μέθοδος για την επεξεργασία και παρουσίαση σε χάρτη της κατανομής των στοιχείων και θα πρέπει να χρησιμοποιείται σε όλες τις περιβαλλοντικές μελέτες. Η γεωστατιστική θα πρέπει να χρησιμοποιείται και στο σχεδιασμό του λεπτομερούς δικτύου δειγματοληψίας για τη μείωση των σφαλμάτων δειγματοληψίας. Στην περίπτωση αυτή, οι γεωστατιστικές παράμετροι του δικτύου δειγματοληψίας μπορούν να καθοριστούν από την προσανατολιστική εδαφο-γεωχημική έρευνα.
14. Η παραγοντική και η ομαδική ανάλυση πρέπει να χρησιμοποιούνται στις περιβαλλοντικές μελέτες για τον καθορισμό περίπλοκων συσχετίσεων μεταξύ των στοιχείων/ μεταβλητών.
15. Για την τελειωτική ερμηνεία των αποτελεσμάτων απαιτείται η λεπτομερής γνώση της περιοχής.
16. Η εκτίμηση της επικινδυνότητας πρέπει να βασίζεται σε τεχνικές αξιολόγησης πολλαπλών κριτηρίων και
17. Όλες οι χωρικές περιβαλλοντικές παράμετροι πρέπει να παρουσιάζονται σε χάρτες, δεδομένου ότι η ρύπανση είναι γεωγραφικό πρόβλημα.

This study has shown that the European Union must set realistic statutory limits for soil. It is stressed, that statutory limits must consider the variable geochemical background against which contamination should be assessed. This fact is also stressed in the book *"Europe's Environment, The Dobříš Assessment"* (Stanners and Bourdeau, 1995, p.164), which was published by the European Environmental Agency. In parallel, the work of the

Στα πλαίσια της μελέτης αυτής διαπιστώθηκε η αναγκαιότητα ότι η Ευρωπαϊκή Ένωση πρέπει να θεσπίσει ρεαλιστικά όρια για τα εδάφη. Τονίζεται, ότι τα νομοθετημένα όρια πρέπει να λαμβάνουν υπ' όψη τη μεταβλητότητα του γεωχημικού υποβάθρου, βάσει του οποίου θα εκτιμηθεί η ρύπανση. Το γεγονός αυτό επισημαίνεται επίσης και στο βιβλίο *«Europe's Environment, The Dobříš Assessment»* (Stanners and Bourdeau,

Geochemistry Group of the Forum of the European Geological Surveys, and the working group on "Global Geochemical Baselines" of the International Union of Geological Sciences, should be taken into account. European results are expected to be available in the year 2001. Further, realistic statutory limits should also be set for house dust, plants and human tissues.

We are all hoping that the techniques used, in the characterisation of contaminated land in Lavrion, will constitute a fundamental axis for the development of a standardised methodology to assess contaminated land. Nevertheless, in order that these results do not remain *"on paper"*, the taking of essential measures and decisions to improve the living conditions of the local population, depend on the will of the State. We are hoping, therefore, that the new century will be marked with co-ordinated efforts from all of us towards environmental protection and upgrading of quality of life. *We have an obligation to offer a better and a healthier environment to the new generation*. Otherwise, it is mathematically certain that we will be led to deadlocks, which to be overcome we will be forced to turn to extreme solutions, which will include, in the case of the seriously contaminated areas of Lavrion and Lavreotiki, the movement and resettlement of the population to another more suitable area. Hence, the whole Lavreotiki peninsula will be converted to a national forest and an open museum of our historical and mining activities.

1995, σελ.164), το οποίο δημοσιεύτηκε από την Ευρωπαϊκή Υπηρεσία Περιβάλλοντος. Παράλληλα, θα πρέπει να ληφθεί υπ' όψη η εργασία της Ομάδας Γεωχημείας της Ένωσης Ευρωπαϊκών Γεωλογικών Υπηρεσιών και της Ομάδας Εργασίας της «Παγκόσμιας Γεωχημικής Χαρτογράφησης» της Διεθνούς Ένωσης Γεωλογικών Επιστημών. Τα αποτελέσματα που αφορούν την Ευρώπη αναμένονται να είναι διαθέσιμα εντός του 2001. Επίσης, ρεαλιστικά νομοθετημένα όρια πρέπει να καθοριστούν για τη σκόνη σπιτιών, τα φυτά και τους ανθρώπινους ιστούς.

Ελπίδα όλων μας είναι οι τεχνικές, που χρησιμοποιήθηκαν για το χαρακτηρισμό της ρυπασμένης γης στο Λαύριο, να αποτελέσουν βασικό άξονα μιας τυποποιημένης μεθοδολογίας για την εκτίμηση της ρύπανσης. Όμως, στη συνέχεια, για να μην μένουν τα αποτελέσματα αυτά *«στα χαρτιά»*, επαφίεται στη βούληση της Πολιτείας η λήψη ουσιαστικών μέτρων και αποφάσεων για τη βελτίωση των συνθηκών διαβίωσης του τοπικού πληθυσμού. Ελπίζουμε, ότι ο νέος αιώνας θα σηματοδοτηθεί από τις συντονισμένες προσπάθειες όλων μας για την προστασία του περιβάλλοντος και της αναβάθμισης της ποιότητας ζωής. *Έχουμε υποχρέωση να προσφέρουμε ένα καλύτερο και υγιέστερο περιβάλλον στη νέα γενιά.* Διαφορετικά, είναι μαθηματικώς βέβαιο ότι θα οδηγηθούμε σε αδιέξοδα, τα οποία για να ξεπεραστούν θα μας αναγκάσουν να καταφύγουμε σε ακραίες λύσεις, που θα περιλαμβάνουν, συγκεκριμένα για την έντονα ρυπασμένη περιοχή του Λαυρίου και της Λαυρεωτικής, τη μετακίνηση και εγκατάσταση του πληθυσμού σε άλλη καταλληλότερη περιοχή. Έτσι, ολόκληρη η περιοχή της Λαυρεωτικής χερσονήσου θα μετατραπεί σε εθνικό δρυμό και ανοικτό μουσείο της ιστορικής και μεταλλευτικής δραστηριότητας.

Blank back page
Λευκή οπίσθια σελίδα

ACKNOWLEDGEMENTS

The authors sincerely thank all the people who helped in the various stages of the project. With a large number of people involved, directly or indirectly, in such a project, it is difficult to be exhaustive. The authors apologise for the involuntary omission of any individual, who contributed to this project.

IGME General Directors:- Dr. Vassilios Andronopoulos, Professor Christos Katagas, Mr. George Katsamankos, Dr. Stavros Kalogeropoulos and Professor Antonios Koussis, whose help was greatly appreciated in the final leg of the project.
Directors of the IGME Division of Geochemistry:- Mr. Costantinos Kouvelos and Mr. Kiriakos Ioannidis, who devoted a considerable part of his time in procedural matters about the project. Further, his interest for the successful completion of the project was greatly appreciated.
Deputy Director of the IGME Division of Geochemistry:- Dr. Penelope Stavrakis for her active participation in the project until her early retirement in June 1998.
IGME Division of Geochemistry scientists:- Mária Kaminari and Sotiris Lampropoulos, whose help was greatly appreciated in the translation of many technical terms from English into Greek. Mária Kaminari is also thanked for her constructive comments on parts of the project report.
IGME Division of Geochemistry technical personnel:- Loukas Savvides for his assistance in the field work, and Constantinos Letsios for the computer entry of data.
Laboratory of the IGME Branch of Eastern Macedonia and Thrace:- (a) Chemists: Georgios Grigoriades and Grigoris Katsanopoulos, (b) Technical personnel: Constantinos Tsouskidis, Evangelia Isaakidou, Christos Sphatos, Vasilio Demenidis and Anastasios Kirmizopoulos for sample preparation and analysis.
Laboratory of the IGME Branch of Preveza:- (a) Chemist: Harry Tzoulis, and (b) Technical personnel: Georgios Ntovas for sample preparation.
IGME Central Laboratory in Athens:- (a) Chemists: Dr. Constantinos Leonis and Theopisti Limperopoulou, and (b) Technical personnel: Panagiotis Papaneofitou, Athanassios Sakkas and Vassiliki Kotsi for analytical determinations.
Laboratory of the IGME Division of Geochemistry:- Varvara Lemonia and Angeliki Karakatsani for the determination of Hg.
IGME Division of Economics:- Antonis Papastilianou, Ioanna Margaritopoulou, Vasilios Nikakis, Georgios Hatzioannou and Mary Vagena for their help in financial and procedural matters.
IGME Public Relations Department:- Dimitris Constantinides, Ioannis Papadakis, Dimitris Vassiliou, Stavroula Havaki, Eleni Kotronia and Kalliopi Katartzi for their help in the organisation of workshops, exhibitions, *etc.*
IGME Photographic Department:- Grigoris Karianakis and Nicolaos Athanassopoulos for the photographic compilation of maps.
PRISMA – Centre for Development Studies: Julia Drossinou, Cynthia Stathaki, George Moussouris and Mary Sifou for their positive input in the project during their employment at the Project Manager's office.
British Geological Survey:- Professor Jane Plant, Dr. John W. Baldock, Dr. John Ridgway, Dr. Mark N. Ingham, Dr. Daug Miles, Dr. Chris McDermott and Dr. Alain C. Mackenzie for their help in data processing with the Arc/Info GIS and the free gratis analysis of samples by XRF.
Institute for Hygiene and Occupational Medicine, Technical University of Aachen:- Dr. Vasilios Makropoulos for the provision of biomedical data and bibliography.
General Child Hospital of Penteli: Alexandra Nicolaou-

ΕΥΧΑΡΙΣΤΙΕΣ

Οι συγγραφείς ευχαριστούν όσους βοήθησαν στα διαφορετικά στάδια του έργου. Με έναν τόσο μεγάλο αριθμό ανθρώπων που βοήθησαν, άμεσα ή έμμεσα, σε ένα τέτοιο έργο, είναι δύσκολο να είμαστε διεξοδικοί. Οι συγγραφείς ζητούν συγγνώμη για την ακούσια παράλειψη οποιουδήποτε ατόμου, που βοήθησε σ' αυτό το έργο.

Γενικοί Διευθυντές ΙΓΜΕ:- Δρ. Βασίλειο Ανδρονόπουλο, Καθηγητή Χρήστο Καταγά, κ. Γεώργιο Κατσαμάγκο, Δρ. Σταύρο Καλογερόπουλο και Καθηγητή Αντώνιο Κούση, η βοήθεια του οποίου στο τελικό στάδιο του έργου εκτιμάται ιδιαίτερα.
Διευθυντές Διεύθυνσης Γεωχημείας ΙΓΜΕ:- κ. Κωνσταντίνο Κούβελο και κ. Κυριάκο Ιωαννίδη, ο οποίος αφιέρωσε σημαντικό μέρος του χρόνου του στα διαδικαστικά θέματα του έργου. Επίσης, το ενδιαφέρον του για την επιτυχή ολοκλήρωση του έργου εκτιμάται ιδιαίτερα.
Αναπληρώτρια Διευθύντρια της Διεύθυνσης Γεωχημείας του ΙΓΜΕ:- Δρ. Πηνελόπη Σταυράκη για την ενεργό συμμετοχή της στο έργο μέχρι την πρόωρη συνταξιοδότησή της τον Ιούνιο του 1998.
Επιστημονικό προσωπικό της Διεύθυνσης Γεωχημείας του ΙΓΜΕ:- Μάρια Καμινάρη και Σωτήρη Λαμπρόπουλο, η βοήθεια των οποίων εκτιμάται ιδιαίτερα στη μετάφραση πολλών τεχνικών όρων από τα Αγγλικά στα Ελληνικά. Την Μάρια Καμινάρη την ευχαριστούμε επίσης για τα εποικοδομητικά της σχόλια επί τμήματος της έκθεσης.
Τεχνικό προσωπικό της Διεύθυνσης Γεωχημείας του ΙΓΜΕ:- Λουκά Σαββίδη για τη βοήθειά του στις υπαίθριες εργασίες και τον Κωνσταντίνο Λέτσιο για την εισαγωγή δεδομένων στον ηλεκτρονικό υπολογιστή.
Χημείο ΙΓΜΕ Παραρτήματος Ανατολικής Μακεδονίας και Θράκης:- (α) Χημικούς: Γεώργιο Γρηγοριάδη και Γρηγόρη Κατσανόπουλο, (β) Τεχνικό προσωπικό: Κωνσταντίνο Τσουσκίδη, Ευαγγελία Ισαακίδου, Χρήστο Σφάτο, Βασίλειο Δεμενίδη και Αναστάσιο Κυρμιζόπουλο για την τυποποίηση και ανάλυση των δειγμάτων.
Χημείο ΙΓΜΕ Παραρτήματος Πρέβεζας:- (α) Χημικό: Χάρη Τζούλη, και (β) Τεχνικό προσωπικό: Γεώργιο Ντόβα για την τυποποίηση των δειγμάτων.
Κεντρικό Χημείο ΙΓΜΕ στην Αθήνα:- (α) Χημικούς: Δρ. Κωνσταντίνο Λεώνη και Θεοπίστη Λυμπεροπούλου, και (β) Τεχνικό προσωπικό: Παναγιώτη Παπανεοφύτου, Αθανάσιο Σακκά, και Βασιλική Κότση.
Εργαστήριο Διεύθυνσης Γεωχημείας ΙΓΜΕ:- Βαρβάρα Λεμονιά και Αγγελική Καρακατσάνη για τον προσδιορισμό του Hg.
Διεύθυνση Οικονομικού ΙΓΜΕ:- Αντώνιο Παπαστυλιανού, Ιωάννα Μαργαριτοπούλου, Βασίλειο Νικάκη, Γεώργιο Χατζηϊωάννου και Μαίρη Βαγενά για τη βοήθειά τους σε οικονομικά και διαδικαστικά θέματα.
Τμήμα Τεκμηρίωσης Διεθνών και Δημοσίων Σχέσεων:- Δημήτριο Κωνσταντινίδη, Ιωάννη Παπαδάκη, Δημήτριο Βασιλείου, Σταυρούλα Χαβάκη, Ελένη Κοτρωνιά και Καλλιόπη Καταρτζή για τη βοήθειά τους στην οργάνωση παρουσιάσεων, εκθέσεων, κ.ά.
Φωτογραφικό Τμήμα ΙΓΜΕ:- Γρηγόρη Καριανάκη και Νικόλαο Αθανασόπουλο για τη φωτογραφική σύνθεση χαρτών.
PRISMA – Κέντρο Αναπτυξιακών Μελετών:- Ιουλία Δροσινού, Κυνθία Σταθάκη, Γεώργιο Μουσούρη και Μαίρη Σίφου για τη θετική συνεισφορά τους στο έργο κατά την περίοδο εργασίας τους στα γραφεία του Προϊσταμένου του Έργου.
Βρεττανική Γεωλογική Υπηρεσία:- Καθηγήτρια Jane Plant, Δρ. John W. Baldock, Δρ. John Ridgway, Δρ. Mark N. Ingham, Δρ. Daug Miles, Δρ. Chris McDermott and Δρ.

Papanagiotou and Georgia Tapaki for the provision of biomedical bibliography.
Imperial College of Science, Technology and Medicine of the University of London:- Mrs. Krystyna St. Clair-Gribble for the careful preparation of the sequential extractions.
Institute of Advanced Studies, University of Malaya:- Dr. Yap Slaw Yang for her work on individual particle characterisation of Lavrion samples during her training at Imperial College.
Nottingham Trent University:- Dr. Paul Constantinos Nathanail for the provision of bibliography on risk assessment, and constructive discussions about the subject.
Geological Survey of Finland:- Professor Reijo Salminen for the provision of bibliography about the Finnish statutory levels on soil.
Geological Survey of The Netherlands:- Dr. Jan Ebbing for the provision of bibliography about the Dutch statutory levels on soil.
OMAC Laboratories Ltd.:- Mike O'Neill is thanked for devoting his time to experiment on the Lavrion samples in order to produce good quality results.
Students:- Manolis Mavrommatis, Eleana Venaki, Dimitris Zisimos, and Sofia Kokkoni for data entry and map digitisation.
Ph.D. student: Panagiota Mpossinakou for her help in map digitisation.
Graduate Trainees: Nikolaos Mpardanis, Maria Amargiotakis and Eleni Douvi for their help in the binding of the volumes.
Lavrion inhabitants:- Constantinos Pogkas (past Mayor) and Ioannis Mpallopoulos (past Chairman of Municipality Council) for information about mining and smelting activities in Lavrion, and Constantinos Manthos (deceased) for assistance in historical information.
Video production:- Mineralogical Museum of Lavrion (Nicos Vourlakos), family of Emmanouel Papadohazaki, Nico Angelopoulo and Marina Demetriadou for their help in the production of the video film.
Lavrion Forestry Office for provision of the boundaries of national forest areas.
Lavrion Port Authorities for provision of boundaries of the state port area.
Ministry of Environment, Planning and Public Works, Division of Aerial Photographs for the provision of aerial photographs at a scale of 1:5000.
Hellenic State Mortgage Company for the provision of the boundaries of state properties in Lavrion.
National Statistics Office for the provision of statistical data of the Municipality of Lavreotiki.
Commission of the European Union, DG XI:- Last but not least, Dr. Theodoros Tharouniatis for his continued interest in the project, and his assistance in various matters.

Alain C. Mackenzie για τη βοήθειά τους σε θέματα επεξεργασίας δεδομένων με το Arc/Info GIS και τη δωρεάν ανάλυση δειγμάτων με φασματομετρία ακτίνων-Χ.
Ινστιτούτο Υγιεινής και Ιατρικής Εργασίας, Τεχνικό Πανεπιστήμιο του Άαχεν:- Δρ. Βασίλειο Μακρόπουλο για τη διάθεση των βιοϊατρικών δεδομένων και βιβλιογραφίας.
Γενικό Νοσοκομείο Παίδων Πεντέλης:- Αλεξάνδρα Νικολάου-Παπαναγιώτου και Γεωργία Ταπάκη για τη διάθεση βιοϊατρικής βιβλιογραφίας.
Βασιλικό Κολλέγιο Επιστήμης, Τεχνολογίας και Ιατρικής του Πανεπιστημίου του Λονδίνου:- Krystyna St. Clair-Gribble για την προσεκτική προπαρασκευή των διαδοχικών εκχυλίσεων.
Ινστιτούτο Προηγμένων Μελετών, Πανεπιστήμιο Μαλαίας:- Δρ. Yap Slaw Yang για την εργασία της στο χαρακτηρισμό σωματιδίων σε δείγματα του Λαυρίου κατά την περίοδο εκπαίδευσής της στο Βασιλικό Κολλέγιο του Πανεπιστημίου του Λονδίνου.
Πανεπιστήμιο Νόττινχαμ Τρεντ:- Δρ. Παύλο Κωνσταντίνο Ναθαναήλ για τη διάθεση βιβλιογραφίας, που αφορά την εκτίμηση της επικινδυνότητας και τις εποικοδομητικές συζητήσεις στο θέμα αυτό.
Γεωλογική Υπηρεσία της Φινλανδίας:- Καθηγητή Reijo Salminen για τη διάθεση βιβλιογραφίας σχετικά με τα Φινλανδικά νομοθετημένα όρια των εδαφών.
Γεωλογική Υπηρεσία Ολλανδίας:- Δρ. Jan Ebbing για τη διάθεση βιβλιογραφίας σχετικά με τα Ολλανδικά νομοθετημένα όρια των εδαφών.
OMAC Laboratories Ltd:- Ευχαριστούμε τον Mike O'Neill για το χρόνο που αφιέρωσε στον πειραματισμό επί των δειγμάτων του Λαυρίου, ούτως ώστε να δώσει καλής ποιότητας αποτελέσματα.
Φοιτητές:- Μανώλη Μαυρομμάτη, Ελεάνα Βενάκη, Δημήτριο Ζήσιμο και Σοφία Κοκκώνη για την εισαγωγή δεδομένων και ψηφιοποίηση χαρτών.
Υποψήφια Διδάκτωρ: Παναγιώτα Μποσινάκου για τη βοήθειά της στη ψηφιοποίηση χαρτών.
Υπό εκπαίδευση πτυχιούχοι: Νικόλαο Μπαρδάνη, Μαρία Αμαργιωτάκη και Ελένη Δουβή για τη βοήθειά τους στη σελιδοποίηση των τόμων.
Κάτοικοι Λαυρίου:- Κωνσταντίνο Πόγκα (πρώην Δήμαρχο) και Ιωάννη Μπαλλόπουλο (πρώην Πρόεδρο Δημοτικού Συμβουλίου) για πληροφορίες επί της μεταλλευτικής και μεταλλουργικής δραστηριότητας στο Λαύριο και τον Κωνσταντίνο Μάνθο (θανόντα) για τη βοήθειά του σε ιστορικές πληροφορίες.
Παραγωγή βιντεοταινίας:- Ορυκτολογικό Μουσείο Λαυρίου (Νίκο Βουρλάκο), την οικογένεια Εμμανουήλ Παπαδοχαζάκη, Νίκο Αγγελόπουλο, Θεόδωρο Σαββίδη και Μαρίνα Δημητριάδου για τη βοήθειά τους στην παραγωγή της βιντεοταινίας του έργου.
Δασαρχείο Λαυρίου για την παροχή των ορίων των δασικών εκτάσεων.
Λιμενικό Ταμείο Λαυρίου για την παροχή των ορίων των ιδιοκτησιών του.
ΥΠΕΧΩΔΕ, Δ/νση Αεροφωτογραφιών για τη διάθεση αεροφωτογραφιών σε κλίμακα 1:5000.
Κτηματική Εταιρεία του Δημοσίου για την παροχή των ορίων των κρατικών ιδιοκτησιών στο Λαύριο.
Εθνική Στατιστική Υπηρεσία για την παροχή στατιστικών δεδομένων για το Δήμο Λαυρεωτικής.
Επιτροπή Ευρωπαϊκής Ένωσης, XI Διεύθυνση:- Δρ. Θεόδωρο Θαρουνιάτη για το συνεχές ενδιαφέρον του στο έργο και τη βοήθεια του σε διάφορα θέματα.

IGME PROJECT ACTIVITIES – Contractual obligations

Alecos Demetriades
Institute of Geology and Mineral Exploration, 70 Messoghion Street, Gr-115 27 Athens, Greece

1. INTRODUCTION

The contractual obligations of the Institute of Geology and Mineral Exploration (IGME) will be concisely described below.

The principal objective of the project is to apply, on a demonstration scale, the appropriate techniques for the rehabilitation of the heavily polluted industrial area of Lavrion.

Project objectives, under the responsibility of the IGME Division of Geochemistry or in collaboration with the other partners [National Technical University of Athens (NTUA) Municipality of Lavrion & PRISMA], as defined in the approved proposal are outlined below:

- Detailed evaluation of the current status of the Lavrion urban area, focusing mainly on soil contamination,
- Identification of the main pollution sources in the area,
- Development of an integrated environmental management scheme for the Lavrion urban area, and
- To inform people and organisations about the available techniques for mitigating similar environmental problems.

It must be appreciated that this was a multi-media and multi-facet project dealing with one of the most heavily contaminated areas in the World. The data generated by the above project objectives are enormous. Data processing required considerable time, under normal circumstances, when everything is working perfectly smoothly. In this case, we had to face a multitude of technical hardware/software problems. These unexpected problems created a chaotic situation, because it was impossible to keep to any strict time schedule, for matters were completely out of hand.

The data generated, their description and discussion are essentially presented in six volumes, there are, however, still some unprocessed data. In conclusion, this project it was too ambitious to be completed within the span of three years.

2. CONTRACTUAL OBLIGATIONS

The above objectives were fulfilled through the different tasks of Phases I to III, which are concisely described below. The contractual obligations are itemised for ease of checking with the approved project proposal, comments made where problems were

encountered with the available data and information, and justifications given when alterations were deemed necessary.

The IGME technical report due to the vast quantity of data is presented in five volumes, i.e.,

Volume 1: Geochemical atlas of the Lavrion urban area for environmental protection and planning: Explanatory text.

Volume 1A: Geochemical atlas of the Lavrion urban area for environmental protection and planning: Tables and figures.

Volume 1B: Geochemical atlas of the Lavrion urban area for environmental protection and planning: Appendix reports.

Volume 2: Geochemical atlas of the Lavrion urban area for environmental protection and planning.

Volume 4: Environmental Management Plan for the Rehabilitation of Soil in the Lavrion urban area (Part I: Greek text and Part II: English text)

*[**Note**: Volume 3 is the report of the National Technical University of Athens]*

Maps quoted in the following description will be found in Volume 2 of the Technical Report *"Geochemical atlas of the Lavrion urban area for environmental protection and planning"*.

PHASE I

Task 1: Definition of areas under study and selection of locations for application of methods (sub-tasks 1.1 to 1.3)

A thorough evaluation of the current state of the Lavrion surface environment was not possible upon starting the project. The reason was that, apart from geochemical data, no detailed geological, metallurgical wastes and digital topography maps were available. At the time of writing the project proposal in 1993 the information was, however, that they were available.

1. The 4 m interval contour lines of the 1:5000 topographical map of the Hellenic Army Geographical Service, spot heights and triangulation stations, were scanned and/or digitised, for the purchased digital elevation model had significant errors at this scale (Map 2.1). Contour lines at 20-m intervals were subsequently selected for constructing the topography layer of the lithology map (Map 2.3), metallurgical wastes map (Map 2.3), land use map (Map 2.4) and sample site maps (Maps 2.7 - 2.15).

2. The town plan of the 1:5000 topographical map was out of date; hence, this was updated with the aid of recent aerial photographs and fieldwork (Map 2.1).

3. Maps of the lithology and metallurgical wastes were prepared following field mapping at a scale of 1:5000 (Maps 2.2 & 2.3).

4. All available soil geochemical data were entered into a database, and single element and composite distribution maps plotted.

5. Additional soil samples from unsampled areas were collected (n=56), making a total of 224 samples in the Lavrion urban area (Map 2.9), and 269 samples for the greater area extending westwards to the village of Ayios Constantinos. Following their analysis by a five-step sequential extraction method at Imperial College of Science, Technology and Medicine (Environmental Geochemistry Research Group, T.H. Huxley School of Environment, Earth Science & Engineering, Royal School of Mines, University of London, United Kingdom), it was found that even residual soil that seemed uncontaminated had high toxic element concentrations. Since, it was not possible to determine the natural background variation of soil in order to make a realistic assessment of the degree of contamination, it was decided to sample bedrock; 140 rock samples were collected (Map 2.7) [sample preparation and analysis by the IGME Branch of Eastern Macedonia and Thrace]. The lithology map was used in planning the rock geochemical sampling survey [Map 2.2]. These data are reported in Volumes 1, 1A and 2. *It is noted that rock sampling was not originally included in the approved project proposal*.

6. Representative samples were collected from all types of metallurgical wastes for their geochemical (n=62) and mineralogical (n=21) characterisation (Maps 2.3 & 2.13). Samples of metallurgical wastes following their preparation at the IGME Branch of Eastern Macedonia and Thrace they were analysed at Omac Laboratories Ltd, Loughrea, Ireland. Mineralogical characterisation by *"Individual particle analysis using computer controlled scanning electron microscopy"* was carried out in collaboration with the Environmental Geochemistry Research Group, T.H. Huxley School of Environment, Earth Science & Engineering, Royal School of Mines, Imperial College of Science, Technology and Medicine, University of London, United Kingdom (Volume 1B: Appendix Report 1).

7. Representative samples were collected from the medium- to fine-grained metallurgical wastes (n=10) and residual soil (n=8) to study their particle-size distribution and element concentrations in the different grain-size fractions (Map 2.11). Particle-size analysis was carried out at the IGME Branch of Eastern Macedonia and Thrace, and analytical determinations at Omac Laboratories Ltd., Loughrea, Ireland. Data reported in Volumes 1, 1A and 2.

8. Samples of residual soil/overburden (n=269) and house dust (n=127) were subjected to sequential extraction and multi-element determination (22 elements) by Inductively-coupled plasma emission at Imperial College of Science, Technology and Medicine [Environmental Geochemistry Research Group, T.H. Huxley School of Environment, Earth Science & Engineering, Royal School of Mines]. Results are reported in Volumes 1, 1A and 2.

9. Surface streams run only after torrential rain. Hence, no stream water samples were taken.

10. Previous ground water studies did not determine toxic elements. Samples of ground water were, therefore, collected from fifteen wells/boreholes (Map 2.12) for a preliminary assessment. Results are reported in Volumes 1, 1B and 2.

11. Climatic data are not available for Lavrion, since in the whole Lavreotiki peninsula there is no weather station. According to our information, a weather station, recording also air pollution, was working until 1989. Following the closure of the smelter, the station was closed down. Several attempts to obtain the data were unsuccessful.

12. Available cross-sectional epidemiological data and information were obtained from the Lavrion Medical Centre and sample locations placed on the 1:5000 topographical map (Map 2.15). Only individual blood-Pb measurements of Lavrion children were recorded on the medical information questionnaire sheets. Other determinants, such as blood-Cd, and the 24 hour urine As, Cr, Ni, Hg, F and phenol, after a thorough search at the Institute of Hygiene and Occupational Health of Technical University of Aachen (Germany), where the analysis was carried out, were not found. Results are reported in Volumes 1, 1B and 2.

13. All spatial information was scanned or digitised and is available in Arc/Info® GIS and Surfer® formats. IGME project scientists were trained at the British Geological Survey (Keyworth, Nottingham, United Kingdom) in the effective use of Arc/Info® GIS, and subsequently at the premises of IGME.

14. Following preliminary assessment of available data and plotting of environmental impact maps, project scientists selected the most suitable locations for field demonstration of rehabilitation techniques developed in the laboratory. This work was carried out in collaboration with the National Technical University of Athens (NTUA), PRISMA and the Municipality of Lavrion. The final selection relied on land availability, which was subject to ownership, public or private. Since, land ownership was one of the problems faced in the selection of suitable test sites, it was decided to compile a property characterisation map (Map 12.5*)*. A map of urban control zones, according to 1997 state legislation was compiled (Map 12.6). These two maps will be very useful for the Municipality of Lavrion for planning purposes, and it is stressed that *they were not part of our contractual obligations*.

15. Advanced statistical techniques, such as R-mode factor analysis was used during the preliminary assessment of X-ray fluorescence (XRF) multi-element soil analytical data (n=50) [analysis at the British Geological Survey, Keyworth, Nottingham, United Kingdom]. Pattern classification, factor and cluster analyses were used in the detailed study of project data sets (refer to Volumes 1 & 2). Further, multi-criteria evaluation maps were plotted during the risk assessment study (Maps 11.15-11.18).

Phase II

Task 3: Development and application of selected remedial technologies

IGME following the assessment of contamination provided possible locations for the demonstration scale application of the rehabilitation techniques developed by NTUA. This task was also included in Sub-task 1.3 of Phase I (refer to item 14 above).

Task 4: Evaluation and assessment of preventive and remedial methods used for the improvement of a heavily polluted environment

IGME, in collaboration with Imperial College of Science, Technology and Medicine [Environmental Geochemistry Research Group, T.H. Huxley School of Environment, Earth Science & Engineering, Royal School of Mines] used project data for making a spatially resolved risk assessment (Maps 11.1-11.18).

For making an effective risk assessment additional data and information were necessary, e.g., land use map (Map 2.4), present and previous stacks (source of aerial contaminants), streams, tar and untarred roads. *These items were not part of our contractual obligations*, but since the work was essential for the risk assessment study, it was carried out. The work is reported in Volumes 1, 1A and 2.

A video film was made in collaboration with NTUA, PRISMA and the Municipality of Lavreotiki about the methods used in the project and their results. The script was written during February-March 1999. On site video filming was carried out intermittently from January to April 1999. The studio work began at the end of March and the video film was finally completed on the 30th May 1999.

An eight-page information leaflet with project results and practical recommendations to the local inhabitants was written during April-May 1999 by project scientists (IGME-NTUA-PRISMA), and was printed in early June 1999.

Phase III

Task 5: Development of an integrated environmental management scheme for the Lavrion urban area

Results obtained during the preceding tasks were assessed, and an integrated environmental management scheme for the Lavrion urban area was developed in collaboration with an external expert, NTUA and PRISMA (Maps 12.1-12.4, Volume 4). Risk assessment results, rehabilitation costs, effectiveness of rehabilitation methods etc. were used in cost-benefit analysis on the different rehabilitation methods developed by NTUA (Maps 12.1, Volume 3).

Project results were communicated to Councillors of the Municipality of Lavrion on the 18th June 1999. Project were results and the video film were presented to the local

population, Municipality Officers, scientists from the Institute of Geology and Mineral Exploration, National Technical University of Athens, Hellenic Universities etc. on the 19th June 1999.

This part of the work in the approved project proposal was going to be carried out in collaboration with RPS Cairns (The Environmental Consultancy). For reasons unknown to us, they did not respond to our communications, following the despatch of project data in January 1997. Hence, this work was carried out in collaboration with different scientists, i.e., Imperial College of Science, Technology and Medicine for the risk assessment study (Chapter 11, Volume 1 & Maps 11.1 to 11.8 in Volume 2), and Dr. Nikos Nikolaidis (external expert from the University of Connecticut, U.S.A.) for the integrated environmental management scheme (Volume 4, Maps 12.1-12.4).

3. ADDITIONAL WORK NOT INCLUDED IN THE PROJECT PROPOSAL

Additional work, deemed necessary, but not was part of our contractual obligations, has already been mentioned in the relevant sections, but is summarised here as well.

Rock geochemical sampling and multi-element analysis of the samples were carried out, as explained above, because it is the only medium able to give natural element concentrations in the Lavrion urban area.

Core-drilling was carried out under the initiative of NTUA, for it was considered significant to obtain depth-related data about the chemical and physical characteristics of sub-surface materials. IGME collaborated in the location of the drill-holes [Map 2.14], core logging, multi-element analysis of samples at Omac Laboratories Ltd., Loughrea, Ireland, data processing and interpretation (Appendix Report 3B, Volume 1B).

Land use is a significant parameter in risk assessment and environmental management. Hence, a detailed land use map at a scale of 1:5000 was prepared for the Lavrion urban area (Map 2.4).

Since, one of the greatest problem faced during the demonstration scale application of rehabilitation techniques was property ownership, it was decided to compile two maps which will help the Lavrion Municipality officers in planning of remediation activities, i.e., a property ownership map (Map 12.5) and a map of urban control zones according to State legislation (Map 12.6).

4. PROJECT REPORTS

During the course of the project four reports were written:

- *"Risk assessment and rehabilitation of contaminated soil at the Phenikodhassos in Lavrion"*, June 1995 (in Greek with a summary in English). The report was written following an official request from the Ministry of Environment, Planning and Public Works.

- *"The release of toxic elements from the Lavrion slags"* , August 1995 (in Greek with a summary in English). The report was written after a formal request from the Mayor of the Municipality of Lavrion.

- *"Environmental Geochemistry, Biomedicine and Data Management"*, November 1996 (in English). This report was the IGME contribution to the interim Technical Report submitted to the XI Directorate in November 1996 by the Project Co-ordinator.

- *"Child blood lead content as a basis for risk assessment of the metallurgical processing residues and contaminated soil in Lavrion Attiki",* March 1998:
  Part I: *"Software, databases, quality control, digital, statistical and geostatistical processing of data, Lavrion Attiki"* (in Greek with a summary in English).
  Part II: *"Evaluation of child exposure to lead in Lavrion as a basis for risk assessment"* (in English).
  The report discusses the background of data management and processing leading to risk assessment. It was submitted to the XI Directorate in June 1998.

5. DISSEMINATION OF PROJECT RESULTS

Project results were disseminated to other scientists in national and international symposia and conferences (oral and poster presentations), workshops, seminars, special meetings, excursions to Lavrion and exhibitions. Further, two in-house workshops were organised by IGME with participation from Greek universities. All these activities are listed below.

5.1. Publications and presentations in national and international symposia

1. A multidisciplinary study on the effects of environmental contamination on the human population of the Lavrion urban area, Hellas
P. Stavrakis, A. Demetriades, K. Vergou-Vichou, I. Thornton, G. Fosse, V. Makropoulos and N. Vlachoyiannis
In: S.P. Varnavas (ed.), Environmental Contamination, 6th International Conference, Delphi, Greece, 10-12 October 1994. CEP Consultants Ltd, Edinburgh, 1994: 20-22.

2. The contribution of geochemical exploration in the study of environmental problems in Greece
A. Demetriades, P. Stavrakis and K. Vergou-Vichou
Workshop on Mineralogy and Geology: Their contribution in environmental protection. Geological Society of Greece, Committee on Economic Geology and Geochemistry. Observatory theatre, Aristotelean University of Thessaloniki, 20.2.1995. Abtract only (in Greek.

3. The relationship between geochemistry and mineralogy and their contribution in environmental studies
A. Demetriades, P. Stavrakis, K. Vergou-Vichou, X. Li, K. Zagkalis, V. Perdikatsis and J. Watt

Workshop on Mineralogy and Geology: Their contribution in environmental protection. Geological Society of Greece, Committee on Economic Geology and Geochemistry. Observatory theatre, Aristotelean University of Thessaloniki, 20.2.1995. Abtract only (in Greek).

4. Soil rehabilitation in the municipality of Lavrion
A. Kontopoulos, N. Papassiopi, P. Stavrakis and A. Demetriades
Recycling Waste Management Remediation of Contaminated Sites, 1995. European Commission, EC Environment and Climate Programme, DGXII/D-1, Technologies for Environmental Protection, Report 8: 570-575.

5. Environmental geochemistry study of Lavrion
P. Stavrakis, K. Vergou-Vichou and A. Demetriades
Environment and Development, Municipality of Lavreotiki, Lavrion, October 1995: 55

6. Risk assessment and rehabilitation of contaminated soil at the Phenikodhassos in Lavrion
Αλ. Δημητρίαδης, Π. Σταυράκη και Αικ. Βέργου-Βήχου
Heleco'95: "Geotechnical Engineering and Environment", Technical Chamber of Greece, Stadium of Peace and Friendship, 9.-10.11.1995. Υπό έκδοση (Text in Greek with a summary in English), in press.

7. Multipurpose geochemical mapping in Greece
A. Demetriades
Workshop: Environmental and Legislative uses of Regional Geochemical Baseline Data for Sustainable Development", British Geological Survey, Keyworth, United Kingdom (U.K.), March 1996 (Abstract only).

8. Distribution of lead and arsenic in the Lavrion urban environment, Greece
P. Stavrakis, A. Demetriades, K. Vergou-Vichou, V. Makropoulos, N. Vlachoyiannis and I. Thornton
14th European Conference, Society of Environmental Geochemistry and Health, Centre for Environmental Technology, Imperial College of Science, Technology and Medicine, London, U.K., 1.-3.4.1996, Book of abstracts: 11.

9. Lead in the surface environment of Lavreotiki peninsula (Attiki, Greece) and its effects on human health
A. Demetriades, P. Stavrakis and K. Vergou-Vichou
In: Aug. Anagnostopoulos, Ph. Day and D. Nicholls (Editors), Proceedings Third International Conference on Environmental Pollution, Sept. 16-20, 1996, University of Thessaloniki, Thessaloniki: 143-146.

10. Exploration geochemistry in environmental impact assessment: Examples from Greece
A. Demetriades, P. Stavrakis and K. Vergou-Vichou
In: P.G. Marinos, G.C. Koukis, G.C. Tsiambaos and G.C. Stournaras (Editors), Proceedings International Symposium on Engineering Geology and The Environment, 23-27 June 1997. A.A. Balkema, Rotterdam, 2 (1997): 1757-1762.

11. Arsenic and antimony in the surface soil of Lavreotiki peninsula, Attiki Prefecture, Greece
A. Demetriades
A one-day Seminar hosted by Imperial College for the Royal Society of Chemistry, Environmental Chemistry Discussion Group, 3.12.1997, Abstract only.

12. Hazard assessment of Pb in soil and dust at Lavrion, Greece, using GIS techniques
E. Tristán, A. Demetriades, M.S. Rosenbaum, M.H. Ramsey, P. Stavrakis, I. Thornton, E. Vassiliades and K. Vergou
16th European Conference of the Society for Environmental Geochemistry and Health, University of Derby, Derby, U.K., 6.-8.4.1998. Abstract only.

13. Spatially resolved hazard and exposure assessments: An example of lead in soil at Lavrion, Greece
E. Tristán, A. Demetriades, M.H. Ramsey, M.S. Rosenbaum, P. Stavrakis, I. Thornton, E. Vassiliades and K. Vergou
Paper has been accepted for publication in Environmental Research.

14. Toxic elements in the soil of Lavreotiki and their effect on the health of the local population
A. Demetriades and K. Vergou
A one-day seminar organised by the Thematic Society of Welfare and Mutual Aid of Eastern Attiki, Pallini, Greece, 9.5.1999 (Abstract only in Greek).

5.2. IGME Workshops

5.2.1. First workshop: Risk Assessment

A two-day workshop was organised on the 17th and 18th March 1998 for transfer of know-how to IGME scientists of the risk assessment methodology. Twenty-two geoscientists attended the workshop.

Tuesday, 17 March 1998

Applied geochemical exploration for environmental purposes in Lavrion
P. Stavrakis

Background data and information for risk assessment in the framework of EU LIFE project “Soil Rehabilitation in the Municipality of Lavrion”: Software, data bases, and data treatment-presentation of results for risk assessment”
A. Demetriades and E. Vassiliades

Uncertainty in mapping hazards: Implications for classification of contaminated land
M.H. Ramsey (Imperial College of Science, Technology and Medicine, London, U.K.)

Spatially resolved exposure assessment using GIS
E. Tristán (Imperial College of Science, Technology and Medicine, London, U.K.)

Uncertainty: Estimation of random component
M.H. Ramsey

Uncertainty: Estimation of systematic component
M.H. Ramsey

Incorporation of uncertainty into hazard classification
M.H. Ramsey

Wednesday, 18 March 1998

Hazard mapping at Lavrion
E. Tristán

Weighted Linear Combination for hazard mapping at Lavrion
E. Tristán

Exposure assessment mapping at Lavrion
E. Tristán

Conclusions, limitations and future possibilities
M.H. Ramsey and E. Tristán

5.2.2. Second workshop: Assessment of environmental contamination and soil rehabilitation in the Municipality of Lavreotiki

A two-day workshop was organised on the 28th and 29th January 1999 for presenting the methodology used in the assessment and management of environmental contamination at Lavrion. It was attended by 58 scientists from IGME, NTUA, PRISMA, University of Athens, Technical University of Crete and the Ministry of Environment, Planning and Public Works

Thursday, 28 January 1999

Methodology for hazardous waste site assessment and remediation
Case study 1: Arsenic contamination from a landfill
Case study 2: Chromium contamination from a metal finishing industry
N.P. Nikolaidis (University of Connecticut, U.S.A.)

Excursion to Lavrion: Sources of environmental contamination and pilot project areas – Excursion leaders: A. Demetriades, N. Papassiopi, P. Theodoratos and K. Vergou-Vichou

Friday, 29 January 1999

Activities and results for the assessment of environmental contamination and risk – A. Demetriades, K. Vergou-Vichou and E. Vassiliades (IGME)

Environmental characterisation of metallurgical wastes: Laboratory tests and pilot scale application of rehabilitation techniques – N. Papassiopi and P. Theodoratos (NTUA).

Framework for planning the soil rehabilitation in the Municipality of Lavreotiki in order to protect human health and the environment –
N.P. Nikolaidis, A. Demetriades, K. Vergou-Vichou, E. Vassiliades (IGME)
N. Papassiopi and P. Theodoratos (NTUA)
N. Varelidis (PRISMA)

5.2.3. Special lectures, meetings and excursions

Lecture: Friday, 27 June 1997

Mapping hazards and calculating risk
M. Rosenbaum (Imperial College of Science Technology and Medicine, University of London, London, U.K.)

The lecture was attended by 25 IGME geoscientists.

Meeting at the Municipality of Lavrion, October 1997

The IGME, NTUA and PRISMA project scientists informed Mr. Th. Tharouniatis (EU LIFE programme supervisor), Mr. Th. Stoikos (Euroconsultants S.A.) and officers of the Municipality of Lavreotiki about the hitherto results, and problems encountered.

Meeting at IGME offices, December 1997

Euroconsultants S.A., LIFE programme supervisors in Greece, arranged a meeting with the Municipality of Evosmos (Thessaloniki) and Environmental Technology Ltd. (INTERGEO), who are also carrying out a LIFE project “Implementation of local environmental policy in the residential development” [ENV/GR/000382]. The purpose was to inform them about the work programme and project results.

Excursion to Lavrion: Tuesday, 30 March 1999

Thirty-eight students of the Technological Educational Institution of Athens studying for the degree of Public Health Inspector were taken to Lavrion, shown the contamination problems caused by the metallurgical processing wastes, the rehabilitation test sites, and were informed about the health related problems.
Excursion leaders: A. Demetriades (IGME) and P. Theodoratos (NTUA).

5.2.4. National and international exhibitions and conferences

- **November 1997. Conference of Greek users of Arc/Info® in Athens**

The land use map of the Lavrion urban area was exhibited, and entered in the map competition. It was awarded the second prize.

- **September 1998. Helexpo´98**

  Maps from the Lavrion urban area were exhibited on a poster.

- **4 June1999. Day of the Environment**
  (organised by the Ministry of the Environment, Planning and Public Works in Athens)

  A poster with Lavrion maps was exhibited.

- **3-6 June, 1999. HELECO'99. Third International Exhibition and Conference of Environmental Technology for the Mediterranean Region, Thessaloniki, Greece** (organised by the Technical Chamber of Greece)

  A poster with Lavrion maps was exhibited.

- **64th HELEXPO – International Exhibition, Thessaloniki, Greece**

  The project Video film was played at the IGME exhibition stand.

6. TIME SCHEDULE

IGME started the project on the 1st June 1994 following the official signing of a contract with the Municipality of Lavreotiki. Due to many problems encountered during the course of the project, that it was impossible to anticipate at its start, the proposed schedule described in the project proposal was not observed. Reasons for the delays were explained in the First Interim Technical Report, and subsequent correspondence, and are not going to be discussed further. In our opinion the delays were justifiable, and it is more significant that the project reached a successful conclusion with results, which are useful to the Municipality of Lavreotiki, and a methodology that could be applied to other areas facing similar environmental contamination problems.

As it can be appreciated the coloured printing of

(a) 35 copies of each of 192 A3-size maps (total 6720 maps),
(b) 35 copies of each of 88 borehole/vertical profile A4-size figures (total 3080 figs), and
(c) 2 copies of each of 192 A1-size maps [scale 1:5000] (total 384 maps)

presented considerable problems. To begin with, the greatest problem encountered, was incompatibility between software and hardware. Maps showing the layer of metallurgical processing wastes with a shading scheme were displayed on the screen by the software used, but could not be printed. For almost a whole year discussions with Hewlett Packard technicians and Microsoft personnel, and the testing of different

suggestions, were not able to solve the incompatibility problem. Consequently, all maps with overlays of the metallurgical processing wastes had to be reconstructed with a different scheme that could be printed. This problem alone caused a significant delay.

The second problem was data processing and interpretation of the enormous amount of data and information produced during the project. Following discussions among project scientists, but also with others acquainted with the project, it was decided to describe and discuss in detail project results, for Lavrion is a unique area, and deserves to have such a special treatment. Project results will also be useful, apart from planning future actions in Lavrion, to other areas facing similar environmental contamination problems.

The third problem involved the personal life of the participating scientists, which had detrimental effects on their psychology. We sincerely thank the LIFE programme supervising-scientists for being so discrete and understanding.

6.1. Report writing

Although parts of the final project report were written between 1997-1998, they had to be revised in 1999. Final report writing began after the presentation of results in Lavrion on the 19th June 1999 and the binding of Volume 2. As it may appreciated the task to describe, discuss and interpret such a vast volume of data was an indeed difficult task, and demanded dedicated work. Many problems were again encountered with the software, e.g., misplaced or disappearing figures and tables from the computer files, report pages not being printed, locked files, etc. All these problems again caused serious delays and despair.

7. COMMENTS

"*A picture is worth a thousand words*" is a truism that has been applied in this project, for environmental contamination is a geographical problem that can only be effectively presented in map form (see Volume 2). Hence, emphasis was given on making different thematic map series, which describe in detail the surface environmental conditions of the Lavrion urban area. The question one had to face, however, was how many maps to present. Individual geographical variables totalled more than 600, an impossible task to process and present. It was finally decided to present as many variables as it was practically possible, because Lavrion is a unique area, which deserves special attention from both the scientific community, and politicians from Greece and Europe.

Considerable effort has been made, therefore, to produce maps with interpretative parameters for scientists and lay persons alike, and maps that will be of practical use to the end users, officers of the Municipality of Lavreotiki, for environmental management.

Further, hundreds of useful tables and figures were compiled and plotted (Volume 1A and tables & figures within Volumes 1, 1A, 1B & 4).

Blank back page
Λευκή οπίσθια σελίδα

Chapter 1

GENERAL INTRODUCTION: Regional geology, Mineralisation, Mining & metallurgical activities, Environmental impact, Regional soil geochemistry and Contamination index maps

Alecos Demetriades and Katerina Vergou-Vichou
Institute of Geology and Mineral Exploration, 70 Messoghion Street, Gr-115 27 Athens, Greece

1.1. INTRODUCTION

Lavrion, a town 55 km to the south-east of Athens, is the seat of the Municipality of Lavreotiki (Map 1.1; Photo 1 in Volume 2). The boundaries of the municipality extend from the village of Legrena in the south to the village of Agios Constantinos (Kamariza) in the north and the Thorikon settlement in the east. The area covered by this study is approximately 7 km^2 (Map 1.1). It includes the main urban area of the town of Lavrion and its immediate surroundings, which extend into the rural part of the Municipality of Lavreotiki.

Lavreotiki peninsula (Map 1.1) is a richly mineralised area with mixed sulphide and iron-manganese ore (Map 1.2) (Marinos and Petrascheck, 1956; Conophagos, 1980; IGME Working Group, 1987). It was one of the largest complexes of intensive mining and smelting activities of polymetallic sulphide ores from ancient to recent times. The evidence of exploitation of ore is the many adits, shafts, washing plants and smelters, as well as the mining and metallurgical wastes, found in many parts of the peninsula (Map 1.2). Within the limits of the study area there are ancient washing plants and an adit (Photos 2-3). Two of the ancient washing plants in the Thorikon area, according to archaeological findings, belonged to Euthidike (daughter of Epiphanos from Elefsis; 5^{th}–4^{th} century BC; Photo 3) and Philokrates (4^{th} century BC).

The study area comprises the industrial part of Lavrion, where the mineral beneficiation wastes were piled, and the local population, and children especially, run the greatest exposure risk (Photos 6-33). The population, according to different ten-year census, was 6,907 in 1951, 6,720 in 1961, 9,034 in 1971, 10,124 in 1981 and 10,293 in 1991 (refer to Volume 4, Appendix 2). There is a significant increase in population from 1951 to 1991. Regarding children up to the age of 14 years old, the last census recorded 1,200 boys and 1,100 girls, *i.e.*, 22.35% of the total population (11.66% boys and 10.69% girls).

Expansion of population since 1951, and its housing over metallurgical processing wastes, is indeed one of the greatest health hazards that officers of the Municipality of Lavreotiki must face. Other future problems are the probable population expansion due to

(a) the State decision to make Lavrion a central port for the Aegean islands, and
(b) the new international airport of Athens at Spata.

Any new housing estate plans in the Lavrion area, and the Lavreotiki peninsula, must take into account the problem of contaminated land, and its effects on the quality of life of the population.

In this chapter the regional geology, mineralisation, mining and smelting activities, their environmental impact, and regional soil geochemical results, are going to be briefly described, because it is considered significant to understand the background information leading to the hazardous situation in the Lavrion urban area. Two composite geochemical maps of the Lavrion area are discussed at this point, so that the reader can understand the seriousness of toxic element soil contamination and its adverse effects on the health of the local population.

1.2. REGIONAL GEOLOGY

Geologically, the Lavreotiki area belongs to the Attico-Cycladic geotectonic zone (Renz, 1940; Auboin, 1959; Marinos and Petrascheck, 1956). The geology of Lavreotiki peninsula is described by Lepsius (1893), Kober (1929), Marinos and Petrascheck (1956), IGME Working Group (1987) and Papadeas (1991). Rock formations are subdivided into two distinct units, *i.e.*,

(a) the autochthonous Attica unit (Katsikatsos, 1986; Papanikolaou, 1986), which consists of a large mass of marble, often dolomitised (the lower marble), the mica schist of Kaesariani or Kamariza with thin intercalated marble horizons and mafic-ultramafic rocks, and the upper marble. The age of part of the metamorphosed and intensely deformed marble sequence, according to some fossil evidence, is considered to be Upper Triassic to Lower Jurassic; and

(b) the overthrust cover or Lavrion unit (Papanikolaou, 1986), is an allochthonous formation, thrust on top of the metamorphosed Attica unit (Marinos and Petrascheck, 1956). It comprises phyllite, quartzite, sericite-chlorite schist, metamorphosed mafic rocks (meta-basalt and meta-gabbro) and marble intercalations. Its most characteristic feature is the occurrence of the mineral glaucophane. Formations at the base of this folded and foliated unit, during overthrusting, have been intermingled with the upper horizons of the underlying autochthonous unit (Triassic and Jurassic limestone, mafic extrusives, *etc.*), thus forming a mélange. At the top of this unit there occurs limestone of Upper Cretaceous age.

After metamorphism and overthrusting of the allochthonous unit, a granodioritic batholith with dykes of granitic porphyry, known as eurite, were intruded in the area of Plaka during the Miocene. These igneous rocks mainly intrude members of the autochthonous unit.

Post-alpine formations, *i.e.*, Tertiary and Quaternary deposits, lie over the overthrust cover. Outcrops of Neogene rocks occupy a small area about cape Sounion, and are made up of mainly marl and conglomerate. Quaternary deposits lie unconformably on older formations, and consist of a coarse-grained, brittle and porous calcareous sandstone, which is found near the coast. Recent sediments occur in valleys and coastal areas.

1.3. MINERALISATION

The Lavreotiki peninsula ore concentrations occur mainly in the form of replacement beds within the marble and at the contacts of marble and schist (Marinos and Petrascheck, 1956; IGME Working Group, 1987; Demetriades, 1992; Gelaude *et al.*, 1996). Three mineralised contacts have been identified, *i.e.*, between

(i) the upper marble and the Athenian schist,
(ii) the upper marble and the Kaesariani schist, and
(iii) the lower marble and the Kaesariani schist, which is the most significant for economic mineralisation.

Mineralisation is related to folding of beds and neighbouring felsic igneous rocks. Mixed sulphide mineralisation is the most important, and comprises argentiferous galena, sphalerite and pyrite. In addition, iron-manganese ores of manganese bearing ankerite or rhodochrosite with baryte, fluorite and quartz, occur in the area as well as stratiform or vein skarn type mineralisation within the hornfels of the Plaka area, which are derived from the contact metamorphism of the two units of Lavreotiki, and in particular the Kaesariani schist. Massive magnetite deposits, which are a characteristic feature of the area, are cross-cut by mixed sulphide ore (Economou *et al.*, 1981).

More than 260 primary and secondary minerals have been identified in the Lavreotiki peninsula (Marinos and Petrascheck, 1956; Demetriades, 1992; Vourlakos, 1992; Katerinopoulos, 1994), most of which are secondary in origin (Gelaude *et al.*, 1996). They consist mainly of sulphides, arsenates, carbonates, chlorides, fluorides, phosphates, hydroxides, molybdates, oxides, silicates, sulphates, sulphosalts, vanadates and native metallic elements. Primary ore is of two types, mixed sulphides of Zn, Fe and Pb, and iron-manganese (Marinos and Petrascheck, 1956; IGME Working Group, 1987).

Mixed sulphide minerals are galena, sphalerite and pyrite. There also occur smaller proportions of minerals of other associated elements, such as As, Bi, Cu, Ni, Co, *etc.* Sphalerite contains some Fe, Mn and a very small quantity of Cd; pyrite includes a little As, and galena variable proportions of Ag, and a very small quantity of Au; the silver content of galena varies from 40 to 25000 g/ton (Marinos and Petrascheck, 1956). The richest argentiferous galena has been mined during ancient times. Present day galena yields 40-250 g/ton Ag and approximately 2 g/ton Au. Accessory and gangue minerals of the mixed sulphides are fluorite, baryte, ankerite, quartz, chalcedony, calcite, kaolinite, *etc.* Baryte and fluorite form also entirely separate deposits.

Iron-manganese ore consists mainly of manganiferous ankerite and rhodochrosite; it is associated with baryte, fluorite and quartz. Oxidation of ore has formed limonite, pyrolusite, *etc.*

Secondary minerals have also been formed in ancient slags which are in contact with the sea (Marinos and Petrascheck, 1956; Katerinopoulos, 1994; Gelaude *et al.*, 1996).

Lavreotiki ores are considered to be hydrothermal, and are believed to be genetically connected to a felsic pluton at depth, the apophyses of which are the Plaka granodiorite and the eurite dykes (Marinos and Petrascheck, 1956). Deposition of ore occurred during Lower Tertiary and continued, to a lesser extent, during Neogene. A

recent hypothesis considers these ores as volcano-sedimentary, and genetically connected to the volcanic activity that formed the Kaesariani schist (Leleu *et al.*, 1973). The metallogenesis may also be related to features of uplift and erosion of the lower marble-schist unit, which resulted in karstification of carbonate rocks, transportation of metals by hydrothermal fluids, and their subsequent deposition into karstic cavities or fractures. Both hypotheses, however, have their weak points, and are not widely accepted.

1.4. MINING AND METALLURGICAL ACTIVITIES

Xenophon, the ancient Greek historian, has written in the 4th century BC that nobody knows exactly when the mining and metallurgical activities in the Lavreotiki peninsula began. According to isotopic dating of ancient lead utensils by archaeologists of the University of Oxford in the United Kingdom and the Max-Planck Institute of Nuclear Physics in Heidelberg, Germany, mining and smelting activities in the Lavreotiki peninsula must have started between 3500 and 3000 BC (Dermatis, 1994). Moreover, archaeological excavations at Thorikon, a settlement to the north of Lavrion (Map 1.1), confirmed the existence of mining activities as early as 3000 BC (Gelaude *et al.*, 1996). It appears, therefore, that all the ancient people of the Mediterranean (Minoans, Mycenaeans, Phoenicians, Greeks, *etc.*) acquired some of their metals (lead, silver, copper and iron) from the Lavreotiki peninsula. The first intensive period of exploitation was during the Golden Age of Athens in the 5th century BC, and the second from 1865 up to 1987 AD.

The Lavreotiki mines began to play a significant role in the development of Athens from the 6th century BC, since the city was able to mint its own silver coins, the famous "Athenian or Lavreotic owls" (Conophagos, 1980) (Photo 2). Their silver content was as high as 97.8%. Athenian silver coins dominated the ancient Mediterranean market for a considerable time. Peisistratus (561-527 BC), the tyrant, used the revenue from the mines to finance public works in Athens. The Athenian fleet that defeated the Persians at Salamis in 480 BC was built from the revenue of the Lavreotiki mines. Even the building of monuments during the Golden Age of Athens in the 5th century BC, relied partly on funds from the Lavreotiki mine concessions. Exploitation of the mines began to wane down from the 4th century BC until it completely ceased in the 1st century BC. Pausanias, during the 2nd century AD, verifies the complete closure of the mines by writing that the Athenian silver mines in Lavrion have been completely forgotten. It appears, however, that some mining may have been carried out at later times, for it is reported that silver from Lavreotiki and Pangaeon (Macedonia, N.E. Greece) has been used for building the church of Saint Sofia in Constantinople during the 6th century AD.

Waste materials generated by ancient Greeks, after exploitation of the richest ores [first- and second-class ore (Jackson, 1997)], were the (a) mine tailings (*εκβολάδες* = *ekvolades*), (b) washing plant debris or flotation tailings (*πλυνίτες* = *plynites*), (c) slag and (c) litharge (PbO). Mine tailings are distinguished into interior and exterior. *Interior mine tailings* were the poor ore left by the ancients, following crushing by hammer and first hand selection of the rich ore, in the longitudinal underground adits; outside the adit the material was hand selected a second time. First-class ore, more than 30% Pb, was directly sent to furnaces for melting and further metallurgical treatment; poorer material was subjected to hand selection. Poor material was thrown away and made the *exterior mine tailings*; comparatively richer material, the second-class ore, was crushed and beneficiated in flat-bed (Photo 3) or helicoidal washing plants. The lighter fine-grained poor wastes, left after

washing the second-class ore, constitute the *washing plant debris* or *flotation tailings*. Slag is the material left in the furnace after melting the ore for recovery of silver bearing lead, and litharge includes the remains of lead bearing silver, following recovery of silver by fire assay (Conophagos, 1975, 1980, 1985).

The Greek government, following the independence of Greece from the Turkish occupation in 1827, attempted to revive mining in Lavreotiki peninsula by calling on foreign experts, Fielder in 1835 and Russegger in 1841; both reported that there is no ore potential for mixed sulphides (Conophagos, 1980). Russegger saw only a potential in the iron ore. In 1861 the Ministry of Economy employed Andreas Cordellas, a Greek mineralogist/mining engineer. He was the first to see the potential of remelting ancient slags, which were very rich in lead (up to 10% Pb). Jean Batiste Serpieri, an Italian mining engineer, after reading Cordellas' report, negotiated in 1863, with the then Greek Government, the exploitation of 1,500,000 tonnes of ancient slag. In addition, Serpieri saw a potential in the mine tailings (*ekvolades*), which the ancient miners, after hand selection, discarded because of poor quality.

Serpieri founded in 1864 the Italian-French company Roux-Serpieri-Fressynet S.A., at the location Ergastiria, which was the area used until recently by the cotton-weaving factory of Aegaeon, *i.e.*, behind the offices of the Lavrion Port Authorities and to the south of the Lavrion Council House. As from 1865 lead was again produced in Lavrion.

Due to illegal exploitation of ancient mine tailings by Serpieri, a problem that reached international dimensions, the company was purchased in 1873 by Andreas Syngros, representative of the Bank of Constantinople. The new company was called Societé des Usines du Laurium. The Greek State granted the company exploitation of ancient slag and tailings (*ekvolades*). The company built large washing plants at the site where the Lavrion Secondary School, Mineralogical Museum and municipal sports area are now situated (Photo 12). In the washing plants about 1000 tonnes of ancient tailings were treated per 24 hour shift. About 250 tonnes were taken for smelting, and 750 tonnes thrown away, and constitute the present day beneficiation/flotation residues, called *"savoura"* by the local inhabitants (Photos 13-15, Map 2.3) (Dermatis, 1994). After the ancient mine tailings were exhausted, the company began beneficiation of poor washing plant debris (*plynites*), left by the ancients after washing the crushed second-class ore. The company, before closing down in 1917, carried out some mining. In 1930 the company sold its premises.

Serpieri founded, in 1876 at Kiprianos, a new company, Compagnie Française des Mines du Laurium (the site of the present day Technological Park) (Photo 4). The French consortium Pennaroya purchased the company in 1930, and continued production of silver bearing lead from Lavreotiki ore until 1977 (Manthos, 1990). It continued to process imported ore from 1977 to 1982, the year when it closed down. In 1984 the installations of Compagnie Française des Mines du Laurium were rented by the Greek State and operated by the Hellenic Metallurgical and Mining Company of Lavrion S.A. The company worked with imported ore until 1989, when it finally closed down. The Greek State purchased in 1992 the premises of Compagnie Française des Mines du Laurium, and the Ministry of Culture by decree decided to convert the whole industrial complex into a Technological-Cultural Park. This operation has been undertaken by the National Technical University of Athens (NTUA).

Mediterranean Mines Inc. was another company processing ore from Lavreotiki peninsula, but also from Kassandra mines in Chalkidhiki (Photo 5). This company

exploited mines, which belonged to Societé des Usines du Laurium. Operations began in mid-1951, but stopped in 1953 due to the low grade of sulphide ore and small capacity of the flotation plant. In 1954 the company began its operations again, and after nine years of work it completely closed down in March 1963 (K.L. Pogkas, person. commun., 1999). Crushing and sieving capacity of the plant was about 20 tonnes of material per hour, and 250 tonnes of crushed material per day was treated by flotation.

The total tonnage of lead produced from exploitation of ore from the Lavreotiki peninsula is 2,260,000 tonnes (Table 1.1). According to Conophagos (1980) a minimum of 1,400,000 tonnes of lead and 3,500,000 kg of silver were produced by the ancient Greeks from at least 13,000,000 tonnes of excavated material; he stressed that this is a very conservative estimate. The 19th and 20th century companies produced only 860,000 tonnes of lead, and approximately 1,000,000 kg of silver. The volume of excavated material has not, however, been estimated. Since, modern underground and open pit mining uses explosives and mechanical equipment, the dimensions of adits and pits were much larger, and the quantity of excavated material should at least be double of what Conophagos (1980) estimated for ancient exploitation. A cautious estimate of excavated material is two to three times the quantity of the ancients, *i.e.*, approximately 30,000,000 tonnes. As it may be appreciated, a considerable amount of waste rock is present in the Lavreotiki peninsula, and is exposed to the processes of erosion and deposition.

Table 1.1. Tonnage of lead produced from the exploitation of Lavreotiki ore (Conophagos, 1980).
Πίνακας 1.1. Ποσότητα μολύβδου που παρήχθη από την εκμετάλλευση των κοιτασμάτων της Λαυρεωτικής χερσονήσου.

Company	*Period*	*Tonnes of lead*
Εταιρεία	*Περίοδος*	*Ποσότητα μολύβδου (σε τόνους)*
Ancient smelting	*3500-0 BC*	*1,400,000*
Roux-Serpieri-Fressynet S.A.	*1865-1873*	*60,000*
Societé des Usines	*1873-1910*	*290,000*
Societé des Usines	*1910-1917*	*20,000*
Compagnie Française des Mines du Laurium	*1877-1910*	*207,000*
Compagnie Française des Mines du Laurium	*1910-1939*	*153,000*
Compagnie Française des Mines du Laurium	*1939-1960*	*60,000*
Compagnie Française des Mines du Laurium	*1960-1977*	*70,000*
Total tonnage for the period 1865-1977 *Συνολική ποσότητα για την περίοδο 1865-1977 (σε τόνους)*		*860,000*
Total tonnage from ancient to recent times *Συνολική ποσότητα από την αρχαιότητα μέχρι σήμερα (σε τόνους)*		*2,260,000*

Apart from lead and silver, other metals produced were zinc concentrate, white arsenic oxide (As_2O_3), various oxides of lead [minium (Pb_3O_4), litharge (PbO)]; other metals of secondary importance were pyrite, copper, iron, iron-manganese ore, fluorite, barite, *etc.* (Marinos and Petrascheck, 1956).

1.5. ENVIRONMENTAL IMPACT

Exploitation of the mineral wealth of Lavreotiki peninsula, from ancient to recent times, resulted in the accumulation of enormous quantities of waste materials, such as waste

rock, mine tailings, slag and other coarse- to fine-grained metallurgical processing residues, found in many parts of the peninsula, and especially the Lavrion urban area (Photos 6-33). The effects, of mining and smelting activities, were the burdening of the already "naturally" contaminated soil with additional amounts of toxic elements.

Ancient exploiters built ore crushing and washing plants in valleys, for they required water for separation of ore-grade material from the waste rock. This practice facilitated transportation of waste rock and mineral processing wastes by erosion processes (fluvial and aeolian), and their subsequent deposition in the flood plains and gulfs of Lavreotiki peninsula. These processes have been going on for at least the past 5,000 years. From 1865 mine and flotation tailings (*ekvolades* and *plynites*) left by the ancients gradually disappeared, and new waste products generated by modern exploiters from ancient waste materials, such as beneficiation/flotation residues (flotation tailings) and slag, and from mining new ore they produced waste rock, mine tailings, and metallurgical wastes. It is stressed, that ancient pits and adits directed modern exploiters, who enlarged the adits, excavated open pits near valleys, and tipped waste rock again on hill slopes and valley bottoms.

In the Lavrion area a number of streams have their outlets. Within their drainage basins, there is a very large number of ancient and recent mining and smelting sites, which are shown on Map 1.2. Hence, the alluvial plains in the Lavrion have been contaminated.

Late 19th and 20th century metallurgical processing wastes have been dumped, mainly in the Lavrion urban area and the nearby gulfs, thus upsetting the natural balance of the local terrestrial and marine ecosystems (Photos 6-33). Their transportation, by erosion (fluvial and aeolian) processes and human activities, resulted in the toxic element contamination of soil in the greater part of the Lavrion urban environment. In fact, houses, schools, parks, playgrounds, sport fields and roads are either situated on or are very close to these wastes (Photos 9, 11-16, 21, 24-28, 30). The consequences are the health related problems of the local population (Nakos, 1985; Maravelias *et al.*, 1989; Eikmann *et al.*, 1991; Makropoulos *et al.*, 1991, 1992; Hadjigeorgiou-Stavrakis and Vergou-Vichou, 1992; Stavrakis *et al.*, 1994b; Demetriades *et al.*, 1996; Kafourou *et al.*, 1997), animals and plants (Nakos, 1979; Chronopoulos and Chronopoulou-Sereli, 1986a, 1986b, 1991; Chronopoulou-Sereli and Chronopoulos, 1991a, 1991b; Xenidis *et al.*, 1997).

1.6. REGIONAL SOIL GEOCHEMISTRY OF LAVREOTIKI PENINSULA

Soil geochemical maps of Lavreotiki peninsula have been included in this report to show that environmental contamination extends far beyond the limits of the Lavrion urban area, which has been studied during this project (Maps 1.3 & 1.4). The reasons for this contamination are (a) the above normal concentrations of elements due to rich and extensive mineralisation, and (b) anthropogenic activities (mining and smelting) (Map 1.2).

Regional soil geochemistry, on a sampling grid of 500 x 500 m, was carried out over 170 km^2 of the Lavreotiki peninsula in 1991-93 by the Institute of Geology and Mineral Exploration (Demetriades, 1997; Demetriades *et al.*, 1994a, 1994b, 1994c, 1996a, 1996b, 1996c; Stavrakis *et al.*, 1994a). For the sake of scientific information it is mentioned that Korre (1997) covered with soil geochemistry 120 km^2 of the peninsula

on a sampling grid of 400 x 500 m for her doctorate thesis (Korre and Durucan, 1995a; 1995b). It should be stressed, however, that such overlaps must definitely be avoided in the future by stricter control of Greek and foreign University geological research by the Institute of Geology and Mineral Exploration.

The geochemical distribution of elements presented on Maps 1.3 and 1.4 show two distinct patterns:

1. elements associated with the mixed sulphide mineralisation (Pb, Zn, Cd, Cu, As an Sb), mining and smelting activities from ancient to recent times, and
2. elements associated with the mafic members of rock formations (Cr and Ni).

It is quite apparent from the results presented on the geochemical maps, that most of Lavreotiki peninsula's surface soil has element concentrations far in excess of stipulated phytotoxic levels, quoted by Kabata-Pendias and Pendias (1984) (Table 1.2). More than 90% of the area covered by the soil geochemical survey exceeds phytotoxic threshold levels for Pb, Zn, As and Cr. Even the tentative "threshold trigger" concentrations set by ICRCL (1987) are exceeded by As, Cd, Cr, Cu, Pb, Ni and Zn. These trigger concentrations are considered as the critical levels above which risk for hazard begins to become significant. According to ICRCL (1987) soil with values in As>40 ppm, Cd>15 ppm, Cr>1000 ppm and Pb>2000 ppm cannot be used for domestic gardens, allotments, parks, playing fields and open space, for contaminants may pose hazards to health. Copper greater than 130 ppm, Ni>70 ppm and Zn>300 ppm do not normally pose health risks to humans, but are phytotoxic, and soil with values over these tentative threshold trigger concentrations should not be used for plant growth.

Table 1.2. Phytotoxic levels and percentage proportion of surface soil (0-10 cm) of the Lavreotiki peninsula considered hazardous to plants (area covered 170 km^2) [From Demetriades *et al.*, 1996a, Table 5, p.13].
Πίνακας 1.2. Φυτοτοξικά επίπεδα και η εκατοστιαία αναλογία του επιφανειακού εδάφους (0-10 cm) της Λαυρεωτικής χερσονήσου που θεωρείται ως επικίνδυνη για φυτά (εμβαδόν περιοχής μελέτης 170 τ.χλμ.)

Element	*Phytotoxic level (ppm)*	*% area affected*	*Element*	*Phytotoxic level (ppm)*	*% area affected*
Στοιχείο	*Φυτοτοξικό επίπεδο (ppm)*	*% εμβαδόν περιοχής*	*Στοιχείο*	*Φυτοτοξικό επίπεδο (ppm)*	*% εμβαδόν περιοχής*
As	*15*	*92.26*	Ni	*100*	*71.35*
	50	*68.77*		-	-
Cd	*3*	*57.31*	Pb	*100*	*96.70*
	8	*29.37*		*400*	*66.05*
Cr	*75*	*96.99*	Sb	*5*	*50.57*
	100	*95.13*		*10*	*42.84*
Cu	*60*	*36.25*	Zn	*70*	*99.57*
	125	*15.62*		*400*	*52.01*

Note: Minimum and maximum phytotoxic levels quoted by Kabata-Pendias and Pendias (1984, Table 6, p.11).

Toxic element limits for residential areas are more stringent for some elements, *i.e.*, As>10 ppm, Cd>3 ppm, Cu>130 ppm, Ni>70 ppm, Pb>500 ppm and Zn>300 ppm (ICRCL, 1987); Cr>100 ppm and Sb>27 (US CT, 1994), suggesting that a far greater proportion of the area of Lavreotiki peninsula is hazardous for a human habitat.

The soil geochemical survey carried out in the Lavreotiki peninsula, including the Lavrion urban area, mapped to the level of its working scale (500 x 500 m sampling grid), the intensity and extent of above normal anthropogenic multi-element contamination. These results should evidently constitute the basis for interdisciplinary collaboration, since the issue of soil contamination by toxic elements is very serious, especially when there are already known cases with

- excessive toxic element concentrations in plants (Chronopoulos and Chronopoulou-Sereli, 1986a, 1986b, 1991; Chronopoulou-Sereli and Chronopoulos, 1991a, 1991b; Xenidis *et al.*, 1997),
- human health problems (Maravelias *et al.*, 1989; Eikmann *et al.*, 1991; Makropoulos, 1991, 1992; Stavrakis *et al.*, 1994b; Kafourou, 1997)
- animal health problems (*personal information from local population, 1992-4*), and
- loss in agricultural production (*personal information from local population, 1992-4*).

Further work is, therefore, required over the whole Lavreotiki peninsula to fully investigate

1. the effects of multi-element soil contamination on groundwater supplies, animals, plants and humans, and
2. cost-effective methods for *in-situ* rehabilitation of soil, stabilisation and permanent revegetation of mine tailings and waste rock heaps.

Meanwhile all agricultural production, animal rearing, and issue of new housing permits should stop, and the local population be informed about the health-related contamination problems. *Otherwise, local authorities, state and private town planners and decision-makers in general, may be legally charged, in the future, with negligence and causing bodily harm in terms of health, for not informing, local inhabitants and other interested parties, about soil contamination and the possible health related hazards to which they may be exposed to.*

The first environmental geochemistry study, carried out by the Institute of Geology and Mineral Exploration, concerned the town of Lavrion and the village of Ayios Constantinos (Hadjigeorgiou-Stavrakis and Vergou-Vichou, 1992). Copies of the report were submitted to the Municipality of Lavreotiki, Community of Ayios Constantinos, Attiki Regional Office, Ministry of Environment, Planning and Public Works, *etc.* The second environmental geochemistry study covered the whole Lavreotiki peninsula (Demetriades 1994a, b, c; Stavrakis *et al.*, 1994a), and copies of the five-volume report submitted to the Municipalities of Lavreotiki and Keratea; the Communities of Ayios Constantinos, Anavissos and Nea Fokaea; Attiki Regional Office, Ministry of Environment, Planning and Public Works, *etc.* Both projects were carried out with finance from the Regional Structural Funds Project of the Attiki Regional Office (Project No.: 202.088.00).

1.7. CONTAMINATION INDEX MAPS OF THE LAVRION URBAN AREA

Two contamination index maps with ten toxic elements (As, Be, Ba, Cd, Cr, Cu, Ni, Pb, V and Zn) in overburden/soil have been compiled by using two different sets of limiting levels for residential areas. Map 1.5 uses statutory levels obtained from the United

Kingdom (ICRCL, 1987), Finland (R. Salminen, pers. com., 1996) and US State of Connecticut (US CT, 1994, 1997), whereas Map 1.6 employs soil action levels developed specifically for the Lavrion urban area (refer to Volume 4 for explanations) [Table 1.3]. The method of computing the contamination index is the same for both maps, and follows the work of Sainsbury *et al.* (1970) for estimating the total geochemical anomaly of a sampling site in mineral exploration.

Table 1.3. Statutory levels and Lavrion "Soil Action Levels" used for computing the contamination index of overburden in the Lavrion urban area.
Πίνακας 1.3. Μέγιστα αποδεκτά νομοθετημένα όρια και «'Ορια Λήψης Μέτρων για το 'Εδαφος» στο Λαύριο, τα οποία χρησιμοποιήθηκαν για τον υπολογισμό του δείκτη ρύπανσης στην αστική περιοχή του Λαυρίου.

Element	*Statutory level (ppm)*	*Soil Action Level (ppm)*	*Element*	*Statutory level (ppm)*	*Soil Action Level (ppm)*
Στοιχείο	*Νομοθετημένα όρια (ppm)*	*'Οριο Λήψης Μέτρων για το 'Εδαφος (ppm)*	*Στοιχείο*	*Νομοθετημένα όρια (ppm)*	*'Οριο Λήψης Μέτρων για το 'Εδαφος (ppm)*
As	10	25	Cu	130	2,300
Ba	600	5,500	Ni	70	1,500
Be	0.14	2	Pb	500	500
Cd	3	40	V	470	550
Cr	100	140	Zn	300	20,000

Note: Statutory guideline or threshold values were obtained from (a) ICRCL (1987) for As, Cd, Cu, Ni, Pb and Zn, (b) Finland (R. Salminen, pers. com., 1996) for Ba and Cr, and (c) the US State of Connecticut (1994) for Be and V.

To begin with, the concentration of each element at a sampling site is divided by its designated baseline value (Statutory Level or Lavrion Soil Action Level); this procedure results in a concentration ratio for each element, in which the baseline is represented by the number 1. The Contamination Index for each sampling site is then calculated by adding the concentration ratios of each element and subtracting from the total, the sum of either the Statutory Level baseline values or the Lavrion Soil Action Level baseline values, which in both cases is 10; or more simply the number of elements used in the computation. The Contamination Index (CI) represents, therefore, the sum of the ratios of selected elements above the preferred baseline values for each element. Values for the contamination index of zero (CI=0) or less than zero (CI<0), *i.e.*, negative values, mean that there is no contamination, or that element concentrations are below the baseline levels used. Values greater than zero (CI>0) suggest contamination. The example, tabulated in Table 1.4, will explain the procedure.

Tables 1.5 and 1.6 tabulate the statistical parameters of the contamination ratios of each element and the contamination index, and the boxplots (Figs. 1.2 & 1.3) show their distributions. As it may be appreciated, elements with high contamination ratios in overburden/soil samples (>100), have the greatest contribution in the contamination index value (Tables 1.5 & 1.6). In the two cases under study, the baseline value of each element, against which its concentration value in the sample is compared, dictates the level of its contamination ratio. Hence, elements with the greatest contribution in the contamination index value for both cases are

- As, Cd, Pb and Zn, when using the Statutory Levels of elements as their baseline (Fig. 1.1), and
- As and Pb when using the Lavrion Soil Action Levels of elements as their baseline values (Fig. 1.2).

The former case has contamination indices varying from 18 to 2882 with a mean of 338.1 (Map 1.5), and the latter from –0.75 to 1121 with a mean of 122.86 (Map 1.6). Although there are significant differences, in the range and mean values of the two contamination indices, the hazard still prevails over the whole area.

Maps 1.5 and 1.6 show the spatial distribution of the two contamination indices. The patterns are essentially the same. Areas with the greatest hazard are situated over or are near to the flotation residues, pyritiferous sand and slag. By using the most conservative approach, which is the case with the Lavrion Soil Action Levels (Map 1.6), 97.5% of the area has contamination indices more than 8. This means that overburden/soil contamination in Lavrion is widespread and is very high with respect to arsenic and lead, the two most hazardous elements to human health.

Table 1.4. Calculation of the Contamination Index at a sampling site using the Statutory and Lavrion "Soil Action Levels".
Πίνακας 1.4. Υπολογισμός του Δείκτη Ρύπανσης σε μία θέση δειγματοληψίας βάσει των Νομοθετημένων Ορίων και των «Ορίων Λήψης Μέτρων για το 'Εδαφος» στο Λαύριο.

Element	*Site element concentration (C) in ppm*	*Statutory Level (SL) in ppm*	*Ratio SL/C*	*Lavrion Soil Action Level (SAL) in ppm*	*Ratio SAL/C*
Στοιχείο	*Σημειακή συγκέντρωση στοιχείου (C) σε ppm*	*Νομοθετημένο 'Οριο (SL) σε ppm*	*Λόγος SL/C*	*'Οριο Λήψης Μέτρων του Λαυρίου (SAL) σε ppm*	*Λόγος SAL/C*
As	2040	10	204.00	25	81.60
Ba	308	600	0.51	5,500	0.06
Be	0.89	0.14	6.36	2	0.45
Cd	36	3	12.00	40	0.91
Cr	189	100	1.89	140	1.35
Cu	240	130	1.85	2,300	0.10
Ni	116	70	1.66	1,500	11.92
Pb	5961	500	11.92	500	0.08
V	71	470	0.15	550	0.13
Zn	7490	300	24.97	20,000	0.38
Total of element concentration ratios Σύνολο των λόγων των συγκεντρώσεων			265.31		96.98
Contamination index of sampling site [Total-10] **Δείκτης ρύπανσης σε μία θέση δειγματοληψίας [Σύνολο-10]**			**255.31**		**86.98**

Table 1.5. Statistical parameters of individual element contamination ratios and contamination index based on *statutory levels*.
Πίνακας 1.5. Στατιστικές παράμετροι των λόγων ρύπανσης του κάθε στοιχείου και του δείκτη ρύπανσης *(Cont. Index)* βάσει των *μέγιστων αποδεκτών νομοθετημένων ορίων για τους ρυπαντές*.

Statistical parameters	*As/10*	*Ba/600*	*Be/0.14*	*Cd/3*	*Cr/100*	*Cu/130*	*Ni/70*	*Pb/500*	*V/470*	*Zn/300*	***Cont. Index***
Number of samples	224	224	224	224	224	224	224	224	224	224.	**224**
Minimum	5.00	0.11	1.73	1.33	0.016	0.33	0.57	1.62	0.06	1.97	**18.02**
Maximum	2400.00	7.59	19.12	308.30	10.83	34.19	8.44	303.16	0.69	254.37	**2881.91**
Mean	249.43	1.11	7.89	22.67	2.64	2.75	2.02	23.16	0.18	36.24	**338.08**
Median	129.00	0.80	7.24	12.60	1.83	1.43	1.81	14.61	0.16	22.23	**184.18**
First quartile	77.50	0.55	5.99	7.09	1.28	0.87	1.42	8.43	0.14	10.56	**110.88**
Third quartile	223.00	1.23	9.43	21.83	3.19	2.35	2.23	26.51	0.20	41.06	**353.01**
Standard error	23.77	0.07	0.18	2.42	0.15	0.31	0.07	2.07	0.01	2.81	**28.84**
95% confidence interval of mean	46.87	0.14	0.36	4.77	0.30	0.60	0.13	4.08	0.01	5.55	**56.85**
99% confidence interval of mean	61.80	0.19	0.48	6.28	0.39	0.80	0.18	5.38	0.01	7.32	**74.96**
Average deviation	217.34	0.65	2.14	18.05	1.74	2.38	0.68	16.48	0.05	27.85	**270.11**
Standard deviation	355.79	1.07	2.77	36.18	2.25	4.58	1.01	30.98	0.08	42.12	**431.57**
Coefficient of variation (%)	142.64	97.15	35.10	159.6	85.06	166.77	50.2	133.79	45.61	116.23	**127.65**
Coefficient of skewness	3.17	3.14	1.05	4.94	1.39	4.61	2.27	5.34	2.77	2.47	**3.03**
Coefficient of kurtosis	11.47	11.47	1.62	28.68	1.15	24.54	8.15	38.50	10.30	6.63	**10.56**

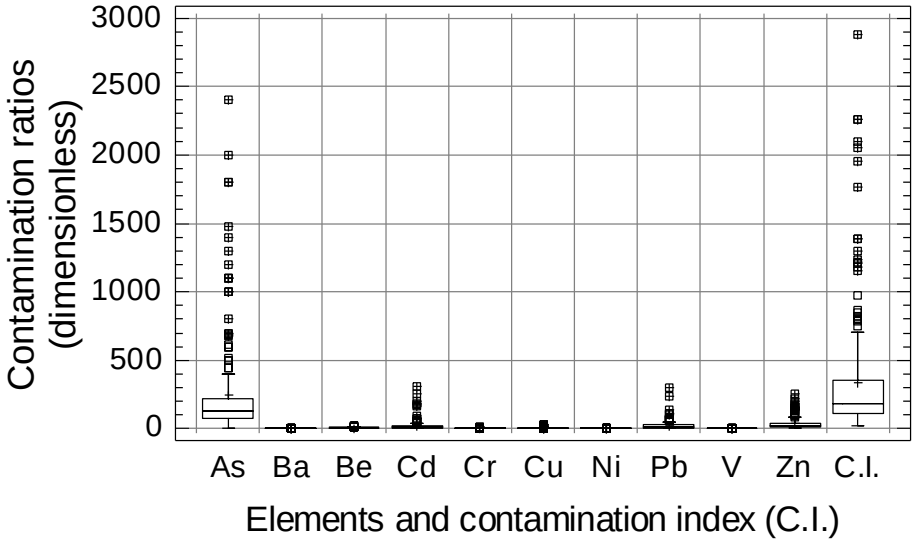

Fig. 1.1. Distribution of contamination ratios of toxic elements and the Contamination Index (C.I.) based on *statutory levels*.
Σχ. 1.1. Κατανομή των λόγων των συγκεντρώσεων των τοξικών στοιχείων και του Δείκτη Ρύπανσης (C.I.) βάσει των *μέγιστων αποδεκτών νομοθετημένων ορίων για τους ρυπαντές*.

Table 1.6. Statistical parameters of individual element contamination ratios and contamination index based on *Lavrion "Soil Action Levels"*.
Πίνακας 1.6. Στατιστικές παράμετροι των λόγων ρύπανσης του κάθε στοιχείου και του δείκτη ρύπανσης *(Cont. Index)* βάσει των *«Ορίων Λήψης Μέτρων για το 'Εδαφος» στο Λαύριο*.

Statistical parameters	*As/5*	*Ba/5500*	*Be/2*	*Cd/40*	*Cr/140*	*Cu/2300*	*Ni/1500*	*Pb/500*	*V/550*	*Zn/20000*	***Cont. Index***
Number of samples	224	224	224	224	224	224	224	224	224	224	**224**
Minimum	2.00	0.01	0.12	0.10	0.04	0.02	0.03	1.62	0.05	0.03	**-0.75**
Maximum	960.00	0.83	1.34	23.12	27.08	1.93	0.39	303.16	0.59	3.82	**1121.03**
Mean	99.77	0.12	0.55	1.70	6.60	0.16	0.09	23.16	0.16	0.54	**122.86**
Median	51.60	0.09	0.51	0.94	4.58	0.08	0.08	14.61	0.14	0.33	**66.24**
First quartile	31.00	0.06	0.42	0.53	3.21	0.05	0.07	8.43	0.12	0.16	**42.79**
Third quartile	89.20	0.13	0.66	1.64	7.99	0.13	0.10	26.51	0.17	0.62	**121.42**
Standard error	9.51	0.01	0.01	0.18	0.38	0.02	0.00	2.07	0.00	0.04	**10.93**
95% confidence interval	18.75	0.02	0.03	0.36	0.74	0.03	0.01	4.08	0.01	0.08	**21.55**
99% confidence interval	24.72	0.02	0.03	0.47	0.98	0.04	0.01	5.38	0.01	0.11	**28.42**
Average deviation	86.94	0.07	0.15	1.35	4.34	0.13	0.03	16.48	0.05	0.42	**100.55**
Standard deviation	142.32	0.12	0.19	2.71	5.62	0.26	0.05	30.98	0.07	0.63	**163.62**
Coefficient of variation (%)	142.64	97.15	35.10	159.60	85.06	166.77	50.20	133.79	45.61	116.23	**133.18**
Coefficient of skewness	3.17	3.14	1.05	4.94	1.39	4.61	2.27	5.34	2.77	2.47	**3.14**
Coefficient of kurtosis	11.47	11.47	1.62	28.68	1.15	24.54	8.15	38.50	10.30	6.63	**11.39**

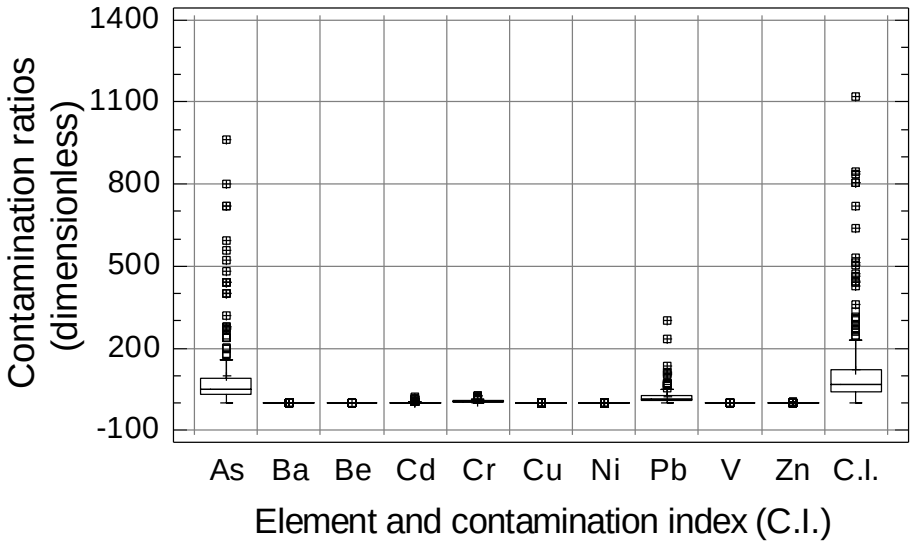

Fig. 1.2. Distribution of contamination ratios of toxic elements and the Contamination Index (C.I.) based on *Lavrion "Soil Action Levels"*.
Σχ. 1.2. Κατανομή των λόγων των συγκεντρώσεων των τοξικών στοιχείων και του Δείκτη Ρύπανσης (C.I.) βάσει των «*Ορίων Λήψης Μέτρων για το Έδαφος» στο Λαύριο*.

Blank back page
Λευκή οπίσθια σελίδα

Chapter 2

GENERAL THEMATIC MAPS OF THE LAVRION URBAN AREA: Digital topography, Lithology, Metallurgical processing residues & contaminated soil, Soil and House dust pH

Alecos Demetriades, Katerina Vergou-Vichou and Evripides Vassiliades
Institute of Geology and Mineral Exploration, 70 Messoghion Street, Gr-115 27 Athens, Greece

2.1. INTRODUCTION

A number of thematic maps of the Lavrion urban area at scale of 1:5000, which are considered essential in the interpretation of geochemical results, environmental assessment and management, have been compiled (refer to Volume 2). These are:

- digital topographical map (Map 2.1),
- lithological map (Map 2.2),
- map of metallurgical processing wastes and overburden (Map 2.3),
- land use map (Map 2.4),
- distribution of pH in overburden (Map 2.5), and
- distribution of pH in house dust (Map 2.6).

In the following paragraphs the above maps will be described and discussed.

2.2. DIGITAL TOPOGRAPHY

The digital topographical map of the Lavrion urban area (Map 2.1) is based on the 1:5000 map sheets 6478/5 and 6478/7 of the Hellenic Army Geographical Service. To begin with, the town plan was revised for the original displayed on the maps was out of date. Revision was done by firstly, examining recent aerial photographs and transferring information to the 1:5000 base maps, and secondly, by field mapping. The revised town plan and topographic contour lines were drafted on separate plastic tracing sheets. They were subsequently scanned and processed with Arc/Info® GIS. Finally, all spot heights and triangulation stations were digitised. Digital information was converted to a form readable by Surfer®, and the topographical map with spot heights and town plan plotted. Contour lines of the 1:5000 map are at 4-m intervals.

Contour lines at 20-m intervals were subsequently selected for constructing the topography layer of the lithology map (Map 2.2), metallurgical wastes map (Map 2.3), land use map (Map 2.4) and sample site maps (Maps 2.7 -2.15).

The digital elevation (DEM) and terrain (DTM) models of the Lavrion urban area can be constructed from these data for modelling of aerial transport of fine-grained materials. In such a case, detailed data of wind direction and velocity are required, as well as the dustiness of surface materials, especially the ones not covered by vegetation.

The landscape of the Lavrion urban area may be described as undulating near the coast with low hillocks at Perdika (29.79 m), Fougara (41.60 m) and Nichtochori (31.90 m), and intervening lowland. Further inland the topography begins to rise to the west of a south-north line from Panormos, Koukos, Neapoli, Ayios Andreas, Santorineika to Kavodokanos. The highest peaks being at Koukos (82.27 m), Prasini Alepou (66.20 m), and to the west of Kavodokanos (124.80 m). The area is drained by a number of seasonal streams (torrents) with outlets in the area of Komobil, to the east of Phenikodassos and Thorikon.

The natural landscape has been altered considerably by deposition of metallurgical processing wastes as is shown on Map 2.3. Drainage channels have been filled with wastes, hills extended with slag and flotation residues, or new hills created from wastes, as is the elongated hill of flotation residues running from southwest (Noria) to northeast (Santorineika).

2.3. LITHOLOGY

The lithology of the Lavrion urban area was mapped at a scale of 1:5000. The technique used was the detailed outcrop mapping of the different rock units occurring in the Lavrion urban area. On completion of field mapping, probable boundaries, between the different units, were drawn. Rock boundaries were digitised, processed with

Arc/Info® GIS, converted to a form readable by Surfer®, and the lithological map plotted (Map 2.2). It is stressed that the stratigraphic succession of different rock units and their structure were not determined, for the objectives were:

(a) to map in detail rock outcrops,
(b) to study if their spatial distribution is satisfactory for rock geochemical sampling, and
(c) to compile rock geochemical maps for baseline information.

Regional stratigraphy and geological structure are discussed by Marinos and Petrascheck (1956), and the IGME Working Group (1987), who classified rock units of the Lavrion urban area as belonging to the Upper Schist System of Mesozoic age (Triassic-Jurassic).

In the Lavrion urban area the following rock units occur:

- Marble with schist intercalations,
- Schist with marble intercalations,
- Schistose-gneiss,
- Prasinite, and
- Sandstone, conglomerate and alluvial deposits of Quaternary to Recent age.

Outcrops of iron and “iron calamine” mineralisation are found in the study area. Marinos and Petrascheck (1956) referred to the occurrence of small outcrops with galena [PbS] at Kiprianos and Nichtochori hills. They also mentioned the existence of an outcrop of granodiorite porphyry (eurite) at Kiprianos.

The area extent of the different rock units is tabulated in Table 2.1. Marble is the dominant rock type, covering 86.22% of the solid geology, followed by schist (13.24%).

Table 2.1. Area covered by different rock units, Lavrion urban area.
Πίνακας 2.1. 'Εκταση που καλύπτουν οι διάφορες λιθολογικές ενότητες, αστική περιοχή Λαυρίου.

Rock unit	*Λιθομονάδα*	*Area (m^2)* *'Εκταση (m^2)*	*(%)*
Marble with schist intercalations	Μάρμαρο με ενστρώσεις σχιστολίθου	6238189.48	86.22
Schist with marble intercalations	Σχιστόλιθος με ενστρώσεις μαρμάρου	957995.00	13.24
Schistose-gneiss	Σχιστογνεύσιος	9713.00	0.13
Prasinite	Πρασινίτης	27301.00	0.38
Iron mineralisation	Σιδηρούχος μεταλλοφορία	1831.00	0.03
Total area of solid geology	**Συνολική έκταση συμπαγών πετρωμάτων**	**7235029.48**	**100.00**
Altered marble	Εξαλλοιωμένο μάρμαρο	555173.00	8.90
Quaternary formations	Τεταρτογενείς σχηματισμοί	2161342.00	29.87

2.3.1. MARBLE WITH SCHIST INTERCALATIONS

Marble is fine- to coarse-grained, varies in colour from white, to creamy white, to pale and dark grey, and is rosy at places. Apart from ubiquitous jointing the marble is fractured, silicified to a variable degree, locally dolomitised [$CaCO_3.MgCO_3$] and ankeritised [$CaCO_3.(Mg,Fe,Mn)CO_3$]. Dolomitised and ankeritised marble, due to the presence of iron, is reddish brown in colour. Approximately 8.9% of the marble is altered to a variable degree. Ankeritised marble at places is enriched in zinc and cadmium, constituting "*iron calamine*" or *monheimite* [$(Zn,Fe)CO_3$], and also lead, possibly *cerussite* [$PbCO_3$]. According to Marinos and Petrascheck (1956) iron calamine is associated with some zinc silicate, such as *willemite* [Zn_2SiO_4] and *hemimorphite* [$(ZnOH)_2SiO_3$]. Mineralised parts of the marble are indicated by rock geochemical anomalies of lead, zinc and cadmium (Maps 3.1, 4.30, 4.9).

Veinlets of (a) white calcite, and (b) brown iron carbonate minerals, possibly siderite [$FeCO_3$], crosscut the brown ankeritised and grey marble respectively. Locally, disseminated small crystals (<1 to 3 mm) of pyrite [FeS_2] have been observed along bedding planes of white to grey marble.

Lenses of mica schist occur within marble. Their dimensions vary from less than a metre to tens of metres. Schist is generally altered to a variable degree.

2.3.2. SCHIST WITH MARBLE INTERCALATIONS

Schist is a foliated and fractured grey- to greyish green metamorphic rock consisting mainly of muscovite, quartz and feldspar. It contains lenses of marble of variable size, and crosscut by calcite veinlets.

2.3.3. SCHISTOSE-GNEISS

Schistose-gneiss occurs as a small outcrop at the summit of Koukos hill. It is a light-coloured, medium- to coarse-grained and foliated metamorphic rock, rich in feldspar and quartz, with femic minerals (possibly amphibole), and white quartz lenses.

2.3.4. PRASINITE

Prasinite occurs as dykes or lenses within marble and schist, and at the contact of marble and schist. It is an altered metamorphosed mafic rock, originally composed of

augite (often titaniferous), basic plagioclase, and pyroxene (diallage); secondary minerals, due to alteration, are mainly albite, chlorite (penninite), epidote, clinozoisite, actinolite, hornblende, glaucophane and leucoxene (Marinos and Petrascheck, 1956). The original rock is considered to be diabase-gabbro, which has been subjected to chlorite-epidote facies metamorphism.

Prasinite is a very hard and massive rock, which is not easily altered by weathering processes. It, therefore, occurs on hills or forms resistant protrusions (minor hillocks) within the marble in the low-lying land.

2.3.5. QUATERNARY FORMATIONS

Quaternary formations comprise the older (Pleistocene) and recent (Holocene) deposits. Calcareous sandstone, occurring at many locations in Lavrion, is considered to be the older formation (Marinos and Petrascheck, 1956). It is a medium-grained yellowish-brown sandstone, mainly consisting from rounded to sub-rounded quartz grains (<2 mm), and cemented by calcareous material.

Calcareous conglomerate occurs in present-day stream beds. Pebbles of marble, schist and prasinite are rounded to sub-rounded, reach sizes of up to 35 cm, and are cemented by yellow-brown to reddish calcareous material. These deposits may also be of Pleistocene age.

Recent deposits comprise the pale-brown to yellow-brown alluvial deposits in the valleys and plains, which consist of unconsolidated sand with a variable proportion of clay.

2.3.6. IRON MINERALISATION

Small lenses of intensely silicified dark-red iron mineralisation occur within the marble at Fougara and Perdika hills (southeastern part of study area, Map 2.2).

2.4. METALLURGICAL PROCESSING WASTES AND OVERBURDEN

Metallurgical processing of ore-grade materials from 1865 to 1989 produced considerable amount of waste materials, which cover a large part of the Lavrion urban area (Map 2.3). Ancient wastes that may have existed are completely masked. Residual soil has been contaminated to a variable degree, and constitutes today the greatest hazard, since it covers the greatest area in Lavrion (74.91% of study area, Table 2.3). Since, residual soil is only found in a few places, and the natural landscape has been altered considerably by deposition of metallurgical wastes, their moving about by the local inhabitants, and importation of soil from other parts of Greece, the term *overburden* is preferred for it describes the situation perfectly well. *Overburden* is defined by Jackson (1997, p.457) as the "*loose soil, silt, sand, gravel, or other unconsolidated material overlying bedrock, either transported or formed in place*".

The different types of metallurgical processing wastes were mapped in detail at a scale of 1:5000. Aerial photographs were used only for the exact delimitation of areas covered by slag about the hills at Perdika and Kavodokanos (Map 2.3). Exact boundaries of the flotation residues were difficult to ascertain especially in agricultural areas, because of their mixing with alluvial sediments.

Boundaries were transferred from the field map onto a new base map, digitised, processed with Arc/Info® GIS, converted to a form readable by Surfer®, and the map of metallurgical processing wastes and contaminated overburden plotted (Map 2.3).

Three main categories of metallurgical processing wastes occur in the Lavrion urban area:

- beneficiation/flotation residues or tailings (they will be referred to in the text as either flotation residues or flotation tailings),
- pyritiferous tailings, and
- slags (lumpy and pelletised).

These three main types of metallurgical processing wastes have been subdivided further into other *sub-categories*, depending on their proportion which is mixed with other wastes or materials, *i.e.*,

- disseminated slag,
- sand-blast material from slag and pelletised slag,
- beneficiation/flotation sand with disseminated pyrite,
- disseminated slag and coarse-grained beneficiation/flotation residues,
- beneficiation/flotation sand and coarse-grained materials, and
- beneficiation/flotation residues and disseminated slag.

The surface area of the metallurgical processing wastes, and contaminated soil or overburden, are tabulated in Table 2.3.

2.4.1. BENEFICIATION/FLOTATION RESIDUES

The beneficiation/flotation residues or tailings are those portions of lighter materials that are washed or floated off during the beneficiation/flotation process, that are too poor for further treatment. Flotation tailings in Lavrion are called *savoura (=σαβούρα)* by the local inhabitants, which means material of no value, *i.e.*, waste. The flotation tailings have the greatest area extent (Table 2.3).

Flotation tailings are yellow-brown to pale brown in colour, and vary in grain-size, *i.e.*, fine- to coarse-grain sand, and sand mixed with angular pebbles and cobbles of marble and schist. The proportion of silt- and clay-size material is variable.

It is noted that the Wentworth classification is used for the description of clastic particle grain-size (Table 2.2).

Table 2.2. Wentworth classification of clastic particles (from Lahee, 1959, Table 1, p.38).
Πίνακας 2.2. Ταξινόμηση Wentworth των κλαστικών μορίων.

Range of dimensions (mm)	*Individual fragments or particles*	*Range of dimensions (mm)*	*Individual fragments or particles*
>256	Boulder	0.25-0.5	Medium sand grain
64-256	Cobble	0.125-0.25	Fine sand grain
4- 64	Pebble	0.0625-0.125	Very fine sand grain
2- 4	Granule	0.0039-0.0625	Silt particle
1- 2	Very coarse sand grain	<0.0039	Clay particle
0.5- 1	Coarse sand grain		

Table 2.3. Area covered by different types of metallurgical processing wastes and contaminated soil in the Lavrion urban area.
Πίνακας 2.3. 'Εκταση που καταλαμβάνουν οι διάφοροι τύποι των μεταλλουργικών απορριμμάτων και το ρυπασμένο έδαφος στην αστική περιοχή του Λαυρίου.

Smelter wastes	*Μεταλλουργικά απορρίμματα*	*Area (m^2) Έκταση (m^2)*	*(%)*
Beneficiation/flotation residues or tailings	Απορρίμματα εμπλουτισμού/επίπλευσης (σαβούρα)	474,211.83	6.55
Slag	Σκουριές	397,568.97	5.50
Slag with sand-blast wastes	Σκουριές και απορρίμματα αμμοβολής	135,764.79	1.88
Disseminated slag	Διάσπαρτες σκουριές	145,008.07	2.00
Sand-blast wastes	Απορρίμματα αμμοβολής	105,813.29	1.46
Beneficiation/flotation sands with disseminated pyrite	'Αμμοι εμπλουτισμού/επίπλευσης με διάσπαρτο πυρίτη	305,047.01	4.22
Pyritiferous beneficiation/flotation residues	Πυριτούχα υλικά εμπλουτισμού/ επίπλευσης	209,029.94	2.89
Disseminated slag and coarse-grained beneficiation/flotation residues	Διάσπαρτες σκουριές και αδρόκοκκα απορρίμματα εμπλουτισμού/επίπλευσης	17,492.64	0.24
Beneficiation/flotation sands and coarse-grained materials	'Αμμοι εμπλουτισμού/επίπλευσης και αδρόκοκκα (απορρίμματα) υλικά	23,279.59	0.32
Beneficiation/flotation residues with disseminated slag	Σαβούρα (απορρίμματα εμπλουτισμού/ επίπλευσης) με διάσπαρτες σκουριές	2,169.52	0.03
Contaminated soil	Ρυπασμένο έδαφος	5,419,643.83	74.91
Total area	**Συνολική έκταση**	**7,235,029.48**	**100.00**

2.4.1.1. Beneficiation/flotation sand with disseminated pyrite

Flotation sand with disseminated pyrite comprises pale brown, fine- to coarse-grain sandy material with scattered crystals of pyrite (<1.5 mm).

2.4.1.2. Beneficiation/flotation sand and coarse-grained materials

Flotation sand with coarse-grain materials, consist of pale brown to yellow-brown, fine- to coarse-grained sandy material with pebbles, cobbles and boulders of marble and schist.

2.4.1.3. Beneficiation/flotation residues and disseminated slag

The beneficiation/flotation residues with disseminated slag are made up from pale brown to yellow brown fine- to coarse-grain flotation sand, and pebble- to boulder-size marble and schist, mixed with scattered fragments of slag.

2.4.2. PYRITIFEROUS TAILINGS

Pyritiferous tailings consist of grey fine- to medium-grain pyrite concentrate. These tailings have been altered by supergene processes to a variable degree, and are brown to brownish-red in colour. At two sites, Komobil and Kavodokanos, lakes with very acid water were formed in the winter period (refer to section 2.6). The pH of water varied from 1.8 to 2.5, indicating that strong sulphuric acid has been formed. Fortunately, for the inhabitants the lakes no longer exist, because they have been covered since 1997 by other materials.

2.4.3. SLAG

Slag is the grey-black solid waste material produced in the furnace during melting of ore for separation of argentiferous lead. There are two types of slag: (a) lumpy slag which is cast into flat cone-shaped vessels and is found today either intact flat cone-shaped blocks or broken-up in large angular fragments (1-35 cm), and (b) pelletised slag, which is slag in small pellets (<3 mm).

It is noted that in the slag heaps there occurs fine- to medium-grain pale brown to yellow-brown earthy material.

2.4.3.1. Sand-blast material from slag and pelletised slag

At Kavodokanos and Thorikon there were two units (Map 2.4), which crushed slag to produce material for sand-blasting the metal of ships, and it was sold to ship-building yards, *e.g.*, Elefsis. Sand-blast material is black coloured and angular in shape, and since is approximately the same size as the pelletised slag (<3 mm), it is difficult to distinguish the two in the field.

2.4.3.2. Disseminated slag and coarse-grained beneficiation/flotation residues

Fragments of angular grey-black lumpy slag are mixed with coarse-sand to boulder-size flotation residues; angular pebbles, cobbles and boulders consist of marble and schist.

2.5. LAND USE

The Lavrion urban area, covered by this study, extends from the residential part of the town into its outskirts, which are either agricultural or forested. The different types of land use were mapped in detail by field mapping at scale of 1:5000. Aerial photography was used only in the exact delimitation of areas covered by forest and olive groves.

The original mapping of land use types had about fifty categories, which were later reduced to thirty by joining similar categories. Land use categories were classified into two broad groups:

1. residential area, tillage, forest and open space, and
2. industrial, commercial.

Both groups have fifteen categories each.

Land use category boundaries were transferred from the field map onto a new base map, digitised, processed with Arc/Info® GIS, converted to a form readable by Surfer®, and the land use map plotted (Map 2.4).

Areas covered by each land use category are tabulated in Table 2.4. Open space with or without bushes and scattered trees cover 53.86% of the study area. Together with the areas covered by pine forest (5.15%), open space with trees (1.54%), olive groves (6.08%), vineyards (1.7%), vegetables (0.2%) and wheat fields (0.16%) make up 68.69% of the total area. All industries cover 16.82% of the total area, and only about 14.5% is utilised for residential and recreational purposes. Hence, the agricultural part dominates the study area, followed by the industrial, and the residential/recreational section of the town covers the smallest area.

In Table 2.5, the percentage proportion (%) of the different land use categories overlying the different types of metallurgical processing wastes and contaminated soil is tabulated. It is stressed that

- a large part of the residential and recreational area of Lavrion is situated over contaminated soil, the flotation residues and slag;
- vineyards are mainly grown over the flotation residues, and
- a large part of the olive groves.

These statistics are not very encouraging, since local inhabitants live, work and play in the most hazardous areas.

Table 2.4. Area covered by the different land use categories in the Lavrion urban area.
Πίνακας 2.4. 'Εκταση που καταλαμβάνουν οι διάφορες κατηγορίες χρήσης γης στην αστική περιοχή του Λαυρίου.

Land use category	*Κατηγορίες χρήσης γης*	*Area (m^2)*	*(%)*
1. Residential area, Tillage, Forest, Open Space	*1. Αστικός χώρος, Καλλιέργειες, Δάσος, Ανοικτός χώρος*	*'Εκταση (m^2)*	
House, shop, church	Κατοικία, κατάστημα, εκκλησία	481186.45	6.65
House with a garden	Κατοικία με περιβόλι	416639.21	5.76
School	Σχολείο	44613.16	0.62
Playground	Παιδική χαρά	6724.61	0.09
Park	Πάρκο	40872.01	0.57
Football pitch, sports field	Γήπεδο, χώρος άθλησης	39537.31	0.55
Olive grove	Ελαιώνας	439975.42	6.08
Vineyard	Αμπελώνας	123200.04	1.70
Vegetables	Κηπευτικά	14681.36	0.20
Wheat	Στάρι	11222.18	0.16
Pine forest	Δάσος με πεύκα	372498.46	5.15
Open space with trees ± (olives, figs, *etc.*)	Ανοικτός χώρος με δένδρα ±(ελιές, συκιές, κ.ά.)	111722.65	1.54
Open space with trees ± (bushes, trees)	Ανοικτός χώρος ±(θάμνοι, δένδρα)	3896642.50	53.86
Archaeological site	Αρχαιολογικός χώρος	4243.66	0.06
Cemetery	Κοιμητήριο	13537.25	0.19
2. Industrial, Commercial	*2. Βιομηχανίες, Εμπορικά*		
Ore treatment plant & storeroom	Εργοστάσιο κατεργασίας μεταλλεύματος & αποθήκη	273223.46	3.78
Smokeduct	Καπναγωγός	23358.94	0.32
Sandblasting units with slag	Μονάδα αμμοβολής με σκουριές	2436.98	0.03
Lead-acid battery factory	Εργοστάσιο υγρών μπαταριών μολύβδου	41403.68	0.57
Factory (ammunition, weapons, matches), storerooms	Εργοστάσιο (πολεμοφόδια, όπλα, σπίρτα), αποθήκη	437996.98	6.05
Petrol station, garage & motor repairs	Πρατήριο βενζίνης, γκαράζ & συνεργείο αυτοκινήτων	12190.98	0.17
Iron converter industry & trading	Σιδηροκατασκευές & εμπορία σιδήρου	119636.64	1.65
Aluminium converter industries	Αλουμινοκατασκευές	3060.38	0.04
Cotton weaving industries	Κλωστοϋφαντουργία	119232.05	1.65
Other industries, storage sites	Λοιπές βιοτεχνίες, αποθήκες υλικών	9906.59	0.14
Building materials storehouses	Αποθήκες οικοδομικών υλικών	27099.37	0.38
Port installations	Λιμενικές εγκαταστάσεις	141574.90	1.96
Marble quarry	Λατομείο μαρμάρου	4659.13	0.06
Old mining works	Παλαιές μεταλλευτικές εργασίες	1057.41	0.01
Waste site	Χωματερή	895.72	0.01
Total area	**Συνολική έκταση**	**7235029.48**	**100.00**

Table 2.5. Table showing the area in square metres and the percentage proportion (%) of the different land use categories covering the different types of smelter wastes and contaminated soil, Lavrion urban area.

Πίνακας 2.5. Πίνακας όπου φαίνεται η έκταση σε τετραγωνικά μέτρα και η ποσοστιαία αναλογία (%) των διαφόρων κατηγοριών χρήσης γης που υπέρκεινται των διαφορετικών τύπων των μεταλλευτικών απορριμμάτων και του ρυπασμένου εδάφους, αστική περιοχή Λαυρίου.

Land use category	*Beneficiation/ flotation residues*	*Slag*	*Slag and sand-blast wastes*	*Disseminated slag*	*Sand- blast wastes*	*Beneficiation/ flotation sands with disseminated pyrite*	*Pyritiferous beneficiation/ Flotation residues*	*Disseminated slag and coarse-grained beneficiaition/ Flotation residues*	*Flotation sands and coarse grained materials*	*Beneficiation/ flotation residues and disseminated slag*	*Contaminated soil*
Χρήση γης	*Απορρίμματα εμπλουτισμού/ Επίπλευσης (σαβούρα)*	*Σκουριές*	*Σκουριές και απορρίμματα αμμοβολής*	*Διάσπαρτες σκουριές*	*Απορρίμματα αμμοβολής*	*Άμμοι εμπλουτισμού/ επίπλευσης με διάσπαρτο πυρίτη*	*Πυριτούχα απορρίμματα εμπλουτισμού/ Επίπλευσης*	*Διάσπαρτες σκουριές με αδρόκοκκα απορρίμματα εμπλουτισμού/ Επίπλευσης*	*Αδρόκοκκα υλικά επίπλευσης και άμμοι*	*Σαβούρα (απορρίμματα εμπλουτισμού/ επίπλευσης) και διάσπαρτες σκουριές*	*Ρυπασμένο έδαφος*
House, shop, church Κατοικία, κατάστημα, εκκλησία	21134.33 (0.2921)	8578.57 (0.1186)	431.53 (0.0060)	6290.20 (0.0869)	2270.96 (0.0314)	2664.05 (0.0368)	3353.50 (0.0464)	-	-	-	436463.31 (6.0326)
House with a garden Κατοικία με περιβόλι	56725.11 (0.7840)	9448.96 (0.1306)	-	1030.78 (0.0142)	637.30 (0.0880)	-	729.18 (0.0101)	146.42 (0.0020)	-	-	347921.46 (4.8088)
School Σχολείο	1546.28 (0.0214)	6867.05 (0.0949)	-	8.91 (0.0001)	-	21397.48 (0.2957)	-	-	-	-	14793.44 (0.2045)
Playground Παιδική χαρά	2159.92 (0.0299)	-	-	-	-	-	-	-	-	-	4564.69 (0.0631)
Park Πάρκο	-	-	-	105.29 (0.0015)	-	4962.74 (0.0686)	-	-	-	-	35803.98 (0.4949)
Football pitch, sports field Γήπεδο, χώρος άθλησης	2992.68 (0.0414)	4987.05 (0.0689)	-	-	-	28825.46 (0.3984)	-	-	-	-	2732.12 (0.0378)
Olive grove Ελαιώνας	32475.22 (0.4489)	1358.63 (0.0188)	1329.72 (0.0184)	4552.25 (0.0629)	626.92 (0.0087)	-	6773.52 (0.0936)	-	-	-	392859.16 (5.4300)
Vineyard Αμπελώνας	64325.71 (0.8891)	-	-	1058.77 (0.0146)	27.01 (0.0004)	-	-	-	-	-	57788.55 (0.7987)
Vegetables Κηπευτικά	-	-	-	-	-	-	-	-	-	-	14681.36 (0.2029)
Wheat Στάρι	-	-	-	-	-	-	-	-	-	-	11222.18 (0.1551)
Pine forest Δάσος με πεύκα	5184.30 (0.0717)	404.89 (0.0056)	-	-	-	141.10 (0.0020)	9.41 (0.0001)	-	-	-	366758.76 (5.0692)
Open space with trees Ανοικτός χώρος με δένδρα	32830.31 (0.4538)	273.34 (0.0038)	-	1387.82 (0.0192)	-	-	-	-	-	-	77231.18 (1.0675)
Open space Ανοικτός χώρος	226319.20 (3.1281)	263317.90 (3.6395)	96513.36 (1.3340)	93252.70 (1.2889)	67878.50 (0.9382)	246937.10 (3.4131)	149967.80 (2.0728)	12215.16 (0.1688)	23208.43 (0.3208)	2169.52 (0.0300)	2714862.83 (37.5239)
Archaeological site Αρχαιολογικός χώρος	-	-	-	-	-	-	-	-	-	-	4243.66 (0.0587)
Cemetery Κοιμητήριο	-	-	-	-	-	-	-	-	-	-	13537.25 (0.1871)

…..Table 2.5. Table showing the area in square metres and the percentage proportion (%) of the different land use categories covering the different types of smelter wastes and contaminated soil, Lavrion urban area.

…..Πίνακας 2.5. Πίνακας όπου φαίνεται η έκταση σε τετραγωνικά μέτρα και η ποσοστιαία αναλογία (%) των διαφόρων κατηγοριών χρήσης γης που υπέρκεινται των διαφορετικών τύπων των μεταλλευτικών απορριμμάτων και του ρυπασμένου εδάφους, αστική περιοχή Λαυρίου.

Land use category	*Beneficiation/ flotation residues*	*Slag*	*Slag and sand-blast wastes*	*Disseminated slag*	*Sand- blast wastes*	*Beneficiation/ flotation sands with disseminated pyrite*	*Pyritiferous beneficiation/ Flotation residues*	*Disseminated slag and coarse-grained beneficiation/ flotation residues*	*Flotation sands and coarse grained materials*	*Beneficiation/ flotation residues and disseminated slag*	*Contaminated soil*
Χρήση γης	*Απορρίμματα εμπλουτισμού/ Επίπλευσης (σαβούρα)*	*Σκουριές*	*Σκουριές και απορρίμματα αμμοβολής*	*Διάσπαρτες σκουριές*	*Απορρίμματα αμμοβολής*	*Άμμοι εμπλουτισμού/ επίπλευσης με διάσπαρτο πυρίτη*	*Πυριτούχα απορρίμματα εμπλουτισμού/ Επίπλευσης*	*Διάσπαρτες σκουριές με αδρόκοκκα απορρίμματα εμπλουτισμού/ Επίπλευσης*	*Αδρόκοκκα υλικά επίπλευσης και άμμοι*	*Σαβούρα (απορρίμματα εμπλουτισμού/ επίπλευσης) και διάσπαρτες σκουριές*	*Ρυπασμένο έδαφος*
Ore treatment plant & storeroom Εργοστάσιο κατεργασίας μεταλλεύματος & αποθήκη	7997.45 (0.1105)	15712.56 (0.2172)	37348.66 (0.5162)	656.82 (0.0091)	28682.82 (0.3964)	42.65 (0.0006)	44935.70 (0.6211)	‘	71.16 (0.0010)	‘	137775.64 (1.9043)
Smokeduct Καπναγωγός	‘	927.09 (0.0128)	‘	‘	‘	‘	2113.96 (0.0292)	‘	‘	‘	20317.89 (0.2808)
Sandblasting unit with slags Μονάδα αμμοβολής από σκουριές	‘	‘	‘	‘	2436.98 (0.0337)	‘	‘	‘	‘	‘	‘
Lead-acid battery Εργοστάσιο υγρών μπαταριών Pb	‘	‘	‘	‘	‘	‘	‘	‘	‘	‘	41403.68 (0.5723)
Factory (ammunition, etc) Εργοστάσιο (πολεμοφόδια, κλπ.)	‘	27370.74 (0.3783)	‘	25422.13 (0.3514)	‘	‘	‘	‘	‘	‘	385204.11 (5.3242)
Petrol station, garage & motor repairs Πρατήριο βενζίνης, γκαράζ, συνεργείο	1040.34 (0.0144)	131.59 (0.0018)	‘	‘	‘	‘	‘	3948.60 (0.0546)	‘	‘	7070.45 (0.0977)
Iron converter industry & trading Σιδηροκατασκευές και εμπορία σιδήρου	6367.88 (0.0880)	1815.31 (0.0251)	‘	9881.61 (0.1366)	‘	‘	‘	‘	‘	‘	101571.84 (1.4039)
Aluminium converter industry Αλουμινοκατασκευές	‘	‘	‘	‘	‘	‘	1146.87 (0.0159)	‘	‘	‘	1913.51 (0.0264)
Cotton-weaving industry Κλωστοϋφαντουργία	‘	4604.09 (0.0636)	‘	‘	3252.80 (0.0450)	76.43 (0.0011)	‘	‘	‘	‘	111298.73 (1.5383)
Other industries, storage sites Λοιπές βιομηχανίες, αποθήκες υλικών	1546.21 (0.0214)	‘	‘	49.42 (0.0007)	‘	‘	‘	‘	‘	‘	8310.96 (0.1149)
Building materials wholesaler Αποθήκη οικοδομικών υλικών	11566.89 (0.1599)	4321.04 (0.0597)	‘	1308.63 (0.0181)	‘	‘	‘	1182.46 (0.0163)	‘	‘	8720.35 (0.1205)
Port installations Λιμενικές εγκαταστάσεις	-	46572.83 (0.6437)	‘	‘	‘	‘	‘	‘	‘	‘	95002.07 (1.3131)
Disused marble quarry Παλαιό λατομείο μαρμάρου	‘	877.33 (0.0121)	‘	2.74 (0.0004)	‘	‘	‘	‘	‘	‘	3779.06 (0.0522)
Disused mining works Παλαιά μεταλλευτική εργασία	‘	‘	141.52 (0.0020)	‘	‘	‘	‘	‘	‘	‘	915.89 (0.0127)
Waste site Χωματερή	‘	‘	‘	‘	‘	‘	‘	‘	‘	‘	895.72 (0.0124)

2.6. DISTRIBUTION OF pH IN OVERBURDEN, MOBILITY AND AVAILABILITY OF ELEMENTS

Overburden pH was determined on the dry, sieved (<2 mm) and pulverised (<0.177 mm) samples. This is in contradiction to normal practice requiring that "soil" samples are kept under or near to field conditions or at worse gently air-dried, since it is known that pH is particularly very sensitive to oxidation-reduction reactions (including microbial activity), which normally affect (a) sulphide-sulphate and (b) nitrogen-nitrate transformations, as well as (c) the balance of carbon dioxide between soil gases and the atmosphere (Fletcher, 1981).

It is widely known that the solubility of most elements, and the stability of their compounds, are extremely sensitive to the pH of the aqueous environment. Only a few elements, the alkali metals (Na, K, Rb), alkaline earths (Ca, Mg, Sr) and some elements that form acid radicals (nitrogen and chlorine), are normally soluble throughout the entire pH range (Levinson, 1974). Most metallic elements are soluble only in acid solutions, and tend to precipitate as hydroxides (or basic salts) with increasing pH. The pH at which these elements precipitate as hydroxides is known as the *pH of hydrolysis* or *pH of hydroxide precipitation*. In Table 2.6 elements are presented in the order of increasing pH of hydrolysis. The following examples will elucidate the principles of *pH of hydrolysis*, *e.g.*, $Fe(OH)_3$ begins to precipitate at a pH of 2.48; $Al(OH)_3$ at 4.1; $Cu(OH)_2$ at 5.3; $Fe(OH)_2$ at 5.5; $Ni(OH)_2$ at 6.7; $Mn(OH)_2$ at 9; $Mg(OH)_2$ at 10.5 (Table 2.6). Consequently, Al^{3+} and Fe^{2+} ions can exist in a weakly acid medium (pH to 4.1 and 5.5), whereas the Mn^{2+} and Mg^{2+} ions are stable even in an alkaline medium (Perel'man, 1977; Levinson *et al.*, 1987). Their precipitation in the form $Mn(OH)_2$ and $Mg(OH)_2$ starts only under strongly alkaline conditions. It is stressed that the *pH of hydrolysis* depends on the metal ion concentration.

Table 2.6. pH of hydrolysis (hydroxide precipitation) of some elements from dilute (0.025-0.0025M) solutions (from [1]Levinson, 1974, Table 3-6, p.128 and [2]Kabata-Pendias and Pendias, 1984, Table 9, p.20).
Πίνακας 2.6. pH υδρόλυσης (κατακρήμνισης υδροξειδίων) μερικών στοιχείων από αραιά (0.025-0.0025M) διαλύματα.

Element	*pH[1]*	*pH[2]*	*Element*	*pH[1]*	*pH[2]*	*Element*	*pH[1]*	*pH[2]*	*Element*	*pH[1]*	*pH[2]*
Fe^{3+}	2.0	2.2-3.2	Al^{3+}	4.1	3.8-4.8	Cd^{2+}	6.7	8.0-9.5	Pr^{3+}	7.1	-
Zr^{4+}	2.0	2.0	U^{6+}	4.2	-	Ni^{2+}	6.7	6.7-8.2	Hg^{2+}	7.3	-
Sn^{2+}	2.0	-	Cr^{3+}	5.3	4.6-5.6	Co^{2+}	6.8	7.2-8.7	Ce^{3+}	7.4	-
Ce^{4+}	2.7	-	Cu^{2+}	5.3	5.4-6.9	Y^{3+}	6.8	-	La^{3+}	8.4	-
Hg^{1+}	3.0	-	Fe^{2+}	5.5	5.1-5.5	Sm^{3+}	6.8	-	Ag^{1+}	7.5-8.0	-
In^{3+}	3.4	-	Be^{2+}	5.7	-	Zn^{2+}	7.0	5.2-8.3	Mn^{2+}	8.5-8.8	7.9-9.4
Th^{4+}	3.5	-	Pb^{2+}	6.0	7.2-8.7	Nd^{3+}	7.0	-	Mg^{2+}	10.5	10.5

Values of *pH of hydrolysis* explain many characteristics of metal migration, *e.g.*, migration of Fe^{2+} in weakly acid waters, the low mobility of Fe^{3+} in such waters, and a wide range of migration for Mg^{2+}. Nevertheless, this parameter should be used with certain reservations when one draws geochemical conclusions, because the supergene geochemical environment is more complex. The actual forms of occurrence of metals in the aqueous environment (*e.g.*, as complex ions), their concentration, and other factors should be taken into account (Perel'man, 1977). Otherwise, one may arrive at conclusions, which do not conform to natural situations. Mobility based on the *pH of hydrolysis* does not take into account such factors as

- the formation of organic and inorganic complexing agents, *e.g.*, formation of uranyl carbonate and sulphate complexes, which extend the solubility of uranium well into the alkaline pH range from the pH of 4.2 shown in Table 2.6;
- the presence of certain elements and radicals can cause almost immediate precipitation of certain other elements considerably before their pH of hydrolysis is reached, *e.g.*, precipitation of insoluble anglesite when sulphate occurs in waters associated with an oxidising lead deposit (Levinson, 1974).

Hence, the *pH of hydrolysis* data should be used as no more than a first approximation to actual situations found in nature.

Apart from the role of pH in the solubility and mobility of elements in solution, it plays a significant part in (a) determining the adsorption capacity of clays, and (b) the elemental uptake by plants. Montmorillonite, for example, in an acid environment will have little if any adsorbed metals, by comparison with an alkaline environment. This is because the hydrogen ion is preferentially adsorbed (or exchanged) in place of metals. Availability of elements in soil, and their uptake by plants, depends on whether elements are in soluble or insoluble forms, and whether and how strongly, elements are adsorbed onto clays (Levinson, 1974).

The distribution of pH in overburden is shown on Map 2.5. Spatial characteristics have been determined by the geostatistical variogram surface (Pennatier, 1996). The dominant structure is from southwest to the northeast, which corresponds with the orientation of the flotation residues; a secondary structure is from southeast to northwest, following again the other direction of the flotation tailings from Santorineika to Prasini Alepou.

Replicate analysis of pH enabled the estimation of sampling and analytical variance, called technical variance by Ramsey (1993), and geochemical variance, which are 17.24% and 87.26% respectively.

Values of overburden pH vary from 2.69 (acid) to 8.56 (alkaline), with a mean of 7.81 and a median of 7.88. The alkaline nature of overburden, due to the dominant rock type which is marble and the carbonates in the flotation residues, is evident, since about 97.5% of the samples have pH values of over 7.0. Approximately 2.5% of overburden samples have pH values between 2.69 and 6.87, and these samples come from the pyritiferous sands. In these areas corrosive acid drainage is generated by reaction of pyrite with air, rain, surface- and ground-water, *i.e.*, (a) reaction of *[pyrite + water + (Fe^{3+} or oxygen)]* produces *[Fe^{2+} + sulphate + acid]*, and (b) *[Fe^{3+} + water]* produces *[iron hydroxides + acid]*. The pH was measured in ponds of water at Komobil and Kavodokanos, formed during the winter period by rainwater, and was found to be between 1.8 and 2.5. As it may be appreciated this acid water dissolves many heavy metals, and toxic elements in general, present in metallurgical processing wastes, to produce fluid-acid drainage, which contains high to extreme concentrations of Fe, Al, Mn, Pb, Zn, Cd, As, Sb, Cu and other metals, thus endangering groundwater supplies.

Effects of acid emissions from the petroleum powered electricity generating plant, which is situated to the north-east of Lavrion, can be seen at high ground areas, such as Ayios Andreas (pH: 7.42-7.66) and Neapoli-Koukos (pH: 7.11-7.66); the latter area may also have been affected by emissions from the lead-acid battery plant (situated to the WSW). These values, although still in the alkaline range, are slightly lower than the pH of the surrounding area (pH>7.88).

The predominantly alkaline nature of overburden solutions (*e.g.*, high proportion of carbonates), suggests that element mobility is generally low to insignificant. Elements that could possibly be mobile in the acid to slightly alkaline environment of the pyritiferous tailings *(pH of hydrolysis>2.69 to 7.11)* are: Hg^{1+}, Al^{3+}, Cr^{3+}, Cu^{2+}, Fe^{2+}, Be^{2+}, Pb^{2+}, Cd^{2+}, Ni^{2+}, Co^{2+} and Zn^{2+}. In the alkaline environment of overburden over marble, schist and metallurgical processing residues, other than the pyritiferous tailings, (*pH of hydrolysis>7.11 to 8.56*) the only elements with some mobility are Mn^{2+} and Mg^{2+}; Zn^{2+} is mobile in the narrow pH range of 6.87-7.11 (*pH of hydrolysis 7.0*), and Hg^{2+} between 7.11-7.42 (*pH of hydrolysis 7.3*).

As it has already been mentioned the local inhabitants are engaged in agricultural activities, *e.g.*, olive groves, vegetables, vineyards and wheat (Map 2.4). Availability of mineral nutrients to plants depends on soil pH, among other factors. Most plants thrive better between a pH of 6.0 to 7.5 (Russell, 1970; Kabata-Pendias and Pendias, 1984). The area having this pH range in Lavrion is indeed very small. Agricultural areas have pH values >7.66.

At a pH of about 7 most elements are available to plants (Mervyn, 1980; 1985). In highly acid soils (pH<6.0) only potassium, iron, manganese, copper and zinc can be absorbed by plants. Whereas, in highly alkaline soils (pH>7.5) phosphorus, potassium, sulphur and boron are freely available for absorption by plants. Even under moderately acid (pH 6.0-6.5) to alkaline (pH 7.5-8.0) conditions elements such as phosphorus, calcium, magnesium, iron and manganese are not fully available for absorption, and deficiency of these nutrients in plants can result.

Apart from pH another factor influencing uptake of elements by plants is the concentration of other elements in soil, which can either stimulate or antagonise the absorption of a particular element. Zinc absorption, for instance, is dependent upon phosphorus, iron and calcium concentrations. These relationships are displayed by Mulder's chart (Fig. 2.1), which shows the interaction of different mineral nutrients. Thus,

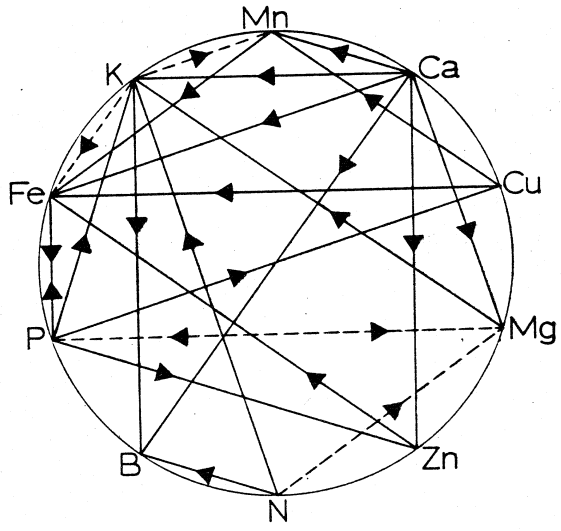

Fig. 2.1. Mulder's chart showing plant uptake of mineral nutrients (from Mervyn, 1980, Fig. 1, p. 12).

Σχ. 2.1. Το σχεδιάγραμμα του Mulder δείχνει την πρόσληψη μεταλλικών θρεπτικών στοιχείων από τα φυτά.

high concentrations of phosphorus in the soil antagonise the uptake of zinc, copper and potassium, while stimulating the uptake of magnesium. In the case of Lavrion *"agricultural soil"* with

- high zinc concentrations antagonise the uptake of iron. Meaning that there may be a deficiency in iron, and the symptoms in plants are: yellowing of veins in young leaves; stems are short and slender; buds remain alive (Mervyn, 1980, 1985).
- high copper concentrations antagonise the uptake of iron and manganese. Hence, high copper concentrations also inhibit the absorption of iron by plants, but also of manganese. Symptoms of manganese deficiency in plants are: yellowing, dead areas between veins; smallest veins remain green.

Such symptoms of yellowing leaves were observed in the vines grown over the flotation tailings.

2.7. DISTRIBUTION OF pH IN HOUSE DUST

House dust pH was determined on the dry and sieved (<1 mm) samples (Map 2.6, Volume 2). The map was plotted using the same geostatistical parameters determined for overburden, since no sensible spatial structure could be obtained from house dust samples.

The reason for determining pH on house dust samples was to study its relationship with that of overburden, and possible differences between them. It is quite apparent from the absolute values of pH that there are differences mainly in the range of values of house dust pH, *i.e.*, 5.45 to 11.70 (overburden 2.69-8.56), and minor differences in the mean, 7.66 (overburden mean 7.81) and median, 7.54 (overburden median 7.88). Similarities between mean and median pH values of overburden and house dust indicate the close relationship between the two sample media. Whereas differences in the range of values is explained by the fact that no houses are built over pyritiferous tailings, and house dust's carbonate content is possibly higher due to input from building materials.

The extremely low pH values (<6.23) at Nichtochori, Neapoli and Perdika are most likely due to acid emissions of the petroleum powered electricity generating plant (situated to the NNE), the lead-acid battery plant (situated to the WSW), and the matches factory (situated to the W) respectively (refer to Map 2.4, Volume 2). The low house dust pH values (<6.84) between Kavodokanos and Thorikon are also possibly explained by acid emissions of the petroleum powered electricity generating plant (situated to the NE). Evidence for the effects of acid emissions from the petroleum powered electricity generating plant can be seen on the concrete structures at Nichtochori.

Chapter 2A

SAMPLING AND SAMPLE PREPARATION

Alecos Demetriades and Katerina Vergou-Vichou
Institute of Geology and Mineral Exploration, 70 Messoghion Street, Gr-115 27, Athens, Greece

2A.1. INTRODUCTION

The following sample types were collected from the Lavrion urban area:

- rock (Map 2.7, Volume 2 of this report),
- metallurgical processing residues (Map 2.8),
- overburden including residual soil (Map 2.9),
- house-dust (Map 2.10),
- metallurgical processing wastes and residual soil for particle-size analysis (Map 2.11),
- ground water (Map 2.12),
- metallurgical wastes for particle characterisation (Map 2.13), and
- overburden from drill-hole core and vertical profiles (Map 2.14).

In addition,

- biomedical sample sites and results were provided by epidemiological researchers (Map 2.15), and
- soil sample sites and results of samples collected for the agronomy study were provided by the Forest Research Institute and the National Technical University of Athens (Map 2.16).

Residual soil occurs in small patches over hilly ground, forested sections, and the northern and southern parts of the Lavrion urban area. Alluvial soil is mainly found in the flood plain of Thorikon, and in some of the smaller valleys. Most of the surface "soil" is a mixture of residual or alluvial soil, *sensu stricto*, and fine-grained metallurgical processing wastes. Hence, the preference to use the term "overburden", which describes better the sampled material. Overburden is defined by Jackson (1997, p.457) as *"the loose soil, silt, sand, gravel, or other unconsolidated material overlying bedrock, either transported or formed in place"*.

Observations for each sample type were recorded on field-sheets.

2A.2. SAMPLING

2A.2.1. ROCK SAMPLING (Map 2.7)

Composite rock chip samples were collected from 3-5 subsites, depending on the surface area of the outcrop. Visible oxidation surfaces and lichens were removed. The total number of rock samples was 140. To evaluate sample variability, 33 duplicate rock samples were collected. Sample weight varied from 1.0 to 1.5 kg.

2A.2.2. SAMPLING OF METALLURGICAL PROCESSING RESIDUES (Map 2.8)

Representative composite samples were collected from the different types of metallurgical processing residues. Sample weight varied from 1.0 to 1.5 kg.

Slag: chips were collected from 15-20 lumpy slag fragments for (a) determination of total element concentrations (n=21), and (b) for use in a five-step sequential extraction procedure (n=10).

Sand-blast wastes (n=8), *earthy material within slag* (n=7*), beneficiation/ flotation residues* (n=8), *pyrite tailings* (n=12) and *pyritiferous sand* (n=6): small scoops of each material were collected from 15-20 subsites.

2A.2.3. OVERBURDEN SAMPLING (Map 2.9)

Composite samples of overburden materials (n=224), including residual and alluvial soil, were collected from *house gardens* (n=138), *playgrounds and parks* (n=13), *school yards* (n=6), and *open space* (n=67).

A composite sample was collected from the surface layer down to a depth of 5 cm, after cleaning the surface debris, from 15-20 random subsites. To evaluate sample variability, 11 field duplicate overburden samples were collected. Sample weight varied from 1-1.5 kg.

2A.2.4. HOUSE-DUST SAMPLING (Map 2.10)

Pre-numbered plastic bags were given to each household, and the landlady was asked to place in it all dust swept for a period of 15-20 days. Households with a vacuum cleaner were asked to use a new bag, and to place the vacuum bag in the pre-numbered plastic bag. Sample weight varied from 0.1 to 0.25 kg. The total number of samples was 127.

2A.2.5. SAMPLING FOR PARTICLE-SIZE ANALYSIS STUDY (Map 2.11)

Representative samples for particle-size analysis were collected from the metallurgical processing wastes, *earthy material within slag* (n=4), *beneficiation/flotation residues* (n=3) and *pyritiferous tailings* (n=3), and residual soil (n=8), *sensu stricto*. In each case, a composite sample was collected from five random subsites. Sample weight, depending on the specific gravity of the material, varied from 2.7-6.8 kg.

2A.2.6. GROUNDWATER SAMPLING (Map 2.12)

Groundwater samples were collected from thirteen wells and two drill-holes (n=15). A bucket was used for the collection of groundwater from the wells. The pH was measured in the field with a graduated Merck paper. To evaluate sample variability, 3 duplicate groundwater samples were collected.

Groundwater samples were placed in clean one-litre plastic bottles, and kept in the refrigerator until despatch to the laboratory. All samples were carefully packed in plastic crates, encased in polystyrene blocks together with ice bags, and sent to the IGME Branch Laboratory of Eastern Macedonia and Thrace in Xanthi for analysis.

2A.2.7. SAMPLING FOR PARTICLE CHARACTERISATION STUDY (Map 2.13)

Representative samples were collected from metallurgical residues (n=21) for the particle characterisation study.

2A.2.8. OVERBURDEN DRILL-HOLE CORE SAMPLING (Map 2.14)

Twenty overburden drill-hole cores were sampled. The core was split in two halves and, after logging, each distinct layer was sampled by collecting a channel section over the total thickness of each layer. Sample weight varied from 1.0 to 1.5 kg. The total number of drill-hole core samples was 147.

2A.2.9. VERTICAL PROFILE OVERBURDEN SAMPLING (Map 2.14)

Two overburden vertical profiles were sampled. Each distinct layer was sampled by collecting a channel section over the total thickness of each layer. The total number of overburden vertical profile samples was 18. Sample weight varied from 1.0 to 1.5 kg.

2A.2.10. BIOMEDICAL SAMPLING (Map 2.15)

Blood and urine samples were collected from 255 Lavrion school-age children in March 1988 for the purposes of a cross-sectional epidemiological study. This was collaborative effort between the Institute of Hygiene and Occupational Medicine of the Technical University of Aachen in Germany, and the Institute of Hygiene of the University of Athens (Makropoulos *et al.*, 1991; Eikmann *et al.*, 1991). Biomedical information sheets, with details about the children that have taken part in this study, were provided, as well as the blood-lead (b-Pb) concentrations.

Biomedical sample sites were placed on the 1:5000 base map during field visits to Lavrion, by using the address information on the record sheets. From the 255 children only 235 live within the limits of the study area.

2A.2.11. SOIL SAMPLING FOR AGRONOMY STUDY (Map 2.16)

According to information provided, unemployed and untrained workers under the supervision of agronomists carried out soil or overburden sampling. Surface samples (0-10 cm) were collected by the workers and placed in pre-numbered plastic bags. The agronomists supervising the work noted the sample sites on aerial photographs at a scale of about 1:10000. These sites were transferred on to the 1:5000 base map used in the present study. The total number of samples collected was 583.

The Forest Research Institute in collaboration with the Municipality of Lavreotiki carried out this work in the autumn of 1992.

2A.3. SAMPLE PREPARATION

It is stressed that during sample preparation, all equipment used was thoroughly cleaned between samples.

2A.3.1. ROCK SAMPLES

Rock chip samples were crushed in a jaw crusher down to 2 mm, and following homogenisation a 50-gram sub-sample was pulverised in an agate mortar to 0.075-mm (200 mesh). Each sample was homogenised and placed in two 25-gram plastic vials.

2A.3.2. SAMPLES OF METALLURGICAL PROCESSING WASTES

Slag samples were first crushed in a jaw-crusher down to 2 mm, and following homogenisation, a sub-sample of 50-gram was pulverised in an agate mortar down to 0.075-mm (200 mesh). Each sample was homogenised and placed in two 25-gram plastic vials.

Sand-blast wastes are generally coarse-grained (<3 mm). Hence, they were first homogenised and a 50-gram sub-sample was pulverised in an agate mortar down to 0.075-mm (200 mesh). Each sample was homogenised and placed in two 25-gram plastic vials.

Samples of *pyrite tailings*, *pyritiferous sand*, *earthy material within slag* and *beneficiation/flotation residues* were first dried at room temperature, disaggregated in a porcelain mortar and sieved through a 0.177-mm (80-mesh) nylon screen. Each <0.177 mm sample was homogenised and placed in two 25-gram plastic vials.

In each case the coarse-grain material was placed in plastic bags and stored for reference.

2A.3.3. OVERBURDEN SAMPLES

Samples were dried at room temperature, and then disaggregated in a porcelain mortar. Afterwards they were sieved through a 2-mm (8-mesh) nylon screen, and pulverised in an agate mortar until all sample material passed through a 0.177-mm (80-mesh) nylon screen. Each sample was homogenised and placed in two 75-gram plastic vials.

2A.3.4. HOUSE-DUST SAMPLES

House-dust samples were generally very fine-grained. They were sieved through a 1-mm nylon screen, and pulverised in an agate mortar until all sample material passed through a 0.177-mm (80-mesh) nylon screen. Each sample was homogenised and placed in two 75-gram plastic vials.

2A.3.5. PARTICLE-SIZE ANALYSIS OF METALLURGICAL RESIDUES AND RESIDUAL SOIL

Samples of fine-grained metallurgical residues (earthy material within slag & beneficiation/flotation residues) and residual soil were first dried at room temperature. Dried samples were weighed and their weight recorded. Following disaggregation of samples in a porcelain mortar, the whole sample was sieved through the following nylon screens:

- <2 mm +1 mm
- <1 mm +0.5 mm
- <0.5 mm +0.25 mm

- <0.25 mm +0.125 mm
- <0.125 mm +0.063 mm
- <0.063 mm.

Each particle-grain size fraction was weighed, and the weight recorded (Map 9.1)

2A.3.6. GROUNDWATER SAMPLES

Groundwater samples immediately after sampling were placed in a refrigerator, and kept at a temperature of <10^{o}C prior to analysis.

2A.3.7. PARTICLE CHARACTERISATION SAMPLES

Sample preparation of these samples is described in Appendix Report 2 of Volume 1B of this study.

2A.3.8. OVERBURDEN DRILL-HOLE CORE SAMPLES

Overburden drill-hole core samples were dried at room temperature, and subsequently disaggregated in a porcelain mortar. Afterwards they were sieved through a 2-mm nylon screen, and following homogenisation, a 50-gram sub-sample was pulverised down to 0.075 mm (200 mesh) in an agate mortar. The ground sample was placed in a plastic bag, and the <2 mm samples were kept for reference.

2A.3.9. VERTICAL PROFILE OVERBURDEN SAMPLES

Vertical profile overburden samples were dried at room temperature, and subsequently disaggregated in a porcelain mortar. Afterwards they were sieved through a 2-mm nylon screen, and following homogenisation, a 50-gram sub-sample was pulverised down to 0.075 mm (200 mesh) in an agate mortar. The ground sample following homogenisation was placed in two 25-gram plastic vials. The remaining <2 mm sample was placed in a plastic bag and kept for reference.

2A.3.10. SOIL SAMPLES FOR AGRONOMY STUDY

Samples were dried at room temperature, and then disaggregated in a porcelain mortar. Afterwards they were sieved through a 2-mm (8-mesh) nylon screen, and a 25-gram aliquot pulverised in an agate mortar until all sample material passed through a 0.075-mm (200-mesh) nylon screen. The <2 mm and <0.075 mm portions of each sample were placed in plastic bags.

Blank back page
Λευκή οπίσθια σελίδα

Chapter 2B

ANALYTICAL METHODS

Alecos Demetriades
Institute of Geology and Mineral Exploration, 70 Messoghion Street, Gr-115 27, Athens, Greece

2B.1. INTRODUCTION

Project samples were analysed at different laboratories for a selected suite of elements. It is stressed that the complete suite of each sample type was analysed at the same laboratory, *i.e.*,

- at the geochemical laboratories of the British Geological Survey (BGS, Keyworth, Nottingham, U.K.) a suite of 50 overburden samples was analysed by X-ray fluorescence (XRF);
- at Imperial College of Science, Technology and Medicine (Environmental Geochemistry Research Group, Royal School of Mines, T.H. Huxley School of Environment, Earth Science & Engineering, University of London, U.K.) the overburden, house dust and metallurgical residues samples were analysed by a sequential extraction method and elements determined by ICP-AES; total element contents were determined on a selected suite of fifty overburden samples;
- at the regional laboratory of the Institute of Geology and Mineral Exploration of Eastern Macedonia and Thrace in Xanthi the rock samples were analysed by atomic absorption spectrometer (AAS) following digestion by different analytical methods; pH was determined on a sludge of soil and house dust, and the ground water samples analysed by different methods;
- at the central laboratory of the Institute of Geology and Mineral Exploration (IGME) in Athens, arsenic (As) was determined on overburden and house dust samples by ICP-AES following an aqua regia extraction;
- at the laboratory of the IGME Geochemistry Division in Athens total mercury was determined on soil and house dust samples;
- at OMAC Laboratories Ltd. (Athenry, Co. Loughrea, Ireland) samples of (a) metallurgical processing wastes, (b) drill-hole overburden core, (c) vertical profile overburden, and (d) particle-grain analysis were analysed by ICP-AES following an aqua regia extraction;
- at the Laboratory of Metallurgy, Department on Mining and Metallurgy, Technical University of Athens, the soil samples for the agronomy study were analysed.

2B.2. ANALYTICAL METHODS

2B.2.1. XRF ANALYTICAL METHOD

The details given below for the XRF analysis of the 50 Lavrion overburden samples were copied from a hand out given to the author by Dr. M.N. Ingham (BGS).

Instrument specifications: Two sequential, fully microprocessor controlled wavelength dispersive X-ray fluorescence spectrometers, each with a 216-position sample changer (Philips® PW1404/10 and PW1480/10 spectrometers with extended PW1500 sample changers). Both spectrometers have 100 kV (3kW) generators, and tube anodes used include tungsten (for all elements, except As, W, Bi, eq. Th), scandium and molybdenum (for As, W, Bi, eq. Th).
Computer Hardware: DEC® Micro VAX®2000, 6 Mbyte memory, 2 x 159 Mbyte Winchester® hard disks, and 90 Mbyte tape system.
Software: DEC® VMS operating system, Philips® X40 Version 3.0B XRF application package and in-house reformatting programs.
Sample preparation: The 50 samples were first pulverised in an agate mortar to <0.075-mm. A 12 g aliquot from each sample and 3 g of Elvacite® 2013 (Dupont® & Co's n-butyl methacrylate copolymer) are ground in agate for 45 minutes using a Fritsch® P5 planetary ball mill. The mixture is then pressed at 25 tons load into 40-mm diameter pellets.
Calibration: Analyte angles are calibrated using 1000 mg/kg single element standards in a silica matrix. Background factors where applicable are calculated by either angular difference (2 theta) or from mean values of 5 Specpure oxide blanks. Line-overlap factors are calculated from high concentration single element standards of the interfering analyte. Internal ratio is used for matrix corrections. Multi-element standards, both synthetic an natural (international an in-house reference materials), are measured with an analytical program and curves fitted using the de Jongh calibration algorithm, producing saved calibration constants (intercept, slope and alpha coefficient of the element upon itself). All backgrounds and peaks are drift corrected using an external ratio monitor. Drift correction intensities from the monitor are stored on hard disc and used to monitor instrumental stability and detect machine faults.
Routine analysis: Required elements are determined using the appropriate tube anode to obtain optimum detection limits and precision. Calibration intercepts are checked weekly and adjusted where necessary. Routine calibrations cater for rocks, soils, stream sediments, panned concentrates, tills and panned tills.
Routine elements determined: Ca, Ti, V, Cr, Mn, Fe, Co, Ni, Cu, Zn, Rb, Sr, Y, Zr, Nb, Mo, Ag, Sn, Sb, Ba, La, Ce, Pb, Th, U, As, W, Bi, eq. Th.

Lower limits of detection, tabulated in Table 2B.1, are theoretical values for the concentration equivalent to three standard deviations above the background count rate for the analyte in a silica matrix. No value is shown where background subtraction is used.

Table 2B.1. XRF lower limits of detection. Element concentrations were determined by a Philips® PW1404/10 XRF spectrometer. The slow program was used, *i.e.*, the analytical time was 68 minutes.
Πίνακας 2Β.1. Χαμηλότερα όρια ανίχνευσης της μεθόδου με φασματομετρία ακτίνων-Χ. Τα στοιχεία προσδιορίστηκαν με το φασματόμετρο ακτίνων-Χ της Philips® PW1404/10. Χρησιμοποίηθηκε το αργό πρόγραμμα για τον προσδιορισμό των στοιχείων, δηλ. ο αναλυτικός χρόνος ήταν 68 λεπτά.

Element	*Lower Limit of Detection (mg/kg or ppm)*	*Maximum Limit of Calibration (%)*	*Element*	*Lower Limit of Detection (mg/kg or ppm)*	*Maximum Limit of Calibration (%)*
Ag	1	1	Ni	1	1
As	2	1	Pb	3	1
Ba	4	69	Rb	1	1
Bi	1	0.25	Sb	2	1
Ca	-	40	Sn	1	1
Ce	6	20	Sr	1	1
Co	1	2	Th	1	1
Cr	1	25	Ti	-	40
Cu	1	1	U	1	1
Fe	-	70	V	1	2
La	2	2.5	W	1	1
Mn	-	25	Y	1	1
Mo	1	0.15	Zn	1	1
Nb	1	1	Zr	1	5

High instrument stability results in practical values for these materials approaching the theoretical. They may, however, be adversely affected to a considerable extent by line overlap and inter-element effects in other matrices and may not be reported to the precision shown in Table 2B.1.

Important comments: Lead and Zn values above 10000 ppm exceed the normal reporting limits of instrument calibration, which is up to 1%. Therefore, the results above 10000 ppm give the order of magnitude, and not precise values. The Y, Zr and W values are affected by inter element interferences, hence the results give again the order of magnitude. Finally, the given Th values were corrected by subtracting the equivalent Th (eq. Th).

2B.2.2. SEQUENTIAL EXTRACTION METHOD

The five-step sequential extraction procedure has appropriately been abstracted from Li (1993) and Li *et al.* (1995), since the method was developed during his doctorate study at the Environmental Geochemistry Group, Centre of Environmental Technology, Royal School of Mines, Imperial College of Science, Technology and Medicine, University of London, U.K.

Analar®-grade chemicals and deionised water (DIW, conductivity >1MΩ cm) were used throughout the analysis of the Lavrion samples. All pipettes, tubes and containers were washed with a detergent (Decon®), then soaked for 24 hours in 2% nitric acid (HNO_3) solution and rinsed repeatedly with DIW. International reference materials were selected, these included: MAG-1 (U.S. Geological Survey, U.S.A.); USGS); SO-1, SO2, SO3 and SO4 (Canadian Certified Reference Material Project, Canada; CCRMP); and BCR-141, BCR-142 and BCR-143 (Community Bureau of Reference, Belgium; BCR). Descriptions of these materials have been given by Potts *et al.* (1992). All the test materials were dried at 105ºC overnight before use. Reference materials, duplicates of samples and reagent blanks were distributed at random throughout the whole extraction procedure to make the most realistic assessments of data quality (Ramsey *et al.*, 1987).

2B.2.2.1. Sequential extraction steps

The sequential extraction scheme was developed from that of Tessier *et al.* (1979), and the same terminology is retained. Since, this is the method that has given results about the possible bioavailability of the elements and their extractability or leachability, it is described in detail.

Extraction was carried out progressively on an initial weight of 1.000 gram of test material. The extractants used and operationally defined chemical fractions are outlined below and illustrated in the flow chart of Fig. 2B.1:

Fraction 1: exchangeable (*exchangeable phase*) – sample extracted with 8 ml of 0.5*M* magnesium chloride ($MgCl_2$) at pH 7.0 for 20 minutes, with continuous agitation, at room temperature.
Fraction 2: bound to carbonate and specifically adsorbed (*carbonate phase*) – residue step (1) leached for 5 hours with 8 ml of 1*M* sodium acetate (NaOAc; adjusted to pH 5.0 with acetic acid, HOAc) at room temperature. Continuous agitation was maintained during the extraction.
Fraction 3: bound to Fe-Mn oxides (*reducible phase*) – residue from step (2) was extracted with 20 ml of 0.04*M* hydroxylammonium hydrochloride ($NH_2.OH.HCl$) in 25% (v/v) HOAc for 6 hours. The extraction was performed at 96ºC with occasional agitation. After extraction, the extract solutions were diluted to 20 ml with DIW and subjected to continuous agitation for 10 minutes.
Fraction 4: bound to organic matter and sulphide (*oxidisable phase*) – to the residue from step (3), 3 ml of 0.02*M* HNO_3 and 5 ml of 30% hydrogen peroxide (H_2O_2; adjusted to pH 2.0 with HNO_3) were added. The sample was heated progressively to 85ºC, and maintained at this temperature for 2 hours with occasional agitation. A second 3-ml aliquot of 30% H_2O_2 (adjusted to pH 2.0 with HNO_3) was then added, and the mixture was heated again at 85ºC for 3 hours with intermittent agitation. After cooling, 5 ml of

3.2*M* ammonium acetate (NH_4OAc) in 20% (v/v) HNO_3 were added, followed by dilution to a final volume of 20 ml with DIW. The tubes were then continuously agitated for 30 minutes.
Fraction 5: residual phase – residue from step (4) was digested with 4 ml concentrated HNO_3 (70% w/w), 3 ml perchloric acid ($HClO_4$, 60% w/w) and 15 ml hydrofluoric acid (HF, 40% w/w) to dryness using the following heating regime: 90°C for 6 hours, 120°C for 10 hours and 190°C for 6 hours. The remaining material was then taken up in 5 ml of 5*M* HCl at 70°C for 1 hour, and diluted to 25 ml with DIW.

Fig. 2B.1. The sequential chemical extraction procedure and the operationally defined geochemical phases used on the Lavrion overburden and house dust samples (from Li, 1993, Fig. 7.1, p.181).
Σχ. 2Β.1. Η μεθοδολογία της διαδοχικής εκχύλισης των στοιχείων και οι καθορισθείσες επιχειρησιακές γεωχημικές φάσεις, που χρησιμοποιήθηκε για την ανάλυση των δειγμάτων του επιφανειακού καλύμματος και της σκόνης σπιτιών από την αστική περιοχή του Λαυρίου.

Sample weight 1.0 g.

addition 8 ml 0.5M $MgCl_2$ (pH 7.0), continuous agitation for 20 minutes at room temperature

Centrifugation

Leachate 1

4 ml aliquot — Adsorbed fraction [***exchangeable phase***]

Residue 1

addition 8 ml 1M NaOAc (pH 5.0), continuous agitation for 5 hours at room temperature

Centrifugation

Leachate 2

1 ml aliquot — Carbonate and Specifically adsorbed fraction [***carbonate phase***]

Residue 2

addition 20 ml 0.04M $NH_2.OH.HCl$ in 25% (v/v) HOAc, intermittent agitation for 6 hours at 96°C. The leachate was diluted with 20 ml deionised water, continuous agitation for 10 minutes

Centrifugation

Leachate 3

15 ml aliquot — Fe-Mn oxide fraction [***reducible phase***]

Residue 3

addition

a) 5 ml 30% H_2O_2 (pH 2.0 with HNO_3) gradual heating to 85°C and maintaining this temperature for 2 hours, intermittent agitation.
b) 3 ml 30% H_2O_2 (pH 2.0 with HNO_3) and repeat heating of mixture at 85°C for 3 hours, intermittent agitation. Room temperature.
c) 5 ml 3.2M NH_4OAc in 20% (v/v) HNO_3 with dilution to 20 ml with deionised water, continuous agitation for 30 minutes.

Centrifugation

Leachate 4

15 ml aliquot — Organic/Sulphide fraction [***oxidisable fraction***]

Residue 4

addition 15 ml HF + 4 ml HNO_3 + 3 ml $HClO_4$ and heating to dryness: 90°C for 6 hours, 120°C for 10 hours and 190°C for 6 hrs. The residue dissolved with 5 ml 5M HCl at 70°C for 1 hour and dilution to 25 ml with deionised water.

Centrifugation

Leachate 5

Residual fraction (silicates, residual crystalline fraction. The refractory minerals may remain in the final residue) [***residual phase***]

Note: "Ac" denotes $C_2H_2O_2^-$ or CH_3COO^-.

The extractions (except the last HF-$HClO_4$-HNO_3 step) were conducted in 50-ml polysulphone centrifuge tubes (28.5x104 mm) with 24-mm polypropylene sealing caps (Nalgene®, Sybron International, Rochester, New York, U.S.A.). When continuous agitation was required, samples were shaken lengthwise on a mechanical shaker at 50 oscillations per minute with a stroke of 8 cm. Heating of the samples was operated using an aluminium-heating block. Following each extraction, the mixtures were centrifuged at 2000 rpm for 20 minutes at room temperature. An aliquot of the supernatant was decanted into clean glass test tubes using a Gilson® pipette. The aliquot used for each extraction step was 4, 1, 15 and 15 ml for steps (1), (2), (3) and (4), respectively. The remainder of the solution was discarded. Prior to the start of the next extraction step, samples were shaken with 8 ml of DIW for 5 minutes, and the wash solution was discarded after 20-minutes centrifuging. The final extraction step (HF-$HClO_4$-HNO_3 digestion) was carried out in large PTFE (PolyteTraFluoro-Ethylene) tubes (140x25 mm) after the residue had been transferred from the polysulphone tubes by repeated suspension of the residue in DIW using a vortex mixer, and subsequent decanting of the suspension.

Matrix adjustment and analysis of extraction solutions

In order to ensure uniform matrix for ICP-AES analysis, the different extraction matrices were digested with concentrated HNO_3. To the aliquots of extractant solutions from steps (1)-(4), 1 ml HNO_3 (concentrated, 70% w/w) was added, and then the solutions were heated to dryness on an aluminium heating block at 140°C. Care should be taken when heating the solution from extraction steps (3) and (4) because of violent reaction of HNO_3 with NH_2.OH.HCl or NH_4OAc may occur. After adding HNO_3, these extract solutions were left overnight on a heating block at 90°C, ant the temperature raised slowly to 140°C and heated to dryness. The residue in the tubes was then leached with 2 ml of 5 ml HCl, and made-up to final volume of 10 ml with DIW.

Multi-element analysis was performed by ICP-AES under the operating conditions given in Table 2B.2 (Ramsey and Thompson, 1987). The calibration scheme was based on that described by Thompson and Walsh (1989) with a matrix of 1*M* HCl and approximate matrix matching at 2000 μg g^{-1} Na in the trace-element calibration solutions. Calibration solutions were also run and at regular intervals throughout each batch and at the end of the analysis, to compensate for drift.

Twenty-two elements were determined Ag, Al, Ba, Be, Ca, Cd, Co, Cr, Cu, Fe, K, La, Li, Mn, Mo, Ni, P, Pb, Sr, Ti, V and Zn on the extractant solution of each of the five steps. Element detection limits for each step are tabulated in Table 2B.3.

For more details on the sequential extraction method, results of reference materials, *etc.* the reader is referred to the research work of Li (1993) and Li *et al.* (1995).

Table 2B.2. Instrumental operating conditions for the determination of elements in the solutions of the five-step sequential and total extraction methods at Imperial College of Science, Technology and Medicine, University of London, U.K.

Πίνακας 2Β.2. Συνθήκες λειτουργίας του οργάνου για τον προσδιορισμό των στοιχείων σε διαλύματα των πέντε σταδίων της διαδοχικής εκχύλισης και ολικής ανάλυσης στο Βασιλικό Κολλέγιο Επιστήμης, Τεχνολογιίας και Ιατρικής του Πανεπιστημίου του Λονδίνου, Ηνωμένο Βασίλειο.

ICP-AES instrument	Applied Research Laboratories®, ARL 34000C, 1-m vacuum polychrometer with PDP® 11/04 computer
Forward power	1.25 kW at 27 MHz
Reflected power	<10 W
Viewing height	4.0-mm square window centred 14 mm above the load coil
Torch	Fassel® type
Gas flow rate:	
Coolant	12.0 l min^{-1}
Auxiliary	0.4 l min^{-1}
Injector	l min^{-1}
Spray chamber	Scott® double-pass type
Nebuliser	Concentric glass (Meinhard® TR-30-3A)
Solution uptake rate	ml min-1 (unpumped)
Uptake tube	310 x 0.5-mm i.d. polyethylene
Nebuliser tip wash	0.5 ml of de-ionised water containing 1% v/v Photo-flo® between sample solutions
Pre-flush, integration time	20 s and 3 x 5 s

Table 2B.3. Instrument and *practical* detection limits of the five-step sequential extraction procedure and total extraction used at Imperial College of Science, Technology and Medicine for the analysis of Lavrion overburden/soil and house dust samples (values in ppm). Instrument detection limits for each element are quoted in the first row, and *practical detection limits* in the second row with *italic numbers* [see also Tables 2C.9A-2C.15A, Volume 1A, p.10-16].
Πίνακας 2Β.3. 'Ορια ανίχνευσης του οργάνου και *τα πρακτικά όρια* των πέντε σταδίων των διαδοχικών εκχυλίσεων και ολικών προσδιορισμών των μεθόδων που εφαρμόστηκαν στο Βασιλικό Κολλέγιο Επιστήμης, Τεχνολογίας και Ιατρικής για την ανάλυση των δειγμάτων του εδαφικού καλύμματος και της σκόνης σπιτιών από την αστική περιοχή του Λαυρίου (τιμές σε ppm). Τα όρια ανίχνευσης του κάθε στοιχείου γράφονται στην πρώτη γραμμή, και τα *πρακτικά όρια ανίχνευσης* στη δεύτερη γραμμή με *πλάγια γράμματα*. [βλ. επίσης Πίν. 2C.9A-2C.15A, Τόμος 1A, σελ. 10-16].

Element	*Step 1*	*Step 2*	*Step 3*	*Step 4*	*Step 5*	*Total*
Ag	0.04	0.16	0.064	0.02	0.38	0.42
	0.06	*0.17*	*0.064*	*0.05*	*0.38*	*0.50*
Al	1.00	8.00	24.50	13.70	0.90	29.20
	1.50	*6.53*	*24.54*	*13.69*	*0.90*	*253.04*
Ba	0.20	0.80	2.00	0.30	1.00	2.40
	0.23	*0.76*	*2.44*	*0.27*	*129.97*	*0.20*
Be	0.002	0.008	0.003	0.0014	0.005	0.01
	0.004	*0.022*	*0.012*	*0.0034*	*0.027*	*0.05*
Ca	1.00	3.10	0.67	0.67	1.25	3.62
	4.14	*3.14*	*425.32*	*11.33*	*585.48*	*196.23*
Cd	0.004	0.001	0.35	0.14	0.38	0.54
	0.004	*0.001*	*0.35*	*0.09*	*0.46*	*0.85*
Co	0.10	0.40	0.07	0.07	0.13	0.44
	0.06	*0.22*	*0.22*	*0.07*	*0.27*	*0.50*
Cr	0.20	0.80	1.00	0.133	1.00	1.64
	0.76	*0.61*	*0.44*	*0.004*	*1.17*	*1.92*
Cu	0.02	0.08	0.07	0.07	0.13	0.18
	0.07	*0.36*	*0.52*	*3.45*	*3.95*	*3.32*
Fe	0.80	1.60	0.27	0.27	0.50	1.90
	6.67	*9.71*	*124.59*	*22.28*	*715.11*	*923.20*
K	2.00	4.00	0.67	0.67	1.25	4.74
	4.96	*19.52*	*10.32*	*0.89*	*133.09*	*594.81*
La	0.10	0.40	0.50	0.07	1.39	1.54
	0.21	*0.71*	*0.15*	*0.07*	*1.40*	*0.88*
Li	0.040	0.16	0.07	0.02	0.13	0.22
	0.047	*0.16*	*0.12*	*0.04*	*0.82*	*0.65*
Mn	0.30	0.80	0.13	0.13	0.25	0.91
	0.63	*9.23*	*43.67*	*1.50*	*3.71*	*18.84*
Mo	0.20	0.80	0.13	0.13	0.25	0.88
	0.02	*0.51*	*0.33*	*0.06*	*0.63*	*0.54*
Ni	0.20	0.80	0.13	0.13	0.25	0.88
	0.12	*0.32*	*0.40*	*0.20*	*0.49*	*0.61*
P	0.40	0.20	0.67	0.20	1.25	1.50
	1.62	*2.74*	*4.00*	*0.12*	*17.10*	*35.55*
Pb	0.60	4.00	0.67	0.67	1.25	4.34
	1.72	*31.28*	*7.59*	*0.48*	*37.64*	*30.15*
Sr	0.14	0.21	0.74	0.12	0.76	1.10
	0.14	*0.21*	*0.74*	*0.12*	*0.75*	*3.31*
Ti	0.04	0.16	0.07	0.07	0.13	0.23
	0.06	*0.38*	*0.34*	*0.28*	*15.74*	*15.10*
V	0.10	0.40	0.07	0.07	0.13	0.44
	0.11	*0.22*	*0.04*	*0.17*	*4.15*	*0.81*
Zn	0.20	0.80	0.13	0.13	0.25	0.88
	0.10	*6.45*	*48.04*	*10.42*	*4.79*	*72.74*

2B.2.3. TOTAL EXTRACTION AND ELEMENT DETERMINATION BY ICP-AES

Total element contents were determined on 50 garden soil samples by the following analytical method at Imperial College of Science, Technology and Medicine:

1. Weigh 0.250 g (±0.001) of sample using the top-pan balance into a clean dry test tube;
2. Add 4.0 ml nitric acid (HNO_3) into each tube from an Oxford® dispenser;
3. Add 1.0 ml perchloric ($HClO_4$) acid into each tube from the dispenser;
4. Place tubes in the aluminium heating block and switch programmer to "manual" mode, set programmer as follows:
5. Turn on the fume cupboard and switch programmer to "auto";
6. The attack cycle is complete when the residue in each tube is dry;
7. Transfer tubes to the stainless steel racks and when cool, add 2.0 ml 5 M hydrochloric acid (HCl) to each tube from an Oxford® dispenser and heat at 60°C for 1 hour;
8. Transfer tubes to wire racks and allow to cool;
9. Add 8.0 ml of deionised water from an Oxford® dispenser and thoroughly mix the solution in each tube using a vortex mixer;
10. Decant into polystyrene tubes and cap. If necessary, centrifuge at 2,000 rpm for 2 minutes;
11. Chemical analysis for trace elements using ICP-AES according to instrumental conditions outlined in Table 2B.2.

Twenty-two elements were determined Ag, Al, Ba, Be, Ca, Cd, Co, Cr, Cu, Fe, K, La, Li, Mn, Mo, Ni, P, Pb, Sr, Ti, V and Zn on the extractant solution. Element detection limits are tabulated in Table 2B.3, and Tables 2C.17 to 2C.21.

2B.2.4. AQUA REGIA EXTRACTION AND ELEMENT DETERMINATION BY AAS

Lavrion house garden "soil", open space "soil" and house dust samples were subjected to the following analytical method for the determination of As by ICP-AES (Jobyn Yvon®, model 80) at the IGME Central Laboratory in Athens. Rock samples were also treated by this method, at the IGME branch Laboratory of Eastern Macedonia and Thrace, for the determination of trace elements (Ba, Cd, Co, Cr, Cu, Li, Mn, Mo, Ni, Pb, Sr, V, Zn) by AAS. The detection limit of the analytical method for the determination of As by ICP-AES is 2 ppm, whereas the detection limits for the determination by AAS of Cd, Co, Cr, Cu, Li, Mn, Mo, Ni, Pb, Sr, V & Zn is 1 ppm, and that of Ag, Ba and Mn is 0.1, 10 and 5 ppm respectively.

An outline of the analytical method is given below (K. Leonis, IGME, pers. commun., 1992):

1. Weigh 2.5 g of sample material and transfer to a high type beaker of 150 ml capacity;
2. Add 20 ml of aqua regia;
3. The beakers with the sample solutions are placed on thermostatically controlled plates, which are inside fume cupboards;
4. Heat under fume cupboard for 45 minutes; samples are stirred intermittently with a glass rod to assist dissolution;
5. Evaporate to near dryness;
6. Add 2 ml of concentrated HCl dropwise on the whole sample surface and evaporate to near dryness;
7. Repeat addition of 2 ml of concentrated HCl and evaporate to near dryness;
8. Allow samples to cool to room temperature;
9. Add 2 ml of concentrated HCl and 2 ml of concentrated H_2O_2 very carefully and under the fume cupboard;
10. Add 25 ml of deionised H_2O;
11. Transfer the contents of the beaker into a volumetric cylinder by washing with deionised H_2O, and add water up to the 50 ml mark;
12. Leave over night for settling or filter;
13. The supernatant solution is aspirated through an atomic absorption spectrophotometer or an inductively coupled plasma spectrophotometer and the required elements determined.

According to IGME chemists the above analytical method is able to bring into solution the geochemically significant portion of the most important elements in an AAS compatible solution, together with small variable amounts of some of the base metals locked in the crystal lattice. The method extracts approximately 85-95% of element contents present in geological materials.

2B.2.5. DETERMINATION OF TOTAL ELEMENT CONTENTS IN ROCK SAMPLES

Total element contents in rock samples were determined at the IGME Branch Laboratory of Eastern Macedonia and Thrace in Xanthi by different analytical digestion methods. An outline of the methods is given below (G. Katsanopoulos and G. Grigoriades, pers. commun., 1998):-

1. **Determination of SiO_2, Al_2O_3, Fe_2O_3, CaO & MgO:** fusion of 0.1 g sample aliquot with a mixture of borax ($Na_2B_4O_7.10H_2O$) and carbonate (K_2CO_3-Na_2CO_3) and uptake with 200 ml of 5% hydrochloric acid (HCl), or 500 ml for SiO_2. Detection limits for SiO_2, Al_2O_3, Fe_2O_3, CaO & MgO are 0.01% for both oxides.
2. **Determination of K_2O and Na_2O:** Hot digestion of 0.1 g sample aliquot with HCl-HF acid, and uptake with 100 ml of 5% hydrochloric acid (HCl). Detection limits for K_2O & Na_2O are 0.01% for both oxides.
3. **Determination of TiO_2:** Hot digestion of 0.2 g sample aliquot with HCl-HNO_3-HF and uptake with 50 ml of 5% hydrochloric acid (HCl). Detection limit for TiO_2 is 0.01%.
4. **Determination of P_2O_5:** Hot digestion of 0.1 g sample aliquot with $HClO_4$-HNO_3, and uptake with 50 ml of deionised water. Addition of ammonium vanadiomolybdate {*i.e.*, ammonium heptamolybdate tetrahydrate [$(NH_4)_6Mo_7O_{24}.4H_2O$] and ammonium monovanadate (NH_4VO_3)} for the development of colour and measurement with an UV-VIS spectrometer (Varian® 634). Detection limit is 0.01% P_2O_5.
5. **Determination of Ag:** 0.5 g of sample weight heated to a temperature of 640ºC, and decomposition with HCl-HNO_3-HF, and uptake by 50 ml with 4:1 HCl:HNO_3 acid. Detection limit for Ag is 0.1 ppm.
6. **Determination of As & Sb:** Hot digestion of 1-g sample aliquot with HCl-HNO_3-HF, and uptake with 100 ml 5% HCl. Detection limit is 0.1% As and 0.01% Sb.
7. **Determination of Li:** Hot digestion of 0.1 g sample aliquot with $HClO_4$-HNO_3-HF, and uptake with 20 ml of 5% HCl. Detection limit is 1 ppm Li.
8. **Determination of Ba, Cd, Co, Cr, Cu, Mn, Mo, Ni, Pb, Sr, V & Zn:** for details refer to the section (above): *"Aqua regia extraction and element determination by AAS"*. The detection limit for all elements was 1 ppm, except Ba 10 ppm and Mn 5 ppm. It is noted that this is a *"near-total"* method. According to IGME chemists, it generally releases 85-95% of trace element contents present in geological samples.
9. **Loss on ignition (LOI):** 1-g sample aliquot was heated at 1000ºC in an oven for 1 hour and the loss in weight measured.

2B.2.6. DETERMINATION OF TOTAL MERCURY

Total Hg contents were measured with a flameless HGG-3 Hg-atomic absorption spectrometer manufactured by Scintrex® (Concord, Ontario, Canada). Technical details of the instrument have already been described by Robbins (1973), and a detailed description of the analytical method is given by Pöppelbaum and Van den Boom (1980a, b).

A 0.1-g aliquot of the sample is accurately weighed in an aluminium boat. The aluminium boat with the sample is subsequently placed in a quartz-glass tube, which fits in an openable small tube furnace. The temperature in the quartz-glass tube is measured with a Ni-Cr/Ni thermocouple. The operation temperature is 700ºC.

The mercury in the sample is vaporised by rapid and strong heating of the substance. The vapour is introduced into the analytical chamber of the spectrometer in a nitrogen gas flow, and the mercury content of the vapour phase can be directly measured.

The lower and upper detection limits of the method are 2.5 and 700 ppb Hg. Analytical precision and variability are monitored continuously by internal reference materials, which are analysed every tenth sample.

2B.2.7. DETERMINATION OF AQUA REGIA EXTRACTABLE ELEMENTS BY ICP-AES

At OMAC Laboratories Ltd. (Athenry, Co. Loughrea, Ireland) samples of (a) metallurgical processing wastes, (b) borehole overburden core, and (c) vertical profile overburden were digested differently from the samples of particle-grain analysis, due to the coarseness of the latter. Element determinations were made, in both cases, with an ICP-AES, Perkin-Elmer Optima 3000 DV. Details of the analytical methods used were supplied by M.J. O'Neill (pers. commun., 1998).

The Perkin-Elmer Optima 3000 DV ICP-AES is a dual view instrument permitting simultaneous radial and axial viewing of the plasma, the axial mode being used to give increased sensitivity for some elements. Spectral interferences are quantified and corrected for, by running a suite of 6 specially formulated interference standards. These are run at the beginning and end of each batch. In-house standards and blanks are run with each batch of up to 50 samples. Repeated analysis is performed on 10% of samples through the whole procedure.

Element detection limits are given in Table 2B.4.

Table 2B.4. Lower detection limits for the elements determined by ICP-AES following an aqua regia extraction at OMAC Laboratories Ltd.
Πίνακας 2B.4. Τα χαμηλότερα όρια ανίχνευσης των στοιχείων που προσδιορίστηκαν με ICP-AES μετά από εκχύλιση με βασιλικό νερό στα εργαστήρια της OMAC.

Element	*Lower Limit of Detection (mg/kg or ppm)*	*Element*	*Lower Limit of Detection (mg/kg or ppm)*	*Element*	*Lower Limit of Detection (mg/kg or ppm)*
Ag	0.5	Hg	1	Sc	1
Al	100	In	2	Se	10
As	5	K	100	Sn	5
B	5	La	2	Sr	2
Ba	2	Li	2	Ta	2
Be	1	Mg	5	Te	5
Bi	5	Mn	5	Th	5
Ca	100	Mo	1	Ti	10
Cd	1	Na	100	U	5
Ce	1	Nb	5	V	2
Co	1	Ni	1	W	5
Cr	1	P	100	Y	1
Cu	1	Pb	1	Zn	1
Fe	100	Rb	50	Zr	1
Ga	5	S	100		
Ge	2	Sb	5		

2B.2.7.1. Digestion of Samples of Metallurgical Processing Wastes, Drill-hole Overburden and Vertical Profile

The following analytical procedure was used:

- 0.2 g ± 0.005 g is weighed into 50 ml Erlenmeyer® flask;
- 4 ml of concentrated Aqua Regia (3:1:2 HCl-HNO_3-H_2O);
- samples covered with watchglass and heated at 95°C for one hour;
- cooled and diluted to 10 ml with distilled water;
- determination by ICP-AES of elements: Ag, Al, As, B, Ba, Be, Bi, Ca, Cd, Ce, Co, Cr, Cu, Fe, Ga, Ge, Hg, In, K, La, Li, Mg, Mn, Mo, Na, Nb, Ni, P, Pb, Rb, S, Sb, Sc, Se, Sn, Sr, Ta, Te, Th, Ti, U, V, W, Y, Zn, Zr.

It is noted that the aqua regia leach is partial for Mn, Fe, Sr, Ca, P, La, Cr, Mg, Ba, Ti, B, W and limited for Na, K and Al.

2B.2.7.2. Digestion of Particle-size Analysis Samples

A larger sample weight was used for the analysis of particle-size analysis samples, because of their coarse-grained nature, *i.e.*, samples were analysed at their natural state without grinding: <2-1 mm, <1-0.5 mm, <0.5-0.25 mm, <0.25-0.125, <0.125-0.063 mm, <0.063 mm.

The following analytical procedure was used:

- 2.00 g ± 0.005 g is weighed into 100 ml Erlenmeyer® flask;
- 20 ml of concentrated Aqua Regia (3:1:2 HCl-HNO_3-H_2O);
- samples covered with watchglass, brought to boil and then simmered for 45 minutes;
- cooled and made up to 100 ml with distilled water;
- samples diluted 1 to 3 with 10% Aqua Regia containing 1000 µg/ml Cs and 1000 µg/ml Triton® (non-ionic surfactant);
- determination by ICP-AES of elements: Ag, Al, As, B, Ba, Be, Bi, Ca, Cd, Ce, Co, Cr, Cu, Fe, Ga, Ge, Hg, In, K, La, Li, Mg, Mn, Mo, Na, Nb, Ni, P, Pb, Rb, S, Sb, Sc, Se, Sn, Sr, Ta, Te, Th, Ti, U, V, W, Y, Zn, Zr.

2B.2.8. DETERMINATION OF pH ON OVERBURDEN AND HOUSE DUST SLUDGE

The following method, used by the Environmental Geochemistry Research Group at Imperial College of Science, Technology and Medicine (M.H. Ramsey, pers. commun.), was used by the IGME Eastern Macedonia and Thrace Branch at Xanthi to determine pH on the sludge of loose overburden materials and house dust:

- Weigh out 4.00 g of soil (air dried) into a disposable 15 ml centrifuge tube;
- Add 5.00 ml of high purity water using an autopipette. Cap and shake to disperse the soil in the water.
- Add a second 5.00 ml of water, cap and place on a shaking machine for 15 minutes;
- Calibrate a pH electrode using buffers at pH 4, 7 and 9, being careful to rinse off these solutions with water between measurements;
- Insert the pH electrode into the soil suspension until a stable reading of pH is achieved (to the nearest 0.1 pH units);
- Check calibration of the electrode after ten samples.

2B.2.9. GROUND WATER ANALYSIS

A number of methods were used for the analysis of the ground water samples, *i.e.*,

- Ca, Mg and Cl were determined by a volumetric method;
- Na and K by AAS;
- NO_2, SO_4, NO_3 and NH_4 by spectrophotometric colorimetry;
- Cd, Cr, Cu, Fe, Mn, Ni, Pb and Zn by AAS;
- hardness by a volumetric method, and
- pH and conductivity were measured by appropriate instruments.

Detection limits of variables determined on ground water samples are given in Table 2B.5.

Table 2B.5. Lower detection limits for the variables determined by different analytical methods on ground water samples at the Eastern Macedonia and Thrace Branch Laboratory of IGME.
Πίνακας 2B.5. Τα χαμηλότερα όρια ανίχνευσης των παραμέτρων που προσδιορίστηκαν με διαφορετικές αναλυτικές μεθόδους στο Εργαστήριο του Παραρτήματος Ανατολικής Μακεδονίας και Θράκης του ΙΓΜΕ.

Cation Radical	*Lower Limit of Detection (mg/l or ppm)*	*Element*	*Lower Limit of Detection (μg/l or ppb)*	*Pollution Indices*	*Lower Limit of Detection (mg/l or ppm)*
Ca^{2+}	0.1	Cd	1	NO_2^-	0.001
Mg^{2+}	0.1	Cr	10	NH_4^+	0.001
Na^+	0.1	Cu	10	O_2	0.100
K^+	0.1	Fe	1	*Hardness*	*°f*
HCO_3^-	0.1	Mn	1		
Cl^-	0.2	Ni	10	Temporary	1.0
SO_4^{2-}	0.1	Pb	10	Permanent	1.0
NO_3^-	0.3	Zn	10	Total	1.0

2B.2.10. COLD EDTA EXTRACTION AND ELEMENT DETERMINATION BY AAS

The 583 soil/overburden samples collected for the agronomic study were analysed by the following method at the Laboratory of Metallurgy, Department of Mining and Metallurgical Engineering, of the National Technical University of Athens.

1. Weigh out 10 grams of soil into a 300 ml conical flask;
2. Add 100 ml of extractant solution [1*M* CH_3COONH_4 + 0.02*M* EDTA, pH 7.0];
3. Agitate mixture for 60 minutes with a horizontal type mechanical shaker at 100 movements/minute;
4. Pass mixture through a Schleicher & Schuel® (Ref. No 300111) filter, and
5. Determine Pb, Zn and Cd with a double beam atomic absorption spectrometer.

Blank back page
Λευκή οπίσθια σελίδα

Chapter 2C

ANALYTICAL AND SAMPLING VARIANCE

Alecos Demetriades
Institute of Geology and Mineral Exploration, 70 Messoghion Street, Gr-115 27, Athens, Greece

2C.1. INTRODUCTION

Routine quality control procedures of geochemical surveys have long been developed (Miesch, 1964, 1967, 1973, 1976; Garrett, 1969, 1973, 1983; Howarth and Lowestein, 1971; Bølviken and Sinding-Larsen, 1973; Thompson and Howarth, 1976, 1978, 1980; Plant *et al.*, 1975; Howarth and Thompson, 1976; Garrett and Goss, 1978; Garrett *et al.*, 1980; Fletcher, 1981; Sinclair, 1983; Reimann, 1989; Thompson and Maguire, 1993; Brandvold and McLemore, 1998). They are based on random submission of all samples, insertion of control reference samples, blind duplicates of project samples and field duplicate samples, and the use of analysis of variance (ANOVA) techniques to estimate sampling, analytical and data or geochemical variance. It is customary in geochemical surveys to use 10% of all samples for quality control purposes. This was not always possible in the sampling of different sample media in Lavrion. Hence, different statistical quality control procedures were used depending on available data. The techniques used are described below. It is noted that Tables 2C1.A to 2C.16A will be found in Appendix 1A of Volume 1A (p.1-17).

2C.2. QUALITY CONTROL STATISTICAL PROCEDURES

Garrett (1969, 1973, 1983) proposed a method to estimate the combined sampling and analytical variance (the technical variance of Ramsey *et al.*, 1992), and overall data variance (the geochemical variance) by the collection and analysis of field duplicate samples. An ANOVA model was suggested to determine the required statistical parameters. He pointed out that it is of utmost importance that sampling and analytical errors be significantly smaller than the overall data variability in order to adequately identify geochemical or spatial data variation. In this case the *F*-test is used to estimate the significance of random errors introduced by field sampling, sample preparation and analysis. According to Garrett (1969), the sampling and analytical variance (the technical variance) should not contribute more than 25% to the total variance. Garrett's method was used to estimate the quality control parameters of overburden samples, analysed by the sequential extraction and total analytical methods (Tables 2C.1A-.16A, Appendix 1A, Volume 1A, p.2-17). No duplicate field samples were collected during the house dust survey and, therefore, the analytical precision could only be estimated by replicate analysis.

Ramsey *et al.* (1992) and Ramsey (1993) considering the significance of estimating both random and systematic errors in analytical measurements for environmental studies, proposed the use of a more robust procedure, the Sampling and Analytical Quality Control (SAX) technique. This requires again the collection of random field sample duplicates. The two field control samples, routine and duplicate, are split in two and are randomly analysed in the batches. Hence, for each field control sample, routine and duplicate, there are two determinations for each element. Robust analysis of

variance, instead of the classical ANOVA technique, is used to separate analytical and sampling errors from "true" geochemical variation in the study area. This method was employed for estimation of quality control parameters of the rock geochemical survey (Table 2C.8A, Appendix 1A, Volume 1A, p.9).

The combined sampling and analytical variance (the technical variance), according to Ramsey *et al.* (1992) and Ramsey (1993), should not exceed the upper limit of 20% of the total variance. An upper limit for analytical variance is set at 4% of the total variance. Hence, the sampling variance should not exceed the upper limit of 16% of the total variance. It is significant, as pointed by all researchers in this field, for the greatest part of the variance to be ascribed to the geochemical data variance or geochemical (spatial) variation, otherwise a contoured geochemical distribution map cannot be produced (Garrett, 1969; Howarth, 1983; Sharp, 1987). In the latter case, where geochemical data show no spatial persistence, element concentrations may be plotted at the sample sites as variable-size dots (Bølviken *et al.*, 1986; Björklund and Gustavsson, 1987; Lahermo *et al.*, 1990), symbols (De Vos *et al.*, 1996), Exploratory Data Analysis symbols (Englund and Sparks, 1988; O'Connor *et al.*, 1988; Demetriades, 1990), or recording on maps the sample site analytical data (Van der Sluys *et al.*, 1997). However, final decisions about geochemical distribution map plotting may be decided upon, following a thorough geostatistical structural analysis of the data (Davis, 1973; Miesch, 1975; Howarth, 1983; Reimann, 1998; refer to Chapter 2D, this report).

Ramsey *et al.* (1992) and Ramsey (1993) stressed that, application of ANOVA and SAX techniques to environmental surveys, is particularly appropriate due to the high degree of heterogeneity often associated with anthropogenic contamination of the environment. They suggested the graphical display of data quality parameters in the form of a pie chart (Fig. 2C.1). Visual representation of variance on all element distribution maps, gives the reader direct access to significant information about the quality and reliability of geochemical data (Maps 3.1, 3.8-3.13, 3.15-3.20, 4.2-4.30, 6.1-6.30).

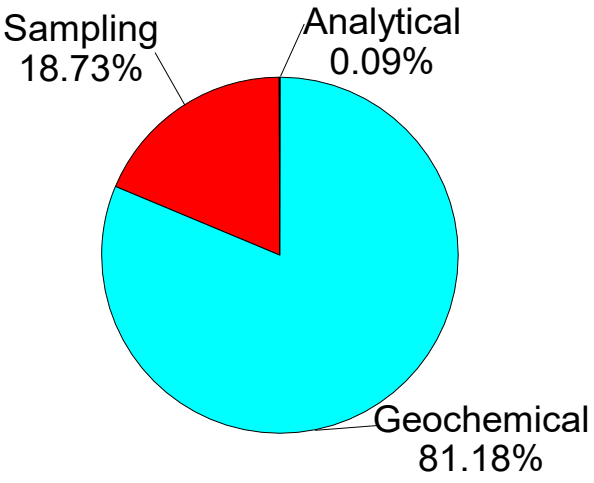

Fig. 2C.1. Proportions of variance contributed by measurement processes of sampling and analysis for Pb in overburden samples of the Lavrion urban area. For geochemical information to be reliable the maximum analytical and sampling variance should be <4% and <16% respectively. The pie chart shows total Pb data to be within the specifications.
Σχ. 2C.1. Ποσοστά της διασποράς που οφείλονται στις διεργασίες μετρήσεων της δειγματοληψίας και ανάλυσης του Pb σε δείγματα εδαφικού καλύμματος της αστικής περιοχής του Λαυρίου. Η πίττα δείχνει ότι τα δεδομένου του Pb είναι μέσα στα προδιαγεγραμμένα όρια.

In the case of only analytical control samples, a simple analysis of variance, fitted regression line and notched-box-and-whisker plots may be employed to study analytical variation of routine and replicate analyses (Figs. 2C.2-3). These procedures were used to process analytical quality control data on samples of house dust, metallurgical processing wastes, drill-hole and particle-size fractions. Examples from the drill-hole analytical data will only be discussed.

Apart from the estimation of sampling, analytical and geochemical variability, it is possible to estimate practical detection limits for each element, and the precision for each individual element for every sample (Thompson and Howarth, 1976; Fletcher, 1981). For estimation of precision the method proposed by Thompson and Howarth (1978) was modified in order to determine the linear regression equation by the reduced major axis method (Till, 1974; Demetriades and Vassiliades, 1998). A software programme, DEPRECIS, was developed for this purpose by Evripides Vassiliades, under the instructions of the author of this study, to estimate all quality control parameters (Tables 2C.9A-.16A in App. 1A, Vol. 1A, p.10-17) (E. Vassiliades, in preparation).

It is again noted that Tables 2C.1A to 2C.16A are in Appendix 1A of Volume 1A (p.1-17) of this report.

2C.2.1. Analysis of Variance on Quality Control Data of Sequential Extraction and Total Element Contents in Overburden Samples

Analysis of variance (ANOVA) for estimation of analytical, sampling and geochemical variation for

(a) each step of the sequential extraction procedure,
(b) the combined data of steps 1 and 2 (exchangeable and carbonate phases), and
(c) total element contents

was carried out on 11 field duplicate overburden samples, and 31 analytical replicate samples. The results are tabulated in Tables 2C.1A to 2C.7A with statistical explanations, and the apportionment of variance displayed on element distribution maps in the form of a pie chart (Maps 3.1, 3.8-3.13, 3.15-3.20, 4.2-4.30, 6.1-6.30, Volume 2 of this report). Since, geochemical data are positively skewed (Ahrens, 1954a, b; Tennant and White, 1959; Sinclair, 1976; Miesch, 1977), all data sets were transformed to logarithms base 10.

The critical F-value at the 95th confidence level for 11 and 10 degrees of freedom is 2.94. For geochemical map plotting, calculated F-ratios of the geochemical variance over the combined sampling and analytical variance should exceed the critical F-value.

2C.2.1.1. Analysis of Variance on Exchangeable Phase Results [Step 1]

(Table 2C.1A, Appendix 1A, Volume 1A, p.2)

ANOVA results for exchangeable phase sampling and analytical control data have shown that the overall data or geochemical variance (variation between sample sites) is significantly larger than the combined sampling and analytical variance (within-site variability) for the majority of elements. For Ag, Be, Cr, K, La and Mo, however, the combined sampling and analytical variance is less than the critical value of F at the 95th confidence level and, therefore, geochemical distribution maps cannot be plotted for

these elements. Further, the analytical variance for elements Co, Li, and V is high, suggesting poor analytical sensitivity, meaning that again no distribution maps can be plotted.

2C.2.1.2. Analysis of Variance on Carbonate Phase Results [Step 2] (Table 2C.2A)

ANOVA results for carbonate phase sampling and analytical control data have shown that the overall data or geochemical variance (variation between sample sites) is significantly larger than the combined sampling and analytical variance (within-site variability) for the majority of elements. For Be, Cr, Cu, K, Mo and Ti, however, the combined sampling and analytical variance is less than the critical value of F at the 95th confidence level and, therefore, geochemical distribution maps cannot be plotted for these elements. Further, the analytical variance for Ag is high, suggesting poor analytical sensitivity, meaning that again no distribution map can be plotted.

2C.2.1.3. Analysis of Variance on Reducible Phase Results [Step 3] (Table 2C.3A)

ANOVA results for reducible phase sampling and analytical control data have shown that the overall data or geochemical variance (variation between sample sites) is significantly larger than the combined sampling and analytical variance (within-site variability) for the majority of elements. For Mo, however, the combined sampling and analytical variance is less than the critical value of F at the 95th confidence level and, therefore, a geochemical distribution map cannot be plotted for this element. Further, the analytical variance for elements Ag, Li and Ti is high, suggesting poor analytical sensitivity, meaning that again no distribution maps can be plotted.

2C.2.1.4. Analysis of Variance on Oxidisable Phase Results [Step 4] (Table 2C.4A)

ANOVA results for oxidisable phase sampling and analytical control data have shown that the overall data or geochemical variance (variation between sample sites) is significantly larger than the combined sampling and analytical variance (within-site variability) for the majority of elements. For Mo, however, the combined sampling and analytical variance is less than the critical value of F at the 95th confidence level and, therefore, a geochemical distribution map cannot be plotted for this element.

2C.2.1.5. Analysis of Variance on Residual Phase Results [Step 5] (Table 2C.5A)

ANOVA results for exchangeable phase sampling and analytical control data have shown that the overall data or geochemical variance (variation between sample sites) is significantly larger than the combined sampling and analytical variance (within-site variability) for the majority of elements. For Mo, however, the combined sampling and analytical variance is less than the critical value of F at the 95th confidence level and, therefore, a geochemical distribution map cannot be plotted for this element.

2C.2.1.6. Analysis of Variance on the Combined Exchangeable and Carbonate Phase Results [Steps 1 & 2] (Table 2C.6A, Appendix 1A, Volume 1A, p.7)

ANOVA results for the combined exchangeable and carbonate phase sampling and analytical control data have shown that the overall data or geochemical variance (variation between sample sites) is significantly larger than the combined sampling and analytical variance (within-site variability) for the majority of elements. For Be, Cr, Cu, K, Mo and V, however, the combined sampling and analytical variance is less than the

critical value of F at the 95th confidence level and, therefore, geochemical distribution maps cannot be plotted for these elements. Further, the analytical variance for elements Ag and Li is high, suggesting poor analytical sensitivity, meaning that again no distribution maps can be plotted.

2C.2.1.7. Analysis of Variance on Total Element Concentrations (Table 2C.7A)

ANOVA results for the "total" sampling and analytical control data have shown that the overall data or geochemical variance (variation between sample sites) is significantly larger than the combined sampling and analytical variance (within-site variability) for the majority of elements. For Mo, however, the combined sampling and analytical variance is less than the critical value of F at the 95th confidence level and, therefore, a geochemical distribution map cannot be plotted for this element.

2C.2.2. Classical and Robust Analysis of Variance on Quality Control Data of Rock Samples (Table 2C.8A, Appendix 1A, Volume 1A, p.9)

Classical and robust analysis of variance parameters on the results of 33 replicated rock samples were estimated with the program ROBCOOP4, provided by M.H. Ramsey (Ramsey *et al.*, 1992; Ramsey 1993). Results are tabulated in Table 2C.8A. The analytical variance, estimated by both classical and robust analysis of variance, is low for all elements, except Ag, which has a high analytical variance by classical, but not robust, statistics. Robust statistics show that the analytical variance for elements is low, meaning that the analytical method is suitable for the determination of these elements on rock samples. The sampling variance (>16% of the total variance) is contributing the greatest error to the technical variance, *i.e.*, the sampling and analytical variance, for the following elements:

- Ba, Cu, Li, Mn, Pb, Ti and V for both classical and robust analysis of variance;
- Co, Cr, Fe, K, Ni and Sr for classical analysis of variance only, and
- Ag and Zn for robust analysis of variance only.

Elements having values of geochemical variability exceeding the limit of 80% of the total variance are:

- Al, Ca, Fe, Ni, P, and Ti for both classical and robust analysis of variance,
- Co, Cr, K, and Sr for robust analysis variance, and
- Zn for classical analysis of variance.

Generally, robust analysis of variance values for geochemical variability are higher than those corresponding to classical analysis of variance.

According to Ramsey *et al.* (1992) and Ramsey (1993) robust analysis of variance estimates are affected less by outlying values, as indicated by the above discussion. Aluminium, Ca, Co, Cr, Fe, K, Ni, P, Sr and Ti have robust estimates of geochemical variability exceeding the limiting value of 80% of the total variance, meaning that rock geochemical distribution maps can be plotted. Although robust estimates of geochemical variability are less than 80% of the total variance for elements Ba, Cd, Cu, Li, Mn, Pb, V and Zn, it was decided to plot their geochemical distribution maps, in order to have even a crude visual representation of the baseline situation.

2C.2.3. ANALYTICAL QUALITY CONTROL

Analytical quality control was monitored by repeat analysis of routine samples and by internal reference materials for all sample types, and especially those without field replicates, such as house dust, metallurgical processing wastes, drill-hole and particle-size analysis. The procedures used on the raw analytical data were one-way analysis of variance, linear regression analysis and notched-box-and-whisker (Figs. 2C.2-.3), performed with Statgraphics® plus software (Manugistics, 1995). Examples from the drill-hole analytical data will be used to show the different procedures. In this case, 34 drill-hole samples were reanalysed for quality control purposes.

2C.2.3.1. One-way Analysis of Variance

One-way analysis of variance compares the mean values of the routine and replicate analyses of 34 drill-hole samples. Tables 2C.1 to 4 tabulate one-way analysis results for As, Cd, Pb and Zn.

Table 2C.1. One-way analysis of variance of routine and replicate analyses of As in overburden samples from drill-holes.
Πίνακας 2C.1. Ανάλυση διασποράς ενός παράγοντα των αναλύσεων ρουτίνας και επαναληπτικών του As σε δείγματα του εδαφικού καλύμματος από γεωτρήσεις.

Source	*Sum of squares*	*Degrees of freedom*	*Mean square*	*F-ratio*	*p-value*
Model	2.52915×10^{-9}	1	2.529115×10^{-9}	68895.94	0.0000
Residual	1.17471×10^{-6}	32	36709.7		
Total (corr.)	2.53032×10^{-9}	33			

Table 2C.2. One-way analysis of variance of routine and replicate analyses of Cd in overburden samples from drill-holes (n=34 pairs).
Πίνακας 2C.2. Ανάλυση διασποράς ενός παράγοντα των αναλύσεων ρουτίνας και επαναληπτικών του Cd σε δείγματα του εδαφικού καλύμματος από γεωτρήσεις (n=34 ζεύγη).

Source	*Sum of squares*	*Degrees of freedom*	*Mean square*	*F-ratio*	*p-value*
Model	1.19367×10^{-6}	1	1.19367×10^{-6}	39481.57	0.0000
Residual	967.471	32	30.2335		
Total (corr.)	1.19463×10^{-6}	33			

Table 2C.3. One-way analysis of variance of routine and replicate analyses of Pb in overburden samples from drill-holes (n=34 pairs).
Πίνακας 2C.3. Ανάλυση διασποράς ενός παράγοντα των αναλύσεων ρουτίνας και επαναληπτικών του Pb σε δείγματα του εδαφικού καλύμματος από γεωτρήσεις (n=34 ζεύγη).

Source	*Sum of squares*	*Degrees of freedom*	*Mean square*	*F-ratio*	*p-value*
Model	6.11308×10^{-9}	1	6.11308×10^{-9}	1090.49	0.0000
Residual	1.79386×10^{-8}	32	5.60582×10^{-6}		
Total (corr.)	6.29246×10^{-9}	33			

Table 2C.4. One-way analysis of variance of routine and replicate analyses of Zn in overburden samples from drill-holes (n=34 pairs).
Πίνακας 2C.4. Ανάλυση διασποράς ενός παράγοντα των αναλύσεων ρουτίνας και επαναληπτικών του Zn σε δείγματα του εδαφικού καλύμματος από γεωτρήσεις (n=34 ζεύγη).

Source	*Sum of squares*	*Degrees of freedom*	*Mean square*	*F-ratio*	*p-value*
Model	4.8776×10^{-10}	1	4.8776×10^{-10}	13430.69	0.0000
Residual	1.14784×10^{-8}	32	3.587×10^{-6}		
Total (corr.)	4.82907×10^{-10}	33			

The p-value in the ANOVA table tests the significance of the calculated F-ratio. Since the p-value for all four elements is less than 0.01 and 0.05, there is a statistically significant relationship between routine and replicate analyses of all four elements at the 99% and 95% confidence levels respectively.

2C.2.3.2. Linear Regression Analysis

For the linear regression model of Y = a + b.X, the dependent variable for all four elements (As, Cd, Pb, Zn) was the replicate analyses (Y), and the independent variable the routine analyses (X). Scatter diagrams were first plotted to examine the linear relationship of the two variates (Fig. 2C.1). The plots show that there is a definite relationship between routine and replicate analyses of As, Cd, Pb and Zn. Following the establishment of linearity, the linear regression parameters were calculated (Tables 2C.5-.8).

Table 2C.5. Linear regression analysis of routine and replicate analyses of As in overburden samples from drill-holes (n=34).
Πίνακας 2C.5. Ανάλυση γραμμικής συμμεταβολής των αναλύσεων ρουτίνας και επαναληπτικών του As σε δείγματα του εδαφικού καλύμματος από γεωτρήσεις (n=34).

Parameter		*Estimate*	*Standard error*	*t-statistic*	*p-value*
Intercept		-5.02237	37.1129	-0.13533	0.8932
Slope		1.00236	0.003819	262.48	0.0000
Correlation coefficient, R	0.999768				
R^2 %	99.9536				
Standard error of estimate	191.598				

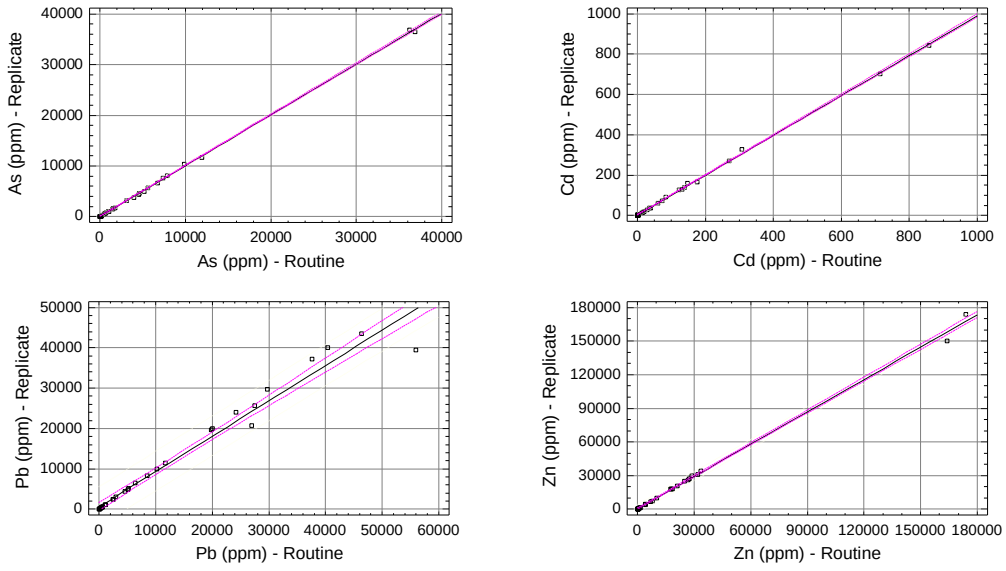

Fig. 2C.1. Scatter diagrams, linear regression lines and 95% confidence limits (dotted lines) of routine and replicate analyses of As, Cd, Pb and Zn in overburden samples from drill-holes (n=34).
Σχ. 2C.1. Διαγράμματα διασποράς, ευθείες γραμμικής συμμεταβολής και τα όρια εμπιστοσύνης στο 95% επίπεδο (διακεκομμένες γραμμές) των αναλύσεων ρουτίνας και επαναληπτικών του As, Cd, Pb και Zn σε δείγματα του εδαφικού καλύμματος από γεωτρήσεις (n=34).

Table 2C.6. Linear regression analysis of routine and replicate analyses of Cd in overburden samples from drill-holes (n=34).
Πίνακας 2C.6. Ανάλυση γραμμικής συμμεταβολής των αναλύσεων ρουτίνας και επαναληπτικών του Cd σε δείγματα του εδαφικού καλύμματος από γεωτρήσεις (n=34).

Parameter		*Estimate*	*Standard error*	*t-statistic*	*p-value*
Intercept		1.67202	1.05725	1.58148	0.1236
Slope		0.98743	0.0049695	198.7	0.0000
Correlation coefficient, R	0.999595				
R^2 %	99.919				
Standard error of estimate	5.4985				

Table 2C.7. Linear regression analysis of routine and replicate analyses of Pb in overburden samples from drill-holes (n=34).
Πίνακας 2C.7. Ανάλυση γραμμικής συμμεταβολής των αναλύσεων ρουτίνας και επαναληπτικών του Pb σε δείγματα του εδαφικού καλύμματος από γεωτρήσεις (n=34).

Parameter		*Estimate*	*Standard error*	*t-statistic*	*p-value*
Intercept		566.659	509.251	1.11273	0.2741
Slope		0.875913	0.26525	33.0225	0.0000
Correlation coefficient, R	0.985643				
R^2 %	97.1492				
Standard error of estimate	2367.66				

Table 2C.8. Linear regression analysis of routine and replicate analyses of Zn in overburden samples from drill-holes (n=34).
Πίνακας 2C.8. Ανάλυση γραμμικής συμμεταβολής των αναλύσεων ρουτίνας και επαναληπτικών του Zn σε δείγματα του εδαφικού καλύμματος από γεωτρήσεις (n=34).

Parameter		*Estimate*	*Standard error*	*t-statistic*	*p-value*
Intercept		278.357	359.565	0.774151	0.4445
Slope		0.961081	0.00829298	115.891	0.0000
Correlation coefficient, R	0.998811				
R^2 %	99.7623				
Standard error of estimate					

The linear correlation coefficient in all cases is very high indicating a strong relationship between the two variates. The coefficient of determination (R^2 %) is also very high, suggesting that almost all the variation is explained by the linear relationship.

2C.2.3.3. Notched-box-and-whisker plots

The notched-box-and-whisker plot is a very powerful Exploration Data Analysis tool for comparing different data sets (Kürzl, 1988; Manugistics, 1997). The rectangular part of the plot extends from the lower quartile (25th percentile) to the upper quartile (75th percentile), covering the centre half of each data set. The centre line within each box shows the location of the median. The plus (+) sign indicates the location of the sample mean. Whiskers extend from the box to the minimum and maximum values in each data set, except for any outside or far outside points, which are plotted separately. Outside points are points, which lie more than 1.5 times the interquartile range, above or below the box, and are shown as small squares. Far outside points are points, which lie more than 3.0 times the interquartile range, above or below the box, and are shown as small squares with plus signs through them. The presence of far outside points may

indicate outliers or a highly skewed distribution. Also included on the plots are notches covering a distance, above and below each median, representing the 95% confidence limits about the median value. If the two notches for any pair of medians overlap, there is not a statistically significant difference between the medians at the 95% confidence level. If the two notches for any pair of medians do not overlap, there is a statistically significant difference between the medians at the 95% confidence level.

In the four cases studied there is a definite overlap of the notches of the box-plots representing the routine and replicate analyses. Therefore, it can be concluded that there is no significant difference between the medians of the routine and replicate analyses of As, Cd, Pb and Zn at the 95% confidence level.

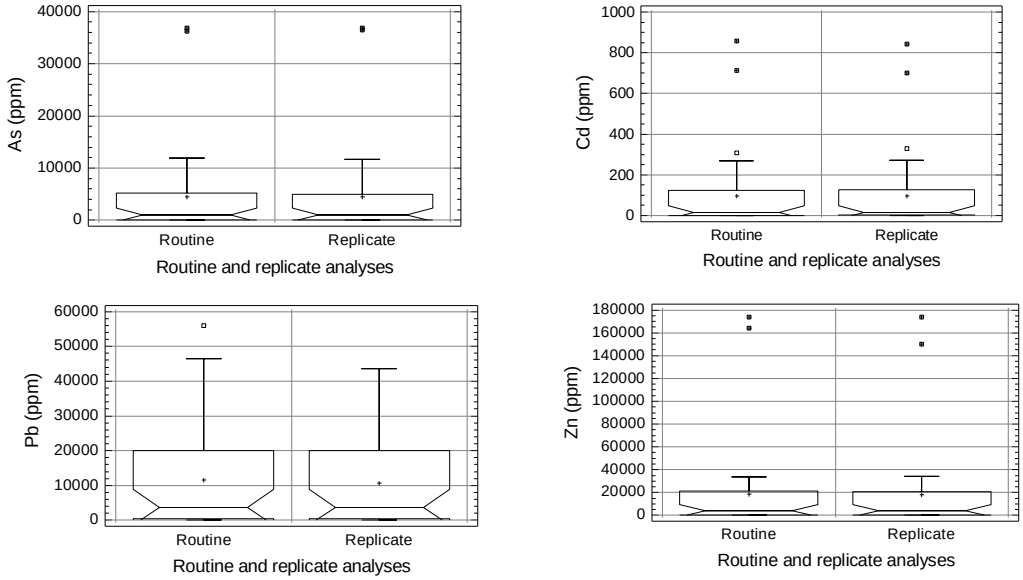

Fig. 2C.3. Notched-box-and-whisker plots of routine and replicate analysis for As, Cd, Pb and Zn on the same drill-hole samples (n=34).
Σχ. 2C.3. Σύγκριση των αναλύσεων ρουτίνας και επαναληπτικών του As, Cd, Pb και Zn σε δείγματα επιφανειακού καλύμματος από γεωτρήσεις με τη βοήθεια θηκογραμμάτων με εγκοπές (n=34).

2C.2.4. PRACTICAL DETECTION LIMIT AND PRECISION (Tables 2C.17-.24)

Practical detection limits, the precision and other parameters were determined for (a) each step of the sequential extraction procedure, (b) the combined data of steps 1 and 2 (exchangeable and carbonate phases), (c) total element contents, and (d) rock geochemical data. The results are tabulated in Tables 2C.9A to 2C.16A (in Appendix 1A, Volume 1A, p.10-17) with statistical explanations.

The program DEPRECIS (E. Vassiliades, in preparation) used the method of Thompson and Howarth (1976, 1978), with modifications made by the author of this study, for the estimation of precision and practical detection limits. Replicated analysis is performed for at least 50 randomly selected samples. Hence, a minimum of 50 pairs of duplicate analyses is available for input in program DEPRECIS. In the Lavrion case study, there were for each element 55 pairs of duplicate analyses for each of the five

sequential extraction steps and totals on overburden samples, and 66 pairs for the rock samples. The steps followed are:

1. Calculate the mean values of the 55 pairs $[(X_1+X_2)/2]$. According to Thompson and Howarth (1978) this mean value is an estimate of true concentration of an element for the particular analytical method used.
2. Calculate the absolute differences between each pair $|X_1-X_2|$. The absolute difference is an estimate of the standard deviation, σ_c, at that particular concentration. $|X_1-X_2|$ is normally distributed and relates to the parent population, with a standard deviation σ_c, such that: $\sigma_d = \sqrt{2\sigma_c}$, where σ_d is the standard deviation of the difference $|X_1-X_2|$;
   $d = 1.128\sigma_c$, where d is the mean value for the difference; and
   $M_d = 0.954\sigma_c$, where M_d is the median value for the difference. σ_c can be obtained from each of these relationships, but the median (M_d) is the most convenient estimator, because it is (i) relatively little affected by wild values; (ii) readily estimated graphically, and (iii) corresponds very closely to σ_c without further calculation (Fletcher, 1981).
3. Arrange list in increasing order of concentration means;
4. From the first 11 results calculate the mean concentration (Group mean) and the median difference (Group median);
5. Repeat step 4 for each successive group of 11 samples, ignoring any remainder less than 11;
6. Calculate the linear regression of the median difference (y-axis, dependent variable) on the means (x-axis, independent variable). At this point the modification has been introduced. In classical regression, (Y = a + bX), a linear relationship is quantified by fulfilling the following requirements of (a) dependency and (b) knowing one variable without error. Thompson and Howarth (1978) assumed that the group means are the independent variable or predictor (X), by which the group median difference (Y) is estimated. The question posed is the following: which is really the dependent variable? Since, both variables are derived from the grouping of the same analytical data set, they are subject to errors of the same order of magnitude. It is concluded, therefore, that the requirements of classical regression cannot be met. To overcome this situation Kermack and Haldane (1950) developed the reduced major axis line, which is the line of best-fit between a set of points (Till, 1974). Essentially, is the best-fit line between the two regression lines of (Y = a + bX) and (X = a + bY). Hence, errors of estimation are minimised;
7. Obtain from the major axis regression line of the group median differences, $|X_1-X_2|$, on the group means, $[(X_1+X_2)/2]$, the intercept, a, and coefficient, b.
8. Multiply by 1.048 (*i.e.*, 1/0.954) the intercept, a, and coefficient, b, to obtain σ_o and k respectively; from the regression $\sigma_c = \sigma_o + kc$, so that the precision, P_c, is given by

$$P_c = [(2.\sigma_o/X_{ci}) + (2.k)],$$

   which is the variation at the two standard deviation (95%) confidence level.
9. Calculate the percentage precision (P_c%) by using the equation

$$P_c\% = [(2.\sigma_o/X_{ci}) + (2.k)] .100 = [(200.\sigma_o/ X_{ci}) + (200.k)],$$

   where X_{ci} is the element concentration determined on individual samples. Hence, it is possible to estimate, by this method, the precision for every determination.
10. Calculate the detection limit. Detection limit is normally defined as the concentration that gives rise to a signal equal to twice the standard deviation of *blank* fluctuations, *i.e.*, at a value of $P_c = 100\%$ and $X_{ci} = 2.\sigma_o$. At concentrations higher than the detection limit, precision falls asymptotically towards the value of 2.k as defined in the expression $Pc = [(2.\sigma_o/X_{ci}) + (2.k)]$. For further information, and the implications involved in the estimation of these quality control parameters, Thompson and Howarth (1976) should be consulted.

It is important to understand the asymptotic nature of precision, and that it is wrong to quote a single value for precision, *i.e.*, at concentrations higher than the detection limit, precision falls asymptotically towards the value of 2k or 200k in the above expressions (refer to Fletcher, 1981, Fig. 2-5, p.32). On the geochemical distribution maps the relative precision equation is given, so the reader can estimate precision at any specific concentration.

Practical detection limits determined by this method are subject to the variation of element concentrations in the selected random samples. In case the samples have a good distribution of element concentrations, approaching a normal Gaussian distribution, the practical detection limits of these elements are either the same or very close to instrument detection limits, *e.g.*, Ag, Cd, Sr (Table 2C.11A). Elements which have non-Gaussian distributions, their practical detection limits are normally very different from those quoted by the analysts, *e.g.*, Ca, Fe, Mn, Pb, Zn (Table 2C.11A in Appendix 1A, Volume1A, p.12).

In Tables 2C.9A-.16A (Appendix 1A, Volume 1A, p.10-17) are tabulated the parameters of the precision equation, practical detection limits, and the variables required to calculate the relative precision of each element at the 95% confidence level for any concentration value.

2C.2.4.1. Detection Limit Used in Data Processing

Since, the Lavrion replicated analysis samples did not satisfy the conditions for determination of practical detection limits for all elements, *i.e.*, too many samples with high element concentrations, it was decided to use those quoted by analysts on blank solutions for each particular analytical method and instrument used.

2.C.2.4.1.1. Handling of values below detection limit

For statistical purposes, it is customary in geochemical surveys, to set all concentration values quoted as “below detection limit” to half the reported limit.

Blank back page
Λευκή οπίσθια σελίδα

Chapter 2D

DATA PROCESSING: STATISTICAL AND GEOSTATISTICAL METHODS AND GEOCHEMICAL MAP PRODUCTION

Alecos Demetriades
Institute of Geology and Mineral Exploration, 70 Messoghion Street, Gr-115 27, Athens, Greece

2D.1. INTRODUCTION

An enormous amount of data were produced from the analysis of different sample types collected from the Lavrion urban area, *i.e.*,

- Rock samples (18 elements),
- Metallurgical processing samples (30 elements),
- Overburden/soil samples [22 elements for each of the five-steps of sequential extraction and totals],
- House dust samples [22 elements for each of the five-steps of sequential extraction and totals],
- Particle-size analysis samples of metallurgical processing wastes and residual soil [grain size distribution of six fractions, and 5 elements for each fraction],
- Groundwater samples (16 variables),
- Drill-hole and vertical overburden profile samples (7 variables), and
- Biomedical samples (blood-Pb only).

Their processing for map production and vertical distribution profiles was indeed a challenging task.

To begin with, all analytical data were subjected to quality control checks discussed in Chapter 2C, and subsequently databases developed for each sample type. Samples treated by different analytical methods, as for example overburden and house dust samples, have databases for each of the five sequential extraction steps, combined and exchangeable steps, and total element determinations. Databases included, apart from the analytical data and sample number, the east and north site co-ordinates, as well as other site characteristics, depending on the data processing performed on the different sample types. The biomedical database included blood-Pb concentrations, and the personal information of children, that participated in the cross-sectional epidemiological study.

Thorough checks were carried out on all databases to ensure the integrity of data entered.

A concise description of all statistical and geostatistical parameters and diagrams presented on the geochemical maps are discussed below. Specific statistical and presentation techniques, used for processing of drill-hole and groundwater data are described in the relevant chapters. Similarly, other statistical techniques, such as factor and cluster analysis, employed in data processing are discussed under the relevant chapters.

2D.2. DATA PROCESSING AND PRESENTATION

The different statistical and map production techniques used will be briefly described. Commercial and public domain software packages employed were Geo-EAS (Englund and Sparks, 1988), Harvard Graphics® (SPC, 1993), Statgraphics® (Manugistics, 1995, 1997), Surfer® (Golden Software, 1995), Variowin (Pennatier, 1996) and MapViewer® (Golden Software, 1997).

2D.2.1. HISTOGRAMS AND STATISTICAL PARAMETERS

Histograms were plotted for all single element or variable maps to show the distribution of values. Next to the histograms a number of statistical parameters are displayed, *i.e.*, number of samples, average value, standard deviation, minimum and maximum values (Maps 3.1, 3.4, 3.5, 3.6, 3.8-13, 3.15-20, 4.2-30, 6.1-30, 6.32-34, Volume 2 of this report). On single element maps with multi-component features, such as metallurgical wastes (Maps 3.2, 5.1-30), sequential extraction (Maps 3.7, 3.14, 7.1-30, 8.1-30), and groundwater (Maps 10.1-4), a large number of statistical parameters are presented, *i.e.*, number of samples, minimum, maximum, mean, median, first quartile, third quartile, standard error of mean, 95% & 99% confidence interval of mean, average deviation, standard deviation, relative coefficient of variation, coefficient of skewness and coefficient of kurtosis. All these parameters are concisely described below.

It is noted that the statistical parameters of the sample data set are estimated, *i.e.*, the sample mean ($\mathbf{0}$), sample standard deviation (s), *etc.*, and *not* the population mean (μ) and population standard deviation (σ). According to statistical theory the population is the parent group from which the sample population is drawn. In the cases studied, representative samples were collected from different sample media.

Number of samples (n) indicates the total number of samples in the data set.

Minimum indicates the minimum concentration value of the element or variable in the sample data set. A point to note is the treatment of element concentration values below the analytical detection limit. As mentioned in Chapter 2C, for statistical purposes element concentration values below detection limit are customarily set by geochemists to half the detection limit. This approach leads, however, to a problem when studying statistical tables, *i.e.*, the minimum class interval, with a value below detection limit. Experienced geochemists will immediately realise that minimum values below detection limit have been set to half their detection limit. *This note is for the non-expert, who is making an in-depth study of the statistical tables and geochemical distribution maps presented in these reports.*

Maximum indicates the maximum concentration value of the element in the sample data set.

Mean is the arithmetic average value of the sample data set. It is the sum of all element concentration values divided by the number of samples, *i.e.*,

Sample mean ($\mathbf{0}$): $$\mathbf{0} = 1/n \sum_{i=1}^{n} x_i$$

Where: n is the number of samples in the data set
x_i is the element concentration value in a sample.

Median is the middle value among the sample data set, which are ordered consecutively from minimum to maximum values, *i.e.*, half of the element concentration values are larger than the median and half are smaller than the median. When there are an even number of samples, the median is the average of the element concentration values of the two middle values.

First quartile *(25th percentile)* is the element concentration value, such that one-fourth of the concentration values are smaller than the quartile, and three-fourths of the values are larger than the first quartile.

Third quartile *(75th percentile)* is the element concentration value, such that three-fourths of the concentration values are smaller than the quartile, and one-fourth of the values are larger than the third quartile.

Standard error of mean. It is common practice to refer to the standard deviation of a sampling distribution of a statistic as the *standard error* of that statistic, the mean in this case, *i.e.*, the *standard error of mean* is an estimate of the standard deviation of means that would be found, if many sample concentration values of n items were repeatedly collected from the same population. More simply, suppose many sample element concentration values of size n were repeatedly collected from the same population, and the mean values of these many samples were calculated. The means of these samples would themselves form a data set. The standard error of mean is an estimate of the standard deviation of this theoretical sample of means.

Standard error of mean (SE): $SE = s / \sqrt{n}$

Where:

s is the sample standard deviation
n is the number of data values (for a sample).

95th and 99th confidence interval (CI) of mean. The range of element concentration values between $\mathbf{0}$ - CI and $\mathbf{0}$ + CI is expected to include the true mean of the underlying population 95% of the time (for the 95% confidence interval) or 99% of the time (for 99% confidence interval). This formula assumes that the data set is sufficiently large for the central limit theorem to apply.

95% confidence interval of mean: $\pm\, t_{(n-1),\alpha=0.05}$ (SE)

99% confidence interval of mean: $\pm\, t_{(n-1),\alpha=0.01}$ (SE)

Where:

$t_{v,\alpha}$ is the value of the Student's t distribution with v degrees of freedom, such that the difference between the cumulative probability function evaluated at $t_{v,\alpha}$ and $-t_{v,\alpha}$ is equal to 1-α.
SE is the standard error of mean.

Average deviation is the average of the absolute values of the differences between each element concentration value and the mean. Sample data set Average deviation (MD) is estimated by:

$$MD = 1/n \sum_{i=1}^{n} \left| (x_i - \mathbf{0}) \right|$$

Where:

$\bar{x}$ is the mean value of element concentrations of the sample data set
x_i is the element concentration value in a sample
n is the number of samples in the data set.

Standard deviation is the square root of the variance, which is the average of the squared deviations from the mean, *i.e.*, the square root of the sum of the squared deviations from the mean divided by one less than the number of samples in the data set.

Standard deviation (s): $s = \sqrt{[1/(n-1)\sum_{i=1}^{n}(x_i - \bar{x})^2]}$

Where:

$\bar{x}$ is the mean value of element concentrations of the sample data set
x_i is the element concentration value in a sample
n is the number of samples in the data set.

Coefficient of variation, the statistic C, is a dimensionless measure of relative dispersion or variation of the distribution of an element. It is the standard deviation divided by the mean, and is normally expressed either as a fraction or as a percentage.

Sample coefficient of variation (C): $C = (s/\bar{x}).100$

Where:

s is the sample standard deviation
$\bar{x}$ is the mean value of element concentrations of the sample data set.

The coefficient of variation can be used to compare the variability between two or more sets of data. The one with the highest coefficient of variation will be the most widely dispersed.

As pointed out by Koch and Link (1971) for substances in small amounts, such as trace elements, the coefficient of variation is extremely high (>200 or 250%), whereas extremely low C values (<20%) are generally found only for geological substances present in amounts measured in a few tens of percent, as for example with major elements. In the case of Lavrion samples, high coefficients of variation are expected in (a) overburden, because of contamination, (b) rock, because of mineralisation and lithology, and (c) metallurgical processing wastes, because of large differences in their chemistry.

Coefficient of skewness is a measure of asymmetry of the data distribution. A positive value indicates a longer tail to the right (positive skewness), while a negative value indicates a longer tail to the left (negative skewness). A perfectly symmetrical distribution, like the normal gaussian distribution, has a coefficient of skewness equal to 0. This statistic is unreliable for small data sets (n<50). Geochemical data are normally positively skewed.

Sample coefficient of skewness (g_1): $g_1 = 1/(ns^3)\sum_{i=1}^{n}(x_i - \bar{0})^3$

Where:

s is the sample standard deviation
$\bar{0}$ is the mean value of element concentrations of the sample data set
x_i is the element concentration value in a sample
n is the number of samples in the data set.

Coefficient of kurtosis is a measure of peakedness, *i.e.*, how sharp is the peak of the distribution curve. Traditionally the value of the coefficient of kurtosis is compared to zero (0), the value of the normal gaussian distribution. A value greater than 0 indicates a peaked distribution, and a value less than 0 indicates a flat distribution. This statistic is again unreliable for small data sets (n<50).

Sample coefficient of kurtosis (g_2): $g_2 = [1/(ns^4)\sum_{i=1}^{n}(x_i - \bar{0})^4] - 3$

Where:

s is the sample standard deviation
$\bar{0}$ is the mean value of element concentrations of the sample data set
x_i is the element concentration value in a sample
n is the number of samples in the data set.

It is noted that the coefficient of kurtosis for the normal gaussian distribution, in some statistical text books, is quoted as having a value of 3. In the above equation, the value of the normal distribution is reduced to zero by subtracting 3.

2D.2.1.1. Percentiles

Percentiles were used for selection of concentration (class) intervals for plotting geochemical distribution maps. The *k*th percentile is defined as the value of the data set, such that *k* percent of element concentration values in the sample data set are less than that value, and 100-*k* percent are greater than that particular value. For example, the 50th percentile is by definition the median value. The percentiles selected are at *0, 2.5, 5, 10, 15, 25, 50, 75, 90, 95, 97.5* and *100*; the 0 and 100 percentiles represent the minimum and maximum element concentration values respectively. Hence, a fairly good idea of the statistical distribution of element concentrations is presented on the geochemical maps.

By extension, percentiles indicate the area coverage of the different element concentration (class) intervals. The area studied in Lavrion is 7.235 km^2. Hence, the 0-2.5, 2.5-5, 5-10 *etc.* percentile intervals represent 0.181 km^2, 0.362 km^2, 0.7235 km^2 *etc.* respectively of the surface area of Lavrion.

2D.2.1.2. Box plots

Box plots (or boxplots) are graphical displays based on quantiles (Tukey, 1977). The *box plot or box-and-whisker plot* is defined by five numbers (Figs. 3.1-3.2; 3.7-3.10, Chapter 3):

- minimum,
- first quartile (25^{th} percentile),
- median (50^{th} percentile),
- third quartile (75^{th} percentile), and
- maximum value of a variable (Kürzl, 1988; Chambers *et al.*, 1983).

The first and third quartiles define the extremes of the box. A line within the box indicates the median. Whiskers extend from the box to the minimum and maximum values in each data set, except for any outside or far outside points, which are plotted separately. Outside points or outliers are points, which lie more than 1.5 times the interquartile range, above or below the box, and are shown as small squares. Far outside points are points, which lie more than 3.0 times the interquartile range, above or below the box, and are shown as small squares with plus signs through them. The presence of far outside points may indicate outliers or a highly skewed distribution. The Statgraphics® (Manugistics, 1995) graphical representation of the box-and-whisker plot displays an additional parameter, the sample mean which is indicated by a plus (+) sign.

2D.2.1.2.1. Notched-box-and-whisker plot

The notched-box-and-whisker plot is a variation of the normal boxplot, and includes a confidence interval on the median, for the purpose of comparing different data sets (see Fig. 3.9). A notch about the median represents the 95th confidence interval on the median. If the two notches for any pair of medians overlap, there is not a statistically significant difference between the medians at the 95% confidence level. If the two notches for any pair of medians do not overlap, there is a statistically significant difference between the medians at the 95% confidence level.

2D.2.2. GEOSTATISTICAL PROCESSING AND MAP PRODUCTION

Geostatistics have been developed for the study of regionalised variables. The foundations of this new theory were laid down by Krige (1951, 1952, 1962, 1970, 1976a, 1976b) and Sichel (1952, 1966, 1973). Krige was responsible for much of the early development. Matheron (1963, 1971) took up the *"yoke"* of earlier workers, formalised and developed the science, by publishing a treatise on the "Theory of Regionalised Variables". The application of this theory to problems in geology and mining has led to the more popular name of *geostatistics*, proposed by Matheron himself. Whereas, the technique producing the *"best"* estimation of an unknown value at some location within an ore deposit as *kriging*, in honour of D.G. Krige (Journel and Huijbregts, 1978; Rendu, 1978; Clark, 1979; Isaaks and Srivastava, 1990).

Although geostatistics are used extensively in ore estimation, and planning of diamond drilling operations, it is not widely used in geochemical exploration (Marshall, 1972; Croissant, 1977; Carignan, 1979). The Environmental Protection Agency of the United States of America recognising the significance of geostatistics for geochemical map plotting in environmental surveys developed Geo-EAS, Geostatistical Environmental Assessment Software (Englund and Sparks, 1988). Environmental

geochemical studies that have used geostatistics for map plotting are *"The Soil Geochemical Atlas of England and Wales"* (McGrath and Loveland, 1992a; 1992b), and the *"Environmental Geochemical Atlas of the Central Barents Region"* (Reimann *et al.*, 1998). The author of this chapter has been using geostatistics for geochemical map plotting in mineral exploration since 1979, and has found them to be very effective and an *"exact interpolator",* to borrow a favourite phrase of A.G. Royle, the author's teacher (pers. commun., 1979). Consequently, all single element, or variable, and composite maps were plotted after a thorough geostatistical structural analysis.

Since, geochemical data are positively skewed (Ahrens, 1954a, 1954b; Tennant and White, 1959; Sinclair, 1976, 1983), it was decided to transform them into logarithms base 10. Log-transformed analytical data were used in geostatistical processing (variograms, validation, *etc.*), and map plotting.

Variograms were constructed with Variowin (Pennatier, 1996). Variogram parameters were subsequently validated with Geo-EAS, and maps plotted using the kriging algorithms of Surfer® (Golden Software, 1995). For map plotting, line spacing in both X- and Y- directions were set to 20 metres. A significant tool in studying the spatial structural characteristics of the data was the experimental variogram surface calculated with Variowin, and the modelled variogram surface. These two surfaces were combined into a single plot, and displayed on the geochemical distribution maps, together with the azimuth direction of the major and minor axes of the range of influence (Maps 1.5, 1.6, 3.1, 3.4-3.6, 3.8-3.13, 3.15-3.20, 4.2-4.30, 6.1-6.30, 6.32-6.34, Volume 2 of this report).

Maps of house dust element distribution (Maps 3.5, 8.1-8.30) and blood-Pb contents (Map 3.6) show actual element concentrations by the variable-size dots, and interpolated coloured contoured values in the unsampled areas. The interpolation for house dust samples is based on soil geostatistical parameters, because sensible variograms could not be obtained from the actual house dust element data. Whereas blood-Pb concentrations were modelled until an optimum distribution was obtained, based on the actual knowledge of the spatial distribution of Pb in the Lavrion surface environment, and the metallurgical processing wastes.

2D.2.2.1. Variable-size dot maps

Two types of variable-size dot maps were plotted, *i.e.*,

1. on single element and composite element geochemical distribution maps, apart from the coloured class intervals, each sample is indicated by a black dot, the diameter of which increases logarithmically with $\log_{10}$-increasing concentration (Maps 1.5, 1.6, 3.1, 3.4-3.6, 3.8-3.13, 3.15-3.20, 4.2-4.30, 6.1-6.30, 6.32-6.34). Similarly, raw pH-values were plotted at each sample site (Maps 2.5 & 2.6). These maps were plotted with Surfer® (Golden Software, 1995). The linear proportional scale option was used to determine the dot diameter, and

2. single element maps were plotted to show concentration values in samples of metallurgical processing wastes. Each sample type is indicated by a different coloured dot, the diameter of which increases proportionally with increasing concentration (Maps 3.2, 5.1-5.30). These maps were plotted with MapViewer® (Golden Software, 1997).

2D.2.2.2. Multiple variable-size bar maps

Multiple variable-size bar maps were plotted with MapViewer® (Golden Software, 1998) for the geographical presentation of

(a) five-step sequential extraction analytical data for overburden and house dust samples (Maps 3.7, 3.14, 7.1-7.30, 8.1-8.30 in Volume 2);
(b) particle-size analysis data (Maps 3.3, 9.1, 9.3, 9.9, 9.14, 9.24, 9.30), and
(c) groundwater analytical data (Maps 10.1-10.4).

Two different variations were used for presentation of element concentrations or variable values, *i.e.*,

(i) length of bars proportional across variables, and
(ii) concentrations considered individually for each variable.

In both variations the centre of the bar chart is positioned at the sample site.

2D.2.2.3. Bars proportional across variables

This option was used to compare element concentrations, or variable values, across the different variables plotted, *e.g.*, element concentrations in each of the five-steps of sequential extraction data, and the particle-size analysis data. In this case, the minimum and maximum bar heights are based on all data sets. The bars are thus scaled proportionally across all variables both within and between variables.

2D.2.2.4. Bars proportional for each variable

This option was used for plotting groundwater analytical data. In this case the bar height is based on the minimum and maximum values of individual variables. Consequently, no comparisons can be made between variables.

Chapter 3

DISTRIBUTION OF LEAD IN THE LAVRION URBAN ENVIRONMENT

Alecos Demetriades and Katerina Vergou-Vichou
Institute of Geology and Mineral Exploration, 70 Messoghion Street, Gr-115 27, Athens, Greece

Nicolaos Vlachoyiannis
Lavrion Medical Centre, Lavrion, Greece

3.1. INTRODUCTION

Argentiferous galena [PbS] was the mineral mined and processed from ancient (*ca.* 3500 BC) to recent times (1989 AD) in the Lavreotiki area. Since lead (Pb) is the major constituent of galena, it is one of the most widespread toxic element in the Lavrion urban environment (Hadjigeorgiou-Stavrakis and Vergou-Vichou, 1992; Hadjigeorgiou-Stavrakis *et al.*, 1993; Stavrakis *et al.*, 1994b; Demetriades *et al.*, 1996c), and its effects on the local population and, children especially, have been studied by cross-sectional epidemiological studies (Drossos *et al.*, 1982; Benetou-Marantidou *et al.*, 1985; Nakos, 1985; Hatzakis *et al.*, 1987; Maravelias *et al.*, 1989; Makropoulos *et al.*, 1991, 1992a, 1992b; Kafourou *et al.*, 1997). Because of the attention, Pb has already received, not only in Lavrion but also worldwide, it is treated separately from other toxic elements occurring in the study area.

Trace amounts of Pb appear to be essential to the health of some animals, but it has never been shown as necessary in human biochemistry (Mervyn, 1980, 1985; Manousakis, 1992). Hippocrates (460-377 BC), the father of medicine, together with other Greek philosophers and physicians, Aristotle (384-322 BC), Dioskourides (1st century BC) and Galenus (128-200 AD), have observed the effects of acute and chronic intoxication of Pb poisoning, and described the classic symptoms of abdominal convulsions, constipation, anaemia and paralysis. Gaius Plinius Secundus, the classical Roman author (23-79 AD) mentioned the toxic effects of Pb, and that vapours, released during smelting of Pb ore, should not be inhaled for *"they are dangerous and could cause death to humans and animals"*. He also warned about the danger to pregnant women in case of exposure; he advised the ones working in the treatment of "red Pb", crocooite ($PbCrO_4$), to protect themselves by wearing masks from animal organs. It appears, therefore, that ancient Greeks and Romans knew that Pb poisoning (plumbism) was a disease contracted by workers in Pb mines and ore processing. Later medical practitioners, such as Paracelsus (1493-1541 AD), described the toxic effects of Pb at the work place. Lead apparently, is the first toxic metal to receive so much attention by the medical profession from ancient to modern times.

3.1.1. TOXIC EFFECTS OF LEAD

The toxic effects of Pb are well documented, and especially for children, who are more susceptible to Pb poisoning than adults (Kazantzis, 1973; Mervyn, 1980, 1985; Thornton and Culbard, 1987; Trattler, 1987; Briskin and Marcus, 1990; Ferguson, 1990; Reagan and Silbergeld, 1990; Manousakis, 1992; Wixson and Davies, 1994; US EPA,

1998). Inorganic Pb is not metabolised, but is directly absorbed, distributed in different parts of the human body and excreted. The rate depends on its chemical and physical form, and on the physiological characteristics of the exposed person (*e.g.*, nutritional status and age). Once in the blood, Pb is primarily distributed among three compartments:

- blood
- soft tissue (kidney, bone marrow, liver, and brain), and
- mineralising tissue (bones and teeth).

Absorption via the gastrointestinal track, following ingestion, is highly dependent upon the levels of calcium, iron, fats and proteins. Long-term exposure to inorganic Pb compounds is known to affect the central nervous system, peripheral nerves, and kidneys. High levels of Pb in the human body have the following effects (Mervyn, 1980,1985; Manousakis, 1992):

- *reduction of vitamin D.* If Pb is removed, however, by some means from the human body, then vitamin D is restored to normal level;
- *decrease in the amount of iron*. Lead inhibits the synthesis of haem and haemoglobin, as well as the activity of certain enzymes. In fact, anaemia is often the first sign of Pb intoxication.
- *reduction in the amount of calcium and phosphorus*. This antagonistic relationship between Pb and (Ca+P) works in the opposite way too. Calcium and phosphorus decrease the gastrointestinal absorption of Pb, and aids in its elimination. Some authors suggest, that people living in high-risk environments in terms of Pb should drink additional quantities of milk. There is, however, contradictory evidence in the use of milk to counteract absorption of Pb and other toxic elements. Trattler (1985) states that milk as a source of calcium is associated with increased Pb levels, and is not advised. He proposes alternatives, such as calcium orotate, calcium lactate or bone meal, and inorganic forms of phosphorus.

3.1.1.1. Effects on Children and Adults

The US Environmental Protection Agency (US EPA, 1998, p.5) stresses that it is important to know that even exposure to low levels of Pb can permanently affect children. Low level exposure of children to Pb can cause:

- nervous system and kidney damage;
- learning disabilities, attention deficit disorder, and decreased intelligence;
- speech, language, and behaviour problems;
- poor muscle co-ordination;
- decreased muscle and bone growth; and
- hearing damage.

While low-level exposure is most common, exposure to high levels of Pb can have devastating effects on children, including seizures, unconsciousness, and, in some cases, death.

Although children are especially susceptible to Pb exposure, it can also be dangerous to adults. In adults, high Pb levels can cause:

- increased chance of illness during pregnancy;
- harm to foetus, including brain damage or death;

- fertility problems (in men and women);
- high blood pressure;
- digestive problems;
- nerve disorders;
- memory and concentration problems, and
- muscle and joint pain.

3.1.3. EPIDEMIOLOGICAL STUDIES IN LAVRION

Cross-sectional epidemiological studies in Lavrion have indicated that

- children who had lived all their life in the close vicinity of the Pb-Zn smelter exhibited a significant excess of pathological features, and persistent evidence of organic brain damage with associated behavioural effects (Benetou-Marandidou *et al.*, 1985);
- there is a highly significant negative relationship between blood-Pb and psychometric intelligence and attentional performance in children (Hatzakis *et al.*, 1987);
- toxic elements, such as Pb, Hg and As, can impair the immune system, and affected children may show a reduced resistance to bacterial infections (Makropoulos *et al.*, 1992a);
- children with high blood-Pb concentrations tended to have, on average, a reduced head and chest circumference and decreased height (Kafourou *et al.*, 1997).

3.1.4. EPILOGUE TO THE INTRODUCTION

It is quite apparent from the aforesaid, that Pb in the Lavrion urban environment is a major potential public health hazard. Mounting medical evidence points to the fact that there is no “zero-effect” level of childhood blood-Pb. ***The overall conclusion is that human exposure to Pb must be reduced to almost the zero level***. This is, of course, wishful thinking for increased Pb concentrations have been found even in remote areas, such as the polar ice cap and oceanic waters. The residence time of Pb compounds in seawater is 400 years (Henderson, 1982), and in soil 400-3000 years (Ferguson, 1990). Its widespread distribution, and long residence time in seawater and soil, threatens, therefore, the ecological stability of the entire biosphere.

In the following paragraphs, the contamination of the Lavrion urban environment by Pb will be described. To begin with, the distribution of Pb in rocks (Map 3.1, Volume 2 of this report) is discussed, since these are the only media that can give data on the natural, baseline, distribution (including geochemically anomalous levels due to mineralisation), before humans began to contaminate the surface environment in Lavrion. Total Pb contents in samples of metallurgical processing wastes (Map 3.2), and its distribution in different grain-size fractions of metallurgical wastes and residual soil (Map 3.3) are then described, in order to understand the contamination of the soil cover. It is followed by the description of total Pb in overburden and house dust, and total Pb in children’s blood (Maps 3.4-3.6). These maps show the contamination of the Lavrion urban environment and its impact on human health. The remaining maps (Maps 3.7-3.20) describe the results of the five sequential extraction steps, and give information about the leachability and bioavailability of Pb.

Regarding the terminology used in this study, the term "*overburden*" is preferred to "*soil*", for it is a collective term, which includes all loose surficial materials and residual soil, that may come in contact with the human population, and especially children. *Overburden* is defined as all unconsolidated surficial deposits overlying bedrock. *Soil* constitutes the naturally occurring, unconsolidated material at the surface of the earth capable of supporting plant growth.

3.2. DISTRIBUTION OF LEAD IN ROCKS

Parent rocks of the Lavrion urban area mainly consist of marble, schist, schistose-gneiss, prasinite, calcareous sandstone, and conglomerate (Map 2.2). Fault breccia and outcrops of iron mineralisation are of minor significance, since they occur at a few locations. Marble and schist are the dominant rock types (Table 2.1). Statistical parameters of Pb concentrations in different rocks, occurring in the Lavrion study area, are tabulated in Table 3.1 and displayed in Fig. 3.1.

Marble has the greatest variation in Pb (0.5-1850 ppm; coefficient of variation, C, 362.2%), with a mean of 54.6 ppm and a median of 18 ppm. High Pb levels in marble occur in areas where it is altered (ankeritised) and slightly mineralised (calamine). Schist has also highly variable Pb concentrations (8-810 ppm; C=172.22%), and more anomalous values than marble, as indicated by the mean, median, first and third quartiles (Table 3.1; Fig. 3.1). Geochemically anomalous Pb levels in schist occur near its contact with altered marble. It is noted that base metal mineralisation occurs at the contact of marble and schist, and is mainly hosted in marble. Schistose-gneiss (6-54 ppm Pb; C=125.56%), prasinite (0.50-60 ppm Pb; C=139.23%), and calcareous sandstone (22-58 ppm Pb; C=41.38%) do not have excessive Pb concentrations. The only departure is by conglomerate (37-1040 ppm Pb; C=85.26%), which locally contains altered-mineralised marble pebbles.

From the geochemical exploration point of view, marble and schist only exhibit anomalous Pb concentrations (Map 3.1). The outliers of the boxplot (Fig. 3.1) display this characteristic (Kürzl, 1988; O'Connor *et al.*, 1988), *i.e.*, for marble there are outlying anomalous values >83.75 ppm Pb, and for schist >155.88 ppm Pb. A major north-east to south-west trending geochemical anomaly extends from Noria to Ayios Andreas, and a minor in the Prasini Alepou area. Slightly elevated Pb contents occur about Fougara hill and Kiprianos. The marble in these areas is oxidised to a variable degree. Lead levels in rock samples from other parts of the Lavrion urban area are within the local geochemical background range (0.5-22 ppm Pb).

3.3. DISTRIBUTION OF LEAD IN SAMPLES OF METALLURGICAL WASTES

Map 3.2 displays the distribution and statistical parameters of Pb in samples of metallurgical processing wastes, *i.e.*, slag (5000-51200 ppm Pb; C=72.09%), sand-blast material (12300-32800 ppm Pb; C=39.30%), earthy-material within slag (5080-30800 ppm Pb; C=44.95%), flotation residues (18500-28100 ppm Pb; C=12.54%), pyrite tailings (9800-85200 ppm Pb; C=52.65%) and pyritiferous sand (3800-41200 ppm Pb; C=89.08%). Slag, pyritiferous tailings and pyritiferous sand, show the greatest variation in Pb levels (Fig. 3.2), because of differences in the original ore, and metallurgical processing method.

Table 3.1. Statistical parameters of lead (ppm Pb) concentrations in all rocks, marble, schist, schistose-gneiss, prasinite, sandstone and conglomerate, Lavrion urban area.
Πίνακας 3.1. Στατιστικές παράμετροι των συγκεντρώσεων του μολύβδου (ppm Pb) στα δείγματα όλων των πετρωμάτων, μαρμάρου, σχιστολίθου, σχιστο-γνευσίου, πρασινίτη, ψαμμίτη και κροκαλοπαγούς από την αστική περιοχή του Λαυρίου.

Statistical parameters	*All rock types*	*Marble*	*Schist*	*Schistose-gneiss*	*Prasinite*	*Sandstone*	*Conglomerate*
	'Ολα τα πετρώματα	*Μάρμαρο*	*Σχιστόλιθος*	*Σχιστο-γνεύσιος*	*Πρασινίτης*	*Ψαμμίτης*	*Κροκαλοπαγές*
*General rock type mean**	*17.00*	*5.00*	*22.00*	-	*4.00*	*10.00*	-
Number of samples	140	88	33	4	4	6	3
Minimum	0.50	0.50	8.00	6.00	0.50	22.00	37.00
Maximum	1,850.00	1,850.00	810.00	54.00	60.00	58.00	1,040.00
Mean	76.85	54.61	111.82	18.75	19.63	35.67	602.33
Median	22.00	18.00	39.00	7.50	9.00	31.00	730.00
First quartile	11.50	10.00	16.50	6.00	3.25	24.00	-
Third quartile	54.00	39.50	72.25	31.50	36.00	48.00	-
Standard error of mean	17.67	21.09	33.52	11.77	13.66	6.03	296.49
95% conf. int. of mean	34.97	41.92	68.29	37.46	43.47	15.49	1,275.81
99% conf. int.of mean	46.20	55.54	91.79	68.76	79.80	24.30	2,942.70
Average deviation	89.08	60.24	125.29	17.63	20.19	12.00	376.89
Standard deviation	209.06	197.81	192.58	23.54	27.32	14.76	513.54
Coef. of variation (%)	272.03	362.20	172.22	125.56	139.23	41.38	85.26
Coefficient of skewness	5.82	8.50	2.52	0.74	0.68	0.40	-0.23
Coefficient of kurtosis	39.68	74.12	5.68	-1.69	-1.73	-1.81	-2.33

*Reimann *et al.* (1998)

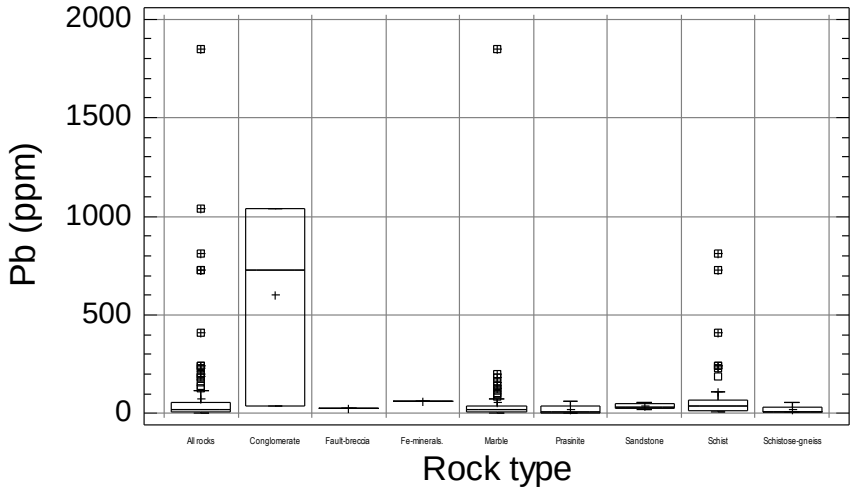

Fig. 3.1. Multiple boxplot of the distribution of lead (Pb) in different rock types occurring in the Lavrion urban area.
Σχ. 3.1. Πολλαπλό θηκόγραμμα της κατανομής του μολύβδου (Pb) στα διάφορα είδη πετρώματος που απαντώνται στην αστική περιοχή του Λαυρίου.

The narrowest range and lowest coefficient of variation of Pb (12.54%) is exhibited by flotation residues, showing that Pb concentrations are fairly uniform in this type of waste. An interesting feature, exhibited in Fig. 3.2, is the elevated mean and median Pb levels in earthy material within slag in comparison to normal slag, and its similarity with sand-blast material, which is, comminuted slag. This feature suggests, that as slag is broken down to finer fractions, Pb is more uniformly distributed (low coefficient of variation) with a concurrent increase in its mean and median values.

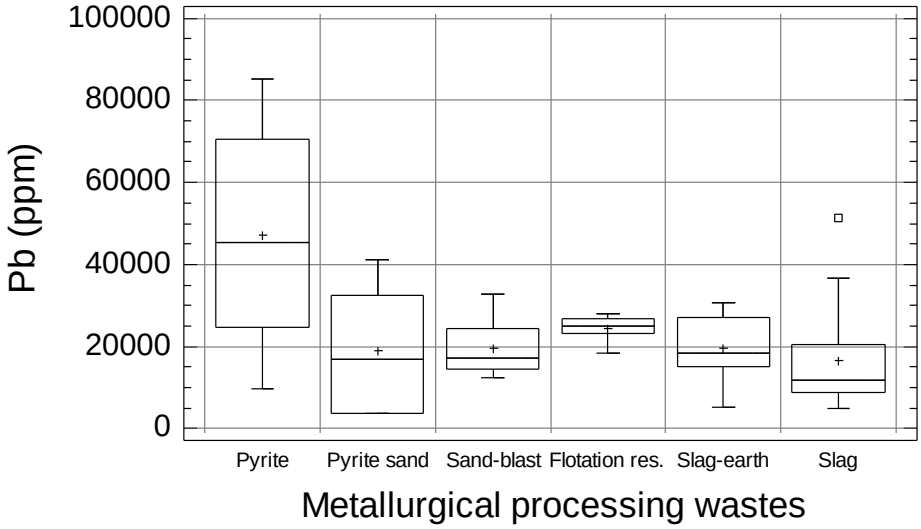

Fig. 3.2. Multiple boxplot of the distribution of lead (Pb) in samples from the different types of metallurgical processing wastes in the Lavrion urban area (refer to Map 3.2).
Σχ. 3.2. Πολλαπλό θηκόγραμμα της κατανομής του μολύβδου (Pb) στα δείγματα των διαφορετικών τύπων μεταλλουργικών απορριμμάτων από την αστική περιοχή του Λαυρίου (βλ. Χάρτη 3.2).

3.4. DISTRIBUTION OF LEAD IN DIFFERENT GRAIN-SIZE FRACTIONS OF METALLURGICAL WASTES AND RESIDUAL SOIL

Map 3.3 displays the distribution of Pb in different grain-size fractions of metallurgical wastes and residual soil, their statistical parameters and boxplot comparisons. The boxplot shows that the greatest variation and highest mean and median concentrations of Pb occur in the finest fraction (<0.063-mm). This feature is in agreement with the observation of increased Pb contents in comminuted slag materials (*e.g.*, sand-blast, and earthy material within slag).

There is a tendency for the greatest concentrations of Pb to be in the finest fraction (<0.063-mm) of flotation residues (68000-112000 ppm), and earthy material within slag (7300-65000 ppm). Pyritiferous sand and residual soil, apparently have approximately a similar range of Pb contents in the two finest fractions, *i.e.*, <0.125+0.063 mm and <0.063 mm.

3.5. DISTRIBUTION OF TOTAL LEAD IN OVERBURDEN

Map 3.4 shows the spatial distribution of total Pb in overburden materials, including residual soil. The dominant features, governing the spatial distribution of Pb in the Lavrion surface environment, are the heaps of metallurgical processing wastes, *i.e.*, flotation residues, pyrite tailings and slag (Map 2.3). Their dominant orientations are north-east to south-west, and north-west to south-east, which are exhibited by the variogram surface (see inset of Map 3.4).

Lead concentrations vary from 810 to 151579 ppm, with a mean of 11578 ppm, median of 7305 ppm, and a coefficient of variation of 133.79%, which indicates the great variability of Pb in overburden. It is quite apparent, that high Pb contents in overburden materials, including residual soil, are mainly due to metallurgical processing activities. Emissions from smelters and the enormous amount of metallurgical wastes, deposited in the Lavrion urban area, and subsequent transportation of fine-grained

fractions by aeolian processes (deflation) have contaminated even the remotest sites in the study area.

The greatest concentrations of Pb occur in areas covered by the metallurgical processing wastes. The smelter and its surrounding area have the highest Pb contents (21615-151579 ppm). The next area with high Pb levels occurs over the flotation residues (13256-33856 ppm).

The legislative upper value of total Pb for residential areas with a garden is 500 ppm (ICRCL, 1987), and the draft soil action guideline value of the Contaminated Land Exposure Assessment Model (CLEA), based on the 95th percentile lifetime exposure distribution at a pH 7.0 and 10% organic matter, is 560 ppm (Ferguson, 1995; Taylor and Langley, 1996). Whichever national guideline value is selected from the international literature, the fact remains that total Pb concentrations in surface overburden materials of the Lavrion urban area are over 810 ppm. The 2.5th percentile is at 1777 ppm Pb, indicating that 97.5% of the area has Pb contents above this value.

According to Kabata-Pendias and Pendias (1984), the maximum concentration of Pb for healthy plant growth is 200 ppm. It, therefore, appears that the Lavrion urban environment is very seriously contaminated with respect to Pb, and is potentially hazardous to plants, animals and humans, especially children.

3.6. DISTRIBUTION OF TOTAL LEAD IN HOUSE DUST

Map 3.5 illustrates the distribution of total Pb in house dust. The highest Pb concentrations in indoor dust occur in houses situated over metallurgical processing wastes and, especially, the flotation residues or tailings. It is indeed very disturbing to have total Pb contents in Lavrion homes varying from 488 to 18617 ppm (mean=4006 ppm Pb; median=3091 ppm Pb).

There appears to be a relationship between total Pb in overburden (Map 3.4) and house dust samples. Linear regression analysis of logarithmically (base 10) transformed Pb concentrations shows that the correlation coefficient is 0.7 (Fig. 3.3).

The coefficient of determination, R^2 % statistic, indicates that the fitted model explains 49.024% of the variability of total Pb in house dust samples. In Tables 3.2 and 3.3 are tabulated the calculated regression and analysis of variance parameters respectively. The equation of the fitted model is

$$\log_{10} \text{Pb in house dust} = 0.781202 + (0.711294 \times \log_{10} \text{Pb in overburden}) \quad \text{[equation 3.1]}.$$

Since, the p-value in the ANOVA table (Table 3.3) is less than 0.01, there is a statistically significant relationship between total Pb in house dust and total Pb in overburden materials at the 99% confidence level. The above equation may be used to predict total house dust Pb concentrations from total overburden Pb in areas where there are no house dust samples. Refer to Chapter 8 for a more detailed analysis of regression relationships between overburden and house dust and Tables 8.111A to 8.116A in Appendix 4A of Volume 1A of this report (p.167-172).

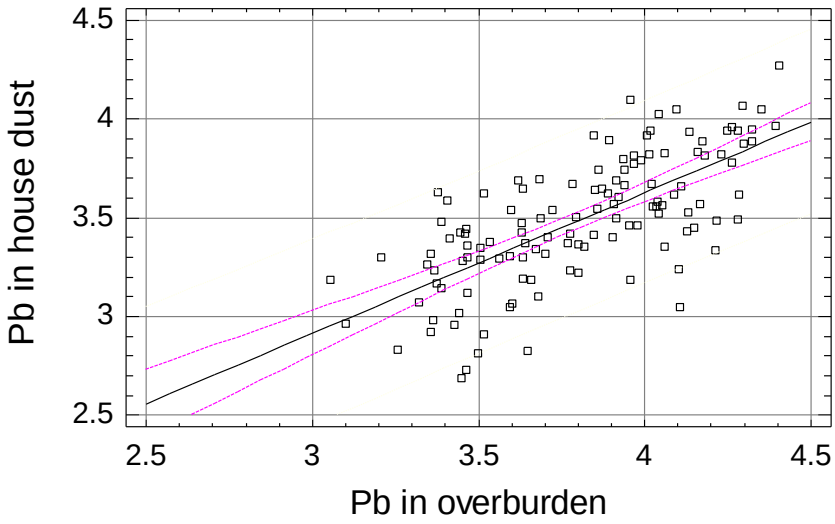

Fig. 3.3. Scatter plot of $\log_{10}$ Pb contents in house dust and overburden samples (n=126), linear regression line and 95% confidence limits (dotted lines) [values in $\log_{10}$ ppm].
Σχ. 3.3. Διάγραμμα διασποράς των λογαριθμημένων τιμών (με βάση το 10) του Pb στα δείγματα σκόνης σπιτιών και εδαφικού καλύμματος (n=126), ευθεία της γραμμικής συμμεταβολής και τα όρια εμπιστοσύνης στο 95% επίπεδο (διακεκομμένες γραμμές) [τιμές σε $\log_{10}$ ppm].

Table 3.2. Linear regression analysis of house dust and overburden total lead (Pb) contents (n=126 pairs).
Πίνακας 3.2. Ανάλυση γραμμικής συμμεταβολής των ολικών συγκεντρώσεων του μολύβδου (Pb) στα δείγματα σκόνης σπιτιών και εδαφικού καλύμματος (n=126 ζεύγη).

Parameter	*Value*	*Estimate*	*Standard error*	*t-statistic*	*p-value*
Intercept		0.78120	0.24891	3.13851	0.0021
Slope		0.71129	0.06514	10.92020	0.0000
Correlation coefficient, R	0.70020				
R^2 %	49.02370				
Standard error of estimate	0.23151				

Table 3.3. One-way analysis of variance of house dust and overburden total lead (Pb) concentrations (n=126 pairs).
Πίνακας 3.3. Μονοπαραγοντική ανάλυση διασποράς των ολικών συγκεντρώσεων του μολύβδου (Pb) στα δείγματα σκόνης σπιτιών και εδαφικού καλύμματος (n=126 ζεύγη).

Source	Sum of squares	Degrees of freedom	Mean square	F-ratio	p-value
Model	6.39155	1	6.39155	119.25	0.0000
Residual	6.64614	124	0.05360		
Total (corr.)	13.03770	125			

3.7. DISTRIBUTION OF BLOOD-LEAD CONTENTS IN NURSERY AND PRIMARY SCHOOL-AGE CHILDREN

Biosensors, bioassays, biomarkers, biological indicators, bioindicators and *biological toxicity testing* are some of the terms used in the assessment of environmental contamination in biological or toxicological terms. Biological toxicity testing is based on exposing test organisms to all bioavailable chemicals in a test sample, and then noting the changes in biological activity (Ribo *et al.*, 1985; Wang *et al.*, 1998). Biological materials used are plants, animals, human hair, teeth, urine and blood. In the present study for Lavrion the biological tissue used, to assess the impact of environmental contamination on the human population, is child blood. There are also data on child urine (Eikmann *et al.*, 1991) and teeth (Stavrakis *et al.*, 1994b), which cannot be used in the geographical assessment of the effects of environmental contamination, due to lack of point data for urine, and sample location for teeth.

Map 3.6 shows the actual and interpolated blood-Pb (b-Pb) contents in 235 nursery and primary school age children in the Lavrion urban area, provided by the medical researchers of the last cross-sectional epidemiological study, which was carried out from the 1st to the 25th March 1988 (Makropoulos *et al.*, 1991, 1992a, b). On the map all the necessary features, required for interpretation of b-Pb levels, have been placed, such as metallurgical processing plants and their wastes, to interpret the blood-Pb levels.

Blood-Pb concentrations vary from 5.98 to 60.49 μg/100 ml, with a mean of 19.43 μg/100 ml and median of 17.83 μg/100 ml (C=43.44%). An astounding 95% of the children have b-Pb levels exceeding 10 μg/100 ml, the level of “concern” (US EPA, 1986, 1998; ATSDR, 1988). This is indeed worrying, but not unexpected, when overburden in the Lavrion urban area has total Pb concentrations varying from 810-151579 ppm (Map 3.4), and house dust 488-18617 ppm (Map 3.5).

Makropoulos *et al.* (1991) concluded that

- the highest b-Pb levels were in children living within a 500-m area around the large smelter at Kiprianos, *i.e.*, children attending the 3rd Primary School (see boxplot, Map 3.6);
- b-Pb contents decrease with increasing distance from the emitter;
- b-Pb levels in children living at a distance of 1500-m from the smelter are significantly higher than those of children living next to other kinds of industrial Pb sources, and
- boys have higher b-Pb contents than girls (Maravelias *et al.*, 1989), because they spent more time in playing outside games and do not observe rules of cleanliness as girls do (see boxplot, Map 3.6).

The first cross-sectional epidemiological study by Nakos (1985) related child b-Pb levels to distance from the smelter at Kiprianos, although she had data from her husband’s study about soil contamination (Nakos, 1979a, 1979b). The second cross-sectional epidemiological study on Lavrion children by Maravelias *et al.* (1989) mentioned, that according to bibliographic sources, Pb in dust and soil represents a significant source of Pb exposure for children. In the third, and final, cross-sectional epidemiological study, Makropoulos *et al.* (1991) assumed that high b-Pb levels in children are only due to emissions from the large metallurgical processing complex at Kiprianos, although they considered a number of other possible socio-economic confounding factors. They, therefore, obtained Lavrion ambient air Pb results, and also

samples for analysis of floor dust, sand pit material and surface soil from the 2nd & 4th Primary Schools, the school furthest away from the smelter (about 1500-m), and drinking water (Makropoulos *et al.*, 1991). The results of the Lavrion ambient air are tabulated in Table 3.4. Lead contents in the different materials collected from the 2nd & 4th Primary Schools were:

- 3780 ppm Pb in floor dust;
- 253.29 ppm Pb in sand pit material, and
- 10283.27 ppm Pb in surface soil outside the school.

Drinking water had a value of 3.4 μg Pb/litre, which was below CEC (50 μg Pb/l) and WHO (10 μg Pb/l) maximum admissible concentrations (CEC, 1980; WHO, 1993). It is stressed that Lavrion is linked, as from the 30th April 1984, to the Athens water supply network. Local ground-water water was used for potable purposes until 29th April 1984 (K.L. Pogkas, Lavrion Mayor, pers. commun., 1999) [Refer to Chapter 10 of this report].

Table 3.4. Lead contents in the Lavrion ambient air during 1987 and the first three months of 1988 (values in μg Pb/m^3) (from Makropoulos *et al.*, 1991).
Πίνακας 3.4. Συγκεντρώσεις μολύβδου στον ατμοσφαρικό αέρα του Λαυρίου για το 1987 και τους τρεις πρώτους μήνες του 1988 (τιμές σε μg Pb/m^3).

Period	*Mean*	*Minimum*	*Maximum*
1987	1.62	0.38	2.54
January, 1988	0.30	-	0.36
February, 1988	5.07	-	22.44
March, 1988	1.59	-	4.04

It was not possible to obtain details of ambient air measurements, despite attempts by different project scientists, such as all measurements of the period the station or stations was/were working, number of stations, height of sensors from ground surface, *etc.* Since, children are the group of main concern, the height of sensors from ground surface is especially important, for there is a definite stratification of the material transported by wind.

Lead contents in the ambient air of Lavrion show considerable variation in the monthly mean and maximal values (Table 3.4). They are all apparently well below the US Clean Air Act regulatory value of 1500 μg Pb/m^3 (Bingham and Lutkenhoff, 1990). Consequently, the validity of these measurements is questioned, and are not discussed further.

Makropoulos *et al.* (1991) did not realise the significance of Pb concentrations in floor dust and surface soil samples from the 2nd & 4th Primary School, which is situated at a distance of approximately 1500-m from the smelter at Kiprianos. Using equation 3.1, and the concentration of 10283.27 ppm Pb determined on soil outside the school, a value of 4315 ppm Pb has been calculated for school dust. This value differs by approximately 14% from the analytical value of 3780 ppm, which is an acceptable difference, after considering analytical and sampling errors, and the correlation coefficient of 0.7. A direct relationship between surface “soil” and house dust or floor dust is thus verified, within the limits of acceptable error variation. As it has been pointed out by many researchers, soil Pb and house dust Pb contribute much more to blood-Pb than does air Pb (Yankel *et al.*, 1977; Schmitt *et al.*, 1979; Roels *et al.*, 1980; Brunekreef *et al.*, 1981; Culbart *et al.*, 1983; Duggan, 1983; Brockhaus *et al.*, 1988;

Reagan and Silbergeld, 1990; Thornton *et al.*, 1990; Cotter-Howells and Thornton, 1991; Ferguson and Marsh, 1993; Watt *et al.*, 1993; Ferguson *et al.*, 1998). Hence, the geostatistical interpolation of actual b-Pb values was based on the knowledge of Pb distribution in overburden materials.

High b-Pb concentrations are indeed found within an 800-m radius from the main smelter at Kiprianos. In this area, however, an enormous amount of metallurgical processing wastes has been deposited. Houses either are built on or are very close to these wastes. Further, overburden materials, residual soil and house dust are seriously contaminated (Maps 3.4, 3.5). These confounding factors play a significant role in the high b-Pb levels of Lavrion children, *e.g.*,

- in the Prasini Alepou area they are attributed to the fact that houses are built on flotation tailings;
- to the south of the disused ore washing plant (central part of the map) they are mainly ascribed to (a) aeolian transportation of fine-grained flotation tailings, and (b) contaminated soil;
- to the north of the smelter in the Kavodokanos area they may be due to (a) contaminated soil, (b) smelter wastes, and (c) father working at the smelter;
- the single high b-Pb value on the coastal road in the Kavodokanos area is most likely due to (a) contaminated soil, and (b) proximity to metallurgical waste heaps; and
- the single high b-Pb value in the Thorikon area (north part of the map) is definitely attributed to (a) contaminated soil, and (b) proximity to the metallurgical waste heap.

It is quite apparent from the above description, that contaminated soil and the metallurgical processing wastes, play a significant role in the b-Pb contents of Lavrion children. There is clearly a correlation between the distribution of total soil Pb (Map 3.4) and b-Pb (Map 3.6). Generally, low b-Pb levels are found in areas where “soil” is not intensely contaminated, *e.g.*, (a) Panormos-Koukos-Neapoli-Ayios Andreas area, (b) Ayia Paraskevi-Nichtochori area, and (c) the area between Santorineika and Phenikodassos.

High Pb levels in overburden and house dust, the components in direct contact with children, are very significant to elevated b-Pb contents when such materials are inhaled or ingested by children. Although soil pica for Lavrion children was mentioned by medical researchers (Maravelias *et al.*, 1989), they did not realise its importance, and persisted to explain observed high b-Pb levels in children to smelter emissions (Makropoulos *et al.*, 1991). Recent studies on soil pica behaviour of children have shown that some children may ingest up to 25-60 grams of soil during a single day (Calabrese *et al.*, 1997). The US EPA on the other hand, for purposes of estimating potential health risks on children, assumed that most children ingest relatively small quantities of soil (*e.g.*, <100 mg/day), while the upper 95th percentile are estimated to ingest 200 mg/day on average (US EPA, 1996). As Calabrese *et al.* (1997) pointed out, soil ingestion studies normally last for about a week or less and, therefore, it is not possible to obtain a clear understanding of intra-individual variability in soil ingestion activity. Their model, however, which is based on their long experience in soil ingestion studies on children (Stanek and Calabrese, 1995) indicates that for 1-2 days/year

- 62% of children will ingest >1 g of soil,
- 42% of children will ingest >5 g of soil, and

- 33% of children will ingest >10 g of soil (Calabrese *et al.*, 1997).

Their conclusions are:

(a) for the majority of children, soil pica may occur only on a few days of the year, but much more frequently for others;
(b) soil pica, although highly variable, is an expected activity in a normal population of young children, rather than an unusual activity in a small subset of the population, and
(c) the implications of soil pica are significant for risk assessment.

In Lavrion, a moderate to strong northerly wind is blowing almost throughout the whole year. The comparatively dry climate for most months aids transportation of dust by wind. Fugitive dust, which is dust released from soil by the action of wind, with or without the assistance of mechanical disturbance (Ferguson *et al.*, 1998) is a major hazard in Lavrion. At the head height of a young child, fugitive dust appears to be considerable, for it was experienced on the face of the sampling team during kneeling down for overburden sampling. Particles of less than 10 μm diameter are normally assumed to be respirable; larger particles are trapped in the upper respiratory tract, from where they are expectorated or swallowed (Ferguson *et al.*, 1998). In a study of Pb exposure in young children from dust and soil in the United Kingdom, Thornton *et al.* (1990) estimated Pb uptake by a young child to be 36 μg Pb/day, of which 1 μg was by inhalation and 35 μg by ingestion.

It is quite apparent from the above discussion that Pb contents in “soil” and “dust” are important to exposure assessment of young children in Lavrion.

3.8. SEQUENTIAL EXTRACTION RESULTS ON OVERBURDEN AND HOUSE DUST SAMPLES

The biochemical and ecotoxicological significance of an element is associated with its specific chemical form and the prevailing local environmental factors (*e.g.*, climate, pH, Eh). Measurement of total element concentrations does not provide, however, enough information to estimate the bioavailable proportion of an element. Consequently, partial chemical extraction methods are used in an attempt to determine the bioavailable fraction. The sequential extraction procedure, developed by Tessier *et al.* (1979) and adapted by Li (1993) for use with ICP-AES, provides a useful analytical method, for the partitioning of particulate trace elements into five geochemical phases including, exchangeable, carbonate, hydrous iron and manganese oxide, organic and sulphides, and residual fractions.

The geochemical phases at each extraction step in the absence of detailed mineralogical studies, as pointed out by Li (1993), Hall *et al.* (1997) and Cohen *et al.* (1998), are largely *“operationally defined”*, and are relative rather than absolute chemical speciation. The amount of trace elements released being dependent on sample type, grain-size fraction chosen for analysis, the degree of crystallinity and purity of the mineral phases present, dissolution conditions (chemicals employed, sample to volume ratio) and digestion time (Hall *et al.*, 1997; Cohen *et al.*, 1998). Interpretation is based on solubility and bioavailability of Pb, rather than its actual mineralogy in overburden and house dust samples (the other elements are similarly treated in Chapters 7 & 8). Step 4, the oxidisable phase, is operationally defined as the organic and sulphide fraction (Tessier *et al.*, 1979), but it has been shown that primary sulphide minerals

(*e.g.*, galena, PbS) cannot be totally leached out in this step (Förstner, 1985). Nevertheless, the term *"organic/sulphide"* fraction is retained on Maps 3.7, 3.14, 7.1-7.30, 8.1-8.30 and in Chapter 2B. It should be regarded, however, as mainly extracting the organic fraction with a partial leach of primary sulphide minerals (Tessier and Cambell, 1989; Kim and Fergusson, 1991; Li, 1993).

3.8.1. PARTITIONING OF THE OPERATIONALLY DEFINED PHASES OF LEAD (Pb) IN OVERBURDEN

Map 3.7 is a comparative plot showing the partitioning patterns of the five operationally defined phases of Pb in overburden samples, *e.g.*, exchangeable (Pb1), carbonate (Pb2), reducible (Pb3), oxidisable (Pb4) and residual (Pb5), obtained by the sequential extraction procedure developed by Li (1993) from that of Tessier *et al.* (1979). Overburden Pb is mainly partitioned among three phases

- carbonate (64.8-58100 ppm Pb),
- reducible, which is associated with Fe-Mn oxides (240-30000 ppm Pb), and
- residual (207-65300 ppm Pb).

The carbonate and reducible phases appear to extract on average 20.62% and 31.99% respectively of the total Pb in overburden (Table 3.5, Fig. 3.4).

Lead in contaminated residual soil appears to be strongly associated with the carbonate phase (step 2; 64.80-58,100 ppm Pb) (Table 3.6, Fig. 3.5). Li (1993) has found a similar association in his study in the historical Pb smelting area in Derbyshire, United Kingdom. An identical behaviour is exhibited by Pb in the earthy material within slag (164-50,400 ppm Pb) (Table 3.8, Fig. 3.5), and pyritiferous sand samples from the Komobil area. The very high Pb levels in some samples of slag earth, and nearby residual soil, from and about the smelter area at Kiprianos, are explained by their association with carbonate minerals and other specific sites within slag minerals, and other wastes associated with the smelting activities. Comparatively high carbonate Pb contents are found in samples of flotation residues and nearby contaminated soil (Noria-Prasini Alepou-Santorineika-Ayios Andreas). In this case, Pb is mainly associated with carbonate minerals.

Apart from areas with pyritiferous sand, pH in overburden varies from 7.11-8.56. According to thermodynamic predictions cerussite ($PbCO_3$) would be the dominant Pb mineral at the prevailing Eh-pH in Lavrion overburden materials, including residual soil, *i.e.*, cerussite is stable at a pH above 6.0 (Garrels and Christ, 1965; Brookins, 1988; Li, 1993). Lead emissions from smelters have been shown to consist of Pb sulphate ($PbSO_4$), Pb monoxide (PbO) and Pb oxysulphate ($PbO.PbSO_4$) (Foster and Lott, 1980; Ferguson, 1990; Clevenger *et al.*, 1991). Clevenger *et al.* (1991) showed that 0.5 M NH_2OAc may dissolve up to 81% of PbO in soil. The reagent used in extraction step 2 (1 M NaOAc) has a similar strength. It can, therefore, be assumed that most Pb in the form of PbO may be extracted in this step. Hence, carbonates, sulphates and oxides may be the major chemical forms of Pb extracted in this step.

Table 3.5. Statistical parameters of the percentage proportion of lead (Pb) extracted by each of the five sequential extraction steps out of the total in overburden materials; the percentage proportion of combined exchangeable & carbonate phases is also tabulated.
Πίνακας 3.5. Στατιστικές παράμετροι της ποσοστιαίας αναλογίας του εκχυλιζομένου μολύβδου (Pb) στο κάθε στάδιο των διαδοχικών εκχυλίσεων στα δείγματα του εδαφικού καλύμματος. Αναγράφονται επίσης οι συνολικές ποσοστιαίες αναλογίες του αθροίσματος της ανταλλάξιμης και ανθρακικής φάσης.

Statistical parameters	*Exchangeable (%)*	*Carbonate (%)*	*Reducible (%)*	*Oxidisable (%)*	*Residual (%)*	*Exchangeable + Carbonate (%)*
Number of samples	224	224	224	224	224	224
Minimum	0.00	0.26	0.64	0.03	9.63	0.30
Maximum	3.29	49.92	73.64	27.19	94.86	50.32
Mean	0.16	20.62	31.99	9.29	37.95	20.77
Median	0.09	18.97	31.04	9.53	36.22	19.02
First quartile	0.06	12.75	26.61	5.06	27.44	12.85
Third quartile	0.17	28.19	36.53	12.92	45.78	28.45
Standard deviation	0.27	10.79	9.65	4.94	14.52	10.83

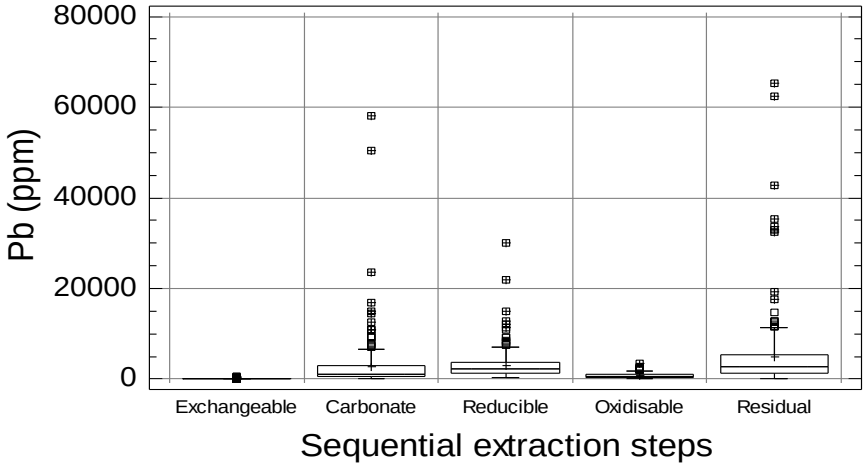

Fig. 3.4. Multiple boxplot of the distribution of overburden lead (Pb) in the five phases of the sequential extraction procedure (n=224).
Σχ. 3.4. Πολλαπλό θηκόγραμμα της κατανομής των συγκεντρώσεων του μολύβδου (Pb) στις πέντε φάσεις των διαδοχικών εκχυλίσεων στα δείγματα του εδαφικού καλύμματος (n=224).

Table 3.6. Statistical parameters of lead (ppm Pb) in ***contaminated soil*** samples for the five sequential extraction steps, combined exchangeable & carbonate phases and total contents.
Πίνακας 3.6. Στατιστικές παράμετροι του μολύβδου (ppm Pb) στα δείγματα ***ρυπασμένου εδάφους*** για τις πέντε φάσεις των διαδοχικών εκχυλίσεων, το άθροισμα της ανταλλάξιμης & ανθρακικής φάσης και τις ολικές συγκεντρώσεις.

Statistical parameters	*Exchangeable*	*Carbonate*	*Reducible*	*Oxidisable*	*Residual*	*Exchangeable +Carbonate*	*Total*
Number of samples	168	168	168	168	168	168	168
Minimum	0.30	64.80	423.00	34.80	207.00	65.40	810.40
Maximum	662.00	58100.00	30000.00	3350.00	62300.00	58762.00	151579.00
Mean	21.39	2269.20	2662.71	712.38	3466.91	2290.59	9132.59
Median	5.85	964.00	1955.00	550.50	2215.00	977.25	6081.60
First quartile	2.10	516.00	1230.00	343.50	1140.00	518.40	3358.15
Third quartile	15.45	2380.00	3115.00	932.50	3965.00	2397.50	11050.05
Standard deviation	64.29	5127.98	2922.63	516.21	5502.98	5187.46	13287.31
Coef. variation (%)	300.55	225.98	109.76	72.46	158.73	226.47	145.49

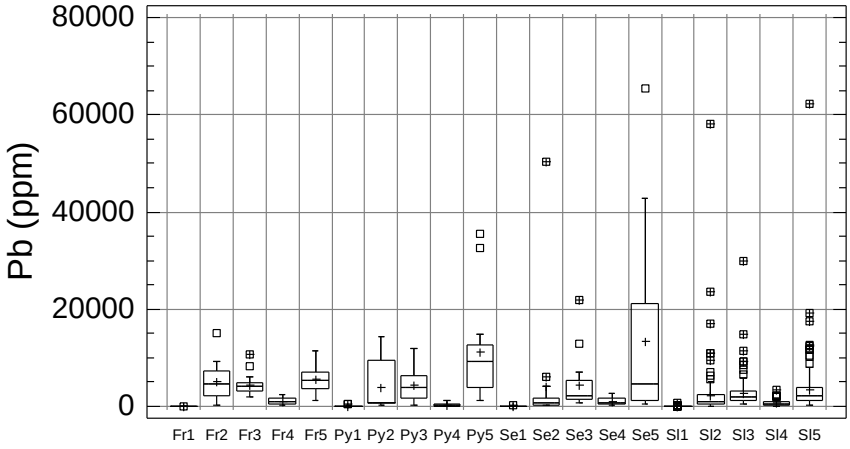

Fig. 3.5. Multiple boxplot of the distribution of lead (Pb) in the five phases (1-5) of the sequential extraction procedure in different sample types [Fr = Flotation residues; Py = pyritiferous sand; Se = earthy material within slag; Sl = contaminated soil].
Σχ. 3.5. Πολλαπλό θηκόγραμμα της κατανομής των συγκεντρώσεων του μολύβδου (Pb) στις πέντε φάσεις (1-5) των διαδοχικών εκχυλίσεων στους διαφορετικούς τύπους δειγμάτων [Fr = απορρίμματα επίπλευσης; Py = πυριτούχοι άμμοι; Se = γαιώδες υλικό σκουριών; Sl = ρυπασμένο έδαφος].

Table 3.7. Statistical parameters of lead (ppm Pb) in samples of ***flotation residues*** for the five sequential extraction steps, combined exchangeable & carbonate phases and total contents.
Πίνακας 3.7. Στατιστικές παράμετροι του μολύβδου (ppm Pb) στα δείγματα των ***απορριμμάτων επίπλευσης*** (σαβούρα) για τις πέντε φάσεις των διαδοχικών εκχυλίσεων, το άθροισμα της ανταλλάξιμης & ανθρακικής φάσης και τις ολικές συγκεντρώσεις.

Statistical parameters	*Exchangeable*	*Carbonate*	*Reducible*	*Oxidisable*	*Residual*	*Exchangeable +Carbonate*	*Total*
Number of values	26	26	26	26	26	26	26
Minimum	1.20	127.00	1950.00	338.00	1210.00	136.30	7256.20
Maximum	86.70	15000.00	10800.00	2450.00	11400.00	15030.90	32984.90
Mean	18.20	4996.42	4265.38	1091.35	5496.15	5014.63	15867.51
Median	14.25	4725.00	4145.00	909.50	5430.00	4773.00	16274.35
First quartile	8.70	2200.00	3050.00	555.00	3600.00	2207.50	9478.20
Third quartile	21.00	7180.00	4760.00	1640.00	7050.00	7192.30	19897.00
Standard deviation	16.41	3319.81	1917.37	610.07	2575.05	3324.92	6582.59
Coef. variation (%)	90.17	66.44	44.95	55.90	46.85	66.30	41.48

Table 3.8. Statistical parameters of lead (ppm Pb) in samples of ***earthy material within slag*** for the five sequential extraction steps, combined exchangeable and carbonate phases and total contents.
Πίνακας 3.8. Στατιστικές παράμετροι του μολύβδου (ppm Pb) στα δείγματα του γαιώδες υλικού των σκουριών για τις πέντε φάσεις των διαδοχικών εκχυλίσεων, το άθροισμα της ανταλλάξιμης & ανθρακικής φάσης και τις ολικές συγκεντρώσεις.

Statistical parameters	*Exchangeable*	*Carbonate*	*Reducible*	*Oxidisable*	*Residual*	*Exchangeable +Carbonate*	*Total*
Number of samples	16	16	16	16	16	16	16
Minimum	0.30	164.00	762.00	277.00	477.00	164.30	2538.30
Maximum	330.00	50400.00	21900.00	2660.00	65300.00	50730.00	117670.00
Mean	27.34	4215.81	4478.44	1054.63	13297.63	4243.16	23073.84
Median	6.75	708.00	2155.00	609.00	4575.00	717.35	10062.10
First quartile	2.25	319.00	1575.00	394.50	1200.00	326.95	4282.25
Third quartile	10.80	1730.00	5405.00	1695.00	21155.00	1736.30	26914.60
Standard deviation	80.92	12399.43	5587.76	851.10	19468.24	12479.68	31847.46
Coef. of variation (%)	295.94	294.12	124.77	80.70	146.40	294.11	138.02

Table 3.9. Statistical parameters of lead (ppm Pb) in samples of ***pyritiferous sand*** for the five sequential extraction steps, combined exchangeable and carbonate phases and total contents.
Πίνακας 3.9. Στατιστικές παράμετροι του μολύβδου (ppm Pb) στα δείγματα ***πυριτούχων άμμων*** για τις πέντε φάσεις των διαδοχικών εκχυλίσεων, το άθροισμα της ανταλλάξιμης & ανθρακικής φάσης και τις ολικές συγκεντρώσεις.

Statistical parameters	*Exchangeable*	*Carbonate*	*Reducible*	*Oxidisable*	*Residual*	*Exchangeable +Carbonate*	*Total*
Number of samples	14	14	14	14	14	14	14
Minimum	0.30	223.00	240.00	2.40	1310.00	223.30	3810.70
Maximum	580.00	14400.00	12000.00	1140.00	35400.00	14465.70	56390.00
Mean	98.34	3927.71	4339.29	338.13	11119.29	4026.05	19822.75
Median	6.00	776.50	3825.00	207.50	9150.00	841.40	14477.05
First quartile	1.80	619.00	1690.00	7.40	3930.00	620.80	7353.20
Third quartile	120.00	9530.00	6360.00	555.00	12700.00	9650.00	31220.80
Standard deviation	175.89	5301.75	3263.62	381.29	10594.16	5365.17	15642.57
Coef. of variation (%)	178.87	134.98	75.21	112.76	95.28	133.26	78.91

The reducible phase (step 3) is associated with Fe-Mn oxides, and is the second significant fraction of Pb in overburden with extractions up to 73.64% of the total concentrations (Table 3.5, Fig. 3.4). Iron-manganese oxides are important scavengers of heavy metals in soil, and particularly at high pH ranges (Chao, 1984; Tipping *et al.*, 1986). Considering, however, the high carbonate (calcite, $CaCO_3$) in overburden (see Chapter 7 & Map 7.8 for the Ca partitioning patterns), the second extraction step [1 M NaOAc, pH 5.0] may not be effective in the removal of all carbonate minerals into solution, an observation noted by other researchers (Tessier *et al.*, 1979; Jouanneau *et al.*, 1983; Pickering, 1986; Kheboian and Bauer, 1987; Li, 1993). It is, therefore, possible that remaining carbonate minerals may be placed into solution in step 3, when the more acidic reagent $NH_2OH.HCl$ in 25% HOAc is used. This appears to be the case, as shown by the partitioning patterns of calcium (Map 7.8), *i.e.*, step 3 extracting most of the carbonate. Consequently, the reducible phase (step 3) may contain a proportion of Pb carbonate as well as the form bound to Fe-Mn oxides (Tables 3.6-3.9; Figs. 3.4, 3.5). An overlap between extraction steps 2 and 3 is quite apparent from the patterns of Pb and Ca (Maps 3.7, 7.8). The reducible phase appears to be a significant extraction phase of Pb in samples of slag earth (Table 3.8; Fig. 3.5) and residual soil, from and about the smelter area at Kiprianos, pyritiferous sand from Komobil (Table 3.9; Fig. 3.5), flotation residues (Table 3.7; Fig. 3.5) and nearby contaminated soil from Noria-Prasini Alepou-Santorineika-Ayios Andreas. In fact, high reducible Pb levels occur in almost the same samples with high carbonate Pb contents.

The oxidisable phase (step 4) is associated with the organic/sulphide fraction, and appears to extract up to 27.19% (mean 9.29%) of total Pb in overburden (2.4-3350 ppm Pb) (Tables 3.5-3.9; Fig. 3.4). All sample types appear to behave in a similar way in this extraction step. It is quite apparent that the oxidisable phase is of minor importance for Pb extraction in comparison to the carbonate, oxidisable and residual phases.

The last extraction, residual phase (step 5: $HF/HClO_4/HNO_3$), accounts for 9.63-94.86% (mean 37.95%) of total Pb in overburden samples. This fraction may represent Pb held in primary minerals, such as galena [PbS], and possibly pyromorphite $[(PbCl)Pb_4(PO_4)_3]$ (Cotter-Howells and Thornton, 1991), in the contaminated overburden materials (see the partitioning patterns of phosphorus in Chapter 7, Map 7.21). The residual phase appears to be important to earthy material within slag, and residual soil over or near to slag heaps (Map 3.7). The greatest Pb contents are extracted in this step (up to 65300 ppm, mean 13298 ppm;

Table 3.8). High Pb concentrations in the residual fraction reflect the nature of contamination from the slag, which has a high Pb content.

The exchangeable phase (step 1) accounts for a very small proportion (up to 3.9%) of total Pb in overburden (0.3-662 ppm) (Tables 3.5-3.9; Figs. 3.4-3.5). Emissions of Pb from the smelters and the Pb-acid battery plant should be the major components of the exchangeable fraction. If this is really the case, then Pb contamination from actual emissions is indeed very small or have been completely masked, since the closure of the smelter in 1989 by the transportation of fugitive dust *etc.* This step appears to be the most significant for Pb in anglesite [$PbSO_4$] (Harrison *et al.*, 1981; Clevenger *et al.*, 1991). Lead in this fraction may represent its sulphate phase in the smelting areas of Lavrion. The proportion of Pb in the exchangeable phase decreases with increase of overburden pH (Fig. 3.6), a feature also found by Li (1993) in his study of contaminated soil in the historical smelting area of Derbyshire, U.K. In the pyritiferous sand area, where the pH is comparatively low, step 1 extracts up to 580 ppm Pb (Table 3.9; mean 98.34 ppm, third quartile 120 ppm).

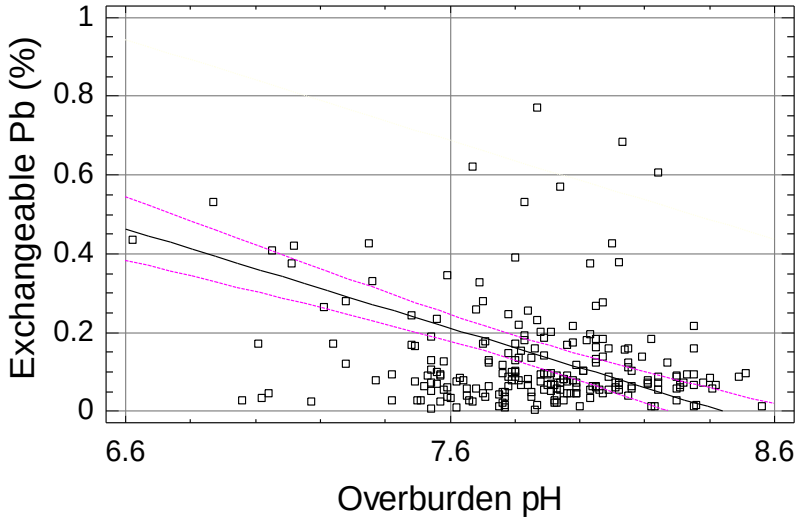

Fig. 3.6. Scatter plot of the percentage proportion of exchangeable Pb extracted from the total overburden Pb in relation to pH (n=224); linear regression line (r= -0.47) and 95% confidence limits (dotted lines).
Σχ. 3.6. Διάγραμμα διασποράς της εκατοστιαίας αναλογίας του ανταλλάξιμου Pb στα δείγματα εδαφικού καλύμματος σε σχέση με το pH (n=224), ευθεία γραμμικής συμμεταβολής και τα όρια εμπιστοσύνης στο 95% επίπεδο (διακεκομμένες γραμμές).

3.8.1.1. Spatial distribution of overburden lead (Pb) in the different operationally defined phases of sequential extraction

The purpose of plotting geochemical distribution maps of overburden Pb for the five operationally defined phases of the sequential extraction procedure (exchangeable, carbonate, reducible, oxidisable, residual, and combined exchangeable-carbonate) was to study the anthropogenic influence and patterns in overburden materials. It is stressed that geogenic patterns, even in residual soil, have completely been eradicated by the intense contamination, as has already been shown by total Pb distribution in overburden (Map 3.4) in comparison to primary Pb distribution in rock samples (Map 3.1).

Experimental and modelled variogram surfaces (Maps 3.8-3.13, insets) show the spatial structural characteristics of overburden Pb distribution in the different operationally defined phases of the sequential extraction scheme. The spatial distribution of exchangeable, carbonate, combined exchangeable & carbonate, reducible and residual Pb in overburden is influenced by the major NE-SW orientation of the flotation residues, and the minor NW-SE trend of again the flotation tailings, slag heaps and pyritiferous tailings (Maps 3.8-3.11, 3.13). Oxidisable Pb in overburden, because of its association with sulphides, exhibits a strong geostatistical NW-SE trend (Map 3.12), which is the orientation of pyritiferous tailings on the beach from Komobil to Kiprianos (Map 2.3), and other pyritiferous wastes.

3.8.1.1.1. Distribution of exchangeable lead (Pb) in overburden (Map 3.8)

The geochemical distribution of exchangeable Pb in overburden shows that concentrations between 120-662 ppm mainly occur in the premises of the smelter at Kiprianos. Exchangeable Pb levels between 7-120 ppm are found in inhabited areas, which are covered by residual or alluvial “soil”, flotation residues, slag and pyritiferous tailings.

Exchangeable Pb, since it is loosely held by overburden materials, may be associated with

(a) emissions from smelters (refer to stacks) and Pb-acid battery factory in the Noria area,
(b) fugitive dust from metallurgical processing wastes that have contaminated residual and alluvial soil, and
(c) fugitive dust from contaminated residual and alluvial soil, and
(d) the fine-grained portion of metallurgical wastes and contaminated soil.

The last three associations are considered to be the most significant, since the closure of the smelter in 1989, although the Pb-acid battery factory still releases hazardous emissions. Even though the exchangeable phase accounts for only a small proportion (up to 3.9%; Table 3.5) of the total Pb in overburden, the extracted amount (0.3-662 ppm) is readily available at a pH of 7.0. About 45% of the study area has Pb concentrations of 7-120 ppm, which are easily available to plants, animals and humans.

Emissions from the smelters and Pb-acid battery factory were expected to play a significant role in the shape of the exchangeable Pb geochemical distribution patterns in overburden materials. It is, however, difficult to solely ascribe the resulting patterns to emissions from these industrial sources. The influence exerted by the loosely bound Pb held on the metallurgical processing wastes and residual soil, due to other processes of deposition, is very great, and essentially masks emission patterns.

3.8.1.1.2. Distribution of carbonate lead (Pb) in overburden (Map 3.9)

Carbonate phase Pb contents in overburden between 9500-58100 ppm mainly occur in the smelter area at Kiprianos and its immediate surroundings. In the inhabited area, covered by flotation residues, carbonate Pb levels vary from 1175-14400 ppm. Residential and agricultural areas with residual soil have carbonate Pb concentrations ranging from 65-9500 ppm.

Carbonate Pb in overburden could be made available at and below a pH of 5. Hence, at the slightly acid conditions prevailing in the root area of plants, a proportion of carbonate Pb is available for absorption. It is also available to animals and humans through inhalation and ingestion of contaminated overburden.

Geochemical carbonate Pb distribution patterns in overburden samples are strongly influenced by the NE-SW and NW-SE orientation of the flotation residues, and the NE-SW trend of slag in the smelter area at Kiprianos.

3.8.1.1.3. Distribution of combined exchangeable & carbonate lead (Pb) in overburden (Map 3.10)

Combined exchangeable & carbonate Pb concentrations in overburden, as has already been mentioned, are considered to represent the readily available Pb to plants, animals and humans. Combined exchangeable and carbonate Pb concentrations of 65-14466 ppm in overburden materials occur in the residential and agricultural areas of Lavrion. Geochemical distribution patterns of combined exchangeable & carbonate overburden Pb are strongly influenced by the NE-SW and NW-SE orientations of flotation tailings, and the NE-SW trend of slag in the smelter area at Kiprianos.

3.8.1.1.4. Distribution of reducible lead (Pb) in overburden (Map 3.11)

The highest reducible Pb concentrations in overburden occur in the smelter area at Kiprianos and its immediate surroundings (5540-30000 ppm). Reducible Pb levels of 2235-11400 ppm occur in the area covered by the flotation tailings. Residual soil has reducible Pb contents of 240-8050 ppm.

Residential and agricultural areas have reducible Pb concentrations in overburden varying from 240 to 11400 ppm. This form of Pb is operationally associated with Fe-Mn oxides, and may be made available under reducing conditions and a pH between 2.0 and 5; it has already been mentioned that due to incomplete solution of carbonates in Step 2, part of the extracted Pb in this phase is associated with carbonates. Trace elements associated with precipitated Mn and Fe oxides are in different forms (Pickering, 1986), *i.e.*,

- loosely adsorbed (exchangeable),
- moderately fixed (*e.g.*, with amorphous oxides), and
- strongly bound (*e.g.*, occluded in goethite, lepidocrocite and other oxide minerals).

Availability of these forms is dependent on pH and Eh conditions. Loosely adsorbed Pb on Fe-Mn oxides is the form easily available as pH is being reduced below 5.0. Moderately fixed and strongly bound Pb is released at pH conditions approaching a value of 2.0. At the prevailing pH conditions of over 6.87 for 97.5% of the study area, the reducible Pb is not available (Map 2.5). This fraction is possibly available only in areas covered by pyritiferous tailings, which have a low pH. Reducible Pb contents of 240-8050 ppm could, however, be made available to animals and humans, when contaminated materials are inhaled or ingested (*i.e.*, gastric fluids have a pH of 1.5-2.5).

Geochemical distribution patterns of reducible overburden Pb are strongly influenced by the NE-SW and NW-SE orientations of flotation tailings, and the NE-SW trend of slag in the smelter area at Kiprianos.

3.8.1.1.5. Distribution of oxidisable lead (Pb) in overburden (Map 3.12)

The spatial distribution pattern of oxidisable Pb in overburden is strongly influenced by the NW-SE orientation of pyritiferous tailings on the beach between Komobil and Kiprianos. Although the pyritiferous wastes have the dominant geostatistical structural feature, they have the lowest Pb concentrations (2 to 1610 ppm). The greatest Pb contents (990-3350 ppm) appear to be in the earthy material within the slag in the Fougara area, and residual soil to the south of the smelter at Kiprianos, which may be influenced by the nearby pyritiferous tailings. Elevated Pb levels, in residual and alluvial soil occur in the Thorikon area (990-2230 ppm).

Flotation tailings have Pb concentrations of 577-1860 ppm, and residual soil from 2 to 2230 ppm. Oxidisable Pb contents (2-3350 ppm) may be made available under oxidising conditions and a pH at or lower than 2.0. Although this fraction is not available to plants, it may be available to animals and humans, when contaminated materials are inhaled or ingested, since gastric fluids have a pH of 1.5 to 2.5, and a completely empty stomach has a pH of 1.0.

3.8.1.1.6. Distribution of residual lead (Pb) in overburden (Map 3.13)

The spatial distribution pattern of residual Pb in overburden is definitely associated with the earthy material within slag and residual soil, which has been contaminated by slag material, *e.g.*, Fougara area and smelter at Kiprianos. The greatest Pb levels occur in these two areas (5365-65300 ppm). As it has been pointed out by Li (1993), a high percentage of Pb in the residual fraction and its definite association with slag, indicates that slag possesses a high Pb content.

Occurrence of high residual phase Pb contents in pyritiferous tailings at Komobil, Nichtochori and Kiprianos (smelter area) indicate that pyrite is moderately decomposed in step 4 (oxidisable phase) (Pickering, 1986). High residual Pb contents in flotation tailings in the Noria to Santorineika area (5365-33000 ppm) and "soil" (207-12700 ppm) may be associated with alumino-silicates (clays and quartz).

3.8.2. PARTITIONING OF THE OPERATIONALLY DEFINED PHASES OF LEAD (Pb) IN HOUSE DUST

Map 3.14 is a comparative plot showing the partitioning of the five operationally defined phases of Pb in house dust, *e.g.*, exchangeable (Pb1), carbonate (Pb2), reducible (Pb3), oxidisable (Pb4) and residual (Pb5). Lead in house dust, appears to behave in a similar manner to overburden Pb, and is mainly partitioned among the same three phases:

- carbonate (107-6880 ppm Pb),
- reducible, which is associated with Fe-Mn oxides (200-6030 ppm Pb), and
- residual (126-5820 ppm Pb).

The carbonate, reducible and residual phases extract on average 21.52%, 37.59% and 33.07% respectively of the total Pb in house dust (Table 3.10, Fig. 3.7).

Comparison of partitioning patterns of the operationally defined phases of Pb between samples of house dust (Map 3.14) and overburden (Map 3.7), show similarities with respect to the percentage of Pb extracted by the exchangeable (step 1), carbonate

(step 2) and residual (step 5) phases (Fig. 3.8). This is discerned from the almost overlapping notches of boxplots, *i.e.*, if two notches for any pair of medians overlap, there is not a statistically significant difference between the medians at the 95% confidence level (Kürzl, 1988; Manugistics, 1997). If, however, two notches for any pair of medians do not overlap, as is the case with the reducible (step 3) and oxidisable (step 4) phases of Pb in house dust and overburden, there is a statistically significant difference between the medians at the 95% confidence level. The geochemical inferences from these statistical observations about the extractability of Pb by the different sequential extraction steps are:

(a) house dust Pb in the exchangeable, carbonate and residual fractions appears to retain most of the physico-chemical characteristics of overburden source materials, and
(b) house dust and overburden Pb in the reducible and oxidisable fractions are associated with Fe-Mn oxides and organic matter/sulphides respectively, which are phases susceptible to changes in environmental conditions. As pointed out by Hall (1998) the relative importance of Fe and Mn oxides as scavengers will depend upon (i) pH-Eh conditions; (ii) degree of crystallinity of the oxides and, hence, their reactivity; (iii) their relative abundance, and (iv) the presence of organic matter as a competing adsorbing and chelating fixing agent. Since, environmental conditions are different between the two sampling media, differences are expected.

In terms of absolute Pb concentrations, the partitioning patterns between house dust and overburden samples are very different (Fig. 3.9). In all cases, Pb levels are higher in samples of overburden than the corresponding house dust samples.

The above are general observations and inferences, which are made for the whole house dust data set. A more detailed picture is given by Fig. 3.10 and Tables 3.11 to 3.13, where house dust samples are classified according to the location of the house, *i.e.*, over pyritiferous tailings, flotation residues, earthy material within slag and contaminated soil. In this classification, it is assumed that the greatest proportion of dust, within the house, is derived from its immediate vicinity. This assumption is based on the moderate to strong wind blowing throughout the year, and the large parts of land in the Lavrion urban area with no vegetation (Map 2.4), which are exposed to deflation. Airborne dust is, therefore, considered to be a major contributor to house dust. Other possible sources of domestic dust, which are not taken into account in the following discussion, are: (a) dust brought at home on clothes, (b) dust from household furniture (paint), carpets, cloths, *etc.*, (c) industrial emissions, (d) automobile emissions, (e) cigarette smoke, *etc.*

According to their location, there are 101 houses over contaminated soil, 21 houses over flotation residues, 4 houses over slag and earthy material within slag, and 1 house over pyritiferous tailings (Map 3.14; Tables 3.11-3.13).

Indoor dust Pb concentrations of exchangeable, carbonate, combined exchangeable & carbonate, and reducible fractions are greater in houses over the area with the flotation residues, followed by houses over contaminated residual soil, and earthy material within slag (Tables 3.11-3.13; Fig. 3.10; Map 3.14). Combined exchangeable & carbonate contents between 410-6896 ppm Pb in dust of houses over the flotation tailings, 115-3575 ppm Pb over contaminated residual soil, and 219-670 ppm Pb over slag, are readily available to tenants if they inhale or ingest indoor dust.

Lead levels in indoor dust, extracted by the oxidisable and residual phases, are higher in houses over contaminated soil, followed by houses over flotation residues, and slag.

It appears that residential areas over the flotation residues are at greater risk, than over contaminated soil and slag.

Table 3.10. Statistical parameters of the percentage proportion of lead (Pb) extracted by each of the five sequential extraction steps out of the total in house dust; the percentage proportion of the combined exchangeable & carbonate phases is also tabulated.
Πίνακας 3.10. Στατιστικές παράμετροι της ποσοστιαίας αναλογίας του εκχυλιζομένου μολύβδου (Pb) στο κάθε στάδιο των διαδοχικών εκχυλίσεων στα δείγματα της σκόνης σπιτιών. Αναγράφονται επίσης οι συνολικές ποσοστιαίες αναλογίες του αθροίσματος της ανταλλάξιμης και ανθρακικής φάσης.

Statistical parameters	*Exchangeable (%)*	*Carbonate (%)*	*Reducible (%)*	*Oxidisable (%)*	*Residual (%)*	*Exchangeable +Carbonate (%)*
Number of samples	127	127	127	127	127	127
Minimum	0.00	4.19	22.59	0.23	16.71	4.29
Maximum	3.11	40.49	63.69	14.26	56.42	41.00
Mean	0.63	21.52	37.39	7.38	33.07	22.15
Median	0.45	21.19	37.31	7.06	33.21	22.55
First quartile	0.26	17.57	34.01	5.16	28.59	18.05
Third quartile	0.83	25.21	39.75	9.29	37.54	25.61
Standard deviation	0.59	6.64	6.00	2.62	6.95	6.67

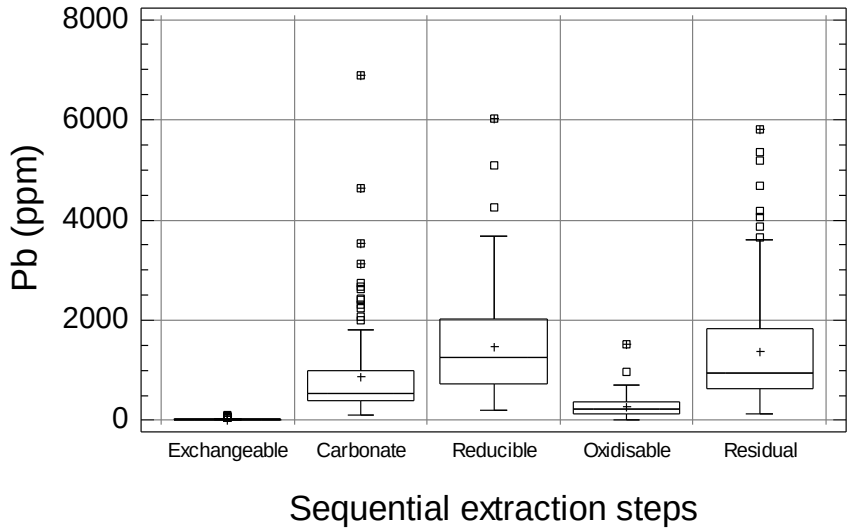

Fig. 3.7. Multiple boxplot of the distribution of house dust lead (Pb) in the five phases of the sequential extraction procedure (n=127).
Σχ. 3.7. Πολλαπλό θηκόγραμμα της κατανομής των συγκεντρώσεων του μολύβδου (Pb) στις πέντε φάσεις των διαδοχικών εκχυλίσεων των δειγμάτων σκόνης σπιτιών (n=127).

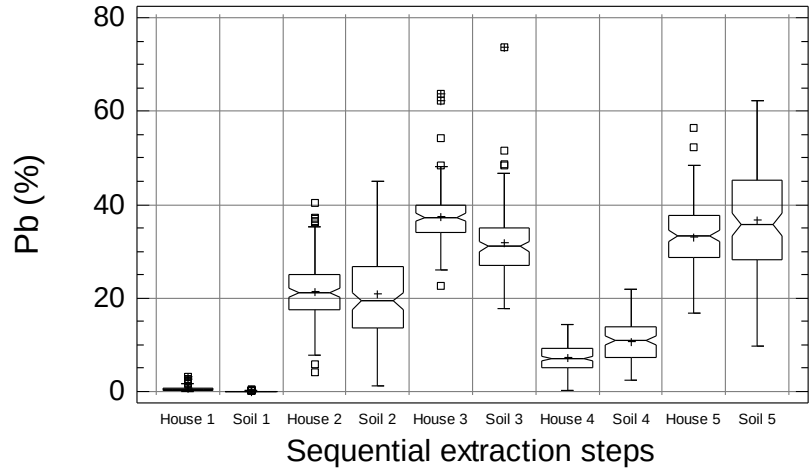

Fig. 3.8. Multiple boxplot comparison of the percentage proportion of Pb, in relation to the total contents, extracted by each of the five sequential extraction phases (1-5) from samples of indoor dust (House) and overburden (Soil) from the same houses (n=126).
Σχ. 3.8. Πολλαπλό θηκόγραμμα με εγκοπές της ποσοστιαίας αναλογίας του Pb σε σχέση με την ολική συγκέντρωση για κάθε μία από τις πέντε (1-5) φάσεις των διαδοχικών εκχυλίσεων στα δείγματα σκόνης σπιτιών (House) και των αντίστοιχων του εδαφικού καλύμματος (Soil) από τα ίδια σπίτια (n=126).

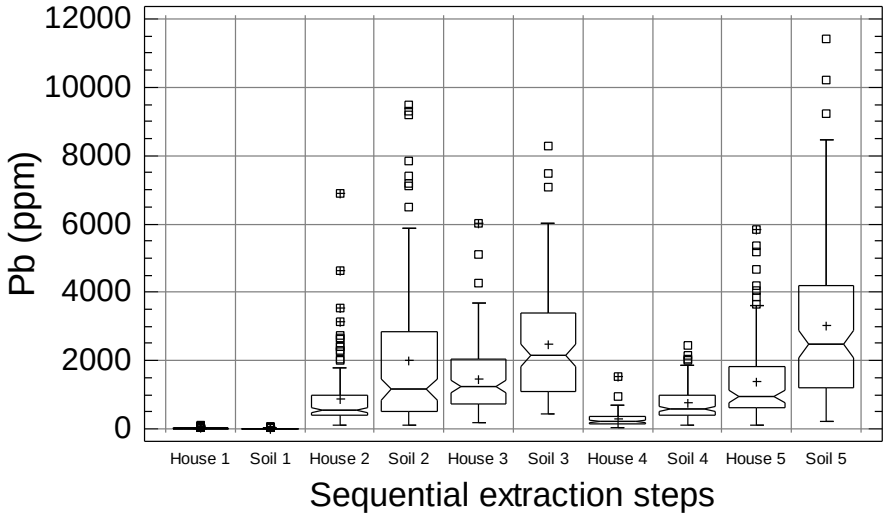

Fig. 3.9. Multiple boxplot comparison of Pb contents extracted by each of the five sequential extraction phases (1-5) from samples of indoor dust (House) and overburden (Soil) from the same houses (n=126).
Σχ. 3.9. Πολλαπλό θηκόγραμμα με εγκοπές των συγκεντρώσεων του Pb για κάθε μία από τις πέντε φάσεις (1-5) των διαδοχικών εκχυλίσεων στα δείγματα της σκόνης σπιτιών (House) και των αντίστοιχων του επιφανειακού καλύμματος (Soil) από τα ίδια σπίτια (n=126).

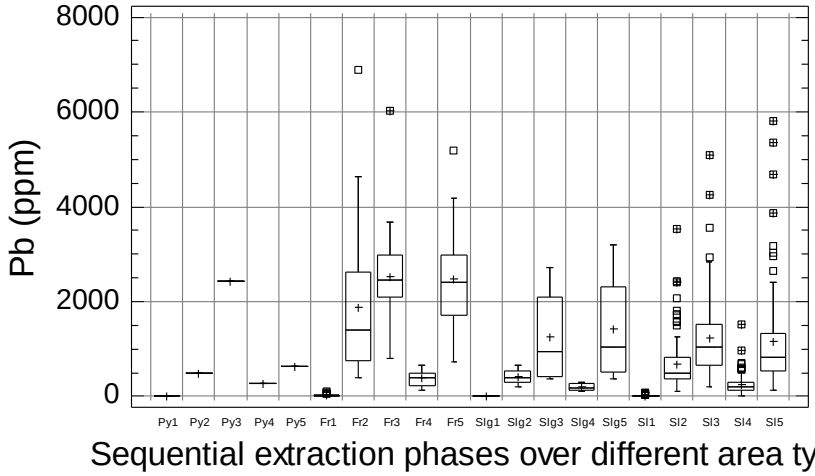

Fig. 3.10. Multiple boxplot of the distribution of indoor dust lead (Pb) in the five phases (1-5) of the sequential extraction procedure in houses built over the metallurgical processing wastes or contaminated soil [Py = pyritiferous sand; Fr = Flotation residues; Slg = Slag and earthy material within slag; Sl = contaminated soil].

Σχ. 3.10. Πολλαπλό θηκόγραμμα της κατανομής των συγκεντρώσεων του μολύβδου (Pb) στις πέντε φάσεις (1-5) των διαδοχικών εκχυλίσεων στα δείγματα σκόνης σπιτιών κτισμένων πάνω σε μεταλλουργικά απορρίμματα ή σε ρυπασμένο έδαφος [Py = πυριτούχοι άμμοι; Fr = απορρίμματα επίπλευσης; Slg = σκουριές και γαιώδες υλικό σκουριών; Sl = ρυπασμένο έδαφος].

Table 3.11. Statistical parameters of indoor dust lead (ppm Pb) in houses built over ***contaminated soil*** for the five sequential extraction steps, combined exchangeable & carbonate phases and total contents.

Πίνακας 3.11. Στατιστικές παράμετροι των συγκεντρώσεων του μολύβδου (ppm Pb) στα δείγματα σκόνης σπιτιών κτισμένων πάνω σε ***ρυπασμένο έδαφος*** για τις πέντε φάσεις των διαδοχικών εκχυλίσεων, το άθροισμα της ανταλλάξιμης & ανθρακικής φάσης και τις ολικές συγκεντρώσεις.

Statistical parameters	*Exchangeable*	*Carbonate*	*Reducible*	*Oxidisable*	*Residual*	*Exchangeable +Carbonate*	*Total*
Number of samples	101	101	101	101	101	101	101
Minimum	0.50	107.00	200.00	19.20	126.00	115.10	488.10
Maximum	88.20	3530.00	5100.00	1530.00	5820.00	3575.00	11649.50
Mean	17.90	692.57	1236.59	253.86	1149.62	710.47	3350.55
Median	13.20	498.00	1040.00	202.00	834.00	523.40	2655.30
First quartile	8.70	379.75	653.75	127.00	536.25	390.95	1808.40
Third quartile	22.35	826.75	1540.00	298.00	1342.50	848.75	4221.35
Standard deviation	15.11	551.17	858.21	212.53	1020.61	556.22	2356.98
Coef. variation (%)	84.44	79.58	69.40	83.72	88.78	78.29	70.35

Table 3.12. Statistical parameters of indoor dust lead (ppm Pb) in houses built over ***flotation residues*** for the five sequential extraction steps, combined exchangeable & carbonate phases and total contents.
Πίνακας 3.12. Στατιστικές παράμετροι του μολύβδου (ppm Pb) στα δείγματα σκόνης σπιτιών κτισμένων πάνω σε ***απορρίμματα επίπλευσης (σαβούρα)*** για τις πέντε φάσεις των διαδοχικών εκχυλίσεων, το άθροισμα της της ανταλλάξιμης & ανθρακικής φάσης και τις ολικές συγκεντρώσεις.

Statistical parameters	*Exchangeable*	*Carbonate*	*Reducible*	*Oxidisable*	*Residual*	*Exchangeable +Carbonate*	*Total*
Number of samples	21	21	21	21	21	21	21
Minimum	5.00	396.00	813.00	138.00	719.00	409.50	2155.50
Maximum	108.00	6880.00	6030.00	650.00	5190.00	6895.50	18616.50
Mean	27.45	1885.05	2537.76	387.14	2471.00	1912.50	7308.40
Median	18.50	1390.00	2450.00	389.00	2409.97	1423.00	6644.40
First quartile	13.28	720.00	1965.00	217.00	1585.00	727.58	5059.53
Third quartile	28.95	2640.00	3010.00	511.75	3127.50	2655.15	8882.95
Standard deviation	25.67	1588.70	1118.74	162.02	1187.78	1592.03	3791.99
Coef. variation (%)	93.53	84.28	44.08	41.85	48.07	83.24	51.89

Table 3.13. Statistical parameters of house dust lead (ppm Pb) over areas with ***slag and earthy material within slag*** for the five sequential extraction steps, combined exchangeable and carbonate phases and total contents.
Πίνακας 3.13. Στατιστικές παράμετροι του μολύβδου (ppm Pb) στα δείγματα σκόνης σπιτιών που βρίσκονται σε περιοχές με ***σκουριές και γαιώδες υλικό των σκουριών*** για τις πέντε φάσεις των διαδοχικών εκχυλίσεων, το άθροισμα της ανταλλάξιμης & ανθρακικής φάσης και τις ολικές συγκεντρώσεις.

Statistical parameters	*Exchangeable*	*Carbonate*	*Reducible*	*Oxidisable*	*Residual*	*Exchangeable +Carbonate*	*Total*
Number of samples	4	4	4	4	4	4	4
Minimum	7.20	210.00	374.00	117.00	378.00	219.30	1161.30
Maximum	15.30	659.00	2720.00	305.00	3200.00	670.10	6626.20
Mean	10.73	409.25	1250.25	196.00	1416.75	419.98	3282.98
Median	10.20	384.00	953.50	181.00	1044.50	395.25	2672.20
First quartile	8.25	292.00	410.50	128.00	523.50	304.30	1408.30
Third quartile	13.20	526.50	2090.00	264.00	2310.00	535.65	5157.65
Standard deviation	3.44	185.79	1098.06	85.83	1267.30	186.30	2482.80
Coef. variation (%)	32.09	45.40	87.83	43.79	89.45	44.36	75.63

3.8.2.1. Spatial distribution of house dust lead (Pb) in the different operationally defined phases of sequential extraction

The purpose of plotting geochemical distribution maps of house dust Pb for the five operationally defined phases of the sequential extraction procedure (exchangeable, carbonate, reducible, oxidisable, residual, and combined exchangeable-carbonate) was twofold. First, to study the spatial distribution of Pb in indoor dust for each of the five sequential extraction phases and combined & exchangeable and, second, to compare patterns between house dust and overburden.

Sensible experimental and modelled variogram surfaces could not be obtained for house dust Pb and, consequently, the spatial structural characteristics of Pb distribution in overburden samples, in the different operationally defined phases of the sequential extraction scheme, were used. As was mentioned above, house dust Pb, in the exchangeable, carbonate and residual fractions, appears to retain most of the physico-chemical characteristics of overburden source materials in terms of extractability.

Distinct differences exist, however, for house dust and overburden Pb in the reducible and oxidisable fractions. Consequently, the majority of house dust Pb phases may have similar geostatistical characteristics to their corresponding overburden Pb phases.

3.8.2.1.1. Distribution of exchangeable lead (Pb) in house dust (Map 3.15)

The geochemical distribution of exchangeable Pb in house dust shows that concentrations between 23.7-108 ppm occur over flotation tailings in the Prasini Alepou area, and contaminated soil at Kavodokanos. Exchangeable house dust Pb levels between 23.7-60.3 ppm are found in areas over flotation residues between Noria and Prasini Alepou, and contaminated soil and pyritiferous tailings between Ayios Andreas and Komobil. High exchangeable Pb levels in household dust to the south of the flotation tailings in the Santorineika area towards Ayios Andreas, are most likely due to dust from the flotation tailings heap behind the sports area and secondary school (Photos 12 & 13, Volume 2 of this report).

The distribution of exchangeable house dust Pb, in the Kavodokanos area, appears to be related to dust from the slag heap (Photos 16, 18-20). Elevated Pb values in the Thorikon area, near a slag heap, indicate a possible hazard from this material.

The very low exchangeable house dust Pb levels in Ayia Paraskevi and Phenikodassos are noted, since the source materials are the nearby slag heaps, only a limited amount of Pb is extracted in this step (refer to Maps 3.16-3.20).

Exchangeable house dust Pb accounts for only a small proportion (up to 3.11%; Table 3.10) of the total, the extracted amount (0.5-108 ppm Pb) is, nevertheless, readily available at a pH of 7.0. About 90% of the study area has indoor dust Pb levels of 5-108 ppm, which are easily available to the human population in their home environment.

Patterns between exchangeable house dust (Map 3.15) and overburden Pb (Map 3.8) have some similarities over the flotation residues in the Noria Prasini Alepou area, and residual soil and pyritiferous tailings between Ayios Andreas and Komobil.

3.8.2.1.2. Distribution of carbonate lead (Pb) in house dust (Map 3.16)

Carbonate phase Pb contents in house dust between 547-6880 ppm mainly occur over the flotation residues from Noria to Prasini Alepou and Santorineika. At Thorikon there are carbonate house dust Pb levels between 547-3130 ppm, which are related to the nearby slag heap. High carbonate Pb levels in household dust to the south of the flotation tailings in the Santorineika area towards Ayios Andreas and Ayia Paraskevi is most likely due to dust from the flotation tailings heap behind the sports area and secondary school (Photos 12 & 13 in Volume 2).

Samples at Ayia Paraskevi and Phenikodassos have carbonate Pb contents of 547-991 ppm, in contrast to the low levels extracted by the exchangeable phase (see Map 3.15).

Carbonate Pb concentrations in house dust (107-6880 ppm) could be made available at and below a pH of 5. Hence, if contaminated dust is inhaled or ingested, it will be attacked by the acid gastric fluids (pH 1.5-2.5), and a certain amount could be made available for absorption by the human population.

Geochemical carbonate Pb distribution patterns in house dust are strongly influenced by the distribution of flotation tailings. Hence, indoor dust patterns (Map 3.16), with respect to these wastes, are similar to those over overburden (Map 3.9).

3.8.2.1.3. Distribution of combined exchangeable & carbonate lead (Pb) in house dust (Map 3.17)

Comparatively high concentrations of combined exchangeable & carbonate Pb (115-6896 ppm) occur in house dust. As has already been mentioned, the levels extracted by these two fractions are considered to represent the readily available Pb to humans. The greatest combined exchangeable & carbonate house dust Pb contents (597-6896 ppm) occur over the flotation tailings from Noria to Prasini Alepou and Santorineika (Map 3.17). At Thorikon, as expected, combined Pb levels between 597-3154 ppm occur, and are related to the nearby slag heap. High combined exchangeable & carbonate house dust Pb levels to the south of the flotation tailings, in the Santorineika area towards Ayios Andreas and Ayia Paraskevi, are possibly ascribed to fugitive dust from the flotation tailings heap behind the sports area and secondary school (Photos 12 & 13).

The combined exchangeable & carbonate house dust Pb geochemical distribution patterns follow the orientation of the flotation tailings (Map 3.17) and are, therefore, similar to those in overburden (Map 3.10).

3.8.2.1.4. Distribution of reducible lead (Pb) in house dust (Map 3.18)

Reducible Pb contents in house dust vary between 200-6030 ppm. The highest reducible house dust Pb concentrations (1250-6030 ppm) occur over the flotation tailings (Noria-Prasini Alepou-Santorineika), flotation residues, pyritiferous wastes and contaminated soil in the Kavodokanos area. The pattern to the south of the flotation tailings in the Santorineika area towards Ayios Andreas and Ayia Paraskevi still persists, verifying its association with dust from the flotation tailings heap behind the sports area and secondary school (Photos 12 & 13). Elevated reducible house dust Pb levels evidently occur at Thorikon and Ayia Paraskevi (1250-2770 ppm). The high reducible house dust Pb contents at Phenikodassos and Ayia Paraskevi are most likely related to dust from the nearby slag heaps.

This form of Pb is operationally associated with Fe-Mn oxides, and may be made available under reducing conditions and a pH between 2.0 and 5.0. Reducible house dust Pb contents of 200-6030 ppm could, however, be made available to household animals and humans, when dust is inhaled or ingested (*i.e.*, gastric fluids have a pH of 1.5-2.5).

Reducible house dust Pb geochemical distribution patterns are strongly influenced by the orientation of flotation tailings (Map 3.18), as are patterns in overburden (Map 3.11).

3.8.2.1.5. Distribution of oxidisable lead (Pb) in house dust (Map 3.19)

The spatial distribution patterns of oxidisable Pb in house dust, although strongly distorted, by the structural geostatistical characteristics of overburden, the raw data variable-size dot pattern shows, however, overall similarities to overburden Pb patterns (Map 3.12). High house dust Pb contents (218-1530 ppm) occur over or in the vicinity of the flotation tailings from Noria to Prasini Alepou and Santorineika, in the Kiprianos-

Kavodokanos area, and at Thorikon (Map 3.19). Elevated oxidisable house dust Pb levels (139-381 ppm) occur at Ayia Paraskevi, Neapoli and Ayios Andreas. The very low oxidisable Pb contents at Phenikodassos may be explained by differences in the chemical composition of the slag.

Oxidisable house dust Pb contents (19-1530 ppm) may be made available under oxidising conditions and a pH at or lower than 2.0. Although this fraction is not completely available to humans, a certain proportion may be available under the very acid environment of gastric fluids (pH of 1.5 to 2.5), and on a completely empty stomach (pH 1.0), if the dust is inhaled or ingested.

3.8.2.1.6. Distribution of residual lead (Pb) in house dust (Map 3.20)

Residual Pb concentrations in house dust vary from 126-5820 ppm. The highest residual indoor dust Pb levels occur over the flotation tailings and nearby areas from Noria to Prasini Alepou and Santorineika (951-5820 ppm Pb), and Phenikodassos to Kiprianos and Kavodokanos (951-4680 ppm Pb). High residual house dust Pb values at Phenikodassos and Ayia Paraskevi indicate that the source material of the dust is mainly from the nearby slag heap. The pattern to the south of the flotation tailings in the Santorineika area towards Ayios Andreas is still present and is, undoubtedly, ascribed to fugitive dust from the flotation tailings heap behind the sports area and secondary school (Photos 12 & 13).

Geochemical distribution patterns of residual house dust Pb (Map 3.20) are again influenced by the orientation of the flotation tailings and, therefore, some similarities exist to those in overburden (Map 3.13).

3.9. DISCUSSION AND CONCLUSIONS

Geochemical distribution maps of Pb in different sampling media have given a detailed picture of the natural state of the Lavrion urban environment, the subsequent contamination caused by human industrial activities, and its effects on child health (Maps 3.1-3.20). Parent rocks have Pb levels ranging from 0.5-1850 ppm, *i.e.*, from natural background to geochemical anomalous levels in mineralised areas (Map 3.1). Natural soil would have had enhanced anomalous Pb contents over primary geochemical anomalies, due to its concentration by pedogenic processes, but certainly not the levels found today, which are solely due to anthropogenic contamination (810-151579 ppm Pb).

Fugitive dust from ore crushing, emissions from smelters and dust from metallurgical processing wastes from 1865 to 1989, were responsible for the contamination of residual soil, which is presently a secondary, but a very significant, source of contamination (Fig. 3.11). As a consequence, the whole surface environment of the Lavrion urban area is completely contaminated, and this is shown by the extremely high Pb levels in house dust 488-18617 ppm (Map 3.5). Life exposure of the human population and, especially children, to this adverse environment, places them at high risk with respect to their health. The effects are shown by high blood-Pb levels in children, 5.98-60.49 μg/100 ml; 95% of the 235 children have b-Pb contents over 10 μg/100 ml, the upper limit set by international organisations (Map 3.6).

Leachability, mobility and bioavailability of Pb depends on its mode of occurrence, and prevailing pH-Eh conditions. The five-step selective extraction procedure, used in the analysis of overburden and house dust samples, has given considerable

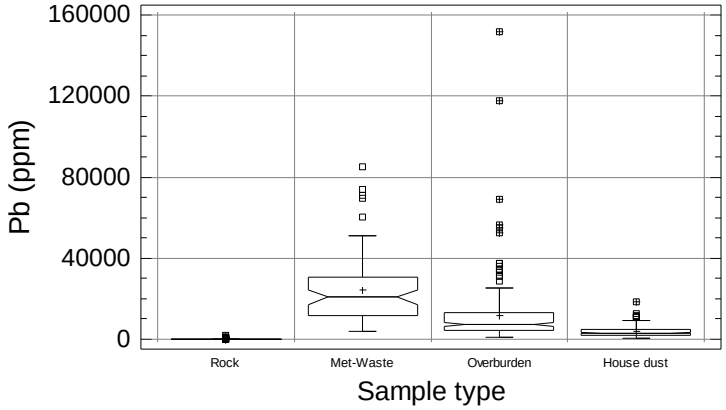

Fig. 3.11. Lead (Pb) contents in samples of rock (n=140), metallurgical processing wastes (n=62), overburden (n=224) and house dust (n=127).
Fig. 3.11. Συγκεντρώσεις μολύβδου (Pb) στα δείγματα πετρώματος (n=140), μεταλλουργικών απορριμμάτων (n=62), εδαφικού καλύμματος (n=224) και σκόνης σπιτιών (n=127).

information about the availability of Pb and other elements determined for this study (refer to Chapters 7 & 8). Mobility and bioavailability of metals decrease approximately in the order of the extraction sequence, from readily available to unavailable, because the strength of extraction reagents used increases in this order (Harrison *et al.* 1981). The exchangeable fraction may indicate the form in which metals are most available for plant and animal uptake. The second step extracts metals bound to carbonate and specifically adsorbed phases, which can become easily mobile and available under conditions of lower soil pH, or in the very acid environment of human gastric fluids with a pH of 1.5-2.5; gastric fluids of a completely empty stomach have a pH of 1. Elements bound to Fe-Mn oxides and organic/sulphide fractions are generally more strongly held within soil constituents than the first two fractions, but could be mobilised under certain conditions, low pH and a reducing or oxidising environment. The residual phase usually represents elements incorporated in the lattice of minerals, which are unavailable to plants and animals.

The easily available exchangeable Pb fraction in the intensely contaminated overburden and house dust is comparatively small in relation to the total metal (Tables 3.5 & 3.10). Nevertheless, levels of up to 662 ppm Pb in overburden and 108 ppm Pb in house dust are still easily available to plants, animals and humans (Maps 3.8 & 3.15). Because ingestion and inhalation are significant pathways for grazing animals and children alike, the combined exchangeable and carbonate phase Pb concentrations should be considered. In this case, the potential exposure hazard is indeed greater for concentrations of 65-58762 ppm Pb in overburden and 115-6896 ppm Pb in house dust may be available (Maps 3.10 & 3.17). These two fractions may also be available for uptake by plants.

Since, ingestion (*e.g.*, via soil, plants), inhalation (*e.g.*, via dust particles, vapour), and percutaneous (*e.g.*, soil) uptake are considered to be three major human exposure pathways (Ferguson *et al.*, 1998), and the fact that gastric fluids have a very low pH (1.5-2.5), higher levels of Pb may be available from the reducible and oxidisable phases *i.e.*, 242-33350 ppm Pb from overburden and 219-7560 ppm Pb from house dust. Consequently, the exposure risk on the animal and human population in Lavrion is indeed greater than hitherto anticipated. Rehabilitation of the Lavrion surface environment is, therefore, one of the most significant and urgent tasks that must be undertaken by the Hellenic State.

Blank back page
Λευκή οπίσθια σελίδα

Chapter 4

GEOCHEMISTRY OF PARENT ROCKS

Alecos Demetriades and Katerina Vergou-Vichou
Institute of Geology and Mineral Exploration, 70 Messoghion Street, Gr-115 27, Athens, Greece

4.1. INTRODUCTION

One of the aims of the present project was to determine the background variation of elements in the Lavrion urban area. An indeed difficult objective, since *"residual soil"* in the Lavrion urban area is seriously contaminated by toxic elements, as it has already been shown by maps of the contamination index (Maps 1.5 & 1.6 in Chapter 1 of Volume 2 of this report, & Chapter 1, Section 1.7, p.9-13 in this Volume). The only natural medium amenable to study natural background variation is surface rock. Rock outcrop mapping during the compilation of the lithological map (Map 2.2; Chapter 2) has shown that there were enough outcrops, well distributed over the whole study area (Map 2.7), to compile rock geochemical maps.

Parent rocks of the Lavrion urban area mainly consist of marble, schist, schistose-gneiss, prasinite, calcareous sandstone, and conglomerate. Outcrops of iron mineralisation and fault breccia are of minor significance, since they occur at a few locations. Marble and schist are the dominant rock types (Table 2.1; Map 2.2).

Rock samples were collected from 140 outcrops (Map 2.7), and analysed for 25 major and trace elements. In this Chapter, only 18 elements are presented, *e.g.*, Al, As, Ba, Ca, Cd, Co, Cr, Cu, Fe, K, Li, Mn, Ni, P, Sr, Ti, V and Zn (Maps 4.1-4.30); the rock geochemical distribution of Pb has already been discussed in Chapter 3 (this Volume, Section 3.2, p.66 & Map 3.1 in Volume 2). Elements, such as Ag, As, and Sb were below the detection limit of the analytical method used, which were 1, 1000 and 100 ppm respectively. Since, arsenic is a significant contaminant of overburden materials aqua regia extractable rock geochemical data were compiled and plotted (Map 4.3). Further, in order to evaluate fully the contamination caused by metallurgical activities with respect to other elements, such as Ag, B, Be, Bi, Hg, La, Mo, S, Sb, Sn and U, statistical parameters on their aqua regia extractable concentrations are tabulated in Table 4.1 (see also Table 4.19A, p.37, in Appendix 2A of Volume 1A).

The analytical methods used for determination of elements on rock geochemical samples are described in Chapter 2C; the analytical and sampling variance in Chapter 2C, and data processing for map plotting in Chapter 2D. All rock geochemical distribution and other maps referred to in this chapter are in Volume 2 (Maps 4.2-4.30).

In the following description, the most significant features of the statistical and spatial element distributions will be discussed. Statistical Tables (Tables 4.1A-4.19A in Appendix 2A of Volume 1A of this report, p.19-38), boxplot comparisons (Figs. 4.1A-4.18A), and geochemical distribution maps (Maps 4.2-4.30 in Volume 2) give the reader all the required information for more detailed interpretations. Statistical tables and boxplots are in Volume 1A of this report, and are distinguished from tables and figures within the text by the suffix "A", *e.g.*, Table 4.1A, Fig. 4.1A. Tables and figures within the text are normally numbered as Table 4.1, Fig. 4.1 *etc.*

Information about the average concentration of elements in different rock types was obtained from Reimann *et al.* (1998), who recently compiled this very useful data from different sources, and the average element concentrations in the upper continental crust from Wedepohl (1995); other sources are cited below the tables. In Tables 4.1A-4.19A (Appendix 2A , Volume 1A, p.19-38) these are referred to as "*Global rock type mean",* and the value of the equivalent rock type has been taken, *i.e.*, *limestone* for marble, *shale/schist* for schist, *gabbro/basalt* for prasinite, and *sandstone* for calcareous sandstone.

4.2. GEOCHEMICAL DISTRIBUTION OF ELEMENTS IN PARENT ROCKS

Geostatistical structural analysis, which is summarised by experimental and modelled variogram surfaces (refer to insets of Maps 4.2-4.30, Volume 2), has shown the following major axial trends of the spatial distribution of elements in rocks:

- NNE-SSW: Cd, Co, Pb, and V;
- ESE-WNW: As, Cr, Fe, Mn, P, and Sr;
- NW-SE: Al, Ba, Ca, Cu, K, Li, Ni, Ti, and
- Isotropic: Zn.

The isotropic variogram of Zn is caused by different structures, almost with the same range in the directions NNE-SSW, NW-SE, SE-NW, which mask the major NE-SW trend (refer to inset of Map 4.30). The above element associations suggest that primary element distribution, in the Lavrion urban area, is governed by lithology and two mineralisation events. The lithology is associated with elements, such as Al, Ba, Ca, Cu, K, Li, Ni and Ti, which have a strong NW-SE trend, the major axial orientation of the regional anticlinal structures (Papadeas, 1991). The two ore-mineral associations are:

(a) Pb-Cd-Zn, which are positively associated with Co and V, follow a NNE-SSW trend. According to Marinos and Petrascheck (1956) the Pb-Zn mineralisation is located in NNE-SSW zones, which are parallel to the major folding in the Lavreotiki peninsula, and
(b) Fe-Mn-As, which are positively associated with Cr and P, and negatively correlated with Sr, follow an ESE-WNW trend.

In Tables 4.1A-4.18A (Volume 1A) the abundance of elements occurring in rocks of the Lavrion urban area (*entry All rocks*) is compared to the mean concentration in rocks of the upper continental crust (Levinson, 1974; Wedepohl, 1995), and are summarised in Table 4.1. This comparison showed that the Lavrion urban area rocks are naturally

- enriched in **As**>**Sb**>**Cd**>**Ag**>**Hg**>**Ni**>Ca>**Pb**>**Zn**>P>Mn>**Cr**>Co>**Cu**>Ba>S>**U**, and
- depleted in Fe>Mo>Li>Sr>La>Ti>Al>V>K>B

with respect to their abundance in rocks of the upper continental crust. Calcium enrichment is explained by the widespread occurrence of marble (Map 2.2 in Volume 2). Enrichment with respect to other elements, the majority of which are classified as toxic (highlighted), is either due to mineralisation or lithology. It is noted that the terms, *depletion* and *enrichment*, are used for mean element concentrations *below* and *above* the *Global rock type mean* respectively.

Since, each rock has a different chemical composition, *mean* element concentrations in marble, schist, prasinite and sandstone of the Lavrion urban area are compared to their respective *Global rock type means* (Table 4.2). This comparison is

Table 4.1. Statistical parameters of element concentrations in rock, overburden and metallurgical processing wastes in Lavrion, Global rock mean of upper continental crust, Global soil mean or median, and enrichment/depletion index of Lavrion rocks with respect to Global rock mean (from Reimann et al., 1998). Median values of Lavrion overburden and metallurgical wastes and Global soil mean or median (Reimann et al., 1998) are given for comparison purposes.
Πίνακας 4.1. Στατιστικές παράμετροι των συγκεντρώσεων των στοιχείων στα δείγματα του πετρώματος, εδαφικού καλύμματος, μεταλλουργικών απορριμμάτων του Λαυρίου, Παγκόσμιες μέσες τιμές των πετρωμάτων του ανωτέρου τμήματος του γήϊνου φλοιού, Παγκόσμιες μέσες ή διάμεσες τιμές των εδαφών, και ο δείκτης εμπλουτισμού/έκπλυσης των πετρωμάτων του Λαυρίου σε σχέση με τις Παγκόσμιες μέσες τιμές των πετρωμάτων. Οι διάμεσες τιμές των συγκεντρώσεων των στοιχείων στα δείγματα εδαφικού καλύμματος και μεταλλουργικών απορριμμάτων του Λαυρίου καθώς και οι Παγκόσμιες μέσες ή διάμεσες τιμές στο έδαφος παραθέτονται για σύγκριση.

Element	*Lavrion rock (n=140)[1], overburden (n=224)[2] and metallurgical wastes (n=62)*							*Global rock mean of upper continental crust (ppm)*	*Global soil mean or median* (ppm)*	*Enrichment/ Depletion Index of Lavrion rocks with respect to Global rock mean*
	All Rocks (n=140) (values in ppm)					*Over-burden (ppm)*	*Metallurgical wastes (ppm)*			
	Minimum	*Maximum.*	*Mean*	*Stand.Dev.*	*Median*	*Median*	*Median*			
Ag*	<0.5	41.00	0.89	3.63	0.50	12.06	18.90	0.055	0.10	16.18
Al	<50	75152.00	19267.00	21375.00	8044.00	32315.00	20074.00	77440.000	80000.00*	0.25
As	<0.5	1032.00	62.80	172.40	15.60	1290.00	2492.00	2.000	5.00	31.40
B**	0.25	5.24	0.52	0.87	0.25	136.00	42.97	17.000	30.00	0.03
Ba	40.00	108000.00	1067.00	9110.00	210.00	479.00	243.00	668.000	500.00	1.60
Be**	<0.5	below detection limit				1.01	0.50	3.100	6.00	-
Bi**	<0.5	below detection limit				11.00	2.50	0.120	0.30	-
Ca	50.00	390938.00	217301.00	125319.00	220.13	93625.00	102603.00	29450.00	14000.00*	7.38
Cd	<1.0	41.00	1.89	5.02	0.50	38.00	20.62	0.102	1.00	18.53
Co	<1.0	104.00	26.90	26.10	20.50	16.00	23.83	11.600	10.00	2.32
Cr	<1.0	610.00	100.40	145.90	20.00	183.00	73.18	35.000	50.00	2.87
Cu	3.00	225.00	32.80	31.00	25.00	186.00	630.50	14.300	20.00	2.29
Fe	979.00	107016.00	23790.00	20660.00	19515.00	44771.00	234500.00	30890.000	35000.00*	0.77
Hg**	<1.0	7.77	0.69	1.05	0.50	0.14	2.35	0.056	0.03	12.32
K	<83	31795.00	5841.00	7552.00	8044.00	9770.00	7100.00	28650.000	14000.00*	0.20
La**	<2.0	30.69	10.21	6.47	8.86	22.70	27.32	32.300	35.00*	0.32
Li	<1.0	106.00	9.10	12.10	5.00	17.40	14.50	22.000	30.00	0.41
Mn	100.00	25000.00	1831.00	2635.00	1200.00	2189.00	9398.00	527.000	530.00*	3.47
Mo*	<0.5	11.00	0.83	1.16	0.50	4.90	3.57	1.400	2.50	0.59
Ni	<1.0	1600.00	168.30	252.20	54.50	127.00	38.52	18.600	30.00	9.05
P	44.00	8510.00	2381.00	1904.00	1855.00	992.00	1103.00	665.000	300.00*	3.58
Pb	<1.0	1850.00	76.85	209.06	22.00	7305.00	20750.00	17.000	20.00	4.52
S**	100.00	3000.00	1100.00	600.00	1200.00	12690.00	20581.19	953.000	800.00	1.15
Sb**	<5.0	71.04	6.94	12.05	2.50	121.00	189.00	0.310	5.00	22.39
Sn**	<5.0	below detection limit				18.50	27.71	2.000	10.00	-
Sr	<1	800.00	121.00	129.00	98.00	118.00	178.69	316.000	67.00*	0.38
Ti	<120	7014.00	920.00	1401.00	300.00	2162.00	737.70	3117.000	4000.00	0.30
U**	2.50	6.06	2.75	0.85	2.50	3.00	2.50	2.500	2.70	1.10
V	<1	71.00	13.10	13.00	9.00	75.00	46.30	53.000	80.00	0.25
Zn	<6	5200.00	210.60	599.60	57.00	6668.00	39800.00	52.000	50.00	4.05

[1]Rock: Ag , Mo (n=155); ** B, Be, Bi, Hg, La, S, Sb, Sn, U (n=48); [2]Overburden: B, Bi, Hg, S, Sn, U (n=50) and Sb (n=90).

made to show geochemical differences between the different Lavrion urban area rocks and their respective global rock averages.

All four rock types are enriched in Cd, Cu, Mn, P and Pb, which are elements associated with the polymetallic mineralisation, and depleted with respect to K and V. Moreover, marble and schist are enriched in Ag, As, Co, Hg, Ni and Zn, elements also associated with base metal mineralisation. It is quite apparent, therefore, that mineralisation is the cause of enrichment, of all rocks occurring in the Lavrion urban area, with respect to major and minor ore elements.

Prasinite, metamorphosed diabasic lava, was expected to be enriched in Fe, Ti, V, Cr, Ni and Co, because of its mafic, and locally ultramafic, mineralogy, but it is

Table 4.2. Comparison of mean element concentrations of Lavrion urban area rocks to Global rock type means. Elements enriched in all rock types are displayed in **bold letters**, and those that are depleted in *underlined letters*. Elements below detection limit are in brackets.
Πίνακας 4.2. Σύγκριση των μέσων συγκεντρώσεων των στοιχείων στα πετρώματα της αστικής περιοχής του Λαυρίου με τις γενικές μέσες τιμές των πετρωμάτων. Στοιχεία που είναι εμπλουτισμένα ή παρουσιάζουν χαμηλές τιμές σε όλους τους τύπους των πετρωμάτων αναγράφονται με έντονη γραφή ή είναι υπογραμμισμένα αντίστοιχα. Στοιχεία κάτω από το όριο ανίχνευσης είναι μέσα σε παρενθέσεις.

	Marble *Μάρμαρο*	*Schist* *Σχιστόλιθος*	*Prasinite** *Πρασινίτης**	*Sandstone* *Ψαμμίτης*
Enriched in: Εμπλουτισμένο σε:	Ag, Al, As, Ba, **Cd**, Co, Cr, **Cu**, Fe, Hg, La, **Mn**, Mo, Ni, **P**, **Pb**, S, Ti, U, Zn	Ag, As, Ca, **Cd**, Co, Cr, **Cu**, Hg, **Mn**, Ni, **P**, **Pb**, Zn	Ca, **Cd**, **Cu**, Li, **Mn**, **P**, **Pb**	Ba, Ca, **Cd**, Co, Cr, **Cu**, Fe, **Mn**, Ni, **P**, **Pb**, Sr, Zn
Depleted in: Πτωχό σε:	B, (Be), (Bi), Ca, K, Li, (Sn), Sr, V,	Al, B, Ba, (Be), (Bi), Fe, K, La, Li, Mo, S, (Sn), Sr, Ti, (U), V	Al, Ba, Co, Cr, Fe, K, Ni, Sr, Ti, V, Zn	Al, K, Li, Ti, V

* Prasinite mineralogy: albite [$NaAlSi_3O_8$], pennine [$H_8(Mg,Fe)_5Al_2Si_3O_8$], epidote [$H_2O.4CaO.3(Al,Fe)_2O_3.6SiO_2$], clinozoisite [$HCa_2(Al,Fe)_3Si_3O_{13}$], actinolite [$Ca_2(Mg,Fe)_5(OH)_2(Si_4O_{11})_2$], horblende {$(Ca,Na)_{2-3}(Mg,Fe^{2+},Fe^{3+},Al)_5(OH)_2.[(Si,Al)_8O_{22}]$}, glaucophane [$Na(Al,Fe,Mg)(SiO_3)_2$] and leucoxene $FeO.TiO_2$ (Marinos and Petrascheck, 1956).

peculiarly depleted with respect to all these elements. The calcium enrichment is explained by its mineralogy, but the abnormal Li level is a local peculiarity, for this is an element normally enriched in granite and pegmatite, and not in mafic rocks.

4.3. FACTOR AND CLUSTER ANALYSES

Factor and cluster analyses were used in order to study element associations in parent rocks of the Lavrion urban environment. These two methods reveal underlying relationships among the variables, which are not normally exposed by simple correlation analysis. In both cases, the R-mode method was used, which deals with similarities among elements determined on the samples. For details of the methods, the reader may refer to specialised literature on factor and cluster analyses (Cattell, 1965; Obial, 1970; Obial and James, 1973; McCammon, 1974; Klovan, 1975; Davis, 1973; Goddard and Kirby, 1976; Jöreskog *et al.*, 1976; Howarth, 1983; Miesch, 1990).

Data were normalised by the 2-parameter log transformation used by Miesch (1990) in the G-PREP module of program G-RFAC. This is the most widely applied transformation in chemometrics. The 2-parameters are the mean log and log variance, which completely define a lognormal distribution.

4.3.1. FACTOR ANALYSIS ON ROCK GEOCHEMICAL DATA

The ten factors of the principal component model are tabulated in Table 4.3. The first five factors, with eigenvalues above 1, explain 80.85% of total variance. Five factors were extracted and the varimax-rotated factor loadings were calculated for 18 elements (Table 4.4).

In the first or *"prasinite-schist"* factor, Ti, Al and K have the strongest positive varimax loadings (>0.8), followed by Li, Cu and P with positive loadings >0.6 to <0.8. These elements occur in prasinite and the femic components of schist. Moderate positive varimax loadings on Co, Cr, Ni and V support this interpretation, since these

Table 4.3. Eigenvalues of the first ten factors of the principal component model of rock geochemical data, the percentage variance explained by each factor and the cumulative percentage variance.
Πίνακας 4.3. Ιδιοτιμές των δέκα πρώτων παραγόντων του μοντέλου κύριων συνιστώσων για τα λιθογεωχημικά δεδομένα, ποσοστιαία μεταβλητότητα ερμηνευομένη από κάθε παράγοντα και ποσοστιαία αθροιστική μεταβλητότητα.

Factor	*Eigenvalue*	*Variance explained by factor* (%)	*Cumulative variance* (%)
1	**7.57**	42.08	42.08
2	**2.52**	13.97	56.05
3	**1.86**	10.34	66.39
4	**1.32**	7.33	73.72
5	**1.28**	7.13	80.85
6	0.70	3.89	84.74
7	0.58	3.22	87.96
8	0.49	2.74	90.70
9	0.34	1.92	92.62
10	0.28	1.55	94.17

Table 4.4. Varimax loadings for the five strongest factors of rock geochemical data (n=140). Correlation between varimax scores and transformed data. [Strong positive loadings (>0.6) are shown by bold numbers, and *the strong negative loading of Ba (<-0.6) in Varimax 5 is italicised*].
Table 4.4. Φορτία περιστροφής "varimax" για τους πέντε ισχυρότερους παράγοντες των λιθογεωχημικών δεδομένων (n=140). Συσχέτιση μεταξύ των φορτίων varimax και των μετασχηματισμένων δεδομένων. [Με έντονη γραφή: ισχυρά θετικά φορτία (>0.6). *Με πλάγια γραφή: ισχυρό αρνητικό φορτίο (<-0.6) του Ba στο πέμπτο φορτίο "varimax"*].

Element	*V a r i m a x l o a d i n g s*				
	Factor 1	*Factor 2*	*Factor 3*	*Factor 4*	*Factor 5*
Al	**0.850**	-0.028	-0.263	0.182	0.060
Ba	0.132	0.074	0.212	0.126	*-0.811*
Ca	-0.176	0.086	**0.880**	-0.031	-0.174
Cd	-0.123	**0.885**	-0.027	0.024	-0.044
Co	0.492	0.136	-0.499	0.547	0.195
Cr	0.337	0.285	-0.045	0.511	**0.605**
Cu	**0.686**	0.107	0.218	0.160	0.003
Fe	**0.552**	0.092	-0.158	**0.763**	0.140
K	**0.837**	0.005	-0.222	0.264	-0.089
Li	**0.775**	0.109	-0.253	0.226	0.371
Mn	-0.023	0.111	0.077	**0.892**	-0.202
Ni	0.386	0.203	-0.059	**0.709**	0.405
P	**0.560**	0.063	-0.076	**0.758**	0.143
Pb	0.145	**0.810**	-0.132	0.048	0.142
Sr	-0.097	-0.065	**0.874**	-0.026	-0.014
Ti	**0.907**	-0.046	-0.137	0.088	0.095
V	0.475	0.183	0.055	0.195	**0.604**
Zn	0.073	**0.872**	0.172	0.164	0.007
Eigenvalue	*7.57*	*2.52*	*1.86*	*1.32*	*1.28*
Variance explained by factor	*42.08%*	*13.97%*	*10.34%*	*7.33%*	*7.13%*
Cumulative variance	*42.08%*	*56.05%*	*66.39%*	*73.72%*	*80.85%*

elements are normally found in mafic rocks and femic minerals. The low negative varimax loading on Ca suggests that these elements occur in areas where there is depletion in calcium, *i.e.*, areas with no marble. Further, the very low positive loadings on Pb, Zn and negative on Cd, indicate that this factor is not related to mineralisation.

The second or *"Pb-Zn mineralisation"* factor has strong positive varimax loadings on Cd, Zn and Pb. Low positive varimax loadings on other elements, including rock forming, suggests that the mineralising event is not directly related to its host rocks, but it has been superimposed on them by mineralising fluids invading the host rocks through fractures. An epigenetic hydrothermal ore-genetic model is thus supported (Marinos and Petrascheck, 1956).

The third or *"carbonate lithology*" factor has strong positive varimax loadings on Ca and Sr, the two elements occurring in marble and calcareous sandstone.

The fourth or *"marble alteration and Fe-Mn mineralisation"* factor has strong positive varimax loadings on Mn, Fe, P and Ni. Moderate positive varimax loadings on Co and Cr support this interpretation. Low negative varimax loadings on Ca and Sr, suggests that this factor is not related to normal marble, but to altered dolomitised and ankeritised marble. According to Marinos and Petrascheck (1956), Fe-Mn mineralisation is accompanied by widespread dolomitisation of marble, *i.e.*, replacement of the original calcium carbonate [calcite, $CaCO_3$] by magnesium carbonate [dolomite, $CaMg(CO_3)_2$]. Ankerite [$Ca(Fe,Mg,Mn)(CO_3)_2$], a reddish iron-rich mineral is related to dolomite and is a major mineral of Fe-Mn mineralisation, and of marble alteration (reddish-brown marble outcrops). Siderite [$FeCO_3$] has also been observed in altered marble. Hence, Fe-Mn mineralisation occurs in areas with Ca and Sr depletion. Altered marble, because of cation exchange to form dolomite, ankerite, siderite, *etc.*, is also comparatively depleted with respect to these two elements.

The fifth or *"mafic lithology"* factor has strong positive varimax loadings on Cr and V, moderate positive loadings on Ni and Li, and very low positive loadings on Fe and Pb, suggesting mafic affinities peculiar to the femic minerals of schist, the mafic prasinite, and altered dolomitised and ankeritised marble. Further, the strong negative varimax loading on Ba, and low negative loadings on Ca and Sr support its association with altered marble. This factor appears to be related to hydrothermal alteration processes. According to Marinos and Petrascheck (1956), chromium (Cr), and also V, are not compatible with hydrothermal Pb-Zn mineralisation connected to an acid magma. These elements, however, can easily be derived from ophiolites. They proposed that ore-bearing solutions leached out some iron from prasinite to produce ankeritisation of marble; ankerite has widespread traces of Cr-talc. Their proposed hydrothermal alteration model of prasinite is supported by its comparative depletion with respect to Cr (Table 4.7A, Volume 1A in this report) and V (Table 4.17A), and its enrichment with Li (Table 4.11A), an element associated with acid rocks.

The above interpretation is supported by the statistical and spatial distribution of elements in rocks of the Lavrion urban area (refer to Tables 4.1A-4.18A, Figs. 4.1A-4.18A, Maps 4.2-4.30).

4.3.2. Cluster Analysis on Rock Geochemical Data

Cluster analysis was performed with the Statgraphics® software package (Manugistics, 1995). The nearest neighbour, single linkage, clustering method was used together

with the squared Euclidean distance. This procedure creates gradually one cluster from “n” variables. Clusters are groups of variables with similar characteristics. To form the clusters, the procedure begins with each variable in a separate group. It then combines the two variables with the greatest similarity, the ones that are closest together. Afterwards, recomputes the distance between groups, and the two groups that are closest together are again combined. The process is repeated until only one group remains. The dendrogram is the graphical representation of cluster analysis.

Two dendrograms were constructed, *i.e.*,

- Fig. 4.1 shows the relationship among the 18 elements, and
- Fig. 4.2 the relationship among the 18 elements and the different rock types occurring in the Lavrion urban area.

The strongest correlations are between Fe-P and Cr-Ni, which are linked to Co, thus forming the first cluster. The second cluster comprises Al-Ti, which is linked to Li and K. The first two clusters are linked together at a lower correlation level, and subsequently to Mn, V and Cu. This element association is similar to the first and fourth factors of factor analysis, and is related to (a) the mafic lithology (prasinite) and femic minerals of schist, and (b) the marble alteration and Fe-Mn mineralisation. The direct relationship with schist is indicated in Fig. 4.2, but not its association with prasinite and Fe-Mn mineralisation, which are linked to this group at a greater distance or lower correlation, possibly suggesting a distant relationship.

The third distinct cluster begins with Cd-Zn, which is linked to Pb, showing that this mineralising event is completely separate (Fig. 4.1). This element association is similar to the second factor of factor analysis. Its relationship with Cu and V, suggests that these elements are distally associated with mineralisation, and elements of the first two clusters, and schist (Fig. 4.2).

The fourth distinct cluster begins with Ca-Sr, which is linked to Ba, the elements mainly associated with marble (Fig. 4.1). The direct relationship of Ca-Sr to marble is indicated in Fig. 4.2, and the association of Ba to this cluster is at a lower link, suggesting that the Ba distribution is possibly superimposed on marble, probably through a mineralising event. This cluster is similar to the third factor of factor analysis.

Calcareous sandstone is related to the above, fourth cluster, indicating that its constituents are mainly derived from marble.

The relationship of conglomerate and prasinite with members of the first three factors, indicates that these are their major constituents (Fig. 4.2).

The relationship of prasinite and schist points to their spatial and temporal association, in contact or intruding the marble (Map 2.2, Volume 2).

Iron-mineralisation appears to be distally associated with the base metals, which is the case in the Lavreotiki peninsula mineralising events.

Schistose-gneiss and fault-breccia do not appear to have a direct relationship to any of the clusters. They are completely distinct, because of their very local occurrence.

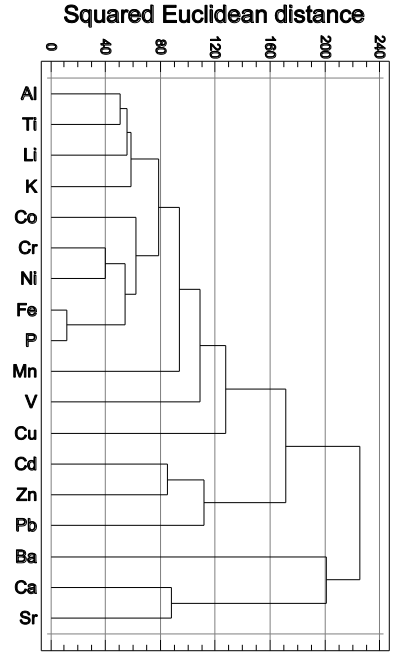

Fig. 4.1. Dendrogram of 18 elements determined on 140 rock samples from the Lavrion urban area. The dendrogram was constructed using the nearest neighbour method and squared Euclidean distance for one cluster.
Σχ. 4.1. Δενδρόγραμμα 18 χημικών στοιχείων που προσδιορίστηκαν στα 140 δείγματα πετρώματος από την αστική περιοχή του Λαυρίου. Το δενδρόγραμμα κατασκευάστηκε με τη μέθοδο του πλησιέστερου γείτονα και το τετράγωνο της Ευκλειδείου απόστασης με τελικό στόχο τη δημιουργία μίας ομάδας.

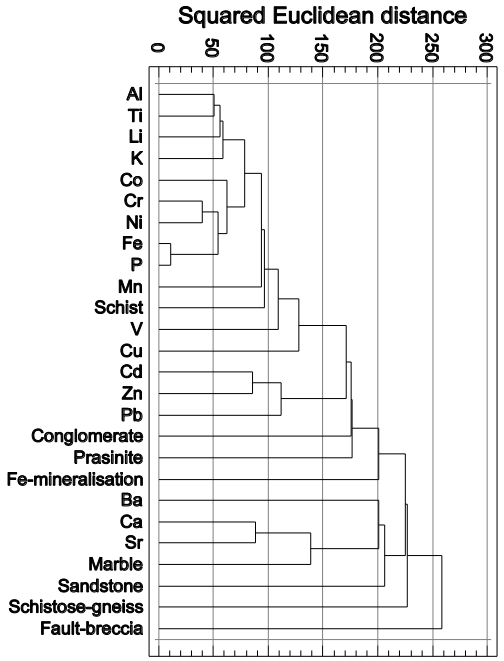

Fig. 4.2. Dendrogram showing the relationship among the 18 elements and the different rock types from the Lavrion urban area (n=140). The dendrogram was constructed using the nearest neighbour method and squared Euclidean distance for one cluster.
Σχ. 4.2. Δενδρόγραμμα που απεικονιζει τη σχέση μεταξύ των 18 χημικών στοιχείων και των διαφορετικών τύπων πετρωμάτων από την αστική περιοχή του Λαυρίου (n=140). Το δενδρόγραμμα κατασκευάστηκε με τη μέθοδο του πλησιέστερου γείτονα και το τετράγωνο της Ευκλειδείου απόστασης με τελικό στόχο τη δημιουργία μίας ομάδας.

4.4. DISCUSSION AND CONCLUSIONS

The primary element distribution in rocks of the Lavrion urban area has given the geochemical background variation of 18 elements, and the anomalous concentrations and trends of ore elements (Pb, Cd, Zn, As, Fe, Mn; Maps 4.2-4.30, Tables 4.1A-4.19A). This natural variation of elements constitutes their *geochemical baseline*, which is defined as *a variable geochemical reference value, including both the natural background variation and abnormal element contents of mineralisation* (Demetriades, 1998). Such information is indeed very significant for the estimation of anthropogenic contamination in the Lavrion urban area.

Geostatistical structural analysis proved very useful in the determination of spatial variability of elements, and their major geochemical trends, which are ascribed to either mineralisation or lithology.

The coefficient of variation, denoting the degree of scatter, was very high (>20%) for almost all elements (Tables 4.1A-4.19A in Volume 1A of this report), indicating the variable chemical composition of Lavrion rocks, and their geochemical anomalous nature with respect to ore elements (Maps 4.2-4.30). Boxplot outliers (Figs. 4.1A-4.18A) also show this feature. The variable chemical composition of Lavrion rocks has been caused, largely, by mineralisation, which caused their alteration through epigenetic hydrothermal processes.

Lavrion rocks, in comparison with Global average element concentrations of the upper continental crust, are enriched in **As**>**Sb**>**Cd**>**Ag**>**Hg**>**Ni**>Ca>**Pb**>**Zn**>P>Mn> **Cr**> Co> **Cu**>Ba>S>**U**, and depleted in Fe>Mo>Li>Sr>La>Ti>Al>V>K>B. The detection limit of the analytical method for Be, Bi and Sn is above the value of their abundance in the upper continental crust. These elements should, therefore, be analysed by a more sensitive method.

Toxic elements that may have given concentrations in *"natural soil"* above statutory threshold levels are: As>10 ppm (Map 4.3), Ba>600 ppm (Map 4.4), Cd>3 ppm (Map 4.9), Cr>100 ppm (Map 4.11), Cu>130 ppm (Map 4.12), Ni>70 ppm (Map 4.20), Pb>500 ppm (Map 3.1), Sb>27 ppm (Table 4.19A), and Zn>300 ppm (Map 4.30). It is quite apparent, therefore, that a large part of "*natural soil*" in Lavrion would have had toxic element concentrations above statutory threshold levels. The extent of geochemically anomalous or *"naturally contaminated"* soil, depending on the toxic element, would have been largely restricted over the geochemically anomalous rocks, covering approximately 10% to 50% of the Lavrion urban area.

R-mode factor and cluster analyses showed interrelations among 18 elements (Tables 4.3 & 4.4; Figs. 4.1 & 4.2). In general, both techniques were useful in the identification of different element associations, and to ascribe such relationships to various geological factors, *i.e.*, elements directly associated with mineralisation, rock alteration and lithology. In fact, factor and cluster analyses effectively highlighted element relationships that are difficult to deduce by means of more conventional geological and geochemical correlation methods.

Blank back page
Λευκή οπίσθια σελίδα

Chapter 5

CHEMISTRY OF METALLURGICAL PROCESSING WASTES

Alecos Demetriades and Katerina Vergou-Vichou
Institute of Geology and Mineral Exploration, 70 Messoghion Street, Gr-115 27, Athens, Greece

5.1. INTRODUCTION

The metallurgical processing wastes cover a large part of the Lavrion urban area, and presently they are the major source of contamination of the surface environment. It is, therefore, significant to understand their environmental impact and implications to the quality of life of the local population (Photos 6-33, Volume 2). Their geographical distribution and macroscopic features were described in Chapter 2 (section 2.4), and the area they cover is shown on Map 2.3 (see Volume 2), and tabulated in Table 2.3 (p.19). In this chapter their chemistry will be discussed. For this purpose, representative samples were collected and analysed from the main metallurgical processing waste categories (Map 2.8, Volume 2), *i.e.*,

- slag (n=21),
- sand-blast material or wastes (n=8),
- earthy material within slag [or *slag-earth*] (n=7),
- beneficiation/flotation residues or tailings (n=8),
- pyrite tailings (n=12), and
- pyritiferous sand (n=6).

Sampling and sample preparation were described in Chapter 2A and the analytical method used is in Chapter 2B.

Since, contamination is a geographical problem, chemical results of thirty elements were plotted as variable-size dot-maps in order to show the chemical variability of metallurgical processing wastes, both between and within each category (refer to Volume 2: Maps 3.2, 5.1-5.30). Different coloured dots are used for each metallurgical processing waste category. Statistical parameters of each element for the different types of metallurgical waste categories are tabulated on the maps. In the following description, dot-maps and accompanying statistical tables are complemented by boxplots, which facilitate the chemical comparison among the different metallurgical processing waste categories. For comparison purposes the range of element concentrations of each category are quoted, and not the medians, for in this case the variation of elements is of interest. It is stressed that the most significant features of each element will be described and discussed and that the following description must be studied in conjunction with the element distribution maps in Volume 2 of this report (Maps 5.1 to 5.30).

5.2. CHEMISTRY OF METALLURGICAL PROCESSING WASTES

5.2.1. DISTRIBUTION OF SILVER (Ag) IN SAMPLES OF METALLURGICAL WASTES (Map 5.1, Fig. 5.1)

Silver varies from 3.2 to 96 ppm in metallurgical wastes. The highest Ag content is in pyritiferous sand (6.85-95.98 ppm) followed by slag (3.19-90.35 ppm), pyrite tailings (16.16-87.75 ppm), flotation residues (35.75-75.41 ppm), slag-earth (6.70-51.11 ppm) and sand-blast material (10.65-23.77 ppm).

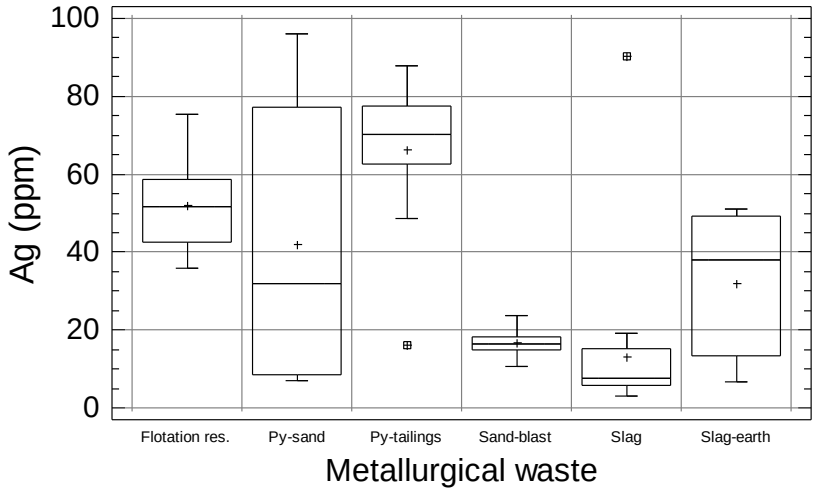

Fig. 5.1. Multiple boxplot of the distribution of silver (Ag) in samples from the different types of metallurgical processing wastes in the Lavrion urban area (refer to Map 5.1).
Σχ. 5.1. Πολλαπλό θηκόγραμμα κατανομής του μολύβδου (Pb) στα δείγματα των διαφορετικών τύπων μεταλλουργικών απορριμμάτων από την αστική περιοχή του Λαυρίου (βλ. Χάρτη 5.1).

Slag, apart from one sample with very high Ag in the Kiprianos area (90.35 ppm Ag), has a very narrow range of Ag values as shown by Map 5.1 and the boxplot (Fig. 5.1). Slag samples to the south of Ayia Paraskevi and Kiprianos have similar Ag contents.

An interesting feature, exhibited in Fig. 5.1, are the elevated mean and median values of Ag in the earthy material within slag (*slag-earth*) and sand-blast material in comparison to normal slag; a direct comparison can be seen in the Kavodokanos and Fougara areas, where samples of slag and slag-earth have been collected from the same site. This feature has already been described with respect to Pb (refer to Chapter 3, Map 3.2, Fig. 3.2).

Pyrite tailings, apart from a single sample low in Ag in the Kavodokanos area, have a fairly uniform Ag content. Silver variation in pyritiferous sand shows distinct differences between samples at the beach, which have the lowest levels, and those further inland, containing Ag about the same level as the pyrite tailings (Map 5.1; area between Komobil and Kiprianos).

Flotation tailings at Noria-Prasini Alepou-Santorineika have lower Ag values than the ones at Kavodokanos.

5.2.2. DISTRIBUTION OF ALUMINIUM (Al) IN SAMPLES OF METALLURGICAL WASTES (Map 5.2, Fig. 5.2)

Aluminium varies from 1,118 to 38,071 ppm in metallurgical wastes. Samples of slag have the highest Al contents (5,437-38,071 ppm) followed by slag-earth (16,406-33,529 ppm), pyritiferous sand (8,396-27,295 ppm), flotation residues (8,687-26,341 ppm), sand-blast material (18,673-23,487 ppm) and pyrite tailings (1,118-7,696 ppm).

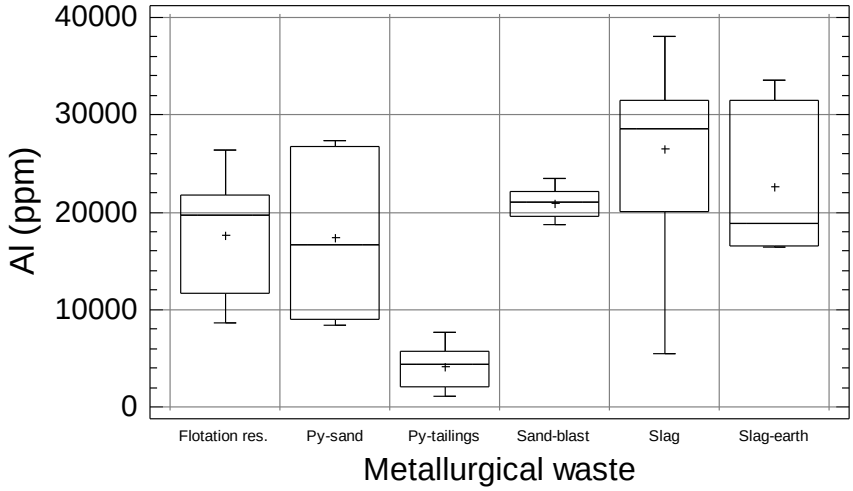

Fig. 5.2. Multiple boxplot of the distribution of aluminium (Al) in samples from the different types of metallurgical processing wastes in the Lavrion urban area (refer to Map 5.2).
Σχ. 5.2. Πολλαπλό θηκόγραμμα κατανομής του αργιλίου (Al) στα δείγματα των διαφορετικών τύπων μεταλλουργικών απορριμμάτων από την αστική περιοχή του Λαυρίου (βλ. Χάρτη 5.2).

Aluminium levels in samples of slag and slag-earth from Fougara have distinctly higher values than those at Kavodokanos. Aluminium levels are approximately in the same order of magnitude in slag from Fougara, Panormos, Neapoli and Ayia Paraskevi. It is noted that slag heaps in the south, about Lavrion harbour, are older the ones at Kavodokanos.

Aluminium is not enriched in samples of slag-earth and sand-blast material with respect to slag.

Pyrite tailings have the lowest Al contents, since they consist of mainly pyrite. There is a fairly distinct difference between Al levels in pyrite tailings at Nichtochori-Komobil and those at Kavodokanos, Kiprianos and Santorineika; the latter have comparatively higher Al values.

The contrast between low and high values in samples of pyritiferous sand from the beach and further inland, between Komobil and Kiprianos, noted for Ag and Pb, still persists with respect to aluminium.

Aluminium levels in samples of flotation residues from Noria-Prasini Alepou-Santorineika have distinctly higher values in comparison to those at Kavodokanos.

5.2.3. DISTRIBUTION OF ARSENIC (AS) IN SAMPLES OF METALLURGICAL WASTES (Map 5.3, Fig. 5.3)

Arsenic levels are considerably high and very variable in samples from the different types of metallurgical processing wastes, *i.e.*, from 283 to 26,063 ppm. The highest range of As values is found in flotation residues (2,470-26,063 ppm), followed by pyritiferous sand (3,875-14,440 ppm), pyrite tailings (2893-14747 ppm) and slag-earth (684-15907 ppm). Slag (283-6,236 ppm As) and sand-blast material (854-2,243 ppm As) have comparatively lower of As contents.

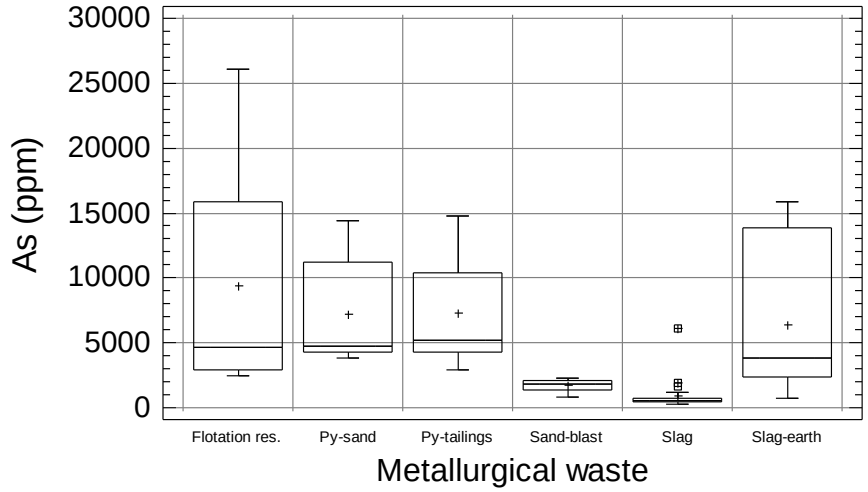

Fig. 5.3. Multiple boxplot of the distribution of arsenic (As) in samples from the different types of metallurgical processing wastes in the Lavrion urban area (refer to Map 5.3).
Σχ. 5.3. Πολλαπλό θηκόγραμμα κατανομής του αρσενικού (As) στα δείγματα των διαφορετικών τύπων μεταλλουργικών απορριμμάτων από την αστική περιοχή του Λαυρίου (βλ. Χάρτη 5.3).

Slag, apart from one sample high in As from Kavodokanos, has the lowest values. Arsenic is enriched in slag-earth and sand-blast material in comparison to samples of slag; a feature already noted for Ag and Pb.

Pyrite tailings of the Nichtochori-Komobil area have higher As contents than the ones at Kavodokanos, Kiprianos and Santorineika.

Pyritiferous sand samples from the beach, between Komobil and Kiprianos, have comparatively higher As levels compared to the ones further inland.

Arsenic levels in samples of flotation residues from Kavodokanos have considerably higher values than those from Noria-Prasini Alepou-Santorineika.

5.2.4. DISTRIBUTION OF BARIUM (BA) IN SAMPLES OF METALLURGICAL WASTES (Map 5.4, Fig. 5.4)

Barium varies from 28 to 2,059 ppm in metallurgical wastes. The highest Ba values are in samples of slag (118-2,059 ppm) followed by slag-earth (97-1,193 ppm), flotation residues (160-800 ppm), and pyritiferous sand (37-461 ppm). Sand blast material (65-141 ppm Ba) and pyrite tailings (28-142 ppm Ba) have comparatively lower Ba contents.

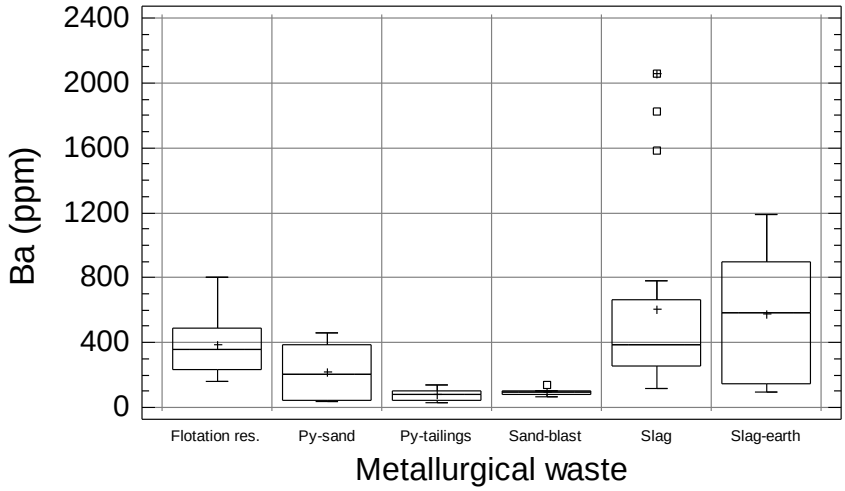

Fig. 5.4. Multiple boxplot of the distribution of barium (Ba) in samples from the different types of metallurgical processing wastes in the Lavrion urban area (refer to Map 5.4).
Σχ. 5.4. Πολλαπλό θηκόγραμμα κατανομής του βαρίου (Ba) στα δείγματα των διαφορετικών τύπων μεταλλουργικών απορριμμάτων από την αστική περιοχή του Λαυρίου (βλ. Χάρτη 5.4).

Slag has a number of outliers (Fig. 5.4, Map 5.4), which give it the greatest range, but a lower median value than slag-earth, which has overall higher Ba levels. Hence, Ba is enriched in samples of slag-earth from Fougara compared to normal slag.

Very high Ba contents in slag occur in samples from the Ayia Paraskevi and Komobil-Kiprianos heaps. Higher Ba values are also found in the slag heaps about Fougara, at Panormos and Neapoli, in comparison to those at Kavodokanos and Kiprianos, which have lower Ba levels. Slag samples to the south of Ayia Paraskevi and Kiprianos have similar Ba contents.

Pyritiferous sand samples from the beach, between Komobil and Kiprianos, have comparatively lower Ba levels than the ones further inland.

There is apparently a distinct difference between Ba levels in samples of flotation residues from Kavodokanos, which have higher values in comparison to the Noria-Prasini Alepou-Santorineika heap.

5.2.5. DISTRIBUTION OF BERYLLIUM (Be) IN SAMPLES OF METALLURGICAL WASTES (Map 5.5, Fig. 5.5)

Beryllium varies from <1.00 to 1.28 ppm in metallurgical wastes. All samples from the flotation residues, pyrite tailings and pyritiferous sand have Be values below the detection limit of the analytical method (<1.00 ppm Be). Samples of sand-blast material have the highest Be levels (<1.00-1.28 ppm), followed by slag (<1.00-1.16 ppm) and slag-earth (<1.00-1.02 ppm).

Higher Be values are found in slag heaps about Fougara, at Panormos and Neapoli, in comparison to those at Kavodokanos and Kiprianos (western part), which have lower Be contents. Slag heaps to the east of Ayia Paraskevi and between Komobil and

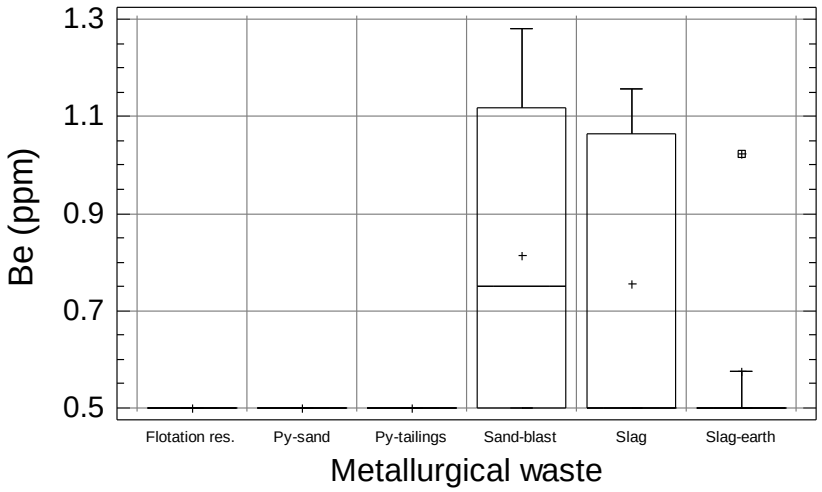

Fig. 5.5. Multiple boxplot of the distribution of beryllium (Be) in samples from the different types of metallurgical processing wastes in the Lavrion urban area (refer to Map 5.5).
Σχ. 5.5. Πολλαπλό θηκόγραμμα κατανομής του βηρυλλίου (Be) στα δείγματα των διαφορετικών τύπων μεταλλουργικών απορριμμάτων από την αστική περιοχή του Λαυρίου (βλ. Χάρτη 5.5).

Kiprianos have one sample with a high Be content. Slag samples to the south of Ayia Paraskevi and Kiprianos have similar Be levels.

5.2.6. DISTRIBUTION OF BISMUTH (Bi) IN SAMPLES OF METALLURGICAL WASTES (Map 5.6, Fig. 5.6)

Bismuth varies from <5.00 to 56.85 ppm in metallurgical wastes. Samples of slag and sand-blast material have Bi values below the detection limit of the analytical method

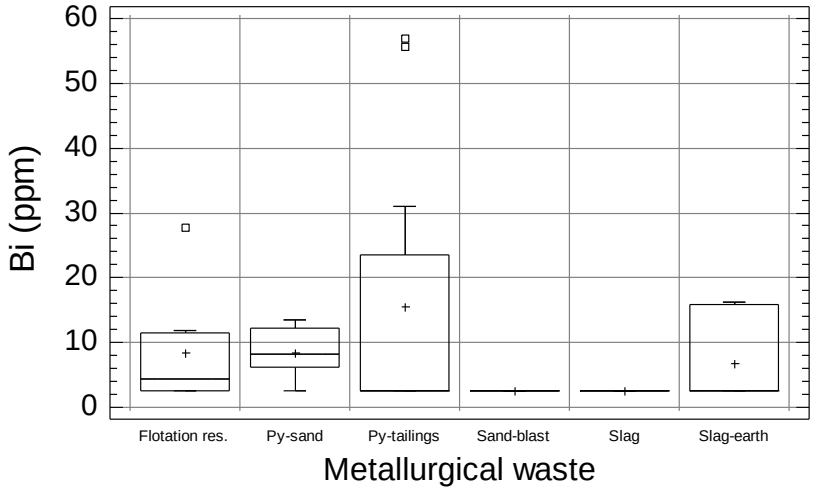

Fig. 5.6. Multiple boxplot of the distribution of bismuth (Bi) in samples from the different types of metallurgical processing wastes in the Lavrion urban area (refer to Map 5.6).
Σχ. 5.6. Πολλαπλό θηκόγραμμα κατανομής του βισμουθίου (Bi) στα δείγματα των διαφορετικών τύπων μεταλλουργικών απορριμμάτων από την αστική περιοχή του Λαυρίου (βλ. Χάρτη 5.6).

(<5.00 ppm Bi). Pyrite tailings have the highest Bi levels (<5.00-56.85 ppm), followed by flotation residues (<5.00-27.66 ppm), slag-earth (<5.00-16.32 ppm) and pyritiferous sand (<5.00-13.47 ppm).

Pyrite tailings at Nichtochori and Komobil have the highest Bi contents in comparison to those at Kavodokanos, Kiprianos and Santorineika. In the Komobil-Kiprianos area, there is again a distinction between higher Bi levels in pyritiferous sand on the beach and the distinctly lower values of further.

Flotation residues at Kavodokanos have higher Bi contents than those at Noria-Prasini Alepou-Santorineika.

5.2.7. DISTRIBUTION OF BORON (B) IN SAMPLES OF METALLURGICAL WASTES (Map 5.7, Fig. 5.7)

Boron varies from <5.00 to 667 ppm in metallurgical wastes. Samples of slag-earth have the highest B levels (34-667 ppm), followed by flotation residues (14-524 ppm), and sand-blast material (32-135 ppm). Samples of slag, pyritiferous sand and pyrite tailings have B contents of <100 ppm.

Slag heaps about Fougara, at Panormos and Neapoli have comparatively higher B contents than the ones at Kavodokanos and Kiprianos. A sample of slag-earth at Fougara has an unexplained very high B value of 667 ppm; similarly, a sample of flotation residues at Noria has a very high B level of 524 ppm (see boxplot outliers, Fig. 5.7).

The distinction between pyritiferous sand samples from the beach of Komobil-Kiprianos and those further inland still persists; the latter have higher values than those at the beach.

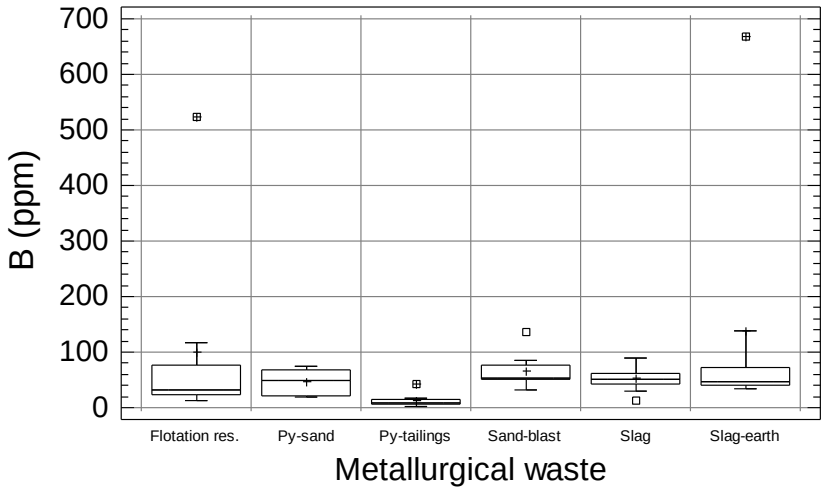

Fig. 5.7. Multiple boxplot of the distribution of boron (B) in samples from the different types of metallurgical processing wastes in the Lavrion urban area (refer to Map 5.7).
Σχ. 5.7. Πολλαπλό θηκόγραμμα κατανομής του βορίου (Β) στα δείγματα των διαφορετικών τύπων μεταλλουργικών απορριμμάτων από την αστική περιοχή του Λαυρίου (βλ. Χάρτη 5.7).

5.2.8. DISTRIBUTION OF CALCIUM (Ca) IN SAMPLES OF METALLURGICAL WASTES (Map 5.8, Fig. 5.8)

Calcium varies from 7,456 to 229,340 ppm in metallurgical wastes. Samples of flotation residues have the highest Ca levels (52,281-229,340 ppm) followed by slag-earth (90,198-178,354 ppm), sand-blast material (94,994-129,408 ppm), slag (24,050-128,840 ppm), pyrite tailings (7,456-122,660 ppm) and pyritiferous sand (89,718-116,217 ppm).

The only distinct geographical difference is between the Ca content of pyrite tailings from Nichtochori-Komobil with very low values, and the high levels in samples from Kavodokanos, Kiprianos and Santorineika (Map 5.8).

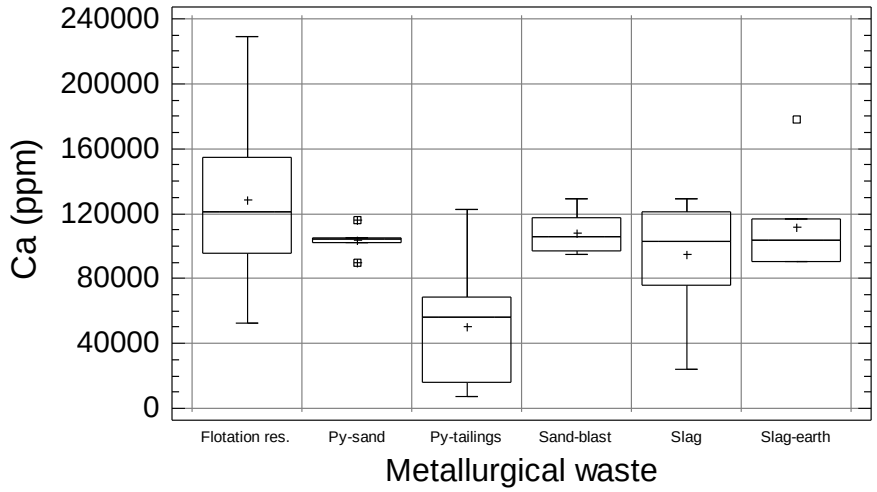

Fig. 5.8. Multiple boxplot of the distribution of calcium (Ca) in samples from the different types of metallurgical processing wastes in the Lavrion urban area (refer to Map 5.8).
Σχ. 5.8. Πολλαπλό θηκόγραμμα κατανομής του ασβεστίου (Ca) στα δείγματα των διαφορετικών τύπων μεταλλουργικών απορριμμάτων από την αστική περιοχή του Λαυρίου (βλ. Χάρτη 5.8).

5.2.9. DISTRIBUTION OF CADMIUM (Cd) IN SAMPLES OF METALLURGICAL WASTES (Map 5.9, Fig. 5.9)

Cadmium varies from 1.8 ppm to 580.84 ppm in metallurgical wastes. Samples of flotation residues have the highest Cd levels (26.61-580.84 ppm) followed by slag-earth (28.90-372.80 ppm), pyrite tailings (4.82-157.48 ppm), pyritiferous sand (29.23-156.83 ppm), sand-blast material (4.20-74.37 ppm), and slag (1.80-10.51 ppm).

Slag-earth has considerably higher Cd contents than slag, indicating a definite enrichment (Fig. 5.9, Map 5.9). Sand-blast material has also higher Cd contents than slag.

There is again a distinct difference among the pyrite tailings at Nichtochori-Komobil with very low Cd contents, and those at Kavodokanos, Kiprianos and Santorineika, which have higher levels.

The distinction between pyritiferous sand samples from the beach of Komobil-Kiprianos and those further inland is a feature that still persists; the latter have higher Cd values than the ones at the beach.

Flotation tailings at Noria-Prasini Alepou-Santorineika have lower Cd values in comparison to the ones at Kavodokanos. Flotation residues have consistently higher Cd values than the other types of metallurgical wastes, with very high levels at Kavodokanos (up to 580 ppm Cd).

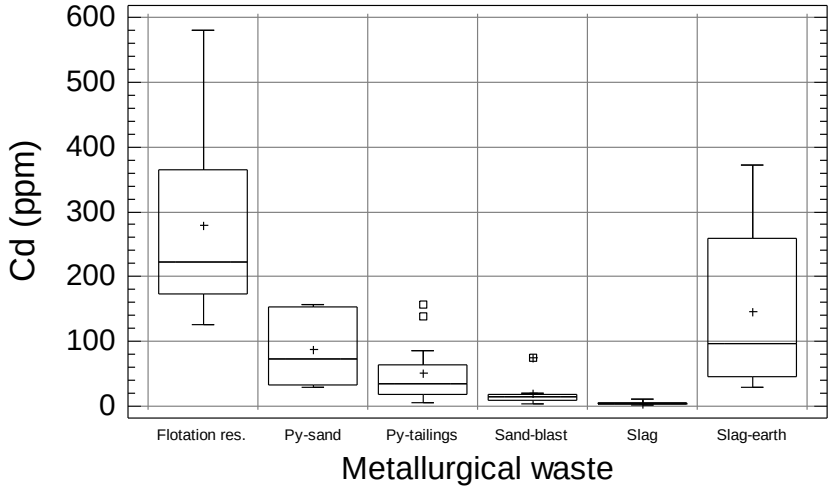

Fig. 5.9. Multiple boxplot of the distribution of cadmium (Cd) in samples from the different types of metallurgical processing wastes in the Lavrion urban area (refer to Map 5.9).
Σχ. 5.9. Πολλαπλό θηκόγραμμα κατανομής του καδμίου (Cd) στα δείγματα των διαφορετικών τύπων μεταλλουργικών απορριμμάτων από την αστική περιοχή του Λαυρίου (βλ. Χάρτη 5.9).

5.2.10. DISTRIBUTION OF COBALT (Co) IN SAMPLES OF METALLURGICAL WASTES (Map 5.10, Fig. 5.10)

Cobalt varies from 2.98 to 83.95 ppm in metallurgical wastes. Samples of pyrite

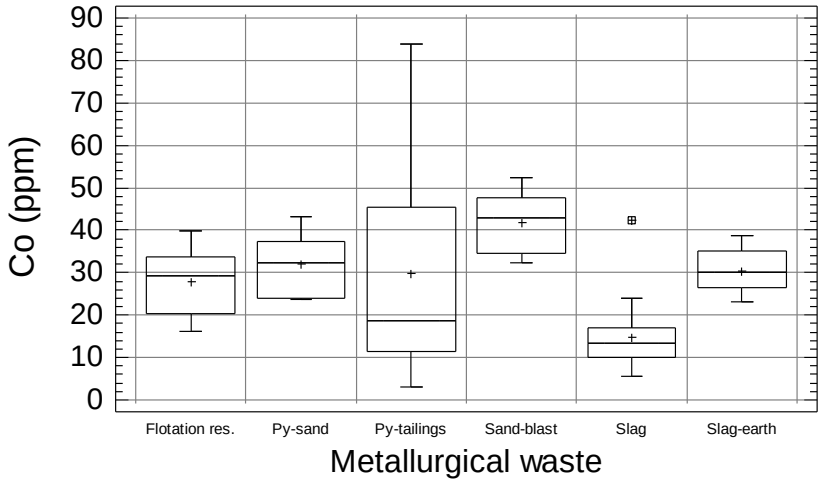

Fig. 5.10. Multiple boxplot of the distribution of cobalt (Co) in samples from the different types of metallurgical processing wastes in the Lavrion urban area (refer to Map 5.10).
Σχ. 5.10. Πολλαπλό θηκόγραμμα κατανομής του κοβαλτίου (Co) στα δείγματα των διαφορετικών τύπων μεταλλουργικών απορριμμάτων από την αστική περιοχή του Λαυρίου (βλ. Χάρτη 5.10).

tailings have the highest Co levels (2.98-83.95 ppm) followed by sand-blast material (32.32-52.37 ppm), pyritiferous sand (23.82-43.24 ppm), slag (5.61-42.26 ppm), flotation residues (16.13-39.87 ppm), and slag-earth (23.16-38.85 ppm).

Cobalt is enriched in slag-earth and sand-blast material compared to slag (Fig. 5.10, Map 5.10).

Pyrite tailings at Nichtochori-Komobil have higher Co levels that those at Kavodokanos, Kiprianos and Santorineika. Samples of pyritiferous sand from the beach of Komobil-Kiprianos have comparatively higher Co contents than those further inland.

Cobalt variation in samples of flotation tailings at Noria-Prasini Alepou-Santorineika and Kavodokanos is approximately similar.

5.2.11. DISTRIBUTION OF CHROMIUM (Cr) IN SAMPLES OF METALLURGICAL WASTES (Map 5.11, Fig. 5.11)

Chromium varies from 8.1 to 297.1 ppm in metallurgical wastes. Samples of sand-blast have the highest Cr levels (41.0-297.1 ppm) followed by slag-earth (61.6-248.9 ppm), slag (15.8-199.1 ppm), flotation residues (28.5-168.3 ppm), pyritiferous sand (25.3-144.1 ppm) and pyrite tailings (8.1-66.8 ppm).

Slag heaps about Fougara, at Neapoli, Ayia Paraskevi (eastern samples) and Komobil-Kiprianos have overall higher Cr levels in comparison to those at Kavodokanos, Kiprianos (south and west), Ayia Paraskevi (south) and Panormos. Slag samples to the south of Ayia Paraskevi and Kiprianos have similar Cr levels.

Slag-earth and sand-blast samples are generally enriched in Cr with respect to slag.

Pyrite tailings at Nichtochori-Komobil have lower Cr levels than those at Kavodokanos and Kiprianos.

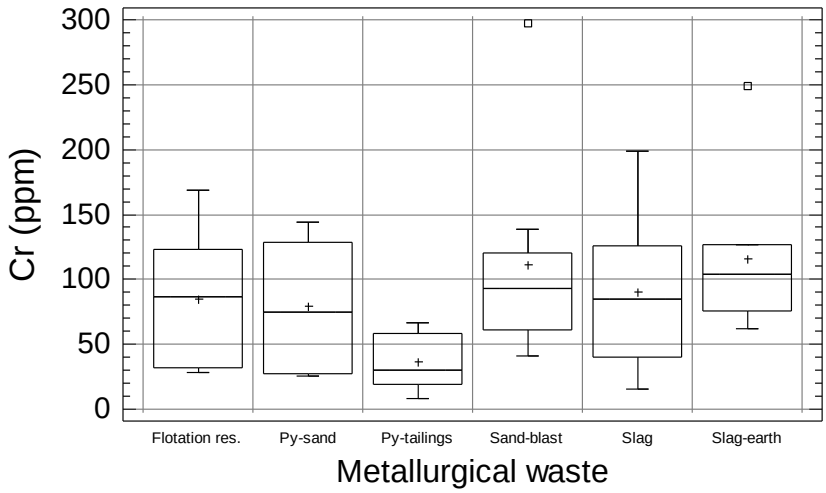

Fig. 5.11. Multiple boxplot of the distribution of chromium (Cr) in samples from the different types of metallurgical processing wastes in the Lavrion urban area (refer to Map 5.11).
Σχ. 5.11. Πολλαπλό θηκόγραμμα κατανομής του χρωμίου (Cr) στα δείγματα των διαφορετικών τύπων μεταλλουργικών απορριμμάτων από την αστική περιοχή του Λαυρίου (βλ. Χάρτη 5.11).

Samples of pyritiferous sand from the beach of Komobil-Kiprianos have comparatively lower Cr contents than the ones further inland.

Flotation tailings at Noria-Prasini Alepou-Santorineika have higher Cr values in comparison to those at Kavodokanos.

5.2.12. DISTRIBUTION OF COPPER (Cu) IN SAMPLES OF METALLURGICAL WASTES (Map 5.12, Fig. 5.12)

Copper varies from 184 to 8,700 ppm in metallurgical wastes. Samples of slag have the highest Cu levels (240-8,700 ppm) followed by sand-blast material (1,080-4,210 ppm), flotation residues (219-3,000 ppm), pyrite tailings (214-2,350 ppm), slag-earth (184-1,960 ppm), and pyritiferous sand (248-451 ppm).

Apart from a slag sample with very high Cu content at Kiprianos, the Kavodokanos slag has comparatively higher Cu levels than those about Fougara, at Panormos, Neapoli and Ayia Paraskevi.

Slag-earth and sand-blast wastes are generally enriched in Cu compared to slag.

Pyrite tailings at Kavodokanos, Kiprianos and Santorineika have generally higher Cu contents than the ones at Nichtochori-Komobil.

Flotation tailings at Noria-Prasini Alepou-Santorineika have lower Cu values in comparison to those at Kavodokanos.

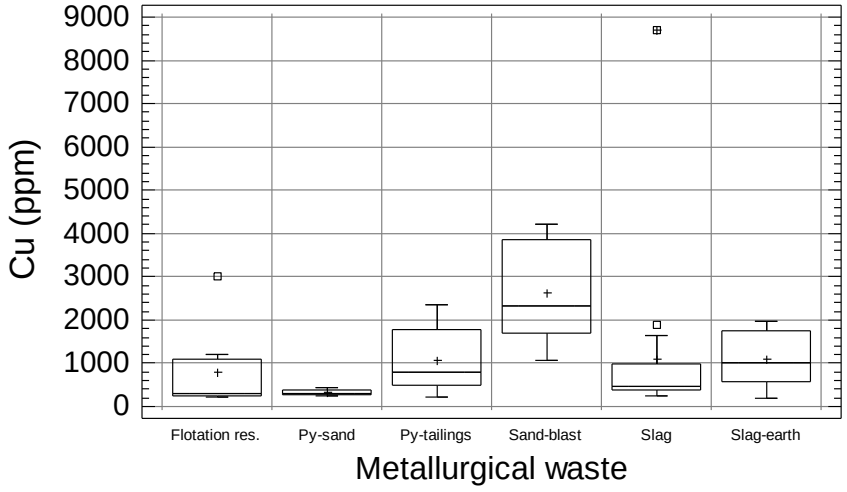

Fig. 5.12. Multiple boxplot of the distribution of copper (Cu) in samples from the different types of metallurgical processing wastes in the Lavrion urban area (refer to Map 5.12).
Σχ. 5.12. Πολλαπλό θηκόγραμμα κατανομής του χαλκού (Cu) στα δείγματα των διαφορετικών τύπων μεταλλουργικών απορριμμάτων από την αστική περιοχή του Λαυρίου (βλ. Χάρτη 5.12).

5.2.13. DISTRIBUTION OF IRON (Fe) IN SAMPLES OF METALLURGICAL WASTES (Map 5.13, Fig. 5.13)

Iron varies from 5.10 to 38.00% in metallurgical wastes. Samples of pyrite tailings have the highest Fe levels (17.30-38.00%) followed by slag (16.20-34.80%), sand-blast material (26.80-33.90%), slag-earth (7.50-25.00%), pyritiferous sand (5.10-24.30%), and flotation residues (3.50-18.50%).

As expected pyrite tailings have the highest Fe contents, and no significant differences exist among the various heaps.

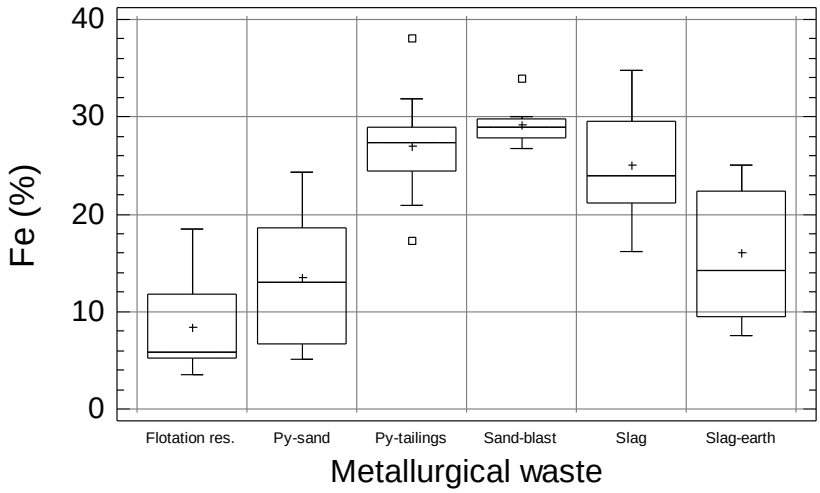

Fig. 5.13. Multiple boxplot of the distribution of iron (Fe) in samples from the different types of metallurgical processing wastes in the Lavrion urban area (refer to Map 5.13).
Σχ. 5.13. Πολλαπλό θηκόγραμμα κατανομής του σιδήρου (Fe) στα δείγματα των διαφορετικών τύπων μεταλλουργικών απορριμμάτων από την αστική περιοχή του Λαυρίου (βλ. Χάρτη 5.13).

Slag heaps about Fougara, at Panormos, Neapoli and Ayia Paraskevi (eastern samples) have overall slightly lower Fe levels than the ones at Kavodokanos, Kiprianos, Komobil-Kiprianos and Ayia Paraskevi (southern sample), which have distinctly higher values.

Sand-blast samples are enriched in Fe with respect to slag.

Samples of pyritiferous sand from the beach of Komobil-Kiprianos have comparatively higher Fe contents than those further inland.

Flotation tailings at Noria-Prasini Alepou-Santorineika have lower Fe values in comparison to those at Kavodokanos.

5.2.14. DISTRIBUTION OF MERCURY (Hg) IN SAMPLES OF METALLURGICAL WASTES (Map 5.14, Fig. 5.14)

Mercury varies from <1.00 to 10.20 ppm in metallurgical wastes. Samples of flotation residues have the highest Hg levels (2.14-10.20 ppm) followed by slag-earth (1.10-5.43 ppm), pyrite tailings (<1.00-5.04 ppm), slag (<1.00-4.55 ppm,), pyritiferous sand (1.41-3.26 ppm), and sand-blast material (1.73-3.25 ppm).

Slag heaps about Fougara, at Panormos, Neapoli, Ayia Paraskevi and Komobil-Kiprianos have overall slightly lower Hg levels than those at Kavodokanos and Kiprianos (western part). Slag samples to the east of Ayia Paraskevi have Hg contents below the detection limit of the analytical method.

Sand-blast and slag-earth samples are slightly enriched in Hg with respect to slag.

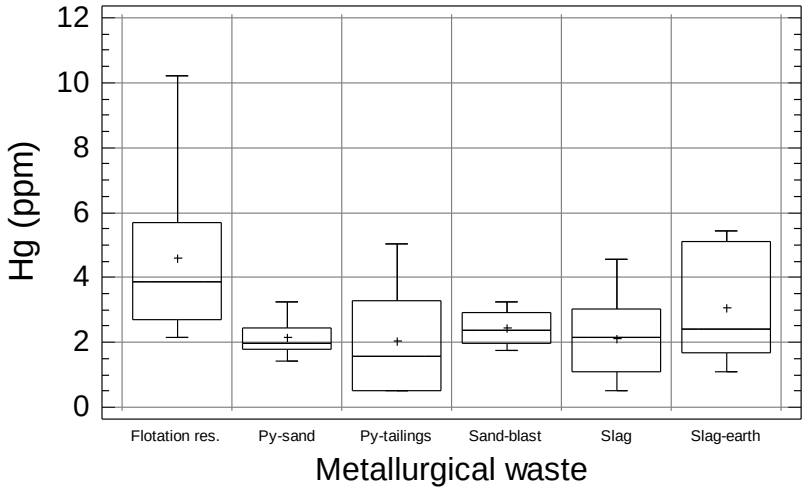

Fig. 5.14. Multiple boxplot of the distribution of mercury (Hg) in samples from the different types of metallurgical processing wastes in the Lavrion urban area (refer to Map 5.14).
Σχ. 5.14. Πολλαπλό θηκόγραμμα κατανομής του υδραργύρου (Hg) στα δείγματα των διαφορετικών τύπων μεταλλουργικών απορριμμάτων από την αστική περιοχή του Λαυρίου (βλ. Χάρτη 5.14).

Pyrite tailings at Nichtochori-Komobil have generally lower Hg levels in comparison to those at Kavodokanos and Kiprianos.

Samples of pyritiferous sand from the beach of Komobil-Kiprianos have comparatively lower Hg contents than those further inland.

Flotation tailings at Noria-Prasini Alepou-Santorineika have lower Hg values than the ones at Kavodokanos.

5.2.15. DISTRIBUTION OF POTASSIUM (K) IN SAMPLES OF METALLURGICAL WASTES (Map 5.15, Fig. 5.15)

Potassium varies from 993 to 13,407 ppm in metallurgical wastes. Samples of slag have the highest K levels (2,587-13,407 ppm) followed by pyritiferous sand (1,338-10,166 ppm), slag-earth (3,282-9,942 ppm), flotation residues (3,311-9,394 ppm), sand-blast material (5,800-7,975 ppm), and pyrite tailings (993-3,668 ppm).

Slag heaps about Fougara, at Panormos, Neapoli, Ayia Paraskevi and Komobil-Kiprianos have higher K levels than those at Kavodokanos and Kiprianos (western part).

Sand-blast and slag-earth samples have lower K contents with respect to.

Pyrite tailings at Nichtochori-Komobil have two samples with higher K levels in comparison to the ones at Kavodokanos, Kiprianos and Santorineika.

Samples of pyritiferous sand from the beach of Komobil-Kiprianos have comparatively lower K contents than the ones further inland.

Flotation tailings at Noria-Prasini Alepou-Santorineika have higher K values compared to those at Kavodokanos.

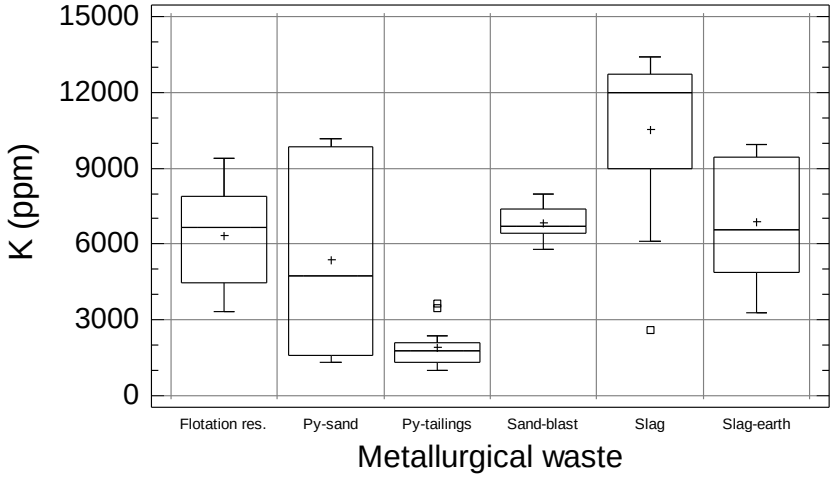

Fig. 5.15. Multiple boxplot of the distribution of potassium (K) in samples from the different types of metallurgical processing wastes in the Lavrion urban area (refer to Map 5.15).
Σχ. 5.15. Πολλαπλό θηκόγραμμα κατανομής του καλίου (K) στα δείγματα των διαφορετικών τύπων μεταλλουργικών απορριμμάτων από την αστική περιοχή του Λαυρίου (βλ. Χάρτη 5.15).

5.2.16. DISTRIBUTION OF LANTHANUM (La) IN SAMPLES OF METALLURGICAL WASTES

(Map 5.16, Fig. 5.16)

Lanthanum varies from <2.00 to 47.25 ppm in metallurgical wastes. Samples of slag have the highest La levels (22.12-47.25 ppm) followed by sand-blast material (25.87-39.46

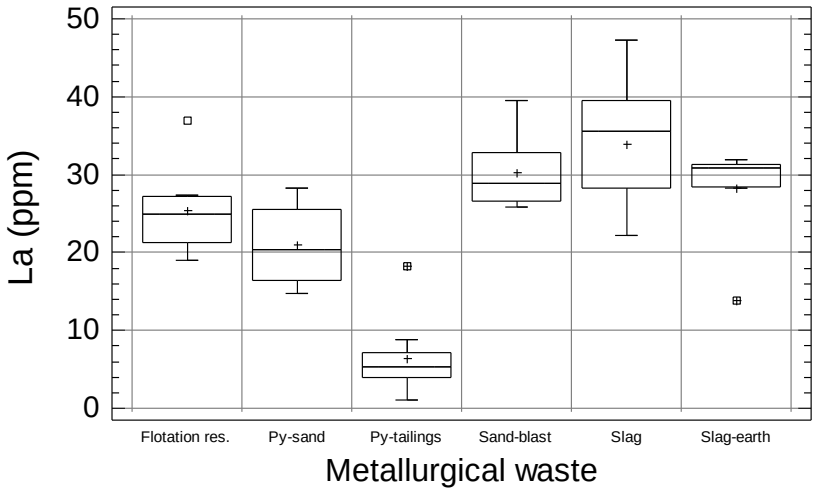

Fig. 5.16. Multiple boxplot of the distribution of lanthanum (La) in samples from the different types of metallurgical processing wastes in the Lavrion urban area (refer to Map 5.16).
Σχ. 5.16. Πολλαπλό θηκόγραμμα κατανομής του λανθανίου (La) στα δείγματα των διαφορετικών τύπων μεταλλουργικών απορριμμάτων από την αστική περιοχή του Λαυρίου (βλ. Χάρτη 5.16).

ppm), flotation residues (18.99-36.99 ppm), slag-earth (13.76-31.94 ppm), pyritiferous sand (14.81-28.21 ppm), and pyrite tailings (<2.00-18.22 ppm).

Slag heaps about Fougara, at Panormos, Neapoli, Ayia Paraskevi (eastern samples) and Komobil-Kiprianos have overall slightly higher La levels than those at Kavodokanos, Kiprianos (western part) and south of Ayia Paraskevi. Slag samples to the south of Ayia Paraskevi and Kiprianos have similar La levels.

Sand-blast and slag-earth samples have lower La contents with respect to.

Pyrite tailings at Nichtochori-Komobil have generally lower La levels in comparison to those at Kavodokanos, Kiprianos and Santorineika.

Samples of pyritiferous sand from the beach of Komobil-Kiprianos have comparatively lower La contents than the ones further inland.

Flotation tailings at Noria-Prasini Alepou-Santorineika have lower La values in comparison to those at Kavodokanos.

5.2.17. DISTRIBUTION OF LITHIUM (Li) IN SAMPLES OF METALLURGICAL WASTES (Map 5.17, Fig. 5.17)

Lithium varies from <2.00 to 25.83 ppm in metallurgical wastes. Samples of slag have the highest Li levels (7.63-25.83 ppm) followed by sand-blast material (16.11-20.23 ppm), slag-earth (6.83-16.93 ppm), pyritiferous sand (5.09-11.89 ppm), flotation residues (2.63-11.27 ppm), and pyrite tailings (<2.00-5.71 ppm).

Slag heaps about Fougara, at Panormos, Neapoli, Ayia Paraskevi (eastern samples) and Komobil-Kiprianos have overall slightly higher Li levels than those at

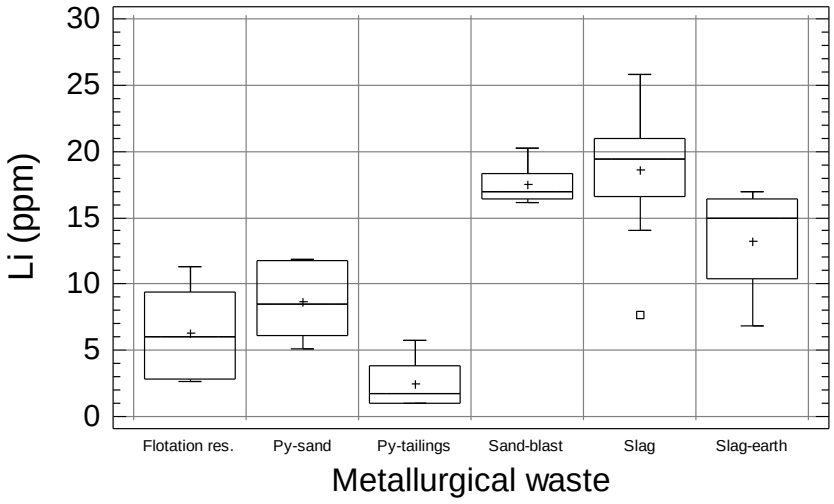

Fig. 5.17. Multiple boxplot of the distribution of lithium (Li) in samples from the different types of metallurgical processing wastes in the Lavrion urban area (refer to Map 5.17).
Σχ. 5.17. Πολλαπλό θηκόγραμμα κατανομής του λιθίου (Li) στα δείγματα των διαφορετικών τύπων μεταλλουργικών απορριμμάτων από την αστική περιοχή του Λαυρίου (βλ. Χάρτη 5.17).

Kavodokanos, Kiprianos (western part) and south of Ayia Paraskevi. Slag samples to the south of Ayia Paraskevi and Kiprianos have similar Li levels.

Sand-blast and slag-earth samples have lower Li contents with respect to.

Pyrite tailings at Nichtochori-Komobil have overall lower Li levels than the ones at Kavodokanos, Kiprianos and Santorineika.

Samples of pyritiferous sand from the beach of Komobil-Kiprianos have comparatively lower Li contents than those further inland.

Flotation tailings at Noria-Prasini Alepou-Santorineika have higher Li values in comparison to those at Kavodokanos.

5.2.18. DISTRIBUTION OF MANGANESE (Mn) IN SAMPLES OF METALLURGICAL WASTES
(Map 5.18, Fig. 5.18)

Manganese varies from 182 to 35,354 ppm in metallurgical wastes. Samples of slag have the highest Mn levels (5,739-35,354 ppm) followed by sand-blast material (13,228-21,981 ppm), slag-earth (3,302-18,311 ppm), pyritiferous sand (2,810-14,906 ppm), pyrite tailings (182-11,256 ppm), and flotation residues (1,736-8,711 ppm).

Slag heaps about Fougara, at Panormos, Neapoli, Ayia Paraskevi and Komobil-Kiprianos have overall slightly lower Mn levels than those at Kavodokanos and Kiprianos (western part).

Sand-blast and slag-earth samples have generally lower Mn contents with respect to slag.

Pyrite tailings at Nichtochori-Komobil have lower Mn levels in comparison to the ones at Kavodokanos, Kiprianos and Santorineika.

Samples of pyritiferous sand from the beach of Komobil-Kiprianos have comparatively higher Mn contents than those further inland.

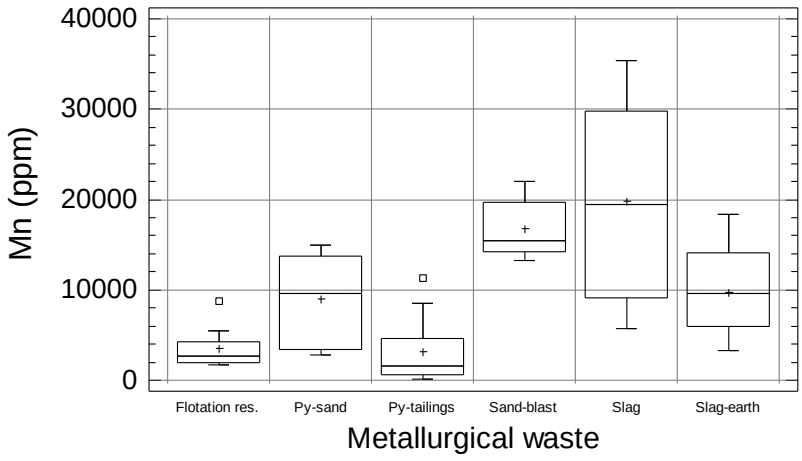

Fig. 5.18. Multiple boxplot of the distribution of manganese (Mn) in samples from the different types of metallurgical processing wastes in the Lavrion urban area (refer to Map 5.18).
Σχ. 5.18. Πολλαπλό θηκόγραμμα κατανομής του μαγγανίου (Mn) στα δείγματα των διαφορετικών τύπων μεταλλουργικών απορριμμάτων από την αστική περιοχή του Λαυρίου (βλ. Χάρτη 5.18).

Flotation tailings at Noria-Prasini Alepou-Santorineika have lower Mn values in comparison to the ones at Kavodokanos.

5.2.19. DISTRIBUTION OF MOLYBDENUM (Mo) IN SAMPLES OF METALLURGICAL WASTES (Map 5.19, Fig. 5.19)

Molybdenum varies from <1.00 to 11.08 ppm in metallurgical wastes. Samples of sand-blast material have the highest Mo levels (5.88-111.08 ppm) followed by slag (1.35-18.74 ppm), pyrite tailings (<1.00-6.81 ppm), slag-earth (2.65-5.77 ppm), flotation residues (1.47-5.09 ppm), and pyritiferous sand (1.70-4.18 ppm).

Patterns are difficult to discern because of the very high contrast between Mo in sand-blast samples and the other types of metallurgical wastes. Nevertheless, slag heaps about Fougara and at Neapoli have overall slightly lower Mo levels than those at Panormos, Ayia Paraskevi, Komobil-Kiprianos, Kiprianos and Kavodokanos.

Sand-blast samples have considerably higher Mo contents with respect to slag.

Flotation tailings at Noria-Prasini Alepou-Santorineika have overall higher Mo values than the ones at Kavodokanos.

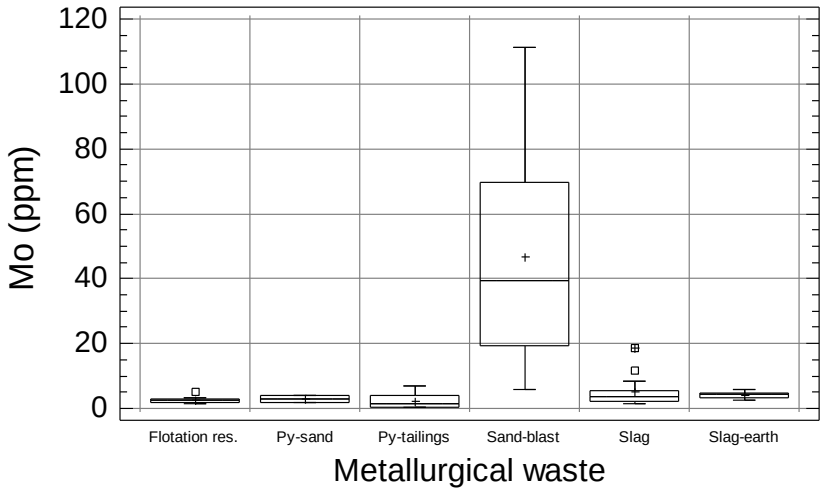

Fig. 5.19. Multiple boxplot of the distribution of molybdenum (Mo) in samples from the different types of metallurgical processing wastes in the Lavrion urban area (refer to Map 5.19).
Σχ. 5.19. Πολλαπλό θηκόγραμμα κατανομής του μολυβδαινίου (Mo) στα δείγματα των διαφορετικών τύπων μεταλλουργικών απορριμμάτων από την αστική περιοχή του Λαυρίου (βλ. Χάρτη 5.19).

5.2.20. DISTRIBUTION OF NICKEL (Ni) IN SAMPLES OF METALLURGICAL WASTES (Map 5.20, Fig. 5.20)

Nickel varies from 5.5 to 205.2 ppm in metallurgical wastes. Samples of slag-earth have the highest Ni levels (30.7-205.2 ppm) followed by flotation residues (28.9-123.8 ppm), pyritiferous sand (39.5-117.1 ppm), sand-blast material (33.8-105.2 ppm), slag (5.5-56.9 ppm), and pyrite tailings (12.9-55.2 ppm).

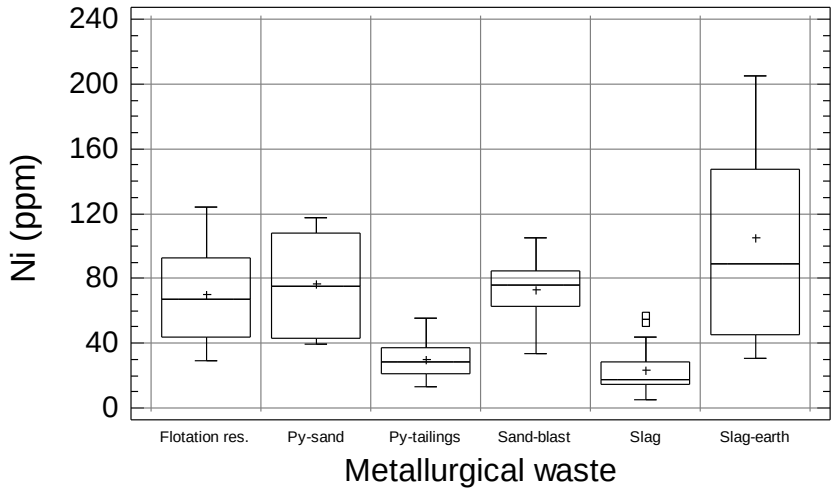

Fig. 5.20. Multiple boxplot of the distribution of nickel (Ni) in samples from the different types of metallurgical processing wastes in the Lavrion urban area (refer to Map 5.20).
Σχ. 5.20. Πολλαπλό θηκόγραμμα κατανομής του νικελίου (Ni) στα δείγματα των διαφορετικών τύπων μεταλλουργικών απορριμμάτων από την αστική περιοχή του Λαυρίου (βλ. Χάρτη 5.20).

Slag heaps about Fougara, at Panormos, Neapoli, Ayia Paraskevi (eastern part) and Komobil-Kiprianos have overall slightly higher Ni levels than those at Ayia Paraskevi (south), Kavodokanos and Kiprianos (western part), with the exception of one sample in each area with slightly elevated Ni contents.

Sand-blast and slag-earth samples are enriched in Ni with respect to slag.

Pyrite tailings at Nichtochori-Komobil have in general slightly lower Ni levels than those at Kavodokanos and Kiprianos; the Santorineika sample has a lower Ni content than the ones from the former area.

Samples of pyritiferous sand from the beach of Komobil-Kiprianos have comparatively lower Ni contents than those further inland.

Flotation tailings at Noria-Prasini Alepou-Santorineika have higher Ni values in comparison to the ones at Kavodokanos.

5.2.21. DISTRIBUTION OF PHOSPHORUS (P) IN SAMPLES OF METALLURGICAL WASTES
(Map 5.21, Fig. 5.21)

Phosphorus varies from <10.00 to 2,116.6 ppm in metallurgical wastes. Samples of pyrite tailings have the highest P levels (<10.0-2,116.6 ppm) followed by slag (332.9-1,904.4 ppm), sand-blast material (947.8-1,286.6 ppm), slag-earth (599.5-1,160.5 ppm), pyritiferous sand (270.7-817.1 ppm), and flotation residues (372.8-605.2 ppm).

Distinctive P patterns do not appear to exist among the different heaps of slag and flotation residues.

Sand-blast and slag-earth samples have lower P contents with respect to slag.

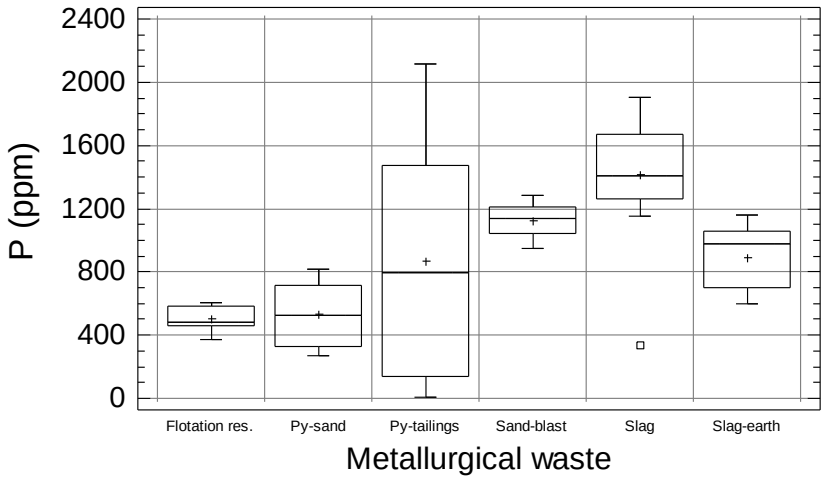

Fig. 5.21. Multiple boxplot of the distribution of phosphorus (P) in samples from the different types of metallurgical processing wastes in the Lavrion urban area (refer to Map 5.21).
Σχ. 5.21. Πολλαπλό θηκόγραμμα κατανομής του φωσφόρου (P) στα δείγματα των διαφορετικών τύπων μεταλλουργικών απορριμμάτων από την αστική περιοχή του Λαυρίου (βλ. Χάρτη 5.21).

Pyrite tailings at Nichtochori-Komobil have considerably lower P levels than those at Kavodokanos, Kiprianos and Santorineika.

Samples of pyritiferous sand from the beach of Komobil-Kiprianos have comparatively lower P contents than the ones further inland.

5.2.22. DISTRIBUTION OF LEAD (Pb) IN SAMPLES OF METALLURGICAL WASTES (Map 3.2)

For the distribution of lead in metallurgical wastes refer to Chapter 3 (pages 66-68).

5.2.23. DISTRIBUTION OF SULPHUR (S) IN SAMPLES OF METALLURGICAL WASTES (Map 5.23, Fig. 5.23)

Sulphur varies from 0.20 to 34.17% in metallurgical wastes. Samples of pyrite tailings have the highest S levels (7.41-34.17%) followed by pyritiferous sand (0.51-16.50%), slag (0.26-5.14%), sand-blast material (1.51-3.20%), slag-earth (0.21-2.17%), and flotation residues (0.20-2.01%).

Pyrite tailings at Nichtochori-Komobil have higher S levels than those at Kavodokanos, Kiprianos and Santorineika.

Samples of pyritiferous sand from the beach of Komobil-Kiprianos have comparatively higher S contents than the ones further inland.

Slag heaps about Fougara, at Panormos, Neapoli, Ayia Paraskevi and Komobil-Kiprianos have overall slightly lower S levels than those at Kavodokanos and Kiprianos (western part).

Sand-blast and slag-earth samples have correspondingly higher and lower S contents in comparison to slag.

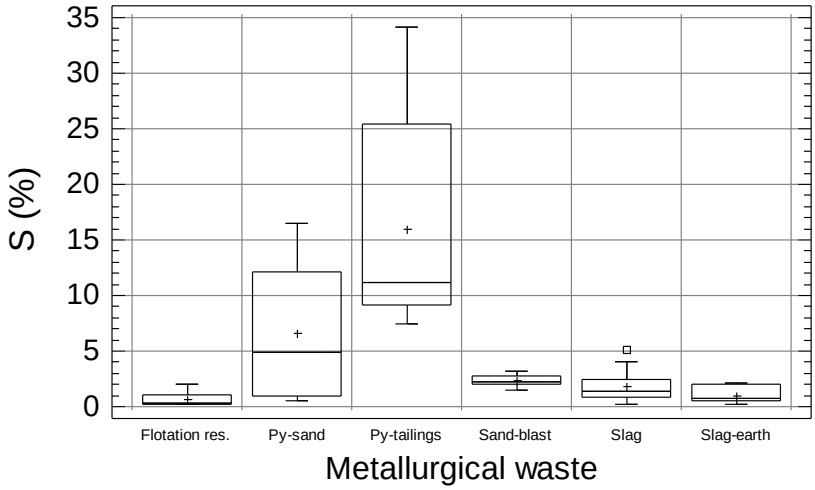

Fig. 5.23. Multiple boxplot of the distribution of sulphur (S) in samples from the different types of metallurgical processing wastes in the Lavrion urban area (refer to Map 5.23).
Σχ. 5.23. Πολλαπλό θηκόγραμμα κατανομής του θείου (S) στα δείγματα των διαφορετικών τύπων μεταλλουργικών απορριμμάτων από την αστική περιοχή του Λαυρίου (βλ. Χάρτη 5.23).

Flotation tailings at Noria-Prasini Alepou-Santorineika have slightly lower S values than those at Kavodokanos.

5.2.24. DISTRIBUTION OF ANTIMONY (Sb) IN SAMPLES OF METALLURGICAL WASTES

(Map 5.24, Fig. 5.24)

Antimony varies from 13 to 851 ppm in metallurgical wastes. Samples of sand-blast material have the highest Sb levels (139-851 ppm) followed by flotation residues (324-609 ppm), slag-earth (66-541 ppm), pyritiferous sand (70-538 ppm), pyrite tailings (84-376 ppm), and slag (13-342 ppm).

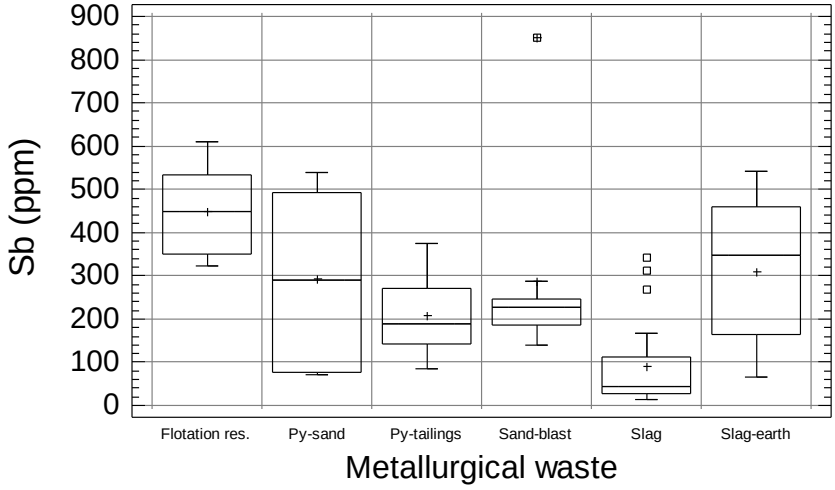

Fig. 5.24. Multiple boxplot of the distribution of antimony (Sb) in samples from the different types of metallurgical processing wastes in the Lavrion urban area (refer to Map 5.24).
Σχ. 5.24. Πολλαπλό θηκόγραμμα κατανομής του αντιμονίου (Sb) στα δείγματα των διαφορετικών τύπων μεταλλουργικών απορριμμάτων από την αστική περιοχή του Λαυρίου (βλ. Χάρτη 5.24).

Slag heaps about Fougara, at Panormos, Ayia Paraskevi (eastern part) and Komobil-Kiprianos have overall slightly higher Sb levels than those at Kavodokanos and Kiprianos (western part). The highest Sb contents in slag are found in two samples to the east of Ayia Paraskevi and the beach between Komobil and Kiprianos.

Sand-blast and slag-earth samples have overall higher contents in comparison to slag.

Pyrite tailings at Nichtochori-Komobil have overall higher Sb levels than the ones at Kavodokanos, Kiprianos and Santorineika.

Samples of pyritiferous sand from the beach at Komobil-Kiprianos have comparatively lower Sb contents than those further inland.

Flotation tailings at Noria-Prasini Alepou-Santorineika have overall lower Sb values in comparison to the ones at Kavodokanos.

5.2.25. DISTRIBUTION OF TIN (Sn) IN SAMPLES OF METALLURGICAL WASTES (Map 5.25, Fig. 5.25)

Tin varies from 5.68 to 332.25 ppm in metallurgical wastes. Samples of sand-blast material have the highest Sn levels (38.96-332.25 ppm) followed by pyrite tailings (7.91-74.75 ppm), slag (15.32-62.22 ppm), slag-earth (20.54-40.08 ppm), pyritiferous sand (5.68-25.48 ppm), and flotation residues (7.36-22.19 ppm).

Slag heaps about Fougara, at Panormos, Neapoli, Ayia Paraskevi and Komobil-Kiprianos have overall slightly higher Sn levels than those at Kavodokanos and Kiprianos.

Sand-blast and slag-earth samples have correspondingly higher and lower Sn contents in comparison to slag.

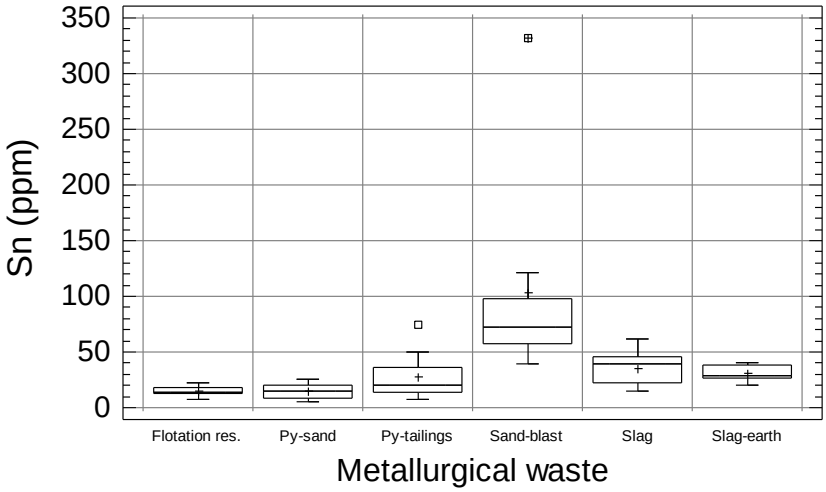

Fig. 5.25. Multiple boxplot of the distribution of tin (Sn) in samples from the different types of metallurgical processing wastes in the Lavrion urban area (refer to Map 5.25).
Σχ. 5.25. Πολλαπλό θηκόγραμμα κατανομής του κασσιτέρου (Sn) στα δείγματα των διαφορετικών τύπων μεταλλουργικών απορριμμάτων από την αστική περιοχή του Λαυρίου (βλ. Χάρτη 5.25).

Pyrite tailings at Nichtochori-Komobil have higher Sn levels than in comparison to the ones at Kavodokanos, Kiprianos and Santorineika.

Samples of pyritiferous sand from the beach at Komobil-Kiprianos have comparatively slightly lower Sn contents than the ones further inland.

Flotation tailings at Noria-Prasini Alepou-Santorineika have slightly lower Sn values than those at Kavodokanos.

5.2.26. DISTRIBUTION OF STRONTIUM (Sr) IN SAMPLES OF METALLURGICAL WASTES

(Map 5.26, Fig. 5.26)

Strontium varies from 10.4 to 798.6 ppm in metallurgical wastes. Samples of sand-blast material have the highest Sr levels (218.8-798.6 ppm) followed by slag-earth (113.4-453.5 ppm), slag (133.1-389.3 ppm), flotation residues (92.1-181.5 ppm), pyritiferous sand (78.6-106.0 ppm), and pyrite tailings (10.4-98.9 ppm).

Slag heaps about Fougara, at Panormos, Ayia Paraskevi and Komobil-Kiprianos have overall slightly higher Sr levels in comparison to those at Kavodokanos, Kiprianos (western part) and Neapoli.

Sand-blast and slag-earth samples have correspondingly higher and lower Sr contents in comparison to slag.

Pyrite tailings at Nichtochori-Komobil have slightly lower Sr levels than those at Kavodokanos, Kiprianos and Santorineika.

No distinct difference in Sr content exists between samples of pyritiferous sand from the beach at Komobil-Kiprianos and the ones further inland.

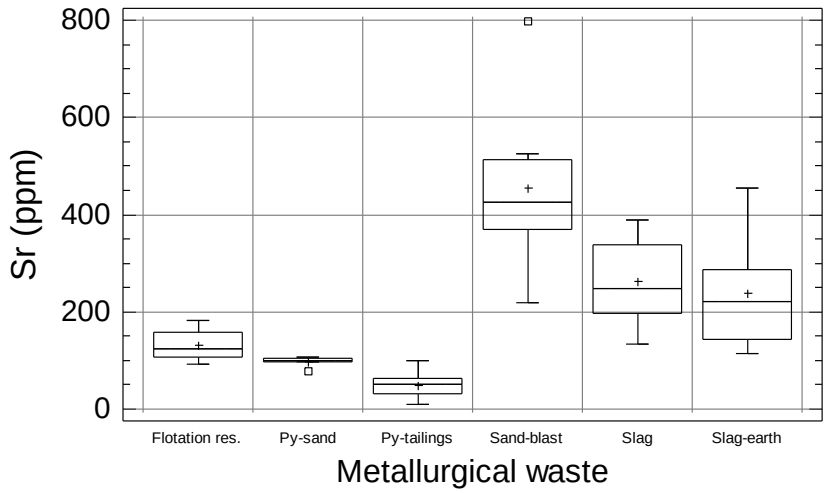

Fig. 5.26. Multiple boxplot of the distribution of strontium (Sr) in samples from the different types of metallurgical processing wastes in the Lavrion urban area (refer to Map 5.26).
Σχ. 5.26. Πολλαπλό θηκόγραμμα κατανομής του στροντίου (Sr) στα δείγματα των διαφορετικών τύπων μεταλλουργικών απορριμμάτων από την αστική περιοχή του Λαυρίου (βλ. Χάρτη 5.26).

Flotation tailings at Noria-Prasini Alepou-Santorineika have slightly lower Sr values in comparison to those at Kavodokanos.

5.2.27. DISTRIBUTION OF TITANIUM (Ti) IN SAMPLES OF METALLURGICAL WASTES (Map 5.27, Fig. 5.27)

Titanium varies from <10.00 to 2,013.1 ppm in metallurgical wastes. Samples of slag have the highest Ti levels (322.9-2013.1 ppm) followed by sand-blast material (973.7-1806.9 ppm), slag-earth (274.1-1519.7 ppm), flotation residues (57.7-564.5 ppm), pyritiferous sand (72.5-455.0 ppm), and pyrite tailings (<10.0-116.8 ppm).

Slag heaps about Fougara, at Panormos, Neapoli, Ayia Paraskevi and Komobil-Kiprianos have distinctly higher Ti levels than those at Kavodokanos and Kiprianos (western part). Sand-blast and slag-earth samples have lower Ti contents with respect to slag.

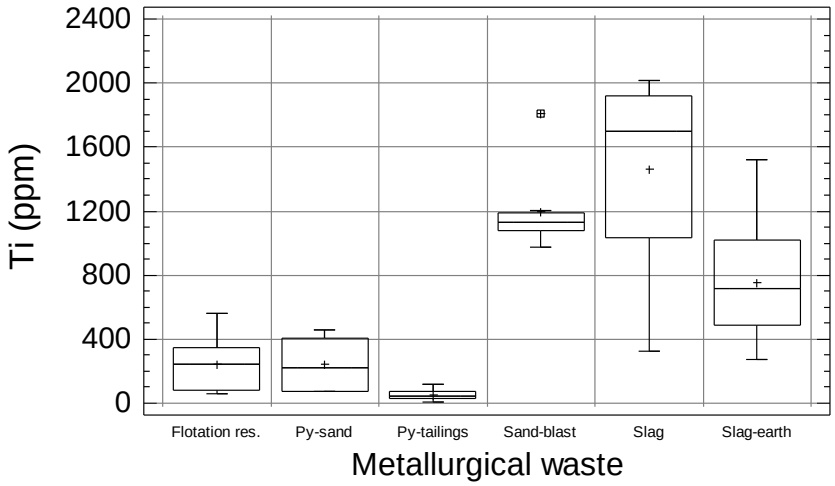

Fig. 5.27. Multiple boxplot of the distribution of titanium (Ti) in samples from the different types of metallurgical processing wastes in the Lavrion urban area (refer to Map 5.27).
Σχ. 5.27. Πολλαπλό θηκόγραμμα κατανομής του τιτανίου (Ti) στα δείγματα των διαφορετικών τύπων μεταλλουργικών απορριμμάτων από την αστική περιοχή του Λαυρίου (βλ. Χάρτη 5.27).

Pyrite tailings at Nichtochori-Komobil, Kiprianos and Santorineika have approximately similar Ti levels.

Samples of pyritiferous sand from the beach at Komobil-Kiprianos have comparatively lower Ti contents than those further inland.

Flotation tailings at Noria-Prasini Alepou-Santorineika have higher Ti values compared to the ones at Kavodokanos.

5.2.28. DISTRIBUTION OF URANIUM (U) IN SAMPLES OF METALLURGICAL WASTES (Map 5.28, Fig. 5.28)

Uranium varies from <5.00 to 12.46 ppm in metallurgical wastes. Samples of sand-blast material have the highest U levels (<5.00-12.46 ppm) followed by slag (<5.00-8.62 ppm), and flotation residues (<5.00-5.63 ppm). Pyrite tailings and pyritiferous sand have values below the detection limit of the analytical method (<5.00 ppm).

Sand-blast wastes have a single sample with high U of 12.46 ppm (west of Phenikodassos), otherwise their range of U values falls within the slag variation.

Slag heaps to the east of Ayia Paraskevi and between Komobil and Kiprianos have similar U values. Slag samples to the south of Ayia Paraskevi and Kiprianos have similar U levels.

Slag-earth has generally lower U contents with respect to slag, except in one case at Kavodokanos where the sample is enriched in comparison to the corresponding slag.

Flotation tailings at Noria-Prasini Alepou-Santorineika have overall lower U values than those at Kavodokanos.

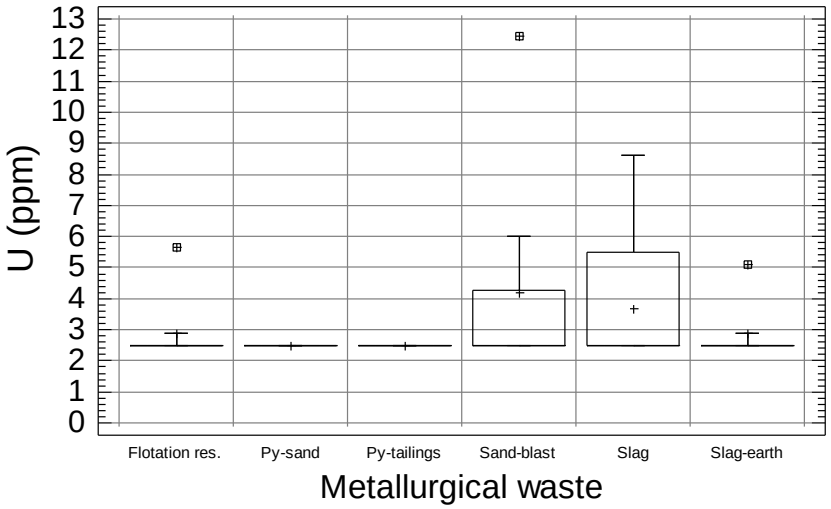

Fig. 5.28. Multiple boxplot of the distribution of uranium (U) in samples from the different types of metallurgical processing wastes in the Lavrion urban area (refer to Map 5.28).
Σχ. 5.28. Πολλαπλό θηκόγραμμα κατανομής του ουρανίου (U) στα δείγματα των διαφορετικών τύπων μεταλλουργικών απορριμμάτων από την αστική περιοχή του Λαυρίου (βλ. Χάρτη 5.28).

5.2.29. DISTRIBUTION OF VANADIUM (V) IN SAMPLES OF METALLURGICAL WASTES (Map 5.29, Fig. 5.29)

Vanadium varies from <2.00 to 104.24 ppm in metallurgical wastes. Samples of slag-earth have the highest V levels (39.25-104.24 ppm) followed by slag (18.45-84.77 ppm), sand-blast material (53.15-80.07 ppm), pyritiferous sand (42.52-77.73 ppm), flotation residues (18.75-51.27 ppm), and pyrite tailings (<2.00-29.70 ppm).

Slag heaps to the east of Ayia Paraskevi and the one between Komobil and Kiprianos have overall higher V levels in comparison to those about Fougara, at Panormos, Neapoli, Kavodokanos, Kiprianos and to the south of Ayia Paraskevi.

Sand-blast and slag-earth samples have generally higher V values with respect to slag.

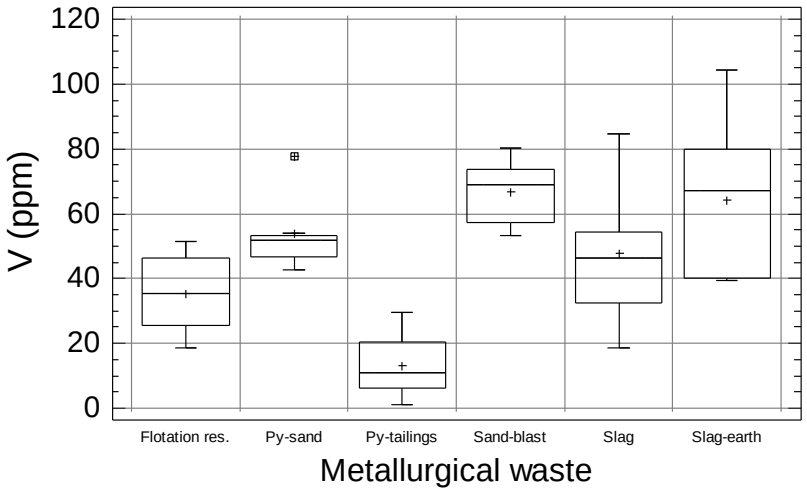

Fig. 5.29. Multiple boxplot of the distribution of vanadium (V) in samples from the different types of metallurgical processing wastes in the Lavrion urban area (refer to Map 5.29).
Σχ. 5.29. Πολλαπλό θηκόγραμμα κατανομής του βαναδίου (V) στα δείγματα των διαφορετικών τύπων μεταλλουργικών απορριμμάτων από την αστική περιοχή του Λαυρίου (βλ. Χάρτη 5.29).

Pyrite tailings at Nichtochori-Komobil have higher V levels in comparison to those at Kavodokanos, Kiprianos and Santorineika.

Samples of pyritiferous sand from the beach at Komobil-Kiprianos have comparatively lower V contents than those further inland.

Flotation tailings at Noria-Prasini Alepou-Santorineika have higher V values than the ones at Kavodokanos.

5.2.30. DISTRIBUTION OF ZINC (Zn) IN SAMPLES OF METALLURGICAL WASTES (Map 5.30, Fig. 5.30)

Zinc varies from 1,500 to 98,000 ppm in metallurgical wastes. Samples of flotation residues have the highest Zn contents (14,000-98,000 ppm) followed by sand-blast material (56,300-97,000 ppm), slag (29,500-76,000 ppm), slag-earth (7,400-69,000 ppm), pyrite tailings (1,500-47,600 ppm), and pyritiferous sand (7,500-24,000 ppm).

Slag heaps about Fougara, at Panormos, Neapoli, Ayia Paraskevi and Komobil-Kiprianos have overall lower Zn levels than those at Kavodokanos and Kiprianos.

Sand-blast samples have generally higher Zn contents with respect to slag. Slag-earth is locally slightly enriched in Zn (see Kavodokanos samples, Map 5.30)

Pyrite tailings at Nichtochori-Komobil have lower Zn levels compared to the ones at Kavodokanos, Kiprianos and Santorineika.

Samples of pyritiferous sand from the beach at Komobil-Kiprianos have comparatively lower Zn contents than the ones further inland.

Flotation tailings at Noria-Prasini Alepou-Santorineika have lower Zn values in comparison to those at Kavodokanos.

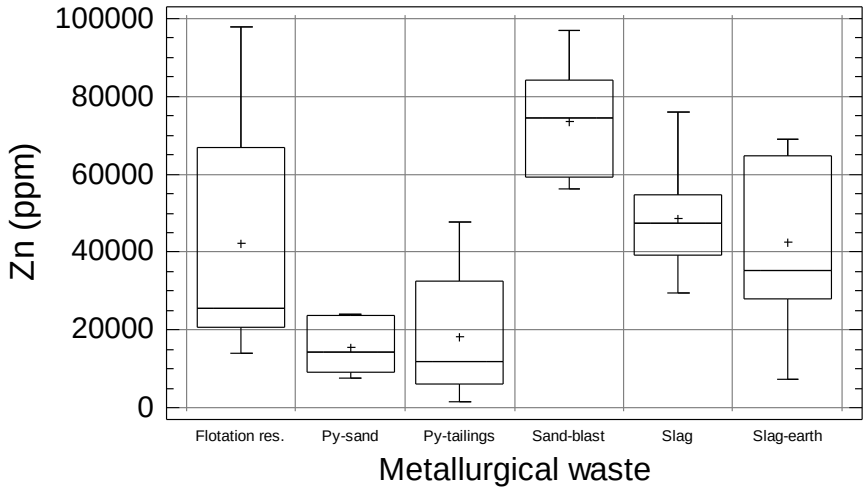

Fig. 5.30. Multiple boxplot of the distribution of zinc (Zn) in samples from the different types of metallurgical processing wastes in the Lavrion urban area (refer to Map 5.30).
Σχ. 5.30. Πολλαπλό θηκόγραμμα κατανομής του ψευδαργύρου (Zn) στα δείγματα των διαφορετικών τύπων μεταλλουργικών απορριμμάτων από την αστική περιοχή του Λαυρίου (βλ. Χάρτη 5.30).

5.3. DISCUSSION AND CONCLUSIONS

It must be appreciated that the metallurgical wastes in the Lavrion urban area are the products of over hundred years of ore processing. Apart from differences in the mineralogy of processed ore, changes made in the metallurgical methods, resulted in the production of wastes of different chemical composition. The above description of the chemistry of metallurgical processing wastes has verified the existence of distinct chemical differences among the six major metallurgical waste categories, but also within each one. The spatial chemical variation has been depicted, in general terms, by the geographical presentation of the results (Maps 5.1 to 5.30, Volume 2).

Slag heaps are distinguished into four different types in terms of their chemical composition, *i.e.*,

1. Fougara, Panormos and Neapoli are characterised by comparatively high levels in Al, (B), Ba, Be, (Cr), K, La, Li, Ni, Sb, Sn, Sr and Ti; *B is enriched in slag samples from Fougara and Panormos, and Cr from Fougara and Neapoli*.

2. Eastern part of Ayia Paraskevi and the beach section of Komobil-Kiprianos are characterised by comparatively high levels in Al, Ba, (Be), Cr, K, La, Li, Mo, Ni, Sb, Sn, Sr, Ti and V; *Be is only enriched in slag samples from Komobil-Kiprianos*.

3. South of Ayia Paraskevi are characterised by comparatively high in Al, Fe, K, Mo, Sn, Sr and Ti, and

4. Kavodokanos and Kiprianos (western part in the metallurgical plant) are characterised by comparatively high levels in (Ag), Cu, Fe, Hg, Mn, Mo, S and Zn; *Ag is only enriched in slag samples from Kavodokanos*.

Apart from the chemical differences, slag heaps can, in fact, be distinguished in the field as well. The lumpy slag to the south of Ayia Paraskevi, behind the old iron pier of

the former French Mining Company is comparatively more weathered than slag from other sites. It has also built on it old store rooms of the same company. The lumpy slag of the heaps about Fougara hill, Panormos and Neapoli is weathered to a variable degree, and should be of similar or slightly later age than that to the south of Ayia Paraskevi. The remaining slag heaps are of younger age, and not so weathered.

Sand-blast material comprises comminuted slag and fine pelletised slag. It is only found in the Kavodokanos area. Although chemically similar to the Kavodokanos slag, it appears when slag is fine- to medium-grained either by metallurgical process or crushing, its chemistry changes, *i.e.*, it is enriched in comparison to normal lumpy slag with respect to most elements, *e.g.*, Ag, As, B, Be, Ca, Cd, Cr, Cu, Fe, Hg, Mo, Ni, Pb, S, Sb, Sn, V and Zn. The earthy material within slag (*slag earth*) is also enriched; the Fougara slag earth is enriched with respect to Ag, Ba, Cd, Co, Cr, Cu, Hg, Ni, Pb, Sb and V, and the Kavodokanos slag earth in Ag, As, Cd, Co, Cr, Cu, Hg, Ni, Pb, Sb and V.

Pyrite tailings can also be distinguished chemically into four broad categories

(i) the Nichtochori-Komobil, which were produced by the Mediterranean Mines company from 1953 to 1963, and are characterised by high levels in Ag, As, Bi, Co, Fe, K, S, Sb, Sn and V, and are weathered to a variable extent.

(ii) Kavodokanos-Kiprianos-Santorineika, which are characterised by high levels in Al, Ca, Cd, (Cr), Cu, Fe, (Hg), La, Li, Mn, (Ni), P, Sr and Zn; *Cr is only enriched in slag samples from Kavodokanos, and Hg and Ni is only enriched in slag samples from Kavodokanos and Kiprianos*.

(iii) Thorikon beach, which are characterised by high levels in As, Bi, Co, Fe, Mn and S, and

(iv) Thorikon inland, which are characterised by high levels in Ag, Al, B, Ba, Cd, Cr, Hg, K, La, Li, Ni, P, Sb, Sn, Ti, V and Zn.

The Kavodokanos pyrite tailings are the most weathered. All pyrite tailings produce acid drainage and are, therefore, more hazardous for polluting groundwater resources.

Flotation residues are chemically distinguished into the large mass extending from Noria to Prasini Alepou and Santorineika, and the smaller heap at Kavodokanos. The former is characterised by high levels in Al, Cr, K, Li, Mo, Ni, Ti and V, and the latter in Ag, As, Ba, Bi, Cd, Cu, Fe, Hg, La, Mn, S, Sb, Sn, Sr, U, and Zn. Their different chemical composition is attributed to differences in the original processed ore and its gangue.

Table 5.1 summarises the chemical features of the metallurgical processing wastes. In the same table are given, for comparison purposes, the median rock and overburden values. This comparison definitely shows that the metallurgical wastes are the major source of “soil” contamination.

It is finally concluded that the metallurgical processing wastes have high toxic element concentrations (As, Be, Cd, Cu, Hg, Pb, Sb, Zn). Their wide distribution in the Lavrion urban area, *i.e.*, they cover approximately 1.8 km^2 of the 7.24 km^2 studied in this project, which represents about 25% of the total area, and transportation by aerial, fluvial and anthropogenic means, resulted in the contamination of residual and alluvial soil. The first priority, therefore, must be the rehabilitation of the metallurgical processing wastes by suitable methods.

Table 5.1. Statistical parameters of element concentrations in metallurgical processing wastes, rock and overburden in Lavrion. Median values of rock and overburden are given for comparison purposes.

Πίνακας 5.1. Στατιστικές παράμετροι των συγκεντρώσεων των στοιχείων στα δείγματα των μεταλλουργικών απορριμμάτων, πετρώματος και εδαφικού καλύμματος του Λαυρίου. Οι διάμεσες τιμές των συγκεντρώσεων των στοιχείων στα δείγματα πετρώματος και εδαφικού καλύμματος παραθέτονται για σύγκριση.

Elements	*All metallurgical processing wastes (n=62) (values in ppm)*						*Rock (n=140)**	*Overburden (n=224)***
	Minimum.	*Maximum*	*Mean*	*Standard deviation*	*Coefficient of variation (%)*	*Median*	*Median (ppm)*	*Median (ppm)*
Ag	3.20	96.00	33.80	28.22	83.49	18.90	0.50	12.06
Al	1118.00	38071.00	18998.00	10302.00	54.23	20074.00	8044.00	32315.00
As	283.00	26063.00	4593.00	5383.00	117.20	2492.00	15.60	1290.00
B	<5.00	667.07	61.78	102.80	166.40	42.97	0.25	136.00
Ba	27.70	2059.00	368.20	419.00	113.80	243.00	210.00	479.00
Be	<1.00	1.28	0.64	0.26	40.63	0.50	-	1.01
Bi	<5.00	56.85	6.83	10.82	158.31	2.50	-	11.00
Ca	7456.00	229340.00	99995.00	39454.00	39.46	102603.00	220.13	93625.00
Cd	116.59	580.84	74.80	116.59	155.87	20.62	0.50	38.00
Co	2.98	83.95	26.35	15.96	60.57	23.83	20.50	16.00
Cr	8.11	299.15	83.47	59.98	71.86	73.18	20.00	183.00
Cu	184.00	8700.00	1172.90	1362.60	116.17	630.50	25.00	186.00
Fe	35000.00	380000.00	217081.00	89238.00	41.11	234500.00	19515.00	44771.00
Hg	<1.00	10.20	2.58	1.73	67.05	2.35	0.50	0.14
K	993.00	13408.00	6942.00	3911.00	56.34	7100.00	8044.00	9770.00
La	<2.00	47.25	25.13	11.64	46.32	27.32	8.86	22.70
Li	<1.00	25.83	12.18	7.17	58.87	14.50	5.00	17.40
Mn	182.00	35354.00	11913.00	9925.00	83.31	9398.00	1200.00	2189.00
Mo	<1.00	111.08	9.25	19.01	205.51	3.57	0.50	4.90
Ni	5.47	205.22	51.36	40.36	78.58	38.52	54.50	127.00
P	<10.00	2117.00	1011.00	515.13	50.95	1103.00	1855.00	992.00
Pb	3800.00	85200.00	24450.97	18085.37	73.97	20750.00	22.00	7305.00
S	1972.06	341731.68	48394.57	73380.14	151.63	20581.19	1200.00	12690.00
Sb	183.30	851.00	229.50	183.30	79.87	189.00	2.50	121.00
Sn	5.68	332.25	37.54	43.67	116.36	27.71	-	18.50
Sr	150.80	798.60	210.60	150.80	71.61	178.69	98.00	118.00
Ti	<10.00	2031.00	799.80	682.50	85.33	737.70	300.00	2162.00
U	<5.00	12.46	3.21	1.85	57.63	2.50	2.50	3.00
V	<2.00	104.24	44.42	23.83	53.65	46.30	9.00	75.00
Zn	1500.00	98000.00	41194.00	25332.00	61.50	39800.00	57.00	6668.00

*Rock: Ag , Mo (n=155); ** B, Be, Bi, Hg, La, S, Sb, Sn, U (n=48); **Overburden: B, Bi, Hg, S, Sn, U (n=50) and Sb (n=90).

Chapter 6

GEOCHEMISTRY OF OVERBURDEN

Alecos Demetriades and Katerina Vergou-Vichou
Institute of Geology and Mineral Exploration, 70 Messoghion Street, Gr-115 27, Athens, Greece

6.1. INTRODUCTION

In Lavrion, it is difficult to sample uncontaminated residual soil *sensu strictu*, due to the presence of an enormous amount of metallurgical processing residues (Map 2.3, Volume 2), which are the result of anthropogenic activities from antiquarian to present times, and certainly since 1866 AD, when the recent, most intensive and environmentally destructive, exploitation began. Most of the surficial "soil" is a mixture of normal soil, and fine-grained metallurgical processing wastes. Hence, the preference to use the term *"overburden"*, which describes better the sampled loose surface material. *"Overburden"* is defined by Jackson (1997, p.457) as *"the loose soil, silt, sand, gravel, or other unconsolidated material overlying bedrock, either transported or formed in place."* Nevertheless, residual soil does occur in small patches over hilly ground, forested sections, and the northern and southern parts of the Lavrion urban area. Since, residual soil is somewhat scarce in Lavrion, soil, when used, is in the *sensu latu* sense.

Another problem encountered in the Municipality of Lavreotiki is that the local inhabitants are transporting themselves the fine- to medium-grained beneficiation/ flotation residues to fill in low ground or to mix-up with their garden soil or to use it instead of sand in concrete. Further, the coarse-grained metallurgical processing wastes, such as slag and sand-blast material, are used as hardcore in local road construction, school yards, new port installations, and to infill foundations of buildings (see Photos in Volume 2). During their loading, transportation and unloading, fine dust is released into the ambient air and made available for transportation by wind. The strong winds blowing in the area, almost throughout the whole year, transport fine- to medium-grained metallurgical processing wastes to distant places. Deposition of these materials, with high toxic element concentrations (see Chapter 5 this volume & Maps 5.1-5.30 in Volume 2), and their subsequent mixing with residual and alluvial soil, caused the alteration of the chemical composition of surface soil.

Overburden samples from previous geochemical surveys, conducted in the area by the Division of Geochemistry of the Institute of Geology and Mineral Exploration (IGME), under the auspices of a European Commission Structural Funds programme of the Attiki Regional Office, have been used (Hadjigeorgiou-Stavrakis and Vergou-Vichou, 1992; Demetriades *et al.*, 1994), together with new samples from unsampled sections of the Lavrion urban area covered by this study. A total of 224 overburden samples have been collected (refer to Chapter 2, this volume & Map 2.9, Volume 2).

Overburden samples were analysed at Imperial College of Science, Technology and Medicine (Environmental Geochemistry Research Group) by the five-step sequential extraction method of Tessier *et al.* (1979), which was adapted by Li (1993) for use for multi-element determinations with ICP-AES (refer to Chapter 2B, this Volume). Total element concentrations for 22 elements were obtained by adding up the

concentrations of the five sequential extraction fractions. The validity of this process was tested, prior to the routine analysis of all samples, by analysing a suite of 50 random samples by a total digestion method (see Chapter 2B, this Volume), and comparing the results. It was found that differences in element concentrations were within the acceptable limits of analytical error, and below 5% absolute variation for most elements.

The analytical methods used for determination of elements on overburden samples are described in Chapter 2C; the analytical and sampling variance in Chapter 2C, and data processing for map plotting in Chapter 2D. All overburden geochemical and other maps referred to in this chapter are in Volume 2 (Maps 6.1-6.30).

In this chapter the spatial distribution of elements will be described and discussed, and comparisons made with their respective element concentrations in parent rocks, metallurgical wastes, and house dust. The following paragraphs explain a number of significant items in order to understand fully the description of the results.

6.1.1. NOTCHED-BOX-AND-WHISKER PLOT

Results of different sample types (rock, metallurgical wastes, overburden and house dust) are compared by means of notched-box-and-whisker plots, an Exploration Data Analysis graphical plot, which is independent of statistical data distribution (Tukey, 1977; Kürzl, 1988; O'Connor *et al.*, 1988; Manugistics, 1997; Reimann *et al.*, 1998). Apart from providing a powerful graphical tool of the statistical data structure of each element in different sample types, it offers an excellent way to compare the different data sets (refer to Chapter 2D for details, p.60). Comparisons can be made between data sets analysed by the same analytical method, *i.e.*, (a) overburden and house dust for total and aqua regia extractable As, and (b) aqua regia extractable elements in samples of rock and metallurgical wastes (see below for more details).

6.1.2. ANALYTICAL METHODS

In this comparison it is important to know that the four sample types were analysed by different analytical methods, *i.e.*,

- Rock samples were subjected to (a) an aqua regia extraction and determination of Ag, As, Ba, Cd, Co, Cr, Cu, Li, Ni, Pb, Sb, Sr, V, Zn by AAS, and (b) total dissolution and determination of Al, Ca, Fe, K, Mn, P, Ti by AAS;
- Samples of metallurgical wastes: aqua regia extraction and determination of Ag, Al, As, Ba, Be, Ca, Cd, Co, Cr, Cu, Fe, Hg, K, La, Li, Mn, Mo, Ni, P, Pb, Sb, Sr, Ti, V and Zn by ICP-AES; Ba, Ca, Cr, Fe, La, Mn, P, Sr and Ti are partially leached, whereas a limited extraction is achieved for Al and K; a *"near-total"* extraction is achieved for Ag, As, Be, Cd, Cu, Hg, Li, Mo, Ni, Sb, V and Zn.
- Overburden and house dust samples were analysed by different methods (a) total by addition of concentrations of the five extraction steps for elements Ag, Al, Ba, Be, Ca, Cd, Co, Cr, Cu, Fe, K, La, Li, Mn, Mo, Ni, P, Pb, Sr, Ti, V and Zn, (b) Hg determined by the Scintrex® flameless HGG-3 Hg-atomic absorption spectrometer with an upper limit of 700 ppb Hg; (c) As extracted by aqua regia and determined by AAS, and (d) total Sb determined by XRF.

Consequently, direct comparisons can only be made between samples of (a) overburden and house dust for all elements, (b) rock and metallurgical wastes for

elements extracted by aqua regia, and (c) rock, overburden and house dust for total element contents. For other cases only a relative comparison can be made.

6.1.3. pH OF HYDROLYSIS

Solubility, mobility and stability of cations in soil solutions depends on Eh (oxidation & reduction potential) and pH (acidity & alkalinity) conditions (Garrels and Christ, 1965; Hansuld, 1966; Levinson, 1974; Rose *et al.*, 1979). Since, pH is a major factor in element mobility, it was measured on all samples of soil and house dust from the Lavrion urban area (see Chapter 2B). Soil pH at and below 4.0 in Lavrion indicates zones of oxidising pyrite, *e.g.*, Nichtochori-Komobil and Kiprianos-Kavodokanos (see Map 2.5, Volume 2). Whereas soil pH at and above 8.0 in Lavrion denotes zones over carbonates, such as marble and calcareous sandstone, but even schist for it has a high carbonate content.

An important parameter, governing the mobility and migration of cations in solution, is the *"pH of hydrolysis"*, which is defined as *"the pH at which elements precipitate as hydroxides"* (Levinson, 1974) (Table 6.1). Geochemical features develop, therefore, as a result of pH changes, which are termed as *pH barriers* or *geochemical barriers*. For example, $Fe(OH)_3$ begins to precipitate at a pH of 2.00; $Al(OH)_3$ at 4.1; $Fe(OH)_2$ at 5.5; $Ni(OH)_2$ at 6.7, $Mn(OH)_2$ at 8.5-8.8 (Perel'man, 1977). Consequently, Fe^{3+} can only exist in a strongly acid medium at pH<2.00; Al^{3+} and Fe^{2+} can exist in a weakly acid medium of pH<4.1 and <5.5 respectively, whereas the Mn^{2+} ions are stable even in alkaline conditions, *i.e.*, they begin to precipitate under strongly alkaline conditions of pH>9.0. The pH of hydrolysis is able, therefore, to explain many characteristics of the migration of cations in solutions, *e.g.*, the migration of Fe^{2+} in weakly acid waters and the low mobility of Fe^{3+} in such waters (Perel'man, 1977).

Table 6.1. pH of hydrolysis (hydroxide precipitation) of some elements from dilute (0.025-0.0025M) solutions (from Levinson, 1974, Table 3-6, p.128).
Πίνακας 6.1. pH υδρόλυσης (κατακρήμνιση υδροξειδίων) μερικών στοιχείων από αραιά (0.025-0.0025M) διαλύματα.

Element	*pH*	*Element*	*pH*	*Element*	*pH*
Fe^{3+}	2.0	Cu^{2+}	5.3	Co^{2+}	6.8
Sn^{2+}	2.0	Fe^{2+}	5.5	Zn^{2+}	7.0
Hg^{1+}	2.0	Be^{2+}	5.7	Hg^{2+}	7.3
Al^{3+}	4.1	Pb^{2+}	6.0	La^{3+}	8.4
U^{6+}	4.2	Cd^{2+}	6.7	Ag^{1+}	7.5-8.0
Cr^{3+}	5.3	Ni^{2+}	6.7	Mn^{2+}	8.5-8.8

It is stressed that interpretations based only on pH (Table 6.2) and pH of hydrolysis (Table 6.1) are just good assumptions, based on field knowledge of the area. They should, therefore, serve as indicators of the real situation, and certain reservations ought to be retained, for organic matter, clay minerals, Fe/Mn oxides, and cation exchange capacity of soil, among others, play a significant role in the solubility, mobility and stability of elements in soil solutions.

Table 6.2. Mobility of some trace elements in the surficial environment (from Hoffman, 1986, Table 3.3, p.55, based on Levinson, 1980).
Πίνακας 6.2. Κινητικότητα ορισμένων ιχνοστοιχείων στο επιφανειακό περιβάλλον.

Element	*pH conditions*			*Immobilization factors*			*Heavy minerals*
	Acid pH < 5.5	*Neutral pH 5.5-7.0*	*Alkaline pH > 7.0*	*Fe/Mn oxides*	*Organic matter*	*Other*	
Antimony	Low	Low	Low	Yes		Sulphide; reducing conditions;	
Arsenic	Medium	Medium	Medium	Yes		Sulphide; clay conditions	
Barium	Low	Low	Low			Sulphate; reducing conditions carbonate; clay	
Beryllium	Low	Low	Low	Yes	Yes	Clay	
Bismuth	Low	Low	Low	Very		Reducing conditions	
Boron	Very High	Very High	Very High				Tourmaline
Cadmium	Medium	Medium	Medium			Reducing conditions	
Cerium	Insoluble	Insoluble	Insoluble				Rare earth minerals
Chromium	Very Low	Very Low	Very Low				Chromite
Cobalt	High	Medium to Low	Very Low			Sulphide; adsorption	
Copper	High	Medium to Low	Very Low	Yes	Yes	Sulphide; adsorption	
Fluorine	High	High	High			CaF_2; adsorption	
Gold	Immobile	Immobile	Immobile				Native gold
Iron- Fe^{++}	High to Very Low	Very Low	Very Low	Yes			Magnetite
Iron- Fe^{++}	High	Medium to Low	Very Low	Yes		Oxidizing condition	
Lead	Low	Low	Low			Insoluble carbonate, sulphate, phosphate; reducing conditions	
Lithium	Low	Low	Low	Yes		Clays	
Manganese	High	High	High to Very Low	Yes		Clays	
Mercury (aq)	Medium	Low	Low	Yes		Sulphide	Cinnabar
Mercury (vap)	High	High	High				
Molybdenum	Low	Medium	High	Yes		Adsorption; in presence of Pb, Fe, Ca, carbonate; sulphide; reducing conditions	
Nickel	High	Medium to Low	Very Low			Sulphide, adsorption, silicate minerals	
Niobium/ Tantalum	Insoluble	Insoluble	Insoluble				Yes
Platinum	Insoluble	Insoluble	Insoluble				Native platinum
Radium	High	High	High	Yes	Yes	Coprecipitation with Ba, Ca, Fe, Mn	
Radon	High	High	High			Limited by half life	
Selenium	High	High	Very High	Yes		Reducing conditions, adsorption	
Silver	High	Medium to Low	Very Low	Yes	Yes	Reducing conditions; sulphide; precipitated by Pb, Cl, chromate, arsenate	
Tellurium	Very Low	Very Low	Very Low				Yes
Thorium	Very Low	Very Low	Very Low			Adsorption by clay, aluminum hydroxides	Yes
Tin	Insoluble	Insoluble	Insoluble				Cassiterite
Tungsten	Insoluble	Insoluble	Insoluble	Yes			Wolframite Sheelite
Uranium	Low to Medium	High	Very High	Yes	Yes	Reducing conditions; special ion precipitates; adsorption	
Vanadium	High	High	Very High			Silicate minerals; reducing conditions, adsorption	V- magnetites
Zinc	High	High to Medium	Low to Very Low	Yes	Yes	Sulphide, precipitated by high carbonate, phosphate	

6.1.4. TERMINOLOGY

In exploration geochemistry the term *"background"* describes the "*normal variation of an element in a particular sample type as measured by a particular analytical method"*. The term *"geochemical anomaly"* is defined as *"an abnormally high or low content of an element or element combination, or an abnormal spatial distribution of an element or element combination in a particular sample type in a particular environment as measured by a particular analytical method"* (Govett, 1983, p.30). These two terms will be used in the cases that an element displays, to a large extent, the normal background and anomalous variation.

"Baseline" or *"natural baseline variation"* is nowadays the preferred terms used in environmental studies. They are, in fact, collective terms for natural "background" and the "anomalous" geochemical variation of an element are combined, in order to define the level of anthropogenic contamination, which is superimposed on the natural baseline element variation.

In the following description of the spatial distribution of elements, V.A. Kovda's term geochemical *"neoanomaly"* which describes *the "substantial enrichment in soil by recent industrial and urban developments"* (Davies, 1980) will be used. In the case of Lavrion the term "neoanomaly" will be employed to describe the substantial enrichment in overburden caused by metallurgical activities. Whereas, "geochemical anomaly" will be reserved to describe enhanced element concentrations due to natural means.

A new term will also be used, *"neohalo"* to describe *"element distribution patterns about the metallurgical processing wastes, which are due to their dispersion by aerial, gravitational and/or fluvial processes or human transportation."*

6.1.5. CONTAMINATION OR ENRICHMENT AND DEPLETION INDEX: NATURAL BASELINE VERSUS STATUTORY TRIGGER VALUES

Since, the natural geochemical background variation for the Lavrion urban area is known from the geochemistry of parent rocks, a *"contamination"* or an *"enrichment index"* will be estimated for each element in overburden and house dust. The term *"contamination index"* will be used for known toxic elements, which have definitely been released from the mining and metallurgical activities, *e.g.*, Ag, Cd, Hg, Pb, Sb Zn *etc.* Whereas the term *"enrichment index"* will be reserved for elements, which have a definite geogenic origin, or their geogenic properties supersede those of contamination, *e.g.*, Al, K, *etc.*

The unweighted median value of each element in parent rocks, as a whole, will be taken as the upper level of background variation. Minimum and maximum concentrations of each element in overburden will be divided by its respective rock median value in order to estimate the variation of the contamination or enrichment index. The contamination or enrichment index will have values >1.00. Unity for a particular element will, therefore, represent baseline conditions. In certain situations, there will be decimal values below unity, meaning that there is depletion with respect to the rock median value of that particular element. Hence, the *"depletion index"* will be recognised by values of <1.00

Lavrion's overburden is seriously contaminated and, therefore, it is impossible to determine the local natural background for each element. The well distributed outcrops

of parent rocks offered, however, a unique opportunity to estimate the natural baseline variation of the studied elements (refer to Chapter 4 this volume and Maps 4.2 to 4.30 in Volume 2). The rock median value (50th percentile) of each element is considered, therefore, to be a logical limit on which to base an estimation of the pragmatic contamination index in the Lavrion urban environment. Statutory trigger levels, on the other hand, are usually set up by scientists, taking into account different parameters, but under the pressure of politicians, industrialists and technocrats in general (see Chapter 1 this volume & Map 1.5, Volume 2). They are undoubtedly not based on rational situations, which take into account the local natural variation of elements. There is indeed sympathy with the problems legislators are facing, since good quality geochemical data are not available for each situation.

The principal objection to statutory trigger levels is that nature itself has set up the limits, and not legislators. There are considerable discussions about sustainability, sustainable development, and the United Nations and European Union have passed resolutions for this purpose (Quarrie, 1992; Stanners and Bordeau, 1995). With all due respect, these are vain discussions and worthless resolutions, for the majority of people do not understand natural earth processes. Life on our planet developed in natural balance with the environment. Toxic element concentrations are, normally, not part of the life cycle of biota. Our planet earth in its own wisdom is depositing ore deposits in permeable, porous or broken-up rocks, but the tendency is

(a) to contain ore bodies with toxic elements by impermeable cover rocks;
(b) to trap them between impermeable layers;
(c) to encase them within alteration zones, *e.g.*, argillisation reduces the permeability of a rock, leaving the ore body enclosed within a relatively impermeable shell;
(d) to emplace them in rocks with high carbonate content, which reduce greatly the mobility of elements even in the secondary environment (as is the case in Lavrion), and
(e) to bury them deeply below the earth's surface (Barnes, 1967; Park and MacDiarmid, 1970; Stanton, 1972; Smirnov, 1976).

Concealing them, therefore, in such a way that they are not readily available. Humans, on the other hand have intervened and disrupted the natural earth processes of containment and concealment of ore masses. The results of their exploitation are, of course, detrimental, *i.e.*, contamination of soil, contamination of water resources (ground and surface), and contamination of the atmosphere, with the final consequences, contamination of our food supplies, and degradation of our quality of life. All these are vital compartments of sustainability of life on earth. We are unfortunately paying the penalty of our misdemeanours by diseases, which are directly related to contamination.

Following the anthropogenic contamination of our planet, due to its abuse, the human race attempts to *"…. establish the basis for the major shift required to put this planet on the path towards a more secure and sustainable future"* (Quarrie, 1992, p.9). Believe it or not this is a statement in the Foreword, of the report on the United Nations Conference on Environment and Development held in Rio de Janeiro in 1992, made by Maurice Strong, the appointed Secretary-General of the UN Conference. The problem, however, is not planet earth, for earth will survive, because it has its own mechanisms of self-protection and self-repair, which we are too naïve to understand. *The question is will the human race survive, and at what cost?*

We should be aiming to move towards the zero anthropogenic contamination level, for our own survival and quality of life. Technocratic statutory trigger levels are, therefore, considered as levels of despair for our own survival. Following this philosophical outcry, for in Lavrion, and in many other seriously contaminated places on earth, the local inhabitants are asked to live in a degraded environment, created by industrialists and politicians alike, we have no choice but to discuss statutory trigger levels in relation to the local estimated rock median value of each element.

The rock median value of each element as the upper level of natural background variation is one option of a conservative limit to compare overburden/soil results. The second option is to subtract the natural baseline variation for each element, which includes both the natural background variation and the lithogeochemical anomalies, from its respective concentrations in overburden. In such a case, the positive residuals at each sample point, or the positive residual surface, will give the actual anthropogenic contamination level. Although the second option is the optimum for estimation of anthropogenic contamination against the spatially variable geochemical baseline, it will not be attempted in this study. The best option is, of course, the estimation of site-specific guideline values (see Volume 4).

6.1.6. CONTAMINATION PATTERNS

Contamination patterns are superimposed on natural element variation patterns. As pointed out by Rose *et al.* (1979) they may form in any type of clastic, hydromorphic, or biogenic environment. Contamination is dispersed from its sources by gravity movement of solid particles, wind-blown material or in aqueous solutions, whereas plants may take up contaminating metals at any stage of their dispersion. Further, human activities may play a role in the dispersion of contamination as is the case in the Lavrion urban area.

The geometrical shape of the source area conditions the form of contamination patterns to begin with. In Lavrion there is a large number of source areas, since contamination goes back to antiquarian times. Map 1.2 shows the old and recent mines and the drainage basins leading into the Lavrion urban area. Most of them are in valleys, indicating that wastes were undoubtedly transported by fluvial processes and deposited in the floodplains and gulfs of Lavrion and Thorikon. Since, 1866 the dominant contamination sources were:

(a) the stacks of metallurgical plants and other industries, such as the lead-acid battery plant, which caused the contamination of ambient air and, subsequently, all forms of dust, surface soil and water;
(b) the dumps of metallurgical processing wastes, which cover a very large part of the Lavrion urban environment (Map 2.3). These wastes are, in fact, the major sources of contamination of the surface environment. Fine- and medium-grained materials are transported by aerial and fluvial processes as well as by human activities.

It should be appreciated, therefore, that contamination patterns would be complex, due to the many different sources. Overburden samples mapped the surface contamination patterns, and core-drilling the sub-surface contamination patterns (see Volume 1B, Chapters 3B & 4B).

6.2. DESCRIPTION OF RESULTS

In the underlying description of the results the following order, with minor deviations, will be followed, *i.e.*,

- statistical parameters of each element in overburden samples of the Lavrion urban area, and comparison with global or global normal soil mean and median values; the statistical parameters that will be mentioned are the minimum and maximum values, the mean, the standard deviation (s) and coefficient of variation in per cent (C) in parentheses, and the median (for explanation of statistical parameters refer to Chapter 2D);
- statistical parameters of each element in samples of rock, metallurgical wastes and house dust in order to show the contribution of metallurgical wastes in the contamination of the Lavrion urban environment. In the case of house dust, there is also a contribution from the contaminated overburden. Notched-box-and-whisker plots display effectively the comparison among the different sample types;
- estimation of the contamination or enrichment index of each element in overburden with respect to its rock median value. The contamination or enrichment index in house dust is mentioned, but will not be discussed;
- description of the spatial distribution of each element, and possible explanations with the aid of rock geochemical maps (Maps 4.2-4.30 in Volume 2), chemistry of metallurgical processing wastes (Maps 5.1-5.30), lithology (Map 2.2), and pH (Map 2.5);
- mobility of element in the secondary environment;
- the residence times of each element in soil, if known, will be mentioned, for it is important to understand the problems created by contamination;
- toxicity of each element, if known, with respect to plants, animals and humans. Area considered to be unfit for plant growth to show the seriousness of the contamination, (it is noted that the area covered by this study is 7.235 km^2), and
- statutory trigger or guide levels set for certain toxic elements. Comments will also be made on the statutory trigger values. The percentage area considered to be unfit for human habitat out of the 7.235 km^2 studied, to show again the gravity of the situation, may or may not be given, depending on the validity of statutory trigger levels, for in some cases the limits are set without taking into account geochemical variability, and quality of life, but only if they are carcinogenic.

6.2.1. DISTRIBUTION OF TOTAL SILVER (Ag) IN OVERBURDEN (Map 6.1, Fig. 6.1)

Silver in overburden samples varies from 1.4 to 204.6 ppm, with a mean of 17.8 ppm (s=±21.88 ppm; C=122.92%), and a median of 12.06 ppm (n=224). In comparison, Ag in normal global soil, away from mineralised areas, does not normally exceed 0.5 ppm (Gough *et al.*, 1979), and has an average of 0.1 (Levinson, 1980), and a median in the <2 mm fraction of 0.07 ppm (Reimann *et al.*, 1998). In Lavrion, these values are greatly exceeded due to contamination from metallurgical activities (Fig. 6.1).

Silver concentrations in rocks of the Lavrion urban area vary from <0.5 to 41 ppm, with a mean of 0.89 ppm (s=±3.63 ppm; C=407.87%) and a median of 0.5 ppm (n=155; note this is a recent compilation of additional data, hence the difference with the values quoted on Map 6.1). Only three mineralised rock samples have high Ag concentrations, *i.e.*, 41 ppm to the

west of Perdika, 20 ppm to the west of Kavodokanos, and 7 ppm at Neapoli; most values are between <0.5 to 5.24 ppm Ag.

Silver levels in metallurgical wastes vary from 3.2 to 96 ppm with a mean of 33.8 ppm (s=±28.22 ppm; C=83.49%) and a median of 18.9 ppm (n=62) (refer to Map 5.1).

House dust Ag varies from 1.39 to 34.81 ppm with a mean of 6.85 (s=±5.08 ppm; C=15.03%) and a median of 4.81 ppm (n=127).

The Ag contamination index in overburden, with respect to its median in parent rocks, varies from 2.8 to 409.2, and in house dust from 2.8 to 69.6.

It is apparent from the statistical distribution of Ag in different sample types, that the metallurgical processing wastes are the major source of contamination of overburden samples (Fig. 6.1). The contribution of Ag from rock samples is almost totally masked by the higher concentrations in metallurgical wastes. Both sample types, metallurgical wastes and overburden, contribute to the contamination of house dust.

Major geochemical neoanomalies, with Ag concentrations above 21 ppm have a NE-SW trend, and occur over the flotation residues (Noria-Prasini Alepou-Santorineika), pyritiferous wastes (Komobil, Nichtochori) and slag/sand-blast material (within the smelter area at Kiprianos and Kavodokanos) (refer to Map 5.1). The strongest geochemical neoanomaly >36 to 205 Ag occurs within the premises of the smelter at Kiprianos. Distinct neohaloes extend about the geochemical neoanomalies down to 12 ppm Ag, although even lower levels, to 1 ppm Ag, may be attributed to aerial dispersion from metallurgical wastes.

Mobility of Ag is generally high under acid conditions, medium under oxidising conditions and very low under reducing conditions (Levinson, 1980; Hoffman, 1986; Reimann *et al.*, 1998) (Table 6.2). The pH of hydrolysis of Ag^{1+} in dilute solutions varies from 7.5 to 8.0, meaning that Ag(OH) precipitates in alkaline environments and Ag

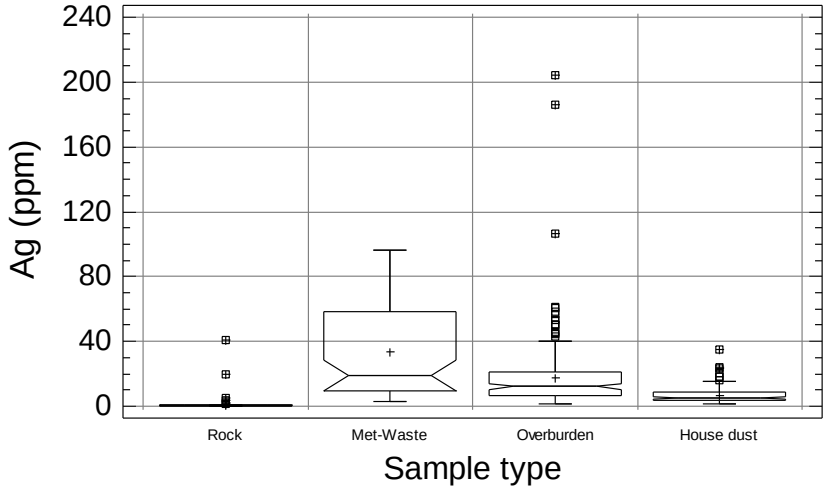

Fig. 6.1. Multiple notched box-and-whisker plot comparing silver (Ag) distribution in different sample types (Met-waste= Metallurgical processing wastes).
Σχ. 6.1. Πολλαπλό θηκόγραμμα με εγκοπές που συγκρίνει την κατανομή του αργύρου (Ag) σε διαφορετικούς τύπους δειγμάτων (Rock = Πέτρωμα, Met-Waste = Μεταλλουργικά απορρίμματα, Overburden = Επιφανεικό κάλυμμα, House dust = Σκόνη σπιτιών).

becomes relatively immobile (Table 6.1). Silver should, therefore, be geochemically immobile in most areas, since soil pH for 85% of the surface area of Lavrion is above 7.54 due to the predominance of marble. In Lavrion Ag may be, however, comparatively mobile in the pyritiferous materials with pH<7.0, as for example, in the areas between Kiprianos and Kavodokanos, and Komobil and Nichtochori; further between Neapoli and Koukos (refer to Map 2.5) the low pH of which is ascribed to the sulphur bearing aerosols released by the petroleum powered electricity generating plant, which is situated to the north-east.

Silver is not an essential element, and is generally toxic to many organisms, and of low toxicity for humans (Gough *et al.*, 1979; Reimann *et al.*, 1998).

According to Kabata-Pendias and Pendias (1984), Ag levels above 2 ppm in soil are considered to be phytotoxic. Consequently, 98.7% of the soil cover of Lavrion, under this premise, is unfit for plant growth (Map 6.1).

The only recommended residential soil statutory limits, quoted in scientific literature, come from Finland and the State of Connecticut and are 2 ppm and 340 ppm Ag respectively (Koljonen, 1992; US CT, 1994, 1997) (Table 6.3). In the opinion of the writers, the Connecticut limit is too high, when the average in normal global soil is about 0.1 ppm (Levinson, 1980), and values do not usually exceed 0.5 ppm (Gough *et al.*, 1979). Silver, apart from being phytotoxic at concentrations above 2 ppm, is also known to be toxic to bacteria and lower life forms, meaning that at high levels as 340 ppm Ag there will be soil degradation, due to reduction in microbial activity. The Finnish maximum concentration of Ag in surface soil is considered to be logical. Consequently, 98.7% of the Lavrion urban area is also considered to be hazardous to the health of the local population.

6.2.2. DISTRIBUTION OF TOTAL ALUMINIUM (Al) IN OVERBURDEN (Map 6.2, Fig. 6.2)

Aluminium in overburden samples varies from 8,076 to 85,161 ppm, with a mean of 35,067 ppm (s=±13,463 ppm; C=38.39%), and a median of 32,315 ppm (n=224). Aluminium in normal global soil has a median value of 80,000 ppm in the <2-mm fraction (Reimann *et al.*, 1998). In Lavrion, overburden/soil Al contents are below the global median due to the predominance of marble (Table 4.1A, Maps 2.2 & 4.2).

Aluminium concentrations in rocks of the Lavrion urban area vary from <50 to 75,152 ppm, with a mean of 19,267 ppm (s=±21,375 ppm; C=110.94%) and a median of 8,044 ppm (n=140) (Map 4.2; Table 4.1A).

Aluminium levels in metallurgical wastes vary from 1,118 to 38,071 ppm with a mean of 18,998 ppm (s=±10,302 ppm; C=54.23%) and a median of 20,074 ppm (n=62) (refer to Map 5.1).

House dust Al varies from 4,844 to 44,162 ppm with a mean of 13,864 (s=±5,803 ppm; C=41.86%) and a median of 13,055 ppm (n=127).

The Al enrichment/contamination index in overburden, with respect to its median in parent rocks, varies from 1.0 to 10.6, and in house dust from 0.6 to 5.5.

It is apparent from the statistical distribution of Al in different sample types, that both rock and metallurgical processing wastes are the major sources of Al in overburden samples (Fig. 6.2). Both sample types, metallurgical wastes and overburden, are the

Table 6.3. Summary table of statutory limits of toxic elements in soil, their phytotoxic levels, and global soil means (values in ppm).
Πίνακας 6.3. Συνοπτικός πίνακας νομοθετημένων ορίων των τοξικών στοιχείων στο έδαφος, τα φυτοτοξικά επίπεδα και παγκόσμιες μέσες τιμές τους στο έδαφος (τιμές σε ppm).

Element	*European Union*		*Canada*		*Denmark*	*Finland*		*Germany*		*Global soil mean*
	Minimum	*Maximum*	*Federal Canada*	*Ontario* Residential*		*Guide value*	*Limit*	*Normal value*	*Limit*	
Ag	-	-	-	-	-	-	2	-	-	0.07
As	-	-	20	25	20	10	20	2-20	20	5
Ba	-	-	-	-	-	600	600	-	-	500
Be	-	-	-	-	-	-	10	-	-	3
Br	-	-	-	-	-	-	10	-	-	
Cd	1	3	3	4	5	0.5	3	0.1-0.2	3	0.3
Co	-	-	40	50	-	50	50	-	-	10
Cr	-	-	750	1000	1000	100	100	30	100	80
Cu	50	140	150	200	500	100	100	30	100	25
F	-	-	-	-	-	-	200	-	-	-
Ga	-	-	-	-	-	-	10	-	-	15**
Hg	1	1.5	0.8	1	3	0.2	2	<0.1	2	0.05
Mn	-	-	-	-	-	-	-	-	-	530
Mo	-	-	5	5	-	5	5	-	-	1.2
Ni	30	75	150	200	30	60	100	30	50	20
Pb	50	300	375	500	400	60	100	30	100	17
Sb	-	-	-	-	-	5	40	-	-	0.5
Sc	-	-	2	2	-	-	-	-	-	12
Se	-	-	-	-	-	-	10	-	-	0.3
Sn	-	-	-	-	-	50	50	-	-	10**
Tl	-	-	-	-	-	-	1	-	-	0.5
U	-	-	-	-	-	-	5	-	-	2.7
V	-	-	-	-	-	-	50	-	-	90
Zn	150	300	600	800	1000	150	300	50	300	70
Zr	-	-	-	-	-	-	300	-	-	300

Element	*Switzerland*		*The Netherlands*			*U.K.*	*US*	*Phytotoxic levels*	
	Trigger Value	*Clean-up Value*	*Definitive*	*Limiting Value*	*Intervention*	*Trigger Value****	*Connecticut Residential*	*Minimum*	*Maximum*
Ag	-	-	-	-	-	-	340	-	2
As	-	-	29	55	55	10	10	15	50
Ba	-	-	-	-	-	-	4700	-	-
Be	-	-	-	-	-	-	2	-	10
Br	-	-	-	-	-	-	-	-	-
Cd	2	20	0.8	2	12	3	34	3	8
Co	-	-	20	20	240	-	-	25	50
Cr	-	-	100	380	380	600	Cr^{6+}: 100	75	100
Cu	150	1000	36	36	190	130	2500	60	125
F	-	-	-	-	-	-	-	-	-
Ga	-	-	-	-	-	-	-	-	-
Hg	-	-	0.3	0.5	10	20	20	0.2	0.5
Mn	-	-	-	-	-	-	-	1500	3000
Mo	-	-	-	-	200	-	-	2	10
Ni	-	-	35	35	210	70	1400	100	100
Pb	200	1000	85	530	530	500	500	100	400
Sb	-	-	-	-	-	-	27	5	10
Sc	-	-	-	-	-	-	-	-	-
Se	-	-	-	-	-	-	340	5	10
Sn	-	-	-	-	-	-	-	50	50
Tl	-	-	-	-	-	-	5.4	-	1
U	-	-	-	-	-	-	-	-	-
V	-	-	-	-	-	-	470	50	100
Zn	-	2000	140	480	720	300	20000	70	400
Zr	-	-	-	-	-	-	-	-	-

* Residential fine-grained soil. ** from Levinson (1980). ***Domestic gardens & allotments. For references refer to text.

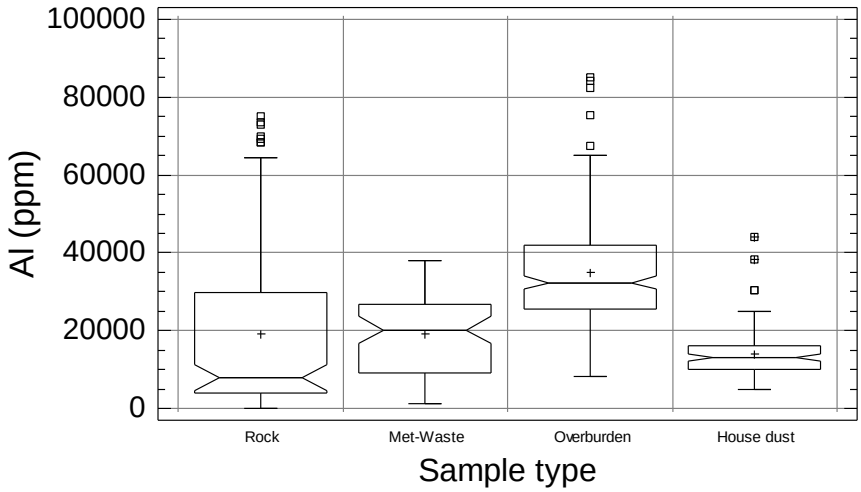

Fig. 6.2. Multiple notched-box-and-whisker plots comparing aluminium (Al) distribution in different sample types.
Σχ. 6.2. Πολλαπλό θηκόγραμμα με εγκοπές που συγκρίνει την κατανομή του αργιλίου (Al) σε διαφορετικούς τύπους δειγμάτων.

sources of Al in house dust. Overburden Al has higher levels than rock and metallurgical wastes, and this may be due to its enrichment in the clay fraction of soil.

Major geochemical "anomalies", with Al concentrations above 41,795 ppm have a NW-SE trend, and occur in the southern, western and northern parts of the study area, and the coastal section to the east of Ayia Paraskevi. The strongest geochemical anomalies >61,593 to 85,161 Al occur from Vilanoira to Panormos and Perdika in the south, and Thorikon in the north. Apart from the strong north-westerly trend of the geochemical anomalies, which is also the major orientation of the lithogeochemical spatial structures (Map 4.2), there are only minor similarities, in the western border part of the study area, between overburden and rock geochemical patterns. There is also some relationship with the metallurgical processing wastes: (a) between Panormos and Fougara, and to the east of Ayia Paraskevi, where the slag/slag earth have high Al levels (>22,000 to 38,071 ppm), and (b) from Noria to Prasini Alepou and Santorineika, where the flotation residues have Al contents >20,000 to 26,341 ppm (refer to Map 5.2). Other explanations about overburden Al patterns are given below, and are due to the behaviour of Al in the secondary environment.

Aluminium is normally enriched in clay-rich soils. Marble does not normally have aluminosilicate minerals and has apparently low Al contents (Table 4.1A in Volume 1A). Schist, however, consists of aluminosilicate minerals, and occurs as intercalations within marble and also as a rock formation. Further, prasinite contains aluminosilicate minerals. Clay-rich soils, and consequently, elevated aluminium concentrations, occur

- over areas with schist and prasinite, and where marble has schist intercalations, *e.g.*, Nichtochori, Neapoli-Noria, Prasini Alepou, west of Kavodokanos and Kiprianos (refer to lithological map, Map 2.2).
- in valleys, where there is deposition of alluvium, which is rich in clay, *e.g.*, the anomalies at Panormos, Vilanoira, Perdika, Santorineika-Phenikodassos, Thorikon, and
- at the base of slopes, where again there is an enrichment in clay, *e.g.*, Perdika, Noria.

It is quite apparent, therefore, that elevated Al concentrations are due to an enrichment of clay in “soil” developed over appropriate rock formations. Clay-rich areas suggest that they may have a high scavenging capability.

Anomalous Al concentrations, since they occur in areas enriched in clay, may be ascribed, therefore, to mainly geogenic sources of the secondary environment. But, as it has already been shown some Al patterns are explained by high contents in metallurgical wastes. Hence, Al patterns in overburden are due to both geogenic and anthropogenic factors.

Mobility of Al is generally low under most conditions (Levinson, 1980; Hoffman, 1986; Reimann *et al.*, 1998). The pH of hydrolysis of Al^{3+} in dilute solutions is 4.1 (Table 6.1), meaning that $Al(OH)_3$ precipitates in an acid environment and Al becomes immobile. Aluminium should, therefore, be geochemically immobile in most areas, since soil pH for 97.5% of the surface area of Lavrion is above 6.87 due to the predominance of carbonates (Map 2.5). In the Lavrion urban area Al may be, however, comparatively mobile in the pyritiferous materials with pH<4, as for example, in the areas between Kiprianos and Kavodokanos, and Komobil and Nichtochori.

Aluminium held in soil is not considered to be toxic to humans. But free Al ions are toxic to humans (Reimann *et al.*, 1998).

Aluminium is an essential element for some organisms, and is toxic to plants at high concentrations in soil with low pH (Gough *et al.*, 1979; Kabata-Pendias and Pendias, 1984; Reimann *et al.*, 1998). Consequently, the area with pyritiferous tailings and a pH<4.0, which covers <1% of the total area, may be unfit for plant growth (Map 6.1).

6.2.3. DISTRIBUTION OF TOTAL ARSENIC (AS) IN OVERBURDEN (Map 6.3, Fig. 6.3)

Arsenic in overburden samples varies from 50 to 24,000 ppm, with a mean of 2,494 ppm (s=±3,558 ppm; C=142.66%), and a median of 1,290 ppm (n=224). Arsenic in normal global soil ranges from <1 to 40 ppm (Gough *et al.*, 1979), or 1 to 50 ppm (Levinson, 1980) with a mean of 5 ppm (Levinson, 1980), and a median of 5 ppm in the <2 mm fraction (Reimann *et al.*, 1998). In Lavrion, these levels are greatly exceeded due to contamination from metallurgical activities (Map 5.3, Fig. 6.3).

Arsenic concentrations in rocks of the Lavrion urban area vary from <0.5 to 1,032 ppm, with a mean of 62.8 ppm (s=±172.4 ppm; C=274.52%) and a median of 15.6 ppm (n=48; note this is a recent compilation of additional data, hence the difference with the values quoted on Map 6.3) (Map 4.3).

Arsenic levels in metallurgical wastes vary from 283 to 26,063 ppm with a mean of 4,593 ppm (s=±5,383 ppm; C=117.20%) and a median of 2,492 ppm (n=62) (refer to Map 5.3).

House dust As varies from 130 to 3,820 ppm with a mean of 5,435 (s=±507.1 ppm; C=9.33%) and a median of 400 ppm (n=127).

The As contamination index in overburden, with respect to its median in parent rocks, varies from 3.2 to 1538.5, and in house dust from 8.3 to 244.9. High As levels in overburden, due to anthropogenic contamination, completely mask primary geochemical patterns (Map 4.3).

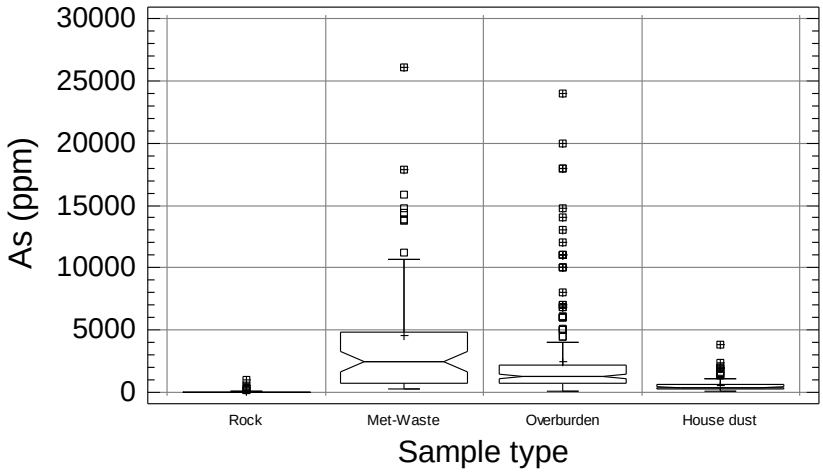

Fig. 6.3. Multiple notched-box-and-whisker plots comparing arsenic (As) distribution in different sample types.
Σχ. 6.3. Πολλαπλό θηκόγραμμα με εγκοπές που συγκρίνει την κατανομή του αρσενικού (As) σε διαφορετικούς τύπους δειγμάτων.

It is apparent from the statistical distribution of As in different sample types, that the metallurgical processing wastes are the major source of contamination of overburden samples (Fig. 6.3). The contribution of As from rock samples is almost totally masked by the higher concentrations in metallurgical wastes. Both sample types, metallurgical wastes and overburden, contribute to the contamination of house dust.

Major geochemical neoanomalies, with As concentrations above 1,290 ppm have NE-SW and NW-SE trends, and occur over and in the immediate neighbourhood of the flotation residues (Noria-Prasini Alepou-Santorineika), pyritiferous wastes (Komobil, Nichtochori) and slag/sand-blast material (at Fougara, Ayia Paraskevi, within the smelter area at Kiprianos and Kavodokanos) (Map 5.3). The strongest geochemical neoanomalies >6,000 to 24,000 As occur over the pyrite tailings and pyritiferous sand from Nichtochori to Komobil and Kiprianos, and within the premises of the smelter. Distinct neohaloes extend about the geochemical neoanomalies down to 380 ppm As, although even lower levels, to 50 ppm As, may be attributed to aerial dispersion from the smelters and metallurgical wastes.

Mobility of As is generally medium under oxidising, acid and neutral to alkaline conditions, and very low under reducing conditions (Levinson, 1980; Hoffman, 1986; Reimann *et al.*, 1998) (Table 6.2). Ferguson (1990), however, states that an increase in pH, as for example by liming, increases the mobility of arsenite salts, presumably by bringing about a change from aluminium [$AlAsO_4$] and iron [$FeAsO_4$] arsenates to calcium arsenates [$Ca_3(AsO_4)_2$]. If this is the case, then Lavrion has a significant problem.

Another significant problem is the long residence times of As in soil, which according to Ferguson (1990) is 2000 years.

Arsenic in minute amounts is an essential element for some organisms, even humans, but in excess is highly toxic with teratogenic properties (Gough *et al.*, 1979; Mervyn, 1985, 1986; Reimann *et al.*, 1998). Toxicity depends on the valency state of As compounds, *e.g.*, As^{5+} compounds are less toxic than As^{3+}.

In Lavrion, As levels in overburden are abnormally high, and may present problems to biota in general. Toxicity, as in all cases, depends on the concentration of soluble, not total, As in soil. According, however, to Kabata-Pendias and Pendias (1984) total element concentrations in soil are quoted for phytotoxicity. Total phytotoxically excessive levels in surface soil vary from 15 to 50 ppm according to different authors. In the case of Lavrion, whichever level is taken the problem remains that 100% of the soil cover is unfit for plant growth (Map 6.3).

The recommended statutory limits for total As in residential soil, quoted in scientific literature, vary from 0.35 to 55 ppm (Table 6.3), *i.e.*,

- 0.35 ppm in the State of Connecticut (US CT, 1994), which was subsequently amended to 10 ppm (US CT, 1997);
- 10 ppm in the United Kingdom (ICRCL, 1987), and Finland (Koljonen, 1992);
- 20 ppm in Germany (Kloke, 1977; Lux, 1993), Federal Canada (Sheppard *et al.*, 1992), and Denmark (Edelgaard and Dahlstrøm, 1999);
- 25 ppm in the State of Ontario (Sheppard *et al.*, 1992), and
- 29 ppm in The Netherlands (VROM, 1983; Lux, 1993; Van den Berg *et al.*, 1993; J. Ebbing, person. commun., 1996).

Further, Finland and The Netherlands have upper limit values of 20 and 55 ppm As. This variation of technocratic statutory limits shows the necessity of setting up internationally agreed limits, based on realistic geochemical and medical principles. The Connecticut limit is too low, when the global soil mean/median value is 5 ppm As. Since, As is a very toxic element to all forms of life, and has teratogenic properties the recommended soil As level of 10 ppm is considered to be logical. However, Lavrion parent rocks, due to mineralisation, are enriched in As (Map 4.3); range <5 to 1032 ppm As, mean 62.8 ppm, median 15.6 ppm, 75th percentile 29 ppm, and 90th percentile 142 ppm As. As it may be appreciated any of the above statutory limits cannot really be applied in Lavrion, for contamination of overburden/soil is not solely due to metallurgical processing activities, but also to parent rocks. The situation with respect to As is indeed difficult, for even the home environment is highly contaminated, *i.e.*, house dust has levels >130 ppm As (mean = 5,435; median = 400 ppm). It can only be stated that the As health hazard in Lavrion is undoubtedly considerable, for the whole surface area has values above the highest limit of 55 ppm As set by legislators in The Netherlands.

6.2.4. DISTRIBUTION OF TOTAL BARIUM (Ba) IN OVERBURDEN (Map 6.4, Fig. 6.4)

Barium in overburden samples varies from 64 to 4,555 ppm, with a mean of 663.2 ppm (s=±644.3 ppm; C=97.15%), and a median of 479 ppm (n=224). In comparison, barium in normal global soil ranges from 100-3000 ppm (Levinson, 1980) with a mean and median of 500 ppm (Rose *et al.*, 1979; Levinson, 1980; Reinmann *et al.*, 1998). The Lavrion overburden/soil Ba mean and median are closed to normal global values.

Barium concentrations in rocks of the Lavrion urban area vary from 40 to 108,000 ppm, with a mean of 1,067 ppm (s=±9,110 ppm; C=853.80%) and a median of 210 ppm (n=140) (Map 4.4). The great variation in rocks is due to a single sample at Fougara. The normal range is from 40 to 1300 ppm Ba.

Barium levels in metallurgical wastes vary from 27.7 to 2,059 ppm with a mean of 368.2 ppm (s=±419 ppm; C=113.80%) and a median of 243 ppm (n=62) (refer to Map 5.4).

House dust Ba varies from 112 to 2,497 ppm with a mean of 655 (s=±505.5 ppm; C=77.18%) and a median of 472.6 ppm (n=127).

The Ba contamination index in overburden, with respect to its median in parent rocks, varies from 0.30 to 21.7, and in house dust from 0.53 to 11.89.

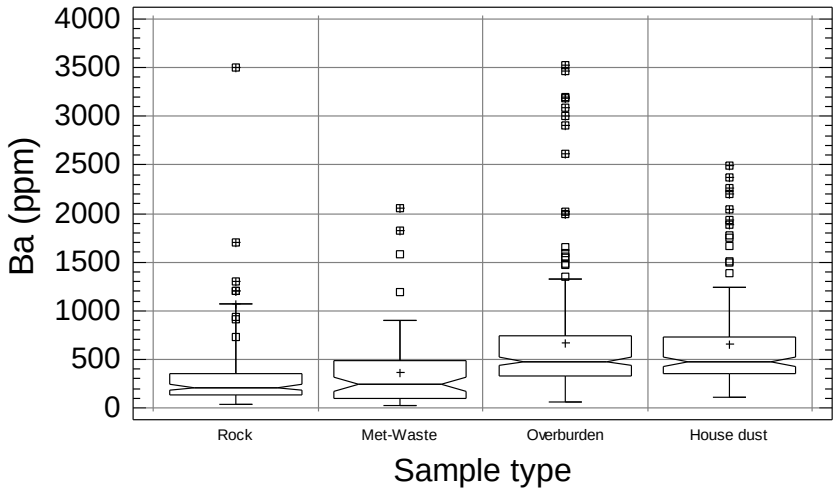

Fig. 6.4. Multiple notched-box-and-whisker plots comparing barium (Ba) distribution in different sample types [one rock sample >4000 ppm Ba].
Σχ. 6.4. Πολλαπλό θηκόγραμμα με εγκοπές που συγκρίνει την κατανομή του βαρίου (Ba) σε διαφορετικούς τύπους δειγμάτων [ένα δείγμα πετρώματος >4000 ppm Ba].

It is apparent from the statistical distribution of Ba in different sample types, that both rock and metallurgical processing wastes are the major sources of Ba in overburden samples (Fig. 6.4); the latter appear, however, to outweigh the former. Both sample types, metallurgical wastes and overburden, are the sources of Ba in house dust. In fact, the correspondence of the median values at the 95th confidence interval, suggests that overburden Ba may be the major source of house dust barium. Overburden Ba has higher levels than rock and metallurgical wastes, and this may be due to its enrichment in the clay fraction of soil by adsorption.

Major geochemical neoanomalies, with Ba concentrations above 739 ppm have a NW-SE trend, and occur over the flotation residues (Noria-Prasini Alepou), and slag/sand-blast material (Kavodokanos-Kiprianos, within the smelter area at Kiprianos, to the east of Ayia Paraskevi and Fougara). The strongest geochemical neoanomalies >1,658 to 4,555 Ba occur at Kavodokanos and Fougara, and appear to be associated with the slag/sand-blast wastes. Distinct neohaloes extend about the geochemical neoanomalies down to 329 ppm Ba. Low Ba concentrations occur in the area, covered by the pyrite tailings and pyritiferous sand, which extends from Nichtochori to Komobil and Kiprianos (Map 6.4).

Regarding the “anomalous” Ba patterns in overburden at Fougara and to the east of Ayia Paraskevi, there appears to be a joint contribution from both geogenic (Map 4.4) and anthropogenic sources (Map 5.4). In both cases, the geogenic contribution appears to be the greater. Moreover, primary dispersion patterns are reflected in the secondary

environment. Other primary dispersion features are not apparently preserved, because of the masking effects of contamination.

Mobility of Ba is generally low under oxidising, acid and neutral to alkaline conditions, and very low under reducing conditions (Levinson, 1980; Hoffman, 1986; Reimann *et al.*, 1998) (Table 6.2).

Barium may be an essential element for some organisms; its soluble compounds may be toxic to humans, animals and plants (Reimann *et al.*, 1998).

According to Kabata-Pendias and Pendias (1984), Ba levels above 220 ppm in soil are considered to be moderately phytotoxic. Consequently, 89.7% of the soil cover of Lavrion, under this premise, may be unfit for plant growth (Map 6.4).

The only countries with statutory guide and limit values of 600 and 4700 ppm Ba for residential soil are Finland (Koljonen, 1992; R. Salminen, person. commun., 1996) and the State of Connecticut (US CT, 1997). Since, (a) the global mean and median in normal soil is 500 ppm Ba, and (b) Lavrion parent rocks have a median of 210 ppm Ba and the 90th percentile is 500 ppm Ba, the value set up by Finland appears to be reasonable. As 33% of the Lavrion overburden has Ba>600 ppm, these areas are considered to be hazardous to human health (Map 6.4).

6.2.5. DISTRIBUTION OF TOTAL BERYLLIUM (Be) IN OVERBURDEN (Map 6.5, Fig. 6.5)

Beryllium in overburden samples varies from 0.24 to 2.68 ppm, with a mean of 1.10 ppm (s=±0.39 ppm; C=35.45%), and a median of 1.01 ppm (n=224). Beryllium in normal global soil has an average value of 6 ppm (Levinson, 1980), and a median of 3 ppm (Reimann *et al.*, 1998). The Lavrion overburden/soil Be levels are below global values.

Beryllium concentrations in rocks of the Lavrion urban area are below the detection limit of the analytical method (<1.0 ppm Be) (Table 4.19A). The average concentration of Be in ordinary limestone is 0.5 and schist 3 ppm (Reimann *et al.*, 1998). It appears, therefore, that Be is definitely not a major trace element in rocks of the Lavrion urban area.

Beryllium levels in metallurgical wastes vary from <1.0 to 1.28 ppm with a mean of 0.64 ppm (s=±0.26 ppm; C=40.63%) and a median of 0.5 ppm (n=62) (refer to Map 5.5). This range of concentrations indicate that Be is not a major trace element in the polymetallic mineralisation of Lavrion.

House dust Be varies from 0.09 to 0.92 ppm with a mean of 0.45 (s=±0.15 ppm; C=33.33%) and a median of 0.46 ppm (n=127).

An enrichment or contamination index cannot be calculated for Be, because of its very low concentrations in Lavrion parent rocks.

The comparative enrichment of Be in overburden with respect to parent rocks should be due to its concentration in the clay fraction of soil (Fig. 6.5). The major source for contamination of overburden/soil is the metallurgical processing wastes. Both sample types, metallurgical wastes and overburden, are the sources of Be in house dust.

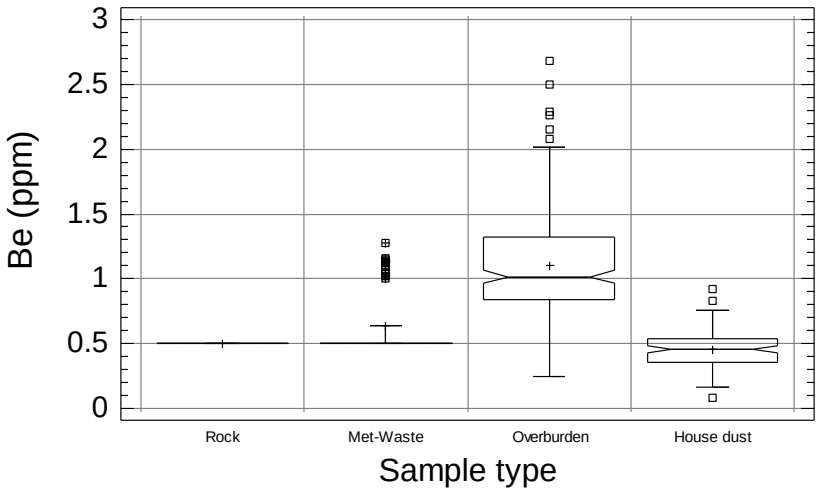

Fig. 6.5. Multiple notched-box-and-whisker plots comparing beryllium (Be) distribution in different sample types.
Σχ. 6.5. Πολλαπλό θηκόγραμμα με εγκοπές που συγκρίνει την κατανομή του βηρυλλίου (Be) σε διαφορετικούς τύπους δειγμάτων.

Major geochemical “anomalies”, with Be concentrations above 1.59 ppm, occur in the southern, western and northern parts of the study area, and the coastal section to the south-east of Ayia Paraskevi. The strongest geochemical anomalies >1.86 to 2.68 ppm Be occur at Vilanoira in the south, and Thorikon in the north. Beryllium anomalous patterns do not appear to be related to the metallurgical processing wastes, for Be is not a major trace element in the polymetallic ore mineral paragenesis (Marinos and Petrascheck, 1956; Demetriades, 1992; Katerinopoulos and Zissimopoulou, 1994;) or in slag (Gelaude *et al.*, 1996). Nevertheless, high Be levels in slag (about 1.2 ppm Be) at Fougara may be responsible for the enhanced values in overburden (>1.32-1.59 ppm Be) (Map 5.5); similarly, part of the elevated Be values in the Kavodokanos overburden may be ascribed to high Be levels in pelletised slag/sand-blast material.

The way the secondary dispersion pattern of Be extends outwards, from west to east (Prasini Alepou-Ayios Andreas; Vilanoira-Panormos), north to south (Thorikon-Kavodokanos), south to north (Panormos-Koukos), with the exception of minor deviations in the areas covered by metallurgical processing wastes (Noria-Prasini Alepou; Kiprianos), suggests that it is associated with normal residual soil, which occurs in the peripheral areas of the Lavrion urban area. Its apparent relationship with Al (Map 6.2) indicates an association with soil clay minerals; Be often substitutes for Al in secondary clay minerals (Gough *et al.*, 1979). Low Be levels (<0.75 ppm Be) occur in areas covered with marble (Ayia Paraskevi), and to the east of Nichtochori, where there is a very thin soil cover. Since, Be is known to be adsorbed on clay minerals (Reimann *et al.*, 1998), this interpretation appears to be valid.

Mobility of Be is generally low under most conditions (Levinson, 1980; Hoffman, 1986; Reimann *et al.*, 1998) (Table 6.2). The pH of hydrolysis of Be^{2+} in dilute solutions is 5.7 (Table 6.1), meaning that $Be(OH)_2$ precipitates in an acid environment and Be becomes immobile. Beryllium should, therefore, be geochemically immobile in most areas, since soil pH for 97.5% of the surface area of Lavrion is above 6.87 due to the predominance of carbonates (Map 2.5). In the Lavrion urban area Be may be, however, comparatively mobile in the pyritiferous materials with pH<4, as for example, in the areas between Kiprianos and Kavodokanos, and Komobil and Nichtochori.

The phytotoxic level of Be, quoted by different authors, is at 10 ppm in soil (Kabata-Pendias and Pendias, 1984) (Table 6.3). But, as pointed out by Gough *et al.* (1979) there are no reports of Be toxicity to plants under field conditions. It is, therefore, concluded, that Be is unlikely to be hazardous to plants in the Lavrion urban area.

The only recommended residential soil statutory limits quoted in scientific literature come from Finland and the State of Connecticut and are 10 ppm and 0.14 ppm Be respectively (Koljonen, 1992; US CT, 1994); the latter was subsequently revised to 2 ppm Be (US CT, 1997). The US Connecticut values are indeed very low, and are a good example of technocratic trigger levels, which do not take into account the natural variation of Be in normal geological materials, *e.g.*, bulk continental crust has on average 1.5-2.8 ppm Be, the upper continental crust 3.1-3.0 ppm Be, shale/schist 3.0 ppm Be, limestone 0.5 ppm Be, and normal global soil has a mean of 3 ppm Be (Reimann *et al.*, 1998).

Nevertheless, the very low trigger level set up for Be by the State of Connecticut is understandable, for Be is considered to be a very toxic metal for all forms of plant and animal life, and a known carcinogen (Gough *et al.*, 1979; Reimann *et al.*, 1998). But, it is unrealistic, for such a level cannot be achieved, when normal geological materials have higher concentrations. In any case, from the low natural levels of Be, only a small part is actually available for absorption by plants, as is pointed out by Gough *et al.* (1979). Further, Be will displace divalent cations in the exchange complex and, therefore, becomes strongly fixed in soil (Gough *et al.*, 1979). Finally, the Finnish soil limit value, on the other hand, may be too high. Hence, this is an element that must be investigated.

6.2.6. DISTRIBUTION OF TOTAL CALCIUM (Ca) IN OVERBURDEN (Map 6.8, Fig. 6.6)

Calcium in overburden samples varies from 4,138 to 239,150 ppm, with a mean of 95,996 ppm (s=±44,539 ppm; C=46.40%), and a median of 93,625 ppm (n=224). Calcium in normal global soil has a median value of 14,000 ppm (Reimann *et al.*, 1998). Hence, in comparison to normal global soil, the Lavrion overburden/soil is enriched in Ca, and this is due to the parent rocks, which are predominantly made of marble.

Calcium concentrations in rocks of the Lavrion urban area vary from 50 to 390,938 ppm, with a mean of 217,301 ppm (s=±125,319 ppm; C=57.67%) and a median of 220,126 ppm (n=140) (Map 4.8).

Calcium levels in metallurgical wastes vary from 7,456 to 229,340 ppm with a mean of 99,995 ppm (s=±39,454 ppm; C=39.46%) and a median of 102,603 ppm (n=62) (refer to Map 5.8).

House dust Ca varies from 44,590 to 242,750 ppm with a mean of 135,860 (s=±39,561 ppm; C=29.12%) and a median of 134,980 ppm (n=127).

The Ca depletion/enrichment index in overburden, with respect to its median in parent rocks, varies from 0.02 to 1.09, and in house dust from 0.20 to 1.10.

It is apparent from the statistical distribution of Ca in different sample types that rock is the major source of Ca in overburden samples (Fig. 6.6), although a contribution from metallurgical processing wastes cannot be precluded. All sample types and mainly the metallurgical wastes and overburden, are the sources of Ca in house dust. The elevated mean and median values of house dust Ca suggest either an enrichment

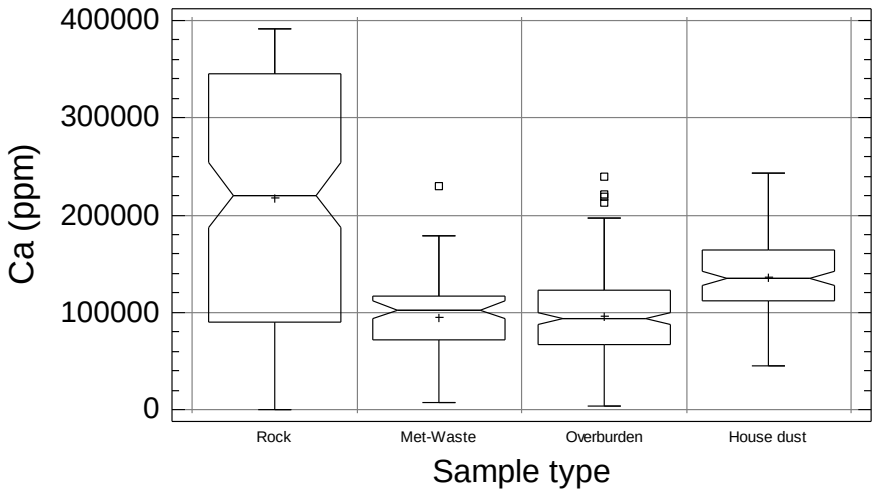

Fig. 6.6. Multiple notched-box-and-whisker plots comparing calcium (Ca) distribution in different sample types.
Σχ. 6.6. Πολλαπλό θηκόγραμμα με εγκοπές που συγκρίνει την κατανομή του ασβεστίου (Ca) σε διαφορετικούς τύπους δειγμάτων.

in the fine-grained household dust or a contribution from other sources in the Lavrion home environment.

Major geochemical “anomalies”, with Ca concentrations above 122,885 ppm have a NW-SE trend, and occur in the central part of the study area from Thorikon in the north to Panormos in the south; from Prasini Alepou-Noria in the west to Ayios Andreas-Lavrion harbour and to Ayia Paraskevi-Nichtochori in the east. The strongest geochemical anomalies >154,300 to 239,150 ppm Ca occur at Ayia Paraskevi, to the south of Santorineika, at Ayios Andreas, and south of Koukos. They appear to be associated with Quaternary formations, which are enriched in carbonates, and unaltered marble (Map 6.8). Overburden samples over schist, dolomitised and ankeritised marble have Ca levels <50,590 ppm. There does not appear to be a distinct relationship between the geochemical distribution patterns of Ca in overburden and parent rocks (Map 4.8). There is also no apparent relationship with the metallurgical processing wastes, even though marble is the host rock of the mineralisation.

Mobility of Ca is generally high under all conditions (Reimann *et al.*, 1998) (Table 6.2).

Calcium is an essential element for most organisms; it is a major plant nutrient, and is not generally toxic (Kabatas-Pendias and Pendias, 1984; and Reimann *et al.*, 1998). Excessive absorption of Ca, however, does cause health problems, such as hypercalcaemia, *i.e.*, abnormally high blood levels of Ca (Mervyn, 1985, 1986).

6.2.7. DISTRIBUTION OF TOTAL CADMIUM (Cd) IN OVERBURDEN (Map 6.9, Fig. 6.7)

Cadmium in overburden samples varies from 4 to 925 ppm, with a mean of 68.02 ppm (s=±108.55 ppm; C=159.59%), and a median of 38 ppm (n=224). In comparison, Cd in global normal soil, away from mineralised areas, has an average of 1 ppm (Levinson, 1980), and a median of 0.3 ppm (Reimann *et al.*, 1998). In Lavrion this level is greatly exceeded due to (a) mineralisation in certain parts of Lavrion (Map 4.9), and (b) contamination from metallurgical activities, which is the major contributor (Map 5.9).

Cadmium concentrations in rocks of the Lavrion urban area vary from <1.0 to 41 ppm, with a mean of 1.89 ppm (s=±5.02 ppm; C=165.61%) and a median of 0.5 ppm (n=140) (Map 4.9).

Cadmium levels in metallurgical wastes vary from 116.59 to 580.84 ppm with a mean of 74.80 ppm (s=±116.59 ppm; C=155.87%) and a median of 20.62 ppm (n=62) (refer to Map 5.9).

House dust Cd varies from 17.19 to 107.48 ppm with a mean of 22.04 (s=±17.19 ppm; C=78.00%) and a median of 16.33 ppm (n=127).

The Cd contamination index in overburden, with respect to its median in parent rocks, varies from 8.0 to 1850.0, and in house dust from 34.4 to 215.0.

It is apparent from the statistical distribution of Cd in different sample types, that the metallurgical processing wastes are the major source of contamination of overburden samples (Fig. 6.7). The contribution of Cd from rock samples is almost totally masked by the higher concentrations in metallurgical wastes. Both sample types, metallurgical wastes and overburden, contribute to the contamination of house dust.

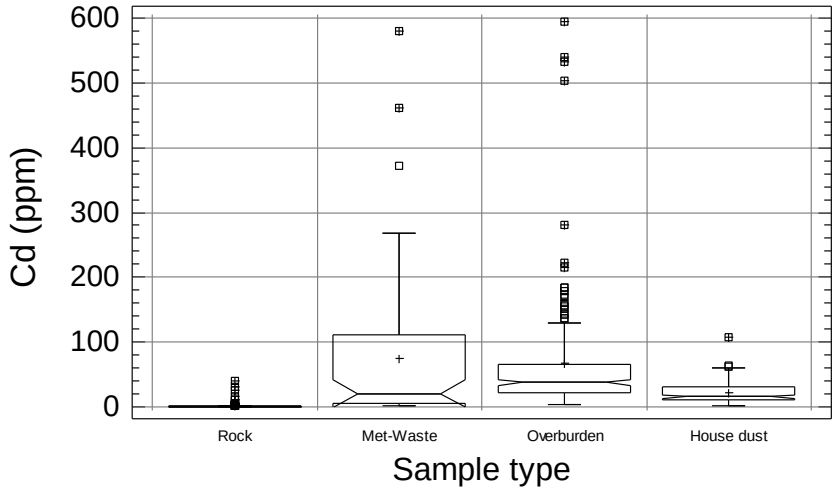

Fig. 6.7. Multiple notched-box-and-whisker plots comparing cadmium (Cd) distribution in different sample types [one soil sample >600 ppm Cd].
Σχ. 6.7. Πολλαπλό θηκόγραμμα με εγκοπές που συγκρίνει την κατανομή του καδμίου (Cd) σε διαφορετικούς τύπους δειγμάτων [ένα δείγμα εδάφους >600 ppm Cd].

Major geochemical neoanomalies, with Cd concentrations above 129 ppm have a NE-SW trend, and occur over the flotation residues (Noria-Prasini Alepou-Santorineika), pyritiferous wastes (Komobil, Nichtochori) and slag/sand-blast material (within the smelter area at Kiprianos, Kavodokanos and Fougara). The strongest geochemical neoanomaly >179 to 925 ppm Cd occurs within the premises of the smelter at Kiprianos, and its immediate surroundings. Distinct neohaloes extend about geochemical neoanomalies down to 38 ppm Cd, although even lower levels, to 6 ppm Cd, may be attributed to aerial dispersion from the smelters and metallurgical wastes.

Mobility of Cd is generally medium under oxidising, acid and neutral to alkaline conditions; very low under reducing conditions (Levinson, 1980; Hoffman, 1986; Reimann *et al.*, 1998) (Table 6.2). The pH of hydrolysis of Cd^{2+} in dilute solutions is 6.7, meaning that $Cd(OH)_2$ precipitates in neutral environments and Cd becomes relatively

immobile (Table 6.1). Cadmium should, therefore, be geochemically immobile in most areas, since soil pH for 97.5% of the surface area of Lavrion is above 6.87 due to the predominance of marble. In the Lavrion urban area Cd may be, however, comparatively mobile in the pyritiferous materials with pH<5.00, as for example, in the areas between Kiprianos and Kavodokanos, and Komobil and Nichtochori (refer to Map 2.5).

Another significant problem is the long residence times of Cd in soil, which according to Ferguson (1990) is 280 years.

Cadmium seems to be an essential element for some animals at low concentrations (Reimann *et al.*, 1998), but is toxic to most animals and humans (Gough *et al.*, 1979; Mervyn, 1985, 1986), and is supposed to be carcinogenic.

According to Kabata-Pendias and Pendias (1984), the maximum permissible level of Cd in soil for healthy plant growth is 8 ppm. Values above this limit are considered to be phytotoxic. Consequently, 96% of the soil cover of Lavrion, under this premise, is unfit for plant growth (Map 6.9).

The recommended statutory limits for total Cd in residential soil, quoted in scientific literature, vary from 2 to 34 ppm, *i.e.*,

- 2 ppm in The Netherlands (VROM, 1983; Lux, 1993; Van den Berg *et al.*, 1993; J. Ebbing, person. commun., 1996),
- 3 ppm in the United Kingdom (ICRCL, 1987), Finland (Koljonen, 1992), Germany (Kloke, 1977; Lux, 1993) and Federal Canada (Sheppard *et al.*, 1992); the European Union recommends an upper Cd level of 3 ppm, when sewage sludge is added to agricultural soil (CEC, 1986).
- 4 ppm in the State of Ontario (Sheppard *et al.*, 1992),
- 5 ppm in Denmark (Edelgaard and Dahlstrøm, 1999),
- 20 ppm in Switzerland (Hämman and Gupta, 1998), and
- 34 ppm in the State of Connecticut (US CT, 1994).

Finland has also an upper limit of 10 ppm for soil Cd (R. Salminen, person. commun., 1996) and The Netherlands an intervention value of 12 ppm Cd. This variation of technocratic statutory limits shows the necessity of setting up internationally agreed limits, based on realistic geochemical and medical principles.

Since, (a) global normal soil has an average of 1 ppm and a median of 0.3 ppm Cd, (b) Lavrion parent rocks have an average of 1.89 ppm Cd, and a median of <1 ppm Cd, and (c) the onset of phytotoxicity may start at 3 ppm Cd, statutory limits between 3 to 4 ppm are considered logical. Hence, the whole Lavrion urban overburden/soil is considered to be a potential health hazard with respect to Cd (Map 6.9).

6.2.8. DISTRIBUTION OF TOTAL COBALT (Co) IN OVERBURDEN (Map 6.10, Fig. 6.8)

Cobalt in overburden samples varies from 3 to 106 ppm, with a mean of 17.7 ppm (s=±9.89 ppm; C=55.88%), and a median of 16 ppm (n=224). In comparison, Co in normal global soil, away from areas of base metal mineralisation and mafic-ultramafic rocks, has a range of 1 to 40 ppm, an average of 10 ppm (Levinson, 1980), and a median of also 10 ppm (Reimann *et al.*, 1998). In Lavrion, the average and median values are slightly exceeded due to (a) mineralisation in certain parts of Lavrion (Map 4.10), (b) mafic

rocks (prasinite) (Map 2.2), and (c) contamination from metallurgical activities (Map 5.10). It appears that overburden Co has both geogenic and anthropogenic sources (Fig. 6.8).

Cobalt concentrations in rocks of the Lavrion urban area vary from <1.0 to 104 ppm, with a mean of 26.9 ppm (s=±26.1 ppm; C=97.03%) and a median of 20.5 ppm (n=140) (Map 4.10).

Cobalt levels in metallurgical wastes vary from 2.98 to 83.95 ppm with a mean of 26.35 ppm (s=±15.96 ppm; C=60.57%) and a median of 23.83 ppm (n=62) (refer to Map 5.10).

House dust Co varies from 3.25 to 69.13 ppm with a mean of 9.61 ppm (s=±7.63 ppm; C=79.40%) and a median of 8.12 ppm (n=127).

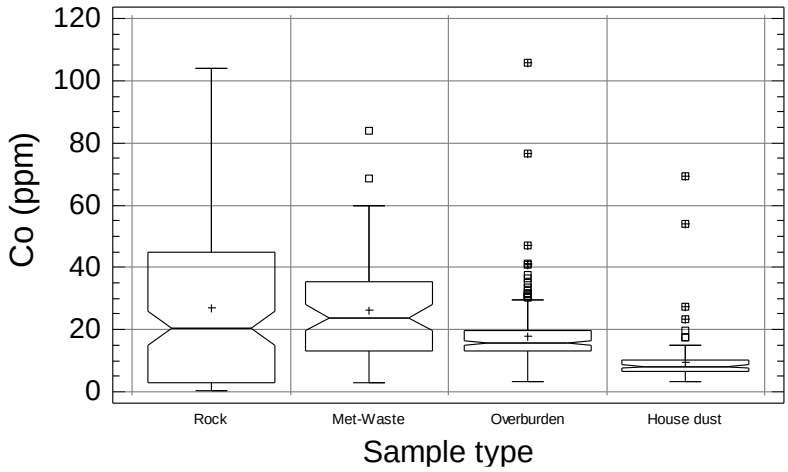

Fig. 6.8. Multiple notched-box-and-whisker plots comparing cobalt (Co) distribution in different sample types.
Σχ. 6.8. Πολλαπλό θηκόγραμμα με εγκοπές που συγκρίνει την κατανομή του κοβαλτίου (Co) σε διαφορετικούς τύπους δειγμάτων.

The Co depletion/“contamination index” in overburden, with respect to its median in parent rocks, varies from 0.15 to 5.17, and in house dust from 0.16 to 3.38.

It is apparent from the statistical distribution of Co in different sample types, that parent rocks and metallurgical processing wastes have contributed to overburden Co (Fig. 6.8). Both sample types, metallurgical wastes and overburden, are sources of house dust contamination.

Major geochemical neoanomalies with Co concentrations above 20 ppm, occur over pyritiferous sand and pyrite tailings (Kiprianos-Phenikodassos-Komobil-Nichtochori, and Kavodokanos), and slag/sand-blast material (within the smelter area at Kiprianos; Kavodokanos and Fougara). The strongest geochemical neoanomaly >32 to 106 ppm Co occurs over pyritiferous sand from Kiprianos to Phenikodassos and Komobil. Distinct Co neohaloes extend about the geochemical neoanomalies down to 16 ppm Co; lower levels are difficult to attribute solely to metallurgical wastes, because of a contribution from geogenic sources (Map 6.10).

The major geochemical Co anomaly over overburden, extending from Noria to Vilanoira-Panormos (>27 to 37 ppm Co), is ascribed to the occurrence of schist, prasinite and marble alteration (Map 2.2), and development of clay rich soil on which Co is adsorbed. The secondary halo extending down to 20 ppm Co from Noria to Panormos and Perdika, and the northerly extension from Noria to Prasini Alepou and west of

Kiprianos-Kavodokanos, are also related to schist, prasinite and marble alteration. Geogenic and anthropogenic dispersion patterns apparently join in the area to the west of Kiprianos and Phenikodassos, because the streams transport weathered materials from outcrops of schist, prasinite and altered marble (Maps 2.2, 4.10 & 6.10).

Since, the secondary geochemical pattern from Koukos to Neapoli, Ayios Andreas and Ayia Paraskevi, with low Co concentrations (<16 ppm), is considered to have more geogenic than anthropogenic affinities, and is generally developed over schist, two types of schist are presumed to occur in Lavrion; one with low and the other with high Co concentrations, although this is not so evident from the lithogeochemical map (Map 4.10).

Mobility of Co is generally moderate under oxidising, high under acid, medium to low under neutral and very low under alkaline and reducing conditions (Levinson, 1980; Hoffman, 1986; Reimann *et al.*, 1998) (Table 6.2). The pH of hydrolysis of Co^{2+} in dilute solutions is 6.8, meaning that $Co(OH)_2$ precipitates in neutral environments and Co becomes relatively immobile (Table 6.1). Cobalt should, therefore, be geochemically immobile in most areas, since soil pH for 97.5% of the surface area of Lavrion is above 6.87 due to the predominance of marble (Map 2.5). In the Lavrion urban area Co may be, however, comparatively mobile in the pyritiferous materials with pH<5.00, as for example, in the areas between Kiprianos and Kavodokanos, and Komobil and Nichtochori.

Cobalt is an essential element for animals and humans only as a constituent of vitamin B_{12} (Mervyn, 1985, 1986). It is, however, toxic to humans at doses of 25 mg/day or more (Reimann *et al.*, 1998).

Phytotoxic levels in surface soil vary from 25 to 50 ppm Co, according to different authors (Kabata-Pendias and Pendias, 1984) (Table 6.3). If the maximum phytotoxic level is taken, then 0.9% of the soil cover of Lavrion, under this premise, is unfit for plant growth (Map 6.10).

Recommended statutory limits for total Co in residential soil, quoted in scientific literature, vary from 20 to 50 ppm, *i.e.*,

- 20 ppm in The Netherlands (VROM, 1983; Lux, 1993; Van den Berg *et al.*, 1993; J. Ebbing, person. commun., 1996),
- 40 ppm in Federal Canada (Sheppard *et al.*, 1992), and
- 50 ppm in Finland (Koljonen, 1992), and the State of Ontario (Sheppard *et al.*, 1992).

Apart from the limit values there is also an intervention value, which in Finland is set at 200 ppm (R. Salminen, person. commun., 1996), and in The Netherlands at 240 ppm Co. This variation of technocratic statutory limits again shows the necessity of setting up internationally agreed limits, based on pragmatic geochemical and medical principles. Normal soil has a range of 1-40 ppm Co (Levinson, 1980), but over mafic and ultramafic rocks values of >45 and >110 ppm Co respectively should occur. It is quite apparent, therefore, that a single statutory trigger value cannot cover all cases. In the case of Lavrion, however, Co is not considered to be a potential health hazard.

6.2.9. DISTRIBUTION OF TOTAL CHROMIUM (Cr) IN OVERBURDEN (Map 6.11, Fig. 6.9)

Chromium in overburden samples varies from 2 to 1083 ppm, with a mean of 264.2 ppm (s=±224.7 ppm; C=85.05%), and a median of 183 ppm (n=224). In comparison, Cr in normal global soil, away from areas of mineralisation and mafic-ultramafic rocks, has an average of 50 ppm (Levinson, 1980), and a median of 80 ppm (Reimann *et al.*, 1998). In Lavrion, the comparatively elevated average and median Cr values in overburden are due to mafic rocks (prasinite) and ferromagnesian minerals in schist (Map 2.2). It appears that overburden Cr has been derived from mainly geogenic sources (Fig. 6.9).

Chromium concentrations in rocks of the Lavrion urban area vary from <1.0 to 610 ppm, with a mean of 100.4 ppm (s=±145.9 ppm; C=145.32%) and a median of 20 ppm (n=140) (Map 4.11).

Chromium levels in metallurgical wastes vary from 8.11 to 299.15 ppm with a mean of 83.47 ppm (s=±59.98 ppm; C=71.86%) and a median of 73.18 ppm (n=62) (refer to Map 5.11).

House dust Cr varies from 48.2 to 1844.9 ppm with a mean of 142.9 ppm (s=±184.3 ppm; C=128.97%) and a median of 113.90 ppm (n=127).

The Cr depletion/anomalous index in overburden, with respect to its median in parent rocks, varies from 0.10 to 54.15, and in house dust from 2.41 to 92.25. In the case of Cr these values should be used with caution, because the aqua regia extraction is not able to bring into solution the total Cr content.

It is apparent from the statistical distribution of Cr in different sample types, that parent rocks and metallurgical processing wastes have contributed to overburden Cr (Fig. 6.9). Both sample types, metallurgical wastes and overburden, are sources of house dust contamination. The higher Cr levels in house dust may be due to anthropogenic sources within the home environment.

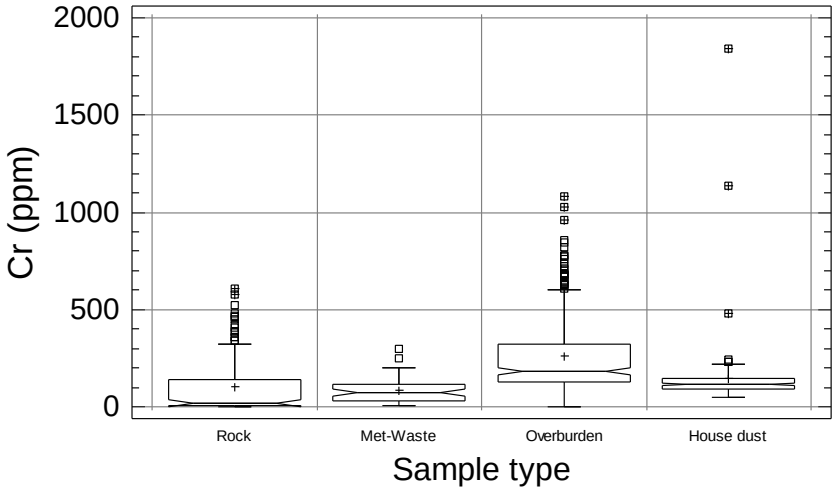

Fig. 6.9. Multiple notched-box-and-whisker plots comparing chromium (Cr) distribution in different sample types.
Σχ. 6.9. Πολλαπλό θηκόγραμμα με εγκοπές που συγκρίνει την κατανομή του χρωμίου (Cr) σε διαφορετικούς τύπους δειγμάτων.

Major geochemical anomalies with Cr concentrations above 319 ppm have a NE-SW trend, and occur over schist, altered marble and prasinite (Vilanoira-Panormos-Koukos-Neapoli-Ayios Andreas-Ayia Paraskevi-Nichtochori; north-west of Noria; Prasini Alepou; Thorikon) (see Map 2.2). The strongest geochemical anomaly >726 to 1083 ppm Cr occurs over altered marble with schist intercalations to the south-west of Panormos. The secondary halo down to 183 ppm Cr is ascribed to a geogenic origin. Overburden samples over marble have Cr concentrations between 61 to 646 ppm, indicating the influence of intercalated schist.

Samples of overburden, over metallurgical processing wastes, have generally Cr levels below 183 ppm (flotation residues: 92-183 ppm Cr), and notably below 61 ppm, especially in the area with pyrite tailings and pyritiferous sand (Nichtochori-Komobil-Kiprianos, and Kavodokanos), and slag/sand-blast wastes (Kavodokanos, Fougara and to the east/south-east of Ayia Paraskevi) (Map 5.11).

Mobility of Cr is generally very low under all conditions (Levinson, 1980; Hoffman, 1986; Reimann *et al.*, 1998) (Table 6.2). The pH of hydrolysis of Cr^{3+} in dilute solutions is 5.3, meaning that $Cr(OH)_3$ precipitates in a slightly acid environment and Cr becomes relatively immobile (Table 6.1). Chromium should, therefore, be geochemically immobile in most areas, since soil pH for 97.5% of the surface area of Lavrion is above 6.87 due to the predominance of marble (Map 2.5). In the Lavrion urban area Cr may be, however, comparatively mobile in pyritiferous materials with pH<5.00, as for example, in the areas between Kiprianos and Kavodokanos, and Komobil and Nichtochori.

Chromium is an essential element for some animals and humans, and especially the trivalent form (Cr^{3+}) for is the only one that can be used by the body (Mervyn, 1985, 1986). Hexavalent chromium (Cr^{6+}) is highly toxic, and its compounds are carcinogenic (Reimann *et al.*, 1998), but fortunately it does not occur in natural minerals (Gough *et al.*, 1979).

Phytotoxic levels of Cr in soil vary from 75 to 100 ppm, according to different authors (Kabata-Pendias and Pendias, 1984) (Table 6.3). If the maximum permissible level of Cr in soil for healthy plant growth is 100 ppm is considered, then 82.6% of the soil cover of Lavrion is unfit for plant growth (Map 6.11).

The recommended residential soil Cr statutory limits, quoted in scientific literature, vary from 25 ppm to 3900 ppm, *i.e.*,

- 25 ppm for Cr^{3+} in the United Kingdom (ICRCL, 1987);
- 100 ppm in Finland (Koljonen, 1992), Germany (Kloke, 1977; Lux, 1993) and State of Connecticut for Cr^{6+};
- 380 ppm in The Netherlands (VROM, 1983; Lux, 1993; Van den Berg *et al.*, 1993; J. Ebbing, person. commun., 1996);
- 600 ppm in the United Kingdom (ICRCL, 1987);
- 750 ppm in Federal Canada (Sheppard *et al.*, 1992);
- 1000 ppm in the State of Ontario (Sheppard *et al.*, 1992), and Denmark (Edelgaard and Dahlstrøm, 1999), and
- 3900 ppm in the State of Connecticut for Cr^{3+} (US CT, 1994, 1997).

This great variation of technocratic statutory limits again shows the necessity of setting up internationally agreed limits, based on pragmatic geochemical and medical principles. However, site specific background values should be estimated.

Global soil mean and median values of Cr are 50 and 80 ppm, respectively. Soil over mafic rocks should have Cr contents >250 ppm, and over ultramafics >2300 ppm. This is another element that shows the necessity of having different statutory limits, which take into account natural geochemical variability. In the case of Lavrion, the United Kingdom (600 ppm Cr) or Federal Canada (750 ppm Cr) statutory limits for chromium are probably the most appropriate. Using these two levels the area considered to be hazardous to human health is 13.8% for the former, and 4.5% for the latter case.

6.2.10. DISTRIBUTION OF TOTAL COPPER (Cu) IN OVERBURDEN (Map 6.12, Fig. 6.10)

Copper in overburden samples varies from 43 to 4,445 ppm, with a mean of 357 ppm (s=±595.4 ppm; C=166.78%), and a median of 186 ppm (n=224). In comparison, Cu in normal global soil, away from areas of mineralisation, mafic-ultramafic rocks and shale/schist, has a range of 2-100 ppm, an average of 20 ppm (Levinson, 1980), and a median of 25 ppm (Reimann *et al.*, 1998). In Lavrion, the high Cu levels in overburden are mainly due to anthropogenic contamination (Map 6.12, Fig. 6.10).

Copper concentrations in rocks of the Lavrion urban area vary from 3 to 225 ppm, with a mean of 32.8 ppm (s=±31.0 ppm; C=94.51%) and a median of 25 ppm (n=140) (Map 4.12).

Copper levels in metallurgical wastes vary from 184 to 8,700 ppm with a mean of 1172.9 ppm (s=±1,362.6 ppm; C=116.17%) and a median of 630.5 ppm (n=62) (refer to Map 5.11).

House dust Cu varies from 34.0 to 4,934 ppm with a mean of 293 ppm (s=±507.6 ppm; C=173.54%) and a median of 179 ppm (n=127).

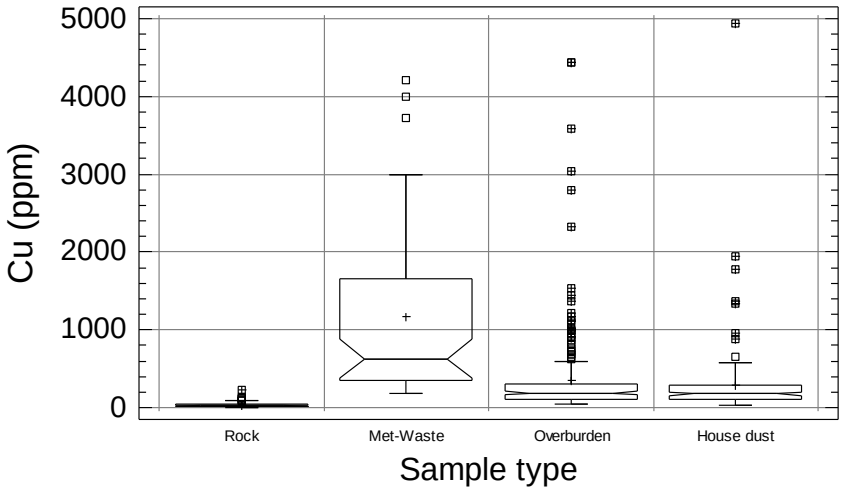

Fig. 6.10. Multiple notched-box-and-whisker plots comparing copper (Cu) distribution in different sample types [two samples of metallurgical wastes >5000 ppm Cu].
Σχ. 6.10. Πολλαπλό θηκόγραμμα με εγκοπές που συγκρίνει την κατανομή του χαλκού (Cu) σε διαφορετικούς τύπους δειγμάτων [δύο δείγματα μεταλλουργικών απορριμμάτων >5000 ppm Cu].

The Cu contamination index in overburden, with respect to its median in parent rocks, varies from 1.72 to 177.8, and in house dust from 1.36 to 197.36.

It is apparent from the statistical distribution of Cu in different sample types, that the metallurgical processing wastes are the main sources of overburden contamination (Fig. 6.10). Both sample types, metallurgical wastes and overburden, should contribute to the contamination of house dust. However, the boxplot comparison shows, by correspondence of the medians at the 95% confidence level, that house dust Cu is largely derived from overburden dust (Fig. 6.10). Further, house dust has higher Cu levels, which may either be due to its finer grain or to anthropogenic sources within the home environment.

Major anthropogenic neoanomalies have a NE-SW trend and Cu concentrations above 306 ppm. They occur over metallurgical processing wastes and, especially, the slag/sand-blast wastes at Kavodokanos and Kiprianos, and the pyrite tailings and pyritiferous sand from Nichtochori-Komobil-Kiprianos. The strongest geochemical neoanomaly >1,122 to 4,445 ppm Cu occurs over slag in the smelter area at Kiprianos (Map 5.12). Over the flotation residues, geochemical neoanomalies vary from 186 to 819 ppm Cu. Neohaloes of Cu appear to extend down to 93 ppm and possibly 76 ppm (Map 6.12). Below the latter Cu level, there is most likely an influence from geogenic sources.

Mobility of Cu is medium under oxidising, high under acid, very low under neutral to alkaline and reducing conditions (Levinson, 1980; Hoffman, 1986; Reimann *et al.*, 1998) (Table 6.2). The pH of hydrolysis of Cu^{2+} in dilute solutions is 5.3, meaning that $Cu(OH)_2$ precipitates in a slightly acid environment, and Cu becomes relatively immobile (Table 6.1). Copper should, therefore, be geochemically immobile in most areas, since soil pH for 97.5% of the surface area of Lavrion is above 6.87 due to the predominance of marble (Map 2.5). In the Lavrion urban area Cu may be, however, comparatively mobile in the pyritiferous materials with pH<5.00, as for example, in the areas between Kiprianos and Kavodokanos, and Komobil and Nichtochori.

Copper is an essential element for all plants and animals (Gough *et al.*, 1979; Reimann *et al.*, 1998), but it is toxic at high doses (Mervyn, 1980, 1985, 1986).

Phytotoxic levels of total Cu in surface soil vary from 60 to 125 ppm, according to different authors (Kabata-Pendias and Pendias, 1984); 100 ppm Cu appears to be the preferred level of most researchers. If this phytotoxic level is taken, then 83.04% of the surface soil cover in Lavrion is unfit for plant growth (Map 6.12).

The recommended residential soil Cu statutory limits, quoted in scientific literature, vary from 36 to 2,500 ppm, *i.e.*,

- 36 ppm in The Netherlands (VROM, 1983; Lux, 1993; Van den Berg *et al.*, 1993; J. Ebbing, person. commun., 1996);
- 100 ppm in Finland (Koljonen, 1992), and Germany (Kloke, 1977; Lux, 1993);
- 130 ppm in the United Kingdom (ICRCL, 1987);
- 150 ppm in Federal Canada (Sheppard *et al.*, 1992), and Switzerland (Hämman and Gupta, 1998);
- 200 ppm in the State of Ontario (Sheppard *et al.*, 1992);
- 500 ppm in Denmark (Edelgaard and Dahlstrøm, 1999), and
- 2,500 ppm in the State of Connecticut (US CT, 1994, 1997).

The European Union recommends a minimum Cu level of 50 ppm and a maximum of 140 ppm, when sewage sludge is added to agricultural soil (CEC, 1986). Apart from the limit values, there are also intervention or clean-up values, which in The Netherlands is set at 190 ppm, in Finland at 400 ppm Cu and in Switzerland at 1000 ppm Cu. This great variation of technocratic statutory limits again shows the necessity of setting up internationally agreed limits, based on sound geochemical and medical principles.

Global normal soil has a range of 2 to 100 ppm Cu, an average of 20 ppm and a median of 25 ppm Cu (Levinson, 1980; Reimann *et al.*, 1998). Different rock types have total Cu contents varying from 2 ppm in sandstone to 90 ppm in gabbro/basalt. Copper concentrations in Lavrion rocks vary from 3 to 225 ppm, with a mean of 32.8 ppm and a median of 25 ppm; the 90th percentile corresponds to 71 ppm Cu. Since, the maximum level of phytotoxicity is 125 ppm Cu, trigger levels of 130 and 150 ppm Cu seem appropriate for Lavrion "soil". In such a case, an area of 68.75% for the former and 60.71% for the latter level is considered to be potentially hazardous to human health (Map 6.12).

6.2.11. DISTRIBUTION OF TOTAL IRON (Fe) IN OVERBURDEN (Map 6.13, Fig. 6.11)

Iron in overburden samples varies from 18,859 to 351,559 ppm, with a mean of 62,398 ppm (s=±51,900 ppm; C=83.18%), and a median of 44,771 ppm (n=224). In comparison, Fe in normal soil, away from areas of mineralisation, mafic-ultramafic rocks and shale/schist, has a median of either 21,000 ppm (Rose *et al.*, 1979) or 35,000 ppm (Reimann *et al.*, 1998). In Lavrion, the comparatively elevated median Fe value in overburden is mainly due to anthropogenic contamination (Fig. 6.11).

Iron concentrations in rocks of the Lavrion urban area vary from 979 to 107,016 ppm, with a mean of 23,790 ppm (s=±20,660 ppm; C=86.84%) and a median of 19,515 ppm (n=140) (Map 4.13).

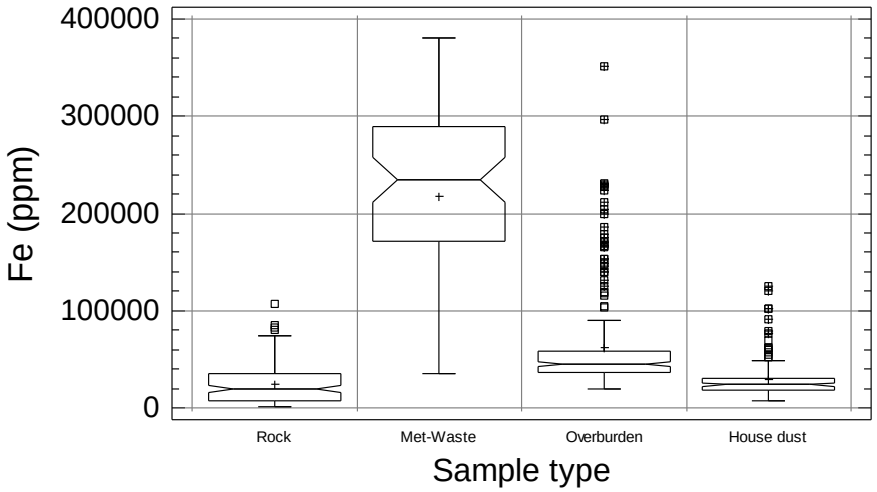

Fig. 6.11. Multiple notched-box-and-whisker plots comparing iron (Fe) distribution in different sample types.
Σχ. 6.11. Πολλαπλό θηκόγραμμα με εγκοπές που συγκρίνει την κατανομή του σιδήρου (Fe) σε διαφορετικούς τύπους δειγμάτων.

Iron in metallurgical wastes varies from 35,000 to 380,000 ppm with a mean of 217,081 ppm (s=±89,238 ppm; C=41.11%) and a median of 234,500 ppm (n=62) (refer to Map 5.13).

House dust Fe varies from 6,745 to 125,009 ppm with a mean of 29,615 ppm (s=±21,285 ppm; C=71.87%) and a median of 23,709 ppm (n=127).

The Fe depletion/contamination index in overburden, with respect to its median in parent rocks, varies from 0.97 to 18.01, and in house dust from 0.35 to 6.41.

It is apparent from the statistical distribution of Fe in different sample types, that the metallurgical processing wastes are the main source of contamination of overburden (Fig. 6.11, Maps 4.13 & 5.13). Both sample types, metallurgical wastes and overburden, should contribute to the contamination of house dust.

Major geochemical neoanomalies with Fe concentrations above 58,261 ppm occur over pyrite tailings, pyritiferous sand, slag/sand-blast wastes from east of Ayia Paraskevi to Nichtochori, Komobil, Phenikodassos, Kiprianos and Kavodokanos (refer also to Map 5.13). About this extensive anomaly there is a neohalo down to 44,771 ppm Fe. The strongest anthropogenic neoanomalies >178.934 to 351,559 ppm Fe occur over pyrite tailings and pyritiferous sand from Nichtochori to Komobil and Kiprianos and at Kavodokanos (Map 6.13). Over the flotation residues (Noria-Prasini Alepou-Santorineika), and the slag heap at Fougara, overburden Fe concentrations vary from 32,168-58,261 and 36,044-139,821 ppm respectively; the lower Fe levels in overburden are explained by the comparatively low Fe contents of flotation residues and slag in both areas (refer to Map 5.13).

Elevated overburden Fe concentrations (>44,771-139,821 ppm) from Panormos-Vilanoira to Neapoli-Noria, and to the west of Prasini Alepou, may be ascribed to the underlying schist, locally to prasinite and altered marble (refer to Maps 2.2 & 4.13). Low overburden Fe concentrations from Perdika to Panormos, Koukos, Neapoli, Ayios Andreas and Ayia Paraskevi are explained by the underlying marble. Hence, overburden Fe has both anthropogenic and geogenic affinities. Anthropogenic contamination, however, masks, to a large extent, geogenic patterns.

Mobility of Fe is generally very low under oxidising, low under acid, neutral to alkaline and reducing conditions (Reimann *et al.*, 1998) (Table 6.2). The valency state of iron plays a very important role in its mobility, *e.g.*, mobility of Fe^{3+} is high to very low in acid, and very low under neutral to alkaline conditions, whereas mobility of Fe^{2+} is high under acid, medium to low under neutral, and very low under alkaline conditions. The pH of hydrolysis of Fe^{3+} and Fe^{2+} in dilute solutions is 2.0 and 5.5 respectively; meaning that $Fe(OH)_3$ and $Fe(OH)_2$ precipitate correspondingly in an acid and slightly acid environment (Table 6.1). Iron should, therefore, be geochemically immobile in most areas, since soil pH for 97.5% of the surface area of Lavrion is above 6.87 due to the predominance of marble (Map 2.5). In the Lavrion urban area, Fe may, however, be comparatively mobile in pyritiferous materials with pH<5.50, as for example, in the areas between Kiprianos and Kavodokanos, and Komobil and Nichtochori.

Iron is an essential element for plants and animals (Mervyn, 1980, 1985, 1986; Reimann *et al.*, 1998). However, at high concentrations in soil there are reports of phytotoxicity problems (Kabata-Pendias and Pendias, 1984).

6.2.12. DISTRIBUTION OF TOTAL MERCURY (Hg) IN OVERBURDEN (Map 6.14, Fig. 6.12)

It should be pointed out at the start, that the analytical method used to determine Hg in overburden samples has a detection limit of 2.5 ppb and an upper limit of 747 ppb (refer to Chapter 2B). Samples with high concentrations of Hg, as is the case with Lavrion samples, do not give correct results, something that was verified recently. Apparently, they furnish a comparative order of magnitude. Hence, the Hg distribution in overburden samples displays geochemical patterns in terms of a comparative order of magnitude, but not the actual total Hg levels, *i.e.*, >500 ppb Hg.

Mercury in overburden samples varies from <2.5 to 747 ppb ppm, with a mean of 204.8 ppb (s=±199.3 ppb; C=97.31%), and a median of 136 ppb (n=194). In comparison, Hg in normal soil, away from mineralised areas, has an average of 30 ppb (Levinson, 1980), and a median of 50 ppb (Reimann *et al.*, 1998). In Lavrion, these levels are exceeded due to (a) mineralisation in certain parts of Lavrion (Table 4.19A), and (b) contamination from metallurgical activities, which is the major contributor (Map 5.14).

Mercury concentrations in rocks of the Lavrion urban area vary from <1.0 to 7.77 ppm (7,770 ppb), with a mean of 0.69 ppm (s=±1.05 ppm; C=152.17%) and a median of 0.5 ppm (n=48; note this is a recent compilation of additional data, hence the difference with the values quoted on Map 6.14) (Table 4.19A). Rock geochemical results give an indication of the range of minimum Hg levels in overburden, since higher levels are expected because of adsorption.

Mercury levels in metallurgical wastes vary from <1.0 to 10.20 ppm (10,200 ppb) with a mean of 2.58 ppm (s=±1.73 ppm; C=67.05%) and a median of 2.35 ppm (n=62) (refer to Map 5.14). Again these results indicate the Hg levels expected in overburden.

House dust Hg varies from <2.5 ppb to 380.0 ppb with a mean of 100 ppb (s=±50 ppb; C=50.00%) and a median of 90 ppb (n=127).

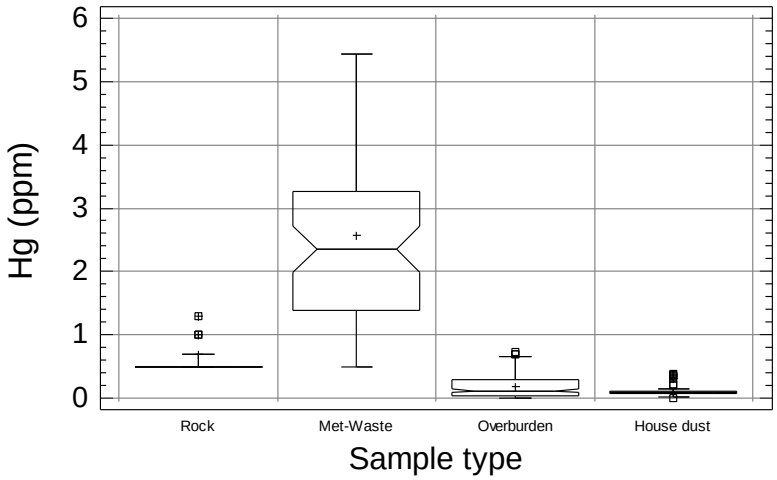

Fig. 6.12. Multiple notched-box-and-whisker plots comparing mercury (Hg) distribution in different sample types. It is stressed that overburden and house dust Hg levels are not correct; refer to text for details [one rock and two metallurgical wastes samples >6 ppm Hg].
Σχ. 6.12. Πολλαπλό θηκόγραμμα με εγκοπές που συγκρίνει την κατανομή του υδραργύρου (Hg) σε διαφορετικούς τύπους δειγμάτων. Σημειώνεται ότι οι συγκεντρώσεις Hg στα δείγματα του εδαφικού καλύμματος και σκόνης σπιτιών δεν δίνουν τις ακριβείς ολικές τιμές. Βλέπετε κείμενο για εξηγήσεις [ένα δείγμα πετρώματος και δύο μεταλλουργικών απορριμμάτων >6 ppm Hg].

The boxplot comparison shows well the analytical problems of Hg determination in samples of overburden and house dust. Concentrations of Hg in rock and metallurgical wastes give correct results; by comparing these results, it is apparent that the metallurgical processing wastes are the main source of Hg contamination of overburden (Fig. 6.12, Maps 5.14).

No contamination index will be estimated due to the analytical problems for determination of overburden and house dust Hg. From the above description of results, it is quite clear that overburden and house dust Hg levels should definitely be higher.

Major geochemical neoanomalies, with Hg concentrations above 346 ppb have a NE-SW trend, and occur over the flotation residues (Noria-Prasini Alepou-Santorineika). Distinct neohaloes extend about the geochemical neoanomalies down to 136 ppb Hg. Unfortunately, considerable information is missing about the geochemical distribution of Hg in overburden, when Maps 5.14 and 6.14 are compared.

Mobility of Hg is generally medium under oxidising, high under acid, very low under neutral to alkaline and reducing conditions (Levinson, 1980; Hoffman, 1986; Reimann *et al.*, 1998) (Table 6.2). The pH of hydrolysis of mercury depends on its valency state; Hg^{1+} and Hg^{2+} in dilute solutions have pH of hydrolysis of 3.0 and 7.3, respectively, meaning that Hg(OH) and $Hg(OH)_2$ precipitate correspondingly in acid and neutral to slightly alkaline environments (Table 6.1). Divalent mercury (Hg^{2+}) should, therefore, be geochemically immobile in most areas, since soil pH for 90% of the surface area of Lavrion is above 7.42 due to the predominance of marble. Monovalent mercury (Hg^{1+}), however, is almost completely immobile for more than 98% of the Lavrion urban area has a pH>5.00. Both monovalent and divalent Hg may be comparatively mobile in pyritiferous materials with pH<6.87 and <3.0, as for example, in the areas between Kiprianos and Kavodokanos, and Komobil and Nichtochori (refer to Map 2.5).

A significant problem is the long residence times of Hg in soil, which according to Ferguson (1990), is 920 years.

Total Hg levels, considered to be phytotoxic, vary from 0.3 to 5 ppm according to different researchers (Kabata-Pendias and Pendias, 1984). Since, overburden Hg data are only indicative of the actual situation, no comments can be made about the problems on plant growth. Nevertheless, results on rock and metallurgical waste samples indicate that there should be hazardous areas in Lavrion with respect to mercury.

The recommended statutory limits of Hg for residential soil, quoted in scientific literature, vary from 0.5 to 20 ppm, *i.e.*,

- 0.5 ppm in The Netherlands (VROM, 1983; Lux, 1993; Van den Berg *et al.*, 1993; J. Ebbing, person. commun., 1996);
- 0.8 ppm in Federal Canada (Sheppard *et al.*, 1992);
- 1 ppm in the State of Ontario (Sheppard *et al.*, 1992);
- 2 ppm in Finland (Koljonen, 1992), and Germany (Kloke, 1977; Lux, 1993);
- 3 ppm in Denmark (Edelgaard and Dahlstrøm, 1999), and
- 20 ppm in the United Kingdom (ICRCL, 1987), and the State of Connecticut (US CT, 1994).

The European Union recommends a minimum of 1 ppm and a maximum of 1.5 ppm Hg, when sewage sludge is added to agricultural soil (CEC, 1986). There is also an

intervention value quoted in some cases, as in Finland, 5 ppm Hg (R. Salminen, 1996, person. commun.), and The Netherlands (10 ppm Hg). The variation of technocratic statutory limits is indeed great for an element, which is considered to be non-essential for plants and animals (Gough *et al.*, 1979; Reimann *et al.*, 1998), and when is known to be very toxic with teratogenic properties (Mervyn 1985, 1986). The necessity of setting up internationally agreed limits, based on realistic geochemical and medical principles, is, therefore, considered to be very urgent for this particular element.

6.2.13. DISTRIBUTION OF TOTAL POTASSIUM (K) IN OVERBURDEN (Map 6.15, Fig. 6.13)

Potassium in overburden samples varies from 3,013 to 22,182 ppm, with a mean of 10,463 ppm (s=±3,585 ppm; C=34.26%), and a median of 9,770 ppm (n=224). Potassium in normal global soil has a median value of 14,000 ppm (Reimann *et al.*, 1998). In comparison, the Lavrion overburden/soil K median is lower. This is explained by the dominance of marble, which does not contain aluminosilicate minerals (Map 2.2).

Potassium concentrations in rocks of the Lavrion urban area vary from <83 to 31,795 ppm, with a mean of 5,841 ppm (s=±7,552 ppm; C=129.29%) and a median of 8,044 ppm (n=140) (Map 4.15).

Potassium levels in metallurgical wastes vary from 993 to 13,408 ppm with a mean of 6,942 ppm (s=±3,911 ppm; C=56.34%) and a median of 7,100 ppm (n=62) (refer to Map 5.15).

House dust K varies from 3,120 to 25,029 ppm with a mean of 5,984 (s=±2,790 ppm; C=46.62%) and a median of 5,574 ppm (n=127).

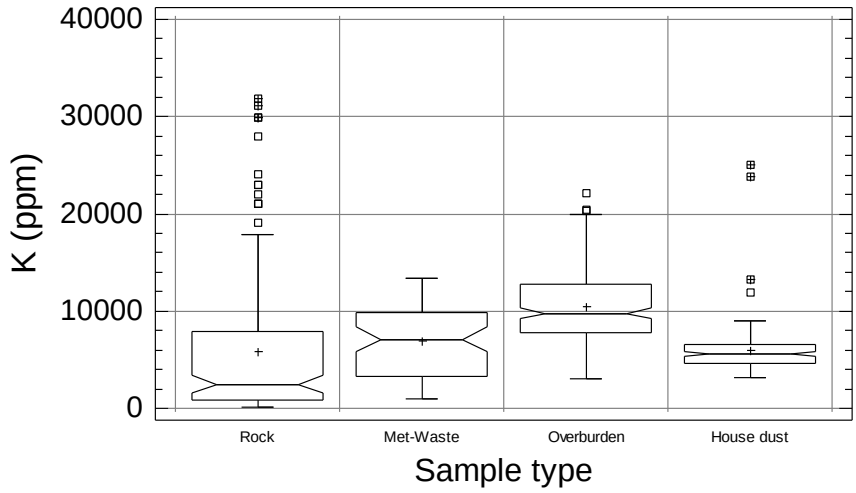

Fig. 6.13. Multiple notched-box-and-whisker plots comparing potassium (K) distribution in different sample types.
Σχ. 6.13. Πολλαπλό θηκόγραμμα με εγκοπές που συγκρίνει την κατανομή του καλίου (K) σε διαφορετικούς τύπους δειγμάτων.

The K depletion/enrichment/contamination index in overburden, with respect to its median in parent rocks, varies from 0.37 to 2.76, and in house dust from 0.39 to 3.11.

It is apparent from the statistical distribution of K in different sample types, that both rock and metallurgical processing wastes are the major sources of K in overburden samples (Fig. 6.13). Both sample types, metallurgical wastes and overburden, are the

sources of K in house dust. Overburden K has higher levels than rock and metallurgical wastes, and this may be due to its enrichment, similar to Al, in the clay fraction of soil.

Major geochemical "anomalies", with K concentrations above 12,714 ppm occur in the southern, western and northern parts of the study area, and the coastal section to the east of Ayia Paraskevi. The strongest geochemical anomalies >17,250 to 22,182 K occur at Vilanoira-Perdika in the south, and Thorikon in the north. There are only minor similarities, in the western border part of the study area, between overburden and rock geochemical patterns (Map 4.15). Minor relationships also exist with the metallurgical processing wastes, and mainly the slag at Fougara and to the east of Ayia Paraskevi, which have elevated K contents (Map 5.15). In both areas there are minor K neoanomalies in overburden. The geochemical anomaly, between Noria and Prasini Alepou with K>12,714 ppm, goes round the flotation residues, because of their lower K contents (Map 6.15).

Potassium, like Al, is normally enriched in clay-rich soils. Marble does not normally have aluminosilicate minerals and has apparently low K contents (Table 4.10A & Fig. 4.10A in Appendix 2A of Volume 1A, p.28; Map 4.15 in Volume 2). Schist, however, consists of aluminosilicate minerals, and occurs as intercalations within marble and also as a rock formation, and is comparatively enriched in potassium. Clay-rich soils, and consequently, elevated potassium (like Al) concentrations, occur

- over areas with schist and schistose-gneiss, and where marble has schist intercalations, *e.g.*, at Nichtochori, Neapoli-Koukos-Noria, Vilanoira, Prasini Alepou, west of Kavodokanos and Kiprianos (refer to lithological map, Map 2.2, Vol. 2), and
- at the base of slopes, where again there is an enrichment in clay, *e.g.*, Perdika, Noria.

It is quite apparent, therefore, that elevated K concentrations are due to an enrichment of clay in overburden. Clay-rich areas suggest that they may have a high scavenging capability.

Major anomalous K concentrations, since they occur in areas enriched in clay, may be ascribed, therefore, to mainly geogenic sources of the secondary environment.

Mobility of K is generally low under all conditions (Reimann *et al.*, 1998).

Potassium is an essential element for plants and animals (Kabata-Pendias and Pendias, 1984; Reimann *et al.*, 1998).

6.2.14. DISTRIBUTION OF TOTAL LANTHANUM (La) IN OVERBURDEN (Map 6.16, Fig. 6.14)

Lanthanum in overburden samples varies from 8.4 to 43.9 ppm, with a mean of 23.05 ppm (s=±5.56 ppm; C=24.12%), and a median of 22.7 ppm (n=224). Lanthanum in normal global soil has a median value of 35 ppm (Reimann *et al.*, 1998). In comparison, the Lavrion overburden/soil La median is lower. This is probably due to the predominance of marble, which has generally low La concentrations. Schist has, however, elevated mean La contents (see Table 4.19A in Appendix 2A of Volume 1A, p.37).

Lanthanum concentrations in rocks of the Lavrion urban area vary from <2.00 to 30.69 ppm, with a mean of 10.21 ppm (s=±6.47 ppm; C=63.37%) and a median of 8.86 ppm (n=48) (Table 4.19A).

Lanthanum levels in metallurgical wastes vary from <2.00 to 47.25 ppm with a mean of 25.13 ppm (s=±11.64 ppm; C=46.32%) and a median of 27.32 ppm (n=62) (refer to Map 5.16).

House dust La varies from 8.05 to 39.07 ppm with a mean of 17.16 (s=±5.70 ppm; C=33.22%) and a median of 16.02 ppm (n=127).

The La depletion/enrichment/contamination index in overburden, with respect to its median in parent rocks, varies from 0.95 to 4.95, and in house dust from 0.91 to 4.41.

It is apparent from the statistical distribution of La in different sample types, that elevated La contents in overburden are principally derived from metallurgical processing wastes (Fig. 6.14), and secondarily from parent rocks (mainly schist). Both sample types, metallurgical wastes and overburden, are the sources of La in house dust.

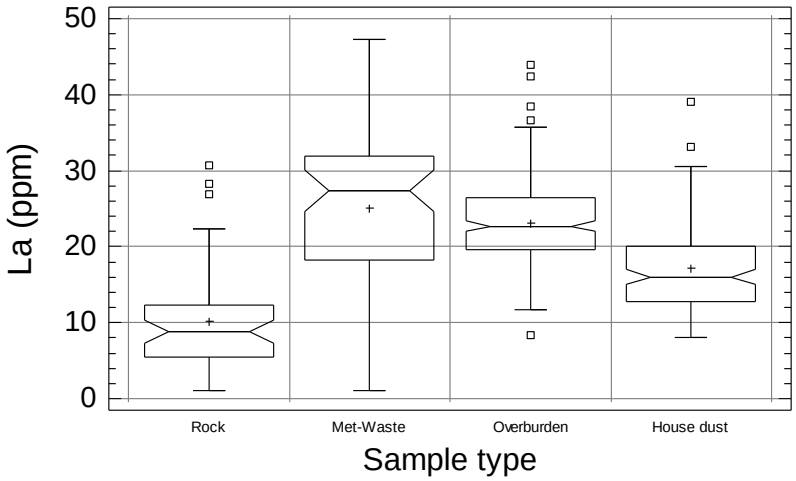

Fig. 6.14. Multiple notched-box-and-whisker plots comparing lanthanum (La) distribution in different sample types.
Σχ. 6.14. Πολλαπλό θηκόγραμμα με εγκοπές που συγκρίνει την κατανομή του λανθανίου (La) σε διαφορετικούς τύπους δειγμάτων.

Major geochemical neoanomalies, with La concentrations above 26.4 ppm occur at Kavodokanos-Kiprianos, Noria-Neapoli-Koukos, to the east of Ayia Paraskevi, and Fougara. The strongest geochemical neoanomaly >32 to 43.9 ppm La occurs at Kavodokanos. The Kavodokanos-Kiprianos La neoanomaly is ascribed to the metallurgical processing wastes, which at Kavodokanos have La levels in (a) flotation residues (28-37 ppm), and slag/slag-earth (32-47 ppm) (Map 5.16). The strong La neoanomaly occurring in the stream valley, indicates that alluvium is enriched with respect to lanthanum. Similarly, the Fougara and Ayia Paraskevi La neoanomalies are attributed to slag and slag-earth, which have comparatively high La contents.

Elevated overburden La concentrations over the flotation tailings vary from 22.7 to 29.7 ppm, where as samples of flotation tailings, *sensu strictu*, have La levels between 19-28 ppm (Map 5.16).

The Koukos-Neapoli-Noria La geochemical anomaly may be due to schist, altered marble and flotation residues.

Overburden La concentrations <22.7 ppm are related to marble and quaternary deposits (Map 2.2).

Mobility of La is generally low under all conditions (Reimann *et al.*, 1998). The pH of hydrolysis of La^{3+} in dilute solutions is 8.4, meaning that $La(OH)_3$ precipitates in an alkaline environment, and La becomes immobile (Table 6.1). Lanthanum should, therefore, be geochemically immobile in a very small part of Lavrion, *i.e.*, for about 5%, since soil pH for 95% of the surface area studied has pH values below 8.4.

Toxicity of La appears to be generally low (Gough, 1979; Reimann *et al.*, 1998).

6.2.15. DISTRIBUTION OF TOTAL LITHIUM (Li) IN OVERBURDEN (Map 6.17, Fig. 6.15)

Lithium in overburden samples varies from 3.8 to 48.3 ppm, with a mean of 18.9 ppm (s=±6.6 ppm; C=34.92%), and a median of 17.4 ppm (n=224). Lithium in normal soil has an average of 30 ppm (Levinson, 1980), and a median of 20 ppm (Reimann *et al.*, 1998). In comparison, the Lavrion overburden/soil Li average and median values are lower. This is due to the predominance of marble, which has generally low Li concentrations. Schist and prasinite have, however, elevated mean Li contents (see Table 4.11A in Appendix 2A of Volume 1A, p.29).

Lithium concentrations in rocks of the Lavrion urban area vary from <1.00 to 106 ppm, with a mean of 9.1 ppm (s=±12.1 ppm; C=132.97%) and a median of 5 ppm (n=140) (Map 4.17).

Lithium levels in metallurgical wastes vary from <1.00 to 25.83 ppm with a mean of 12.18 ppm (s=±7.17 ppm; C=58.87%) and a median of 14.50 ppm (n=62) (refer to Map 5.17).

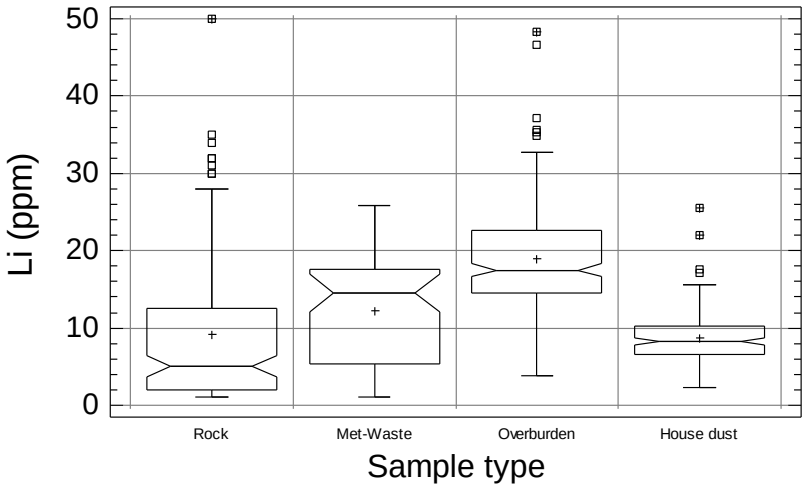

Fig. 6.15. Multiple notched-box-and-whisker plots comparing lithium (Li) distribution in different sample types [one rock sample >500 ppm Li].
Σχ. 6.15. Πολλαπλό θηκόγραμμα με εγκοπές που συγκρίνει την κατανομή του λιθίου (Li) σε διαφορετικούς τύπους δειγμάτων [ένα δείγμα πετρώματος >500 ppm Li].

House dust Li varies from 2.24 to 25.60 ppm with a mean of 8.76 ppm (s=±3.40 ppm; C=38.81%) and a median of 8.25 ppm (n=127).

The Li depletion/enrichment index in overburden, with respect to its median in parent rocks, varies from 0.76 to 9.66, and in house dust from 0.45 to 5.12.

It is apparent from the statistical distribution of Li in different sample types, that elevated Li contents in overburden are principally derived from parent rocks, with a

minor contribution from metallurgical processing wastes (Fig. 6.15). Both sample types, metallurgical wastes and overburden, are the sources of Li in house dust.

Major geochemical anomalies, with Li concentrations above 26.9 ppm occur at Kavodokanos-Thorikon, to the north of Prasini Alepou, at Neapoli and Panormos-Vilanoira. The strongest geochemical anomalies >29.5 to 48.3 ppm Li occur in the same areas. Their strong north-westerly trend suggests, that Li is not associated with metallurgical processing wastes, but with lithology. However, the lithogeochemical distribution map of Li (Map 4.17) does not explain overburden Li anomalies, and Li levels in metallurgical processing wastes may account only for elevated contents at Fougara (slag), Komobil-Phenikodassos (pyritiferous sand), and Kavodokanos (slag/sand-blast wastes) (Map 5.17).

Lithium anomalies in overburden (>26.9 ppm), and enhanced values >22.7 ppm, are apparently related to Al and K anomalous patterns (Maps 6.2 and 6.15), suggesting that elevated Li values occur in areas with comparatively high clay content. In fact, clays are reported to be geochemical barriers for Li (Boyle, 1974; Levinson, 1980; Reimann *et al.*, 1998). Minor anomalies between Neapoli and Noria (>22.7 to 29.5 ppm Li), and to north-west of Noria (>22.7 to 26.9 ppm Li) may be explained by the occurrence of schist, prasinite and marble alteration in the former area, and schist in the latter (Map 2.2), and the development of clay rich soil.

Mobility of Li is low under oxidising, acid and neutral to alkaline conditions, and very low under reducing conditions (Levinson, 1980; Hoffman, 1986; Reimann *et al.*, 1998) (Table 6.2).

Lithium is considered nonessential for higher plants and animals, but an essential element for some micro-organisms (Gough, 1979). Its toxicity is reckoned to be low (Gough, 1979; Reimann *et al.*, 1998).

6.2.16. DISTRIBUTION OF TOTAL MANGANESE (Mn) IN OVERBURDEN (Map 6.18, Fig. 6.16)

Manganese in overburden samples varies from 625 to 35,679 ppm, with a mean of 3,348 ppm (s=±3,757 ppm; C=112.22%), and a median of 2,189 ppm (n=224). In comparison, Mn in normal global soil has a median of 320 ppm, and 530 ppm for the <2 mm fraction according to Rose *et al.* (1979) and Reimann *et al.* (1998) respectively. In Lavrion the elevated median Mn value in overburden is ascribed to both geogenic and anthropogenic factors (Maps 4.18 & 5.18; Fig. 6.16).

Manganese concentrations in rocks of the Lavrion urban area vary from 100 to 25,000 ppm, with a mean of 1,831 ppm (s=±2,635 ppm; C=143.91%) and a median of 1,200 ppm (n=140) (Map 4.18, Fig. 6.16).

Manganese levels in metallurgical wastes vary from 182 to 35,354 ppm with a mean of 11,913 ppm (s=±9,925 ppm; C=83.31%) and a median of 9,398 ppm (n=62) (refer to Map 5.18).

House dust Mn varies from 224 to 14,325 ppm with a mean of 1,539 ppm (s=±1,921 ppm; C=124.82%) and a median of 970 ppm (n=127).

The Mn depletion/contamination index in overburden, with respect to its median in parent rocks, varies from 0.52 to 29.73, and in house dust from 0.19 to 11.94.

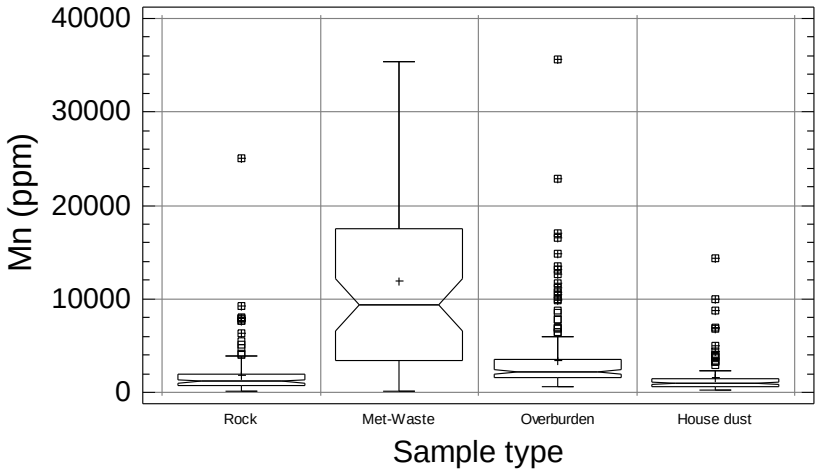

Fig. 6.16. Multiple notched-box-and-whisker plots comparing manganese (Mn) distribution in different sample types.
Σχ. 6.16. Πολλαπλό θηκόγραμμα με εγκοπές που συγκρίνει την κατανομή του μαγγανίου (Mn) σε διαφορετικούς τύπους δειγμάτων.

It is apparent from the statistical distribution of Mn in different sample types, that elevated Mn contents in overburden are principally due to contamination from metallurgical processing wastes, with a minor contribution from parent rocks (Fig. 6.16). Both sample types, metallurgical wastes and overburden, are the sources of Mn in house dust.

Major geochemical neoanomalies with Mn concentrations above 6,402 ppm occur over slag/sand-blast wastes, pyrite tailings and pyritiferous sand from east of Ayia Paraskevi to Nichtochori, Komobil, Phenikodassos, Kiprianos and Kavodokanos, and Fougara. About this extensive neoanomaly there is a neohalo down to 3,475 ppm Mn. The strongest anthropogenic neoanomalies >10,481 to 35,679 ppm Mn occur over slag/sand-blast in the smelter area at Kiprianos, at Kavodokanos and the pyritiferous sand at Komobil (Map 6.18). Over the flotation residues Mn levels vary from 1,563 to 6,402 ppm.

At Fougara and Ayia Paraskevi, apart from the relationship with metallurgical processing wastes, there is also a correlation between overburden and rock geochemical patterns. Hence, in these areas it is difficult to evaluate the contribution of rock and metallurgical wastes to the anomalous patterns in overburden.

Elevated overburden Mn concentrations from Panormos-Vilanoira to Neapoli-Noria and to the west of Prasini Alepou may be ascribed to the underlying schist, locally to prasinite and altered marble (refer to Map 2.2). Low overburden Mn concentrations from Perdika to Panormos, Koukos, Neapoli, Ayios Andreas and Ayia Paraskevi are explained by the underlying marble. Overburden Mn has, therefore, both anthropogenic and geogenic affinities, with the former having a greater contribution in overburden geochemical patterns.

Mobility of Mn is generally very low under oxidising, low under acid, neutral to alkaline and reducing conditions (Reimann *et al.*, 1998), except in the acid, reducing environment of organic swamps and bogs where Mn can move very readily (Rose *et al.*, 1979). Levinson (1980) and Hoffman (1986), on the basis of the pH of hydrolysis, state that the mobility of Mn is high under acid to neutral conditions, and high to very low in

alkaline conditions. The pH of hydrolysis of Mn^{2+} in dilute solutions varies from 8.5 to 8.8; meaning that $Mn(OH)_2$ precipitates in an alkaline environment (Table 6.1). Manganese should, therefore, be geochemically mobile in most areas, since soil pH for about 99% of the surface area of Lavrion is below 8.5 (Map 2.5). In the Lavrion urban area Mn should be very mobile in pyritiferous materials with pH<5.50, as for example, in the areas between Kiprianos and Kavodokanos, and Komobil and Nichtochori.

Manganese is an essential element for plants and animals (Gough *et al.*, 1979; Mervyn, 1980, 1985, 1986; Reimann *et al.*, 1998). However, at high soil Mn concentrations (>3,000 ppm), there are reports of phytotoxicity problems (Gough *et al.*, 1979; Kabata-Pendias and Pendias, 1984). Consequently, about 31% of the Lavrion urban area soil is considered to be unfit for plant growth.

6.2.17. DISTRIBUTION OF TOTAL MOLYBDENUM (Mo) IN OVERBURDEN (Map 6.19, Fig. 6.17)

Molybdenum in overburden samples varies from 1.7 to 108.9 ppm, with a mean of 6.94 ppm (s=±10.63 ppm; C=153.17%), and a median of 4.9 ppm (n=224). In comparison, Mo in normal global soil, away from mineralised areas, has an average of 2.5 ppm (Levinson, 1980) and a median of 1.2 ppm (Reimann *et al.*, 1998). In Lavrion, the global average and median values are exceeded due to contamination from metallurgical activities.

Molybdenum concentrations in rocks of the Lavrion urban area vary from <0.5 to 11 ppm, with a mean of 0.83 ppm (s=±1.16 ppm; C=139.76%) and a median of 0.5 ppm (n=155; note this is a recent compilation of additional data, hence the difference with the values quoted on Map 6.19) (Table 4.19A in Appendix 2A of Volume 1A, p.37).

Molybdenum levels in metallurgical wastes vary from <1.00 to 111.08 ppm with a mean of 9.25 ppm (s=±19.01 ppm; C=205.51%) and a median of 3.57 ppm (n=62) (refer to Map 5.19; Fig. 6.17). It is quite apparent that Mo contamination of overburden is directly related to the metallurgical processing wastes.

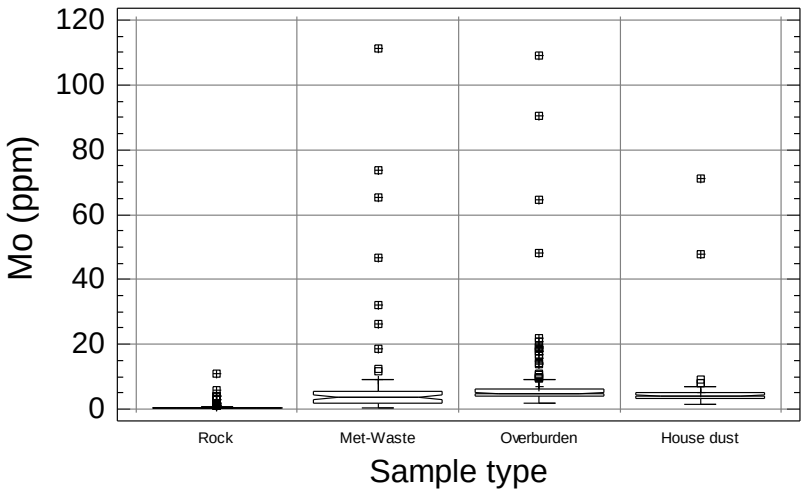

Fig. 6.17. Multiple notched box-and-whisker plots comparing molybdenum (Mo) distribution in different sample types.
Σχ. 6.17. Πολλαπλό θηκόγραμμα με εγκοπές που συγκρίνει την κατανομή του μολυβδαινίου (Mo) σε διαφορετικούς τύπους δειγμάτων.

House dust Mo varies from 1.57 to 70.97 ppm with a mean of 5.12 ppm (s=±7.18 ppm; C=140.23%) and a median of 4.10 ppm (n=127).

The Mo contamination index in overburden, with respect to its median in parent rocks, varies from 3.4 to 217.8, and in house dust from 3.14 to 141.94.

It is apparent from the statistical distribution of Mo in different sample types, that elevated Mo contents in overburden are principally due to contamination from metallurgical processing wastes (Fig. 6.17). Both sample types, metallurgical wastes and overburden, are the sources of Mo in house dust.

Major geochemical neoanomalies, with Mo concentrations above 9.4 ppm have a NE-SW trend, and occur over pelletised slag/sand-blast material and pyrite tailings within the smelter area at Kiprianos and Kavodokanos. The strongest geochemical neoanomaly with Mo levels >16.7 to 108.9 ppm, occurs again within the premises of the smelter at Kiprianos, and extends to Kavodokanos over pelletised slag/sand-blast material (see also Map 5.19). Distinct neohaloes extend about the geochemical neoanomalies down to 6.1 ppm Mo, although even lower levels, to 4.9 ppm Mo, may be attributed to aerial dispersion from metallurgical wastes. Over the flotation residues from Noria to Prasini Alepou and Santorineika, pyrite tailings at Nichtochori, and pyritiferous sand from Komobil and Kiprianos, there are Mo levels between >4.0 to 9.4 ppm.

Mobility of Mo is high in oxidising, alkaline environments, but low in acidic and reducing environments, and moderate in neutral (Levinson, 1980; Hoffman, 1986) (Table 6.2). Reimann *et al.* (1998) postulate, on the other hand, a high mobility under oxidising and acid, very high under neutral to alkaline conditions, and very low under reducing conditions. Mobility in the secondary environment is restricted, however, by presence of Pb, Fe, Ca, carbonates and sulphides, and adsorption on clay minerals (Levinson, 1980; Reimann *et al.*, 1998). It appears, therefore, that mobility of Mo is independent of pH variations in the natural environment (Rose *et al.*, 1979). Because of the restrictions on mobility posed by geochemical barriers, which exist in the Lavrion overburden, mobility of Mo should be moderate to low.

Molybdenum is an essential trace element for plants and animals, but considered to be toxic at high concentrations (Gough *et al.*, 1979; Reimann *et al.*, 1998). Phytotoxic levels, according to different researchers, vary from 2 to 10 ppm Mo (Kabata-Pendias and Pendias, 1984). Taking the maximum permissible level of 10 ppm Mo, about 8% of the soil cover of Lavrion is considered to be unfit for plant growth (Map 6.19).

The recommended statutory limits of Mo for residential soil, quoted in scientific literature, vary from 5 to 200 ppm (Table 6.3), *i.e.*,

- 5 ppm Mo in Finland (Koljonen, 1992), Federal Canada and State of Ontario (Sheppard et al., 1992), and
- 200 ppm Mo in The Netherlands (VROM, 1983; Lux, 1993; Van den Berg *et al.*, 1993; J. Ebbing, person. commun., 1996); this is also the intervention value in Finland (R. Salminen, person. commun., 1996).

The 200 ppm Mo limit is indeed very high, when normal global soil has an average of 2.5 ppm and a median of 1.2 ppm Mo. If the Finnish Mo guide soil value is used, then about 45% of the soil cover in Lavrion may be potentially hazardous to human health.

6.2.18. DISTRIBUTION OF TOTAL NICKEL (Ni) IN OVERBURDEN (Map 6.20, Fig. 6.18)

Nickel in overburden samples varies from 40 to 591 ppm, with a mean of 141.4 ppm (s=±71.0 ppm; C=50.21%), and a median of 127 ppm (n=224). In comparison, Ni in normal soil, away from areas of base metal mineralisation and mafic-ultramafic rocks, has an average of 30 ppm (Levinson, 1980), and a median of also 20 ppm (Reimann *et al.*, 1998). In Lavrion, the normal global soil average and median values are greatly exceeded due to (a) mineralisation in certain parts of Lavrion (Map 4.10), (b) mafic rocks (prasinite) (Map 2.2) and (c) contamination from metallurgical activities (Map 5.10). It appears that overburden Ni, like Co, has both geogenic and anthropogenic affinities (Fig. 6.18; Maps 4.20, 5.20, 6.20).

Nickel concentrations in rocks of the Lavrion urban area vary from <1.0 to 1,600 ppm, with a mean of 168.3 ppm (s=±252.2 ppm; C=149.85%) and a median of 54.5 ppm (n=140) (Map 4.20).

Nickel levels in metallurgical wastes vary from 5.47 to 205.22 ppm with a mean of 51.36 ppm (s=±40.36 ppm; C=78.58%) and a median of 38.52 ppm (n=62) (refer to Map 5.20).

House dust Ni varies from 27.33 to 1,243 ppm with a mean of 107.7 ppm (s=±135.2 ppm; C=125.53%) and a median of 84.07 ppm (n=127).

The Ni depletion/enrichment/"contamination" index in overburden, with respect to its median in parent rocks, varies from 0.73 to 10.84, and in house dust from 0.50 to 22.80.

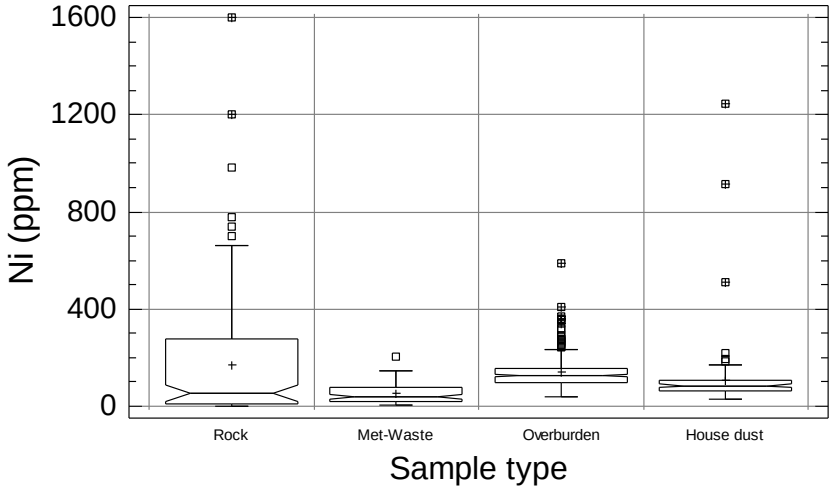

Fig. 6.18. Multiple notched-box-and-whisker plots comparing nickel (Ni) distribution in different sample types.
Σχ. 6.18. Πολλαπλό θηκόγραμμα με εγκοπές που συγκρίνει την κατανομή του νικελίου (Ni) σε διαφορετικούς τύπους δειγμάτων.

The very high level of Ni contamination of house dust, compared to overburden, suggests that there are other sources in the home environment or Ni is enhanced in the finer grained dust.

It is apparent from the statistical distribution of Ni in different sample types, that elevated Ni contents in overburden are principally due to parent rocks, with a minor contribution from metallurgical processing wastes (Fig. 6.18). Both sample types, metallurgical wastes and overburden, are the sources of Ni in house dust, although the outlying values suggest that other factors come into play in the home environment.

Comparison of Ni distribution in parent rocks and overburden shows that there is good correlation between the primary dispersion of Ni>54.5 ppm and its secondary >127 ppm Ni (Maps 4.20 & 6.20). Differences occur in areas where Ni levels are higher in overburden. The major geochemical Ni anomaly in overburden, extending from Noria to Vilanoira-Panormos (>230 to 591 ppm Ni), is ascribed to the occurrence of schist, prasinite and marble alteration (Map 2.2), and development of soil enriched in clay, which has the property to adsorb trace elements (refer to the distribution of Ni & K, Maps 6.2 & 6.15). The secondary halo extending down to 127 ppm Ni from Noria to Koukos and Fougara, and its northerly extension from Noria to Prasini Alepou and west of Kiprianos-Kavodokanos, are also related to schist, prasinite and marble alteration. Geogenic and anthropogenic dispersion patterns apparently join in the area to the west of Kiprianos and Phenikodassos, because the streams transport weathered materials from outcrops of schist, prasinite and altered marble (Maps 2.2, 4.20 & 6.20).

Geochemical neoanomalies with Ni concentrations >156 to 230 ppm, occur over pyritiferous sand and pyrite tailings at Phenikodassos-Komobil, and slag/sand-blast material within the smelter area at Kiprianos and Fougara. Distinct Ni neohaloes, which merge with secondary geogenic haloes, extend about the geochemical neoanomalies down to 127 ppm Ni; lower levels are difficult to attribute solely to the metallurgical wastes (Map 5.10), because of a major contribution from geogenic sources (Map 4.10).

Mobility of Ni is generally medium under oxidising, high under acid, very low under neutral to alkaline and reducing conditions (Levinson, 1980; Hoffman, 1986; Reimann *et al.*, 1998) (Table 6.2). The pH of hydrolysis of Ni^{2+} in dilute solutions is 6.7, meaning that $Ni(OH)_2$ precipitates in neutral environments and Ni becomes relatively immobile (Table 6.1). Nickel should, therefore, be geochemically immobile in most areas, since soil pH for 97.5% of the surface area of Lavrion is above 6.87 due to the predominance of marble (Map 2.5). In the Lavrion urban area Ni may be, however, comparatively mobile in pyritiferous materials with pH<5.00, as for example, in the areas between Kiprianos and Kavodokanos, and Komobil and Nichtochori.

Nickel is essential for some plants and animals (Gough *et al.*, 1979; Reimann *et al.*, 1998). Toxicity of Ni to humans is generally low (Mervyn, 1985, 1986).

According to Kabata-Pendias and Pendias (1984), the maximum permissible level of Ni in soil for healthy plant growth is 100 ppm. Values above this limit are considered to be phytotoxic. Consequently, about 75% of the soil cover in Lavrion, under this premise, is unfit for plant growth (Map 6.20).

The recommended residential soil Ni statutory limits quoted in scientific literature vary from 30 to 1400 ppm, *i.e.*,

- 30 ppm in Denmark (Edelgaard and Dahlstrøm, 1999);
- 35 ppm in The Netherlands (VROM, 1983; Lux, 1993; Van den Berg *et al.*, 1993; J. Ebbing, person. commun., 1996);
- 50 ppm in Germany (Kloke, 1977; Lux, 1993);
- 70 ppm in the United Kingdom (ICRCL, 1987);
- 100 ppm in Finland (Koljonen, 1992);
- 150 ppm in Federal Canada (Sheppard *et al.*, 1992);
- 200 ppm in the State of Ontario (Sheppard *et al.*, 1992), and
- 1400 ppm in the State of Connecticut (US CT, 1997).

Apart from the limit values, there is also an intervention value, which in The Netherlands is set at 210 ppm Ni (Table 6.3). This variation of technocratic statutory limits again shows the necessity of setting up internationally agreed limits, based on pragmatic geochemical and medical principles. Taking into consideration the normal global soil mean and median values, the Lavrion rock median, and the phytotoxic level, the 150 ppm Ni trigger value set by Federal Canada seems to be reasonable. Under this premise, about 28% of the Lavrion soil cover may be potentially hazardous to human health (Map 6.20).

6.2.19. DISTRIBUTION OF TOTAL PHOSPHORUS (P) IN OVERBURDEN (Map 6.21, Fig. 6.19)

Phosphorus in overburden samples varies from 198 to 5,433 ppm, with a mean of 1356.5 ppm (s=±1016.3 ppm; C=74.92%), and a median of 992 ppm (n=224). Phosphorus in normal global soil has a median value of 300 ppm (Rose *et al.*, 1979), and in the <2-mm soil fraction a median of 750 ppm (Reimann *et al.*, 1998). Hence, in comparison to normal soil, the Lavrion overburden/soil is enriched in phosphorus (Table 4.14a, Fig. 4.14a, Map 4.21).

Phosphorus concentrations in rocks of the Lavrion urban area vary from 44 to 8,510 ppm, with a mean of 2,381 ppm (s=±1,904 ppm; C=79.97%) and a median of 1,855 ppm (n=140) (Map 4.21).

Phosphorus levels in metallurgical wastes vary from 5 to 2,117 ppm with a mean of 1,011 ppm (s=±515.13 ppm; C=50.95%) and a median of 1,103 ppm (n=62) (refer to Map 5.21).

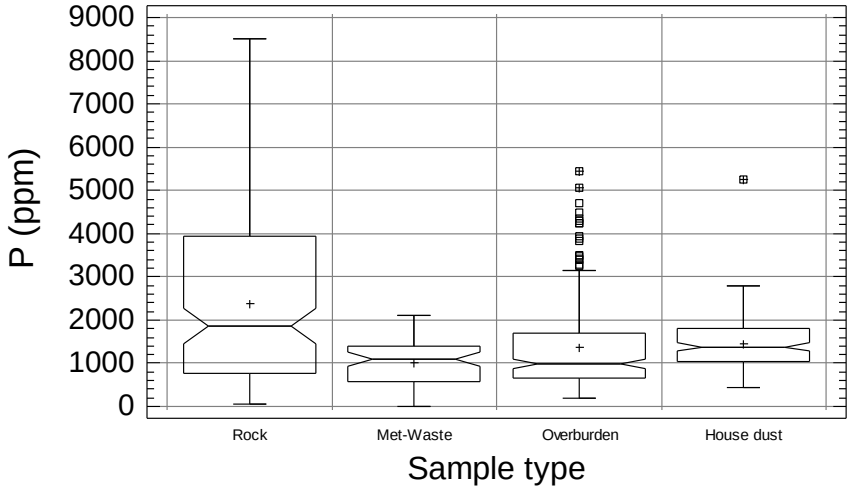

Fig. 6.19. Multiple notched-box-and-whisker plots comparing phosphorus (P) distribution in different sample types.
Σχ. 6.19. Πολλαπλό θηκόγραμμα με εγκοπές που συγκρίνει την κατανομή του φωσφόρου (P) σε διαφορετικούς τύπους δειγμάτων.

House dust P varies from 435 to 5,252 ppm with a mean of 1,439 ppm (s=±624.23 ppm; C=43.38%) and a median of 1,380 ppm (n=127).

The P depletion/enrichment index in overburden, with respect to its median in parent rocks, varies from 0.11 to 2.93, and in house dust from 0.23 to 2.83.

It is apparent from the statistical distribution of P in different sample types, that elevated P contents in overburden should be mainly due to parent rocks, with a minor contribution from metallurgical processing wastes (Fig. 6.19). The outlying values, however, suggest the possibility of other factors contributing to the high P levels in overburden. Both sample types, metallurgical wastes and overburden, should be the sources of P in house dust.

Major geochemical "anomalous" patterns, with P concentrations above 992 ppm occur in the central part of the study area from Thorikon, in the north, to Koukos, in the south, and from Ayios Andreas to Ayia Paraskevi, the predominantly residential area. The secondary halo extends down to 546 ppm phosphorus. There does not appear to be a distinct relationship between geochemical distribution patterns of P in overburden and parent rocks (Map 4.21). There is also no apparent relationship with metallurgical processing wastes. Nevertheless, the pattern from Fougara to Koukos, Ayios Andreas and Ayia Paraskevi is closely related to schist and the contact zone between schist and marble. Hence, this anomalous pattern may be partly ascribed to lithology. The northerly extension, however, from Ayios Andreas to Thorikon is difficult to explain.

The extensive "anomalous" P pattern is closely associated with the predominantly residential area of Lavrion. Apart from vegetable gardens, local inhabitants have small flower gardens (refer to land use map, Map 2.4, Volume 2). Phosphate fertilisers are commonly used in all cultivation activities. A possible explanation is, therefore, suggested for this peculiar P pattern in overburden, which is not strongly related to either lithology or metallurgical processing wastes.

Phosphorus is an essential element for all organisms and plants (Fairbridge, 1972; Mervyn, 1985, 1986; Reimann *et al.*, 1998). It is toxic at high doses, *i.e.*, 60-100 mg are lethal to humans (Reimann *et al.*, 1998).

6.2.20. DISTRIBUTION OF TOTAL LEAD (Pb) IN OVERBURDEN (see Chapter 3, Section 3.5, p.68)

6.2.21. DISTRIBUTION OF TOTAL ANTIMONY (Sb) IN OVERBURDEN (Map 6.24, Fig. 6.20)

Antimony in overburden samples varies from <6.76 to 567 ppm, with a mean of 152.1 ppm (s=±125 ppm; C=82.18%), and a median of 121 ppm (n=90). Antimony in normal global soil has a mean of 5 ppm (Levinson *et al.*, 1979) and a median of 0.5 ppm in the <2-mm fraction (Reimann *et al.*, 1998). In Lavrion, the average and median values of the normal global soil are greatly exceeded due to contamination from metallurgical activities (Map 5.24, Fig. 5.24).

Antimony concentrations in rocks of the Lavrion urban area vary from <5.0 to 71.04 ppm, with a mean of 6.94 ppm (s=±12.05 ppm; C=173.63%) and a median of 2.5 ppm (n=48) (Table 4.19A in Appendix 2A of Volume 1A, p.37).

Antimony levels in metallurgical wastes vary from 183.3 to 851 ppm with a mean of 229.5 ppm (s=±183.3 ppm; C=79.87%) and a median of 189 ppm (n=62) (refer to Map 5.24).

The Sb contamination index in overburden, with respect to its median in parent rocks, varies from 1.0 to 226.8.

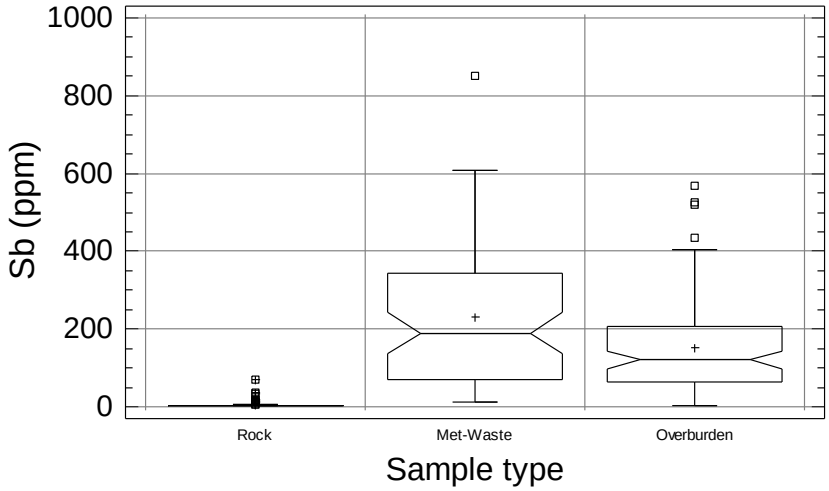

Fig. 6.20. Multiple notched-box-and-whisker plots comparing antimony (Sb) distribution in different sample types.
Σχ. 6.20. Πολλαπλό θηκόγραμμα με εγκοπές που συγκρίνει την κατανομή του αντιμονίου (Sb) σε διαφορετικούς τύπους δειγμάτων.

It is quite apparent from the statistical distribution of Sb in different sample types, that elevated Sb contents in overburden are mainly due to the metallurgical processing wastes (Fig. 6.20).

Major geochemical neoanomalies, with Sb concentrations above 121 ppm have NE-SW and NW-SE trends, and occur over, and in the immediate neighbourhood, of flotation residues (Noria-Prasini Alepou-Santorineika), pyritiferous wastes (Komobil, Nichtochori), and slag/sand-blast material (within the smelter area at Kiprianos and Kavodokanos). The strongest geochemical neoanomalies >206 to 567 ppm Sb occur over flotation residues between Prasini Alepou and Santorineika and at Kavodokanos. Distinct neohaloes extend about geochemical neoanomalies down to 63 ppm Sb, although even lower levels, to 28 ppm Sb, may be attributed to aerial dispersion from metallurgical wastes.

Mobility of Sb is generally low under oxidising, acid and neutral to alkaline conditions, and very low under reducing conditions (Levinson, 1980; Hoffman, 1986; Reimann *et al.*, 1998) (Table 6.2).

Antimony is a nonessential element for plants and animals (Gough *et al.*, 1979; Reimann *et al.*, 1998). At high concentrations Sb is more toxic than As or Pb (Reimann *et al.*, 1998). In Lavrion, Sb levels in overburden are abnormally high, and may present problems to biota in general. Toxicity, as in all cases, depends on the concentration of soluble, not total, Sb in soil. According, however, to Kabata-Pendias and Pendias (1984), total Sb levels above 10 ppm in soil are considered to be phytotoxic. Consequently, 95% of the soil cover of Lavrion, under this premise, is unfit for plant growth (Map 6.24).

The recommended residential soil Sb statutory limits, quoted in scientific literature, vary from 27 to 40 ppm (Table 6.3), *i.e.*,

- 27 ppm in the State of Connecticut (US CT, 1994, 1997), and
- 40 ppm in Finland (Koljonen, 1992).

Since, Sb is more hazardous than As, its legislative limit should be lower, or at worse, equal. In any case, whichever, of the existing statutory values, is used, the fact remains that a large part of the Lavrion overburden is potentially hazardous to human health with respect to Sb, *i.e.*, approximately 90% has concentrations >27 ppm, and 80% >40 ppm.

6.2.22. DISTRIBUTION OF TOTAL STRONTIUM (Sr) IN OVERBURDEN (Map 6.26, Fig. 6.21)

Strontium in overburden samples varies from 17 to 496 ppm, with a mean of 127.2 ppm (s=±58.8 ppm; C=46.23%), and a median of 118 ppm (n=224). Strontium in normal global soil has a median value of 67 ppm (Rose *et al.*, 1979), and in the <2-mm soil fraction a median of 240 ppm (Reimann *et al.*, 1998). Hence, in comparison to normal global soil, the Lavrion overburden/soil is enriched in strontium (Table 4.15a, Fig. 4.15a, Map 4.26).

Strontium concentrations in rocks of the Lavrion urban area vary from <1 to 800 ppm, with a mean of 121 ppm (s=±129 ppm; C=106.61%) and a median of 98 ppm (n=140) (Map 4.26).

Strontium levels in metallurgical wastes vary from 150.8 to 798.6 ppm with a mean of 210.6 ppm (s=±150.8 ppm; C=71.61%) and a median of 178.69 ppm (n=62) (refer to Map 5.26).

House dust Sr varies from 71.2 to 582.8 ppm with a mean of 134.9 ppm (s=±71.2 ppm; C=52.78%) and a median of 119.9 ppm (n=127).

The Sr depletion/enrichment/contamination index in overburden, with respect to its median in parent rocks, varies from 0.17 to 5.06, and in house dust from 0.73 to 5.95.

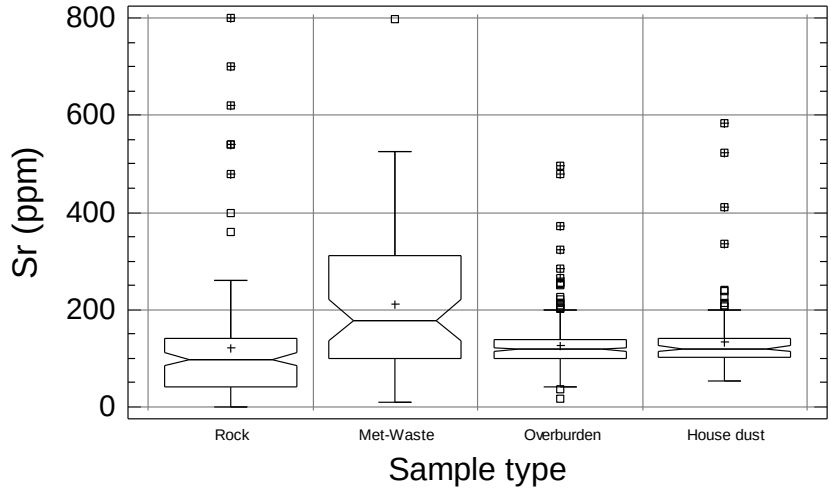

Fig. 6.21. Multiple notched-box-and-whisker plots comparing strontium (Sr) distribution in different sample types.
Σχ. 6.21. Πολλαπλό θηκόγραμμα με εγκοπές που συγκρίνει την κατανομή του στροντίου (Sr) σε διαφορετικούς τύπους δειγμάτων.

It is apparent from the statistical distribution of Sr in different sample types, that elevated Sr contents in overburden are due to both the Lavrion parent rocks and metallurgical processing wastes (Fig. 6.21). Although both, overburden and metallurgical processing wastes, must contribute to house dust Sr, the correspondence of the median values at the 95th confidence level between overburden and house dust, suggests that the contribution from overburden is greater.

Major north-easterly trending geochemical “anomalous” patterns, with Sr concentrations above 140 ppm occur

(a) from Prasini Alepou to Kiprianos and Kavodokanos over altered marble and about its contact with schist and fluvial sediments (Prasini Alepou), and the metallurgical processing wastes (Kiprianos and Kavodokanos slag) (Map 5.26, Table 5.26),
(b) from Ayios Andreas to Ayia Paraskevi and Nichtochori over Quaternary to Recent fluvial deposits, and
(c) to the west of Thorikon, over areas covered with marble and Quaternary to Recent fluvial deposits (Maps 2.2, 4.26), and

A geochemical pattern, with Sr levels >118 to 191 ppm extends, from Koukos-Neapoli-Ayios Andreas to the Lavrion harbour, over areas covered by Quaternary to Recent fluvial deposits.

The strongest geochemical anomalies with Sr >220 to 496 ppm occur

(i) near the marble/schist contact, and the valley with alluvial sediments (Prasini Alepou), and
(ii) over metallurgical processing wastes in the smelter area at Kiprianos and Kavodokanos.

Hence, normal Sr geochemical anomalies, due to lithology, apparently unite with anthropogenic neoanomalies.

Mobility of Sr is generally high under all conditions (Reimann *et al.*, 1998).

Strontium is considered to be a nonessential element for most organisms (Reimann *et al.*, 1998).

6.2.23. DISTRIBUTION OF TOTAL TITANIUM (Ti) IN OVERBURDEN (Map 6.27, Fig. 6.22)

Titanium in overburden samples varies from 584 to 5,297 ppm, with a mean of 2,249 ppm (s=±812 ppm; C=36.10%), and a median of 2,162 ppm (n=224). Normal global soil has a median value of 4,000 ppm Ti in the <2-mm fraction (Reimann *et al.*, 1998). Hence, the Lavrion overburden/soil appears to be depleted with respect to titanium.

Titanium concentrations in rocks of the Lavrion urban area vary from <120 to 7,014 ppm, with a mean of 920 ppm (s=±1,401 ppm; C=152.28%) and a median of 300 ppm (n=140) (Map 4.27).

Titanium levels in metallurgical wastes vary from 40 to 2,031 ppm with a mean of 799.8 ppm (s=±682.5 ppm; C=85.33%) and a median of 737.7 ppm (n=62) (refer to Map 5.27).

House dust Ti varies from 790.6 to 4,686 ppm with a mean of 1,636 ppm (s=±647.9 ppm; C=39.60%) and a median of 1,494 ppm (n=127).

The Ti enrichment index in overburden, with respect to its median in parent rocks, varies from 1.95 to 17.7, and in house dust from 2.6 to 15.6.

It is apparent from the statistical distribution of Ti in different sample types, that elevated Ti contents in overburden are due to both the Lavrion parent rocks and

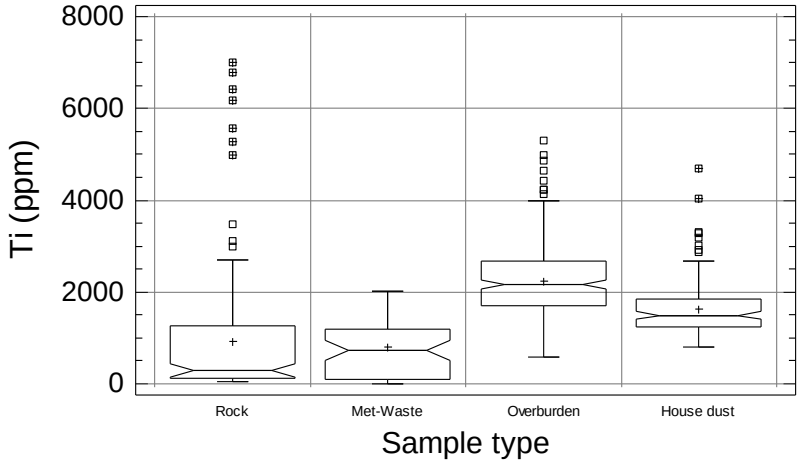

Fig. 6.22. Multiple notched-box-and-whisker plots comparing titanium (Ti) distribution in different sample types.
Σχ. 6.22. Πολλαπλό θηκόγραμμα με εγκοπές που συγκρίνει την κατανομή του τιτανίου (Ti) σε διαφορετικούς τύπους δειγμάτων.

metallurgical processing wastes (Fig. 6.20); the former having a greater contribution. Higher Ti levels in overburden suggest an enrichment. Although both, overburden and metallurgical processing wastes, must contribute to house dust Sr, the former appear to play a more significant part.

Major geochemical "anomalies", with Ti concentrations above 3,281 ppm occur at Vilanoira-Panormos, Fougara, to the west of Kiprianos-Kavodokanos and Thorikon. The strongest geochemical anomalies >3,728 to 5,297 ppm Ti occur from Vilanoira to Panormos in the south, and to the west of Kiprianos in the north. Apart from the north-westerly trend of secondary geochemical anomalies, which is also the major orientation of lithogeochemical spatial structures, there does not appear to be a clear similarity between overburden and rock geochemical patterns. Nevertheless, the anomalous pattern at Noria (>2672 ppm Ti) envelops the flotation residues indicating a possible geogenic relationship. There is also no apparent relationship with metallurgical processing wastes in general, for Ti is not an element of mineralisation. But, the Fougara, Panormos, Neapoli and Ayia Paraskevi slag heaps have elevated Ti concentrations (Map 5.27), varying between 1168-2013 ppm suggesting, therefore, that there may be a relationship. This possibility is strengthened by the low Ti values over the Kavodokanos slag/sand-blast material heaps, which have low Ti levels (<1200 ppm Ti).

Titanium commonly occurs in femic minerals and is, therefore, enriched in schist and prasinite (Table 4.16A in Appendix 2A of Volume 1A, p.34). Marble does not normally have femic minerals, and is expected to have low Ti contents. However, the Lavrion marble, because of alteration and schist intercalations, has above normal Ti levels (Table 4.16A). Clay-rich soils, and consequently, elevated Ti concentrations, occur

- over areas with schist and prasinite, and where marble has schist intercalations, *e.g.*, Nichtochori, Neapoli-Noria, Prasini Alepou, west of Kavodokanos and Kiprianos (refer to lithological map, Map 2.2).
- in valleys, where there is deposition of alluvium, which is rich in clay, *e.g.*, the anomalies at Panormos, Vilanoira, Perdika, Santorineika-Phenikodassos, Thorikon, and

- at the base of slopes, where again there is an enrichment in clay, *e.g.*, Perdika, Noria.

It is quite clear, therefore, that elevated Ti, like Al, concentrations occur in areas with an enrichment of clay in overburden. Clay-rich areas suggest that they may have a high scavenging capability.

Anomalous Ti concentrations, since they occur in areas enriched in clay, may be ascribed, therefore, to mainly geogenic sources of the secondary environment. The Panormos-Fougara and Ayia Paraskevi patterns, however, are explained by the release of Ti from the weathering of slag.

Mobility of Ti is very low under most conditions (Reimann *et al.*, 1998).

Titanium is considered as a nonessential element for plants and animals (Reimann *et al.*, 1998).

6.2.24. DISTRIBUTION OF TOTAL VANADIUM (V) IN OVERBURDEN (Map 6.29, Fig. 6.23)

Vanadium in overburden samples varies from 26 to 325 ppm, with a mean of 86.1 ppm (s=±39.3 ppm; C=45.64%), and a median of 75 ppm (n=224). Normal global soil has an average of 80 ppm V (Levinson, 1980), a median value of 57 ppm (Rose *et al.*, 1979), and a median of 90 ppm in the <2 mm fraction (Reimann *et al.*, 1998). Hence, Lavrion overburden/soil appears to be close to the global average soil with respect to its V content.

Vanadium concentrations in rocks of the Lavrion urban area vary from <1 to 71 ppm, with a mean of 13.1 ppm (s=±13 ppm; C=99.24%) and a median of 9 ppm (n=140) (Map 4.29 in Volume 2; Table 4.17A in Appendix 2A of Volume 1A, p.35).

Vanadium levels in metallurgical wastes vary from <2.0 to 104.24 ppm with a mean of 44.42 ppm (s=±23.83 ppm; C=53.65%) and a median of 46.3 ppm (n=62) (refer to Map 5.29).

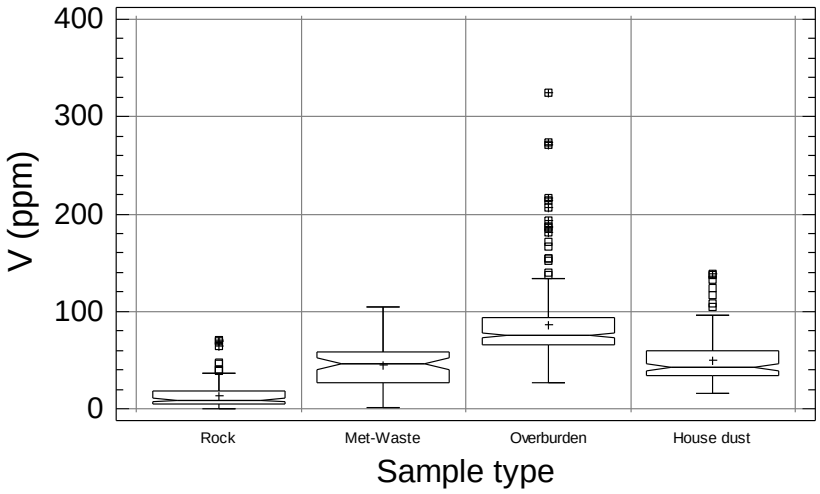

Fig. 6.23. Multiple notched-box-and-whisker plots comparing vanadium (V) distribution in different sample types.
Σχ. 6.23. Πολλαπλό θηκόγραμμα με εγκοπές που συγκρίνει την κατανομή του βαναδίου (V) σε διαφορετικούς τύπους δειγμάτων.

House dust V varies from 15.35 to 139.15 ppm with a mean of 49.95 (s=±25.3 ppm; C=50.65%) and a median of 42.48 ppm (n=127).

The V enrichment/contamination index in overburden, with respect to its median in parent rocks, varies from 2.9 to 36.1, and in house dust from 1.7 to 15.5.

It is apparent from the statistical distribution of V in different sample types, that elevated V contents in overburden are due to both the Lavrion parent rocks and metallurgical processing wastes (Fig. 6.23); the latter having a greater contribution. The higher V levels in overburden suggest an enrichment. Although both, overburden and metallurgical processing wastes, must contribute to house dust V, the former appears to play a more significant part.

Major geochemical “anomalies” patterns, with V concentrations above 93 ppm occur along the coastal section from Ayia Paraskevi to Nichtochori, Komobil, Phenikodassos and Kiprianos, at Vilanoira-Panormos, Fougara and Noria, to the west of Kiprianos-Kavodokanos and Thorikon. The strongest geochemical anomalies >166 to 325 ppm V occur along the coastal section from Ayia Paraskevi, Nichtochori, Komobil and Phenikodassos. Secondary geochemical anomalous patterns are related to both geogenic and anthropogenic sources, which are intermixed in some parts of Lavrion.

The secondary anomalies at Noria (>63 ppm V), to the east of Neapoli, and to the west of Kiprianos-Kavodokanos are related to rock geochemical patterns (Map 4.29). The pattern along the coast from Ayia Paraskevi to Kiprianos is ascribed to metallurgical wastes (slag, slag earth, pyrite tailings and pyritiferous sand), which have elevated V contents (>50 to 85 ppm V); whereas the pattern from Panormos to Fougara is associated with slag/slag earth (Map 5.29). In the smelter area at Kiprianos patterns >63 to 125 ppm V are related to slag/pelletised slag/sand-blast wastes, and at Kavodokanos to pelletised slag/sand-blast wastes.

Chemical differences, in the level of V between the slag heaps about Fougara, the coastal section of Ayia Paraskevi and Komobil to Kiprianos, and pyrite tailings/pyritiferous sand from Nichtochori to Kiprianos, and those at Kavodokanos, are well shown in the secondary geochemical patterns in overburden, *e.g.*, the Kavodokanos slag and pyrite tailings have comparatively low V contents (Maps 5.29 & 6.29).

Vanadium is commonly enriched in gabbro/basalt and shale/schist, but not marble and sandstone. Prasinite and schist in Lavrion, although they have elevated V values compared to marble, are generally depleted in V when compared to global averages (Table 4.17A in Appendix 2A of Volume 1A, p.35). Extensive secondary anomalous geogenic patterns of V, like Al and Ti, are generally associated with clay-rich residual and alluvial soil, as shown by the patterns (a) from Noria to Vilanoira and Panormos, (b) west of Phenikodassos, (c) to the north-west of Kavodokanos, and (d) Thorikon.

Mobility of V is high under oxidising and acid to neutral conditions, very high under alkaline, and very low under reducing conditions (Levinson, 1980; Hoffman, 1986; Reimann *et al.*, 1998) (Table 6.2).

Vanadium is reckoned to be nonessential for higher plants and the majority of higher animals, although reported to be beneficial for some (Gough *et al.*, 1979; Reimann *et al.*, 1998). It is toxic, and levels above 100 ppm are phytotoxic (Kabata-

Pendias and Pendias, 1984). Therefore, under this premise, approximately 19% of the Lavrion urban soil is considered to be unfit for plant growth.

The only statutory limits, quoted in scientific literature, for soil in residential areas come from Finland (Koljonen, 1992) and the State of Connecticut (US CT, 1994, 1997), and are 50 ppm and 470 ppm V. The latter limit is considered too high, when V is considered to be a nonessential element, and normal global soil has an average and a median of 90 ppm and 57 ppm respectively. The Finnish statutory level seems reasonable. Hence, if it is used in the Lavrion case, about 95% of the Lavrion overburden/soil may be potentially hazardous to human health.

6.2.25. DISTRIBUTION OF TOTAL ZINC (Zn) IN OVERBURDEN (Map 6.30, Fig. 6.24)

Zinc in overburden samples varies from 591 to 76,310 ppm, with a mean of 10,872 ppm (s=±12,636 ppm; C=116.2%), and a median of 6,668 ppm (n=224). In comparison, Zn in global normal soil, away from mineralised areas, has an average of 50 ppm (Levinson, 1980), a median of 36 ppm (Rose *et al.*, 1979), and in the <2 mm fraction a median of 70 ppm (Reimann *et al.*, 1998). In Lavrion, these levels are greatly exceeded due to (a) mineralisation in certain parts of Lavrion (Map 4.30), and (b) contamination from metallurgical activities, which is the major contributor (Map 5.30).

Zinc concentrations in rocks of the Lavrion urban area vary from <6 to 5,200 ppm, with a mean of 210.6 ppm (s=±599.6 ppm; C=284.7%) and a median of 57 ppm (n=140) (Map 4.30, Fig. 6.24).

Zinc levels in metallurgical wastes vary from 1,500 to 98,000 ppm with a mean of 41,194 ppm (s=±25,332 ppm; C=61.5%) and a median of 39,800 ppm (n=62) (refer to Map 5.30).

House dust Zn varies from 511.5 to 35,602 ppm with a mean of 4,623 (s=±4,859 ppm; C=105.1%) and a median of 3,044 ppm (n=127).

The Zn contamination index in overburden, with respect to its median in parent rocks, varies from 10.4 to 1,338.8, and in house dust from 9.0 to 624.6. It is quite clear

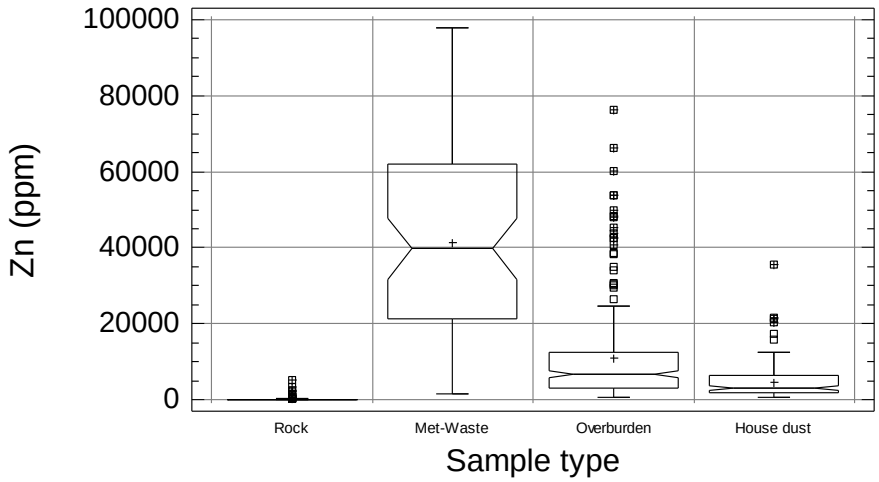

Fig. 6.24. Multiple notched-box-and-whisker plots comparing zinc (Zn) distribution in different sample types.
Σχ. 6.24. Πολλαπλό θηκόγραμμα με εγκοπές που συγκρίνει την κατανομή του ψευδαργύρου (Zn) σε διαφορετικούς τύπους δειγμάτων.

from the statistical distribution of Zn that metallurgical processing wastes are the major source of contamination of overburden (Maps 5.30, 6.30, Fig. 6.24). Although both, overburden and metallurgical processing wastes, must contribute to house dust Zn, the former appears to play a more significant part.

Primary geochemical patterns of Zn are almost completely masked from the contamination of overburden by the metallurgical processing activities. The only exceptions are the geochemical anomalies to the east of Nichtochori and Ayia Paraskevi (Maps 4.30, 6.30), although the latter is more extensive due to Zn contamination from slag (Map 5.30).

Major geochemical neoanomalies, with Zn concentrations above 12,319 ppm have a NE-SW trend, and occur over flotation residues (Noria-Prasini Alepou-Santorineika), pyritiferous wastes (Komobil) and slag/sand-blast material (within the smelter area at Kiprianos and Kavodokanos). The strongest geochemical neoanomaly, >24,576 to 76,310 ppm Zn, occurs within the premises of the smelter at Kiprianos, and its immediate surroundings towards Kavodokanos. This neoanomaly occurs over metallurgical processing wastes, which as shown on Map 5.30 have high Zn contents. Distinct neohaloes extend about the geochemical neoanomalies down to 6,668 ppm Zn, although even lower levels, to 591 ppm Zn, may be attributed to aerial dispersion from the smelters and metallurgical processing wastes.

Mobility of Zn is generally high under oxidising and acid conditions, high to moderately low under neutral, and low to very low under alkaline and reducing conditions (Levinson, 1980; Hoffman, 1986; Reimann *et al.*, 1998) (Table 6.2). The pH of hydrolysis of Zn^{2+} in dilute solutions is 7.0, meaning that $Zn(OH)_2$ precipitates in neutral environments and Zn becomes relatively immobile (Table 6.1). Zinc should, therefore, be geochemically immobile in most areas, since soil pH for 97.5% of the surface area of Lavrion is above 6.87 due to the predominance of marble. In the Lavrion urban area Zn may be, however, comparatively mobile in pyritiferous materials with pH<5.00, as for example, in the areas between Kiprianos and Kavodokanos, and Komobil and Nichtochori (refer to Map 2.5).

Zinc is an essential element for plants and animals (Gough *et al.*, 1979; Reimann *et al.*, 1998). Its toxicity is generally low (Mervyn, 1985, 1987), and is supposed to be non-carcinogenic (Reimann *et al.*, 1998).

According to Kabata-Pendias and Pendias (1984), the maximum permissible level of Zn in soil for healthy plant growth is 400 ppm. Values above this limit are considered to be phytotoxic. Consequently, 100% of the soil cover of Lavrion, under this premise, is unfit for plant growth (Map 6.30).

The recommended residential soil Zn statutory limits, quoted in scientific literature, vary from 300 to 20,000 ppm (Table 6.3), *i.e.*,

- 300 ppm in the United Kingdom (ICRCL, 1987), Finland (Koljonen, 1992), and Germany (Kloke, 1977; Lux, 1993); the European Union also recommends an upper Zn level of 300 ppm, when sewage sludge is added to agricultural soil (CEC, 1986);
- 480 ppm in The Netherlands (VROM, 1983; Lux, 1993; Van den Berg *et al.*, 1993; J. Ebbing, person. commun., 1996);
- 600 ppm in Federal Canada (Sheppard *et al.*, 1992);
- 800 ppm in the State of Ontario (Sheppard *et al.*, 1992);

- 1,000 ppm in Denmark (Edelgaard and Dahlstrøm, 1999);
- 2,000 ppm in Switzerland (Hämman and Gupta, 1998), and
- 20,000 ppm in the State of Connecticut (US CT, 1994).

Apart from the limiting values, Finland (R. Salminen, person. commun., 1996) and The Netherlands have intervention values for residential soil, which are 700 and 720 ppm Zn respectively. This great variation of technocratic statutory limits shows the necessity of setting up internationally agreed limits, based on realistic geochemical and medical principles. The extremely high limit set by the State of Connecticut is based on the fact that Zn is not carcinogenic. It is, however, unrealistically too high, and shows the naive reasoning of technocrats, who do not take into account natural geochemical variability, the requirements of biota and quality of life in particular.

Statutory limits from 300 to 500 ppm are considered logical. Unfortunately, the Lavrion overburden/soil has very high Zn contents (>591 ppm), and is considered to be potentially hazardous to human health.

6.3. GEOSTATISTICAL STRUCTURAL ANALYSIS

Geostatistical structural analysis, which is summarised by experimental and modelled variogram surfaces (refer to insets of Maps 6.1-6.30, Volume 2), has shown the following major axial trends of the spatial distribution of elements in overburden (elements having the same trend as in parent rocks are in bold & underlined letters):

- N-S: Co
- NNE-SSW: Hg, Mo, **Pb**
- NE-SW: Ag, As, Ba, Be, Cd, Cr, Cu, K, Sr, V, Zn
- ENE-WSW: Fe, Mn, P
- ESE-WNW: La, **Li**, Ti
- NW-SE: **Al**, **Ca**, **Ni**, Sb

The only elements which follow geogenic trends of parent rocks are Al, Ca, Li and Ni. Although overburden Pb has a similar trend as its geogenic counterpart, this is due to pure coincidence of primary Pb mineralised structures with the major trend of flotation residues (refer to Maps 2.3, 3.1 & 3.4 in Volume 2). It, therefore, appears that elements, which are strongly associated with lithology, retain their original trends, despite the strong masking effects of anthropogenic contamination.

Some elements have completely the reverse trend, Cu, for example, with a strong north-westerly trend in parent rocks, has a strong north-easterly orientation in overburden (Maps 4.12 & 6.12, Volume 2).

6.4. FACTOR AND CLUSTER ANALYSES ON OVERBURDEN GEOCHEMICAL DATA

Factor and cluster analyses were used in order to study element associations in overburden samples of the Lavrion urban environment. These two methods reveal underlying relationships among variables, which are not normally exposed by simple correlation analysis. In both cases, the R-mode method was used, which deals with similarities among variables determined on the samples. For details of the methods, the reader may refer to specialised literature on factor and cluster analysis (Obial, 1970;

Davies, 1973; Obial and James, 1973; Goddard, and Kirby, 1976; Jöreskog *et al.*, 1976; Howarth, 1983).

Data were normalised by the 2-parameter log transformation used by Miesch (1990) in the G-PREP module of program G-RFAC. This is the most widely applied transformation in chemometrics. The 2-parameters are the mean log and log variance, which completely define a lognormal distribution.

6.4.1. FACTOR ANALYSIS ON OVEBURDEN GEOCHEMICAL DATA

The ten factors of the principal component model are tabulated in Table 6.4. The first six factors, with eigenvalues above 1, explain 79.11% of total variance. Six factors were extracted, and the varimax-rotated factor loadings were calculated for 26 parameters, 25 chemical elements and pH (Table 6.5).

Table 6.4. Eigenvalues of the first ten factors of the principal component model of overburden geochemical data, the percentage variance explained by each factor and the cumulative percentage variance.
Πίνακας 6.4. Ιδιοτιμές των δέκα πρώτων παραγόντων του μοντέλου κύριων συνιστώσων για τα γεωχημικά δεδομένα του εδαφικού καλύμματος, ποσοστιαία μεταβλητότητα ερμηνευομένη από κάθε παράγοντα και ποσοστιαία αθροιστική μεταβλητότητα.

Factor	Eigenvalue	Variance explained by factor (%)	Cumulative variance (%)
1	**7.82**	30.06	30.06
2	**5.87**	22.59	52.65
3	**2.83**	10.89	63.54
4	**1.64**	6.32	69.86
5	**1.28**	4.92	74.78
6	**1.12**	4.33	79.11
7	0.85	3.27	82.38
8	0.74	2.86	85.24
9	0.60	2.30	87.54
10	0.51	1.97	89.51

The first or *"contamination"* factor, explains 30% of the total variance. Lead, Ag, Cd and Zn have the strongest positive varimax loadings (>0.8), followed by As, Cu and Sb with positive loadings >0.6 to <0.8. These are the principle toxic elements that occur in metallurgical processing wastes and, of course, the Lavrion polymetallic mineralisation. Moderate positive varimax loadings on Mo, Hg, Fe and Mn, give essentially the full suite of main elements occurring in metallurgical wastes, and the contaminants of Lavrion overburden/soil. Low negative varimax loadings on Cr, Ti, Al and K suggest that there is a negative relationship or an antipathetic (reverse) covariance with contaminant elements. A possible interpretation is that contaminant elements have not yet been adsorbed on the clay fraction of soil, implying, therefore, that they are readily available.

The second or *"clay"* factor, explains 22.6% of the total variance, and has strong positive varimax loadings on Al, Be, K, Li, Ti, V and La. Moderate positive varimax loadings on Ni, Co, and Cr support the interpretation that these elements are adsorbed on soil clay. Whereas, negative loadings on Ag, As, Cd, Cu, Fe, Pb, Sb and Zn imply, that there is a negative relationship, or an antipathetic covariance, between soil clay and contaminant elements. This relationship strengthens the inference made above, that

Table 6.5. Varimax loadings for the six strongest factors of overburden geochemical data [(n=224, except Hg (n=168) and Sb (n=56)]. Correlation between varimax scores and transformed data. [Strong positive loadings (>0.6) are shown by bold numbers, and the strong negative loadings (<-0.6) in italicised numbers].

Table 6.5. Φορτία περιστροφής "varimax" για τους έξι ισχυρότερους παράγοντες των λιθογεωχημικών δεδομένων [(n=224, εκτός του Hg (n=168) και Sb (n=56)]. Συσχέτιση μεταξύ των φορτίων varimax και των μετασχηματισμένων δεδομένων. [Με έντονη γραφή: ισχυρά θετικά φορτία (>0.6). Με πλάγια γραφή: ισχυρά αρνητικά φορτία (<-0.6)].

Element	*Varimax loadings*					
	Factor 1	*Factor 2*	*Factor 3*	*Factor 4*	*Factor 5*	*Factor 6*
Ag	**0.925**	-0.113	0.026	-0.044	-0.061	0.120
Al	-0.206	**0.919**	-0.057	0.146	0.142	-0.063
As	**0.772**	-0.193	-0.097	0.052	-0.111	0.321
Ba	0.121	0.246	**0.741**	-0.145	0.095	0.219
Be	-0.055	**0.907**	0.193	0.072	0.041	0.051
Ca	0.016	*-0.550*	0.469	-0.073	0.247	-0.425
Cd	**0.899**	-0.031	-0.010	-0.025	0.173	0.165
Co	0.154	0.405	-0.184	**0.587**	0.214	0.469
Cr	-0.274	0.264	0.276	0.140	0.296	*-0.639*
Cu	**0.694**	-0.190	0.236	0.109	-0.127	0.548
Fe	0.409	-0.008	0.007	0.078	-0.183	**0.830**
Hg	0.415	0.109	-0.241	-0.407	0.458	0.082
K	-0.105	**0.906**	-0.104	0.106	0.040	-0.152
La	0.280	***0.548***	0.431	-0.342	0.113	0.032
Li	-0.096	**0.857**	0.030	-0.035	-0.023	0.174
Mn	0.359	0.065	0.165	0.026	0.150	**0.817**
Mo	0.463	0.191	0.313	0.214	-0.177	0.509
Ni	-0.023	0.515	-0.145	**0.732**	0.131	-0.104
P	0.016	-0.191	**0.601**	0.034	-0.249	-0.446
Pb	**0.938**	-0.036	0.034	-0.006	-0.035	0.178
Sb	***0.537***	-0.133	0.189	-0.374	-0.043	-0.129
Sr	0.090	-0.203	**0.810**	-0.057	0.096	0.035
Ti	-0.260	**0.842**	-0.109	0.229	0.050	-0.160
V	0.010	**0.562**	-0.206	0.405	-0.234	0.245
Zn	**0.823**	-0.200	0.219	-0.098	0.088	0.378
PH	-0.116	0.029	0.136	0.121	**0.867**	-0.131
Eigenvalue	*7.82*	*5.87*	*2.83*	*1.64*	*1.28*	*1.12*
Variance explained by factor	*30.06%*	*22.59%*	*10.89%*	*6.32%*	*4.92%*	*4.33%*
Cumulative variance	*30.06%*	*52.65%*	*63.54%*	*69.86%*	*74.78%*	*79.11%*

these elements have not yet been adsorbed on clay minerals. The strong negative loading on Ca suggests, that elements adsorbed on clay have an antipathetic covariance with carbonates.

The third or *"carbonates*" factor explains 10.9% of the total variance, and has strong positive varimax loadings on Sr, Ba and P, and moderate positive loadings on Ca and La, suggesting that these elements are associated with overburden comparatively enriched in carbonates.

The fourth or *"mafic lithology"* factor explains 6.3% of the total variance, and has strong positive varimax loadings on Ni and Co, and moderate loadings on V, and suggest a relationship with prasinite and the femic minerals in schist. Moderately strong negative varimax loadings on Hg, Sb and La suggest that these elements have an antipathetic covariance with this factor. This is, in fact, the case, since these elements are not normally associated with mafic rocks.

The fifth or *"pH"* factor explains 4.9% of the total variance, and has strong positive varimax loadings on pH only, implying that pH does not play a significant role in the Lavrion secondary environment, natural or anthropogenic. Moderate positive loadings on Hg, Cr and Ca, suggest a weak relationship with pH. The moderate positive covariance between pH and Ca indicates that there is an influence from the soil calcium carbonate content.

The sixth or *"Fe-Mn"* factor explains 4.3% of the total variance, and has strong positive varimax loadings on Fe and Mn, and moderate positive loadings on Cu, Mo, Co, and weak on Zn, As, V and Ba, suggesting that these elements are possibly scavenged by Fe and Mn oxides. Strong to moderate negative loadings on Cr, P and Ca indicate a negative relationship, and an antipathetic covariance, with elements associated with this factor.

The above interpretation is supported by the statistical and spatial distribution of elements in overburden samples of the Lavrion urban area (refer to Maps 6.1-6.30).

6.4.2. CLUSTER ANALYSIS ON OVERBURDEN GEOCHEMICAL DATA

Cluster analysis was performed with the Statgraphics® software package (Manugistics, 1995). The nearest neighbour, single linkage, clustering method was used together with the squared Euclidean distance. This procedure creates gradually one cluster from "n" variables. Clusters are groups of variables with similar characteristics. To form the clusters, the procedure begins with each variable in a separate group. It then combines the two variables with the greatest similarity, *i.e.*, the ones that are closest together. Afterwards, recomputes the distance between groups, and the two groups that are closest together are again combined. The process is repeated until only one group remains. The dendrogram is the graphical representation of cluster analysis (Fig. 6.25).

The following eight clusters and their interlinked variables have been identified (major clusters of variables are joined by hyphons, interlinked elements by commas, and closely correlated clusters by semicolons):

- Ag-Sb, Pb, Cd; Cu-Zn; As:- it is comprised from two main clusters, which make up the contaminant elements represented by factor 1;
- Fe-Mn cluster is linked to the above clusters at a lower correlation level (factor 6), suggesting that the above elements are possibly scavenged by Fe-Mn oxides;
- Ba, La: these two elements are related to the Lavrion polymetallic mineralisation, and are, of course, linked at a lower correlation with the above two clusters;
- Ca-Sr:- these are two elements related to marble (factor 3), and are linked at a lower level to the above clusters;
- P, Mo, Hg, pH:- these four variables are weakly related to the above clusters. At this point end the clusters of variables, which are related to the Lavrion polymetallic mineralisation, metallurgical processing and contamination;
- Ti-V; Al-K; Be-Li:- these are the three main lithogenic clusters, which are related to the clay fraction of soil (factor 2);
- Co-Ni, Cr:- are the elements associated with the mafic lithology (factor 4).

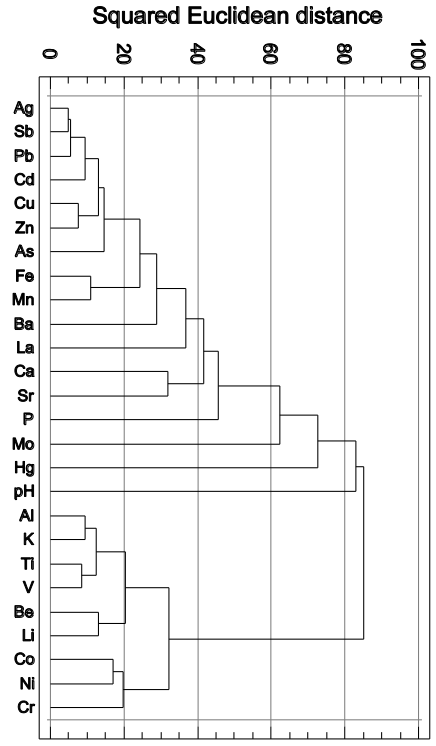

Fig. 6.25. Dendrogram of 25 elements and pH determined on 224 overburden samples from the Lavrion urban area (except Hg = 168 & Sb = 56 samples). The dendrogram was constructed using the nearest neighbour method and squared Euclidean distance for one cluster.
Σχ. 6.25. Δενδρόγραμμα 25 χημικών στοιχείων και του pH που προσδιορίστηκαν στα 224 δείγματα του επιφανειακού καλύμματος από την αστική περιοχή του Λαυρίου (εκτός του Hg = 168 & Sb = 56 δείγματα). Το δενδρόγραμμα κατασκευάστηκε με τη μέθοδο του πλησιέστερου γείτονα και το τετράγωνο της Ευκλειδείου απόστασης με τελικό στόχο τη δημιουργία μίας ομάδας.

It is quite apparent from the above relationships that contaminant and lithogenic elements and variables are completely separate and their correlation is at a very low level. The first main group of clusters essentially comprise the contaminant/ mineralising elements of overburden/soil, and the second group lithogenic elements.

6.5. DISCUSSION AND CONCLUSIONS

In this study it has been shown that overburden has been contaminated to an extremely high degree by metallurgical processing activities. Although mining and smelting activities in the greater Lavrion area date back to *ca.* 3500 BC, the multi-element contamination described is largely due to the wastes produced by the intensive metallurgical processing of the last hundred years. These wastes cover approximately 25% of the area studied in this project (7.235 km^2) (see also Map 2.3 in Volume 2 & Table 2.3, p.19 in this volume). Their subsequent redistribution by aerial, fluvial and anthropogenic processes, has caused the contamination of surficial residual soil, and house dust.

Generally, the mobility of cations in the largest part of Lavrion is comparatively low to moderate due the alkaline pH of soil water. However, in the area of pyritiferous tailings the action of air and rainwater cause the oxidation of pyrite and generation of acid drainage (sulphuric acid, H_2SO_4) which is very corrosive. It leaches metals from the wastes, and a fluid-acid drainage is produced, containing high to extreme concentrations of toxic elements, which have harmful effects on humans, animals and

plants. This acid drainage is also a potential hazard to groundwater supplies. Fortunately, the area covered is relatively small, *i.e.*, the coastal area from Nichtochori-Komobil to Kiprianos, and Kavodokanos.

The extreme multi-element soil contamination in Lavrion can be said that it is a permanent feature, since the residence time of heavy elements in soil is very high, *i.e.*, As 2000 years, Hg 920 years, Cd 280 years and Pb 400-3000 years (Ferguson, 1990).

It has been shown in this study that statutory levels, set up by different authorities, vary considerably. Hence, this is a matter that requires a serious study by a multi-disciplinary team of experts in order to set up internationally accepted statutory levels, based on sound geochemical, biological and medical principles.

Table 6.6 summarises the results already described. The order of the enrichment/depletion/ or contamination index with respect to different levels (a) the Lavrion rock median values, (b) Global soil means/medians and (c) Statutory levels for soil is shown below (toxic elements are highlighted):

Lavrion rock median:	Ca>	**Pb**>	**Zn**>	**As**>	**Cd**>	**Sb**>	**Ag**>	**Mo**>	**Cr**>	**V**>	**Cu**>	Ti>	Al>	Li>	La>	**Ni**>	Fe>	**Ba**>	**Be**>	Mn>	K>	Sr	
Global mean/median:	**Pb**>	**As**>	**Zn**>	**Ag**>	**Cd**>	**Sb**>	**Cu**>	**Hg**>	Ca>	**Cr**>	**Ni**>	Mn>	P>	**Mo**>	Co>	Sr>	**Ba**>	Fe>	**V**					
Statutory level:	**As**>	**Zn**>	**Pb**>	**Cd**>	**Ag**>	**Sb**>	**V**>	**Cu**															

Table 6.6. Statistical parameters of element concentrations in overburden, rock and metallurgical processing wastes in Lavrion, Global soil mean or median, statutory levels and enrichment/depletion/or contamination index.
Πίνακας 6.6. Στατιστικές παράμετροι των συγκεντρώσεων των στοιχείων στα δείγματα του εδαφικού καλύμματος, πετρώματος και μεταλλουργικών απορριμμάτων του Λαυρίου, Παγκόσμιες μέσες ή διάμεσες τιμές, νομοθετημένα όρια και δείκτης εμπλουτισμού/ανεπάρκειας/ ή ρύπανσης.

Element	*Lavrion overburden (n=224)**, rock (n=140)*** and Metallurgical wastes (n=62)*							*Global soil mean or median* (ppm)*	*Statutory level (ppm)*	*Enrichment/Depletion/ or Contamination Index with respect to*		
	Overburden materials (ppm)					*Rock (ppm)*	*Metallurgical wastes (ppm)*			*Lavrion rock median*	*Global soil mean or median**	*Statutory level*
	Min.	*Max.*	*Mean*	*S.Dev.*	*Median*	*Median*	*Median*					
Ag	1.4	204.6	17.8	21.88	12.06	0.5	18.9	0.1	2	**24.12**	**178**	**6.03**
Al	8076.0	85161.0	35067.0	13463.0	32315.0	8044.0	20074.0	80000*	-	**4.02**	0.40*	-
As	50.0	24000.0	2194.0	3558.0	1290.0	15.6	2492.0	5	10	**82.69**	**438.80**	**129.00**
Ba	64.0	4555.0	663.2	644.3	479.0	210.0	243.0	500	600	**2.28**	**1.33**	0.80
Be	0.2	2.7	1.1	0.4	1.0	0.5	0.5	6	10	**2.02**	0.18	0.10
Ca	4138.0	239150.0	95996.0	44539.0	93625.0	220.1	102603.0	14000*	-	**425.32**	**6.69***	-
Cd	4.0	925.0	68.0	108.6	38.0	0.5	20.6	1	4	**76.00**	**68.02**	**9.50**
Co	3.0	106.0	17.7	9.9	16.0	20.5	23.8	10	50	0.78	**1.77**	0.32
Cr	2.0	1083.0	264.2	224.7	183.0	20.0	73.2	50	600	**9.15**	**5.28**	0.31
Cu	43.0	4445.0	357.0	595.4	186.0	25.0	630.5	20	130	**7.44**	**17.85**	**1.43**
Fe	18859.0	351559.0	62398.0	51900.0	44771.0	19515.0	234500.0	35000*	-	**2.29**	**1.28***	-
Hg*	2.5	>747	204.8	199.3	136.0	500.0	2350.0	30	500	0.27	**6.83**	0.27
K	3013.0	22182.0	10463.0	3585.0	9770.0	8044.0	7100.0	14000*	-	**1.21**	0.70*	-
La	8.4	43.9	23.1	5.6	22.7	8.9	27.3	35*	-	**2.56**	0.65*	-
Li	3.8	48.3	18.9	6.6	17.4	5.0	14.5	30	-	**3.48**	0.63	-
Mn	625.0	35679.0	3348.0	3757.0	2189.0	1200.0	9398.0	530*	-	**1.82**	**4.13***	-
Mo	1.7	108.9	6.9	10.6	4.9	0.5	3.6	2.5	5	**9.80**	**2.78**	0.98
Ni	40.0	591.0	141.4	71.0	127.0	54.5	38.5	30	150	**2.33**	**4.71**	0.85
P	198.0	5433.0	1356.5	1016.3	992.0	1855.0	1103.0	300*	-	0.53	**3.31***	-
Pb	810.0	151579.0	11578.0	15491.0	7305.0	22.0	20750.0	20	500	**332.05**	**578.90**	**14.61**
Sb	<6.8	567.0	121.0	125.0	121.0	2.5	189.0	5	27	**48.40**	**24.20**	**4.48**
Sr	17.0	496.0	127.2	58.8	118.0	98.0	178.7	67*	-	**1.20**	**1.76***	-
Ti	584.0	5297.0	2249.0	812.0	2162.0	300.0	737.7	4000	-	**7.21**	0.54	-
V	26.0	325.0	86.1	39.3	75.0	9.0	46.3	80	50	**8.33**	**1.08**	**1.50**
Zn	591.0	76310.0	10872.0	12636.0	6668.0	57.0	39800.0	50	300	**116.98**	**217.44**	**22.23**

* Hg in ppb **Overburden: B, Bi, Hg, S, Sn, U (n=50) and Sb (n=90); *** *Rock: Ag , Mo (n=155); B, Be, Bi, Hg, La, S, Sb, Sn, U (n=48).

A greater number of elements have above normal levels, when overburden results are compared to Lavrion rock median than to Global mean/median values. Both comparisons indicate that toxic elements have above normal values in overburden. Comparison with statutory levels shows that the Lavrion overburden has potentially hazardous levels for human health with respect to As, Zn, Pb, Cd, Ag, Sb, V and Cu.

In Table 6.7 the % area of potentially hazardous elements to human and animal health is tabulated. These figures are indeed very worrying for a large part of the area is hazardous to

(a) human health:

- 100% of the area has hazardous As, Pb, Cd and Zn levels,
- >90% to 99% of the area has hazardous Ag, V and Sb levels,
- 45 to 68.8% of the area has hazardous Cu and Mo levels,
- 13.8 to 33% of the area has hazardous Ba, Ni and Cr levels, and

(b) healthy plant growth:

- 100% of the area has phytotoxic As, Pb and Zn levels,
- >90 to 99% of the area has phytotoxic Ag, Cd and Sb levels,
- >75 to 90% of the area has phytotoxic Ba, Cu, Cr and Ni levels, and
- >19 to 31% of the area has phytotoxic Mn and V levels.

Possible health related problems to such a high degree of multi-element contamination are well documented in scientific literature (*e.g.*, Kazantzis, 1973; Mervyn, 1980, 1985; 1986, 1989, 1996; Thornton and Culbard, 1987; Trattler, 1987; Thornton, 1988; Briskin

Table 6.7. Percentage of potentially hazardous area with respect to human and animal health (study area 7.235 km^2).
Πίνακας 6.6. Ποσοστιαία αναλογία της δυνητικά επικίνδυνης περιοχής για την υγεία του ανθρώπου και υγειή ανάπτυξη των φυτών (έκταση περιοχής 7.235 km^2).

Element	*% of area potentially hazardous to*	
	Humans	*Plants*
Ag	98.7	98.7
Al	-	<1.0
As	100.0	100.0
Ba	33.0	89.7
Be	-	-
Ca	-	-
Cd	100.0	96.0
Co	-	0.9
Cr	13.8	82.6
Cu	68.8	83.0
Fe	-	-
Hg	Should be further investigated	
K	-	-
La	-	-
Li	-	-
Mn	-	31.0
Mo	45.0	8.0
Ni	28.0	75.0
P	-	-
Pb	100.0	100.0
Sb	90.0	95.0
Sr	-	-
Ti	-	-
V	95.0	19.0
Zn	100.0	100.0

and Marcus, 1990; Ferguson, 1990; Hemphill, 1990; Reagan and Silbergeld, 1990; Manousakis, 1992; Wixson and Davies, 1994; Appleton, 1995; Appleton *et al.*, 1996; US EPA, 1998), and the cross-sectional epidemiological studies carried out in Lavrion (Benetou-Marantidou *et al.*, 1985; Nakos, 1985; Hatzakis *et al.*, 1987; Maravelias *et al.*, 1989; Eikmann *et al.*, 1991; Makropoulos *et al.*, 1991, 1992; Kafourou *et al.*, 1997).

The solution to the extreme multi-element contamination mapped in Lavrion is the immediate rehabilitation of the whole area by suitable remediation techniques. However, such a drastic solution cannot be foreseen in the near future. Consequently, the toxic elements in the metallurgical processing wastes and contaminated soil will continuously migrate and disperse into the Lavrion urban environment, and contamination will progressively be worse, and the risks to human, animal and plant health will be greater.

Another practical solution to the problem is resettlement of the population. The Portsmouth City Council in the United Kingdom took such action very recently. Immediately upon discovering that the *"infamous Lumsden Road (Glory Hole) estate"* was contaminated by As, Cd, Cu, Pb, Hg and Zn the residents were re-housed (Walton and Higgins, 1998). This difficult decision, as stated by the authors, was taken at a time when there was not much experience in terms of toxic elements impact on health risks to the residents from exposure to the identified contaminants. Table 6.8 compares toxic element concentrations between the Lumsden Road estate and the Lavrion urban area. It is quite evident that toxic element levels, except Cu and Hg, are much higher in Lavrion. The decision to re-house the residents was considered to be a *"conservative judgement"*, due to the many uncertainties involved at that time (Walton and Higgins, 1998).

Table 6.8. Comparison of toxic element concentrations in soil between the Lumsden Road estate, Portsmouth, U.K. and the Lavrion urban area.
Πίνακας 6.8. Σύγκριση των συγκεντρώσεων τοξικών στοιχείων στο έδαφος μεταξύ του οικισμού Lumsden στην πόλη Πόρτσμουθ της Αγγλίας και της αστικής περιοχής του Λαυρίου.

Element	*Lumsden Road estate, Portsmouth, U.K.**			*Lavrion urban area (this study)*		
	Min.	*Max.*	*Mean*	*Min.*	*Max.*	*Mean*
As:	<3	700	13	50	24000	2194
Cd:	<1	17	1	4	925	68
Cu:	<6	10000	230	43	4445	357
Pb	<20	96000	1400	810	151579	11578
Hg:	<1	590	7	<0.005	>0.75	0.21
Zn:	<11	11000	440	591	76310	10872

* (From Walton and Higgins, 1998, Table 1, p.32)

Four years later the Portsmouth City Council debated about the politically sensitive issue of the optimum location for a proposed new school. This equally difficult decision was taken with the benefit of a full risk assessment methodology, based upon exposure pathways for the identified contaminants of Pb, As, and polynuclear aromatic hydrocarbons (PAH). The result of the quantitative risk assessment model (US EPA, 1989) determined that the exposure hazard presented an unacceptable risk to school children, and so the proposed new school was located elsewhere (Walton and Higgins, 1998). This case study is indeed very interesting for it shows that the Portsmouth City

Council values the quality of life of its citizens, and had the courage to take a politically sound decision.

It is finally concluded, that multi-element contamination of the Lavrion overburden presents unacceptable risk on the quality of life of the local population. These results together with those of house dust (Chapter 8), lead (Chapter 3) and the risk assessment based only Pb data (Chapter 11) must be seriously taken into account by the Municipality of Lavrion councillors for the health of local residents is a truly very valuable gift, which undoubtedly supersedes financial and other profits. Although the decision based on *"the quality of life"* issue is socially, politically and financially difficult, it must be taken through transparent procedures and public agreement.

Blank back page
Λευκή οπίσθια σελίδα

Chapter 6A

DISTRIBUTION OF EDTA EXTRACTABLE ELEMENTS IN OVERBURDEN

Editor's note
Institute of Geology and Mineral Exploration, 70 Messoghion Street, Gr-115 27 Athens, Greece

The distribution of EDTA extractable Cd, Pb and Zn is presented respectively on Maps 6.32, 6.33 and 6.34 in Chapter 6A of Volume 2. This work was carried out in the autumn of 1992 during an unemployed workers training programme instituted by the Lavrion Labour Centre in collaboration with PRISMA. The workers were trained in soil sampling to begin with. Then soil sampling was carried under the supervision of George Nakos, a scientist of the Forest Research Institute in Athens, and other agronomists.

The purpose of this survey was to evaluate soil contamination in order to decide upon the types of plants to be grown. Sample sites are presented on Map 2.16 in Volume 2 of this report. Sampling and sample preparation are described in Chapter 2A (Section 2A.2.11, p.30 & 2A.3.10, p.32), and the analytical method in Chapter 2B (Section 2B.2.10, p.43).

Cold extraction by EthyleneDiamineTetraAcetic acid (EDTA), a chelating agent used for determining plant-available trace elements in soils, is used by soil scientists to simulate uptake by plants (Kabata-Pendias and Pendias, 1984; Pickering, 1986). The extent of dissolution of elements, however, is controlled by many factors, including extraction time, nature and size of solid particles, pH, reagent concentration, and the effective stability of the chelate formed (Pickering, 1986). The pH of the solution is kept at 7, since extraction appears to be stable at a narrow range about this value, i.e., from about pH 6.5 to 7.5 (Kabata-Pendias and Pendias, 1984). Apparently, there is a variation in the capacity of plants to retrieve metal ions sorbed on different soil components. Some take up ions held on ion-exchange sites (e.g., exchange between H^+ on root hairs and cations on clay particles. Other plants appear to favour the fraction bound to organic material, while in other cases the correlation studies imply that the total hydrogenous fraction is available to living matter. Another limitation in simulating plant behaviour is the different time scales involved. Plant uptakes occur over a prolonged time period, whereas tests are usually short lived.

According to Pickering (1986) plants have been grown on contaminated soil, with observed uptake of selected elements being subsequently compared with the amount of elements released by different chemical extractants. The reagents found to give the best correlation (in different studies) include water, 1M $MgCl_2$ *(Step 1 of the sequential extraction procedure used in this project – refer to Chapter 7, p.191-234)*, 1M NH_4NO_3, 1M CH_3COONH_4, acidified $(NH_4)_2C_2O_4$, 0.1N H_3PO_4, 0.1N HCl and DTPA (Diethylene-TriaminePentaAcetic acid). EDTA cold extraction does not appear to give a good correlation.

Although there are serious objections about the quality of the procedures used, the Municipality of Lavreotiki insisted that these soil samples be analysed and maps plotted. It is stressed that the EDTA cold extraction method is approximately equivalent to the $MgCl_2$ step of sequential leaching, which is considered by applied geochemists as a better extraction for the determination of bioavailable trace elements in soil.

Following IGME and NTUA detailed studies, and the collaboration with medical practitioners, it has become quite obvious that planting of trees alone is not the answer to the health-related problems facing the local population. The solution is the immediate isolation of contaminated soil and medium- to fine-grained metallurgical processing residues by uncontaminated material in order to stop their aerial transportation, and subsequent inhalation and ingestion by children and adults alike. Medical evidence points that inhalation of dust is the major route and hands-to-mouth activity secondary.

For those interested in studying these maps, it is mentioned that the threshold trigger concentration for EDTA extractable Zn is 130 ppm (ICRCL, 1987). This means that 66.6% of the area covered by this study has Zn contents over this limit, which is considered phytotoxic to plants (Map 6.34).

Blank back page
Λευκή οπίσθια σελίδα

Chapter 7

PARTITIONING OF THE OPERATIONALLY DEFINED PHASES IN OVERBURDEN – Sequential extraction results

Alecos Demetriades and Katerina Vergou-Vichou
Institute of Geology and Mineral Exploration, 70 Messoghion Street, Gr-115 27, Athens, Greece

Xiangdong Li, Michael H. Ramsey, Brian J. Coles and Iain Thornton
Environmental Geochemistry Research Group, T.H. Huxley School of Environment, Earth Science & Engineering, Royal School of Mines, Imperial College of Science, Technology & Medicine, Prince Consort Road, London SW7 2BP, U.K.

7.1. INTRODUCTION

Metal speciation has been an important area of research for both mineral exploration (Gatehouse *et al.*, 1977; Dijkstra *et al.*, 1979; Hoffman and Fletcher, 1979; Fletcher, 1981; Chao *et al.*, 1984; Pickering, 1986; Hall and Bonham-Carter, 1998) and environmental studies (Leschber *et al.*, 1985; Beckett, 1988; Li, 1993; Li *et al.*, 1995; Kiratli and Ergin, 1996; Wang *et al.*, 1998; Song *et al.*, 1999; Ullrich *et al.*, 1999). In mineral exploration, the objective is to isolate and quantify the portion of the element in a sample, which is relatively loosely bound, indicating prior mobility, presumably from depth. The aim is to improve geochemical contrast by screening out trace element components not derived from local mineralised sources, and to detect subtle leakage haloes emanating from deeply buried mineralisation (Cohen, *et al.*, 1998). Hence, the possibility of locating concealed mineralisation. In environmental studies, the aim is to examine the fate and effect of metals in soil samples, since it is important to know something about the availability of toxic elements to plants, animals and humans.

Previous geochemical studies in Lavrion (Hadjigeorgiou-Stavrakis and Vergou-Vichou, 1992; Hadjigeorgiou-Stavrakis *et al.*, 1993) have shown the complexity of environmental contamination. Hence, it was considered significant to analyse samples of overburden and house dust by an analytical method, which will provide information about mobility and availability of elements. Although an adequate number of elements were determined, it was not possible to analyse As and Sb, two toxic elements known to occur at comparatively high concentrations in the study area (see Chapter 6, this study; Maps 6.1 & 6.26 Volume 2 of this study).

The sequential extraction method used in this study is that of Tessier *et al.* (1979), modified and refined by Li (1993) for multi-element analysis by ICP-AES (Li *et al.*, 1995) (see Chapter 2B). Twenty-two elements were determined on the solution of each of the five sequential extraction steps, *i.e.*, Ag, Al, Ba, Be, Ca, Cd, Co, Cr, Cu, Fe, K, La, Li, Mn, Mo, Ni, P, Pb, Sr, Ti, V and Zn. The sequential extraction results of Pb have already been discussed in Chapter 3 (Volumes 1 & 2).

7.2. BACKGROUND TO THE MODE OF OCCURRENCE OF METALS IN SOIL

Primary minerals of igneous and metamorphic rocks through the action of weathering agents decompose at variable rates to form new products, especially clays and hydrous oxides of iron, manganese and aluminium. Elements held in primary minerals are dispersed mechanically until their host mineral is sufficiently decomposed to release them into solution. Their mobility in the secondary environment is then determined by the chemical stability of dissolved species. Among the many processes, whereby dissolved elements become re-associated with solid phases of soils, and sediments, are:

- changes in solution chemistry, especially Eh and pH;
- exchange reactions on clays and colloids, and
- fixation by organic matter.

Consequently, distribution of trace elements in these media, because of the above processes, is extremely complex.

Conceptually, metals in soil may be present in several different physicochemical phases that act as sinks of elements in the environment (Jenne, 1977; Tessier *et al.*, 1979; Beckett, 1988). These phases, according to Li (1993) include the following forms:

1. **Soluble**: present as free ions, or as soluble complexes with inorganic or organic ligands in soil solutions.
2. **Exchangeable**: held by predominantly electrostatic forces on negatively charged sites on clays, other minerals or organic matter. Exchangeable cations are *isotopically exchangeable**, and may be displaced by the basic cations commonly present in soil solutions. The activation energy of exchange must be low, because this exchange is usually rapid and complete. *[*Isotopic exchange is the transfer of isotopically tagged atoms from one chemical form or valence state to another, without net chemical reaction (Lapedes, 1978)*].
3. **Specific adsorption**: held at sites (usually assumed to be inorganic) on which the trace elements are bound strongly by predominantly covalent or co-ordinate forces. Ions held in this way are taken up and released slower than exchangeable ions, and are more easily displaced by other trace metals or hydro-ions than by basic cations. The number of specific adsorption sites usually varies with pH, and there may be sites, that can hold H_3O^+ or trace metals, but not alkaline or alkaline earth cations. Many but varied adsorption sites occur on the surfaces of amorphous precipitates of iron, aluminium or manganese oxides, alumino-silicates, silica, and micro-crystalline precipitates of oxides, carbonates and phosphates.
4. **Occluded in oxides of iron, aluminium, or manganese**: these oxides are rarely pure; they usually contain cations from each other and, probably trace metal cations as well. Iron and manganese oxides have also been distinguished as “easily”, “moderately” or “difficulty” reducible according to the reagents that dissolve them. The ease of release of occluded trace metal cations is thought to depend on the solubility of oxides that contain them.
5. **Organic bond**: held on insoluble organic materials. This category includes trace metal cations in, or immobilised on, living or recently dead cells, but consists mainly of cations complexed or chelated by organic materials, either recently synthesised or the resistant residues from microbial metabolism. This group includes both specific and non-specific sites. Some of the organic matter of this group will be intrinsically insoluble; some of it will have flocculated or precipitated by complexing cations,

notably iron or aluminium, but also by basic cations like calcium or trace metals such as copper.

6. **Secondary minerals**: including carbonates, sulphates, phosphates, hydroxides, *etc.*, but often not specified. These precipitates may be newly formed compounds, containing the metal as a principal component; they may contain more than one trace metal, and often form mixed crystals or a mixture of crystallites with the corresponding salts of major elements, usually calcium or iron.
7. **Primary minerals**: held in the crystal lattice of primary, non-oxide minerals; this group includes the sites of the crystal lattice within a mineral. They can be the lattice position of trace element minerals itself, but more often is a substitute lattice site within the primary mineral of the major elements.

Soils, sediments and natural dusts contain, therefore, a range of individual components, and each component binds trace elements in more than one way. With such heterogeneity and variety of bonding site types and strengths, different analytical methods have been devised to recover or identify trace elements from natural solid samples. These methods will be concisely described below, ending with the description of the sequential extraction procedure used in this study.

7.3. METHODS OF DETERMINING CHEMICAL SPECIES OF ELEMENTS

Methods of determining the chemical species of trace elements in soils include direct measurement using X-ray diffraction (XRD) and scanning electron microscopy with energy dispersive X-ray spectroscopy (SEM/EDXRA), and indirect estimation, *e.g.*, model calculation and partial chemical extraction.

Trace element solid phases usually form a minor fraction of the total solid matrix of a soil. Therefore, direct identification of these phases can be achieved only through pre-concentration of these phases by non-destructive, physical separation techniques, *e.g.*, density separation (Mattigod *et al.*, 1986; Essington and Mattigod, 1990; Cotter-Howells, 1993). After pre-concentration, soil material can be analysed by XRD or SEM/EDXRA. The major limitation of the XRD technique, however, is that only crystalline material can be analysed, and amorphous substances cannot be readily detected by this method (Lindholm, 1987; Vanloon and Barefoot, 1989; Cotter-Howells, 1991). There are a very large number of soil particles existing as amorphous materials, which may contain a large amount of trace elements, *e.g.*, some secondary precipitates, Fe-Mn oxides and organic compounds.

The SEM/EDXRA technique has recently been used in the study of heavy metal solid phases in sludge-amended soil and mine-waste contaminated soils (Mattigod *et al.*, 1986; Essington and Mattigod, 1991; Cotter-Howells and Thorton, 1991). This method has proved to be very useful in determining the solid species of trace elements (Pb, Ba and Zn) in the heavy density fractions of these soils. However, many trace elements may be adsorbed evenly on to the light soil matrix, such as clay minerals and organic matter, and the concentrations of some elements (*e.g.*, Cd and Cu) are usually not high enough to be detected in soil particles by SEM/EDXRA. These facts limit the usefulness of this technique to analyse heavy metal species in the whole soil system. Nevertheless, an advanced SEM and EDS technique, combined with automated image analysis software, was used for particle-by-particle measurement on a selected number of samples for this study (for details refer to Appendix Report 1B in Volume 1B of this report).

Another important approach to metal speciation in soils is chemical equilibrium modelling, using models such as *SOILCHEM*, which is an extended version of *GEOCHEM* (Sposito and Coves, 1988). *SOILCHEM* is a multi-purpose chemical equilibrium computer program that was developed for soil systems. It is able to calculate the speciation of chemical elements among the aqueous, solid and adsorbed forms in soil (Sposito and Coves, 1988). The program can consider mixed solid phases, redox reaction and simple mineral solubility equilibria. Certain characteristics of a soil, *e.g.*, cation exchange capacity (CEC) and solute concentrations are entered into the program, which then runs through a series of interactions until all equations are satisfied. The result is a list of the percentage distribution of each metal and ligand between aqueous species (free ions and complexes), solid phases and adsorbed forms. There are several studies using *GEOCHEM* in water and soil research showing good results for metal speciation, especially in aquatic phases (Mattigod and Page, 1983; McGrath *et al.*, 1986).

SOILCHEM is, however, just a model and undoubtedly has its limitations (McGrath *et al.*, 1984; Cotter-Howells, 1991). Results produced by *SOILCHEM* depend on the thermodynamic data it contains, which are subject to availability, and may contain inconsistencies with respect to stability constants of trace elements in the environment. Major limitations of *SOILCHEM* are the poorly defined models for organic chelation of metals (Cotter-Howells, 1991). It has been proven, therefore, not to be applicable in metal speciation studies in organic rich soils in temperate areas such as England (McGrath *et al.*, 1984).

Due to difficulties involved in the direct physical determination of trace element solid phases in soil, analytical measurement has usually been approached by phase-selective chemical extraction based on chemical reactivity. Extraction of elements may involve single or multiple extracting chemical reagents. Multi-step sequential extraction schemes appear more promising, and of greater value than single extractant methods, providing more detailed information on possible metal chemical forms in soil (Tessier *et al.*, 1979; Pickering, 1986; Li, 1993; Hall *et al.*, 1993, 1996; Li *et al.*, 1995; Breward *et al.*, 1996; Hall and Bonham-Carter, 1998).

The reagents utilised in sequential extraction have been selected on the basis of their selectivity and specificity towards particular physicochemical forms, although variations in reagent strength, volume and extraction time between schemes are apparent (Lake *et al.*, 1984; Pickering, 1986; Tessier and Cambell, 1988). More than ten different sequential extraction procedures have been developed for partitioning trace elements in sediments, soils and sludge (Tessier *et al.*, 1979; Lake *et al.*, 1984; Shuman, 1985; Förstner, 1985; Pickering, 1986; Hall and Bonham-Carter, 1998). In particular, the protocol of Tessier *et al.* (1979) has been thoroughly researched and is well documented (Tessier *et al.*, 1979; Valin and Morse, 1982; Förstner, 1985; Pickering, 1986; Martin *et al.*, 1987; Kim and Ferguson, 1991; Li, 1993; Li *et al.*, 1995). This method is nowadays applied widely in sediment and soil studies by many researchers (Harrison *et al.*, 1981; Hamilton, 1984; Xian, 1989; Dudka and Chlopecka, 1990; Li, 1993; Li *et al.*, 1995; Song *et al.*, 1999).

The limitations of the Tessier *et al.* (1979) sequential extraction method have, however, been addressed by several researchers (Rendall *et al.*, 1980; Tipping *et al.*, 1985; Kheboian and Bauer, 1987; Martin *et al.*, 1987; Bermond, 1992). These include, technical difficulties associated with achieving complete and selective dissolution, and high recovery of trace elements from the target geochemical phases, and reabsorption

on the remaining phases in soil and sediment (Jouanneau *et al.*, 1983; Kheboian and Bauer, 1987). Despite these inherent limitations, the sequential extraction scheme by Tessier *et al.* (1979) is a very useful method for characterising solid phase associated trace elements in soil, especially if used for comparison between a composite set of soils (Belzile *et al.*, 1989; Tessier and Campbell, 1988; Kim and Ferguson, 1991).

7.4. THE SEQUENTIAL EXTRACTION METHOD USING ICP-AES

The sequential extraction method of Tessier *et al.* (1979) was selected, because it was thoroughly researched by one of the co-authors of this study (Li, 1993). It is also the best-documented procedure, and is widely used in soil and sediment studies. Further, it contains the desired *"operationally defined"* geochemical fractions, such as carbonate and Fe-Mn oxides, which makes it suitable for samples of overburden and house dust collected from the Lavrion urban area. The method examines the possible "*operationally defined*" geochemical phases of major and trace elements in overburden materials, which include metallurgical processing wastes, and residual and alluvial soil contaminated by past mining and smelting activities.

The simplified extraction steps and operationally defined fractions of this method are discussed in Chapter 2B (Section 2B.2.2, p.35) and presented in Fig. 2B.1 (p.36).

Although the sequential extraction procedure of Tessier *et al.* (1979) has been widely used, the accuracy and precision of the technique in each study has rarely been estimated. Comparability of the results produced by different authors is, therefore, very difficult. Furthermore, the analysis of extraction solutions has used flame atomic absorption spectrophotometry (AAS), which is only appropriate in the determination of a relatively small number of elements. The investigation of soil contamination normally requires analysis of a substantial number of samples and determination of a large suite of elements. The method of Tessier *et al.* (1979) has been developed by Xiangdong Li (a co-author of this Chapter) for sequential extraction of soils using ICP-AES to analyse the extractant solutions for some 22 elements (Li, 1993). This development has increased the productivity of the sequential extraction method, and enabled a broader study of geochemical associations in overburden and house dust samples collected from the Lavrion urban area. Technical modification to the procedure for ICP-AES analysis has been outlined in Chapter 2B (Section 2B.2.2., p.35). Li (1993) and Li et al. (1995) discuss the analytical performance of this method in detail.

The modified sequential extraction procedure using ICP-AES enabled simultaneous determination of a large number of elements. Multi-element determinations on the five sequential extraction steps for soil samples were achieved by using a single calibration with acceptable precision and accuracy by ICP-AES. Precision of each extraction step according to Li (1993) and Li *et al.* (1995) is good with values typically about 5% (2s) estimated from the analysis of duplicate samples. Overall recovery rates of the international reference material, USGS MAG-1, by the five steps compared with recommended total element concentrations are in the range of 80-105% for most elements determined, with an average of 92%. The accuracy is acceptable for each extraction step compared with the published values for USGS MAG-1.

7.4.1. OPERATIONALLY DEFINED PHASES

In the absence of detailed mineralogical studies, most extractions are, in effect, only "*operationally defined*" (Hall *et al.*, 1996), since selectivity is not 100%, *e.g.*, *metal or element extracted by magnesium chloride*, $MgCl_2$, *etc.*, or according to the geochemical phase operation, *exchangeable element* or *metal, etc.* The amount of trace elements released is dependent on such factors as:

- chemicals employed,
- time and nature of contact,
- sample to volume ratio,
- on the degree of crystallinity and purity of the mineral phases present,
- the grain-size fraction chosen for analysis, and
- whether coarser grains have been made finer by ball-milling, thus increasing exposure to attack (Hall *et al.*, 1993).

The five *"operationally defined"* geochemical phases of the Tessier *et al.* (1979) method are described below. Information was mainly abstracted from the work of Pickering (1986) and Hall (1998), and will not be quoted in the following description. Material, however, obtained from other authors will be cited.

7.4.1.1. Exchangeable Fraction

The distribution of an element between soil solution and solid phases at equilibrium is governed by:

1. the density of surface binding sites for each component (*e.g.*, clay mineral, hydrous Fe oxide);
2. the binding intensity of the metal ion to each component;
3. the abundance of each component;
4. the chemical characteristics (*e.g.*, pH, ligands and their concentration) of the solution phase, and
5. the concentration of other ions, major or trace, competing for binding sites.

In order to dissolve selectively adsorbed elements in exchange sites on surfaces of clays and colloids, without dissolving the substrate itself (*i.e.*, clays, hydrous oxides, humics), the adsorption equilibrium must be shifted to the free-ion side.

Cations loosely adsorbed or associated with exchange sites on clay mineral surfaces are relatively readily removed by competition with hydrogen ions, or an excess of some other cation, by ion exchange (Fletcher, 1981). Divalent ions are normally more effective in removing exchangeable ions than univalent ions. Leaching, therefore, of soil by a neutral electrolyte, such as $MgCl_2$, promotes displacement of adsorbed metal ions held by electrostatic attraction to negative sites on particle surfaces. The ion-exchange process may be represented as:

$$R - Me^{2+} + Mg^{2+} \longleftrightarrow R - Mg^{2+} + Me^{2+}$$

The affinity of cations of Group I and II cations, such as NH_4^+, Na^+, K^+, Mg^{2+}, Ca^{2+} and Ba^{2+}, for most sites is usually very much less than the affinity of other metal ions. Consequently, the amount of electrostatically bound metal displaced is determined, largely, by the concentration and charge of competing ions. The cation displacement efficiency for oxic soils and sediments has been demonstrated to decrease in the order

Cd > Zn > Cu ~ Pb, which is consistent with the decreasing pH values of their adsorption edges. The solid-to-solution ratio (or "dilution factor") is an important influence on desorption efficiency; the higher the dilution factor, the greater the amount of metal extracted.

In soil extraction studies, dilute solutions (*e.g.*, 0.5*M* $MgCl_2$) are preferred, for they more closely resemble the salt inputs that occur in real systems. Divalent cations (Mg^{2+}) are more effective than monovalent in removing exchangeable ions. Provided that exchange sites are not protected by a coating of iron or manganese oxides or organic colloids, ion exchange proceeds very rapidly (Fletcher, 1981). Presence of alkali or alkaline earth salts (nitrate or chloride) should not result in disintegration of rock mineral fragments, or dissolution of sparingly soluble components (such as hydrous oxides or organic matter), and their influence on the pH of aqueous suspension should be minimal. Magnesium chloride ($MgCl_2$) leachates typically extract very low amounts of Al, Si, Fe and organic matter, showing that attack on the substrates (*e.g.*, clay minerals, organic matter, oxides and sulphides) is minimal.

7.4.1.2. Carbonate and Specifically Adsorbed Fraction

Depending upon climate and local conditions, carbonates may be the dominant sink for some trace elements. The major control on trace element uptake by carbonates, often in metastable and polymorphic forms, is pH. Trace elements may be co-precipitated as their carbonates or, like Cd, may actually replace Ca^{2+} in the lattice. The preferred method of selective dissolution of the carbonate phase is an acidified sodium acetate-buffered extraction, namely 1M CH_3COONa [NaOAc], at a pH of 5. This reagent is classified as *"selectively dissolving"* the carbonate fraction of soils and sediments. The time required for total dissolution of the carbonate phase depends on such factors as particle size, sample size, type of carbonate and percentage of carbonate present. It has been shown that this buffering capacity is sufficient to extract >99% of the total $CaCO_3$-bound Ca^{2+}, present in a carbonate-rich (68% $CaCO_3$) sediment, resulting in a final pH of 5.5. Nevertheless, samples with a high carbonate content, as was the case with the Lavrion samples, may require a longer leaching time than 5 hours, and possibly adjustments of pH (Tzoulis and Kaminari, 1999). Since, the conditions were not changed calcium carbonate was not completely extracted by this step.

Interaction with dolomite ($CaCO_3.MgCO_3$) was demonstrated by the disappearance of the characteristic mineral peak from X-ray diffraction spectra of samples (Tessier *et al.*, 1979).

Sodium acetate at pH 5 recovers most of the metal present in carbonate minerals. In soils, the greatest affinity for reaction with carbonates has been observed for Co, Cd, Cu, Fe, Mn, Ni, Pb, Sr, U and Zn; up to 1000 ppm of Sr and Co may occur in secondary calcite minerals.

In this particular phase, elements occurring at specifically adsorbed sites, not displaced by $MgCl_2$ during the first extraction step, are also released, since the presence of acetate (CH_3COOH^-) promotes desorption from the surfaces of amorphous precipitates of iron, aluminium or manganese oxides (oxyhydroxides), alumino-silicates (clays), silica, and micro-crystalline precipitates of oxides, carbonates and phosphates in soils and sediments. Hence, this phase is described as the *"carbonate and specifically adsorbed fraction"*. Tessier *et al.* (1979) have observed that appreciable amounts of Fe and Mn were extracted by this phase, which were ascribed to dissolution of Fe^{2+} and Mn carbonates. Apparently, there is no evidence of dissolution of fresh,

less well-crystallised ferromanganese oxyhydroxides. Low levels of Si, Al and S, found in leachates of this phase, indicate that attack on silicate and sulphide minerals was minimal (<1%).

7.4.1.3. Fe-Mn Oxide Fraction

Iron and manganese oxides are known to be excellent scavengers of trace elements. In soil they occur as nodules, concretions, matrix component, cement between particles or as a coating on particles. Soil generally contains much greater amounts of Fe oxides than Mn oxides. The latter, however, possess greater sorption capability for trace elements. This reactivity of Mn is due to such characteristics as:

1. it exists in several oxidation states (II, III, IV);
2. it forms non-stoichiometric oxides with different valencies;
3. its higher valence oxides exist in several crystalline forms {*e.g.*, birnessite [$(Na,Ca)Mn_7O_{14}.3H_2O$], lithiophorite [$Li_6Al_{14}O_6(OH)_{36}(Mn_{21}^{4+}O_{42})$], pyrolusite [$MnO_2$] or pseudocrystalline [manganite ($Mn_2O_3.H_2O$)], and
4. it forms co-precipitates and solid solutions with Fe oxides, owing to their similar chemical properties.

The association of trace elements with precipitated Mn and Fe oxides ranges from exchangeable (loosely adsorbed) forms, through moderately fixed (*e.g.*, with amorphous oxides) to relatively strongly bound {*e.g.*, occluded in goethite [α-FeO(OH)], lepidocrocite [γ-FeO(OH)] and other oxide minerals}. Although crystalline forms of Mn oxide do occur in soil, the predominant species are amorphous. Manganese oxides can have surface areas of several hundred m^2/g and larger cation exchange capacities (CEC) than some clay minerals (*e.g.*, in the order of 150 meq/100g). The internal structure of poorly crystallised Mn oxides can have an effect on the uptake of trace elements. The uptake of Ag by such Mn oxides, for example, depends upon the amount of internal Na and K, indicating exchange of these elements by Ag. In an experimental study of the adsorption, by synthetic hydrous Mn oxide, of Co, Zn, Ca and Na, manganese was released to solution during the adsorption of the first two elements, but not the latter. It was deduced, therefore, that Co interchanged with surface-bound hydrogen, and structural Mn^{2+} and Mn^{3+}, Zn with hydrogen, Mn^{2+}, and Ca only with hydrogen.

The degree of fixation of trace elements by Fe oxides ranges from adsorption at the surface, through co-precipitation, to relatively strong binding within the oxide structure. Similar to Mn, the geochemistry of Fe in the terrestrial environment is complex. Its behaviour being closely linked with the cycling of oxygen, carbon and sulphur. Amorphous Fe oxide [$(Fe(OH)_3.nH_2O)$] is chemically more reactive than its pseudocrystalline and crystalline forms, and provides the basis for its chemical separation. Moderate reducing conditions are required, for example, for dissolution of amorphous Fe oxides compared to those for poorly crystallised goethite [α-FeO(OH)] or lepidocrocite [γ-FeO(OH)], whereas highly crystallised magnetite [Fe_3O_4] and haematite [Fe_2O_3] require a strong reductant or aggressive attack.

Crystalline Fe and Mn oxides are more resistant to attack than non-crystalline oxyhydroxides. Manganese oxides dissolve, with moderate ease, in acid solutions containing a reducing agent. A reducing agent, such as hydroxylammonium hydrochloride ($NH_2.OH.HCl$) dissolved in acetic acid (HOAc), is used for the extraction of trace elements adsorbed on Fe and Mn oxides. This reagent preferentially reduces Mn-oxyhydroxides, and is considered to dissolve loosely adsorbed elements. The rate

of attack on Mn^{4+} oxides [*e.g.*, pyrolusite (MnO_2) and bog Mn-oxide] is somewhat slower than for Mn oxyhydroxides. As with other acidic solutions, hydroxylamine reagent dissolves calcite [$CaCO_3$], partially dissolves dolomite [$CaMg(CO_3)_2$], disrupts the zeolite mineral phillipsite {$(K_2,Na_2,Ca)[Al_2Si_4O_{12}].4\text{-}5H2O$}, extracts low levels of Si from opal and river sediments, and releases Al from soil and sediment.

Hydrous aluminium oxides are also scavengers of element ions, but are not normally reported in published sequential extraction procedures. In the Lavrion samples, element ions released during this extraction step, appear to have a strong correlation with Al. It is assumed, therefore, that they are related to hydrous aluminium oxides occurring in overburden samples.

The relative importance of Mn, Fe and Al oxides as scavengers will depend upon:

- pH-Eh conditions;
- degree of crystallinity of the oxides and hence their reactivity;
- their relative abundance, and
- the presence of organic matter as a competing adsorbing and chelating fixing agent.

Thus, elements will show a preference for uptake by either Mn or Fe or Al oxide depending upon local conditions.

7.4.1.4. Organic/Sulphide Fraction

Trace elements become bound to, or incorporated in, many forms of organic matter including living organisms, organic coatings on mineral particles, and biotic detritus. The organic content of soil consists, *inter alia*, of complex polymeric materials known as fulvic and humic acids (with high metal adsorptive capacity), and non-humic substances, such as carbohydrates, proteins, peptides, amino acids, fats, waxes and resins. Adsorption, complexation and chelation are some of the binding mechanisms of trace elements with organic matter. The high scavenging capacity of organic substances is usually attributed to their carboxylic acid (COOH) functional groups, with contributions from other groups, such as $–NH_2$ (amino) and –SH (thiol). The maximum amount, based on equivalents, of any given element bound is approximately equal to the number of carboxyl groups.

This fraction releases, apart from organically bound metals, trace elements incorporated in the structure of sulphide minerals.

Selective destruction of organic matter, and oxidation of sulphides, can be achieved by including an oxidising acid in the reagent mixture. The strong oxidising properties of nitric acid are enhanced by the addition of H_2O_2, *i.e.*, 30% H_2O_2 is added to a suspension of 0.02 *M* in HNO_3 (pH 2). Since, released metal ions may resorb on other components, the oxidised solid residue is subsequently attacked by an electrolyte solution of ammonium acetate in nitric acid (CH_3COONH_4/HNO_3). Use of an acidic solution, prevents scavenging of metal ions by any Fe^{3+} hydroxide precipitates formed at higher pH values. Nevertheless, this extraction phase does not completely oxidise all forms of organic matter present, and does not dissolve all metal sulphides, as apparently is the case with the Lavrion overburden samples. It is reported that dissolution of galena (PbS), cinnabar (HgS), orpiment (AsS_3), stibnite (SbS_3), sphalerite [Zn,Fe)S] and tetrahedrite [$(Cu,Fe)_{12}S(SbS_3)_4$] to be near total, whereas pyrite (FeS_2) and chalcopyrite ($CuFeS_2$) may be only moderately decomposed (40-70%), and

molybdenite (MoS_2) is scarcely affected. Consequently, the incompletely digested organic matter and sulphides of this step are completely decomposed in the final step of the sequential extraction procedure, the residual.

Recovery of elements associated with organic matter and sulphides poses, however, some problems, for there is a violent reaction of HNO_3 with H_2O_2. Soils and sediments having comparatively high $CaCO_3$ contents, not completely digested by the previous phases, enhance the violent reaction when the acid mixture is added. To avoid this violent exothermic reaction, an initial decalcification of the solids is recommended. However, in this study placing the test tubes, with the sample solution, in an ice bath slowed the chemical attack down. The volume of the acid mixture was added dropwise, waiting until the reaction was over before adding the next drop.

7.4.1.5. Residual Fraction

Elements incorporated in the crystal structure of silicate and refractory minerals are released by attacking the residue from the previous step with a dissolution agent, which completely destroys the basic crystal lattice of minerals. Such complete destruction of the final residue, comprised of silicates and resistant mineral species, is effected by a triple acid mixture (HNO_3/$HClO_4$/HF) and subsequently by HCl. It is noted that in this study, sulphide minerals, incompletely dissolved during the previous extraction step, are completely decomposed too. This attack by strong acids, although considered to be total, in some cases it may not be able to dissolve completely the most refractory silicate and oxide minerals, such as tourmaline [$(Na,Ca)(Mg,Fe^{2+},Fe^{3+},Al,Li)_3Al_6(OH)_4(BO_3)_3(Si_6O_{18})$], beryl [$Al_2(Be_3Si_6O_{18})$], chromite [$(Cr,Al)_2(Fe,Mg)O_4$] sphene or titanite [$Ca(TiO)(SiO_4)$], cassiterite ($SnO_2$), and scheelite ($CaWO_4$), thus leaving a small residue (Fletcher, 1981; Hall *et al.*, 1996).

7.5. PARTITIONING OF OPERATIONALLY DEFINED PHASES IN OVERBURDEN

Concentrations of elements for each of the five operationally defined selective extraction phases, *i.e.*,

- adsorbed and exchangeable forms *(step 1: exchangeable phase)*,
- bound to carbonates and to specifically adsorbed sites *(step 2: carbonate phase)*,
- bound to Fe and Mn oxides *(step 3: reducible phase)*,
- bound to organic matter and sulphides *(step 4: oxidisable phase)*, and
- within the structure of silicate and refractory minerals *(step 5: residual phase)*,

are presented as coloured five-bar plots for each of the 224 samples at their respective sampling sites on maps with the three major categories of metallurgical processing wastes (Maps 7.1 to 7.30 in Volume 2) . This method shows pictorially the actual levels of elements in each of the five sequential extraction phases for every sample, and spatial variability. Hence, within and between sample comparisons can be made with ease, and related to the metallurgical processing wastes and contaminated soil (residual or alluvial). Statistical parameters of each of the five phases are also presented on the maps, and a summary of the sequential extraction scheme in a flow diagram. Hence, the reader has all the necessary information to study in detail the variation of element concentrations of each of the five extraction phases without referring to the following description of results.

For a detailed study of the sequential extraction results on overburden samples, the following tables and figures have been compiled/drawn for each element, and will be found in Appendix 3A of Volume 1A (p. 39-102) of this report:

- table showing the percentage proportion of the element extracted by each of the five sequential extraction steps out of the total;
- tables of statistical parameters of overburden samples taken from (a) contaminated soil, (b) flotation residues, (c) earthy material within slag, and (d) pyritiferous wastes (including pyrite tailings and pyritiferous sand).
- multiple boxplot of the distribution of each element in the five phases of the sequential extraction procedure (the statistical parameters of this particular plot are tabulated on Maps 7.1 to 7.30, Chapter 7 in Volume 2 of this report), and
- multiple boxplots of the distribution of element concentrations in the five phases of the sequential extraction procedure in the different sample types, *i.e.*, (a) contaminated soil, (b) flotation residues, (c) earthy material within slag, and (d) pyritiferous wastes. These plots should be studied in conjunction with the respective statistical tables.
- Pearson's linear correlation coefficient was calculated for each of the five steps for 22 elements and pH, and the correlation matrices are presented in Tables 7.106A-.110A in Appendix 3A of Volume 1A (p.93-101). Data were normalised by the 2-parameter log transformation used by Miesch (1990) in the G-PREP module of program G-RFAC. This is the most widely applied transformation in chemometrics. The 2-parameters are the mean log and log variance, which completely define a lognormal distribution. Correlation coefficients range between –1 and +1 and measure the strength of the linear relationship between the variables.
- R-mode cluster and factor analyses were performed on log transformed results of each of the five extraction steps for 22 elements and pH, and presented in the form of dendrograms (Figs. 7.1 to 7.5 in this Chapter, and 7.43A-.47A in Appendix 3A, Volume 1A, p.94-102) and Tables 7.1 to 7.5. Since, element data are in different concentration ranges, they were standardised after being transformed by the 2-parameter log transformation, but prior to calculation of dendrogram and factor parameters. This step was necessary in order to equalise the influence of the variables during R-mode cluster analysis.

The statistical significance of the estimated correlation coefficients is normally tested by the p-values test. P-values, for example, below 0.05 indicate statistically significant non-zero correlation coefficients at the 95% confidence level. The following pairs of variables from Table 7.110A have p-values below 0.05:

Ag and Al (r=-0.37; p=0.0000), Ag and Be (r=-0.281; p=0.0000), Ag and Ca (r=0.600; p=0.0000), Ag and Cd (r=0.718; p=0.0000), Ag and Cr (r=-0.385; p=0.0000), Ag and Cu (r=0.736; p=0.0000), Ag and Fe (r=0.460; p=0.0000), Ag and K (r=-0.262; p=0.0001), Ag and La (r=0.213; p=0.0014), Ag and Li (r=-0.236; 0.0004), Ag and Mn (r=0.152; p=0.0231), Ag and Mo (r=0.302; p=0.0000), Ag and Ni (r=-0.258; p=0.0001), Ag and P (r=0.288; p=0.0000), Ag and Pb (r=0.882; p=0.0000), Ag and pH (r=-0.155; p=0.0206), Ag and Sr (r=0.366; p=0.0000), Ag and Ti (r=-0.399; p=0.0000), Ag and Zn (r=0.872; p=0.0000).

The following pairs of variables indicate non-significant correlation coefficients at the 95% confidence level, because they have p-values over 0.05:

- Ag and Ba (r=0.0403; p=0.5487), Ag and Co (r= -0.0267; p= 0.6910), and
- Ag and V (r= -0.0744; p=0.2678).

The above analysis concerns statistical significance testing of non-zero correlation coefficients at the 95% confidence level, but it does not help, however, in the geochemical interpretation of correlation coefficients. Hence, the following qualitative scale has been devised for geochemical interpretation:

- high or strong positive correlation coefficient: r > 0.60;
- moderate positive correlation coefficient: r > 0.40 to <0.60;
- low or weak positive correlation coefficient: r > 0.20 to <0.40;
- low or weak *negative* correlation coefficient: r <-0.20 to >-0.40;
- moderate *negative* correlation coefficient: r <-0.40 to >-0.60, and
- high or strong *negative* correlation coefficient: r <-0.60.

It is noted that tables and figures with the suffix "A" will be found in Appendix 3A of Volume 1A of this report (p. 39-102); normal numbered tables and figures are within the text of this chapter. The following description and discussion of overburden sequential extraction results is made with reference to the distribution map, tables and figures for each element, the lithological and overburden pH maps (Maps 2.2, 2.5; Volume 2). *For better reading, the geochemical distribution map, tables and figures of each element will be mentioned after the title, and not in the descriptive text, except reference to dendrograms, correlation matrices (Appendix 3A in Volume 1A), and other maps in Volume 2.*

Since, the results presented, may be interpreted in different ways, depending on the interests of the end-user, the following description and discussion of results should serve as a guide to the most significant parts of the distribution of element contents in the five operationally defined geochemical phases.

7.5.1. PARTITIONING OF SILVER (Ag) IN OVERBURDEN (Map 7.1, Tables 7.1A-.5A, Figs. 7.1A-.2A)

The most significant fraction for Ag in overburden is extraction step 5 (residual phase), which accounts for 30.72 to 98.60% of the total content (median=93.20%; <1-198 ppm; Ag; median=11.30 ppm Ag). This indicates that Ag mainly occurs in the crystal lattice of minerals. The second important fraction for Ag appears to be the exchangeable phase in samples of pyritiferous wastes (including pyrite tailings and pyritiferous sand) in the Komobil area, with values from 4 to 21.7 ppm Ag. The association of comparatively high Ag contents in pyritiferous wastes suggests that pyrite has been oxidised, and released some of its trace elements, which have been loosely adsorbed on overburden particles.

Silver (Ag) is associated with

(a) Pb (r=0.88), Zn (r=0.87), Cu (r=0.74), Cd (r=0.72) and Fe (r=0.46) in the residual phase (sequential extraction step 5); Table 7.110A; Fig. 7.47A), and
(b) Pb (r=0.56), Cd (r=0.54) and Zn (r=0.52) in the exchangeable phase (step 1; Table 7.106A; Fig. 7.43A).

In the other steps, it is weakly associated with some elements (Tables 7.107A-.108A, Figs. 7.44A-.46A). The correlation of Ag with elements Pb, Zn, Cu, Cd and Fe in the residual phase suggests that sulphides were not completely dissolved in step 4 (organic/ sulphide phase).

According to Kabata-Pendias and Pendias (1984), total Ag levels above 2 ppm in soil are considered to be phytotoxic. The combined exchangeable and carbonate Ag concentrations, which are regarded to be easily available to plants, have the following ranges in samples of

- contaminated soil from 0.10 to 2.58 ppm (mean=0.46 ppm; median=0.36 ppm);
- flotation residues from 0.10 to 4.14 ppm (mean=0.57 ppm; median=0.42 ppm)
- earthy material within slag from 0.10 to 6.24 (mean=0.63 ppm; median=0.28 ppm), and
- pyritiferous sand from 0.10 to 22.42 ppm (mean=3.31 ppm; median=0.62 ppm).

Hence, part of the overburden in Lavrion is unfit for plant growth with respect to Ag.

7.5.2. PARTITIONING OF ALUMINIUM (Al) IN OVERBURDEN (Map 7.2, Tables 7.6A-.10A, Figs. 7.2A-.4A)

The greatest proportion of Al is found in the residual fraction, which accounts for 57.69 to 99.10% of the total content (median=96.61%; 7,510-83,200 ppm Al; median=30,850 ppm). This indicates that Al occurs in the crystal lattice of mainly rock forming minerals. Low levels of Al are found in the reducible phase – the Fe-Mn fraction (130-4840 ppm Al; median=550 ppm Al), oxidisable phase (81-3440 ppm Al; median=562.5 ppm Al), and carbonate phase (4-1580 ppm Al; median=28.0 ppm Al). Very low levels of Al occur in the exchangeable phase (<1-212 ppm Al; median=9 ppm Al).

The highest Al levels in the carbonate and reducible phases are found at Kavodokanos over pyritiferous tailings, flotation residues, slag and nearby contaminated garden soil.

Aluminium is associated with

(a) Fe in the carbonate phase (step 2; r=0.93, Table 7.107A; Fig. 7.44A), reducible phase (step 3, Fe-Mn oxide phase; r=0.79, Table 7.108A; Fig. 7.45A), and exchangeable phase (step 1; r=0.57; Table 7.107A; Fig. 7.43A);
(b) K (r=0.91), Ti (r=0.91), Be (r=0.90), Li (r=0.84), Ni (r=0.64), V (r=0.63) and La (r=0.48) in the residual phase (step 5; Table 7.110A; Fig. 7.47A), and
(c) Be (r=0.74), Li (r=0.73), K (r=0.66) and La (r=0.64) in the oxidisable phase (step 4, organics/sulphides; Table 7.109A, Fig. 7.46A).

Oxides of Al, especially the hydroxides, can bind some heavy metals in soil in the same manner as Fe oxides (Beckett, 1988), and a strong correlation has been shown to exist between heavy metals, such as Pb, with Al extracted in step 3, the Fe-Mn oxide fraction (Li, 1993). In the Lavrion overburden, there is also a high positive correlation in the Fe-Mn oxide phase between Al-Fe (r=0.79), Al-Be (r=0.75), Al-Zn (r=0.59), Al-Pb (r=0.56), Al-Mn (r=0.55) and Al-Ni (r=0.52) (Table 7.108A, Fig. 7.45A), suggesting that Al hydroxide/oxide is an important binding agent.

7.5.3. PARTITIONING OF BARIUM (Ba) IN OVERBURDEN (Map 7.4, Tables 7.11A-.15A, Figs. 7.5A-.6A)

The partitioning patterns of Ba have a large variation in the different phases, and are dependent on sample types, and differences in the chemistry of metallurgical processing wastes and contaminated soil. Overall the residual fraction accounts for 0.78 to 93.88% of the total content (median=78.58%; 20.4-4040 ppm Ba; median=346.5 ppm Ba).

The second and third most important fractions are the reducible (0.38-80.94% of the total; median=9.86%; 1-2130 ppm Ba; median=39.2 ppm Ba), and the carbonate (0.59-58.94% of the total; median=5.68%; 1.6-1370 ppm Ba; median 23.7 ppm Ba) phases. It appears, therefore, that the largest proportion of Ba occurs in

(a) the crystal lattice of mainly rock-forming minerals, referring to the comparatively moderate positive correlation in the residual fraction with Ti (r=0.55) and Sr (r=0.42), (Table 8.110A, Fig. 8.47A);
(b) Fe-Mn and Al oxides, since it has a high to moderate correlation coefficient in the reducible (Fe-Mn oxide) phase with Fe (r=0.83), Mn (r=0.59), and Al (r=0.57), and other elements associated with this phase, such as Zn (r=0.70), K (r=0.69), Li (r=0.46), Pb (r=0.45), (Table 8.108A, Fig. 8.45A), and
(c) the specifically adsorbed sites of the carbonate phase, and to a lesser extent with calcium minerals, because of its low correlation with Ca (r=0.09), and its high correlation with Al (r=0.83), Fe (r=0.83), Mn (r=0.83), Ti (r=0.75), K (r=0.66), Mo (r=0.61), Be (r=0.61), Co (r=0.59) and Zn (r=0.52) (Table 7.107A, Fig. 7.44A), suggesting a relationship with adsorption sites occurring on the surfaces of amorphous precipitates of alumino-silicates, aluminium, iron and manganese oxides, other micro-crystalline precipitates of oxides, but not phosphates, for it has a negative correlation with P (r=-0.05).

The first case is the dominant one, for it concerns most of the Lavrion overburden samples. The second and third cases refer to samples of flotation residues, earthy material within slag (*slag earth*), and contaminated soil collected from Kavodokanos, and to a lesser extent within the premises of the smelter at Kiprianos and Phenikodassos.

Regarding the readily available (combined exchangeable and carbonates fractions) concentrations of Ba to plants, these vary from <1.0 to 1413 ppm Ba. According to Kabata-Pendias and Pendias (1984), total Ba levels above 220 ppm in soil are considered moderately phytotoxic. Consequently, part of the Lavrion overburden (*e.g.*, contaminated soil and flotation residues), under this premise, is unfit for plant growth (Map 6.4). Further, referring to the Finnish statutory guide and limiting value of 600 ppm total Ba for residential soil (Koljonen, 1992; R. Salminen, person. commun., 1996), there is apparently a hazard to human health.

7.5.4. PARTITIONING OF BERYLLIUM (Be) IN OVERBURDEN (Map 7.5, Tables 7.16A-.20A, Figs. 7.7A-.8A)

The largest proportion of Be occurs in the residual phase, which accounts for 21.64 to 88.39% of the total content (median=80.25%; 0.1 to 1.9 ppm Be; median=0.8 ppm Be). The second and third most significant fractions are the reducible (4.06-49.96% of the total; median=12.75%; 0.03-0.6 ppm Be; median=0.13 ppm Be) and carbonate (0.24-31.13% of the total; 0.004-0.3 ppm Be; median=0.036 ppm Be) phases. It is apparent that, like Ba, the largest proportion of Be occurs in

(a) the crystal lattice of mainly rock-forming minerals, referring to its high to moderate positive correlation with K (r=0.88), Li (r=0.86), Ti (r=0.79), Ni (r=0.57), La (r=0.54) and V (r=0.54) (Table 7.110A, Fig. 7.47A);
(b) Al and Fe-Mn oxides, since it has a high to moderate positive correlation in the reducible (Fe-Mn oxide) phase with Al (r=0.75), Fe (r=0.50), Mn (r=0.47), Li (r=0.72), Co (r=0.59) and Ni (r=0.55) (Table 7.108A, Fig. 7.45A), and

(c) the specifically adsorbed sites of the carbonate phase, and not with calcium carbonate minerals, because of its negative correlation with Ca (r=-0.006), and its high positive correlation with Ti (r=0.75), Al (r=0.64), Fe (r=0.64), V (r=0.62), Mo (r=0.60), Mn (r=0.59), Li (r=0.55), La (r=0.53), and Co (r=0.52) (Table 7.107A, Fig. 7.44A), suggesting a relationship with adsorption sites occurring on the surfaces of amorphous precipitates of alumino-silicates, aluminium, iron and manganese oxides, other micro-crystalline precipitates of oxides, but not so much with phosphates, for it has an insignificant positive correlation with P (r=0.03).

The first case is the dominant one, for it concerns most of the Lavrion overburden samples. The second (Fe-Mn phase) and third (carbonate phase) cases, refer to samples from slag earth, flotation residues, contaminated residual soil and pyritiferous sand, collected from different parts of Lavrion, and in particular Kavodokanos, and to a lesser extent within the premises of the smelter at Kiprianos, Fougara, Ayios Andreas and Phenikodassos.

Regarding the readily available (combined exchangeable and carbonate fractions) concentrations of Be to plants, these vary from <0.001 to 0.35 ppm Be. The levels are very low, but as discussed in Chapter 6, this is an element that requires further investigation, because it is a known carcinogen (Gough *et al.*, 1979; Reimann *et al.*, 1998).

7.5.5. PARTITIONING OF CALCIUM (Ca) IN OVERBURDEN (Map 7.8, Tables 7.21A-.25A, Figs. 7.9A-.10A)

The partitioning patterns of Ca show that the carbonate and reducible phases account for 7.29-78.90% (median=32.32%) and 0.77-77.73% (median=46.40%) of the total content respectively, *i.e.*, their corresponding levels being 451-55,300 ppm Ca (median=31,500 ppm Ca) and 206-179,000 ppm Ca (median=43,600 ppm Ca). The most important phase, with respect to the level of Ca, is the reducible (Fe-Mn oxide) phase, and not the carbonate phase. It appears, therefore, that CH_3COONa (*NaOAc*) was not able to extract the greatest proportion of the total $CaCO_3$-bound calcium, which is present in carbonate rich soil and flotation residues. According to Tessier *et al.* (1979) the attack by CH_3COONa is able to dissolve successfully even dolomite ($CaCO_3MgCO_3$). Assuming that this is true, then the apparent incomplete dissolution of Ca from calcite and dolomite by CH_3COONa, suggests that either there are other modes of occurrence of Ca in Lavrion or the proportion of calcium carbonate minerals was very high, and could not be totally digested.

Calcium occurs in ankerite [$Ca(Fe^{2+},Mg)(CO_3)_2$], aragonite ($CaCO_3$), gypsum ($CaSO_4.2H_2O$) and other less common minerals in Lavrion, as well as in slag and sand blast material. Minerals requiring a stronger dissolution agent, such as hydroxylammonium hydrochloride ($NH_2.OH.HCl$) dissolved in acetic acid (HOAc), used in extraction step 3 (Fe-Mn oxide phase).

Li (1993) in his interpretation of Ca levels in the Fe-Mn oxide fraction of the smelting area studied, he suggested the presence of $CaSO_4$. The Lavrion overburden materials appear to be more complex in their mineralogy. It is interesting to note that in the Fe-Mn phase, Ca has a low negative correlation with Fe (r=-0.13) and Mn (r=-0.19) indicating that it is not related to either Fe or Mn oxides. Thus, supporting the interpretation of incomplete dissolution of calcium carbonate minerals in step 2 (carbonate phase) of the sequential extraction procedure.

The levels of Ca in the exchangeable and residual phases are of local significance, and depend on its mode of occurrence in contaminated soil and pyritiferous wastes (pyrite tailings and pyritiferous sand). The comparatively high exchangeable phase Ca contents in samples of pyritiferous wastes at Komobil, Kiprianos and Kavodokanos reflect the influence of low pH, a feature also noted by Li (1993). Whereas the relatively low residual phase Ca levels, even in earthy material within slag (*slag earth*), which is directly related to slag, probably indicates that low amounts of Ca are incorporated in silicate glass during the smelting process.

Calcium is strongly related to Sr in extraction steps 1 to 4, indicating the diadochic substitution of Ca by Sr in such minerals as aragonite and dolomite (Rankama and Sahama, 1952; Mason, 1966; Goldschmidt, 1970) (Figs. 7.43A-.46A; Tables 7.106A-.109A). In the two dominant phases, Ca has the following linear correlation coefficient with other elements:

- carbonate phase: Sr (r=0.80); La (r=0.51) and pH (r=0.31), and
- reducible (Fe-Mn oxide) phase: Sr (r=0.87); P (r=0.63); La (r=0.62); pH (r=0.33).

The relationship of Ca with La in both phases is again explained by diadochic substitution in calcium carbonate minerals (Rankama and Sahama, 1952; Goldschmidt, 1970). Correlation of Ca with P is considered to be anthropogenically induced, by the application of phosphate fertilisers in the “garden soils” of Lavrion. This inference is supported by the distribution of comparatively high reducible phase Ca levels in inhabited areas, which have gardens. The moderate positive correlation of pH with Ca, indicates the dependency of the former on the concentration of the latter.

Although Ca is essential for most organisms and a major plant nutrient, and is generally not toxic, excessive absorption may cause problems, such as hypercalcaemia, *i.e.*, abnormally high blood levels of Ca (Mervyn, 1985, 1986). The range of readily available Ca (exchangeable and carbonate phases) varies from 838 to 72,200 ppm. This suggests that the medical effects of abnormally high Ca absorption should be studied.

7.5.6. PARTITIONING OF CADMIUM (Cd) IN OVERBURDEN (Map 7.9, Tables 7.26A-.30A, Figs. 7.11A-.12A)

Cadmium shows highly variable partitioning patterns in all five steps, which depend on the mineralogical composition of overburden. Although the reducible phase is the most significant, since it accounts for 7.72-77.97% of the total (median=42.55%; 1 to 327 ppm Cd; median=16 ppm Cd), the other phases also extract considerable amounts of Cd, *i.e.*,

- residual: 1.10-65.22% of the total (median=12.44%; 0.20-360 ppm Cd; median=5 ppm Cd),
- oxidisable: 1.38-61.30% of the total (median=5.20%; 0.07-201 ppm Cd; median=2 ppm Cd),
- carbonate: 0.54-54.67% of the total (median=29.38%; 0.40-221 ppm Cd; 10.2 ppm Cd), and
- exchangeable: 0.73-42.18% of the total (median=6.30%; 0.05-79.7 ppm Cd; median=2.6 ppm Cd).

Contaminated soil, in almost the whole of the study area, has generally the lowest Cd contents in all five phases. Exceptions, to this general observation, are soil samples near to metallurgical processing wastes, which have definitely a strong influence through aerial transportation of contaminants, *e.g.*, Fougara, Prasini Alepou, Kiprianos.

The most significant phases for comparatively high Cd levels, in samples of flotation residues, slag earth and pyritiferous wastes, are the carbonate and reducible phases. The residual phase is important only for samples of slag earth.

Cadmium has the following linear correlation coefficients with other elements in the different phases (Tables 7.106A-.110A; Figs. 7.43A-.47A):

- exchangeable phase: r_{Cd-Pb}=0.74; r_{Cd-Zn}=0.73; r_{Cd-Ag}=0.54;
- carbonate phase: r_{Cd-Pb}=0.72; r_{Cd-Zn}=0.58; r_{Cd-Cu}=0.53;
- reducible phase: r_{Cd-Zn}=0.82; r_{Cd-Pb}=0.75; r_{Cd-Mn}=0.47; r_{Cd-Fe}=0.36; r_{Cd-Cu}=0.36;
- oxidisable phase: r_{Cd-Zn}=0.88; r_{Cd-Cu}=0.81; r_{Cd-Mn}=0.56;
- residual phase: r_{Cd-Pb}=0.83; r_{Cd-Zn}=0.77; r_{Cd-Cu}=0.72; r_{Cd-Ag}=0.72; r_{Cd-Fe}=0.56;

Cadmium in all phases has a high correlation coefficient with Zn; in the exchangeable phase has also a high correlation with Pb and Ag; in the carbonate phase with Pb and Cu; in the reducible phase with Pb, Mn and Fe; in the oxidisable phase with Cu and Mn, and in the residual phase with Pb, Cu, Ag and Fe. The above associations suggest that Cd is related to the smelting activities of sulphide ore. Weathering processes have released Cd and the other ore elements, which were subsequently adsorbed at exchangeable sites, bound with carbonates and adsorbed on Fe-Mn oxides. Cadmium in the organic/sulphide and residual phases is mainly related to sulphides.

According to Kabata-Pendias and Pendias (1984), the maximum permissible level of total Cd in soil for healthy plant growth is 8 ppm, and values above this limit are reckoned to be phytotoxic. The combined exchangeable and carbonate phase Cd contents, which are considered to be readily available vary from 0.45 to 301 ppm, meaning that most of the Lavrion overburden is toxic to plants. Further, available overburden Cd contents exceed statutory residential limits, which vary from 2-34 ppm total Cd depending on the country of origin (refer to Chapter 6, Table 6.3, p.139). Hence, the greatest part of the Lavrion urban overburden/soil is regarded to be a potential health hazard with respect to cadmium.

7.5.7. PARTITIONING OF COBALT (Co) IN OVERBURDEN (Map 7.10, Tables 7.31A-.35A, Figs. 7.13A-.14A)

The partitioning patterns of Co indicate that the most significant phases are the residual and reducible (Fe-Mn oxide fraction), which account for 21.18-83.79% and 3.90-71.25% of the total content respectively, *i.e.* 2.0-82.3 ppm Co (median=7.75 ppm) and 0.3-22.9 ppm Co (median=4.87 ppm). The readily available exchangeable and carbonate phase Co contents, as well as total levels (see Chapter 6), are low, hence this element is not regarded to be hazardous to plants, animals and humans. Geochemically, however, its relationships with other elements are interesting, even at such low concentrations.

In the exchangeable phase Co has a moderate positive correlation coefficient with Ni (r=0.42), and both elements have a strong negative correlation with pH (r_{Co-pH}=-0.54; r_{Ni-pH}=-0.45; Table 7.106A), indicating their relationship with the acidic environment occurring in the pyritiferous wastes at Nichtochori and Komobil.

Cobalt in the carbonate phase is not related to Ca, and to carbonates, but to elements such as Al, Mn, Fe, Zn, Ba, Ti and Be (Table 7.107A, Fig. 7.44A), suggesting,

therefore, a relationship with specific adsorption sites occurring on the surfaces of amorphous precipitates of alumino-silicates, aluminium, iron and manganese oxides, other micro-crystalline precipitates of oxides, but not phosphates, for it has almost no correlation with P (r=0.01).

Reducible phase Co, apart from its association with Mn (r=0.54), and very weak positive correlation with Fe (r=0.15), it is positively correlated with Ni (r=0.76) and Be (r=0.59) (Table 7.108A, Fig. 7.45A), suggesting, therefore, adsorption mainly by Mn oxides, and to a far lesser extent by Fe oxides.

Cobalt in the oxidisable phase is strongly correlated with Ni, Fe and Mn, elements associated with sulphides (*e.g.*, pyrite) (Table 7.109A, Fig. 7.46A).

Finally, Co in the residual phase is strongly correlated with Pb, Zn and Cu, and moderately related to Fe, Mn and Mo (Table 7.110A, Fig. 7.47A), suggesting that sulphides were not completely attacked by the oxidisable phase extraction.

7.5.8. PARTITIONING OF CHROMIUM (Cr) IN OVERBURDEN (Map 7.11, Tables 7.36A-.40A, Figs. 7.15-.16)

The dominant phase of Cr is the residual, which accounts for 1.25-99.59% of the total content (median=93.38%; <1 to 922 ppm Cr; median=171.5 ppm Cr). The next two comparatively important phases of Cr are the carbonate and reducible, especially for samples of contaminated soil.

Chromium in the residual phase is negatively correlated with Cu (r=-0.56) and Fe (r=-0.65), and has a positive correlation with Ni (r=0.44) and Ti (r=0.42) (Table 7.110A, Fig. 7.47A). This relationship suggests that Cr is related not to sulphides, but to femic and mafic rock forming minerals occurring in weathered detritus in residual soil developing over schist, and prasinite.

In the carbonate phase, Cr is negatively correlated with Pb (r=-0.26), Zn (r=-0.14) and Cu (r=-0.34), indicating that it is not related to the smelting operations of sulphide ore. It has a low, but significant, positive correlation with Ca (r=0.27), moderately positive correlation with La (r=0.55), P (r=0.46) and V (r=0.32), and low negative correlation with Al (r=-0.10) and Fe (r=-0.02). This relationship suggests that Cr is weakly related to calcium carbonate minerals, and has a stronger relationship with calcium phosphates. Chromium is present in femic minerals, such as amphibole, biotite and chlorite, occurring in schist, and pyroxene in prasinite, and is released during weathering (Rankama and Sahama, 1952). As pointed out by Goldschmidt (1970) a high pH value might favour oxidation of chromic ions to chromate, which may be the case in Lavrion.

Soil developing over schist should, therefore, explain the chromium levels of step 2 (0.4-210 ppm Cr; median=23.2 ppm Cr). However, the carbonate phase Cr patterns are not directly related to soil developing over schist and prasinite (refer to the lithological map, Map 2.2, Volume 2). In fact, soil samples directly over schist have very low Cr levels in the carbonate phase. Consequently, another explanation must be sought to interpret these patterns. The moderate correlation of Cr with P and their approximately similar distribution patterns in the carbonate phase (Map 7.21), which occur in the inhabited area of Lavrion with gardens, suggest that it is related to phosphate fertilisers. According to Kabata-Pendias and Pendias (1984) phosphate fertilisers have Cr contents between 66-245 ppm.

Reducible Cr contents are negatively correlated with Fe (r=-0.33), Mn (r=-0.33), and Al (r=-0.29), suggesting that they are not adsorbed on Fe-Mn oxides and Al oxides. Chromium has also a negative correlation with Cu (r=-0.39), Pb (r=-0.34), Zn (r=-0.25), indicating that it is not associated with contaminants from the smelting of sulphide ore. Its moderately strong positive correlation with P (r=0.53) and similar distribution pattern, suggests again a relationship with phosphate fertilisers used in houses with gardens (refer to land use map, Map 2.4, Volume 2). Further, its moderate positive correlation with K (r=0.38), possibly implies that it occurs as potassium chromate ($K_2Cr_2O_7$).

Readily available contents of Cr vary from 0.5 to 248.6 ppm (exchangeable and carbonate phase), suggesting that continuous use of phosphate fertilisers resulted in the abnormal concentration of bioavailable Cr in soil. In case chromium is in the form of chromates, because of alkaline conditions, then the hazards are greater for it is particularly phytotoxic even at levels of 10-15 ppm Cr (Gough *et al.*, 1979). For total Cr contents, onset of phytotoxicity appears to begin from 75 ppm (Kabatas-Pendias and Pendias, 1984). Chromium has been reported as a possible factor in causing "yellow leaf" disease (chlorosis) in citrus plants (Goldschmidt, 1970), and reduced growth in tomatoes and potatoes (Gough *et al.*, 1979).

Regarding the residential soil statutory limits for total Cr contents they vary from 100 to 3900 ppm (see Chapter 6), hence some areas in Lavrion are potentially hazardous to human health, for the combined exchangeable and carbonate phase contents are considered to be bioavailable.

7.5.9. PARTITIONING OF COPPER (Cu) IN OVERBURDEN (Map 7.12, Tables 7.41A-.45A, Figs. 7.17A-.18A)

The important phases of Cu are the residual and oxidisable, which account for 17.12-83.59% (median=55.17%) and 4.22-74.85% (median=39.18%) of the total content, respectively (*i.e.*, residual: 30.1-2520 ppm Cu; median=90.6 ppm Cu; oxidisable: 5.2-2480 ppm Cu; median=72 ppm Cu). The other phases are not significant, *e.g.*, the exchangeable phase extracts up to 15.3 ppm Cu, and the carbonate and reducible phases are of local importance, for two-three samples have levels up to 100 and 271 ppm Cu respectively.

Samples of slag earth, pyrite, and nearby residual contaminated soil within the premises of the smelter at Kiprianos and Kavodokanos have given the greatest Cu concentrations. Other samples, with slightly elevated Cu levels, in these two phases, are from pyritiferous wastes at Nichtochori-Komobil-Kiprianos, and nearby contaminated soil, slag earth to the east of Ayia Paraskevi, and contaminated soil at Noria-Neapoli, near to slag heaps, or developed over altered marble. It is worth noting that slag earth and adjoining soil from the Fougara area have low Cu contents in all five phases in comparison to similar samples from Kiprianos and Kavodokanos. This observation suggests that the chemical composition of processed ore was different or the smelting process has changed over time (refer to Chapter 5); in the case of Lavrion both alternatives apply. Similarly, the flotation residues at Kavodokanos have higher Cu concentrations in the residual and oxidisable phases in comparison to samples from Noria-Prasini Alepou-Santorineika.

The distribution patterns suggest that extraction step 4 (organic/sulphide phase), did not completely leach all Cu held in sulphides, even from samples of pyrite tailings, and part of it was extracted in the residual phase. Hence, because of incomplete dissolution of sulphides by the oxidisable phase, it is difficult to differentiate the amount of Cu held

in the glassy part of slag, which was released by the residual phase extraction. This inference is supported by the association of Cu with other elements as indicated for

(a) the organic/sulphide phase by the strong positive correlation of Cu with Zn (r=0.91), and Cd (r=0.81), and moderately strong with Mn (r=0.56), and Fe (r=0.42), elements occurring in pyrite and other sulphides, and
(b) the residual phase by the strong positive correlation of Cu with Zn (r=0.90), Fe (r=0.80), Pb (r=0.78), Ag (r=0.74) and Cd (r=0.72), and moderately strong with Mn (r=0.55) and Mo (r=0.46), elements again occurring in pyrite and other sulphides (Tables 7.109A-.110A; Figs. 7.46A-.47A).

The low to moderate positive correlation of Cu with Mn, Zn, P and Pb (Table 7.106A), and its weak relationship with the cluster of elements of Ca-Sr-K-La-Mn-P-V (Fig. 7.43A) in the exchangeable phase, point to its adsorption on clay minerals in soil, and other detrital calcium-bearing minerals occurring in metallurgical processing wastes.

In the carbonate fraction, the negative correlation of Cu with Ca (r=-0.12) indicates that it is not related to calcium carbonate, but to other specific adsorption sites, such as on surfaces of amorphous precipitates of Mn (r=0.25), Al (r=0.21) or Fe (r=0.13) oxides, alumino-silicates (clays), silica, and micro-crystalline precipitates of oxides, and carbonates, but not to phosphates due to the negative correlation with P (r=-0.29) (Table 7.107A).

In the reducible phase, Cu appears to be weakly associated with Fe-Mn oxides, and other elements adsorbed on them, such as Cd, Co, Pb and Zn (Table 7.108A). This weak relationship is shown by the dendrogram (Fig. 7.45A).

Phytotoxic levels of total Cu in surface soil vary from 60 to 125 ppm (Kabata-Pendias and Pendias, 1984), EDTA extractable Cu has a threshold trigger concentration of 50 ppm (ICRCL, 1987), and trigger levels for soil, which were considered appropriate for Lavrion are 130 and 150 ppm total Cu (refer to Chapter 6, Table 6.3, p.139). Readily available Cu contents (exchangeable and carbonate phase) vary from 0.31 to 286.3 ppm. Hence, some parts of Lavrion are regarded to be toxic for plants and hazardous to human health, for these concentrations exceed total statutory limits.

7.5.10. PARTITIONING OF IRON (Fe) IN OVERBURDEN (Map 7.13, Tables 7.46A-.50A, Figs. 7.19A-.20A)

Iron oxides, as has already been mentioned above, are important in binding trace elements in soil (Buckman and Brady, 1970; Russel, 1970; Jenne, 1977; Alloway, 1990; Levinson, 1974; Rose *et al.*, 1979). The first step, exchangeable phase, extracts very minor amounts of Fe from the Lavrion overburden (up to 0.67% of the total; 0.4-408 ppm Fe; median=11 ppm Fe). The second step, carbonate phase, extracts up to 29.73% of the total (2-30,500 ppm Fe; median=22 ppm Fe). The Fe-Mn oxide fraction, reducible phase, accounts for 1.26-42.67% (median=0.02%) of the total Fe content in overburden samples (628-79,800 ppm Fe; median=2015 ppm Fe), which probably is mainly derived from amorphous Fe oxides as suggested by Tipping *et al.* (1986) and Kim and Ferguson (1991). The organic/ sulphide, oxidisable phase, leaches up to 31.38% (25-37,000 ppm Fe; median=426.5 ppm Fe). The most important phase with respect to Fe is, however, the residual, which accounts for 36.4-98.11% (median=93.80%) of the total Fe (17,500-310,000 ppm Fe; median=41,750 ppm Fe).

Samples from pyritiferous tailings and sand, flotation residues, slag earth and nearby contaminated soil (Nichtochori-Komobil-Kiprianos-Kavodokanos) have the greatest concentrations of Fe in the residual phase, the highest proportion being in the pyritiferous wastes. Overburden samples from the same areas have also the highest Fe contents in the reducible phase (Fe-Mn oxide fraction).

In the residual phase Fe has a high positive correlation with Cu (r=0.80), Mn (r=0.71), Zn (r=0.66), Cd (r=0.56) and Pb (r=0.55), and a moderate correlation with Ag (r=0.46), Mo (r=0.46) and Co (r=0.40), elements normally occurring in pyrite (Table 7.110A; Fig. 7.47A). This element association supports the observation, already made above, about the incomplete destruction of primary sulphide minerals in step 4 (organic/sulphide phase).

Iron in the reducible (Fe-Mn oxide) phase has a high positive correlation with Al (r=0.788), Zn (r=0.69), Ba (r=0.65), Mn (r=0.59) and Pb (r=0.55), and a moderate positive correlation with Be (r=0.50), Ti (r=0.47), V (r=0.45) and Li (r=0.44) (Table 7.108A; Fig. 7.45A). This association suggests that Fe is associated with Al and Fe-Mn oxides in samples of slag earth and contaminated soil, and that a minor proportion is derived from oxidised pyrite.

Exchangeable Fe has strong to moderate positive correlation coefficients with Al (r=0.57), Ni (r=0.48), Zn (r=0.48) and Pb (r=0.44), showing that Fe is adsorbed on easily exchangeable sites, but also that $MgCl_2$ has extracted very low amounts of Al, suggesting a minor attack on the substrates (*e.g.*, clay minerals, organic matter, oxides and sulphides) (Table 7.106A; Fig. 7.43A).

In the carbonate phase Fe has a strong positive correlation with Al (r=0.93), Mn (r=0.87), Ba (r=0.83), Ti (r=0.80), Co (r=0.73), Li (r=0.67), Be (r=0.64), Zn (r=0.62) and Mo (r=0.60), and a moderate positive correlation with K (r=0.53), Ni (r=0.44) and V (r=0.42) (Table 7.107A; Fig. 7.44A). Since, it is not correlated with Ca (r=0.004) the above association indicates that they are all adsorbed on the surfaces of amorphous precipitates of iron, aluminium or manganese oxides, alumino-silicates (clays), silica, and micro-crystalline precipitates of oxides, carbonates, but not phosphates, since Fe is negatively correlated with P (r=-0.01).

Oxidisable phase Fe has a high to moderate positive correlation with Co (r=0.61), Mn (r=0.49), Ni (r=0.35) and Zn (r=0.34), elements occurring in sulphides, and especially pyrite (Table 7.109A; Fig. 7.46A).

Readily available Fe contents (exchangeable and carbonate phase) vary from 2.4 to 30,908 ppm, concentrations which are below the total Fe median value of 35,000 ppm of normal world soil (Reimann *et al.*, 1998). Hence, phytotoxicity problems with respect to Fe may occur in some parts of Lavrion, because the readily available contents are high.

7.5.11. PARTITIONING OF POTASSIUM (K) IN OVERBURDEN (Map 7.15, Tables 7.51A-.55A,Figs.7.21A-.22A)

The most significant phase of K is the residual, which accounts for 37.14-98.80% of the total (median=92.51%; 2270-21369 ppm K; median=9025 ppm K). In the residual phase K is strongly correlated with Al (r=0.91), Be (r=0.88), Ti (r=0.85), Li (r=0.80), Ni (r=0.63) and V (r=0.63), moderately correlated with La (r=0.49), and weakly with Cr (r=34); it has also negative correlation coefficients with Cu (r=-0.38), Zn (r=-36), Ag (r=-0.26) and Pb (r=-0.24) (Table 7.110A; Fig. 7.47A). These element associations suggest that K in the residual

phase is related to alumino-silicate minerals occurring in overburden samples, including flotation residues and slag earth, and not to ore-related elements of smelter wastes.

The other steps are not so important, and are not discussed further. Nevertheless, it is worth mentioning that K is related mainly to rock forming elements, such as La, Li, Mn, P, Sr and Ti, suggesting a relationship with alumino-silicate minerals (Tables 7.106A-.109A; Figs. 7.43A-.46A).

Differences with respect to the partitioning patterns of K in samples of slag earth, flotation residues and nearby contaminated soil at Kavodokanos and Kiprianos, compared to samples from other parts of Lavrion, are ascribed to differences in the chemical composition of these materials, and fertilisers.

7.5.12. PARTITIONING OF LANTHANUM (La) IN OVERBURDEN (Map 7.16, Tables 7.56A-.60A, Figs.7.23A-.24A)

The most significant step for La is the residual phase, which accounts for 19.80-85.48% of the total (median=57.09%; 4.8-36.3 ppm La; median=12.75 ppm La). The next two important steps are the reducible and carbonate, which account for 1.94-36.91% (median=18.01%; 0.3-11.0 ppm La; median=4.0 ppm La) and 1.73-40.73% (median=15.54%; 0.4-10.8 ppm La; median=3.40 ppm La) of the total respectively. It is worth noting that La has approximately a similar partitioning pattern in almost all sample types.

Lanthanum in the residual phase has a moderate positive correlation with Sr (r=0.55), Be (r=0.54), K (r=0.49), Al (r=0.48), Li (r=0.47), Ba (r=0.41) and Ti (r=0.37), suggesting a relationship with rock forming alumino-silicate minerals (Table 7.110A; Fig. 7.47A).

Reducible (Fe-Mn oxide) phase La has a high positive correlation with Sr (r=0.69) and Ca (r=0.62), a moderate with Cr (r=0.43), Ba (r=0.43), Ti (r=0.40), and a weak with Zn (r=0.38), K (r=0.38), P (r=0.36), Mo (r=0.33), pH (r=0.33), Mn (r=0.29), Cd (r=0.27), Fe (r=0.26), Pb (r=0.23) and Al (r=0.20) (Table 7.108A; Fig. 7.45A). The weak positive correlation of La with Fe, Mn and Al, and the strong positive correlation with Sr and Ca, implies that only a minor proportion of La is adsorbed by Fe, Mn and Al oxides, and that the greatest proportion is associated with calcium carbonate minerals, *e.g.*, calcite [$CaCO_3$] and dolomite [$CaMg(CO_3)_2$], which are dissolved by the hydroxylamine reagent.

Carbonate phase La has a moderate positive correlation with Cr (r=0.55), Sr (r=0.55), Be (r=0.53), Ca (r=0.51), Ti (r=0.46), Ag (r=0.40), and a weak positive correlation with Co (r=0.38), Zn (r=0.37), Mn (r=0.35), Fe (r=0.32) and Al (r=0.31) (Table 7.107A; Fig. 7.44A). This association suggests that La is moderately associated with calcium carbonate minerals, but is also adsorbed on the surfaces of amorphous precipitates of manganese, iron or aluminium oxides, alumino-silicates, silica, and micro-crystalline precipitates of oxides, carbonates, and even loosely with phosphates, since La has a weak positive correlation with P (r= 0.16).

In the oxidisable (organic/sulphide) phase La has a high to moderate positive correlation with Be (r=0.65), Al (r=0.64), Li (r=0.56), Ni (r=0.46) and K (r=0.41); it has a weak correlation with Ag (r=0.32), Mn (r= 0.22) and Pb (r=0.17), and a negative correlation with Zn (r=-0.09), Cd (r=-0.12) and Cu (r=-0.22), and is not correlated with Fe (r=0.08) or Ca (r=-0.197) (Table 7.109A; Fig. 7.46A). This element association suggests that La is not related to sulphides, but to alumino-silicates.

Exchangeable phase La concentrations are very low in the Lavrion overburden samples (0.05-1.1 ppm La), and are not considered significant for further discussion.

7.5.13. PARTITIONING OF LITHIUM (Li) IN OVERBURDEN (Map 7.17, Tables 7.61A-.65A, Figs. 7.25A-.26A)

The greatest proportion of Li is in the residual phase, which accounts for 30.24-96.72% of the total (median=92.12%; 3.1-46.0 ppm Li; median=15.85 ppm Li). The next two important extraction steps are the reducible and carbonate, which account for 1.16-41.73% (median=4.47%; 0.20-6.90 ppm Li; median=0.90 ppm Li) and 0.17-31.21% (median=1.76%; 0.08-4.80 ppm Li; median=0.32 ppm Li) of the total respectively, but with comparatively low concentrations.

Samples of slag earth, flotation residues and nearby residual soil from Kavodokanos and Kiprianos have overall distinctly different partitioning patterns in comparison to all sample types from the other parts of Lavrion. These are, in fact, the samples giving the comparatively elevated reducible and carbonate phase Li contents. However, some samples of slag earth and residual contaminated soil from Fougara and Panormos have slightly elevated reducible phase Li concentrations.

In the residual phase Li has a strong positive correlation with Be (r=0.86), Al (r=0.84), K (r=0.80) and Ti (r=0.74) and a moderate correlation with V (r=0.56), Ni (r=0.51) and La (r=0.47) (Table 7.110A; Fig. 7.47A). This association suggests a relationship with alumino-silicate minerals.

The reducible phase Li has a strong positive correlation with Be (r=0.72) and Al (r=0.62), and a moderate correlation with Ba (r=0.53), Fe (r=0.44) and Ti (r=0.42), and a weak correlation with Ni (r=0.314) and Mn (r=0.31) (Table 7.108A; Fig. 7.45A). This element association suggests that Li is adsorbed on Al, Fe and Mn oxides.

Carbonate phase Li has a strong positive correlation with Ba (r=0.70), K (r=0.68), Fe (r=0.67), Mn (r=0.67) and Al (r=0.64), and a moderate correlation with Ti (r=0.57), Be (r=0.55), Mo (r=0.53), Co (r=0.47) and Zn (r=0.46) (Table 7.107A; Fig. 7.44A). This element association and the very low positive correlation with Ca (r=0.10) suggests that Li is not related to calcium carbonate minerals, but is adsorbed on the surfaces of amorphous precipitates of iron, manganese or aluminium oxides, alumino-silicates, silica, and micro-crystalline precipitates of oxides, carbonates, and even phosphates, since Li has a weak positive correlation with P (r=0.23).

Exchangeable and oxidisable phase Li concentrations are very low in the Lavrion overburden samples, *i.e.*, 0.02-1.16 ppm Li and 0.01-1.35 ppm Li respectively, and they are not considered significant for further discussion.

7.5.14. PARTITIONING OF MANGANESE (Mn) IN OVERBURDEN (Map 7.18, Tables 7.66A-.70A, Figs. 7.27A-.28A)

Partitioning patterns of Mn, in samples of overburden, vary according to the chemical composition of smelter wastes and contaminated soil. Reducible (Fe-Mn oxide) phase Mn is the most significant, because it accounts for 7.97-85.98% of the total (median=60.26%; 50-17,300 ppm Mn; median=1350 ppm Mn). The next important phase is the residual, which accounts for 5.49-69.32% of the total (median=19.37%; 143-16,200 ppm Mn; median=409.5 ppm Mn). Carbonate and oxidisable phase Mn account for 0.92-57.66% and

0.57-19.90% of the total respectively; their corresponding median values are 13.91% and 2.7%. Exchangeable phase Mn is not significant, since minor amounts are extracted, *i.e.*, 1-213 Mn ppm.

The reducible (Fe-Mn oxide) phase is the most important for Mn in all sample types, *i.e.*,

(a) contaminated residual soil (406-17,300 ppm Mn; median=1150 ppm Mn);
(b) flotation residues (936-5,760 ppm Mn; median=1,585 ppm Mn);
(c) slag earth (848-9,100 ppm Mn; median=2,900 ppm Mn), and
(d) pyritiferous wastes (49.80-10,600 ppm Mn; median=2,970 ppm Mn).

Significant Mn concentrations are extracted by the carbonate phase from samples of slag earth, and nearby contaminated soil, from the Kavodokanos and Kiprianos areas, and the pyritiferous wastes from Komobil and Kavodokanos.

Reducible phase Mn has a high to moderate positive correlation with Pb (r=0.62), Zn (r=0.60), Fe (r=0.59), Al (r=0.55), Co (r=0.54), Ba (r=0.53), Be (r=0.47), Cd (r=0.47), Ni (r=0.45) and Cu (r=0.40) (Table 7.108A; Fig. 7.45A). This element association suggests that Mn is related to Fe and Al oxides, and elements Pb, Zn, Co, Ba, Be, Cd, Ni and Cu are adsorbed on Mn oxides.

Carbonate phase Mn has a strong to moderate positive correlation with Fe (r=0.87), Ba (r=0.83), Al (r=0.82), Co (r=0.77), Ti (r=0.71), Zn (r=0.69), Li (r=0.67), Be (r=0.59), Mo (r=0.57), K (r=0.56) and Ni (r=0.53). This element association and the insignificant correlation with Ca (r=0.10) suggests that Mn is not related to calcium carbonate, but to amorphous precipitates of manganese, iron or aluminium oxides, alumino-silicates, silica, and micro-crystalline precipitates of oxides, carbonates, but not phosphates, since Mn has an insignificant negative correlation with P (r= -0.002) (Table 7.107A; Fig. 7.44A).

Residual phase Mn has a high to moderate positive correlation with Fe (r=0.71), Cu (r=0.55), Mo (r=0.44), Cd (r=0.44) and Zn (r=0.41) (Table 7.110A; Fig. 7.47A). These are elements which occur is sulphides, indicating that primary sulphide minerals were not completely dissolved by the organic/sulphide phase.

Oxidisable phase Mn has a strong to moderate positive correlation with Co (r=0.61), Zn (r=0.58), Cu (r=0.56), Cd (r=0.56) and Fe (r=0.49), elements which normally occur in sulphide minerals (Table 7.109A; Fig. 7.46A).

Manganese is an essential element for plants and animals (Gough *et al.*, 1979; Mervyn, 1980, 1985, 1986; Reimann *et al.*, 1998). However, at high soil Mn concentrations (>3,000 ppm), there are reports of phytotoxicity problems (Gough *et al.*, 1979; Kabata-Pendias and Pendias, 1984). Since, the readily available Mn (exchangeable and carbonate phase) varies from 17 to 5,343 ppm Mn, some parts of Lavrion are considered to be unfit for plant growth.

7.5.15. PARTITIONING OF MOLYBDENUM (MO) IN OVERBURDEN (Map 7.19, Tables 7.71A-.75A, Figs. 7.29A-.30A)

The most significant phase of Mo is the residual, which accounts for 2.45-91.84% of the total (median=67.40%; 0.13-84.00 ppm Mo; median=3.25 ppm Mo). The next important phase is the carbonate, which accounts for 1.91-53.56% of the total (median=9.01%; 0.40-16.00 ppm

Mo; median=0.40 ppm Mo). Extracted concentrations by the other phases are comparatively low, hence are not considered in this discussion.

Generally, the concentrations of Mo in all five phases, extracted from almost all sample types are comparatively low, since it is not a major component of the base metal mineralisation and, consequently, the metallurgical processing wastes. The highest Mo concentrations in the residual phase are of local significance, and mainly occur in samples of slag earth, pyrite and nearby contaminated soil from Kiprianos and Kavodokanos.

Residual phase Mo has a moderate positive correlation with Cu (r=0.46), Fe (r=0.46), Mn (r=0.44), Cd (r=0.41), Pb (r=0.36) and Zn (r=0.35), elements normally associated with sulphides (Table 7.110A; Fig. 7.47A). This again supports the interpretation of incomplete dissolution of primary sulphide minerals by the organic/sulphide phase.

Carbonate phase Mo has a strong to moderate positive correlation with Ti (r=0.68), Al (r=0.63), Ba (r=0.61), Be (r=0.60), Fe (r=0.60), Mn (r=0.57) and Zn (r=0.44) (Table 7.107A; Fig. 7.44A). This element association and the negative correlation of Mo with Ca (r=-0.1), suggest that it is not related to calcium carbonate minerals, but is adsorbed on the surfaces of amorphous precipitates of aluminium, iron or manganese oxides, alumino-silicates, silica, and micro-crystalline precipitates of oxides, and carbonates, but not phosphates, since Mo has an insignificant negative correlation with P (r=-0.002).

Readily available Mo contents (exchangeable and carbonate phase) vary from 0.50 to 20.1 ppm. If the Finnish total soil Mo guide value of 5 ppm is used (Koljonen, 1992), then some parts of the Lavrion overburden may be hazardous to human health.

7.5.16. PARTITIONING OF NICKEL (Ni) IN OVERBURDEN (Map 7.20, Tables 7.76A-.80A, Figs. 7.31A-.32A)

The most significant phase of Ni for all sample types is the residual, which accounts for 39.53-91.77% of the total (median=79.49%; 27.0-452 ppm Ni; median=101.0 ppm Ni). The second comparatively important phase, again for all sample types, is the reducible, accounting for 2.27-41.40% of the total (median=12.60%; 1.0-90.4 ppm Ni; median=19.67 ppm Ni). The remaining phases are of minor importance.

Residual phase Ni has a high to moderate correlation with Ti (r=0.65), Al (r=0.64), K (r=0.63), Co (r=0.62), V (r=0.59), Be (r=0.57), Li (r=0.51) and Cr (r=0.44) (Table 7.11A; Fig. 7.47A). This element association suggests that Ni is related to (a) refractory alumino-silicate minerals, and (b) sulphides.

Carbonate phase Ni has a strong to moderate positive correlation with Co (r=0.76), Be (r=0.55), Al (r=0.52), Mn (r=0.45), Pb (r=0.40) and Fe (r=0.32) (Table 7.107A; Fig. 7.44A). This element association and the negative correlation of Ni with Ca (r=-0.25), suggest that it is not related to calcium carbonate minerals, but is adsorbed on the surfaces of amorphous precipitates of aluminium, manganese or iron oxides, alumino-silicates, silica, and micro-crystalline precipitates of oxides, and carbonates, but not phosphates, since Ni has a moderate negative correlation with P (r=-0.42).

Readily available Ni concentrations (exchangeable and carbonate phase) vary from 0.5 to 26.3 ppm, levels which are below (a) the maximum phytotoxic limit of total Ni (Kabata-Pendias and Pendias, 1984), and (b) the lowest residential soil limit of 30 ppm total Ni (Edelgaard and Dahlstrøm, 1999), but exceed the EDTA extractable threshold

trigger concentration of 20 ppm Ni (ICRCL, 1987). Consequently, some parts of Lavrion are considered to be both phytotoxic and hazardous to human health.

7.5.17. PARTITIONING OF PHOSPHORUS (P) IN OVERBURDEN (Map 7.21A, Tables 7.81A-.85A, Figs. 7.33A-.34A)

Phosphorus shows variable partitioning patterns, which depend on the chemical composition of wastes and the mineralogy of contaminated soil. The most significant phase is the residual, which accounts for 16.43-99.16% of the total (median=69.78%; 151-3,120 ppm P; median=691.5 ppm P). The next three important phases of P are the

(a) oxidisable (0.02-36.01%; median=12.12%; 0.1-1110 ppm P; median=114.5 ppm P),
(b) reducible (0.54-32.03%; median=11.43%; 2.7-1170 ppm P; median=118 ppm P), and
(c) carbonate (0.01-32.96%; median=3.25%; 0.1-1420 ppm P; median=31.2 ppm P).

The residual phase is the most significant for samples of

- pyritiferous wastes;
- slag earth from the Fougara area;
- flotation residues, which are *not* in residential areas with gardens, and
- contaminated soil, which is *not* close to metallurgical processing wastes, and the inhabited area with gardens.

Variable partitioning patterns, with the residual phase still being the most significant for P, but with comparatively important amounts being extracted by other phases, are found in samples of

- slag earth from Kavodokanos, which has a different chemical composition from that at Fougara;
- flotation residues from inhabited areas with gardens, and
- contaminated soil from again inhabited areas with gardens.

The latter two have been affected by phosphate fertilisers used in both flower and vegetable gardens (refer to land use map, Map 2.4, Volume 2).

Residual phase P has a weak positive correlation with Ba (r=0.31), Ag (r=0.29), Ca (r=0.23), Cu (r=0.22), and Cd (r=0.21) (Table 7.110A; Fig. 7.47A), which suggests a weak relationship with silicate minerals, and pyrite.

Oxidisable phase P has a strong positive correlation coefficient with Cr (r=0.67), and moderate correlation with V (r=0.47), Ba (r=0.43), Ti (r=0.42), Pb (r=0.38), and Sr (r=0.36). It has also moderate to weak negative correlation coefficients with Mn (r=-0.55), Cu (r=-0.34), Zn (r=-0.33), and Cd (r=-0.33) (Table 7.109A; Fig. 7.46A), suggesting an antipathetic relationship with sulphide minerals. It appears, therefore, that P is bound to the organic fraction.

Reducible phase P has a strong positive correlation coefficient with Ca (r=0.63), and moderate correlation with Cr (r=0.53), K (r=0.41), and Sr (r=0.36). It has also moderate to weak negative correlation coefficients with Co (r=-0.49), Cu (r=-0.47), Be (r=-0.44), Ni (r=-0.42), Al (r=-0.42), Mn (r=-0.40), Fe (r=-0.40), La (r=-0.36), Cu (r=-0.34), Zn (r=-0.33), and Ag (r=-0.26) (Table 7.108A; Fig. 7.45A). This suite of elements with negative co-variation with P, indicates that it is not associated with Al, Mn and Fe oxides, whereas the positively correlated elements suggest an association with calcium carbonate minerals, *e.g.*,

calcite [$CaCO_3$] and dolomite [$CaMg(CO_3)_2$], which are dissolved by the hydroxylamine reagent.

Carbonate phase P has moderate to weak positive correlation coefficients with Cr (r=0.46) and Sr (r=0.31) (Table 7.107A; Fig. 7.44A). It has also moderate to weak negative correlation coefficients with Cu (r=-0.29), Cd (r=-0.26), and Pb (r=-0.27). These relationships suggest that P is weakly related to calcium carbonate minerals, because of its very low correlation coefficient with Ca (r=0.12); it is not adsorbed on the surfaces of amorphous precipitates of Al (r=-0.14), Fe (r=-0.01) and Mn (r=-0.002) oxides, because of the very low negative relationship. Consequently, P may be associated with other carbonate minerals, and phosphates, which are present in phosphate fertilisers. Chromium and Sr are elements, which are found in considerable amounts in phosphate fertilisers (Kabata-Pendias and Pendias, 1984).

Exchangeable phase P has moderate to weak positive correlation coefficients with Mn (r=0.52), K (r=0.53), Sr (r=0.53), Cu (r=0.38), V (r=0.32), and Ca (r=0.29), (Table 7.106A; Fig. 7.43A). It has also moderate to weak negative correlation coefficients with Cd (r=-0.43), Ag (r=-0.41), Ba (r=-0.38), Pb (r=-0.29), and Zn (r=-0.26). These relationships suggest that P is weakly related to exchangeable sites, which are not associated with ore elements.

7.5.18. PARTITIONING OF LEAD (Pb) IN OVERBURDEN (refer to Chapter 3, p.75-82)

7.5.19. PARTITIONING OF STRONTIUM (Sr) IN OVERBURDEN (Map 7.26, Tables 7.86A-.90A, Figs. 7.35A-.36A)

One of the peculiar partitioning characteristics of Sr is the variability shown in all sample types. The most significant extraction steps of Sr are the

- residual, 6.15-88.26% of the total (median=35.83%; 10.6-138 ppm Sr; median=36.6 ppm Sr);
- carbonate 1.24-70.97% of the total (median=28.83%; 0.8-352 ppm Sr; median=33 ppm Sr), and
- reducible, 2.82-62.15% of the total (median=26.21%; 1.3-212 ppm Sr; median=29.45 ppm Sr).

Strontium in the residual phase has a moderate positive correlation with La (r=0.55), Ba (r=0.44), Cu (r=0.43), Pb (r=0.42), Cd (r=0.42) and Zn (r=0.40) (Table 7.110A; Fig. 7.47A). This element association suggests that Sr is related to both alumino-silicate and sulphide minerals. The latter were not completely digested in step 4.

In the carbonate phase, Sr has a high to moderate positive correlation with Ca (r= 0.804), La (r=0.55) and K (r=0.42) (Table 7.107A; Fig. 7.44A). This element association suggests that Sr is related to both calcium carbonate, but also other specific adsorption sites, such as adsorbed on the surfaces of amorphous precipitates of manganese (r= 0.30), iron (r= 0.23) or aluminium (r= 0.15) oxides, alumino-silicates, silica, and micro-crystalline precipitates of oxides, and carbonates, and even phosphates, since Sr has a weak positive correlation with P (r=0.31).

Reducible (Fe-Mn oxide) phase Sr has a high positive correlation with Ca (r=0.87) and La (r=0.69); a moderate positive correlation with P (r=0.56) and Ti (r=0.47), and a weak positive correlation with Zn (r=0.31) (Table 7.108A; Fig. 7.45A). This association suggests that Sr is related to

- calcium carbonates, thus indicating the incomplete dissociation of carbonates during the second step;
- phosphates, and
- amorphous silicates.

Strontium is also very weakly adsorbed on Fe oxides (r=0.18), but not Al (r=0.08) and Mn (r=-0.01) oxides. The moderate negative relationship of Sr with Ag (r=-0.51) and Cu (r=-0.43) shows that there is no relationship with these two elements, which mainly occur in sulphides.

7.5.20. PARTITIONING OF TITANIUM (Ti) IN OVERBURDEN (Map 7.27, Tables 7.91A-.95A, Figs. 7.37A-.38A)

The greatest proportion of Ti is found in the residual phase, which accounts for 86.19-99.97% of the total (median=99.70%; 582-5280 ppm Ti; median=2155 ppm Ti). The remaining phases are not very significant with respect to Ti levels.

Residual phase Ti has a high positive correlation with Al (r=0.91), K (r=0.85), Be (r=0.79), Li (r=0.74) and V (r=0.69), and low to moderate negative correlation with Cd (r=-0.22), Pb (r=-0.35), Ag (r=-0.40), Cu (r=-0.44) and Zn (r=-0.45) (Table 7.110A; Fig. 7.47A). These element relationships with (a) rock forming elements, and (b) ore elements, suggest that Ti is associated with alumino-silicate and not sulphide minerals.

7.5.21. PARTITIONING OF VANADIUM (V) IN OVERBURDEN (Map 7.29, Tables 7.96A-.100A, Figs. 7.39A-.40A)

The most significant phase of V for all sample types is the residual, which accounts for 50.55-92.78% (median=83.11%; 18.8-203.0 ppm V; median=61.55 ppm V). The next two comparatively important phases of V are the reducible and oxidisable, which account for 3.64-30.54% and 0.20-27.89% of the total respectively; their corresponding median values are 9.51% and 5.65%.

Vanadium in the residual phase has strong to weak positive correlation coefficients with Ti (r=0.69), Al (r=0.63), K (r=0.63), Ni (r=0.59), Li (r=0.56), Be (r=0.54), Co (r=0.53), La (r=0.33), Mn (r=0.31), Mo (r=0.31), and a weak negative correlation with Ca (r=-0.31). This element association suggests that residual phase V is mainly found in aluminosilicate minerals.

The highest levels of reducible (Fe-Mn oxide) phase V contents occur in the pyritiferous wastes, followed by slag earth and contaminated soil, which is near to metallurgical processing wastes. In the flotation residues, reducible phase V contents are generally lower. The moderate to low positive correlation with Fe (r=0.45), Al (r=0.38), Mn (r=0.29) and Be (r=0.29), supports the interpretation that V is mainly adsorbed on Fe, Al and Mn oxides.

The highest levels of oxidisable (organic/sulphide) phase V are found in samples of contaminated soil, and to a lesser extent in slag earth and pyritiferous wastes. Vanadium has moderate to low positive and negative correlation coefficients with P (r=0.47), Mo (r=0.39), Ni (r=0.31), Cd (r=-0.32), Zn (r=-0.40) and Cu (r=-0.43). These element relationships indicate that V is mostly related to the organic and not the sulphide fraction.

7.5.22. PARTITIONING OF ZINC (Zn) IN OVERBURDEN (Map 7.30, Tables 7.96A-.100A, Figs. 7.41A-.42A)

The partitioning patterns of Zn are variable in all sample types, and especially in slag earth, flotation residues, and nearby contaminated soil from Kavodokanos and Kiprianos. The most significant phase for Zn is the reducible (Fe-Mn oxide) phase, which accounts for 5.73-82.46% of the total (median=44.22%; 245-50,500 ppm Zn; median=2940 ppm Zn). The other important phases are

- the residual, which accounts for 6.96-78.27% of the total (median=23.88%; 218-20,400 ppm Zn; median=1475 ppm Zn);
- the carbonate, which accounts for 0.73-53.27% of the total (median=20.81%; 21.3-16,400 ppm Zn; median=1335 ppm Zn), and
- the oxidisable (organic/sulphide), which accounts for 1.25-52.08% of the total (median=7.89%; 19.1-13,500 ppm Zn; median=525 ppm Zn).

Considerably lower amounts of Zn are extracted by the exchangeable phase (0.6-1360 ppm Zn; median 15.1 ppm Zn), but they are important for when combined with the carbonate phase contents, make up the readily available Zn concentrations.

Differences in the chemistry of slag, and the resulting earthy material within slag or slag earth, between Kavodokanos-Kiprianos and Fougara, have already been noted with respect to other elements. Nevertheless, Zn shows these differences more distinctly. Samples of slag earth, flotation residues and nearby contaminated soil, from these two areas have generally higher Zn levels in the carbonate, reducible, oxidisable and residual phases, than samples from other areas in Lavrion.

The flotation residues, which extend from Noria to Prasini Alepou and Santorineika, the pyritiferous wastes at Nichtochori-Komobil-Kiprianos-Kavodokanos, and nearby contaminated soil, have high Zn contents in the carbonate, reducible and residual phases.

Contaminated soil, which is not directly under the influence of aerial transportation of fine-grained material from the wastes, has generally lower Zn concentrations in the different phases, *e.g.*, Thorikon in the north and Vilanoira-Panormos-Perdika in the south.

Zinc has the following correlation coefficients with other elements in the different phases:

- *exchangeable:* Pb (r=0.75), Cd (r=0.73), Ag (r=0.52), Fe (r=0.48), Co (r=0.40), Cu (r=0.39), Be (r=0.39) and Ni (r=0.37) (Table 7.106A; Fig. 7.43A); this element association together with the antipathetic correlation with pH (r=-0.48), K (r=-0.38), P (r=-0.26), Li (r=-0.14), suggest that (i) Zn, together with the other positively correlated elements, is adsorbed on easily exchangeable sites, (ii) elevated Zn contents occur in areas with a low pH (pyritiferous wastes), and (iii) comparatively lower Zn concentrations are found in areas with high levels of K, P and Li;
- *carbonate:* Mn (r=0.69), Pb (r=0.68), Al (r=0.65), Fe (r=0.62), Co (r=0.61), Cd (r=0.58), Cu (r=0.56), Ba (r=0.52), Ti (r=0.48), Li (r=0.46), Mo (r=0.44), Be (r=0.43), Ni (r=0.43) and La (r=0.37) (Table 7.107A; Fig. 7.44A); this element association together with the very low correlation coefficient between Zn and Ca (r=0.131), suggest that Zn is weakly related to calcium carbonates, and is mainly adsorbed on other specific adsorption sites, such as on the surfaces of amorphous precipitates of manganese, aluminium or iron

oxides, alumino-silicates, silica, and micro-crystalline precipitates of oxides, and carbonates, but not phosphates, since Zn has an insignificant negative correlation with P (r=-0.08).

- *reducible (Fe-Mn oxide):* Cd (r=0.82), Pb (r=0.80), Fe (r=0.69), Mn (r=0.60), Al (r=0.59), Ba (r=0.51), La (r=0.38) and Cu (r=0.37) (Table 7.108A; Fig. 7.45A); this element association suggests that Zn is adsorbed on Fe, Mn and Al oxides;
- *oxidisable (organic/sulphide):* Cu (r=0.91), Cd (r=0.88), Mn (r=0.58) and Ca (r=0.44) (Table 7.109A; Fig. 7.46A); this element association suggests that Zn is mainly related to the sulphide phase; and
- *residual:* Cu (r=0.90), Ag (r=0.87), Pb (r=0.85), Cd (r=0.77), Fe (r=0.66), Ca (r=0.49), Mn (r=0.41) and Sr (r=0.40) have positive correlation with Zn; it has also an antipathetic correlation with Cr (r=-0.45), Ti (r=-0.45), Al (r=-0.43), Be (r=-0.38) and K (r=-0.36) (Table 7.110A; Fig. 7.47A); these two element relationships suggest that Zn occurs in sulphide minerals, which were not completely dissolved in step 4, and is definitely not associated with alumino-silicate and refractory minerals.

According to Kabata-Pendias and Pendias (1984), the maximum permissible level of total Zn in soil for healthy plant growth is 400 ppm. Values above this total Zn limit are considered to be phytotoxic. Recommended residential soil total Zn statutory limits, quoted in scientific literature, vary from 300 to 20,000 ppm depending on the sensitivity of the legislative body and country of origin (refer to Chapter 6, Table 6.2, p. 139). The EDTA extractable threshold trigger concentration for Zn is set at 130 ppm (ICRCL, 1987). Since, readily available Zn contents (exchangeable and carbonate phase) vary from 21.9 to 17,760 ppm, zinc is considered to be potentially hazardous to plants, animals and humans in the Lavrion urban area.

7.6. CLUSTER AND FACTOR ANALYSES

In the above description and discussion of the results, the element associations given relied on Pearson's linear correlation coefficient on the log transformed data. This is a measure of the linear relationship between two elements, and essentially, it may be said, that it quantifies the co-linear relationship or similarity between them. Although the dendrograms were cited, the depicted element associations were not discussed. Since, the sequential extraction phases are operationally defined, multi-element determinations on the samples, and the relationships obtained from the statistical treatment of data, validate indirectly the assumptions made about mineralogical composition of overburden samples. Ideally, validation of the mineralogy of samples, and the proportion of minerals present in each, should be made by direct physical methods, such as SEM/EDSX, XRD *etc.* methods, described earlier. This is, however, impractical and costly when dealing with a large number of samples (refer to Appendix Report 1B in Volume 1B of this report). Hence, one should resort on multi-element analysis of samples, and an exhaustive statistical study, to define relationships between and among the elements, as has been done in this study, with linear correlation coefficients, R-mode cluster and factor analyses.

R-mode cluster analysis with the aid of the dendrogram is a process of coalescing progressively less similar variables (McCammon, 1968, 1969, 1974; Obial, 1970; Davis, 1973; Hesp and Rigby, 1973; Obial and James, 1973; Howarth and Sinding-Larsen, 1983). It uses as input the presence or absence of similarity between variables compared in pairs, either as individual elements to begin with, or clusters (groups) of elements as the process continues to join less similar single or groups of variables at a

greater distance. A process known as hierarchical clustering. Evidently, the dendrogram is a powerful tool of cluster analysis, classifying the entire set of variables (or elements), and thus facilitating the discovery of hidden relationships. When applied on multivariate data sets, it helps to resolve geochemical relationships between individual or groups of variables, and may ultimately offer likely solutions to the geological, or in this case the environmental contamination, problem.

R-mode mode factor analysis reduces the complexity of a given set of inter-correlated data by accounting for the observed correlation among the variables in terms of the fewest possible underlying number of factors (Cattell, 1965; Obial, 1970; Obial and James, 1973; McCammon, 1974; Klovan, 1975; Davis, 1973; Goddard and Kirby, 1976; Jöreskog *et al.*, 1976; Howarth, 1983; Miesch, 1990). The problem in factor analysis is to determine the number of factors, and factor loadings, which best reproduce observed correlation coefficients. The initial principal component analysis model (Daultrey, 1976; Miesch, 1990) is reduced to a simpler structure by varimax rotation. This rotation places the highest possible loadings on the fewest number of variables of each factor, while preserving the independence of each factor, and reduces the complexity further by allowing the factors to become slightly correlated (McCammon, 1974; Miesch, 1990). Although the mathematical theory and calculations are very complex, the final factor analysis matrix gives geologically-geochemically interpretable results, and assists in discovering underlying inter-relationships among the variables of a data set. It is stressed that for the interpretation a good knowledge of the study area is required.

What is the problem that requires the use of both cluster and factor analysis? Multi-element determinations (22 variables) were performed on five sequential extraction steps of overburden and house dust (see Chapter 8) samples from the Lavrion urban area. Since, there is no mineralogical back up, the relationships are explained in terms of the operationally defined phases of the sequential extraction procedure. The calculated linear correlation coefficients have revealed relationships between pairs of elements, but not interelement relationships. Therefore, the objective of cluster and factor analysis is to identify interelement correlations, and essentially to reveal hidden relationships, with the purpose to associate them, if possible, to discrete mineralogical phases and source materials. Further, to identify factors explaining the greatest variation, and in a sense define the major phases (mineralogical-geochemical), or even contamination sources, which may explain the variability of each extraction step.

The number of factors were selected at the point where there was a distinct break in the slope of the line plotted between factors against eigenvalues (Fig. 7.1) , *i.e.*, this plot is known as the Cattell scree or eigenvalue diagram (Goddard, 1968; Goddard and Kirby, 1976; Miesch, 1990). The convention of selecting the number of factors according to the point where eigenvalues are above 1 was not followed. The reason for this deviation is that in a number of cases, the gradient of the factor-eigenvalues plot slope was very low, pointing to minor differences between factors. This defies, in fact, the objective of factor analysis, which is to identify distinctive different and meaningful factors.

Observed minor differences in correlation between variables, occurring in the clusters of dendrograms and factors, are due to the clustering method (nearest neighbour and squared Euclidean distance – refer to Chapter 4 for more details). It is stressed that cluster and factor analyses were performed on data transformed by the 2-parameter log transformation (Miesch,1990); this is a common transformation used in chemometrics.

The 2-parameters are the mean log and log variance, which completely define a lognormal distribution.

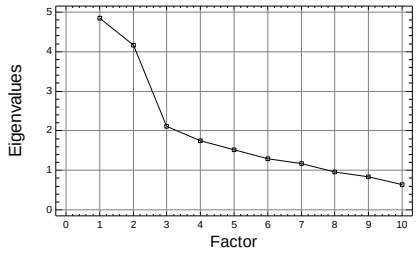

Fig. 7.1. Cattell scree plot of factors against eigenvalues of exchangeable phase overburden data. Note the distinct break of slope at factor 3.
Σχ. 7.1. «Cattell scree» διάγραμμα των παραγόντων με τις αντίστοιχες «eigenvalues» της ανταλλάξιμης φάσης των δεδομένων του εδαφικού καλύμματος. Επισημαίνεται το εμφανές σπάσιμο της κλίσης της καμπύλης στον 3ο παράγοντα.

In Tables 7.1 to 7.5, the following notation is used for the varimax loadings of the 23 variables, *i.e.*, 22 elements and pH:

- strong positive varimax loadings >**0.6** are printed in bold letters
- moderate positive varimax loadings >0.4 to <0.6 are underlined
- strong negative varimax loadings <***-0.6*** are in bold italic letters, and
- moderate negative varimax loadings >-0.6 to <*-0.4* are in underlined italic letters.

7.6.1. Cluster and Factor Analyses on the Exchangeable Phase Data of Overburden

There are seven factors with eigenvalues >1, but only three were retained, because at this point there is a distinct break between the factors and eigenvalues (Fig. 7.1). The variation accounted for by the three-factor varimax model is 48.36% of the total (Table 7.1, Fig. 7.2).

Factor 1 or the *"exchangeable factor"* explains 21.07% of the total variance, and has strong positive loadings (>0.6) on Zn, Pb, Ag, Cd, Be and Co, moderate loadings (>0.4-0.6) on Ni and Fe, a strong negative loading of –0.61 on pH, and moderate negative loadings on (<-0.35 >-0.54) on K and P. The negative covariation of this particular suite of elements with pH, suggests that they are held on easily exchangeable sites, and are adsorbed on overburden particles with a comparatively low (acid) pH; the negative covariation with K and P, implies that they are not associated with these two elements, which are added to soil in the form of chemical fertilisers. The elements of factor 1 are found in the dendrogram in three different clusters, *i.e.*, (a) Pb-Zn, Cd and Ag, (b) Al-Fe, Ti, Ni and Co, and (c) Be-Mo, which are all linked at a lower correlation level.

Factor 2 or the *"carbonates factor"* explains 18.13% of the total variance, and has strong positive loadings (>0.6) on Ca, Mn, La, P and Sr, moderate loadings (>0.4-0.6) K, V and Cu, and moderate negative loadings (<-0.4 >-0.6) on Ba and pH. The negative loadings on pH and Ba, suggests that this suite of elements occurs in overburden with comparatively low pH values, and is not associated with Ba. The dendrogram shows a cluster made-up from Ca-Sr, K, La, Mn, P, Cu and V. This association suggests that $MgCl_2$ has digested some calcium carbonate overburden particles.

Table 7.1. Varimax loadings for the three strongest factors of exchangeable phase overburden geochemical data (n=224). Correlation between varimax scores and transformed data.
[For notation used refer to text].
Table 7.1. Φορτία περιστροφής "varimax" για τους τρεις ισχυρότερους παράγοντες της ανταλλάξιμης φάσης (1ου σταδίου) των γεωχημικών δεδομένων του εδαφικού καλύμματος (n=224). Συσχέτιση μεταξύ των φορτίων varimax και των μετασχηματισμένων δεδομένων. [Για τη σημειογραφία βλέπετε το κείμενο].

Element	*Varimax loadings*		
	Factor 1	*Factor 2*	*Factor 3*
Ag-1	**0.669**	-0.197	-0.075
Al-1	-0.064	0.133	**0.844**
Ba-1	-0.041	-0.520	0.581
Be-1	**0.638**	0.014	-0.211
Ca-1	0.053	**0.773**	0.069
Cd-1	**0.656**	-0.277	0.213
Co-1	**0.598**	0.206	0.065
Cr-1	0.262	-0.135	0.111
Cu-1	0.217	0.432	0.375
Fe-1	0.451	0.065	**0.704**
K-1	*-0.536*	0.493	0.192
La-1	0.134	**0.676**	0.029
Li-1	-0.215	0.286	0.137
Mn-1	0.213	**0.741**	0.207
Mo-1	0.237	0.083	-0.103
Ni-1	0.507	0.153	0.403
P-1	*-0.352*	**0.674**	-0.060
Pb-1	**0.727**	-0.176	0.308
Sr-1	-0.278	**0.673**	0.019
Ti-1	-0.055	0.247	**0.622**
V-1	-0.012	0.469	0.022
Zn-1	**0.854**	0.020	0.197
pH	***-0.602***	-0.431	-0.052
Eigenvalue	*4.85*	*4.17*	*2.11*
Variance explained by factor	*21.07%*	*18.13%*	*9.16%*
Cumulative variance	*21.07%*	*39.20%*	*48.36%*

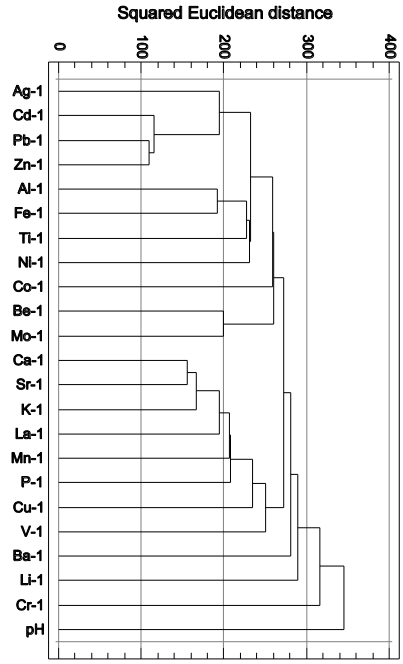

Fig. 7.2. Dendrogram showing the relationship of 22 elements and pH in samples of overburden for sequential extraction step 1 – exchangeable phase (n=224).
Σχ. 7.2. Δενδρόγραμμα που δείχνει τη σχέση μεταξύ 22 στοιχείων και pH στα δείγματα του εδαφικού καλύμματος για το 1ο στάδιο της διαδοχικής εκχύλισης – ανταλλάξιμη φάση (n=224).

Factor 3 or *"Al-Fe oxides factor"* explains 9.16% of the total variance, and has strong positive loadings (>0.6) on Al, Fe and Ti, moderate positive loadings (>0.4-0.6) on Ba, Ni, Cu, and weak loadings (>0.2-0.4) on Pb, Cd, Mn and Zn. A similar cluster is shown by the dendrogram among Al-Fe, Ti, Ni and Co. This element association suggests contaminant elements to be adsorbed on Al-Fe oxides, and $MgCl_2$ extracts a small proportion.

7.6.2. Cluster and Factor Analyses on the Carbonate Phase Data of Overburden

The retention of factors with eigenvalues >1 resulted in the selection of a five factor model for the carbonate phase analytical data. The variation accounted for by this five-factor varimax model is 74.35% of the total (Table 7.2, Fig. 7.3).

Factor 1 or the *"specifically adsorbed Fe-Al-Mn oxides factor"* explains 35.86% of the total variance, and has strong positive loadings (>0.6) on Fe, Al, Ba, Mn, Ti, Li, Be, Mo, Co and K, moderate loadings (>0.4-0.6) on Zn, V and Ni. The dendrogram shows a cluster of elements consisting of Al-Fe, Mn, Ba, Ti, Co, Be, Li and Zn. It is suggested, therefore, that the specifically adsorbed element fraction in overburden samples is more important than the carbonate part. These elements may occur on the surfaces of amorphous precipitates of Fe, Al or Mn oxides, alumino-silicates, silica, and micro-crystalline precipitates of oxides, but not phosphates, because of the insignificant negative loading on phosphorus (-0.005).

Factor 2 or *"specifically adsorbed contaminants factor"* explains 14.87% of the total variance, and has strong positive loadings (>0.6) on Cd, Pb, Cu and Zn, moderate loadings (>0.4-0.6) on Ag and Ni, which are weakly associated with Co (0.32) and Mn (0.20). Chromium, P and V have moderate to weak negative loadings. The dendrogram shows a cluster between Cd and Pb, which is connected to the suite of elements of the first factor or cluster. A possible interpretation is that these contaminant elements are also found at specifically adsorbed sites in soil, and are not related to phosphates, because of the moderate negative loading on P (-0.32).

Factor 3 or *"carbonates factor"* explains 11.05% of the total variance, and has strong positive loadings (>0.6) on Sr and Ca, moderate loadings (>0.4-0.6) on La, K and P. The dendrogram shows two clusters with Ca-Sr, and Cr-La, which are linked at a lower level with P. It appears that calcium carbonates are not the dominant phase of the second extraction step, since only 11.05% of the variation is explained by the "carbonates" factor.

Factor 4 or *"La-Ag-Cr specifically adsorbed sites factor"* explains 8.21% of the total variance, and has strong positive loadings (>0.6) on La, Ag and Cr, moderate loadings (>0.4-0.5) on V and Be, a weak loading of 0.31 on P, and a moderate negative loading of –0.41 on K. The dendrogram shows a cluster with Cr-La, which is linked at a lower correlation to Ag, and the elements of the first, second and third factors. This element association suggests that it is related to soil developed over schist (weathered pyroxenes) and schist intercalations in marble, which has been contaminated by Ag possibly through airborne transportation of wastes. The negative loading on K does not agree, however, with this interpretation. Consequently, there must be another explanation, such as specifically adsorbed sites for the preferential adsorption of La, Ag, Cr, V, Be and P.

Table 7.2. Varimax loadings for the five strongest factors of carbonate phase overburden geochemical data (n=224). Correlation between varimax scores and transformed data.
[For notation used refer to text].
Table 7.2. Φορτία περιστροφής "varimax" για τους πέντε ισχυρότερους παράγοντες της ανθρακικής φάσης (2ου σταδίου) των γεωχημικών δεδομένων του εδαφικού καλύμματος (n=224). Συσχέτιση μεταξύ των φορτίων varimax και των μετασχηματισμένων δεδομένων. [Για τη σημειογραφία βλέπετε το κείμενο].

Element	*V a r i m a x l o a d i n g s*				
	Factor 1	*Factor 2*	*Factor 3*	*Factor 4*	*Factor 5*
Ag-2	0.007	0.418	-0.067	**0.678**	-0.184
Al-2	**0.907**	0.203	-0.052	0.011	0.071
Ba-2	**0.906**	-0.034	0.125	-0.120	0.236
Be-2	**0.748**	0.023	-0.021	0.438	-0.098
Ca-2	-0.050	0.011	**0.868**	0.065	0.234
Cd-2	-0.111	**0.860**	0.048	-0.054	0.166
Co-2	**0.714**	0.316	0.034	0.195	0.092
Cr-2	-0.060	*-0.413*	0.335	**0.628**	0.106
Cu-2	0.105	**0.773**	-0.164	-0.003	-0.108
Fe-2	**0.926**	0.107	0.051	0.014	0.016
K-2	**0.626**	-0.223	0.444	*-0.406*	-0.059
La-2	0.289	0.108	0.470	**0.698**	0.165
Li-2	**0.775**	0.009	0.223	-0.205	-0.176
Mn-2	**0.882**	0.204	0.142	-0.014	0.141
Mo-2	**0.730**	0.068	-0.011	0.058	-0.215
Ni-2	0.487	0.384	-0.195	0.166	0.187
P-2	-0.005	-0.319	0.427	0.314	*-0.397*
Pb-2	0.183	**0.859**	0.053	0.099	0.044
Sr-2	0.209	0.023	**0.892**	0.109	0.054
Ti-2	**0.843**	-0.030	0.080	0.253	-0.098
V-2	0.552	-0.256	-0.013	0.453	0.021
Zn-2	0.569	**0.678**	0.203	0.057	0.070
pH	-0.056	0.039	0.251	0.026	**0.822**
Eigenvalue	*8.25*	*3.42*	*2.54*	*1.89*	*1.00*
Variance explained by factor	*35.86%*	*14.87%*	*11.05%*	*8.21%*	*4.36%*
Cumulative variance	*35.86%*	*50.73%*	*61.78%*	*69.99%*	*74.35%*

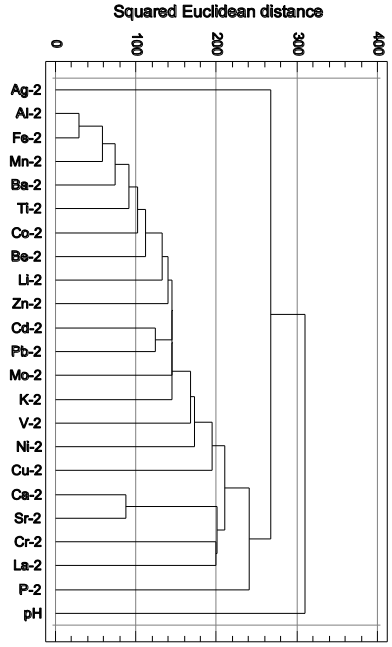

Fig. 7.3. Dendrogram showing the relationship of 22 elements and pH in samples of overburden for sequential extraction step 2 – carbonate phase (n=224).
Σχ. 7.3. Δενδρόγραμμα που δείχνει τη σχέση μεταξύ 22 στοιχείων και pH στα δείγματα του εδαφικού καλύμματος για το 2ο στάδιο της διαδοχικής εκχύλισης – ανθρακική φάση (n=224).

Factor 5 or *"pH factor"* explains 4.36% of the total variance, and has a strong positive loading of 0.82 on pH, and a moderate negative loading of –0.40 on P. The dendrogram shows pH loosely correlated at a lower level with elements of previous clusters and factors. The low association with Ca (0.24) suggests that it occurs in areas with carbonates. The negative covariation with P implies that the addition of phosphate fertilisers lowers soil pH, which is in fact the case (compare Maps 2.5, 6.21 & 7.21 in Vol. 2).

7.6.3. Cluster and Factor Analyses on the Reducible Phase Data of Overburden

There are six factors with eigenvalues >1, but only five were retained, because at this point there is a distinct break between factors and eigenvalues. The variation accounted for by the five-factor varimax model is 72.85% of the total (Table 7.3, Fig. 7.4).

Factor 1 or the *"Al-Fe oxides factor"* explains 28.77% of the total variance, and has strong positive loadings (>0.6) on Li, Al, Fe, Ba, Be and Ti, a moderate loading of 0.55 on V, and low positive loadings (>0.2-0.35) on Mn, K, Ni, Mo, Zn, Sr and Pb. The dendrogram, for this particular element association shows a cluster among Al-Fe, Be, Ba and Li, which is linked to another cluster with Cd-Zn, Pb and Mn. It is interpreted as an Al-Fe oxide factor, which is related to the smelter wastes, and especially slag and to a lesser extent pyritiferous sands.

Factor 2 or *"carbonates factor"* explains 20.69% of the total variance, and has strong positive loadings (>0.6) on Ca, Sr and La, and moderate loadings (>0.55-6) on P and pH. It has also a strong negative loading of –0.76 on Ag, and a moderate negative loading of –0.53 on Cu. The dendrogram shows a cluster among Ca-Sr, La, P and Cr. This factor shows that carbonates were not completely digested in step 2. The negative covariation with Ag and Cu, suggests that these carbonates may be derived from unmineralised marble or soil developed on it.

Factor 3 or *"Mn-Fe-Al oxides factor"* explains 10.17% of the total variance, and has strong positive loadings (>0.6) on Zn, Cd, Pb and Mn, moderate loadings (>0.45-0.6) on Fe, Cu and Al. The dendrogram shows a cluster with Cd-Zn, Pb and Mn, which is linked to elements belonging to the first factor. Contaminant elements may be weakly adsorbed on Mn, Fe and Al oxides. It is interesting to note that this suite of elements has a negative covariation with P and Cr, implying that intense toxic element contamination occurs mainly in areas with low P and Cr contents.

Factor 4 or *"Co-Ni factor"* explains 8.00% of the total variance, and has strong positive loadings (>0.6) on Co, Ni and pH, and moderate loadings (>0.4-0.6) on Be and Mn. It is interesting to note that all ore or contaminant elements have low or negative loadings, implying that they are not correlated with these elements. The dendrogram shows a cluster with Co-Ni and Ti. This is an interesting association, for Co and Ni occur in areas with alkaline pH values, where there is a negative covariation with Ca (-0.18).

Factor 5 or *"fertiliser factor"* explains 5.22% of the total variance, and has strong positive loadings (>0.6) on K and Cr, moderate loadings (>0.4-0.6) on P and La, and a moderate negative loading of –0.5 on V. It is again interesting to note that all ore or contaminant elements have negative loadings, indicating that they are not correlated to these elements. The dendrogram does not show a distinct cluster, except that Cr, V and K are weakly related. This element association together with its weak positive relationship

Table 7.3. Varimax loadings for the five strongest factors of reducible phase overburden geochemical data (n=224). Correlation between varimax scores and transformed data.
[For notation used refer to text].
Table 7.3. Φορτία περιστροφής "varimax" για τους πέντε ισχυρότερους παράγοντες της αναγώγιμης φάσης των γεωχημικών δεδομένων του εδαφικού καλύμματος (n=224). Συσχέτιση μεταξύ των φορτίων varimax και των μετασχηματισμένων δεδομένων. [Για τη σημειογραφία βλέπετε το κείμενο].

Element	*Varimax loadings*				
	Factor 1	*Factor 2*	*Factor 3*	*Factor 4*	*Factor 5*
Ag-3	0.076	***-0.755***	-0.094	-0.103	0.214
Al-3	**0.764**	-0.080	0.432	0.267	-0.038
Ba-3	**0.711**	0.235	0.312	0.210	0.196
Be-3	**0.699**	-0.292	0.122	0.473	-0.080
Ca-3	-0.129	**0.893**	0.075	-0.184	0.220
Cd-3	-0.076	0.157	**0.870**	0.121	-0.076
Co-3	0.116	-0.348	0.171	**0.806**	-0.137
Cr-3	-0.197	0.305	-0.280	-0.128	**0.626**
Cu-3	-0.090	*-0.533*	0.553	0.014	-0.252
Fe-3	**0.714**	-0.064	0.565	-0.072	-0.106
K-3	0.316	0.086	0.037	0.032	**0.792**
La-3	0.244	**0.640**	0.287	-0.015	0.387
Li-3	**0.782**	-0.119	-0.014	0.196	0.070
Mn-3	0.337	-0.040	**0.611**	0.414	-0.145
Mo-3	0.255	0.141	0.325	-0.114	0.157
Ni-3	0.298	-0.115	0.187	**0.772**	-0.080
P-3	-0.180	0.510	-0.218	-0.271	0.572
Pb-3	0.170	0.041	**0.851**	0.230	-0.058
Sr-3	0.209	**0.825**	0.162	-0.178	0.273
Ti-3	**0.697**	0.353	0.019	-0.218	0.043
V-3	0.546	0.057	0.027	-0.108	*-0.502*
Zn-3	0.246	0.167	**0.905**	0.030	0.010
pH	-0.170	0.462	0.027	**0.677**	0.169
Eigenvalue	*6.62*	*4.76*	*2.34*	*1.84*	*1.20*
Variance explained by factor	*28.77%*	*20.69%*	*10.17%*	*8.00%*	*5.22%*
Cumulative variance	*28.77%*	*49.46%*	*59.63%*	*67.63%*	*72.85%*

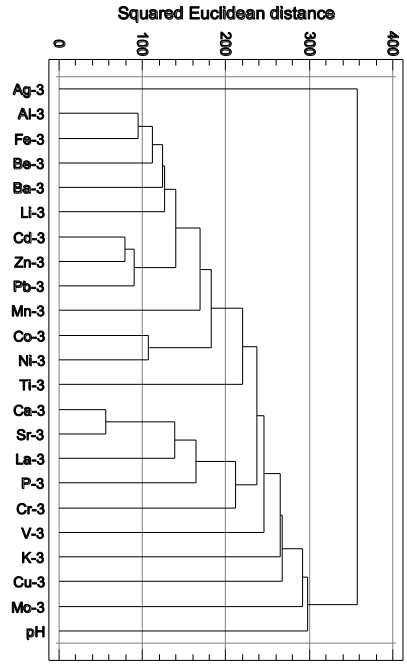

Fig. 7.4. Dendrogram showing the relationship of 22 elements and pH in samples of overburden for sequential extraction step 3 – reducible phase (n=224).
Σχ. 7.4. Δενδρόγραμμα που δείχνει τη σχέση μεταξύ 22 στοιχείων και pH στα δείγματα του εδαφικού καλύμματος για το 3ο στάδιο της διαδοχικής εκχύλισης – αναγώγιμη φάση (n=224).

with pH, suggests that it may be due to contamination by chemical fertilisers used in the cultivated plots of land.

7.6.4. Cluster and Factor Analyses on the Oxidisable Phase Data of Overburden

There are six factors with eigenvalues >1, but only five were retained, because at this point there is a distinct break between factors and eigenvalues. The variation accounted for by the five-factor varimax model is 73.46% of the total (Table 7.4, Fig. 7.5).

Factor 1 or the *"sulphides factor"* explains 23.47% of the total variance, and has strong positive (>0.6) loadings on Zn, Cd, Cu and Mn, weak loadings (>0.2-0.3) on Ca, Fe, Al, Sr and Pb. It is noted that this suite of elements has a strong to moderate negative covariation with Cr, Ti, P and V. The dendrogram, for this particular element association shows two principal clusters: (a) Cu-Zn and Cd, and (b) Co-Ni, Mn and Fe, which are linked at a lower level. The principal elements of this factor are associated with sulphides, and not with the organic phase, because of their negative covariation with P and V.

Factor 2 or *"alumino-silicates factor"* explains 20.12% of the total variance, and has strong positive loadings (>0.6) on Al, Be, La, Li, Ni and K, moderate loadings (>0.4-0.6) on Co and Mn. The dendrogram shows a cluster among Al-Be, Li, K and La, which is linked at a lower level with elements of factor 1. This suite of elements suggests a possible clay mineral association, which is related weakly to contaminant elements.

Factor 3 or *"carbonates factor"* explains 14.03% of the total variance, and has strong positive loadings (>0.6) on Sr, Ca, Ba and P, and moderate loadings (>0.4-0.6) on Cr and Pb. The dendrogram shows two principal clusters of elements: (a) Ca-Sr, which are correlated at a lower level with Pb and Ba, and (b) Cr-P, Ti and V, which are linked to the first cluster at still lower level. It is interesting to note that, apart from Pb, other ore or contaminant elements have very low or negative loadings, implying that there is no or low correlation with Sr, Ca, Ba and P. A possible interpretation is that some resistant carbonate minerals, which survived the attacks by the previous steps are digested in this phase. The source of these particular soil particles is probably unmineralised and uncontaminated material, derived from marble or soil developed on it, which has been contaminated by airborne particulates from the smelting processes, with Pb as the main element.

Factor 4 or *"pyrite factor"* explains 10.15% of the total variance, and has strong positive loadings (>0.6) on Co and Fe, and moderate loadings (>0.4-0.6) on Ni and Mn. It has also strong to moderate negative loadings on Ag, Pb and Ti. Other ore or contaminant elements have weak positive loadings. The dendrogram shows a similar cluster with Co-Ni, Mn and Fe, which has a relationship with also the first factor. The strong negative loadings on Ag and Pb, together with the low negative loading on pH, imply that Co-Fe-Ni-Mn occur in an area with a low pH. It is interpreted, therefore, that this suite of elements is associated with the pyritiferous tailings.

Factor 5 or *"organic factor"* explains 5.69% of the total variance, and has strong positive loadings (>0.6) on Mo and V, moderate loadings (>0.39-0.6) on Ti and P, and weak positive loadings (>0.2-0.35) on Pb, K, and Ni. The dendrogram shows a cluster with Cr-P, Ti, V and Mo, which has already been related to the third factor. Other contaminant elements have very low positive or negative loadings. This element

Table 7.4. Varimax loadings for the five strongest factors of oxidisable phase overburden geochemical data (n=224). Correlation between varimax scores and transformed data.
[For notation used refer to text].
Table 7.4. Φορτία περιστροφής "varimax" για τους πέντε ισχυρότερους παράγοντες της οξειδώσιμης φάσης (4ης φάσης) των γεωχημικών δεδομένων του εδαφικού καλύμματος (n=224). Συσχέτιση μεταξύ των φορτίων varimax και των μετασχηματισμένων δεδομένων. [Για τη σημειογραφία βλέπετε το κείμενο].

Element	*Varimax loadings*				
	Factor 1	*Factor 2*	*Factor 3*	*Factor 4*	*Factor 5*
Ag-4	-0.073	0.193	-0.280	***-0.696***	0.004
Al-4	0.239	**0.878**	0.166	0.029	0.153
Ba-4	-0.038	0.284	**0.694**	-0.348	0.003
Be-4	-0.034	**0.843**	0.202	0.075	-0.048
Ca-4	0.319	-0.139	**0.750**	0.249	-0.016
Cd-4	**0.917**	0.066	0.075	0.010	0.084
Co-4	0.167	0.417	-0.070	**0.762**	0.077
Cr-4	***-0.686***	0.159	0.470	-0.016	0.166
Cu-4	**0.897**	-0.018	0.178	0.218	-0.059
Fe-4	0.279	0.169	-0.074	**0.755**	0.037
K-4	-0.012	**0.650**	0.293	-0.372	0.255
La-4	-0.192	**0.816**	-0.049	-0.092	-0.016
Li-4	0.144	**0.805**	-0.307	0.056	0.002
Mn-4	**0.612**	0.402	-0.217	0.407	-0.196
Mo-4	0.062	0.046	0.074	-0.064	**0.843**
Ni-4	-0.105	**0.681**	0.063	0.425	0.225
P-4	*-0.494*	-0.048	**0.613**	-0.058	0.386
Pb-4	0.212	0.173	0.435	***-0.631***	0.313
Sr-4	0.234	-0.018	**0.826**	0.173	0.091
Ti-4	*-0.542*	0.234	0.066	*-0.447*	0.402
V-4	*-0.461*	0.141	-0.122	0.169	**0.694**
Zn-4	**0.939**	0.076	0.158	0.054	-0.007
pH	-0.140	0.029	0.294	-0.153	-0.094
Eigenvalue	*5.4*	*4.63*	*3.23*	*2.33*	*1.31*
Variance explained by factor	*23.47%*	*20.12%*	*14.03%*	*10.15%*	*5.69%*
Cumulative variance	*23.47%*	*43.59%*	*57.62%*	*67.77%*	*73.46%*

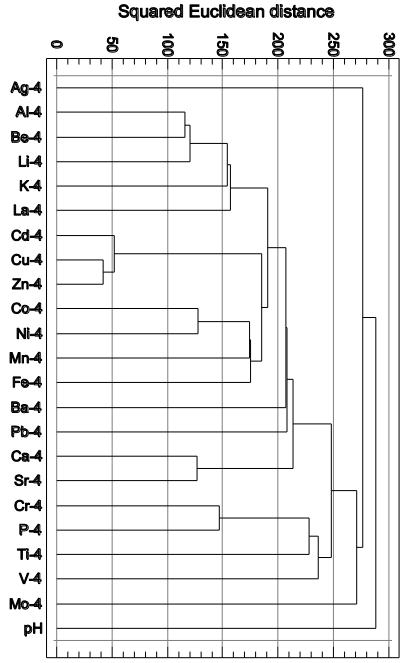

Fig. 7.5. Dendrogram showing the relationship of 22 elements and pH in samples of overburden for sequential extraction step 4 – oxidisable phase (n=224).
Σχ. 7.5. Δενδρόγραμμα που δείχνει τη σχέση μεταξύ 22 στοιχείων και pH στα δείγματα του εδαφικού καλύμματος για το 4ο στάδιο της διαδοχικής εκχύλισης – οξειδώσιμη φάση (n=224).

association suggests that they are related to the organic phase, and Pb is probably derived from airborne dust particles and stack emissions.

7.6.5. Cluster and Factor Analyses on the Residual Phase Data of Overburden

There are five factors with eigenvalues >1, but only four were retained, because at this point there is a distinct break between factors and eigenvalues. The variation accounted for by the four-factor varimax model is 73.27% of the total (Table 7.5, Fig. 7.6).

Factor 1 or *"alumino-silicates factor"* explains 32.83% of the total variance, and has strong positive loadings (>0.6) on Al, K, Ti, Be, Li, V and Ni, moderate loadings (>0.4-0.6) on La and Co, and weak loadings (>0.2-0.4) on Ba and Sr. It is noted that all contaminant elements have negative loadings. The dendrogram shows this suite of elements in one cluster, *i.e.*, Al-K, Ti, Be, Li, V, Ni, Co, La, Sr, Cr, Ba and pH. A possible interpretation is that this particular suite of elements is associated with the operationally defined alumino-silicate phase.

Factor 2 or the *"sulphides factor"* explains 22.43% of the total variance, and has strong positive (>0.6) loadings on Zn, Pb, Ag, Cd, Cu and Fe, moderate loadings (>0.5-0.6) on Ca, Mn, Mo and Sr. The dendrogram shows these elements in two clusters, *i.e.*, (a) Cu-Zn linked to (b) Ag-Pb, and then to Cd, Fe, Mn, Ca and Mo. This suite of elements suggests that it is associated with sulphides, which were not completely digested in step 4 of the sequential extraction procedure.

Factor 3 or *"Ba-Sr factor"* explains 12.17% of the total variance, and has strong positive loadings (>0.6) on Ba and Sr, moderate loadings (>0.4-0.6) on La, Ca and P. This factor has also a strong negative loading of –0.68 on Co, and a moderate negative of –0.39 on Ni. Contaminant elements have low positive loadings. It is noted that the dendrogram does not show this relationship. It is suggested that this factor is related to baryte particles or soil particles rich in Ba.

Factor 4 or *"pyrite factor"* explains 5.84% of the total variance, and has strong positive loadings (>0.6) on Fe, moderate loadings (>0.4-0.6) on Mn, Mo, and Cu. It has also strong negative loadings (<-0.6) on Cr and pH, and a moderate negative loading of -0.43 on Ca. Again, this association is not clearly shown by the dendrogram. The negative covariation with pH and Ca, suggests that the suite of elements with positive loadings occurs in overburden samples with a low pH and Ca contents. Such samples are found in the pyritiferous wastes. The weak positive loadings on contaminant elements, strengthen this inference.

7.6.6. Summary of Factor Analysis Results on Overburden Samples

Table 7.6 summarises the results of factor analysis on the sequential extraction geochemical data of overburden samples. It is quite clear that the specificity and selectivity of the Tessier *et al.* (1979) method on these very complex geochemical overburden samples was not satisfactory to the very demanding researcher. However, from the practical point of view it has provided useful data about the extractability, mobility, possible bioavailability and potential toxicity of the elements studied, as well as their classification into likely mineralogical phases.

Table 7.5. Varimax loadings for the four strongest factors of residual phase overburden geochemical data (n=224). Correlation between varimax scores and transformed data. [For notation used refer to text].

Table 7.5. Φορτία περιστροφής "varimax" για τους τέσσερεις ισχυρότερους παράγοντες της υπολειμματικής φάσης (5ου σταδίου) των γεωχημικών δεδομένων του εδαφικού καλύμματος (n=224). Συσχέτιση μεταξύ των φορτίων varimax και των μετασχηματισμένων δεδομένων. [Για τη σημειογραφία βλέπετε το κείμενο].

Element	*Varimax loadings*			
	Factor 1	*Factor 2*	*Factor 3*	*Factor 4*
Ag-5	-0.223	**0.868**	0.193	-0.010
Al-5	**0.937**	-0.210	0.074	-0.095
Ba-5	0.324	0.007	**0.677**	-0.104
Be-5	**0.885**	-0.178	0.233	-0.143
Ca-5	-0.214	0.507	0.491	*-0.430*
Cd-5	0.003	**0.868**	0.059	0.137
Co-5	0.510	0.274	***-0.675***	0.023
Cr-5	0.322	-0.316	0.175	***-0.682***
Cu-5	-0.230	**0.834**	-0.027	0.389
Fe-5	0.020	**0.627**	-0.262	**0.645**
K-5	**0.895**	-0.157	0.077	-0.089
La-5	0.549	0.302	0.527	0.022
Li-5	**0.855**	-0.130	0.105	0.101
Mn-5	0.172	0.420	-0.128	0.568
Mo-5	0.161	0.419	0.007	0.426
Ni-5	**0.732**	-0.037	*-0.393*	-0.279
P-5	-0.118	0.286	0.420	-0.122
Pb-5	-0.170	**0.879**	0.195	0.145
Sr-5	0.277	0.416	**0.612**	0.301
Ti-5	**0.893**	-0.248	0.011	-0.061
V-5	**0.788**	0.156	-0.223	0.262
Zn-5	-0.265	**0.897**	0.089	0.167
pH	0.126	0.005	-0.098	***-0.658***
Eigenvalue	*7.55*	*5.16*	*2.80*	*1.34*
Variance explained by factor	*32.83%*	*22.43%*	*12.17%*	*5.84%*
Cumulative variance	*32.83%*	*55.26%*	*67.43%*	*73.27%*

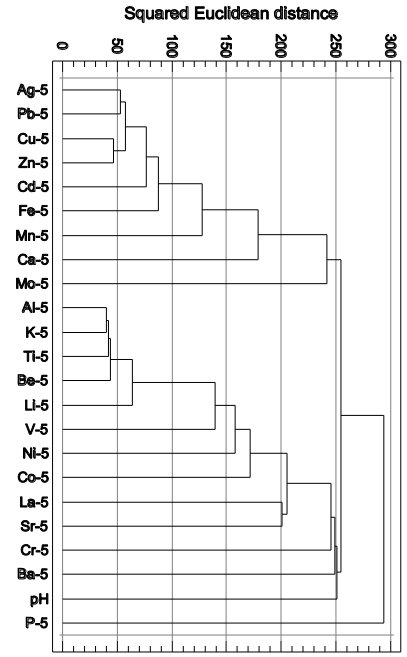

Fig. 7.6. Dendrogram showing the relationship of 22 elements and pH in samples of overburden for sequential extraction step 5 – residual phase (n=224).

Σχ. 7.6. Δενδρόγραμμα που δείχνει τη σχέση μεταξύ 22 στοιχείων και pH στα δείγματα του εδαφικού καλύμματος για το 5ο στάδιο της διαδοχικής εκχύλισης – υπολειμματική φάση (n=224).

Linear regression quantified correlation between pairs of elements, whereas cluster and factor analyses were able to identify interelement correlation, and essentially revealed hidden relationships. Factor analysis distinguished subtle differences for each sequential extraction step, with respect to the different element associations, which are related to distinct mineral phases or source materials. Further, it quantified the variation explained by each. Although the unexplained variation varies from 25.5 to 27.1% for the carbonate, reducible, oxidisable and residual phases, and 51.6% for the exchangeable phase, it does not present problems in the interpretation of results, because the most significant phases have been identified.

Table 7.6. Interpretation table of factor analysis results on the sequential extraction data of overburden samples (n=224). The elements in parentheses have factor loadings >0.55.
Πίνακας 7.6. Ερμηνευτικός πίνακας των αποτελεσμάτων της παραγοντικής ανάλυσης των δεδομένων των διαδοχικών εκχυλίσεων των δειγμάτων επιφανειακού εδάφους (n=224). Τα στοιχεία μέσα στις παρενθέσεις έχουν παραγοντικά φορτία >0.55.

Factor	*Exchangeable*		*Carbonate*		*Reducible*		*Oxidisable*		*Residual*	
	Form, etc.	*%*	*Form, etc.*	*%*	*Form, etc.*	*%*	*Form, etc.*	*%*	*Form, etc.*	*%*
1	Exchangeable (Zn,Pb,Ag,Cd, Co)	21.1	Specifically adsorbed Fe-Al-Mn oxides (Fe,Al,Ba,Mn, Ti,Li,Be,Mo,Co, K,Zn,V)	35.9	Al-Fe oxides (Li,Al,Fe,Ba, Be,Ti,V)	28.8	Sulphides (Zn,Cd,Cu,Mn)	23.5	Alumino-silicates (Al,K,Ti,Be, Li,V,Ni,La)	32.8
2	Carbonates (Ca,Mn,La,P,Sr)	18.1	Specifically adsorbed contaminants (Cd,Pb,Cu,Zn)	14.9	Carbonates (Ca,Sr,La)	20.7	Alumino-silicates (Al,Be,La,Li,Ni, K)	20.1	Sulphides (Zn,Pb,Ag, Cd,Cu,Fe)	22.4
3	Al-Fe oxides (Al,Fe,Ti,Ba)	9.2	Carbonates (Sr,Ca)	11.1	Mn-Fe-Al oxides (Zn,Cd,Pb,Mn, Fe,Cu)	10.2	Carbonates (Sr,Ca,Ba,P)	14.0	Ba-Sr (Ba,Sr)	12.2
4	-	-	La-Ag-Cr specifically adsorbed sites (La,Ag,Cr)	8.2	Co-Ni (Co,Ni,pH)	8.0	Pyrite (Co,Fe)	10.2	Pyrite (Fe,Mn)	5.8
5	-	-	pH	4.4	Fertiliser (K,Cr,P)	5.2	Organic (Ni,V)	5.7	-	-
Total explained variation		48.4		74.5		72.9		73.5		73.2
Unexplained variation		51.6		25.5		27.1		26.5		26.8

7.7. DISCUSSION AND CONCLUSIONS

The Tessier *et al.* (1979) sequential extraction procedure, adapted by Li (1993) for multi-element determinations by ICP-AES, regardless of its limitations of not being completely selective and specific in the dissolution of mineral phases, has proven to be a valuable tool in providing information on the distribution of elements within the Lavrion overburden samples and, hence, on factors influencing their dispersion. Limitations inherent to the method itself were exceeded by other problems, due to the unusual mineralogical composition of the samples themselves. Nevertheless, determination of 22 elements on the extractant solution of each of the five steps enabled a broader study of geochemical associations in overburden samples to be made, and assisted greatly in the effective interpretation of results.

Such a study would have been unthinkable some years ago with atomic absorption instrumentation, because it is too time-consuming to be routinely used and, of course, too costly. To our knowledge this is the first study to analyse *routinely* a large number of overburden samples (n=224) by a sequential extraction method, and to present the results geographically. Thus, enabling the comparative study of element concentrations in the five fractions within and between samples. Interpretation of such a large number

of variables required a good knowledge of lithology, mineralisation, rock alteration, chemistry and mineralogy of the different types of metallurgical processing wastes, and land uses. Otherwise, due to the unusual primary and secondary mineral phases present in the Lavrion overburden samples, results of sequential extractions would have been difficult to interpret.

Ideally, the sequential extraction procedure should be adapted to the particular sample types under study. However, this is not practical, for experimentation in routine investigations is time-consuming and costly, because even under the simplest geological situation there would be more than two sample types. In an area such as Lavrion, where mining and smelting operations have altered greatly the mineralogy of soils and sediments, the variability is far greater. Another plausible approach is to determine the mineralogy of the residue of each extraction phase, before proceeding to the next extraction. In this case, samples should be grouped, and representative samples from the different groups examined. Such mineralogical information would be very useful in the interpretation of results. Nevertheless, such a study is again impractical to be carried out on a routine basis, because again of time and cost.

The only alternative remaining is to accept the drawbacks of selectivity and specificity of reagents used in the sequential extraction procedure selected, and to routinely determine a larger number of elements on the extractant solutions, which will help in the interpretation of results. This proposal is not costly or time consuming, for nowadays modern ICP-AES or ICP-MS instruments are calibrated to determine, at very low detection limits, more than 40 major and trace elements on a routine basis. For this study, interpretation of results would have been facilitated if the following additional elements were determined on each of the extractant solutions, *i.e.*, As, Bi, Hg, S, Sb, Mg, Na, Si and Zr. Further, it is significant to determine total organic matter on all samples to be able to interpret effectively the results of the organic/sulphide phase.

As it has been shown in this study, a detailed knowledge of the area is required to be able to interpret the results. For environmental studies, apart from lithology and mineralisation, it is important to have information about the distribution of mining and metallurgical wastes, their chemistry and mineralogy, and all types of land use.

Despite peculiarities of individual sample types, which undoubtedly account for some of the observed differences in the response of the extractants employed by the sequential extraction method, several conclusive comments can be made on the method used and data processing:

- The high proportion of calcium carbonate, and possibly magnesium carbonate, in overburden samples, resulted in their incomplete dissolution in the second step (carbonate phase). The complete digestion of carbonates was not effected even in the third step (Fe-Mn oxide phase), for the violent exothermic reaction in the fourth step (organic/sulphide phase) is partly explained by the presence of carbonates in the samples. A certain proportion of the element contents occurring in the reducible and oxidisable phases belongs, therefore, to the carbonate phase. This means that the "*bioavailable*" fraction of elements, *i.e.*, exchangeable and carbonate phase contents, is greater.
- Incomplete digestion of sulphide minerals in the fourth step is partly ascribed to the presence of some carbonates. Whatever the mechanism of incomplete decomposition of sulphides in the fourth step, they were completely dissolved in the fifth step. Consequently, a certain proportion of element contents, occurring in the residual phase, belongs to the oxidisable phase.

- The carbonate minerals originating from the parent rocks, which are mainly marble and schist with marble intercalations, largely control pH. Carbonate minerals, play a role as a buffer by reacting with the sulphate radical (SO_4^{2-}), and precipitating $CaSO_4$ in the form of gypsum.
- The generally high pH conditions, except in the area of the pyritiferous wastes, prevailing in the study area, governs the behaviour of heavy metals by keeping the metal forms as hydroxyl species, aqueous metal complexes, and carbonate-bound forms, preventing metal speciation into free ionic form, *e.g.*, exchangeable form (Lindsay, 1979; Chuan *et al.*, 1996; Gee *et al.*, 1997; Song *et al.*, 1999).
- The high pH conditions in the Lavrion area, except the section covered by the pyritiferous tailings, reduce the mobility of heavy metals by decreasing the proportion of the exchangeable form, which is the highly mobile form. This is the reason that has hitherto safeguarded the heavy metal contamination of ground water resources (refer to Chapter 10).
- Interpretation of results would have been more effective if a few additional elements (As, Bi, Hg, S, Sb, Mg, Na, Si, Zr) were determined, and total organic matter.
- Investigation of overburden contamination undoubtedly requires analysis of a substantial number of samples and determination of a large suite of elements.
- Sequential extraction methods should not be applied selectively, therefore, on a few samples, and conclusions drawn for the whole area under investigation. This study has shown that all samples should be analysed by sequential extraction, and the spatial variation of the results examined in conjunction with advanced statistical data processing.
- Sequential extraction methods can provide significant information to understand geochemical dispersion processes in the surficial environment. This can be applied either to determine the origin of trace elements in a single sample or to solve other problems. In environmental studies sequential extraction methods provide, for example, important information about the "*leachability*", "*mobility*" and "*bioavailability*" of elements in soils and sediments, or overburden in general.
- Interpretation of such a large number of variables requires the use of advance statistical techniques, such as regression, cluster and factor analyses. Boxplot comparisons were also very effective in the pictorial presentation of results.

Finally, it has been proven that high concentrations of toxic elements are bioavailable and undoubtedly potentially hazardous to plant, animal and human health. The rehabilitation of contaminated land must be, therefore, the principal objective of the Municipality of Lavrion Officers, for they have the responsibility to improve living conditions, and make the environment safer for children and adults alike. Consequently, apart from the rehabilitation methods, which have been tested by this project (refer to Volume 3 of this report), other cheaper methods should be examined. The Municipality of Lavrion should, in fact, learn from the sensibility shown by other municipalities with similar problems, such as the Portsmouth City Council in the United Kingdom (Walton and Higgins, 1998), and the Trail community of British Columbia in Canada (Hilts, 1996). It should also observe the recommendations made by this project (refer to Volumes 4 & 5 of this report), and the wishes of the local community as outlined in the Environmental Charter of Lavrion, which was compiled in May 1995 (Lavrion 1995a, 1995b), *i.e.*, the people considered as one of the first priorities the rehabilitation of soil by suitable methods, and the inhabitants to be informed about contamination problems.

Chapter 8

PARTITIONING OF THE OPERATIONALLY DEFINED PHASES IN HOUSE DUST – SEQUENTIAL EXTRACTION RESULTS

Alecos Demetriades and Katerina Vergou-Vichou
Institute of Geology and Mineral Exploration, 70 Messoghion Street, Gr-115 27, Athens, Greece

Michael H. Ramsey, Brian J. Coles and Iain Thornton
Environmental Geochemistry Research Group, T.H. Huxley School of Environment, Earth Science & Engineering, Royal School of Mines, Imperial College of Science, Technology & Medicine, Prince Consort Road, London SW7 2BP, U.K.

8.1. INTRODUCTION

Household floor dust is recognised as an important source of toxic elements, especially for young children who spend a lot of their time playing on the floor (Duggan, 1983; Thornton *et al.*, 1985; Davies, 1987; Davies and Thornton, 1987; Laxen *et al.*, 1988; Cotter-Howells and Thornton, 1991). Lead was the element studied extensively on household dust (Thornton and Culbard, 1987), because these studies were concerned with its occurrence in urban indoor dust, contaminated by leaded petrol and paints. In an urban area, like Lavrion, with base metal smelters, a lead-acid battery, a petrol-powered electricity-generating plant and a vast quantity of metallurgical processing wastes, indoor dust is enriched, apart from Pb, with other toxic elements, such as As, Sb, Cd, Hg, Cu, Zn *etc.* Consequently, the hazard to the health of children and adults alike is considerably greater.

In order to evaluate potential health related hazards in the home environment, household floor dust was collected from 127 houses in Lavrion. The sampling, sample preparation and sequential extraction methods have already been described in Chapters 2A and 2B (this Volume) respectively. In Chapter 7, the "operationally defined" geochemical phases of the sequential extraction procedure were discussed with respect to overburden samples. However, this information, apart from the principles, cannot be used to interpret house dust sequential extraction results, because they are completely different media in terms of their physical and chemical properties.

Household floor dust is made up from a variety of particles, including soil, road dust, vehicle exhaust emissions, industrial emissions, atmospheric fallout, aerosols, building materials (cement, paint, *etc.*), furniture, clothes, carpets, tapestry, liquid fuel burning, wood burning (smoke and ash), cigarette (smoke and ash), food, *etc.* Lavrion household floor dust is also comprised of fine particles derived from the metallurgical processing wastes, municipal refuse burning, and petrol-powered electricity-generating plant. Hence, floor dust is a very complex composite medium. Each house, depending on its location, building materials, furniture, *etc.*, produces its own peculiar dust particles. It may be said, that residents leave their own personal signature in their house dust, *e.g.*, father working at the smelter used to bring with him heavy metal dust in his home, a confounding factor for high blood-lead (b-Pb) levels in children, found by epidemiologists (Eikmann *et al.*, 1991; Makropoulos *et al.*, 1991). Apart from the type of work, other confounding factors include parents' cigarette smoking or not, pets (dogs

and cats), which can bring into the house particles of wastes and contaminated soil, and many others.

Since, one of the confounding factors, related to the degree of contamination of indoor dust, is house location, each household floor dust sample was classified according to whether the house is over

- contaminated soil,
- flotation residues,
- slag and earthy material within slag, or
- pyritiferous tailings (Table 8.1).

In Table 8.1, the area covered by each type of waste and contaminated soil, grouped according to the house location category, is also given. The actual area and percentage coverage of the ten metallurgical processing waste categories and contaminated soil are tabulated in Table 2.3 in Chapter 2 (p.19).

Table 8.1. Area covered by the major sources of contamination, and number of houses sampled over each.
Πίνακας 8.1. Εμβαδόν των κύριων πηγών ρύπανσης και ο αριθμός των δειγματισθέντων σπιτιών που είναι κτισμένα πάνω από κάθε κατηγορία.

Sources of contamination	*Area (m^2)*	*Area (%)*	*Houses sampled*	*Samples (%)*
Contaminated soil	5,419,643.83	74.91	101	79.53
Beneficiation/flotation residues	499,660.94	6.90	21	16.53
Slag and sand-blast wastes	801,647.76	11.08	4	3.15
Pyritiferous tailings	514,076.95	7.11	1	0.79
Total	**7,235,029.48**	**100.00**	**127**	**100.0**

Contaminated soil covers the greatest part of the Lavrion urban area, and most houses are situated on it. Although the beneficiation/flotation residues cover a smaller area than slag/sand-blast wastes and pyritiferous tailings, they are more important with respect to house siting, and the number of houses sampled reflects this.

To our knowledge this is the first systematic sequential extraction study on household floor dusts. For this reason, and to facilitate an in-depth study, a considerable number of tables have been compiled, and figures plotted for each of the four major categories of contaminated land (Tables 8.1A-.105A & Figs. 8.1A-.42A are in Appendix 4A of Volume 1A, p.103-156). Although there was only one house over pyritiferous tailings the results are tabulated, for even this minor information is considered significant for the health-related environmental problems in Lavrion.

8.2. PARTITIONING OF OPERATIONALLY DEFINED PHASES IN HOUSE DUST

Concentrations of elements for each of the five operationally defined selective extraction phases, *i.e.*,

- adsorbed and exchangeable forms *(step 1: exchangeable phase)*,
- bound to carbonates and to specifically adsorbed sites *(step 2: carbonate phase)*,

- bound to Fe and Mn oxides *(step 3: reducible phase)*,
- bound to organic matter and sulphides *(step 4: oxidisable phase)*, and
- within the structure of silicate and refractory minerals *(step 5: residual phase)*,

are presented as coloured five-bar plots for each of the 127 house dust samples at their respective sampling sites on maps with the three major categories of metallurgical processing wastes (Maps 8.1 to 8.30 in Volume 2 of this report) . This method shows pictorially the actual levels of elements in each of the five sequential extraction phases for every sample, and spatial variability. Hence, within and between sample comparisons can be made with ease, and related to the outdoor environment, *e.g.*, the different types of metallurgical processing wastes and contaminated soil (residual or alluvial). Statistical parameters of each of the five phases are also presented on the maps, and a summary of the sequential extraction scheme in a flow diagram. Hence, the reader has all the necessary information to study in detail the variation of element concentrations of each of the five extraction phases without referring to the following description of results.

For a detailed study of the sequential extraction results on house dust samples, the following tables and figures have been compiled/drawn for each element, and are presented in Appendix 4A of Volume 1A of this report (p.103-193):

- table showing the percentage proportion of the element extracted by each of the five sequential extraction steps out of the total;
- tables of statistical parameters of house dust samples taken over areas with (a) contaminated soil, (b) flotation residues, (c) earthy material within slag, and (d) pyritiferous wastes (including pyrite tailings and pyritiferous sand).
- multiple boxplot of the distribution of each element in the five phases of the sequential extraction procedure (the statistical parameters of this particular plot are tabulated on Maps 8.1 to 8.30, Chapter 8, Volume 2 of this report), and
- multiple boxplots of the distribution of element concentrations in the five phases of the sequential extraction procedure on house dust samples collected from houses situated over different types of wastes, *i.e.*, (a) contaminated soil, (b) flotation residues, (c) earthy material within slag, and (d) pyritiferous wastes. These plots should be studied in conjunction with the respective statistical tables.
- Pearson's linear correlation coefficient was calculated for each of the five steps for 22 elements and pH, and the correlation matrices are presented in Tables 8.106A-8.110A (Appendix 4A in Volume 1A, p.157-165). Data were normalised by the 2-parameter log transformation used by Miesch (1990) in the G-PREP module of program G-RFAC. This is the most widely applied transformation in chemometrics. The 2-parameters are the mean log and log variance, which completely define a lognormal distribution. Correlation coefficients range between –1 and +1 and measure the strength of the linear relationship between the variables.
- R-mode cluster and factor analyses were performed on log transformed results of each of the five extraction steps for 22 elements and pH, and are presented in the form of dendrograms (Figs. 8.2 to 8.6 in this Chapter and 8.43A-.47A in Appendix 4A, Volume 1A, p.158-166) and Tables 8.106A to 8.110A; since, element data are in different concentration ranges, they were standardised after being transformed by the 2-parameter log transformation, but prior to the calculation of dendrogram parameters. This step was necessary in order to equalise the influence of the variables during R-mode cluster analyses.

  These can be compared with the corresponding Tables 7.106A-.110A and Figures 7.43A-.47A for overburden (refer to Appendix 3A in Volume 1A, p.93-101). For ease of reference to the two sets of tables and figures, the same decimal numbering is

followed; additional Tables and Figures plotted for the comparison of house dust and garden soil samples are appended, *i.e.*, Tables 8.111A to 8.116A (p.167-172) and Figs. 8.48A to 8.89A (p.173-193) in Appendix 4A of Volume 1A of this report.

From each house two samples were taken, a floor dust and a soil/overburden from its yard or garden (called in the following description "*garden soil*"). The total number of houses sampled in this way was 126. Since, house location is regarded as one of the major factors, contributing to the level of contamination of household floor dust, the five step sequential extraction results of house dust, and its corresponding garden soil sample, are compared by means of boxplots in terms of

(a) element concentrations levels, and
(b) the percentage proportion of each element, in relation to the total content (Figs. 8.48A to 8.89A, which are in Appendix 4A of Volume 1A of this report, p.173-193).

The former plots compare the range of element concentrations extracted by each of the five sequential extraction steps in samples of house dust and garden soil. The latter plots are useful for they give an idea of the relative proportion of element contents, extracted by each of the five sequential extraction steps from samples of house dust and garden soil. They essentially depict the different behaviour of the two sample types to the extractant solutions of each step, which are mainly dependent on

- mineralogical composition of samples,
- physico-chemical properties of samples,
- mode of occurrence of each element in the samples,
- leachability of each element by the extractant solutions, and
- concentration of the element associated with the operationally defined geochemical phases of the sequential extraction procedure.

Differences do also exist within each sample type, because their parent materials are very variable, *e.g.*, garden soil samples have been collected from (a) residual or alluvial soil contaminated to a different degree, and (b) metallurgical processing wastes (flotation residues, slag, pyrite), which may or may not have been mixed with clean soil, manure, or chemical fertiliser, *etc.* Nevertheless, it is assumed that differences between the two sample types are larger.

For the detailed study of relationships between house dust and garden soil samples, the linear correlation coefficient, on the log (base 10) transformed data, was calculated for total element contents, and for each of the five extraction steps (Tables 8. 111A-.8.116A in Appendix 4A, Volume 1A, p.167-172). The comparison of total element contents shows the variability in house dust samples that could be explained by garden soil as the source material. Whereas, the comparison between each of the five extraction steps, exhibits the proportion of element variation in house dust, that can be explained by a similar mode of occurrence as in garden soil. Essentially it reveals subtle relationships between house dust and garden soil, which are largely dependent on the above mentioned factors.

8.3. DESCRIPTION AND DISCUSSION OF RESULTS

The results of each element will be described and discussed in three sections, *i.e.*,

(a) partitioning patterns in terms of the most significant fraction or fractions, spatial variability and correlation with other elements,

(b) comparison between house dust and garden soil samples, and
(c) bioavailability and biological effects of each element.

The latter is very important for cross-sectional epidemiological studies in Lavrion have hitherto examined Pb, As and Cd. As it has already been shown the number of contaminant elements is greater. In the following description as "*contaminant elements*" are considered, not only the known toxic elements, but all those that occur in excessive amounts in the home environment, and could be made available to children. Essentially, all trace elements are toxic if ingested or inhaled at sufficiently high levels for a long enough period. Elements in our body are all in balance with another, so that excess or otherwise of one or more will affect the levels of others. Their relationships are summed up in the element wheel shown in Figure 8.1 (Mervyn, 1980, 1985, 1996).

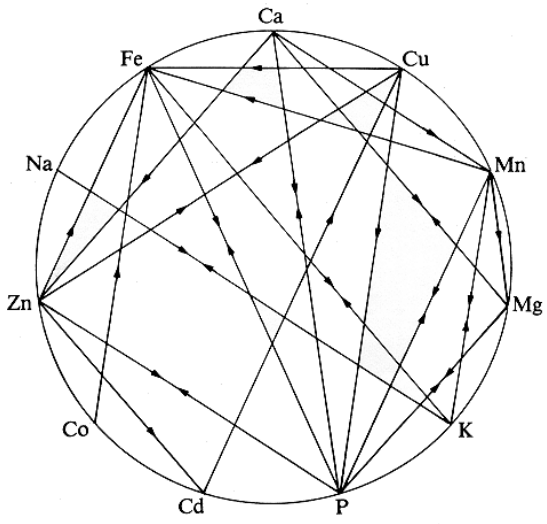

Fig. 8.1. Element relationships in the human body (from Mervyn, 1985, Fig. 1, p.130).
Σχ. 8.1. Σχέσεις χημικών στοιχείων στο ανθρώπινο σώμα.

On this wheel, a tie line with an arrow pointing to a particular element means that an excess of the element, from whence the arrow comes, may cause a deficiency of that particular element. Tie lines with two opposing arrows show elements that may influence one another, *i.e.*, each element in excess or deficiency may influence the level of the other. For example, in the case of a connecting line with

(a) one arrow:

- a high Ca intake may reduce the amount of Zn and Mn;
- a high Cd intake will cause Cu levels to drop;
- a high Cu and Zn intake will reduce the level of Fe, and

(b) two opposing arrows:

- an excess of Na will cause the lowering of K levels in the body; a low K intake will allow Na to accumulate;
- Zn in excess will depress P levels; a low P level will, therefore, allow Zn to accumulate; but an excess of P will lower Zn levels;
- high levels of Zn will also depress Cu levels, or the reverse.

It may be said that it is a *"vicious circle"*, but it illustrates well that elements in our body must be in the correct balance, otherwise health related problems are caused. Contamination of the Lavrion urban environment is more complex than was originally anticipated by epidemiologists. The obvious diseases associated with Pb and As have been identified, but the more subtle sub-clinical level diseases, possibly related to other elements, are more difficult to diagnose. New epidemiological studies in Lavrion must study, therefore, the effects of a large number of elements.

A point that must be remembered is that the pH of fluids in the human stomach is between 1 and 3, due to the presence of hydrochloric acid (Ferguson, 1990). In a completely empty stomach, the fluids have a pH of about 1 (George Kazantzis, person. commun., 1998). Hence, in such an environment heavy metals will become cationic or anionic (*e.g.*, chloro-complex anions) in chemical form. Digested material moves into the duodenum and the small intestine, where the pH is around 6 to 7. Much of the absorption occurs in the duodenum, jejunum and ileum. Materials on the surface of the gastrointestinal tract may be absorbed into the walls and, hence, into the blood stream. Numerous factors influence the absorption process and, of course, the fraction of a metal intake that is absorbed. These, according to Ferguson (1990), include:

- the chemistry of the metal, especially its speciation of the metal at the time of absorption, and
- the solubility of the metal species.

Solubility is controlled by pH at the specific segment of the intestine where the absorption takes place. The time taken for digestion, and the rate of movement in the intestine, influence the kinetics of conversion of cations or anions at pH 1 to 3 (in the stomach) to other species in the intestine at pH 6 to 7. The amount of food eaten, and the type of diet can also influence the absorption of metals. Microbial influences are also important for food digestion, as are the presence of organic chelating agents, and other metals that compete for absorption sites. Since, many factors are involved, it is not possible to generalise over the fraction of metals absorbed. The point that will be stressed in the following discussion will be the amount of metal that could be made available down to a pH of approximately 2, which is the pH of the oxidisable phase extractants (Step 4).

It is hoped that the following description and discussion of results will give the impetus for a new systematic epidemiological study, because it is strongly believed that children should not grow in such an adverse environment. The principal priority is, of course, the rehabilitation of contaminated land, for this is the only way to improve living conditions in Lavrion. Since, this is not something that can be done immediately due to the large cost (refer to Volumes 4 & 5 of this report), it is important to know all the health related problems that are affecting the children.

It is noted that Tables and Figures with suffix "A" will be found in Appendix 4A of Volume 1A of this report (p.103-193). Whereas, *normal numbered,* Tables and Figures are within the text of this Chapter. The following description and discussion of house dust sequential extraction results is made with reference to the distribution map (Maps 8.1 to 8.30 in Volume 2), tables and figures for each element (in this Chapter and in Appendix 4A of Volume 1A), the lithological and house dust pH maps (Maps 2.2 & 2.6 in Volume 2). *For better reading, the geochemical distribution map, tables and figures of each element will be mentioned after the title, and not in the descriptive text, except the reference to dendrograms, correlation matrices (Appendix 4A in Volume 1A), and other maps in Volume 2.*

Since, the results presented, may be interpreted in different ways, depending on the interests of the end-user, the following description and discussion of results should serve as a guide to the most significant parts of the distribution of element contents in the five operationally defined geochemical phases.

8.3.1. PARTITIONING OF SILVER (Ag) IN HOUSE DUST (Map 8.1, Tables 8.1A-.5A, Figs. 8.1A-.2A)

The most significant fraction for Ag in house dust, as in overburden, is extraction step 5 (residual phase), which accounts for 35.02 to 99.39% of the total content (median=90.28%; <1-34.6 ppm; Ag; median=4.37 ppm Ag). The exchangeable and oxidisable phases are of lesser importance, extracting up to 2.1 and 2.2 ppm of Ag respectively.

Silver in the residual phase is associated with Pb (r=0.78), Cd (r=0.76), Zn (r=0.74), Ca (r=0.64), Be (r=0.57), Li (r=0.51), K (r=0.51), Fe (r=0.50), P (r=0.47), Al (r=0.47), Cu (r=0.46) and La (r=0.45) (Table 8.110A; Fig. 8.47A in Appendix 4A, Vol. 1A), indicating that it occurs in the crystal lattice of silicate minerals and sulphides, which were not totally decomposed in step 4 of the sequential extraction procedure.

The highest Ag levels in the residual phase are in floor dust samples of houses over metallurgical processing wastes or contaminated soil near to the wastes. Two houses with comparatively high exchangeable Ag contents (up to 2.1 ppm Ag) are to the south of the Santorineika flotation residues. Houses over contaminated residual soil, in areas away from smelter wastes have comparatively lower residual Ag contents.

8.3.1.1. Comparison of silver (Ag) in house dust and garden soil

Apart from similarities in the residual Ag patterns between house dust and garden soil, the overall partitioning patterns show minor, but distinct differences on a sample by sample comparison (Fig. 8.48A; Maps 7.1 & 8.1 in Volume 2 of this report). These differences can be seen with respect to the *relative* leachability of Ag in the different extraction phases of the two sampling media (Fig. 8.49A). The leachability or extractability patterns are approximately similar only for the residual phase. The other phases show minor differences, except step 2, for which the differences are great, house dust extracts a larger amount of its total silver content.

It is again stressed, that garden soil has higher absolute Ag contents than house dust. Although this observation applies to almost all elements, differences do exist and will be noted in the following description and discussion of results. The comparison essentially refers to the relative leachability or extractability of elements between the two sampling media, which gives an indication of differences in the behaviour of house dust and garden soil to the extractant solutions of the sequential extraction procedure. Differences indicating that the mode of occurrence of elements in the two sampling media is different.

Minor differences in the partitioning patterns of Ag between house dust and garden soil, were quantified by Pearson's linear correlation coefficient, which was determined on the log (base 10) transformed data (n=126). Thus, the linear correlation coefficients between Ag in house dust and garden soil for total and sequential extraction contents are:

- total Ag r = 0.516 (Table 8.111A)
- exchangeable Ag r = 0.131 (Table 8.112A)

- carbonate Ag r = -0.162 (Table 8.113A)
- reducible Ag r = -0.010 (Table 8.114A)
- oxidisable Ag r = 0.295 (Table 8.115A)
- residual Ag r = 0.513 (Table 8.116A).

It is apparent from the correlation coefficients of Ag between house dust and garden soil that there is only a moderately strong positive correlation for total and residual phase Ag contents. For total Ag contents, 26.58% of the variability in household dust could be explained by garden soil Ag. These data, however, imply that the greatest part of house dust total Ag contents are not derived from exterior garden soil, but from other sources either within the home environment or distant outdoor, such as fugitive dust from metallurgical processing wastes, *etc.* Possible internal sources are brazing jewellery, silverware, alloys, coins *etc.* (Lapedes, 1978; Reimann *et al.*, 1998).

The correlation coefficients of the five extraction phases show that there are distinct differences in the extractability of Ag between samples of house dust and garden soil. These differences in geochemical behaviour suggest that the mode of occurrence of Ag in the two sampling media is different and, especially for extraction steps 1 to 4. For residual Ag contents, 26.35% of the variability in household dust could be explained by a similar geochemical behaviour of residual Ag in garden soil. Implying, however, that the greatest part of residual Ag in house dust is explained by extraction from other particles, not related to garden soil. This is supported by the correlation of house dust residual Ag with a larger number of elements (r>0.45) than garden soil residual Ag.

8.3.1.2. Bioavailability and biological effects of silver (Ag)

Readily available amounts of Ag in house dust vary from 0.1 to 3.1 mg/kg Ag (steps 1+2). A child's gastric fluids, in a completely empty stomach, have a pH of 1.0, which means that they can digest element contents held even in the oxidisable phase fractions, which are extracted at a pH of 2.0, *i.e.*, from 0.18 to 5.8 mg/kg Ag (steps 1+2+3+4), and possibly a minor proportion of the residual phase contents.

Silver appears to be of low toxicity for humans, although is toxic for many micro-organisms and fish. Silver compounds can prevent uptake of Se, Cu and vitamin E (Reimann *et al.*, 1998). Long regular consumption of Ag can lead to argyria, a blue-grey skin disease, which is not dangerous (Hanssen and Marsden, 1985). According to Mervyn (1985, 1986, 1996) the acceptable daily intake for Ag has not yet been determined.

8.3.2. PARTITIONING OF ALUMINIUM (Al) IN HOUSE DUST (Map 8.2, Tables 8.6A-.10A, Figs. 8.2A-.4A)

The greatest proportion of Al in house dust is found, as in overburden, in the residual fraction, which accounts for 46.45 to 98.27% of the total content (median=92.15%; 2,250-43,400 ppm Al; median=11,700 ppm). Low levels of Al are found in the reducible – the Fe-Mn fraction (130-3,300 ppm Al; median=615 ppm Al), carbonate (4-2,140 ppm Al; median=32 ppm Al), and oxidisable phases (59-1050 ppm Al; median=290 ppm Al). Very low levels of Al occur in the exchangeable phase (<1-151 ppm Al; median=9 ppm Al).

Aluminium in the residual phase is associated with Li (r=0.93), K (r=0.91), Be (r=0.90), V (r=0.71), Sr (r=0.59), Fe (r=0.55), La (r=0.55), Pb (r=0.53), Zn (r=0.53), Co (r=0.53), Mn (r=0.46) and Ti (r=0.45) (Table 8.110A; Fig. 8.47A). This association indicates that Al in house dust

mainly occurs in the crystal lattice of silicate minerals, but is also related to sulphides, which were not completely digested in step 4 of the sequential extraction procedure.

The highest Al levels in the carbonate and reducible phases are found at Kavodokanos over pyritiferous tailings, flotation residues, slag and nearby contaminated garden soil; this pattern is also found in garden soil samples (see Map 7.2).

8.3.2.1. Comparison of aluminium (Al) in house dust and garden soil

The partitioning patterns between house dust and garden soil Al are approximately similar, but they differ in terms of absolute concentrations (Fig. 8.50A, Maps 7.2 & 8.2); house dust has generally lower levels except in the carbonate phase (house dust: 4-2140 ppm Al; median=32 ppm Al; garden soil: 4-1580 ppm Al; median=28 ppm Al). This feature is shown in Figure 8.51A of the relative leachability of Al, which also depicts that the reducible phase (step 3) extracts more metal from the total house dust content in comparison to garden soil.

House dust residual Al appears to be correlated with more elements (r>0.45) than garden soil residual Al. This observation suggests that the mode occurrence of Al in the two sampling media is different.

The linear correlation coefficients between Al in house dust and garden soil for total and sequential extraction contents are:

- total Al r = 0.026 (Table 8.111A)
- exchangeable Al r = 0.060 (Table 8.112A)
- carbonate Al r = 0.675 (Table 8.113A)
- reducible Al r = 0.492 (Table 8.114A)
- oxidisable Al r = 0.188 (Table 8.115A)
- residual Al r = 0.017 (Table 8.116A).

The above correlation coefficients show that there is no correlation for total Al contents between house dust and garden soil samples, suggesting that the source of household Al is different, *i.e.*, windblown dust from the metallurgical processing wastes and other outdoor and indoor sources. Possible indoor sources are aluminium kitchenware, aluminium foil, textiles, paints, soap, glass, doors, windows, cement, concrete, *etc.* (Lapedes, 1978; Reimann *et al.*, 1998); other probable outdoor sources are the aluminium converter industries in Lavrion. Aluminium has moderately strong positive correlation coefficients in the carbonate and reducible phases, indicating that 45.56% and 24.22% of the variation in house dust respectively is explained by a similar mode of occurrence as in garden soil (samples from Kavodokanos and Phenikodassos).

8.3.2.2. Bioavailability and biological effects of aluminium (Al)

Readily available amounts of Al in house dust vary from 4.5 to 2,291 ppm Al (steps 1+2). The very low pH of a child's gastric fluids in an empty stomach can, however, attack element contents held even in the oxidisable phase fractions, *i.e.*, from 193.5-6,641 ppm Al (steps 1+2+3+4).

The major effects of aluminium toxicity seem to be on the central nervous system, though it does have effects on the parathyroid gland, influencing the degree to which it responds to low serum calcium by excreting parathyroid hormone (Davies and Stewart, 1987). Presenile dementia (Alzheimer's disease) is a condition in which an individual

becomes senile before his time, *i.e.*, brain degeneration. It appears to be associated with high levels of aluminium intake. Levels of 12 μg Al per gram of brain tissue giving rise to brain deterioration in experimental animals, are the same as those found in the brains of human beings, who suffered from Alzheimer's disease (Mervyn, 1985, 1986, 1996).

Aluminium can accumulate in the liver, interfering with its working, and its effects on the kidneys, include nephritis and degeneration (Davies and Stewart, 1987). The element can cause phosphate depletion and skeletal demineralisation resembling osteomalacia in those undergoing kidney dialysis; brain dysfunction in those undergoing kidney dialysis; slow learning in the young, an effect normally ascribed to Pb; epileptic-type fits in experimental animals, and exacerbation of osteoporosis are some of the known diseases that are associated with aluminium toxicity (Mervyn, 1985, 1986, 1996).

Toxic effects of aluminium on the skin include contact dermatitis and irritation in sensitive people (Mervyn, 1985, 1986, 1996).

8.3.3. PARTITIONING OF BARIUM (Ba) IN HOUSE DUST (Map 8.4, Tables 8.11A-.15A, Figs. 8.5A-.6A)

The partitioning patterns of Ba in house dust, as in overburden, have a large variation in the different phases, and are dependent on differences in the chemistry of metallurgical processing wastes and contaminated soil. Overall the residual fraction accounts for 1.87 to 98.10% of the total content (median=85.19%; 36.1-2,450 ppm Ba; median=368 ppm Ba). Similar to overburden, the second and third most important fractions of indoor dust for houses over the flotation residues, slag and contaminated soil (Fig. 8.6A), are the reducible (0.86-74.29% of the total; median=8.26%; 10.6-1190 ppm Ba; median=31.5 ppm Ba), and the carbonate (0.32-49.34% of the total; median=3.52%; 4.3-824 ppm Ba; median 13.4 ppm Ba) phases. It appears, therefore, that the largest proportion of Ba occurs in

(a) the crystal lattice of mainly silicate minerals, referring to the comparatively low positive, but significant, correlation in the residual fraction with Al, K, Ti, Be, Li, V, Ni, Co, La, Sr and Cr (Table 8.110A, Fig. 8.47A in Appendix 4A, Vol. 1A);
(b) Al and Fe-Mn oxides, since it has a high correlation in the reducible (Fe-Mn oxide) phase with Al (r=0.72), Fe (r=0.65) and Mn (r=0.53) (Table 8.108A, Fig. 8.45A), and
(c) the specifically adsorbed sites of the carbonate phase, and not with calcium minerals, because of its low correlation with Ca (r=0.09), and its high correlation with Al (r=0.87), Mn (r=0.86), Fe (r=0.79), Ti (r=0.71), Zn (r=0.64), Mo (r=0.51), Be (r=0.49), Li (r=0.48) and K (r=0.46) (Table 8.107A, Fig. 8.44A), suggesting a relationship with adsorption sites occurring on the surfaces of amorphous precipitates of alumino-silicates, aluminium, iron and manganese oxides, other micro-crystalline precipitates of oxides, but not phosphates, for it has a negative correlation with P (r=-0.36).

The first case is the dominant one, for it concerns most of the Lavrion house dust samples. The second and third cases refer to samples of house dust over flotation residues, earthy material within slag (*slag earth*), and contaminated soil collected from Kavodokanos, and over contaminated soil at Phenikodassos.

8.3.3.1. Comparison of barium (Ba) in house dust and garden soil

Although element associations of Ba in house dust and garden soil are approximately the same, possibly suggesting similar source materials, there are differences in the absolute values of correlation coefficients. This indicates that the mode of occurrence of Ba is different in the two sampling. In terms of absolute Ba concentrations, the residual phase of house dust has higher levels than the corresponding garden soil samples (Fig. 8.52A); this feature is also shown in terms of the relative extractability (Fig. 8.53A). Differences, in the majority of cases, are also shown by the linear correlation coefficients between Ba in house dust and garden soil for total and sequential extraction contents, *i.e.*,

- total Ba r = 0.303 (Table 8.111A)
- exchangeable Ba r = 0.091 (Table 8.112A)
- carbonate Ba r = 0.795 (Table 8.113A)
- reducible Ba r = 0.782 (Table 8.114A)
- oxidisable Ba r = 0.250 (Table 8.115A)
- residual Ba r = 0.136 (Table 8.116A).

The above correlation coefficients show, that there is very weak positive correlation for total Ba contents between house dust and garden soil samples, suggesting that only a very small proportion (9.18%) of house dust variation can be explained by outside garden soil. House dust Ba is derived, therefore, from other sources within the home environment and windblown dust from the metallurgical processing wastes, *etc.* Possible sources within the home environment are paints, rubber, paper, ceramics, glass, *etc.* (Lapedes, 1978; Reimann *et al.*, 1998). With respect to the sequential extraction steps, barium, in house dust and garden soil, has only strong positive correlation coefficients in the carbonate and reducible phases, suggesting that 63.17% and 61.23% of the variation in house dust respectively is explained by a similar mode of occurrence as in garden soil. Therefore, Ba in household dust is not directly related to outdoor garden soil, suggesting that it is brought into the home environment by other means.

8.3.3.2. Bioavailability and biological effects of barium (Ba)

Readily available amounts of Ba in house dust vary from 5.3 to 841 ppm Ba (steps 1+2). A child's gastric fluids in an empty stomach can, however, attack element contents held even in the oxidisable phase fractions, *i.e.*, from 17.7- 2,080 ppm Ba (steps 1+2+3+4).

Soluble barium salts are highly toxic (Mervyn, 1985, 1986, 1996). A fatal dose of barium chloride may be as low as 1 gram. Symptoms of poisoning include vomiting; colic; diarrhoea; slow irregular pulse; high blood pressure; convulsive tremors; muscular paralysis.

8.3.4. PARTITIONING OF BERYLLIUM (Be) IN HOUSE DUST (Map 8.5, Tables 8.16A-.20A, Figs. 8.7A-.8A)

The largest proportion of house dust Be occurs, as in overburden, in the residual phase, which accounts between 33.76-90.83% of the total content (median=75.20%; 0.07 to 0.6 ppm Be; median=0.33 ppm Be). The second and third most significant fractions are the reducible (3.24-44.03% of the total; median=16.00%; <0.012-0.37 ppm Be; median=0.075 ppm Be) and

carbonate (0.55-26.03% of the total; <0.022-0.24 ppm Be; median=0.024 ppm Be) phases. It appears that there are similarities between house dust and garden soil Be; the largest proportion of Be, like Ba, occurs in

(a) the crystal lattice of mainly silicate minerals and sulphides, referring to its high to moderate positive correlation with K (r=0.92), Al (r=0.90), Li (r=0.86), V (r=0.70), Sr (r=0.60), Pb (r=0.59), Zn (r=0.57), Ag (r=0.57),La (r=0.55), Cd (r=0.50), P (r=0.48), Fe (r=0.48), Ca (r=0.47) and Ti (r=0.44) (Table 8.110A, Fig. 8.47A);
(b) Al and Fe-Mn oxides, since it has a high to moderate positive correlation in the reducible (Fe-Mn oxide) phase with Al (r=0.53), Mn (r=0.49) and Fe (r=0.45), and other elements adsorbed by these oxides, such as Ti (r=0.65), Li (r=0.59), K (r=0.56), Sr (r=0.54), Pb (r=0.54), Zn (r=0.53), Ba (r=0.50), Co (r=0.43) and Ca (r=0.43) (Table 8.108A, Fig. 8.45A), and
(c) the specifically adsorbed sites of the carbonate phase, and not so much with calcium carbonate minerals, because of its very low positive correlation with Ca (r=0.15), and its moderate positive correlation with Fe (r=0.55), Mn (r=0.52), Zn (r=0.51), Ba (r=0.49), Ti (r=0.45), Li (r=0.45) and Al (r=0.44) (Table 8.107A, Fig. 8.44A), suggesting a relationship with adsorption sites occurring on the surfaces of amorphous precipitates of alumino-silicates, aluminium, iron and manganese oxides, other micro-crystalline precipitates of oxides, but not with phosphates, for it has a weak negative correlation with P (r=-0.27).

Similar to overburden, the first case is the dominant one, for it concerns most of the Lavrion house dust samples. The second (Fe-Mn phase) and third (carbonate phase) cases, refer to indoor dust samples of houses over slag earth, flotation residues, contaminated residual soil and pyritiferous sand, collected from different parts of Lavrion, and in particular Kavodokanos, and to a lesser extent from Fougara, Ayios Andreas and Phenikodassos.

8.3.4.1. Comparison of beryllium (Be) in house dust and garden soil

Although element associations of Be in house dust and garden soil are similar, there are differences with respect to their correlation level, especially in the suite of elements with moderate to strong correlation coefficients. In terms of absolute Be concentrations, garden soil samples have higher levels than house dust (Fig. 8.54A). With respect to the relative extractability of Be, it is apparently held more loosely in the carbonate and reducible phases of house dust (Fig. 8.55A).

The linear correlation coefficients between Be in house dust and garden soil for total and sequential extraction contents are:

- total Be r = 0.033 (Table 8.111A)
- exchangeable Be r = 0.292 (Table 8.112A)
- carbonate Be r = 0.329 (Table 8.113A)
- reducible Be r = 0.105 (Table 8.114A)
- oxidisable Be r = 0.172 (Table 8.115A)
- residual Be r = 0.027 (Table 8.116A).

The above correlation coefficients show that there is no correlation for total Be contents between house dust and garden soil samples, suggesting that the source is not the outside garden soil, but other interior or exterior sources. The low to almost no

correlation shown, in the sequential extraction steps, suggests that the mode of occurrence between the two sampling media is different.

8.3.4.2. Bioavailability and biological effects of beryllium (Be)

Readily available amounts of Be in house dust vary from 0.005 to 0.27 ppm Be (steps 1+2). A child's gastric fluids in an empty stomach can, however, attack element contents held even in the oxidisable phase fractions, *i.e.*, from 0.011-0.71 ppm Be (steps 1+2+3+4).

Recommended daily oral intake is 0.005 mg Be/kg/day (US EPA, 1991) as a maximum for both sub-chronic and chronic cases.

Beryllium is considered carcinogenic, especially affecting bones; it also causes severe rickets or rachitis (Mervyn, 1989, 1996). The latter illness is thought to be the result of binding of phosphate to Be in the gut and the subsequent depletion of phosphorus in the body (Daugherty, 1992).

8.3.5. PARTITIONING OF CALCIUM (Ca) IN HOUSE DUST (Map 8.8, Tables 8.21A-.25A, Figs. 8.9A-.10A)

The Ca partitioning patterns are approximately similar in almost all house dust samples. House dust Ca shows, like overburden, that the carbonate and reducible phases are the major phases, and account for 8.03-55.3% (median=17.39%) and 34.04-82.89% (median=71.33%) of the total content respectively, *i.e.*, their corresponding levels being 9,180-58,200 ppm Ca (median=22,000 ppm Ca) and 22,100-191,000 ppm Ca (median=94,400 ppm Ca). The most important phase, with respect to the level of Ca, is the reducible (Fe-Mn oxide), and not the carbonate. Similar to overburden, CH_3COONa (*NaOAc*) was not able to extract the greatest proportion of total $CaCO_3$-bound calcium, which is present in carbonate rich house dust samples. According to Tessier *et al.* (1979) the attack by CH_3COONa is able to dissolve successfully even dolomite ($CaCO_3MgCO_3$). Assuming that this is true, then the apparent incomplete dissolution of Ca from calcite and dolomite by CH_3COONa, suggests that there are other modes of occurrence of Ca in Lavrion or the proportion of calcium carbonate minerals was very high, and could not be totally digested. For other possible explanations, the reader is referred to Chapter 7.

It is interesting to note that in the Fe-Mn phase, Ca has a low negative correlation with Fe (r=-0.16) and no correlation with Mn (r=0.04) indicating, as in overburden, that it is not related to either Fe or Mn oxides. Thus, supporting the interpretation of incomplete dissolution of calcium carbonate minerals in step 2 (carbonate phase) of the sequential extraction procedure.

The levels of house dust Ca in the exchangeable and residual phases are of local significance, and depend on its mode of occurrence.

House dust calcium is strongly related to Sr in extraction steps 1 to 4, indicating the diadochic substitution of Ca by Sr in such minerals as aragonite and dolomite (Rankama and Sahama, 1952; Mason, 1966; Goldschmidt, 1970) (Figs. 8.43A-.46A; Tables 8.106A-.109A). In the two dominant phases, house dust Ca has the following linear correlation coefficient with other elements:

- carbonate phase: pH (r=0.54), Sr (r=0.53) and La (r=0.45), and
- reducible (Fe-Mn oxide) phase: Sr (r=0.67), pH (r=0.49) and Be (r=0.43).

The relationship of house dust Ca with La in both phases is again explained by diadochic substitution in calcium carbonate minerals (Rankama and Sahama, 1952; Goldschmidt, 1970). The moderate positive correlation of pH with Ca, indicates the dependency of the former on the concentration of the latter.

8.3.5.1. Comparison of calcium (Ca) in house dust and garden soil

Although the overall partitioning patterns of Ca in house dust and garden soil are approximately similar, there are distinct differences in absolute concentrations. The levels of house dust Ca extracted by the carbonate (step 2) and reducible (step 3) phases are higher than those in the corresponding garden soil samples (Fig. 8.56A). The relative extractability of house dust Ca by the reducible phase is also higher (Fig. 8.57A). The mode of occurrence of house dust Ca in these two phases is presumed, therefore, to be different from that in garden soil.

The linear correlation coefficients between Ca in house dust and garden soil for total and sequential extraction contents are:

- total Ca r = 0.189 (Table 8.111A)
- exchangeable Ca r = 0.140 (Table 8.112A)
- carbonate Ca r = 0.001 (Table 8.113A)
- reducible Ca r = 0.183 (Table 8.114A)
- oxidisable Ca r = 0.240 (Table 8.115A)
- residual Ca r = 0.630 (Table 8.116A).

The above correlation coefficients show that there is no or very low positive correlation between Ca in house dust and garden soil samples, apart from the residual phase. Only 3.56% of the variability of total Ca in the home environment is explained by garden soil, the remaining 96.44% is not derived from the immediate exterior surroundings of the house, but from other sources, perhaps internal ones such as lime, cement, marble floors, textiles and paper, and external as wind-borne dust from metallurgical wastes, rock weathering *etc.* The strong positive correlation coefficient in the residual phase explains 39.62% of the variation of house dust samples to similarities in the mode of occurrence of residual phase Ca to garden soil. This is one explanation, but in this case, it may be a chance correlation, because there is also coincidence of medians of extracted Ca contents at the 95% confidence level (Fig. 8.56). After studying in more detail the residual Ca patterns between the two sampling media the former explanation is apparently preferred (refer to Maps 7.8 & 8.8).

8.3.5.2. Bioavailability and biological effects of calcium (Ca)

Readily available amounts of Ca in house dust vary from 9,863 to 72,500 ppm Ca (steps 1+2). The very low pH of a child's gastric fluids in an empty stomach can, however, attack element contents held even in the oxidisable phase fractions, *i.e.*, from 32,764-290,200 ppm Ca (steps 1+2+3+4).

Recommended daily intakes vary throughout the world reflecting, therefore, different conclusions based on a variety of nutritional studies. It may also reflect varying protein intakes and those of vitamin D, provided by the diet and produced in the skin (Mervyn, 1985, 1986, 1996). The World Health Organisation (WHO) recommendations are (Mervyn, 1985):

Children 0-1 years:	500- 600 mg Ca/day;
Children 1-9 years:	400- 500 mg Ca/day;
Adolescents 10-15 years:	600- 700 mg Ca/day;
Teenagers 16-19 years:	500- 600 mg Ca/day;
Pregnant women and during breast-feeding:	1000-1200 mg Ca/day.

United Kingdom (UK) and United States of America (USA) recommendations are (Mervyn, 1985):

	UK	USA
	(mg Ca/day)	
Children 0-0.5 years:	600	360
Children 0.5-1 years:	600	540
Children 1- 8 years:	600	800
Children 9-10 years:	700	800
Adolescents 11-14 years:	700	800
Teenagers 15-17 years:	600	1200
Adults 18 years:	500	1200
Adults 19 to 75+ years:	500	800
Pregnant women and during breast-feeding:	1200	1200

Excessive absorption of calcium gives rise to a condition of hypercalcaemia, *i.e.*, abnormally high blood levels of calcium (Mervyn, 1985, 1986, 1996). Symptoms are loss of appetite, nausea, vomiting, wasting, constipation, abdominal pains, kidney stones, deposition of calcium in sites outside bone flabby muscles and characteristic facial appearance (Mervyn, 1985, 1986, 1996; Davies and Stewart, 1987). Blood calcium, urea and cholesterol are often raised, as in the blood pressure. There may be mental retardation and brain damage. Fatality rate is high if not diagnosed early.

In adults, hypercalcaemia results from excessive doses of vitamin D or increased production of parathyroid hormone. It is also reported in patients with peptic ulcer and impaired kidney function who are treated with high milk diets and antacids. These conditions promote excessive calcium absorption giving rise to kidney failure.

In healthy adults there is no danger of hypercalcaemia, since controlling mechanisms of the body ensure that calcium from food does not exceed the amount lost elsewhere. Excessive amounts are readily excreted.

8.3.6. PARTITIONING OF CADMIUM (Cd) IN HOUSE DUST (Map 8.9, Tables 8.26A-.30A, Figs. 8.11A-.12A)

House dust cadmium, as in overburden, shows highly variable partitioning patterns in all five steps, which depend on the mineralogical composition of source materials. Although the reducible phase is, as in overburden, the most significant for house dust samples, since it accounts for 16.57-73.93% of the total (median=43.71%; <1 to 57.6 ppm Cd; median=7.25 ppm Cd), the other phases comparatively extract fairly large amounts of Cd, *i.e.*,

- residual: 3.96-42.55% of the total (median=15.63%; <0.5-25.6 ppm Cd; median=2.75 ppm Cd),
- oxidisable: 0.86-34.17% of the total (median=6.25%; <0.09-9.4 ppm Cd; median=1.2 ppm Cd),
- carbonate: 1.94-56.65% of the total (median=25.58%; 0.2-35.2 ppm Cd; 3.4 ppm Cd), and
- exchangeable: 0.40-34.04% of the total (median=6.86%; 0.05-8.35 ppm Cd; median=1.0 ppm Cd).

Indoor dust of houses over contaminated soil, in almost the whole study area, has generally the lowest Cd contents in all five phases. Exceptions, to this general observation, are samples of indoor dust in houses near to metallurgical processing wastes, which have definitely a strong influence through aerial transportation of contaminants, *e.g.*, south of Santorineika.

Similar to garden soil, the carbonate and reducible phases are the most significant for indoor dust, in terms of high Cd concentrations, for houses situated over flotation residues and slag earth. The residual phase is important only for a few house dust samples, which are over flotation residues and slag at Kavodokanos, and contaminated soil at Ayia Paraskevi.

Cadmium has the following linear correlation coefficients with other elements in the different phases (Tables 8.106A-.110A; Figs. 8.43A-.47A):

- exchangeable phase: Zn (r=0.67), Mn (r=0.58);
- carbonate phase: Pb (r=0.72); Zn (r=0.37);
- reducible phase: Pb (r=0.89); Zn (r=0.85); Mn (r=0.71); Co (r=0.47); Be (r=0.39); Fe (r=0.33);
- oxidisable phase: Zn (r=0.73); Mn (r=0.65); Pb (r=0.52); Cu (r=0.49); Be (r=0.48);
- residual phase: Pb (r=0.86); Zn (r=0.83); Fe (r=0.67); P (r=0.65); Mn (r=0.60), Cu (r=0.55); La (r=0.49); Li (r=0.47).

House dust Cd, almost in all phases, has a high correlation coefficient with Zn, except in the carbonate where the correlation is moderately strong. Further, in the exchangeable phase Cd has also a high correlation with Mn; in the carbonate phase with Pb; in the reducible phase with Pb, Mn, Co, Be and Fe; in the oxidisable phase with Mn, Pb, Cu and Be, and in the residual phase with Pb, Fe, P, Mn, Cu, La and Li. The above element associations, although slightly different from those in overburden samples (see Chapter 7), suggest that Cd is related to the smelting activities of sulphide ore, and the wastes.

8.3.6.1. Comparison of cadmium (Cd) in house dust and garden soil

In terms of absolute Cd concentrations, garden soil samples have the highest values (Fig. 8.58A). Comparison of the relative extractability, between the two sampling media, shows that a greater amount of Cd is extracted from samples of house dust in steps 1, 4 and 5 (Fig. 8.59A), which possibly suggests that a large proportion of Cd has a different mode of occurrence. The different element associations in the five sequential extraction steps of Cd in house dust and garden soil support these differences.

The linear correlation coefficients between Cd in house dust and garden soil for total and sequential extraction contents are:

- total Cd r = 0.701 (Table 8.111A)
- exchangeable Cd r = 0.363 (Table 8.112A)
- carbonate Cd r = 0.556 (Table 8.113A)
- reducible Cd r = 0.712 (Table 8.114A)
- oxidisable Cd r = 0.639 (Table 8.115A)
- residual Cd r = 0.576 (Table 8.116A).

The above correlation coefficients show that, apart from the exchangeable phase, there is a strong positive correlation of Cd between house dust and garden soil samples. For total Cd, 49.21% of the variability in house dust could be explained by garden soil, and a comparatively large proportion of Cd has a similar mode of occurrence in the carbonate (30.96%), reducible (50.71%), oxidisable (40.82%) and residual phases (33.15%). The low variability (13.18%) of exchangeable Cd, which is explained by a similar mode of occurrence as in garden soil, is attributed, apart from differences in the mode of occurrence, to differences in the physico-chemical conditions of the two sampling media, which have affected the extractability of Cd. The pH, for example, has a moderately strong negative correlation coefficient with exchangeable phase house dust Cd (r=-0.531), suggesting that higher amounts of Cd are extracted by $MgCl_2$ at pH 7.0 (step 1). Whereas exchangeable phase garden soil Cd has a low negative correlation coefficient with pH (r=-0.126) and, consequently, comparatively lower amounts of Cd are extracted. This feature is well illustrated in Fig. 8.59A, which shows the relative leachability of exchangeable phase Cd in house dust and garden soil.

8.3.6.2. Bioavailability and biological effects of cadmium (Cd)

Readily available amounts of Cd in house dust vary from 0.25 to 43.5 ppm Cd (steps 1+2). The very low pH of a child's gastric fluids in an empty stomach can, however, attack element contents held even in the oxidisable phase fractions, *i.e.*, from 0.78-110.4 ppm Cd (steps 1+2+3+4). The absorption factor of Cd from the gastrointestinal tract into the blood varies, according to different researchers, from 3-8% and 4.7-7%; the suggested value is 6% (Ferguson, 1990).

Daily intakes of 55-70 µg/day have been proposed by the World Health Organisation (WHO) as tolerable. Calculated intakes have been reported as 60-90 µg/day for young adult female New Zealanders; from 27-64 µg/day in children confined to institutions; as 26 µg/day in daily food intakes of USA individuals; as ranging from 50-150 µg/day amongst various countries (Mervyn, 1985, 1986, 1996).

Cadmium competes with Zn, Cu (Fig. 1), Ca and Se in absorption and metabolism, probably by virtue of competition for some protein-binding sites (Mervyn, 1985; Ferguson, 1990); these elements if taken as supplements, provide a protection against excessive accumulation of Cd (Mervyn, 1985, 1986, 1996). Excessive amounts of Cd are toxic, and prolonged exposure may cause a variety of diseases, such as emphysema, kidney damage (nephritis), hypertension, arteriosclerosis, abdominal cramps (colic), nausea, vomiting, diarrhoea, liver disease, acne, slow healing (zinc deficiency), and anaemia (Trattler, 1985). Anaemia is probably caused by excessive intakes of Cd antagonising Cu and Fe functions in blood formation (Fig. 1), and kidney damage is observed at a concentration of 22.4 mg Cd/100 g (Mervyn, 1985, 1986, 1996). Apart from the above diseases, Cd is considered to be carcinogenic (Reimann *et al.*, 1998).

8.3.7. PARTITIONING OF COBALT (Co) IN HOUSE DUST (Map 8.10, Tables 8.31A-.35A, Figs. 8.13A-.14A)

The partitioning patterns of Co indicate that the most significant phases in house dust, as in overburden, are the residual and reducible (Fe-Mn oxide fraction), which account for 26.86-78.43% (median=51.09%) and 3.09-58.35% (median=19.08%) of the total content respectively, *i.e.* 1.8-36.0 ppm Co (median=4 ppm Co) and 0.25-25.8 ppm Co (median=1.5 ppm Co). The partitioning patterns of house dust samples are variable as is shown on

Map 8.10 (Volume 2 of this report). Two samples, at Koukos and Prasini Alepou, have high Co contents in the carbonate, reducible and residual phases, and both houses are over residual soil, which has developed over schist (refer to Map 2.2 in Volume 2 of this report). Although in these two cases there appears to be a clear relationship between indoor dust and its immediate exterior environment, the partitioning patterns of garden soil are different.

Generally, the readily available, exchangeable and carbonate phase Co contents, as well as the total levels (see Chapter 6), are low. Hence, this element is not regarded to be hazardous to humans. Geochemically, however, its relationships with other elements are interesting, even at such low concentrations.

In the exchangeable phase Co has a moderate positive correlation coefficient with Ni (r=0.53), Cu (r=0.50), Zn (r=0.49), Mn (r=0.44) and Li (r=0.39) (Table 8.106A, Fig. 8.43A). The higher levels of exchangeable Co occur over pyritiferous wastes at Kavodokanos.

Cobalt in the carbonate phase has a very low positive relationship with Ca, and calcium carbonates. It is moderately correlated with Cr (r=0.43), V (r=0.43) and La (r=0.41), suggesting, therefore, an association with specific adsorption sites occurring on the surfaces of amorphous precipitates of alumino-silicates, aluminium (r=0.28), iron (r=0.24) and manganese (r=0.25) oxides, other micro-crystalline precipitates of oxides, but not phosphates, for it has no correlation with P (r=0.02) (Table 8.107A, Fig. 8.44A).

Reducible phase Co, apart from its association with Mn (r=0.57) and weak correlation with Fe (r=0.37), it is positively correlated with Pb (r=0.58) and Zn (r=0.51), Be (r=0.43) (Table 8.108A, Fig. 8.45A), suggesting adsorption mainly by Mn oxides, and to a lesser extent by Fe oxides.

Cobalt in the oxidisable phase has a strong to moderate correlation with Fe (r=0.78), Mn (r=0.76), La (r=0.59), Zn (r=0.55), Li (r=0.51), Be (r=0.48), Cd (r=0.44), Ni (r=0.39), Al (r=0.36) and Cu (r=0.36), elements mainly associated with sulphides (*e.g.*, pyrite) (Table 8.109A, Fig. 8.46A).

Finally, Co in the residual phase has a strong to moderate correlation with Cr (r=0.75), Fe (r=0.66), Ni (r=0.62), Mn (r=0.60), Li (r=0.58), V (r=0.52), K (r=0.42), Cu (r=0.39) and Zn (r=0.34) (Table 8.110A, Fig. 8.47A), suggesting that Co does not only occur in silicate, but is mainly associated with mafic and femic minerals and sulphides. The latter, are incompletely digested, in step 4 (oxidisable phase).

8.3.7.1. Comparison of cobalt (Co) in house dust and garden soil

In terms of absolute Co concentrations, garden soil has the highest values in the exchangeable, oxidisable and residual phases, whereas house dust in the carbonate and reducible phases (Fig. 8.60A). Comparison of the relative extractability, between the two sampling media, shows that there is a greater amount of Co extracted from samples of house dust in steps 1, 2, 4 and 5 (Fig. 8.61A). This possibly suggests that a large proportion of Co has a different mode of occurrence. Different element associations in the five sequential extraction steps of Co in house dust and garden soil support these differences.

The linear correlation coefficients between Co in house dust and garden soil for total and sequential extraction contents are:

- total Co r = 0.120 (Table 8.111A)
- exchangeable Co r = -0.108 (Table 8.112A)
- carbonate Co r = -0.159 (Table 8.113A)
- reducible Co r = 0.195 (Table 8.114A)
- oxidisable Co r = 0.159 (Table 8.115A)
- residual Co r = 0.028 (Table 8.116A).

The above correlation coefficients show that there is essentially no correlation between Co in house dust and garden soil. This feature is well illustrated in the partitioning patterns of the two sampling media (refer to Maps 7.10 & 8.10 in Volume 2 of this report), and the relative proportion of Co extracted in the different phases of house dust and garden soil (Fig. 8.61A), and the different element associations (Tables 7.106A-.110A, Figs. 7.43A-.47A; Tables 8.106A-.110A, Figs. 8.43A-.47A). Hence, the source of indoor Co is not garden soil, and its mode occurrence in household dust is completely different from that in garden soil. Sources of house dust Co are either in the home environment [paints, stainless steel, alloys, plastics, toothpaste, hair dyes, glass, *etc.* (Földvári-Vogl, 1978; Lapedes, 1978; Reinmann *et al.*, 1998) or brought by wind borne dust from distant sources, mainly from the metallurgical processing wastes and soil developed on schist and prasinite.

8.3.7.2. Bioavailability and biological effects of cobalt (Co)

Readily available amounts of Co in house dust vary from 0.25 to 14.3 ppm Co (steps 1+2). The very low pH of a child's gastric fluids in an empty stomach can, however, attack element contents held even in the oxidisable phase fractions, *i.e.*, from 0.7-46.7 ppm Co (steps 1+2+3+4).

WHO recommends a minimum daily intake of 1 µg Co to be absorbed (Mervyn, 1985, 1986, 1996).

A high Co intake may reduce the amount of Fe (Fig. 8.1). Cobalt levels in house dust are comparatively low, and no health-related diseases are expected. However, therapeutic doses of 29.5 mg Co given to patients did produce side effects, such as goitre, hypothyroidism and heart failure (Mervyn, 1985, 1986, 1996). Hence, at doses of 25 mg/day or more it is considered as toxic to humans (Reimann *et al.*, 1998).

High intake of Co may result in heart failure and death, caused by a condition called cardiomyopathy. This condition was first diagnosed in 1966 in heavy beer drinkers in Canada, Belgium and U.S.A. (Davies and Stewart 1997). Levels of about 17.7 mg of Co was the daily intake of heavy beer drinkers drinking up to 12 litres of beer, with a content of 1.5 mg of Co per litre (Mervyn 1985, 1986, 1996). It appears that there is an inverse relationship between protein intake and cobalt. The protein intake of these people was low.

An excess intake of Co can also cause overproduction of red blood cells in animals and humans, a condition known as polycythaemia vera.

8.3.8. PARTITIONING OF CHROMIUM (Cr) IN HOUSE DUST (Map 8.11, Tables 8.36A-.40A, Figs. 8.15-.16)

The dominant phase of Cr in house dust, as in overburden, is the residual, which accounts for 41.25-95.92% of the total content (median=73.67%; 23.5-1,610 ppm Cr;

median=81.0 ppm Cr). The next comparatively important phase of Cr in house dust is the reducible. Overall, partitioning patterns of indoor dust Cr are similar over all types of contaminated land. Three house dust samples over residual soil have distinctly different patterns with respect to residual and in one case the reducible phase Cr contents, *e.g.*, at Koukos, Prasini Alepou, and to the north of Ayios Andreas. It is noted, that Koukos and Prasini Alepou house dust samples have similar Co patterns.

House dust Cr in the residual phase has strong to moderate positive correlation coefficients with Ni (r=0.83), Co (r=0.75), V (r=0.43) and K (r=0.40) (Table 8.110A, Fig. 8.47A). This relationship suggests that Cr is related to dust particles derived from femic and mafic rock forming minerals. In fact the two samples with the highest residual Cr content at Koukos and Prasini Alepou are over soil, developed over schist (refer to Map 2.2 in Volume 2 of this report). Although these particular house garden soil samples have high residual Cr contents (up to 350 ppm), their corresponding indoor dust Cr contents have even higher values of up to 1610 ppm.

In the reducible phase, Cr is not correlated with Cu (r=0.09), Pb (r=0.02), Zn (r=-0.08) and Cd (r=-0.07), indicating that it is not related to the smelting operations of sulphide ore. It has moderate to low positive correlation coefficients with Ni (r=0.47, Mo (r=0.34), V (r=0.33) and Al (r=0.31), indicating that Cr is present in femic minerals, such as amphibole, biotite and chlorite, occurring in schist, and pyroxene in prasinite, and is released during weathering (Rankama and Sahama, 1952). As pointed out by Goldschmidt (1970) a high pH value might favour oxidation of chromic ions to chromate, which may be the case in Lavrion.

8.3.8.1. Comparison of chromium (Cr) in house dust and garden soil

Garden soil has lower total Cr levels than house dust (Fig. 6.9, Chapter 6, p.153), and higher concentrations in the exchangeable, carbonate, reducible and oxidisable phases, but not the residual (Fig. 8.62A). Comparison of the relative extractability between the two sampling media shows that a greater amount of Cr is extracted from samples of house dust in steps 1, 3, 4 and 5 (Fig. 8.63A), which possibly suggests that a large proportion of Cr has a different mode of occurrence. The different element associations in the five sequential extraction steps of Cr in house dust and garden soil support these differences.

The linear correlation coefficients between Cr in house dust and garden soil for total and sequential extraction contents are:

- total Cr r = 0.097 (Table 8.111A)
- exchangeable Cr r = -0.158 (Table 8.112A)
- carbonate Cr r = 0.119 (Table 8.113A)
- reducible Cr r = 0.003 (Table 8.114A)
- oxidisable Cr r = 0.249 (Table 8.115A)
- residual Cr r = 0.070 (Table 8.116A).

The above correlation coefficients show that there is essentially no correlation between Cr in house dust and garden soil. This feature is well illustrated in the partitioning patterns of the two sampling media (refer to Maps 8.11 & 8.11 in Volume 2 of this report), the relative proportion of Cr extracted in the different phases of house dust and garden soil (Fig. 8.63A), and the different element associations (Tables 7.106A-.110A, Figs. 7.43A-.47A; Tables 8.106A-.110A, Figs. 8.43A-.47A). The source of indoor Cr is not, therefore, garden

soil. Its mode occurrence in household dust is also completely different from that in garden soil. Sources of house dust Cr are either in the home environment [stainless steel, alloys, chrome plating, dyes, pigments, wood impregnation, refractory bricks, magnetic tapes, glass, pottery, *etc.* (Parkes, 1967; Földvári-Vogl, 1978; Reimann *et al.*, 1998)] or brought by wind borne dust from distant sources.

8.3.8.2. Bioavailability and biological effects of chromium (Cr)

Readily available amounts of Cr in house dust vary from 1.3 to 34.6 ppm Cr (steps 1+2). The very low pH of a child's gastric fluids in an empty stomach can, however, attack element contents held even in the oxidisable phase fractions, *i.e.*, from 6.6-265.5 ppm Cr (steps 1+2+3+4).

Recommended dietary intakes of Cr are suggested by the US Food and Nutrition Board, National Research Council – National Academy of Sciences (Mervyn, 1985):

Infants 0-0.5 year:	10-40 µg Cr/day;
Infants 0.5-1 year:	20-60 µg Cr/day;
children 1-3 years:	20-80 µg Cr/day;
children 4-6 years:	30-120 µg Cr/day;
children 7-10 years:	50-200 µg Cr/day;
adolescents 11+ years:	50-200 µg Cr/day;
adults:	50-200 µg Cr/day.

The above suggestions take into consideration absorption of different Cr sources. Whilst a diet containing 30 µg or less of glucose tolerance factor (GTF) may be adequate, several hundred µg of inorganic trivalent chromium (Cr^{3+}) may be required (Mervyn, 1985).

Toxicity of chromium is low, because so little of it is absorbed (Mervyn 1985, 1986, 1996). Cats can tolerate up to 1000 mg per day of trivalent chromium salts; rats showed no adverse effects from 100 mg per kg diet. Lifetime exposure to 5 mg per litre of trivalent chromium in drinking water induced no toxic effects in rats and mice. Exposure of mice for three generations to chromium oxide, at levels up to 20 mg per kg of the diet, had no effect upon mortality, growth or fertility of the animals.

Chronic exposure to chromium dust (in the form of chromate) has been associated with increased incidence of lung cancer. Oral administration of 50 mg of chromate per kg has been associated with growth depression, and liver and kidney damage in experimental animals.

Hexavalent (Cr^{6+}) is much more toxic than trivalent (Cr^{3+}), but the former is never used in therapy or in supplementation, nor does it occur in natural foods.

8.3.9. PARTITIONING OF COPPER (Cu) IN HOUSE DUST (Map 8.12, Tables 8.41A-.45A, Figs. 8.17A-.18A)

The important phases of house dust Cu are the residual and oxidisable, which account for 9.84-76.87% (median=36.61%) and 13.79-80.91% (median=50.82%) of the total content respectively (*i.e.*, residual: 6.6-1,410 ppm Cu; median=59.7 ppm Cu; oxidisable: 9.1-1,010 ppm Cu; median=85.6 ppm Cu). The carbonate phase is important only for one sample from Phenikodassos (1440 ppm Cu), and the other two phases are of local significance, *e.g.*, the exchangeable phase extracts up to 252 ppm Cu (median=9.02 ppm), and the reducible

extracts up to 835 ppm Cu (median=2.25 ppm). Copper, in the residual and oxidisable phases of indoor dust, has comparatively higher levels in houses at Prasini Alepou and Santorineika, which are situated over flotation residues and contaminated soil, Phenikodassos over contaminated soil, and at Kavodokanos they are situated over all types of contaminated land.

House dust Cu in the residual phase has strong to moderate positive correlation coefficients with Zn (r=0.66), Fe (r=0.61), Mn (r=0.55), Cd (r=0.55), Pb (r=0.51), Ag (r=0.46), and P (r=0.43), elements occurring in pyrite and other sulphides (Tables 8.110A; Fig. 8.47A).

Copper in the oxidisable phase has a moderate positive correlation with Zn (r=0.55), Cd (r=0.49), Be (r=0.44), Mn (r=0.43), and Co (r=0.36), elements occurring in pyrite and other sulphides (Tables 8.109A; Fig. 8.46A).

Carbonate phase Cu in house dust has a weak positive correlation coefficient with Cd (r=0.31), a moderate negative correlation with Be (r=-0.48), and Al (r=-0.45), and no correlation with Ca (r=-0.001). Copper is not related to calcium carbonate minerals, but is associated with other specific adsorption sites, such as on surfaces of amorphous precipitates of oxides, micro-crystalline precipitates, but not alumino-silicates (clays), phosphates due to the negative correlation with Al and very low positive correlation with P (r=0.05) (Table 8.107A; Fig. 8.44A).

Copper in the exchangeable phase has strong to moderate positive correlation coefficients with Zn (r=0.62), Ni (r=0.59), Mn (r=0.58), Cr (r=0.54), P (r=0.51), Co (r=0.50), K (r=0.45), Pb (r=0.38), Ba (r=0.37), and Cd (r=0.35), suggesting that it is adsorbed on a variety of adsorption sites (Tables 8.106A; Fig. 8.43A).

Reducible phase Cu is not correlated with any elements (Tables 8.107A; Fig. 8.45A).

8.3.9.1. Comparison of copper (Cu) in house dust and garden soil

House dust samples have higher Cu levels in all five extraction steps (Fig. 8.64A) and total Cu (Fig. 6.10, p.155) in comparison to the corresponding garden soil samples (n=126). Comparison of the relative extractability between the two sampling media, shows that a greater amount of Cu is extracted from samples of house dust in steps 1, 2, 3 and 4 (Fig. 8.65A), which possibly suggests that a large proportion of Cu has a different mode of occurrence. The different element associations in the five sequential extraction steps of Cu in house dust and garden soil support these differences.

The linear correlation coefficients between Cu in house dust and garden soil for total and sequential extraction contents are:

- total Cu r = 0.358 (Table 8.111A)
- exchangeable Cu r = 0.020 (Table 8.112A)
- carbonate Cu r = 0.071 (Table 8.113A)
- reducible Cu r = 0.142 (Table 8.114A)
- oxidisable Cu r = 0.351 (Table 8.115A)
- residual Cu r = 0.354 (Table 8.116A).

The above correlation coefficients show, that there is weak correlation between total Cu in house dust and garden soil, which suggests that a very large part (87.22%) of indoor dust is not derived from the exterior garden soil. Apparently, there is very weak to no correlation between the sequential extraction steps, indicating that the mode of

occurrence of Cu in the operationally defined phases is largely different. This feature is well illustrated in the partitioning patterns of the two sampling media (refer to Maps 8.12 & 7.12 in Volume 2 of this report), the relative proportion of Cu extracted in the different phases of house dust and garden soil (Fig. 8.65A), and the different element associations (Tables 7.106A-.110A, Figs. 7.43A-.47A; Tables 8.106A-.110A, Figs. 8.43A-.47A). Sources of house dust Cu are either in the home environment [household utensils, electrical wires *etc.*, water pipes, pigments, plastics copper alloys (bronze, brass), (Parkes, 1967; Reimann *et al.*, 1998)] or brought by wind borne dust from distant sources.

8.3.9.2. Bioavailability and biological effects of copper (Cu)

Readily available amounts of Cu in house dust vary from 1.34 to 1,692 ppm Cu (steps 1+2). The very low pH of a child's gastric fluids in an empty stomach can, however, attack element contents held even in the oxidisable phase fractions, *i.e.*, from 10.74-3,537 ppm Cu (steps 1+2+3+4).

Recommended dietary intakes of Cu are suggested by the US Food and Nutrition Board, National Research Council – National Academy of Sciences (Mervyn, 1985):

Infants 0-0.5 year:	0.5-0.7 mg Cu/day;
Infants 0.5-1 year:	0.7-1.0 mg Cu/day;
children 1-3 years:	1.0-1.5 mg Cu/day;
children 4-6 years:	1.5-2.0 mg Cu/day;
children 7-10 years:	2.0-2.5 mg Cu/day;
adolescents 11+ years:	2.0-3.0 mg Cu/day;
adults:	2.0-3.0 mg Cu/day.

High Cu intake will lower P and Zn levels in the body (Fig. 8.1), and possibly, cause deficiency diseases associated with these two elements. In fact Zn deficiency is attributed, in many cases, to a P excess (Mervyn, 1985). Among the diseases associated high levels of Cu intake are mental disorders, schizophrenia, anaemia; copper deposits in kidney, liver, brain and eyes; arthritis, insomnia, hypertension, nausea, vomiting, autism, hyperactivity, stuttering, rheumatoid arthritis (high copper levels), myocardial infarction, postpartum psychosis, toxaemia of pregnancy, Wilson's disease and Indian childhood cirrhosis, inflammation and enlargement of liver, cystic fibrosis (high copper levels) (Mervyn 1985, 1986, 1996; Trattler, 1985).

8.3.10. PARTITIONING OF IRON (Fe) IN HOUSE DUST (Map 7.13, Tables 7.46A-.50A, Figs. 7.19A-.20A)

The most significant phase for Fe, as in overburden, is the residual for all samples of house dust extracting 45.41-96.91% of the total metal (median=86.54%; 5,270-104,000 ppm Fe; median=20,736 ppm Fe). The carbonate, reducible and oxidisable phases are of local importance, *e.g.*, for some samples at Kavodokanos, Prasini Alepou, Santorineika and Phenikodassos. The exchangeable phase extracts very small amounts of Fe (0-1.69%; median=0.08% of the total; 1.2-226 ppm Fe; median=20.5 ppm Fe). At Kavodokanos houses are situated over all types of wastes, including contaminated soil; at Prasini Alepou, Santorineika and Phenikodassos they are located mainly over contaminated soil.

In the residual phase house dust Fe has a strong to moderate positive correlation coefficient with Mn (r=0.91), Zn (r=0.75), Cd (r=0.67), Co (r=0.66), Pb (r=0.65), Cu (r=0.61) P (r=0.59), Li (r=0.58), Al (r=0.55), V (r=0.52), Ag (r=0.50), Be (r=0.48), La (r=0.44), K (r=0.41), Mo

(r=0.40), Sr (r=0.37) (Table 8.110A; Fig. 8.47A). This element association suggests that Fe occurs in both silicate and sulphide minerals. The latter association indicates that sulphides were not completely digested during step 4 (organic/sulphide phase).

House dust Fe in the reducible (Fe-Mn oxide) phase has a high to moderate positive correlation coefficient with Ba (r=0.83), Zn (r=0.65), Al (r=0.61), Mn (r=0.61), K (r=0.53), Be (r=0.45), Pb (r=0.42), Ti (r=0.38), and Li (r=0.35) (Table 8.108A; Fig. 8.45A). This association suggests that Fe is associated with Al and Fe-Mn oxides in dust particles derived from slag earth and contaminated soil, and that a minor proportion is derived from oxidised pyrite, since this a phase occurring mainly at Kavodokanos.

In the carbonate phase house dust Fe has a strong positive correlation with Al (r=0.83), Ba (r=0.79), Ti (r=0.74), Mn (r=0.67), Mo (r=0.56), Be (r=0.55), Zn (r=0.51), Li (r=0.37) and V (r=0.37) (Table 8.107A; Fig. 8.44A). Since, Fe has a low positive correlation with Ca (r=0.13), its association with calcium carbonate minerals should be comparatively minor. The above element association indicates that Fe is adsorbed on the surfaces of amorphous precipitates of iron, aluminium or manganese oxides, alumino-silicates (clays), silica, and micro-crystalline precipitates of oxides, carbonates, but not phosphates, since Fe is negatively correlated with P (r=-0.36). Iron has a moderately strong negative correlation with Cu (r=-0.56); it has also a low negative correlation with Cd (r=-0.28). This antipathetic behaviour indicates that house dust Fe in the carbonate phase occurs in samples with comparatively low Cu and Cd contents.

Oxidisable phase house dust Fe has a high to moderate positive correlation coefficient with Co (r=0.78), Mn (r=0.74), La (r=0.50), Li (r=0.41), Be (r=0.41), Cd (r=0.40), and Zn (r=0.39), Al (r=0.37), Cu (r=0.33), Ni (r=0.33), elements mainly occurring in sulphides, and especially pyrite (Table 8.109A; Fig. 8.46A).

Exchangeable house dust Fe has strong to moderate positive correlation coefficients with Al (r=0.84), Ti (r=0.62), Pb (r=0.53), Zn (r=0.51), P (r=0.45), Ba (r=0.46), Ni (r=0.42), and Mn (r=0.41), showing that Fe is adsorbed on easily exchangeable sites, but also that $MgCl_2$ has extracted very low amounts of Al, suggesting a minor attack on the substrates (*e.g.*, clay minerals, organic matter, oxides and sulphides) (Table 8.106A; Fig. 8.43A).

8.3.10.1. Comparison of iron (Fe) in house dust and garden soil

House dust samples have generally lower Fe levels in all five extraction steps (Fig. 8.66A) and total Fe (Fig. 6.11, p.157) in comparison to the corresponding garden soil samples (n=126). Comparison of median values of the relative extractability between the two sampling media, shows that a greater amount of Fe is extracted from samples of house dust in steps 1, 2, 3 and 4 (Fig. 8.67A), suggesting that a large proportion of Fe has a different mode of occurrence. These differences are supported, up to a certain extent, by different element associations in the five sequential extraction steps of Fe in house dust and garden soil.

The linear correlation coefficients between Fe in house dust and garden soil for total and sequential extraction contents are:

- total Fe r = 0.636 (Table 8.111A)
- exchangeable Fe r = -0.078 (Table 8.112A)
- carbonate Fe r = 0.608 (Table 8.113A)
- reducible Fe r = 0.772 (Table 8.114A)

- oxidisable Fe r = 0.199 (Table 8.115A)
- residual Fe r = 0.489 (Table 8.116A).

The above correlation coefficients show, that there is a moderately strong correlation between total Fe in house dust and garden soil, which suggests that a large part (40.41%) of dust Fe is derived from exterior garden soil. Nevertheless, a very high amount (59.90%) is due to sources within the home environment or distant ones, transported by wind. Significant parts of house dust Fe in the carbonate (36.97%), and reducible (59.59%), and a minor in the residual (23.92%) have a similar mode of occurrence as in garden soil. Sources of house dust Fe in the home environment are household utensils, steel, pigments, *etc.*

8.3.10.2. Bioavailability and biological effects of iron (Fe)

Readily available amounts of Fe in house dust vary from 7 to 24,626 ppm Fe (steps 1+2). The very low pH of a child's gastric fluids in an empty stomach can, however, attack element contents held even in the oxidisable phase fractions, *i.e.*, from 740-73,196 ppm Fe (steps 1+2+3+4).

Recommended daily intakes of Fe in the United Kingdom (UK) and in the United States of America (USA) are tabulated below:

		UK	USA
		(mg Fe/day)	
Children 0-1 year:		6	10
Children 1-3 years:		7	15
Children 4-6 years:		9	10
Children 7-10 years:		10	10
Adolescents 11-14 years:	Males:	12	18
	Females:	12	18
Teenagers 15-18 years:	Males:	12	18
	Females:	12	18
Adults 19-22 years:	Males:	10	10
	Females:	12	18
Adults 23-50 years:	Males:	10	10
	Females:	12	10
Adults 51+ years:	Males:	10	10
	Females:	10	10
Pregnant women:		13	18
Breast feeding women:		15	18

High Fe intake lowers P and K levels in the body (Fig. 8.1), and possibly causes deficiency diseases associated with these two elements. Excessive Fe intakes may lead to a disease called haemosiderosis, a generalised deposition of iron within body tissues, or haemochromatosis when such deposition is associated with tissue injury (Mervyn, 1985, 1986, 1996). Haemochromatosis is uncommon, and is of a hereditary nature. Typical manifestations are cirrhosis of the liver; bronze pigmentation of the skin; diabetes mellitus; heart disease especially congestive failure, arrhythmias and conduction disturbances; loss of libido; abdominal pain; arthritis and liver cancer.

8.3.11. PARTITIONING OF POTASSIUM (K) IN HOUSE DUST (Map 8.15, Tables 8.51A-.55A,Figs.8.21A-.22A)

The most significant phases of house dust K are the residual and exchangeable, which account for 7.23-96.08% (median=57.95%), and 1.22-83.50 (median=33.19%) of the total. In terms of element concentrations the residual phase varies from 545-7,780 ppm K (median=3,010 ppm K) and the exchangeable 71-20,900 ppm K (median=1,700 ppm K). The other phases are of local importance, and are not discussed further.

In the residual phase, house dust K has a strong to moderate correlation coefficient with Be (r=0.92), Al (r=0.91), Li (r=0.88), V (r=0.68), La (r=0.53), Pb (r=0.53), Ag (r=0.51), Zn (r=0.45), Sr (r=0.43), Ca (r=0.43), Co (r=0.42), Ti (r=0.41), Fe (r=0.41), Cr (r=0.40), Cd (r=0.39), and P (r=0.36) (Table 8.110A; Fig. 8.47A). These element associations suggest that K in the residual phase is related to alumino-silicate minerals occurring in household dust and sulphide particles from the smelter wastes.

In the exchangeable phase, house dust K has a strong to moderate correlation coefficient with Li (r=0.69), Cr (r=0.52), P (r=0.48), Cu (r=0.45), Sr (r=0.45), Pb (r=0.42), Ni (r=0.42), Ba (r=0.42), Ca (r=0.41), Ti (r=0.39), Co (r=0.37), Fe (r=0.34), and Al (r=0.32), (Table 8.110A; Fig. 8.47A). These element associations suggest that Fe is adsorbed on easily exchangeable sites, but also that $MgCl_2$ has extracted very low amounts of Al, pointing to a minor attack on the substrates (*e.g.*, clay minerals, organic matter, oxides and sulphides) (Table 8.106A; Fig. 8.43A).

8.3.11.1. Comparison of potassium (K) in house dust and garden soil

The partitioning patterns of K in house dust and garden soil are distinctly different in all samples (Maps 7.15 & 8.15). Compared to garden soil samples (n=126), house dust has lower K levels in the reducible and residual, and higher contents in the exchangeable, carbonate and oxidisable phases (Fig. 8.68A). Comparison of median values of the relative extractability between the two sampling media, shows that a greater amount of K is extracted from samples of house dust in steps 1 and 3 (Fig. 8.69A), which possibly suggests that a large proportion of K has a different mode of occurrence. These differences are supported, up to a certain extent, by the different element associations in the five sequential extraction steps of K in house dust and garden soil.

The linear correlation coefficients between K in house dust and garden soil for total and sequential extraction contents are:

- total K r = 0.076 (Table 8.111A)
- exchangeable K r = 0.239 (Table 8.112A)
- carbonate K r = 0.412 (Table 8.113A)
- reducible K r = 0.420 (Table 8.114A)
- oxidisable K r = 0.146 (Table 8.115A)
- residual K r = 0.143 (Table 8.116A).

There appears to be no correlation between total K contents in house dust and garden soil, suggesting, therefore, that the latter is not the source of indoor dust potassium. The above correlation coefficients indicate that there is some minor correlation with respect to the mode of occurrence of K in the carbonate and reducible phases between house dust and garden soil samples. The greatest proportion, however, has a different mode of occurrence. Although airborne dust cannot be precluded, it appears that the main sources of floor dust K are in the home environment, and occur in easily

extractable forms, *e.g.*, food stuffs, food additives, plants, soap, detergents, dyes, insecticides, *etc.* (Lapedes, 1978).

8.3.11.2. Bioavailability and biological effects of potassium (K)

Readily available amounts of K in house dust vary from 187 to 25,180 ppm K (steps 1+2). The very low pH of a child's gastric fluids in an empty stomach can, however, attack element contents held even in the oxidisable phase fractions, *i.e.*, from 232-27,326 ppm K (steps 1+2+3+4).

Dietary intakes of K are between 1,960 and 5,870 mg/day, with a usual intake of 2.54 g equivalent to 4.85 g potassium chloride (Mervyn, 1985, 1986, 1996). A high K intake may reduce the levels of Fe, Na and Mn in the body (Fig. 8.1), and possibly cause deficiency diseases associated with these three elements. Excess of potassium causes effects first on the muscles of the skeleton and of the heart, giving rise to muscular weakness and mental apathy (Mervyn, 1985, 1986, 1996). High oral doses can cause ulceration of the small bowel. Lower intakes of potassium salts may cause nausea, vomiting, diarrhoea and abdominal cramps.

8.3.12. PARTITIONING OF LANTHANUM (La) IN HOUSE DUST (Map 7.16, Tables 7.56A-.60A, Figs.7.23A-.24A)

The most significant step for house dust La, as in overburden, is the residual phase, which accounts for 21.49-70.98% of the total (median=52.82%; 3.0-22.5 ppm La; median=8.25 ppm La). The next two important steps for house dust La, as again for overburden, are the reducible and carbonate, which account for 14.12-52.32% (median=24.03%; 1.9-14.3 ppm La; median=3.75 ppm La) and 1.50-37.80% (median=16.30%; 0.2-8.4 ppm La; median=3.20 ppm La) of the total respectively. It is worth noting that indoor dust La, independent of house dust location, has approximately a similar partitioning pattern in almost all sample types (Map 8.16, Fig. 8.24A). The deviations that exist are with respect to the levels of La in the different sequential extraction fractions.

Lanthanum in the residual phase of house dust samples has a moderate positive correlation with Li (r=0.59), P (r=0.59), Be (r=0.55), Al (r=0.55), Pb (r=0.49), Cd (r=0.49), Ag (r=0.45), Zn (r=0.41), Mn (r=0.39), and V (r=0.38), suggesting a relationship with alumino-silicate minerals, but also sulphides, which were not completely dissolved in step 4 (Table 8.110A; Fig. 8.47A).

Reducible (Fe-Mn oxide) phase La in house dust samples has a moderate to weak positive correlation with K (r=0.45), Be (r=0.39), Al (r=0.35), Li (r=0.35), Fe (r=0.34), Ti (r=0.32), Sr (r=0.30), Zn (r=0.28), Mn (r=0.26), and Pb (r=0.25) (Table 8.108A; Fig. 8.45A). The weak positive correlation of La with Al, Fe and Mn, and the moderate to weak positive correlation with K, Be, Al and Li, suggests that only a minor proportion of La is adsorbed by Al, Fe and Mn oxides, and that the greatest proportion is associated with oxyhydroxides.

Carbonate phase La in house dust samples has a high to weak positive correlation with Ag (r=0.81), Ti (r=0.47), Ca (r=0.45), Co (r=0.41), Mo (r=0.41), Sr (r=0.32), V (r=0.30), Al (r=0.30), Li (r=0.29), and Fe (r=0.25) (Table 8.107A; Fig. 8.44A). This association suggests that La is related to the carbonate phase, but is also adsorbed on the surfaces of amorphous precipitates of aluminium and iron oxides, alumino-silicates, silica, and micro-crystalline

precipitates of oxides, carbonates, but not Mn oxides, and phosphates, since La has insignificant correlation coefficients with Mn (r=0.09), and P (r= 0.08).

In the oxidisable (organic/sulphide) phase La in house dust samples has a strong to weak positive correlation with Mn (r=0.60), Co (r=0.59), Fe (r=0.50), Be (r=0.47), Li (r=0.39), Cd (r=0.36), Zn (r= 0.33) Al (r=0.24), Sr (r=0.23), Ca (r=0.23), and Cu (r=0.19), and a negative correlation with P (r=-0.36), Cr (r=-0.33), Ti (r=-0.30), and Mo (r=-0.27) (Table 8.109A; Fig. 8.46A). This element association suggests that La is not related to sulphides, but is strongly bound to the organic fraction, which is complexed with such cations as Mn, Fe, Al, Ca and Cu.

Exchangeable phase La concentrations are very low in the Lavrion house dust, as in overburden, samples (0.05-0.9 ppm La), and are not considered significant for further discussion.

8.3.12.1. Comparison of lanthanum (La) in house dust and garden soil

The partitioning patterns of La in house dust and garden soil show similarities, but differences in absolute concentrations (Maps 7.16 & 8.16). Compared to garden soil samples (n=126), house dust has lower La levels with respect to total contents (Fig. 6.14, p.163), and in almost all the sequential extraction steps, except the reducible phase (Fig. 8.70A). Comparison of median values of the relative extractability between the two sampling media, shows that a greater amount of La is extracted from samples of house dust in steps 1 and 3 (Fig. 8.71A), implying that a large proportion of La has a different mode of occurrence. These differences are supported, up to a certain extent, by the different element associations in the five sequential extraction steps of La in house dust and garden soil.

The linear correlation coefficients between La in house dust and garden soil for total and sequential extraction contents are:

- total La r = 0.047 (Table 8.111A)
- exchangeable La r = 0.136 (Table 8.112A)
- carbonate La r = 0.198 (Table 8.113A)
- reducible La r = -0.038 (Table 8.114A)
- oxidisable La r = -0.027 (Table 8.115A)
- residual La r = 0.006 (Table 8.116A).

There appears to be no correlation between total La contents in house dust and garden soil, suggesting, therefore, that the latter is not the source of indoor dust lanthanum. The above correlation coefficients indicate that there is some minor to no correlation, with respect to the mode of occurrence of La in the different sequential extraction phases, between house dust and garden soil samples, despite the visual similarities shown in the patterns. Although airborne dust cannot be precluded, it appears that the main sources of floor dust La are in the home environment, *e.g.*, lighters, glass additives, ceramics, batteries (Reimann *et al.*, 1998), antiseptics (Lapedes, 1978), *etc.*

8.3.12.2. Bioavailability and biological effects of lanthanum (La)

Readily available amounts of La in house dust vary from 0.25 to 9.3 ppm La (steps 1+2). The very low pH of a child's gastric fluids in an empty stomach can, however, attack element contents held even in the oxidisable phase fractions, *i.e.*, from 2.25-26.1 ppm La (steps 1+2+3+4).

Lanthanum is considered a non-essential element for humans, and it is the most toxic of the rare earth elements (REE). Its toxicity is considered generally low, but no data have been found in scientific literature to be able to assess its biological effects (Reimann *et al.*, 1998). It is reported, however, that high intakes of La delay blood clotting, leading to haemorrhages; inhalation and ingestion cause readily reversible symptoms, which disappear at the end of exposure (Gough *et al.*, 1979).

8.3.13. PARTITIONING OF LITHIUM (Li) IN HOUSE DUST (Map 8.17, Tables 8.61A-.65A, Figs. 8.25A-.26A)

The greatest proportion of Li in house dust samples, as in overburden, is in the residual phase, which accounts for 27.49-97.39% of the total (median=78.52%; 1.2-21.4 ppm Li; median=6.2 ppm Li). The next two important extraction steps are the reducible and carbonate, which account for 0.9-42.26% (median=9.26%; 0.1-8.12 ppm Li; median=0.70 ppm Li) and 0.47-27.13% (median=5.04%; 0.08-3.84 ppm Li; median=0.40 ppm Li) of the total respectively, but with comparatively low concentrations. The most distinct partitioning patterns in terms of Li levels are in the Kavodokanos area over all types of contaminated land. The remaining house dust samples have approximately similar partitioning patterns, apart from local deviations, *e.g.*, at Phenikodassos, Ayia Paraskevi and Ayios Andreas.

In the residual phase Li in house dust samples has a strong positive correlation with Al (r=0.93), K (r=0.89), Be (r=0.86) and V (r=0.69), and a moderate correlation with La (r=0.59), Fe (r=0.58), Co (r=0.58), V (r=0.51), Zn (r=0.51), Pb (r=0.51), Mn (r=0.50), Sr (r=0.49), Cd (r=0.47), P (r=0.46) and Ti (r=0.44) (Table 8.110A; Fig. 8.47A). This association suggests a relationship with dust particles from alumino-silicate minerals, but also from sulphides, indicating that they were not completely digested in step 4.

The reducible phase Li in house dust samples has a strong positive correlation with K (r=0.69), Al (r=0.65) and Be (r=0.59), and a moderate correlation with Ba (r=0.46), Fe (r=0.35), Ti (r=0.43) and Sr (r=0.40), and a weak correlation with Fe (r=0.35), V (r=0.30) and Cr (r=0.26) (Table 8.108A; Fig. 8.45A). This element association suggests that Li is associated with K and Al bearing minerals or adsorbed on Al, and to a lesser extent, on Fe oxides, but not Mn oxides, because the correlation coefficient is very low (r=0.04).

Carbonate phase Li in house dust samples has a moderate positive correlation with K (r=0.49), Mn (r=0.48), Ba (r=0.48), Be (r=0.45), Al (r=0.38), Fe (r=0.37), and a weak correlation with Ti (r=0.38), Zn (r=0.33), Mo (r=0.32), La (r=0.29) Cr (r=0.27), Ca (r=0.24) and Sr (r=0.23) (Table 8.107A; Fig. 8.44A). This element association and the weak positive correlation with Ca suggests that Li is weakly related to calcium carbonate minerals, but is adsorbed on the surfaces of amorphous precipitates of manganese, aluminium or iron oxides, alumino-silicates, silica, and micro-crystalline precipitates of oxides, carbonates, but not phosphates, since Li is not correlated with P (r=-0.084).

Exchangeable phase Li in house dust samples has a moderate positive correlation with K (r=0.69), Ni (r=0.44) and Sr (r=0.41), and a weak correlation with Co (r=0.39), Ca (r=0.38), Cu (r=0.38), Cr (r=0.36), Ba (r=0.35), V (r=0.33), and P (r=0.31), (Table 8.107A; Fig. 8.44A). This element association with moderate to weak positive correlation coefficients suggests Li to be weakly adsorbed on easily exchangeable sites of clay minerals.

Oxidisable phase Li concentrations are very low in the Lavrion house dust samples, *i.e.*, 0.01-1.64 ppm Li with a median of 0.34 ppm Li, and are not considered significant for further discussion.

8.3.13.1. Comparison of lithium (Li) in house dust and garden soil

The partitioning patterns of Li in house dust and garden soil show similarities, but differences in their absolute concentrations (Maps 7.17 & 8.17). Compared to garden soil samples (n=126), house dust has lower Li levels with respect to total contents (Fig. 6.15, p.164), as well as in the carbonate and residual phases of sequential extraction, but higher concentrations in the exchangeable, reducible and oxidisable steps (Fig. 8.72A). Comparison of median values of the relative extractability between the two sampling media, shows that a greater amount of Li is extracted from samples of house dust in steps 1, 2, 3 and 4 (Fig. 8.73A), which possibly suggests that a large proportion of Li has a different mode of occurrence. These differences are supported, up to a certain extent, by the different element associations in the five sequential extraction steps of Li in house dust and garden soil.

The linear correlation coefficients between Li in house dust and garden soil for total and sequential extraction contents are:

- total Li r = -0.073 (Table 8.111A)
- exchangeable Li r = -0.009 (Table 8.112A)
- carbonate Li r = 0.261 (Table 8.113A)
- reducible Li r = 0.217 (Table 8.114A)
- oxidisable Li r = 0.317 (Table 8.115A)
- residual Li r = -0.088 (Table 8.116A).

There appears to be a non-significant negative correlation between total Li contents in house dust and garden soil, suggesting, therefore, that the latter is not the major source of indoor dust lithium. The above correlation coefficients indicate that there is some minor to no correlation with respect to the mode of occurrence of Li in the different sequential extraction phases between house dust and garden soil samples, despite visual similarities shown in the patterns. Although airborne dust cannot be precluded, it appears that the main sources of floor dust Li are in the home environment, *e.g.*, glass, ceramics, batteries, lubricants, greases, coolant in some refrigerating and air conditioning units, pharmaceutical products (Földvári-Vogl, 1978; Reimann *et al.*, 1998) *etc.*

8.3.13.2. Bioavailability and biological effects of lithium (Li)

Readily available amounts of Li in house dust vary from 0.1 to 9.08 ppm Li (steps 1+2). The very low pH of a child's gastric fluids in an empty stomach can, however, attack element contents held even in the oxidisable phase fractions, *i.e.*, from 0.21-18.84 ppm Li (steps 1+2+3+4).

Excess Li disturbs element transport across cell membranes as well as fluid balance (Davies and Stewart, 1987). Excessive intakes of lithium give rise to nausea, vomiting, diarrhoea, coarse tremor, thirst, excessive urination, thyroid swelling, weight gain, sluggishness, drowsiness, confusion, disorientation, delirium, skin eruptions, defective speech at blood plasma levels greater than 1.05 mg Li/100 ml, *etc.* (Mervyn, 1985, 1986, 1996; Davies and Stewart, 1987). At higher levels, *i.e.*, greater than 1.4 mg

Li/100 ml, the element gives rise to manifestations of impaired consciousness, abnormal muscle tenseness, coarse tremor, twitchings, increased reflex action, epileptic fits; "coma vigil", where the individual can react when spoken to only by moving the head or eyes (Mervyn, 1985, 1986, 1996). The worse effects are seizures, coma and even death (Davies and Stewart, 1987).

8.3.14. PARTITIONING OF MANGANESE (Mn) IN HOUSE DUST (Map 8.18, Tables 8.66A-.70A, Figs. 8.27A-.28A)

The most significant phase of Mn in house dust samples, as in overburden, is the reducible (Fe-Mn oxide), which accounts for 22.59-81.44% of the total (median=50.93%; 89-11,600 ppm Mn; median=496 ppm Mn). The next important phase, as in overburden, is the residual, which accounts for 6.56-63.89% of the total (median=22.11%; 45.5-2,610 ppm Mn; median=208 ppm Mn). Carbonate phase Mn is important in some samples of house dust over flotation residues, pyritiferous tailings and contaminated soil at Kavodokanos, extracting up to 51.30% of the total Mn (2,240 ppm Mn). Similarly, the exchangeable Mn is important only for one sample over contaminated soil at Phenikodassos, which extracts up to 22.18% of the total Mn (1,510 ppm Mn). The same applies to the oxidisable phase, with one sample at Kavodokanos over slag extracting up to 17.19% of the total Mn (1,200 ppm Mn), and another at Ayia Paraskevi.

As in overburden, the reducible (Fe-Mn oxide) phase is the most important for Mn in house dust samples occurring over all types of contaminated land, *i.e.*,

(a) contaminated residual soil (89-11,600 ppm Mn; median=429 ppm Mn);
(b) flotation residues (317-3,130 ppm Mn; median=794 ppm Mn);
(c) slag earth (197-2,410 ppm Mn; median=1,298 ppm Mn), and
(d) pyritiferous wastes (1,500 ppm Mn).

Reducible phase Mn in house dust samples has a high to moderate positive correlation with Zn (r=0.85), Pb (r=0.72), Fe (r=0.61), Cd (r=0.71), Ba (r=0.59), Co (r=0.56), and Be (r=0.49) (Table 8.108A; Fig. 8.45A). This element association suggests that Mn is related to Fe oxides and weakly to Al oxides (r=0.23), and to elements Zn, Pb, Cd, Ba, Co and Be, which are probably adsorbed on Mn oxides.

Residual phase Mn in house dust samples has a high to moderate positive correlation with Fe (r=0.91), Pb (r=0.66), Cd (r=0.60), Co (r=0.60), Cu (r=0.55), Pb (r=0.55), P (r=0.51), Li (r=0.50), and Al (r=0.46), (Table 8.110A; Fig. 8.47A). These are elements, which occur in sulphides, indicating that dust particles rich in sulphides were not completely dissolved by the organic/sulphide phase (step 4).

Carbonate phase Mn in house dust samples has a strong to moderate positive correlation with Ba (r=0.86), Al (r=0.72), Zn (r=0.72), Fe (r=0.69), Ti (r=0.60), Mo (r=0.69), Be (r=0.52), Li (r=0.48), K (r=0.39), and V (r=0.38) (Table 8.107A; Fig. 8.44A). This element association, and the very low positive correlation with Ca (r=0.15), suggests that Mn is not related to calcium carbonate minerals, but to amorphous precipitates of manganese, aluminium or iron oxides, alumino-silicates, silica, and micro-crystalline precipitates of oxides, carbonates, but not phosphates, since Mn has a weak negative correlation with P (r= -0.36). It is interesting to note that Mn has a weak antipathetic correlation with Ag (r=-0.26) and Cu (r=-0.21).

Oxidisable phase Mn in house samples has a strong to moderate positive correlation with Co (r=0.76), Fe (r=0.74), Cd (r=0.65), Zn (r=0.62), La (r=0.60), Be (r=0.47), Cu

(r=0.43), and Li (r=0.37), elements normally occurring in sulphide minerals (Table 8.109A; Fig. 8.46A). It is interesting to note that Mn has a moderate antipathetic correlation with P (r=-0.54), Ti (r=-0.41), Cr (r=-0.40), V (r=-0.39), and a weak negative covariation with Mo (r=-0.30), suggesting that is not related to particles from mafic minerals.

8.3.14.1. Comparison of manganese (Mn) in house dust and garden soil

The partitioning patterns of Mn in house dust and garden soil show similarities, but differences in the absolute concentrations (Maps 7.18 & 8.18). Compared to garden soil samples (n=126), house dust has lower Mn levels with respect to total (Fig. 6.16, p.166) as well as in the carbonate, reducible, oxidisable and residual phase contents, but higher concentrations in the exchangeable step (Fig. 8.74A). Comparison of median values of the relative extractability between the two sampling media, shows that a greater amount of Mn is extracted from samples of house dust in steps 1, 2, 4 and 5 (Fig. 8.75A), possibly suggesting that a certain proportion of Mn has a different mode of occurrence. These differences are supported, up to a certain extent, by different element associations in the five sequential extraction steps of Mn in house dust and garden soil.

The linear correlation coefficients between Mn in house dust and garden soil for total and sequential extraction contents are:

- total Mn r = 0.660 (Table 8.111A)
- exchangeable Mn r = 0.126 (Table 8.112A)
- carbonate Mn r = 0.748 (Table 8.113A)
- reducible Mn r = 0.545 (Table 8.114A)
- oxidisable Mn r = 0.536 (Table 8.115A)
- residual Mn r = 0.459 (Table 8.116A).

Total Mn in house dust and garden soil has a strong positive correlation. This suggests that 43.60% of the variability in household dust Mn could be explained by garden soil Mn. A large proportion of dust Mn, however, is not derived from exterior garden soil, but from other sources, both internal ones and airborne dust from distant sources, including unleaded automobile exhaust emissions, the petrol-powered electricity-generating plant, lead-acid battery factory, artillery industries, *etc.* Possible internal sources of Mn are steel house-ware, alloys, batteries, pigments, wood preservatives, fungicide, bronze utensils, glass, varnish, paints, disinfectants, medicines, textiles, *etc.* (Parkes, 1967; Lapedes, 1978; Reimann *et al.*, 1998).

The above correlation coefficients of the sequential extraction steps between house dust and garden soil Mn, indicate that there is a very low positive relationship in the extractable phase, suggesting that the mode of occurrence is largely different. In the other phases, however, there is a moderate to strong correlation and, consequently, a significant proportion of Mn in house dust is explained by a similar mode of occurrence as in garden soil. Similarities in terms of extractability (Fig. 8.75A), the partitioning patterns and element associations between the two sampling media support this inference.

8.3.14.2. Bioavailability and biological effects of manganese (Mn)

Readily available amounts of Mn in house dust vary from 26.5 to 3,750 ppm Mn (steps 1+2). The very low pH of a child's gastric fluids in an empty stomach can, however,

attack element contents held even in the oxidisable phase fractions, *i.e.*, from 120.1-16,500 ppm Mn (steps 1+2+3+4).

Suggested dietary intakes by WHO are 2.5 mg/day for adults. Authorities in the U.S.A. suggest the following daily intakes (Mervyn, 1985):

infants of 0-0.5 year:	0.5-0.7 mg Mn/day;
infants of 0.5-1 year:	0.7-1.0 mg Mn/day;
children of 1-3 years:	1.0-1.5 mg Mn/day;
children of 4-6 years:	1.5-2.0 mg Mn/day;
children of 7-10 years:	2.0-3.0 mg Mn/day;
children of 11+ years:	2.5-5.0 mg Mn/day;
adults:	2.5-5.0 mg Mn/day.

These figures are considered as both adequate and safe.

A high intake of Mn will lower Fe, K, Mg and P levels in the body (Fig. 8.1), which may cause diseases related to deficiency with respect to these elements. Excessive intakes of Mn from oral ingestion are rare (Gough *et al.*, 1979; Mervyn, 1985, 1986, 1996). In case, however, the daily intake exceeds normal amounts the symptoms include lethargy, involuntary movements, impairment of voluntary movement, changes in muscle tone, postural changes and coma (Mervyn, 1985).

Chronic poisoning from inhalation of manganese dust is an industrial hazard (Mervyn, 1985, 1986, 1996). Symptoms include irritation and infections of the respiratory system, headache, sleep disturbances, dermatitis, irritability, liver enlargement, nerve degeneration similar to Parkinson's disease. Other symptoms include weakness in the legs, hand tremor, slurred speech, muscular cramps, fixed facial expression, mental deterioration, gastrointestinal irritation, excessive perspiration, excessive salivation, sexual disturbances, and blood diseases. Maximum permissible atmospheric concentration is 5 mg Mn/m^3.

8.3.15. PARTITIONING OF MOLYBDENUM (MO) IN HOUSE DUST (Map 8.19, Tables 8.71A-.75A, Figs. 8.29A-.30A)

The most significant phase of Mo in house dust, as in overburden, is the residual, which accounts for 1.81-81.03% of the total (median=51.73%; 0.13-57.50 ppm Mo; median=2.0 ppm Mo). The next important phase, again as in overburden, is the carbonate, which accounts for 4.51-37.28% of the total (median=12.9%; 0.40-14.4 ppm Mo; median=0.40 ppm Mo).

Generally, the concentrations of house dust Mo in all five phases, extracted from dust over almost all types of contaminated land are comparatively low. The highest house dust Mo concentrations occurring in all phases are of local significance, and mainly occur in houses over samples of slag earth, pyrite, flotation residues and nearby contaminated soil at Kavodokanos, and one sample at Prasini Alepou. Five houses, in the Phenikodassos-Santorineika area and one at Ayia Paraskevi and another at Thorikon, have extractable Mo levels of up to 3 ppm. Although elevated concentrations are generally low for all extraction phases, to be in line with the description of overburden Mo results, the residual and carbonate phases will be discussed below.

Residual phase Mo in house dust samples has a moderate to weak positive correlation with Fe (r=0.40), Cr (r=0.35), Mn (r=0.34), V (r=0.33), Co (r=0.29), Ti (r=0.29), Li (r=0.28), Cd (r=0.27), Ba (r=0.26), and Cu (r=0.26), elements normally associated with

sulphides and silicate minerals (Table 8.110A; Fig. 8.47A). This again supports the interpretation of incomplete dissolution of primary sulphide minerals by the organic/sulphide phase.

Carbonate phase Mo has a strong to moderate positive correlation with Ti (r=0.73), Al (r=0.59), Fe (r=0.56), Ba (r=0.51), Mn (r=0.47), La (r=0.41), Be (r=0.38), and Zn (r=0.31) (Table 8.107A; Fig. 8.44A). This element association and the weak correlation of Mo with Ca (r=-0.25), suggest that only a very small proportion is related to calcium carbonate minerals, and the major part is adsorbed on the surfaces of amorphous precipitates of aluminium, iron or manganese oxides, alumino-silicates, silica, and micro-crystalline precipitates of oxides, and carbonates, but not phosphates, since Mo has a very low negative correlation with P (r=-0.103).

8.3.15.1. Comparison of molybdenum (Mo) in house dust and garden soil

The partitioning patterns of Mo in house dust and garden soil show similarities, but differences in the absolute concentrations (Maps 7.19 & 8.19), which are higher in garden soil samples for total contents only (n=224; Fig. 6.17, p.167). In all five sequential extraction phases, Mo in house dust samples has higher concentrations than the corresponding garden soil samples (Fig. 8.76A; n=126). Comparison of median values of the relative extractability between the two sampling media, shows that a greater amount of Mo is extracted from samples of house dust in steps 1, 2 and 4 (Fig. 8.77A), which possibly suggests that a certain proportion of Mo has a different mode of occurrence. These differences are supported, up to a certain extent, by different element associations in the five sequential extraction steps of Mo in house dust and garden soil.

The linear correlation coefficients between Mo in house dust and garden soil for total and sequential extraction contents are:

- total Mo r = 0.263 (Table 8.111A)
- exchangeable Mo r = 0.238 (Table 8.112A)
- carbonate Mo r = 0.478 (Table 8.113A)
- reducible Mo r = -0.005 (Table 8.114A)
- oxidisable Mo r = -0.012 (Table 8.115A)
- residual Mo r = 0.076 (Table 8.116A).

Total Mo in house dust and garden soil has a weak positive correlation coefficient, implying that 93.07% of the variability in household dust Mo is not derived from exterior garden soil, but from other sources, perhaps internal ones, such as alloys, lubricants, pigments, phosphate detergents, porcelain painting, silk and woollen dyed fabrics, *etc.* (Parkes, 1967; Lapedes, 1978; Reimann *et al.*, 1998). Possible distant external sources are airborne dust, and emissions from the petrol-powered electricity-generating plant.

The above correlation coefficients of the sequential extraction steps between house dust and garden soil Mo indicate that there is a moderate positive to no relationship with respect to the mode of occurrence in the two sample types. This inference is well illustrated by the different behaviour in the extractability of Mo (Fig. 8.77A), the partitioning patterns and element associations between the two sampling media.

8.3.15.2. Bioavailability and biological effects of molybdenum (Mo)

Readily available amounts of Mo in house dust vary from 0.5 to 18.6 ppm Mo (steps 1+2). The very low pH of a child's gastric fluids in an empty stomach can, however,

attack element contents held even in the oxidisable phase fractions, *i.e.*, from 0.64-28.77 ppm Mo (steps 1+2+3+4).

Suggested dietary intakes by the U.S.A. Food and Nutrition Board, National Research Council – National Academy of Sciences are (Mervyn, 1985):

infants of 0-0.5 year:	30- 60 µg Mo/day;
infants of 0.5-1 year:	40- 80 µg Mo/day;
children of 1-3 years:	50-100 µg Mo/day;
children of 4-6 years:	60-150 µg Mo/day;
children of 7-10 years:	100-300 µg Mo/day;
adolescents of 11+ years:	150-500 µg Mo/day;
adults:	150-500 µg Mo/day.

Molybdenum toxicity from inhalation is unknown. Nevertheless, excessive intakes of Mo, according to Mervyn (1985, 1986, 1996) have been reported as causing:

(a) gout (at intakes of 1,015 mg Mo/day) in areas of molybdenum-rich soil. High blood levels of uric acid are produced in the affected individuals; and
(b) increased urinary excretion of Cu, producing deficiency of this trace element. High intakes of Mo from foods grown in molybdenum-rich soils were to blame.

8.3.16. PARTITIONING OF NICKEL (Ni) IN HOUSE DUST (Map 8.20, Tables 8.76A-.80A, Figs. 8.31A-.32A)

The most significant phase of house dust Ni over all types of contaminated land, as in overburden, is the residual, which accounts for 32.04-91.86% of the total (median=69.39%; 21.5-1,140 ppm Ni; median=101.0 ppm Ni). The second comparatively important phase, again over all types of contaminated land, is the reducible, accounting for 5.2-32.24% of the total (median=15.09%; 3-86.5 ppm Ni; median=12.0 ppm Ni). The remaining phases, similar to overburden, are of minor importance. Essentially the partitioning patterns are the same for all samples, except three distinctly different samples at Koukos, to the north of Ayios Andreas and Prasini Alepou, which have very high residual Ni levels and elevated reducible contents. These three samples have also similar patterns with respect to Co and Cr (refer to Maps 8.10 & 8.11), and the latter two have similarities with Cu (Map 8.12).

Residual phase Ni in house dust samples has a high correlation with Cr (r=0.83), and Co (r=0.62), (Table 8.11A; Fig. 8.47A). This element association suggests that Ni is related to dust particles from refractory alumino-silicate minerals, and pyrite, but not polymetallic sulphides, such as Pb-Zn-Cu, with Ag, Cd *etc.*, because its correlation with these elements is very low positive or negative.

Carbonate phase Ni in house dust is weakly correlated to Co (r=0.35) and V (r=0.28) (Table 8.107A; Fig. 8.44A). This element association and the negative correlation of Ni with Ca (r=-0.22), suggest that it is not related to calcium carbonate minerals, and a very small proportion is adsorbed on the surfaces of amorphous precipitates of aluminium (r=0.11), and iron (r=0.15) oxides, micro-crystalline precipitates of oxides, carbonates, and very weakly with phosphates, since Ni has a very low positive correlation with P (r=0.11).

8.3.16.1. Comparison of nickel (Ni) in house dust and garden soil

The partitioning patterns of Ni in house dust and garden soil show distinct differences, especially in the residual phase with consistent higher levels in garden soil (Maps 7.20 & 8.20; Fig. 8.78A). House dust, compared to its corresponding samples of garden soil (n=126), has higher Ni contents in the carbonate, reducible and residual phases (Fig. 8.78A; n=126). Comparison of median values of the relative extractability between the two sampling media, shows that a greater amount of Ni is extracted from samples of house dust in steps 1, 2 and 3 (Fig. 8.78A), which possibly suggests that a certain proportion of Ni has a different mode of occurrence. These differences are supported, up to a certain extent, by different element associations in the five sequential extraction steps of Ni in house dust and garden soil.

The linear correlation coefficients between Ni in house dust and garden soil for total and sequential extraction contents are:

- total Ni r = 0.104 (Table 8.111A)
- exchangeable Ni r = -0.170 (Table 8.112A)
- carbonate Ni r = -0.060 (Table 8.113A)
- reducible Ni r = 0.099 (Table 8.114A)
- oxidisable Ni r = 0.108 (Table 8.115A)
- residual Ni r = 0.151 (Table 8.116A).

Total Ni in house dust and garden soil has a very low positive correlation coefficient, implying that 98.92% of the variability in household dust Ni is not derived from exterior garden soil, but from other sources, perhaps internal ones, such as alloys lining cooking utensils, margarine, cigarette smoke and ash, chrome-nickel plating, batteries, pigments, coins, ceramics, magnetic tapes, dyed textiles *etc.* (Parkes, 1967; Lapedes, 1978; Mervyn, 1985; Reimann *et al.*, 1998). Possible distant external sources are airborne dust, emissions from chemical industries, traffic, fuel combustion, petrol-powered electricity-generating plant, particles from incineration at the municipal waste dump site, *etc.*

The above correlation coefficients of the sequential extraction steps between house dust and garden soil Ni, indicate that there is a very low positive to no relationship with respect to the mode of occurrence in the two sample types. This inference is well illustrated by the different behaviour in the extractability of Ni (Fig. 8.79A), the partitioning patterns and element associations between the two sampling media.

8.3.16.2. Bioavailability and biological effects of nickel (Ni)

Readily available amounts of Ni in house dust vary from 1.3 to 48.1 ppm Ni (steps 1+2). The very low pH of a child's gastric fluids in an empty stomach can, however, attack element contents held even in the oxidisable phase fractions, *i.e.*, from 5.2-161 ppm Ni (steps 1+2+3+4).

Exposure to non-dietary sources of nickel is widespread, and it can be highly toxic if absorbed in large quantities (Stanway, 1983). Serious ill effects range from dermatitis to lung cancer. In tobacco some Ni combines with carbon monoxide to form the toxic nickel carbonyl, a known carcinogen (Manousakis, 1992). Mervyn (1985, 1986, 1996) on the other hand states that toxic effects of excess oral Ni intakes in humans are unknown.

8.3.17. PARTITIONING OF PHOSPHORUS (P) IN HOUSE DUST (Map 8.21, Tables 8.81-.85, Figs. 8.33-.34)

Phosphorus shows variable partitioning patterns in house dust samples over all types of contaminated land. The most significant phase is the exchangeable, which accounts for 0.56-71.40% of the total (median=21.15%; 2.8-3,750 ppm P; median=251 ppm P). Comparatively high dust P contents are also extracted by the other phases, *i.e.*,

(a) residual (6.63-94.57%; median=32.74%; 95-1,530 ppm P; median=425 ppm P),
(b) oxidisable (0.03-46.36%; median=14.39%; 0.3-1,120 ppm P; median=208 ppm P),
(c) carbonate (0.48-28.85%; median=12.65%; 2.4-734 ppm P; median=160 ppm P), and
(d) reducible (4.18-39.08%; median=15.97%; 21-450 ppm; median=227 ppm P).

Exchangeable phase P has moderate to weak positive correlation coefficients with Mn (r=0.55), Ni (r=0.58), Cr (r=0.53), Cu (r=0.51), Zn (r=0.50), K (r=0.48), Fe (r=0.45), Al (r=0.41), Pb (r=0.41), Co (r=0.38), Li (r=0.31), Ba (r=0.29), and Ti (r=0.28), (Table 8.106A; Fig. 8.43A). It has also a strong negative correlation coefficient with pH (r=-0.62), and weak negative correlation with Ag (r=-0.29) and Mo (r=-0.19). These relationships suggest P to be moderately related to exchangeable sites, which are used by contaminant elements. The strong negative correlation of exchangeable P in house dust samples with pH is interesting, for it indicates that the amount of easily extractable P decreases with increasing pH, *e.g.*, over the flotation residues from Noria to Prasini Alepou and Santorineika where the pH is in the alkaline range comparatively low extractable P levels occur.

Residual phase P in house dust samples has a strong to weak positive correlation coefficients with Cd (r=0.65), Pb (r=0.63), Zn (r=0.60), Fe (r=0.59), La (r=0.59), Mn (r=0.51), Be (r=0.48), Ag (r=0.47), Li (r=0.46), Cu (r=0.43), V (r=0.43), Ca (r=0.40), Al (r=0.39), K (r=0.36), and Sr (r=0.33), (Table 8.110A; Fig. 8.47A). This element association suggests that P in the residual phase is primarily related to non-digested particles of sulphides in step 4, and secondarily to silicates, which suggests a relationship with silicate particles.

Oxidisable phase P in house dust samples has a strong positive correlation coefficient with Cr (r=0.66), Mo (r=0.63) and V (r=0.57), a moderate correlation with Ti (r=0.43), and a weak with Sr (r=0.20). It has also moderate to weak negative correlation coefficients with Mn (r=-0.54), Zn (r=-0.39), La (r=-0.36), Co (r=-0.35), Cd (r=-0.34), Fe (r=-0.28), Cu (r=-0.26), (Table 8.109A; Fig. 8.46A), suggesting an antipathetic relationship with dust particles of sulphide minerals. It appears, therefore, that P is bound to the organic fraction.

Carbonate phase P in house dust has moderate to weak positive correlation coefficients with Ag (r=0.44) and Cr (r=0.31), showing that P is adsorbed on similar sites as these two elements (Table 8.107A; Fig. 8.44A). It has also moderate to weak negative correlation coefficients with Ca (r=-0.46), Ba (r=-0.36), Zn (r=-0.36), Mn (r=-0.36), Fe (r=-0.36), Pb (r=-0.31), Al (r=-0.31), Sr (r=-0.28), Be (r=-0.27), and Cd (r=-0.23). These relationships suggest that P is not related to calcium carbonate minerals, because of its negative coefficient with Ca and Sr; it is also not adsorbed on the surfaces of amorphous precipitates of Al (r=-0.14), Fe (r=-0.01) and Mn (r=-0.002) oxides, because again of the weak negative relationship. Consequently, P may be associated with other carbonate minerals, and phosphates. It is noted that the range of total chromium in phosphate fertilisers is 66-245 ppm (Kabata-Pendias and Pendias, 1984).

Reducible phase P in house dust samples has only a weak positive correlation coefficient with Ca (r=0.28). It has also weak negative correlation coefficients with Mn (r=-0.29), Co (r=-0.32), Fe (r=-0.24), Zn (r=-0.21), and Cu (r=-0.21), and Al (r=-0.14) (Table 8.108A; Fig. 8.45A). This suite of elements with negative co-variation with P, indicates that it is not associated with Al, Mn and Fe oxides, whereas the weak positive correlation with Ca suggests a minor association with calcium carbonate minerals, *e.g.*, calcite [$CaCO_3$] and dolomite [$CaMg(CO_3)_2$], which are dissolved by the hydroxylamine reagent.

8.3.17.1. Comparison of phosphorus (P) in house dust and garden soil

The partitioning patterns of P in house dust and garden soil show distinct differences, especially in the exchangeable and residual phases, with comparatively higher levels of exchangeable P in house dust, and lower contents in the residual phase (Maps 7.21 & 8.21; Fig. 8.80A). House dust, compared to its corresponding samples of garden soil (n=126), has also lower P contents in the carbonate, reducible and oxidisable phases (Fig. 8.80, n=126). Comparison of median values of the relative extractability between the two sampling media, shows that a greater amount of P is extracted from samples of house dust in steps 1, 2 and 3 (Fig. 8.81A). This possibly suggests that a certain proportion of P has a different mode of occurrence. These differences are supported, up to a certain extent, by different element associations in the five sequential extraction steps of P in house dust and garden soil.

The linear correlation coefficients between P in house dust and garden soil for total and sequential extraction contents are:

- total P r = 0.153 (Table 8.111A)
- exchangeable P r = -0.150 (Table 8.112A)
- carbonate P r = 0.296 (Table 8.113A)
- reducible P r = 0.359 (Table 8.114A)
- oxidisable P r = 0.474 (Table 8.115A)
- residual P r = 0.377 (Table 8.116A).

Total P in house dust and garden soil has a very low positive correlation coefficient, implying that 97.96% of the variability in household dust P is not derived from exterior garden soil, but from other sources, perhaps internal ones, such as food stuffs, detergents, *etc.* Possible distant external sources are airborne dust, insecticides, herbicides, fungicides, and industries, such as matches, military (explosives and warfare chemicals), *etc.* (Lapedes, 1978; Reimann *et al.*, 1998).

The above correlation coefficients of the sequential extraction steps between house dust and garden soil P, indicate that with respect to its mode of occurrence in the two sample types there is (a) no correlation in the exchangeable phase, and (b) a moderate to weak positive relationship in the oxidisable, residual, reducible and carbonate phases. This inference is supported by the extractability of P (Fig. 8.81A), the partitioning patterns and element associations between the two sampling media.

8.3.17.2. Bioavailability and biological effects of phosphorus (P)

Readily available amounts of P in house dust vary from 5.2 to 4,484 ppm P (steps 1+2). The very low pH of a child's gastric fluids in an empty stomach can, however, attack element contents held even in the oxidisable phase fractions, *i.e.*, from 26.5-6,054 ppm P (steps 1+2+3+4).

United Kingdom and WHO authorities make no recommendations about recommended dietary intakes of P, but USA authorities have suggested the following (Mervyn, 1985):

infants of 0-0.5 year:		240 mg P/day;
infants of 0.5-1 year:		400 mg P/day;
children of 1-3 years:		800 mg P/day;
children of 4-6 years:		800 mg P/day;
children of 7-10 years:		800 mg P/day;
adolescents 11-14 years	Males:	1200 mg P/day;
	Females:	1200 mg P/day;
teenagers 15-18 years	Males:	1200 mg P/day;
	Females:	1200 mg P/day;
adults 19-22 years	Males:	800 mg P/day;
	Females:	800 mg P/day;
adults 23-50 years	Males:	800 mg P/day;
	Females:	800 mg P/day;
adults 51+ years	Males:	800 mg P/day;
	Females:	800 mg P/day;
pregnant women:		1200 mg P/day;
breast-feeding women:		1200 mg P/day.

Excessive oral intakes of P can prevent the absorption of Fe, Ca, Mg and Zn (Fig. 8.1) by formation of insoluble phosphates (Mervyn, 1985, 1986, 1996). Too much oral phosphates can cause diarrhoea. If blood levels of phosphate are too high, calcification in the soft tissues can occur and blood levels of Ca will fall.

8.3.18. PARTITIONING OF LEAD (Pb) IN HOUSE DUST (see Chapter 3, p.82-90)

8.3.19. PARTITIONING OF STRONTIUM (Sr) IN HOUSE DUST (Map 8.26, Tables 8.86A-.90A, Figs. 8.35A-.36A)

Strontium in house dust shows, as in overburden, variable partitioning patterns over all types of metallurgical processing wastes. The most significant extraction steps of Sr, as in overburden, are the

- residual, 3.69-68.96% of the total (median=19.69%; 4.2-284 ppm Sr; median=23.4 ppm Sr);
- carbonate 9.18-65.72% of the total (median=25.8%; 11.3-383 ppm Sr; median=29.8 ppm Sr), and
- reducible, 15.66-59.29% of the total (median=39.84%; 14.4-195 ppm Sr; median=48.7 ppm Sr).

Strontium in the residual phase of house dust samples has a strong to moderate positive correlation with Be (r=0.60), Al (r=0.59), Zn (r=0.57), Ti (r=0.55), V (r=0.53), Li (r=0.49), K (r=0.43), Ba (r=0.42), Ag (r=0.41), Pb (r=0.39), Ca (r=0.39), Cd (r=0.38), and Fe (r=0.37), (Table 8.110A; Fig. 8.47A). This element association suggests that Sr is related to dust particles of both alumino-silicate and sulphide minerals. The latter were not completely digested in step 4.

In the carbonate phase, house dust Sr has a moderate positive correlation with Ag (r= 0.44) and Cr (r=0.31) (Table 8.107A; Fig. 8.44A). Strontium has a moderate to weak negative correlation coefficient with Ca (r=-0.46), Fe (r=-0.36), Mn (r=-0.36), Ba (r=-0.36), Zn (r=-0.36), Pb (r=-0.31) and Al (r=-0.31). This element association suggests that Sr is neither

related to dust particles of calcium carbonate minerals, nor to other specific adsorption sites, such as adsorbed on the surfaces of amorphous precipitates of iron, manganese, and aluminium oxides, alumino-silicates, and phosphates due to its non- correlation with P (r=-0.05). Consequently, it must be adsorbed on dust particles of possibly other carbonate minerals, amorphous silica, and micro-crystalline precipitates of oxides.

House dust reducible (Fe-Mn oxide) phase Sr has a high positive correlation with Ca (r=0.67) and pH (r=0.55); a moderate positive correlation with Be (r=0.54), Ti (r=0.43), Li (r=0.40), K (r=0.38), and Al (r=0.36), and a weak positive correlation with La (r=0.30) and Mo (r=0.29), (Table 8.108A; Fig. 8.45A). This association suggests that Sr is related to

- calcium carbonates, thus indicating the incomplete dissociation of carbonates during the second step, and
- amorphous silicates.

Strontium may also be moderately adsorbed on Al oxides (r=0.36), and very weakly adsorbed on Mn (r=0.22) and Fe oxides (r=0.15).

8.3.19.1. Comparison of strontium (Sr) in house dust and garden soil

The partitioning patterns of Sr in house dust and garden soil show some relationship (Maps 7.26 & 8.26; Fig. 8.82A). House dust, compared to its corresponding samples of garden soil (n=126), has higher Sr contents in the carbonate and residual phases (Fig. 8.82A, n=126). Comparison of median values of the relative extractability, between the two sampling media, shows that a greater amount of Sr is extracted from samples of house dust in steps 1, 3 and 4 (Fig. 8.83A), which possibly suggests that a certain proportion of Sr has a different mode of occurrence. These differences are supported, up to a certain extent, by different element associations in the five sequential extraction steps of Sr in house dust and garden soil.

The linear correlation coefficients between Sr in house dust and garden soil for total and sequential extraction contents are:

- total Sr r = 0.234 (Table 8.111A)
- exchangeable Sr r = 0.228 (Table 8.112A)
- carbonate Sr r = 0.147 (Table 8.113A)
- reducible Sr r = 0.095 (Table 8.114A)
- oxidisable Sr r = 0.317 (Table 8.115A)
- residual Sr r = 0.356 (Table 8.116A).

Total Sr in house dust and garden soil has a very low positive correlation coefficient, implying that 94.53% of the variability in household dust Sr is not derived from exterior garden soil, but from other sources, perhaps internal ones, such as alloys, plastics, lubricants, soap, matches, corrosion resistant pigment used in metal coating, bleaches, medicines, food stuffs (Lapedes, 1978). Possible distant external sources are airborne dust, sea spray, pyrotechnic materials, *etc.* (Reimann *et al.*, 1998).

The above correlation coefficients of the sequential extraction steps, between house dust and garden soil Sr, indicate that with respect to its mode of occurrence in the two sample types there is (a) no correlation in the reducible phase, and (b) a weak to low positive relationship in the residual, oxidisable, exchangeable and carbonate phases. This inference is also shown by the extractability of Sr (Fig. 8.83A), the partitioning patterns and element associations between the two sampling media.

8.3.19.2. Bioavailability and biological effects of strontium (Sr)

Readily available amounts of Sr in house dust vary from 13.2 to 401.5 ppm Sr (steps 1+2). The very low pH of a child's gastric fluids in an empty stomach can, however, attack element contents held even in the oxidisable phase fractions, *i.e.*, from 28.7-613.9 ppm Sr (steps 1+2+3+4).

Daily intakes of up to 4 mg Sr/day do not appear to produce negative health effects (Mervyn, 1996). The most serious toxic effect of Sr in comparatively high doses is the observed absence of bone mineralisation, which can be treated by high doses of calcium.

The non-radioactive form of Sr appears to be perfectly safe according to Mervyn (1985, 1986, 1996). The radioactive form of strontium, Sr-90, with a half-life of 28 years is very toxic and dangerous to health.

8.3.20. PARTITIONING OF TITANIUM (Ti) IN HOUSE DUST (Map 8.27, Tables 8.91A-.95A, Figs. 8.37A-.38A)

The greatest amount of Ti in house dust samples, as in overburden, is found in the residual phase, which accounts for 88.64-99.91% of the total (median=99.44%; 786-4,680 ppm Ti; median=1,480 ppm Ti). The remaining phases, again as in overburden, are not very significant with respect to household dust Ti levels.

Residual phase house dust Ti has a moderate positive correlation with Ba (r=0.55), Sr (r=0.55), V (r=0.47), Al (r=0.45), Be (r=0.44), Li (r=0.44) and K (r=0.41), and weak positive correlation with Mo (r=0.29), Co (r=0.28), La (r=0.28), Cr (r=0.27), Mn (r=0.28), Ag (r=0.26), Ni (r=0.23), Fe (r=0.21), and Pb (r=0.21) (Table 8.110A; Fig. 8.47A). These element relationships with (a) rock forming elements, and (b) ore elements, suggest that Ti is associated with alumino-silicate dust particles, but also with sulphide dust particles, since the latter were not completely digested in step 4.

8.3.20.1. Comparison of titanium (Ti) in house dust and garden soil

The partitioning patterns of Ti in house dust and garden soil show a definite relationship (Maps 7.27 & 8.27; Fig. 8.84A). House dust, compared to its corresponding samples of garden soil (n=126), has higher Ti contents in the exchangeable, reducible and oxidisable phases.

Although the patterns appear similar, the linear correlation coefficients between Ti in house dust and garden soil for total and sequential extraction contents reveal the absolute relationships, and are:

- total Ti r = -0.042 (Table 8.111A)
- exchangeable Ti r = -0.161 (Table 8.112A)
- carbonate Ti r = 0.731 (Table 8.113A)
- reducible Ti r = 0.099 (Table 8.114A)
- oxidisable Ti r = 0.286 (Table 8.115A)
- residual Ti r = -0.034 (Table 8.116A).

Total Ti in house dust and garden soil has a very low negative correlation coefficient, implying that 99.82% of the variability in household dust Ti is not derived from exterior garden soil, but from other sources, perhaps internal ones, such as alloys, paints,

pigments, laundry chemical, cosmetics, toothpaste, food additives, and certain sugar and jam products (Lapedes, 1978; Mervyn, 1985, 1986, 1996; Reimann *et al.*, 1998). A possible distant external source is airborne dust from geogenic sources (Reimann *et al.*, 1998).

The above correlation coefficients of the sequential extraction steps between house dust and garden soil Ti, indicate that with respect to its mode of occurrence in the two sample types there is (a) a strong positive correlation in the carbonate phase only, and (b) a weak to low positive or negative relationship in the oxidisable, reducible, residual and exchangeable phases.

8.3.20.2. Bioavailability and biological effects of titanium (Ti)

Readily available amounts of Ti in house dust vary from 0.44 to 113.94 ppm Ti (steps 1+2). The very low pH of a child's gastric fluids in an empty stomach can, however, attack element contents held even in the oxidisable phase fractions, *i.e.*, from 0.81-211.7 ppm Ti (steps 1+2+3+4).

In the United Kingdom daily dietary intakes of Ti are approximately 800 mg/day. According to Mervyn (1985, 1986, 1996) no limits are given for its acceptable daily intake, and there are no reports of titanium toxicity (Gough *et al.*, 1979).

8.3.21. PARTITIONING OF VANADIUM (V) IN HOUSE DUST (Map 8.29, Tables 8.96A-.100A, Figs. 8.39A-.40A)

The most significant phase of V for all house dust samples, as in overburden, is the residual, which accounts for 44.58-88.21% (median=68.01%; 7.25-98 ppm V; median=29 ppm V). The next two comparatively important phases of house dust V, as in overburden, are the reducible and oxidisable, which account for 7.62-29.11% and 1.06-34.69% of the total respectively; their corresponding median values are 16.64% and 12.21%.

House dust V in the residual phase has strong to weak correlation coefficients with Al (r=0.71), Be (r=0.70), Li (r=0.69), K (r=0.68), Sr (r=0.53), Co (r=0.52), Fe (r=0.52), Ti (r=0.47), P (r=0.43), Cr (r=0.43), Zn (r=0.41), Mn (r=0.39), La (r=0.38), Ni (r=0.36), Pb (r=0.35), Ag (r=0.33), Mo (r=0.33), and Cd (r=0.29). This element association suggests that, residual phase V in house dust samples, is mainly found in dust particles of alumino-silicate minerals, but it is also related, to a lesser extent, to dust particles of sulphides, which were not completely digested in step 4.

The highest levels of reducible (Fe-Mn oxide) phase indoor dust V contents occur in houses between Ayia Paraskevi and Nichtochori, which are situated over contaminated residual soil. Similar levels of dust V are found in a few samples at Neapoli. House dust samples in other areas have generally lower levels of reducible phase V contents. Reducible phase V in house dust samples has weak positive correlation coefficients with Ca (r=0.34), Cr (r=0.33), Li (r=0.30), Be (r=0.27), and Al (r=0.21), which suggests a weak relationship with dust particles of calcium carbonate and Al oxide minerals, but not Mn (r=0.08) and Fe (r=0.01), because of the insignificant positive correlation.

The highest levels of oxidisable (organic/sulphide) phase V in floor dust samples is found again in houses over contaminated soil between Ayia Paraskevi and Nichtochori, and in a few houses at Neapoli. Oxidisable phase V in house dust samples has a strong to weak positive correlation coefficients with Cr (r=0.66), Mo (r=0.62), P (r=0.57), Al

(r=0.34), and Ti (r=-0.32); it has also weak to low negative correlation coefficients with Mn (r=-0.39), Cd (r=-0.27), Ag (r=-0.17), and Zn (r=-0.16). This element association indicates that V is mostly related to the organic and not the sulphide fraction.

8.3.21.1. Comparison of vanadium (V) in house dust and garden soil

The partitioning patterns of V in house dust and garden soil show distinct differences (Maps 7.29 & 8.29; Fig. 8.86A). House dust, compared to its corresponding samples of garden soil (n=126), has higher V contents in the exchangeable, reducible and oxidisable phases.

The linear correlation coefficients between V in house dust and garden soil for total and sequential extraction contents reveal the absolute relationships, and are:

- total V r = 0.011 (Table 8.111A)
- exchangeable V r = 0.448 (Table 8.112A)
- carbonate V r = 0.375 (Table 8.113A)
- reducible V r = 0.305 (Table 8.114A)
- oxidisable V r = 0.526 (Table 8.115A)
- residual V r = -0.101 (Table 8.116A).

Total V in house dust and garden soil has a very low positive correlation coefficient, implying that 99.99% of the variability in household dust V is not derived from exterior garden soil, but from other sources, perhaps internal ones, such as alloys, synthetic rubber, pigments, dyes, textiles, glass, ceramics, food stuffs (Földvári-Vogl, 1978; Lapedes, 1978; Mervyn, 1985, 1986, 1996; Reimann *et al.*, 1998). Possible distant external sources are airborne dust from geogenic materials, petrol-powered electricity-generating plant, *etc.* (Reimann *et al.*, 1998). The comparatively high levels of indoor dust V in the reducible and oxidisable phases in houses, which are situated on hilly ground at Ayia Paraskevi, Nichtochori and Neapoli, down wind from the petrol-powered electricity-generating plant, suggests that it may be one of the major sources of airborne contaminants.

The above correlation coefficients of the sequential extraction steps between house dust and garden soil V, indicate that with respect to its mode of occurrence in the two sample types there is (a) a moderate positive correlation in the oxidisable and exchangeable phases, and (b) a weak to low positive or negative relationship in the carbonate, reducible, and residual phases. Similarities or differences in the element associations, and extractability of V also support these relationships in the sequential extraction phases of the two sample types.

8.3.21.2. Bioavailability and biological effects of vanadium (V)

Readily available amounts of Ti in house dust vary from 0.25 to 12.45 ppm V (steps 1+2). The very low pH of a child's gastric fluids in an empty stomach can, however, attack element contents held even in the oxidisable phase fractions, *i.e.*, from 2.95-86.65 ppm V (steps 1+2+3+4).

Toxic effects have not been reported, except the possibility that V may be related to manic depression (Mervyn 1985, 1986, 1996). Researchers at the University of Dundee, U.K., have in fact shown, that elevated levels of V in hair tissue were present in manic depression patients (Davies and Stewart, 1987).

8.3.22. PARTITIONING OF ZINC (Zn) IN HOUSE DUST (Map 8.30, Tables 8.96A-.100A, Figs. 8.41A-.42A)

The partitioning patterns of house dust Zn, as in overburden, are variable in all samples and, especially, in houses over slag earth, flotation residues, and nearby contaminated soil at Kavodokanos. These patterns indicate a direct relationship to outdoor sources, an observation supported by lower indoor dust Zn contents, which occur in houses over contaminated soil. The most significant phase for house dust Zn, as in overburden, is the reducible (Fe-Mn oxide) phase, which accounts for 9.46-58.34% of the total (median=37.87%; 149-12,900 ppm Zn; median=1,140 ppm Zn). The other important phases for house dust samples, as in overburden, are:

- the residual, which accounts for 5.18-49.41% of the total (median=21.92%; 72.6-10,300 ppm Zn; median=675 ppm Zn);
- the carbonate, which accounts for 6.14-44.23% of the total (median=27.93%; 136-6,830 ppm Zn; median=760 ppm Zn), and
- the oxidisable (organic/sulphide), which accounts for 1.85-44.91% of the total (median=10.48%; 27.9-6,560 ppm Zn; median=331 ppm Zn).

Considerably lower amounts of house dust Zn are extracted by the exchangeable phase (1.2-122 ppm Zn; median 26.5 ppm Zn), but they are important for when combined with the carbonate phase contents, make up the readily available Zn contents, *i.e.*, 137.2-6,952 ppm Zn.

House dust Zn has the following correlation coefficients with other elements in the different phases:

- *exchangeable:* Mn (r=0.70),Cd (r=0.67), Cu (r=0.62), Pb (r=0.60), Ni (r=0.51), Fe (r=0.51), P (r=0.50), Co (r=0.49), Ba (r=0.41), Al (r=0.37), and Cr (r=0.34) (Table 8.106A; Fig. 8.43A); this element association together with the antipathetic correlation with pH (r=-0.68), suggest that (i) Zn, together with other positively correlated elements, is adsorbed on easily exchangeable sites, and (ii) elevated Zn contents occur in areas with a comparatively low pH;
- *carbonate:* Mn (r=0.72), Pb (r=0.68), Ba (r=0.64), Al (r=0.56), Be (r=0.51), Fe (r=0.51), Ti (r=0.48), Cd (r=0.37), Li (r=0.33), and Mo (r=0.31) (Table 8.107A; Fig. 8.44A); this element association together with the insignificant correlation coefficient between Zn and Ca (r=0.01), suggest that house dust Zn, as in overburden, is weakly related to calcium carbonates, and is mainly adsorbed on other specific adsorption sites, such as on the surfaces of amorphous precipitates of manganese, aluminium or iron oxides, alumino-silicates, silica, and micro-crystalline precipitates of oxides, and carbonates, but not phosphates, since dust Zn has a moderate negative correlation with P (r=-0.36).
- *reducible (Fe-Mn oxide):* Pb (r=0.87), Cd (r=0.85), Mn (r=0.85), Ba (r=0.70), Fe (r=0.65), Be (r=0.53), Co (r=0.51), K (r=0.37), Al (r=0.37), and Ti (r=0.36); and a moderate negative correlation with Ag (r=-0.33) and P (r=-0.21) (Table 8.108A; Fig. 8.45A); this element association suggests that Zn is adsorbed on Fe, Mn and Al oxides;
- *oxidisable (organic/sulphide):* Cd (r=0.73), Mn (r=0.62), Cu (r=0.55), Co (r=0.55),Be (r=0.44), Li (r=0.42), Pb (r=0.41), Fe (r=0.39), K (r=0.34), La (r=0.33), and Al (r=0.30), (Table 8.109A; Fig. 8.46A); it has also moderate negative correlation coefficients with P (r=-0.39) and Cr (r=-0.30); this element association suggests that house dust Zn is mainly related to the sulphide phase; and

- *residual:* Pb (r=0.86), Cd (r=0.83), Fe (r=0.75), Ag (r=0.74), Mn (r=0.66), Cu (r=0.66), Ca (r=0.64), P (r=0.60), Sr (r=0.57), Be (r=0.57), Al (r=0.53), Li (r=0.51), K (r=0.45), V (r=0.41), La (r=0.41), and Co (r=0.34) have positive correlation coefficients with house dust Zn (Table 8.110A; Fig. 8.47A); this element association suggests that house dust Zn probably occurs in both particles of sulphide minerals, which were not completely dissolved in step 4, and in particles of alumino-silicate minerals.

8.3.22.1. Comparison of zinc (Zn) in house dust and garden soil

The partitioning patterns of Zn in house dust and garden soil show distinct similarities in many cases (Maps 7.30 & 8.30; Fig. 8.88A). House dust, compared to its corresponding samples of garden soil (n=126), has lower Zn contents in all five sequential extraction phases.

The linear correlation coefficients between Zn in house dust and garden soil for total and sequential extraction contents reveal the absolute relationships, and are:

- total Zn r = 0.778 (Table 8.111A)
- exchangeable Zn r = 0.151 (Table 8.112A)
- carbonate Zn r = 0.735 (Table 8.113A)
- reducible Zn r = 0.768 (Table 8.114A)
- oxidisable Zn r = 0.668 (Table 8.115A)
- residual Zn r = 0.689 (Table 8.116A).

Total Zn in house dust and garden soil has a strong positive correlation coefficient, implying that 60.56% of the variability in household dust Zn is possibly derived from exterior garden soil, and only 39.44% is due to other internal or external sources. Possible internal sources are alloys, galvanised metals, paint, pigments, batteries, electrical fuses, wood preservatives, ceramics, plastics, glass, textiles, cosmetics, *etc.* (Lapedes, 1978; Reimann *et al.*, 1998). Possible distant external sources are airborne dust from geogenic materials, metallurgical wastes, insecticides, fungicides, gutters, drains, *etc.* (Reimann *et al.*, 1998).

The above correlation coefficients of the sequential extraction steps between house dust and garden soil Zn, indicate that with respect to its mode of occurrence in the two sample types there is (a) a very low positive correlation in the exchangeable phase, and (b) a strong positive relationship in the carbonate, reducible, oxidisable and residual phases. Similarities or differences in element associations, and extractability of Zn also support these relationships in the sequential extraction phases of the two sample types. With respect to extractability in the two sampling media, steps 1, 2 and 4 (Fig. 8.89A) leach a greater percentage proportion of house dust Zn out of the total.

8.3.22.2. Bioavailability and biological effects of zinc (Zn)

Readily available amounts of Zn in house dust vary from 137.2 to 6,952 ppm Zn (steps 1+2). The very low pH of a child's gastric fluids in an empty stomach can, however, attack element contents held even in the oxidisable phase fractions, *i.e.*, from 314.1-26,412 ppm Zn (steps 1+2+3+4).

The recommended daily dietary allowances of Zn by the Food and Nutrition Board of the USA, assuming a 20% absorption (Mervyn, 1985), are:

Infants of 0-0.5 year:	3 mg Zn/day;

Infants of 0.5-1 year:	5 mg Zn/day;
children of 1-10 years:	10 mg Zn/day;
adults 11-51+:	15 mg Zn/day;
pregnant women:	20 mg Zn/day;
breast-feeding women:	25 mg Zn/day.

United Kingdom and WHO authorities make no recommendation for Zn intakes. Canada suggests, however, the following intakes:

Infants of 0-0.5 year:		4 mg Zn/day;
Infants of 0.5-1 year:		5 mg Zn/day;
Children of 1-3 years:		5 mg Zn/day;
Children of 4-6 years:		6 mg Zn/day;
Children of 7-9 years	Male:	7 mg Zn/day;
	Female:	7 mg Zn/day;
Adolescents 10-12 years	Male:	8 mg Zn/day;
	Female:	9 mg Zn/day;
Adolescents 13-15 years	Male:	12 mg Zn/day;
	Female:	10 mg Zn/day;
Teenagers 16-18 years	Male:	10 mg Zn/day;
	Female:	11 mg Zn/day;
Adults 19-35 years	Male:	10 mg Zn/day;
	Female:	9 mg Zn/day;
Adults 36-50 years	Male:	10 mg Zn/day;
	Female:	9 mg Zn/day;
Adults 51+ years	Male:	10 mg Zn/day;
	Female:	9 mg Zn/day;
Pregnant women:		12 mg Zn/day;
Breast-feeding women:		16 mg Zn/day.

Chech and Slovak authorities recommend 8 mg Zn/day for adults; Danish and Italian authorities recommend 15 mg Zn/day for adults (Mervyn, 1985).

Excess intake of Zn will lower Cd, Cu, Fe and P levels in the body (Fig. 8.1). The toxicity of zinc is low. Compared with some other elements, like Cu, Se, Pb, Cd and Hg, Zn is non-toxic (Mervyn 1985, 1986, 1996). However, it is reported that the growth rate of tumours is affected by dietary Zn intake (Reimann *et al.*, 1998).

8.4. CLUSTER AND FACTOR ANALYSES

For details about cluster and factor analyses refer to the relevant section in Chapter 7 of this volume (section 7.6, p.220-222).

8.4.1. CLUSTER AND FACTOR ANALYSES ON THE EXCHANGEABLE PHASE DATA OF HOUSE DUST

The retention of factors with eigenvalues >1 resulted in the selection of a six factor model for the exchangeable phase analytical data. The variation accounted for by this six-factor varimax model is 76.34% of the total (Table 8.2, Fig. 8.2).

Factor 1 or the *"exchangeable factor"* explains 30.60% of the total variance, and has strong positive loadings (>0.7) on Mn, Cd and Zn, moderate loadings (>0.4-0.6) on Cu, Co, P and Ni, and a strong negative loading of –0.84 on pH. The negative covariation of this particular suite of elements with pH, suggests that they are held on easily

exchangeable sites, and are adsorbed on dust particles with very low pH values. The dendrogram has a cluster of elements consisting of Mn-Zn, Cd, Cu, Pb, Ni and P, which is essentially the same as factor 1 elements.

Factor 2 or the *"carbonates factor"* explains 13.51% of the total variance, and has strong positive loadings (>0.7) on Ca and Sr, and a moderate loading of 0.5 on La. The dendrogram shows a cluster made-up from Ca and Sr, which is linked at a lower level to V and La. This association suggests that $MgCl_2$ has extracted some calcium carbonate from dust particles.

Factor 3 or *"Be-Mo slag factor"* explains 11.55% of the total variance, and has strong positive loadings (>0.6) on Be, Mo, La and Ag. A similar cluster is shown by the dendrogram among Be-Mo, Ag, with a distant correlation with La. It is noted that there is a negative covariance with Pb and Mn. This element association suggests that dust particles are mainly derived from slag (or slag earth or sand-blast wastes from Kavodokanos), and flotation tailings rich in Be, Mo and Ag, but with low Pb and Mn contents.

Factor 4 or *"Fe-Al oxides factor"* explains 8.91% of the total variance, with strong positive loadings (>0.7) on Fe, Al and Ti, and moderate loadings (>0.5-0.6) on Pb and Ba. It is noted that this suite of elements has a low negative covariation with pH (-0.18). An Al-Fe and Ti cluster is shown by the dendrogram, which is linked, at a lower correlation, to the contaminant elements group. This association suggests that $MgCl_2$ extracts very low amounts of Al-Fe oxides, and their loosely adsorbed elements, and this mainly occurs in house dust samples with comparatively low pH values.

Factor 5 or *"schist factor"* explains 6.47% of the total variance, and has strong positive loadings (>0.7) on K, Cr, Li and Cu, moderate loadings (>0.5-0.6) on P, Ni and Co, and a moderate negative loading of -0.45 on Ag. The dendrogram shows a cluster with K-Li, Co, Cr, P and Ba. This element association suggests that some dust particles originate from weathered schist or soil developed on this rock type.

Factor 6 or *"vanadium factor"* explains 5.30% of the total variance, and has a strong positive loading of 0.82 on only V, which is associated with moderate loadings (>0.37-0.43) on Ni and Al. It is interesting to note that there is a negative covariance with Pb, Cd, Ag, Zn, Cu and pH. Vanadium is known to occur in schist, and soils developed over it, but silicate slag contains noteworthy quantities (Rankama and Sahama, 1952), and is also present in petroleum. It has already been noted that stack emissions from the petrol-powered electricity-generating plant, impart a lower pH value to indoor dust. Since, pH has a low and not a strong negative covariance in this factor, the preferred interpretation is that it is related to dust particles of slag (or slag earth or sand-blast

Table 8.2. Varimax loadings for the six strongest factors of exchangeable phase house dust geochemical data (n=127). Correlation between varimax scores and transformed data.
[For notation used refer to text in Chapter 7].
Table 8.2. Φορτία περιστροφής "varimax" για τους έξι ισχυρότερους παράγοντες της ανταλλάξιμης φάσης των γεωχημικών δεδομένων της σκόνης σπιτιών (n=127). Συσχέτιση μεταξύ των φορτίων varimax και των μετασχηματισμένων δεδομένων. [Για τη σημειογραφία βλέπετε το κείμενο στο Κεφάλαιο 7].

Element	*Varimax loadings*					
	Factor 1	*Factor 2*	*Factor 3*	*Factor 4*	*Factor 5*	*Factor 6*
Ag-1	0.196	0.228	0.585	0.155	*-0.449*	-0.211
Al-1	0.169	0.036	-0.122	**0.862**	0.035	0.367
Ba-1	0.179	0.279	-0.047	0.558	0.308	0.009
Be-1	-0.022	-0.212	**0.910**	-0.040	-0.031	-0.017
Ca-1	-0.094	**0.860**	-0.128	0.035	0.233	0.099
Cd-1	**0.823**	0.132	0.125	-0.049	-0.159	-0.351
Co-1	0.474	0.258	-0.015	-0.044	0.508	0.008
Cr-1	0.151	0.110	0.143	0.168	**0.725**	0.108
Cu-1	0.505	0.121	0.052	0.111	**0.640**	-0.152
Fe-1	0.276	-0.036	-0.086	**0.868**	0.100	0.115
K-1	-0.029	0.300	-0.118	0.331	**0.741**	-0.043
La-1	-0.037	0.499	**0.625**	0.023	0.234	0.139
Li-1	-0.075	0.353	-0.200	0.111	**0.658**	0.122
Mn-1	**0.850**	0.058	-0.202	0.147	0.155	0.085
Mo-1	-0.121	-0.203	**0.883**	-0.062	-0.060	0.063
Ni-1	0.459	0.134	-0.037	0.212	0.538	0.425
P-1	0.468	-0.207	-0.116	0.292	0.578	0.204
Pb-1	0.340	0.086	-0.254	0.564	0.240	-0.398
Sr-1	0.229	**0.819**	-0.099	0.092	0.170	0.112
Ti-1	-0.152	0.057	0.333	**0.775**	0.257	-0.096
V-1	-0.115	0.320	0.043	0.171	0.175	**0.824**
Zn-1	**0.797**	0.067	0.025	0.342	0.238	-0.195
pH	***-0.843***	0.164	0.048	-0.182	-0.083	-0.180
Eigenvalue	*7.04*	*3.11*	*2.66*	*2.05*	*1.49*	*1.22*
Variance explained by factor	*30.60%*	*13.51%*	*11.55%*	*8.91%*	*6.47%*	*5.30%*
Cumulative variance	*30.60%*	*44.11%*	*55.66%*	*64.57%*	*71.04%*	*76.34%*

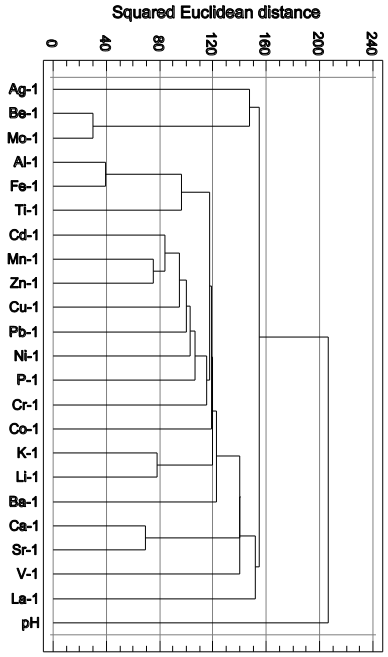

Fig. 8.2. Dendrogram showing the relationship of 22 elements and pH in samples of house dust for sequential extraction step 1 – exchangeable phase (n=127).
Σχ. 8.2. Δενδρόγραμμα που δείχνει τη σχέση μεταξύ 22 στοιχείων και pH στα δείγματα της σκόνης σπιτιών για το 1ο στάδιο της διαδοχικής εκχύλισης – ανταλλάξιμη φάση (n=127).
wastes), and possibly of soil derived from schist, with very low concentrations in Pb, Cd, Ag and Zn.

8.4.2. CLUSTER AND FACTOR ANALYSES ON THE CARBONATE PHASE DATA OF HOUSE DUST

The retention of factors with eigenvalues >1 resulted in the selection of a six factor model for the carbonate phase analytical data. The variation accounted for by this six-factor varimax model is 74.87% of the total (Table 8.3, Fig. 8.3).

Factor 1 or the *"specifically adsorbed elements factor"* explains 29.52% of the total variance, and has strong positive loadings (>0.7) on Ba, Al, Fe, Ti, Mn, Mo and Zn, moderate loadings (>0.4-0.6) on Be, K and Li, and a weak to low negative loadings on Cu (-0.58) and Cd (-0.31), P (-0.28) and pH (-0.19). The dendrogram shows a cluster of elements consisting of Al-Ba, Mn, Fe, Ti, Mo and Zn. It is suggested, therefore, that the specifically adsorbed element fraction in house dust samples is more important than the carbonate part. These elements may occur on the surfaces of amorphous precipitates of Fe, Al or Mn oxides, alumino-silicates, silica, and micro-crystalline precipitates of oxides, but not phosphates because of the negative loading with phosphorus (-0.28); further they are adsorbed on dust particles with a comparatively low pH, and low Cu and Cd contents.

Factor 2 or *"specifically adsorbed contaminants factor"* explains 15.03% of the total variance, and has strong positive loadings (>0.7) on Pb, Cd and Zn, which are weakly associated with Mn (0.27); Cu and Be have low positive loadings of 0.25 and 0.23 respectively. It is also noted that P, K, Ag and Cr have low negative loadings (<-0.17 to –0.28). The dendrogram shows a cluster between Cd and Pb, which is connected, at a lower correlation level, to the suite of elements of the first factor or cluster. A possible interpretation is that these elements are associated with dust particles originating from metallurgical processing wastes, and mainly the flotation tailings.

Factor 3 or *"carbonates-pH factor"* explains 9.74% of the total variance, and has strong positive loadings (>0.6) on Ca and Sr, a moderate loading of 0.51 on pH, and a strong negative covariance with P (-0.65). Noteworthy, are the very low positive or negative loadings on Pb, Cu, Cd, Zn and Ag. The dendrogram shows a cluster with Ca-pH and Sr, which is linked at a lower level to elements of factors 1 and 2. It appears that calcium carbonates are not the dominant phase of the second extraction step, since only 9.74% of the variation is explained by the "carbonates-pH" factor. Calcium and Sr occur in dust particles with an alkaline pH, and are not related to P, as indicated by its strong negative loading, but neither to contaminant elements.

Factor 4 or *"pH-fertiliser factor"* explains 8.70% of the total variance, and has strong positive loadings (>0.6) on Li, Cr, pH and K, moderate loadings (>0.4-0.5) on V and Be, and a low positive loading of 0.2 on P. Noteworthy, are again the very low positive or negative loadings on Zn, Cu, Pb, Ag and Cd. The dendrogram shows a cluster with Li-V and K, which is linked at a lower correlation to Be and the elements of the first and second factors. This element association suggests the fourth factor to be related to dust particles with alkaline pH values, which are derived from garden soil rich in chemical fertilisers, and with insignificant amounts in contaminant elements.

Table 8.3. Varimax loadings for the six strongest factors of carbonate phase house dust geochemical data (n=127). Correlation between varimax scores and transformed data.
[For notation used refer to text in Chapter 7].
Table 8.3. Φορτία περιστροφής "varimax" για τους έξι ισχυρότερους παράγοντες της ανθρακικής φάσης των γεωχημικών δεδομένων της σκόνης σπιτιών (n=127). Συσχέτιση μεταξύ των φορτίων varimax και των μετασχηματισμένων δεδομένων. [Για τη σημειογραφία βλέπετε το κείμενο στο Κεφάλαιο 7].

Element	*V a r i m a x l o a d I n g s*					
	Factor 1	*Factor 2*	*Factor 3*	*Factor 4*	*Factor 5*	*Factor 6*
Ag-2	-0.116	-0.219	-0.053	-0.019	**0.920**	0.113
Al-2	**0.918**	0.009	0.028	0.027	0.074	0.139
Ba-2	**0.920**	0.080	0.054	0.144	-0.128	0.075
Be-2	0.525	0.233	0.157	0.400	-0.151	0.027
Ca-2	0.030	0.011	**0.891**	0.162	0.250	-0.083
Cd-2	-0.308	**0.860**	-0.008	-0.136	-0.106	-0.063
Co-2	0.137	0.090	0.056	0.163	0.396	**0.703**
Cr-2	-0.114	-0.174	-0.168	**0.669**	0.116	0.395
Cu-2	*-0.580*	0.252	0.042	0.057	-0.038	0.045
Fe-2	**0.876**	-0.030	0.148	0.044	-0.046	0.221
K-2	0.395	-0.240	-0.306	**0.615**	0.015	-0.051
La-2	0.226	-0.123	0.289	0.056	**0.857**	0.136
Li-2	0.375	0.098	0.167	**0.705**	0.064	0.078
Mn-2	**0.788**	0.267	0.123	0.227	-0.131	0.098
Mo-2	**0.638**	-0.038	0.184	0.137	0.324	0.079
Ni-2	0.019	-0.062	-0.160	-0.029	-0.026	**0.792**
P-2	-0.282	-0.275	***-0.653***	0.203	0.406	-0.078
Pb-2	0.096	**0.895**	0.010	-0.006	-0.159	0.004
Sr-2	0.274	-0.134	**0.666**	-0.025	0.103	-0.011
Ti-2	**0.832**	-0.019	0.145	0.106	0.338	-0.104
V-2	0.264	-0.002	0.129	0.498	0.053	0.541
Zn-2	**0.626**	**0.695**	-0.024	0.099	-0.119	-0.055
pH	-0.185	0.074	0.511	**0.618**	-0.054	-0.205
Eigenvalue	*6.79*	*3.46*	*2.24*	*2.00*	*1.60*	*1.13*
Variance explained by factor	*29.52%*	*15.03%*	*9.74%*	*8.70%*	*6.95%*	*4.93%*
Cumulative variance	*29.52%*	*44.55%*	*54.29%*	*62.99%*	*69.94%*	*74.87%*

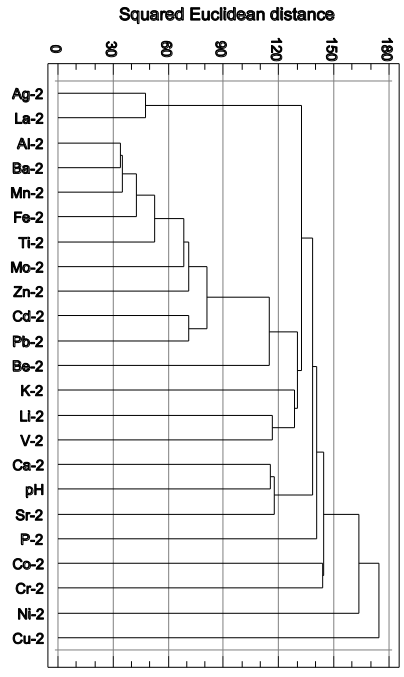

Fig. 8.3. Dendrogram showing the relationship of 22 elements and pH in samples of house dust for sequential extraction step 2 – carbonate phase (n=127).
Σχ. 8.3. Δενδρόγραμμα που δείχνει τη σχέση μεταξύ 22 στοιχείων και pH στα δείγματα της σκόνης σπιτιών για το 2ο στάδιο της διαδοχικής εκχύλισης – ανθρακική φάση (n=127).

Factor 5 or *"contaminated soil factor"* explains 6.95% of the total variance, and has strong positive loadings (>0.7) on Ag and La, moderate loadings (>0.4-0.6) on P and Co, and low loadings (>0.25-0.4) on Co, Ti and Ca. Noteworthy, are again the very low negative loadings on Cu, Cd, Zn and Pb. The dendrogram shows a cluster with Ag-La, which is correlated at a lower level with elements of factors 1, 2 and 4. This element association suggests an anthropogenic source, and since there is an indirect link to contaminant elements, it is interpreted that a small proportion of household dust particles was derived from contaminated residual or alluvial soil.

Factor 6 or *"Ni-Co factor"* explains 4.93% of the total variance, and has strong positive loadings (>0.7) on Ni and Co, and moderate loadings (>0.4-0.6) on V and Cr. . Noteworthy, are again the very low positive or negative loadings on Ag, Cu, Pb, Zn, P, Ca and Cd, and the low negative loading of –0.21 on pH. The dendrogram also shows that the weakest correlation is between Co-Cr and Ni. This element association could be explained by dust particles derived from either (a) weathered schist and prasinite or soil developed on these rocks, (b) pyritiferous wastes, and (c) slag, slag earth or sand-blast wastes, or (d) from all of them. Since, there is no correlation with contaminant elements, P and Ca, a possible interpretation is that a small proportion of indoor dust particles was derived from soil developed over schist, and these particular samples have comparatively low pH values.

8.4.3. Cluster and Factor Analyses on the Reducible Phase Data of House Dust

The retention of factors with eigenvalues >1 resulted in the selection of a six factor model for the reducible (Fe-Mn oxide) phase analytical data. The variation accounted for by this six-factor varimax model is 73.49% of the total (Table 8.4, Fig. 8.4).

Factor 1 or the *"Mn-Fe oxide factor"* explains 29.41% of the total variance, and has strong positive loadings (>0.7) on Cd, Pb, Zn and Mn, and moderate loadings (>0.4-0.6) on Co, Ba and Fe; these elements have a low negative covariance with Ag (-0.21). The dendrogram, for this particular element association shows two clusters of elements: (a) Cd-Pb, Zn and Mn, and (b) Ba-Fe. Manganese oxides appear to be more important than Fe-oxides in scavenging base metals, and with respect to dust particles, they seem to be independent of pH, *i.e.*, very low negative loading of –0.02.

Factor 2 or *"carbonates-pH factor"* explains 15.15% of the total variance, and has strong positive loadings (>0.7) on Ca, pH and Sr, and moderate loadings (>0.55-6) on Be and Ti. Noteworthy, are the low positive or negative loadings on Ag, Pb, Cd, Zn and Cu. The dendrogram shows a cluster among Ca-Sr and pH, and another with Be-Ti, which are not linked directly, but through Co. A possible interpretation is that a small proportion of the reducible phase elements of the second factor are associated with carbonate dust particles from either residual soil or smelter wastes, and that they are related to house dust samples with high alkaline pH values.

Factor 3 or *"Al-Fe oxides factor"* explains 9.6% of the total variance, and has strong positive loadings (>0.7) on K, Ba, Al, Li and Fe, and moderate loadings (>0.45-0.6) on Be, Ti and La; it has also low positive loadings on Zn, Sr, Mn and pH, and low negative loadings on Cd, Ca and Ag. The dendrogram shows Al linked to elements of the first and second clusters or factors. Aluminium and Fe oxides appear to be the principal scavengers of elements in this factor with minor adsorption on Mn oxides. Although house dust pH has comparatively a low positive loading, it plays a significant role on the reducible phase elements of factor 3.

Table 8.4. Varimax loadings for the six strongest factors of reducible phase house dust geochemical data (n=127). Correlation between varimax scores and transformed data.
[For notation used refer to text in Chapter 7].
Table 8.4. Φορτία περιστροφής "varimax" για τους έξι ισχυρότερους παράγοντες της αναγώγιμης φάσης των γεωχημικών δεδομένων της σκόνης σπιτιών (n=127). Συσχέτιση μεταξύ των φορτίων varimax και των μετασχηματισμένων δεδομένων. [Για τη σημειογραφία βλέπετε το κείμενο στο Κεφάλαιο 7].

Element	*Varimax loadings*					
	Factor 1	*Factor 2*	*Factor 3*	*Factor 4*	*Factor 5*	*Factor 6*
Ag-3	-0.208	0.217	-0.145	-0.129	**0.772**	0.017
Al-3	0.100	0.301	**0.768**	0.123	0.021	0.142
Ba-3	0.473	-0.159	**0.794**	-0.028	0.016	0.018
Be-3	0.401	0.598	0.517	0.104	-0.091	-0.011
Ca-3	0.067	**0.800**	-0.110	0.138	0.248	*-0.307*
Cd-3	**0.917**	0.117	-0.026	-0.021	-0.131	-0.052
Co-3	0.555	0.241	0.036	0.301	-0.127	0.498
Cr-3	-0.105	0.100	0.189	**0.810**	0.123	0.017
Cu-3	0.015	-0.193	0.162	0.236	-0.013	0.572
Fe-3	0.468	-0.161	**0.705**	0.069	0.193	0.272
K-3	0.093	0.115	**0.875**	0.086	-0.097	-0.140
La-3	0.130	0.229	0.462	-0.010	0.079	0.276
Li-3	-0.113	0.341	**0.763**	0.214	-0.077	-0.120
Mn-3	**0.854**	0.066	0.207	-0.084	0.054	0.233
Mo-3	-0.111	0.047	0.096	0.275	**0.838**	-0.060
Ni-3	0.106	-0.166	0.024	**0.766**	-0.145	0.179
P-3	-0.145	-0.001	0.056	0.226	0.022	***-0.791***
Pb-3	**0.912**	0.164	0.095	0.083	-0.153	0.028
Sr-3	0.102	**0.714**	0.289	-0.037	0.304	-0.110
Ti-3	0.192	0.580	0.481	-0.120	-0.171	0.174
V-3	0.050	0.226	0.061	0.521	0.134	-0.231
Zn-3	**0.904**	-0.030	0.347	-0.049	-0.112	0.083
pH	-0.022	**0.789**	0.169	0.047	-0.018	0.108
Eigenvalue	6.76	3.48	2.21	1.74	1.43	1.28
Variance explained by factor	*29.41%*	*15.15%*	*9.60%*	*7.55%*	*6.21%*	*5.57%*
Cumulative variance	*29.41%*	*44.56%*	*54.16%*	*61.71%*	*67.92%*	*73.49%*

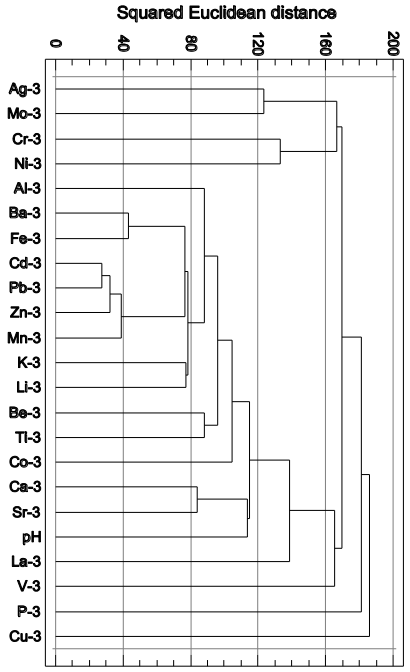

Fig. 8.4. Dendrogram showing the relationship of 22 elements and pH in samples of house dust for sequential extraction step 3 – reducible phase (n=127).
Σχ. 8.4. Δενδρόγραμμα που δείχνει τη σχέση μεταξύ 22 στοιχείων και pH στα δείγματα της σκόνης σπιτιών για το 3ο στάδιο της διαδοχικής εκχύλισης – αναγώγιμη φάση (n=127).

Factor 4 or *"Cr-Ni factor"* explains 7.55% of the total variance, and has strong positive loadings (>0.7) on Cr, Ni, a moderate loading of 0.52 on V, and weak loadings on Cu and P. The insignificant positive or negative loadings on Pb (0.08), Cd (-0.02), Zn (-0.05) and Ag (-0.13), imply that there is no dependency with the strong positively related reducible elements of factor 4, which are also independent of pH, because of the insignificant loading of 0.05. The dendrogram shows a cluster with Cr-Ni, which is linked at a lower level, and at some distance, with V. This is mafic element association, implying that it is related to dust particles derived mainly from weathered schist or soil developed on this rock type, but also any other overburden material rich in Cr, Ni and V.

Factor 5 or *"Mo-Ag factor"* explains 6.21% of the total variance, and has strong positive loadings (>0.7) on Mo and Ag. It is again interesting to note that all ore or contaminant elements have low negative loadings, indicating that they are not correlated with these elements. There is, however, a weak positive correlation with Sr (0.30) and Ca (0.25), implying that they are weakly related to calcium carbonate dust particles. Reducible phase Mo and Ag appear to be independent from pH, because of the insignificant negative loading of –0.02. The dendrogram shows a cluster with Ag-Mo, which is linked to the Cr-Ni cluster. Reducible phase elements of factor 5 are possibly derived from dust particles of overburden materials rich in Mo and Ag, with low Sr and Ca contents, and insignificant amounts of contaminant elements.

Factor 6 or *"Cu-Co factor"* explains 5.57% of the total variance, and has moderate positive loadings (>0.5-0.6) on Cu and Co, weak loadings (>0.2-0.3) on Fe and Mn, and a strong negative loading of –0.79 on P. Reducible phase factor 6 elements are independent of Zn, Pb, Ag and Cd, as indicated by their insignificant positive or negative loadings. The low negative loadings of –0.31 on Ca, and –0.11 on Sr, suggest that factor 6 elements have a negative covariation with calcium carbonates. The dendrogram relationships are complex, because the correlation between Cu and Co is not direct. There is, however, a weak positive relationship with Fe and Mn, suggesting that Cu and Co may be weakly adsorbed on their oxides. Reducible phase elements of factor 6 are possibly derived from dust particles of overburden materials rich in Cu and Co, which may be adsorbed on Fe and Mn oxides, with a minor dependency on pH (loading 0.11), but negatively correlated with Ca and Sr. Such relationships are found in house dust samples over soil developing on schist, and houses near to slag and pyritiferous wastes.

8.4.4. Cluster and Factor Analyses on the Oxidisable Phase Data of House Dust

The retention of factors with eigenvalues >1 resulted in the selection of a six factor model for the oxidisable (organic/sulphides) phase analytical data. The variation accounted for by this six-factor varimax model is 75.21% of the total (Table 8.5, Fig. 8.5).

Factor 1 or the *"Al-Fe-Mn oxides factor"* explains 25.59% of the total variance, and has strong positive (>0.6) loadings on Li, Al, Be and Co, moderate loadings (>0.45-0.6) on La, Fe, K, Mn and Ni, and weak loadings (>0.2-0.4) on Zn, Cu, Cd and Ti. It is noted that these elements have a negative covariation with Ca and P. It is apparent that the elements of these factor are mainly related to crystalline Al, Fe and Mn oxides, and not to the organic phase, since they are not correlated with P or V, elements regarded to be bound to organic matter. They may also be partly related to sulphides, because of the low positive loadings on Zn, Cu and Cd. The dendrogram, for this particular element association shows two principal clusters: (a) Be-Li, and (b) Al-K, which are linked to a complicated group of clusters, *i.e.*, Cd-Zn, Co-Fe, Mn, La, Cu, Pb, and Ba. A possible

interpretation is that this is the Al-Fe-Mn oxide fraction, and is related to ore or contaminant elements. The negative loadings on Ca and P suggest that factor 1 elements of the oxidisable phase are related to dust particles derived from mainly pyritiferous wastes, and other sulphide bearing wastes.

Factor 2 or *"organic factor"* explains 19.56% of the total variance, and has strong positive loadings (>0.7) on Cr, P, Mo and V, a moderate loading of 0.54 on Ti, and a weak loading of 0.4 on Ni; it has also a moderate negative loading of -0.46 on Mn, and weak negative loadings on Ca, pH, Cd, Zn and La. The dendrogram shows a cluster among Cr-Mo, P, Ti and Ni. A possible interpretation is that the elements of the second factor are associated with the operationally defined organic phase.

Factor 3 or *"carbonates-pH factor"* explains 11.65% of the total variance, and has strong positive loadings (>0.65) on Sr, Ca and pH. The dendrogram shows also a similar cluster. It is interesting to note that the ore or contaminant elements have very low or negative loadings, implying that there is low or no correlation with Sr, Ca and pH. An interpretation, which is supported by other observations, including chemical leaching in the laboratory, is that some resistant carbonate minerals, which survived the dissolution by the previous steps are digested in this phase. The source of these particular dust particles is probably unmineralised and uncontaminated material derived from marble or soil developed on it.

Factor 4 or *"pyrite factor"* explains 7.43% of the total variance, and has moderate positive loadings (>0.4-0.6) on Fe, Co, Mn and La. It has also a strong negative loading of –0.77 on Ag and a moderate negative loading of –0.05 on Ti. Other ore or contaminant elements have low negative or positive loadings. It has also a weak negative loading of –0.28 on pH. The dendrogram shows a similar cluster with Co-Fe linked to Mn and La. The low positive varimax loadings on Cu (0.24) and Ni (0.14) and the negative loading on pH, possibly indicate that this factor is related to dust particles derived from the pyritiferous wastes.

Factor 5 or *"sulphides factor"* explains 6.72% of the total variance, and has strong positive loadings (>0.7) on Cd, Pb and Zn, and moderate loadings (>0.4-0.6) on Cu and Mn. The dendrogram shows a cluster with Cd-Zn, which is linked to other clusters and to Pb at a lower level. This element association, together with the negative covariation with pH, suggests dust particles derived from base metal sulphides.

Factor 6 or *"baryte factor"* explains 4.76% of the total variance, and has a strong positive loading of 0.84 on Ba, moderate positive loadings (>0.4-0.6) on Cu and K, and low loadings on Sr, Ti, Mo and Zn ; it has also low negative loadings on Fe, Co, Ag, Mn and Pb. The dendrogram shows that Ba is related at a low level with elements of previous factors. It is noted that ore or contaminant elements have very low or negative loadings. Because of the strong positive varimax loading on Ba, this factor is interpreted as being due to either baryte dust particles, or particles rich in Ba.

Table 8.5. Varimax loadings for the six strongest factors of oxidisable phase house dust geochemical data (n=127). Correlation between varimax scores and transformed data.
[For notation used refer to text in Chapter 7].
Table 8.5. Φορτία περιστροφής "varimax" για τους έξι ισχυρότερους παράγοντες της οξειδώσιμης φάσης των γεωχημικών δεδομένων της σκόνης σπιτιών (n=127). Συσχέτιση μεταξύ των φορτίων varimax και των μετασχηματισμένων δεδομένων. [Για τη σημειογραφία βλέπετε το κείμενο στο Κεφάλαιο 7].

Element	*V a r i m a x l o a d I n g s*					
	Factor 1	*Factor 2*	*Factor 3*	*Factor 4*	*Factor 5*	*Factor 6*
Ag-4	0.020	-0.169	-0.177	***-0.772***	0.116	-0.171
Al-4	**0.756**	0.340	0.000	-0.058	0.090	0.155
Ba-4	0.110	0.112	0.218	0.011	-0.063	**0.841**
Be-4	**0.752**	-0.041	-0.033	-0.048	0.315	0.091
Ca-4	-0.262	-0.144	**0.826**	0.203	0.029	0.035
Cd-4	0.243	-0.260	0.084	0.133	**0.827**	-0.029
Co-4	**0.661**	-0.127	-0.181	0.469	0.266	-0.255
Cr-4	0.108	**0.867**	-0.160	0.015	-0.171	0.052
Cu-4	0.286	-0.094	-0.264	0.235	0.526	0.482
Fe-4	0.572	-0.103	-0.228	0.563	0.208	-0.287
K-4	0.554	0.276	0.255	-0.202	0.287	0.396
La-4	0.594	-0.336	0.319	0.379	0.088	-0.118
Li-4	**0.818**	-0.010	-0.051	-0.069	0.134	0.186
Mn-4	0.507	*-0.459*	-0.084	0.391	0.449	-0.146
Mo-4	0.067	**0.833**	-0.164	0.028	0.148	0.163
Ni-4	0.483	0.399	-0.389	0.139	-0.109	-0.052
P-4	-0.214	**0.839**	0.144	-0.057	-0.104	0.016
Pb-4	0.090	0.262	0.146	-0.158	**0.785**	-0.130
Sr-4	-0.012	0.128	**0.850**	0.143	0.136	0.257
Ti-4	0.224	0.537	-0.104	*-0.496*	-0.233	0.207
V-4	0.005	**0.815**	0.019	0.067	-0.048	-0.071
Zn-4	0.372	-0.257	-0.082	0.075	**0.720**	0.146
pH	0.220	-0.207	**0.663**	-0.281	-0.170	-0.048
Eigenvalue	*5.89*	*4.38*	*2.68*	*1.71*	*1.55*	*1.09*
Variance explained by factor	*25.59%*	*19.56%*	*11.65%*	*7.43%*	*6.72%*	*4.76%*
Cumulative variance	*25.59%*	*44.65%*	*56.30%*	*63.73%*	*70.45%*	*75.21%*

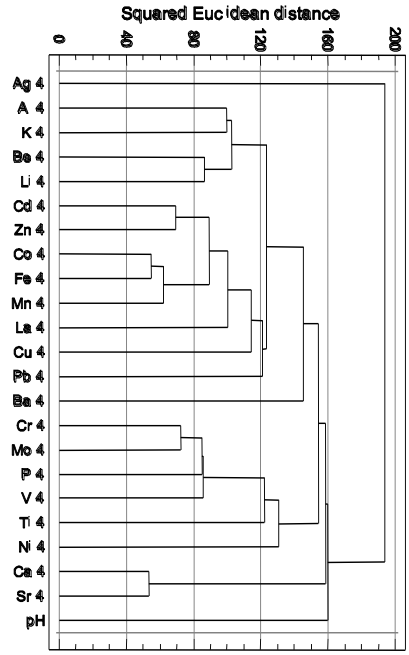

Fig. 8.5. Dendrogram showing the relationship of 22 elements and pH in samples of house dust for sequential extraction step 4 – oxidisable phase (n=127).
Σχ. 8.5. Δενδρόγραμμα που δείχνει τη σχέση μεταξύ 22 στοιχείων και pH στα δείγματα της σκόνης σπιτιών για το 4ο στάδιο της διαδοχικής εκχύλισης – οξειδώσιμη φάση (n=127).

8.4.5. CLUSTER AND FACTOR ANALYSES ON THE RESIDUAL PHASE DATA OF HOUSE DUST

The retention of factors with eigenvalues >1 resulted in the selection of a five factor model for the residual phase analytical data. The variation accounted for by this five-factor varimax model is 76.78% of the total (Table 8.6, Fig. 8.6).

Factor 1 or the *"flotation tailings factor"* explains 42.12% of the total variance, and has strong positive (>0.6) loadings on Pb, Ca, Ag, Cd and Zn, moderate loadings (>0.5-0.6) on Cu and P, and low positive loadings (>0.2-0.4) on La, Be, Fe, K, Sr, Mn, Li and Al. The dendrogram shows that this suite of elements occurs in two main clusters, *i.e.*, (a) Fe-Mn, and (b) Cd-Pb-Zn, Ag, Ca, which are linked at a lower level to Cu and P. This variable suite of elements, which in independent of pH (loading 0.01), suggests that it is related to dust particles from mainly flotation/beneficiation tailings.

Factor 2 or *"alumino-silicates factor"* explains 13.03% of the total variance, and has strong positive loadings (>0.7) on Al, K, Be, Li and V, and moderate loadings (>0.4-0.6) on La, pH and Sr. It has also weak positive loadings (>0.2-0.4) on Co, P, Pb, Fe, Zn, Ca, Cr, Ag and Mn. The dendrogram shows two main clusters between Al-Li and Be-K, which are joined at a lower level to V, Sr and La. A possible interpretation is this suite of elements is associated with the operationally defined alumino-silicate phase.

Factor 3 or *"Ni-Cr-Co factor"* explains 9.59% of the total variance, and has strong positive loadings (>0.65) on Ni, Cr and Co, and weak loadings (>0.17-0.35) on Mo, V, K, Cu and Fe. The dendrogram shows also a similar cluster. It is interesting to note that the ore or contaminant elements and pH (Ag, pH, Pb, Zn, Cd) have almost zero loadings (0.07 to –0.07), indicating that there is no correlation with factor 3 elements. The source of these particular dust particles is probably weathered schist or soil developed on it.

Factor 4 or *"baryte factor"* explains 6.68% of the total variance, and has strong positive loadings (>0.6) on Ba, Ti and Sr, a moderate loading of 0.45 on Mo, and a weak of 0.34 on V. The dendrogram shows a similar cluster with Ba-Ti, which is linked at lower level to Mo. It is suggested that this factor is related to baryte dust particles or particles rich in Ba.

Factor 5 or *"pyrite factor"* explains 5.36% of the total variance, and has strong positive loadings (>0.7) on Mn and Fe, moderate loadings (>0.4-0.6) on Co, Cu, Zn, P, Cd and Mo, and weak loadings (>0.2-0.3) on V, Pb, Li, La, and Sr. The dendrogram shows a cluster with Mn-Fe, which is linked to other clusters comprising Cd-Pb-Zn, already ascribed to the first factor. This association suggests that dust particles were derived from mainly pyritiferous tailings and other pyrite bearing overburden.

Table 8.6. Varimax loadings for the five strongest factors of residual phase house dust geochemical data (n=127). Correlation between varimax scores and transformed data.
[For notation used refer to text in Chapter 7].
Table 8.6. Φορτία περιστροφής "varimax" για τους πέντε ισχυρότερους παράγοντες της υπολειμματικής φάσης των γεωχημικών δεδομένων της σκόνης σπιτιών (n=127). Συσχέτιση μεταξύ των φορτίων varimax και των μετασχηματισμένων δεδομένων. [Για τη σημειογραφία βλέπετε το κείμενο στο Κεφάλαιο 7].

Element	*Varimax loadings*				
	Factor 1	*Factor 2*	*Factor 3*	*Factor 4*	*Factor 5*
Ag-5	**0.833**	0.231	0.073	0.179	0.119
Al-5	0.232	**0.879**	0.089	0.176	0.251
Ba-5	-0.019	0.002	0.062	**0.882**	-0.281
Be-5	0.368	**0.854**	0.066	0.186	0.118
Ca-5	**0.839**	0.239	0.006	0.007	-0.104
Cd-5	**0.817**	0.167	-0.065	0.038	0.409
Co-5	-0.009	0.360	**0.667**	-0.005	0.549
Cr-5	0.056	0.239	**0.905**	0.072	0.119
Cu-5	0.511	-0.037	0.169	0.090	0.542
Fe-5	0.364	0.270	0.168	0.040	**0.828**
K-5	0.319	**0.866**	0.218	0.136	-0.006
La-5	0.372	0.510	0.008	0.023	0.251
Li-5	0.242	**0.837**	0.161	0.159	0.286
Mn-5	0.244	0.204	0.036	-0.030	**0.899**
Mo-5	0.135	-0.051	0.330	0.451	0.393
Ni-5	-0.038	0.088	**0.947**	0.081	-0.044
P-5	0.498	0.291	-0.055	0.023	0.457
Pb-5	**0.840**	0.279	-0.020	0.010	0.310
Sr-5	0.275	0.431	-0.185	**0.619**	0.222
Ti-5	0.042	0.319	0.127	**0.758**	0.131
V-5	0.093	**0.644**	0.277	0.336	0.303
Zn-5	**0.754**	0.243	-0.057	0.096	0.486
pH	0.012	0.436	0.045	-0.041	-0.022
Eigenvalue	*9.69*	*3.00*	*2.21*	*1.54*	*1.23*
Variance explained by factor	*42.12%*	*13.03%*	*9.59%*	*6.68%*	*5.36%*
Cumulative variance	*42.12%*	*55.15%*	*64.74%*	*71.42%*	*76.78%*

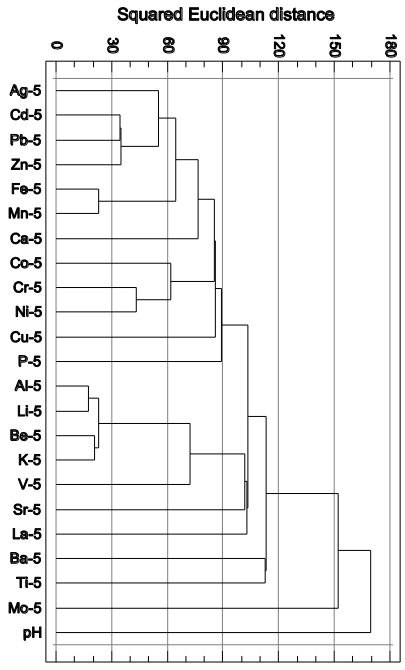

Fig. 8.6. Dendrogram showing the relationship of 22 elements and pH in samples of house dust for sequential extraction step 5 – residual phase (n=127).
Σχ. 8.6. Δενδρόγραμμα που δείχνει τη σχέση μεταξύ 22 στοιχείων και pH στα δείγματα της σκόνης σπιτιών για το 5ο στάδιο της διαδοχικής εκχύλισης – υπολειμματική φάση (n=127).

Summary of Factor Analysis Results on House Dust Samples

Table 8.7 summarises the results of factor analysis on the sequential extraction geochemical data of overburden samples. It is quite clear that the specificity and selectivity of the Tessier et al. (1979) method on these very complex geochemical house dust, as on overburden, samples was not satisfactory to the very demanding researcher. However, from the practical point of view it has provided useful data about the extractability, possible bioavailability and potential toxicity of the elements studied, as well as their classification into likely mineralogical phases.

Linear regression quantified correlation between pairs of elements, whereas cluster and factor analyses were able to identify inter-element correlation, and essentially revealed hidden relationships. Factor analysis distinguished subtle differences for each sequential extraction step, with respect to the different element associations, which are related to distinct mineral phases and source materials. Further, it quantified the variation explained by each. Although the unexplained variation of the five sequential extraction phases varies from 23.2 to 26.4%, it does not present problems in the interpretation of results, because the most significant phases have been identified.

Table 8.7. Interpretation table of factor analysis results on the sequential extraction data of house dust samples (n=127). The elements in parentheses have factor loadings >0.55.
Πίνακας 8.7. Ερμηνευτικός πίνακας των αποτελεσμάτων της παραγοντικής ανάλυσης των δεδομένων των διαδοχικών εκχυλίσεων των δειγμάτων σκόνης σπιτιών (n=127). Τα στοιχεία μέσα στις παρενθέσεις έχουν παραγοντικά φορτία >0.55.

Factor	*Exchangeable*		*Carbonate*		*Reducible*		*Oxidisable*		*Residual*	
	Form	*%*	*Form*	*%*	*Form*	*%*	*Form*	*%*	*Form*	*%*
1	Exchangeable (Mn,Cd,Zn)	30.6	Specifically adsorbed elements (Ba,Al,Fe,Ti, Mn,Mo,Zn)	29.5	Mn-Fe oxides (Cd,Pb,Zn,Mn, Co)	29.4	Al-Fe-Mn oxides (Li,Al,Be,Co,La, Fe,K)	25.6	Flotation tailings (Pb,Ca,Ag, Cd,Zn)	42.1
2	Carbonates (Ca,Sr)	13.5	Specifically adsorbed contaminants (Pb,Cd,Zn)	15.0	Carbonates-pH (Ca,pH,Sr,Be, Ti)	15.2	Organic (Cr,P,Mo,V)	19.6	Alumino-silicates (Al,K,Be,Li, V)	13.0
3	Be-Mo slag (Be,Mo,La)	11.6	Carbonates-pH (Ca,Sr)	9.7	Al-Fe oxides (K,Ba,Al,Li,Fe)	9.6	Carbonates-pH (Sr,Ca.pH)	11.7	Ni-Cr-Co (Ni,Cr,Co)	9.6
4	Fe-Al oxides (Fe,Al,Ti,Pb,Ba)	8.9	pH-fertiliser (Li,Cr,pH,K,)	8.7	Cr-Ni (Cr,Ni)	7.6	Pyrite (Fe only)	7.4	Baryte (Ba,Ti,Sr)	6.7
5	Schist (K,Cr,Li,Cu,P)	6.5	Contaminated soil (Ag,La)	7.0	Mo-Ag (Mo,Ag)	6.2	Sulphides (Cd,Pb,Zn)	6.7	Pyrite (Mn,Fe,Co, Cu)	5.4
6	Vanadium (V only)	5.3	Ni-Co (Ni,Co)	4.9	Cu-Co (Cu only)	5.6	Baryte (Ba only)	4.8	-	-
Total explained variation		76.4		74.8		73.6		75.8		76.8
Unexplained variation		23.6		25.2		26.4		24.2		23.2

8.5. DISCUSSION, CONCLUSIONS AND HEALTH RELATED RECOMMENDATIONS

Part of the discussion about the sequential extraction results on overburden samples in Chapter 7 applies also to house dust, and will not be repeated here. An important aspect, which will be discussed, however, is the relationship between house dust and their corresponding garden soil samples. Comparison between total element contents of the two sampling media has shown, that only the ore/smelter waste elements have a comparatively high proportion of their variability in house dust that could be explained by garden soil, *i.e.*, Ag (r^2=26.58%), As (r^2=36.57%), Cd (r^2=49.21%), Fe (r^2=40.41%), Mn (r^2=43.60%), Pb (r^2=49.02%) and Zn (r^2=60.56%). However, even these data indicate, that a

great part of their concentrations in house dust is not derived directly from exterior garden soil, but from other sources either internal or distant external.

Comparison between each of the sequential extraction phases of the two sampling media has shown the proportion of house dust variability that could be explained by a similar mode of occurrence of the elements as in garden soil, *i.e.*,

- exchangeable phase: all elements have r^2% values between 0.04 to 20.08%;
- carbonate phase: Al (r^2=45.56%), Ba (r^2=63.17%), **Cd** (r^2=30.96%), Fe (r^2=36.97%), Mn (r^2=55.95%), **Pb** (r^2=33.02%), Ti (r^2=53.40%) and **Zn** (r^2=49.21%);
- reducible phase: Ba (r^2=61.23%), **Cd** (r^2=50.21%), Fe (r^2=59.59%), Mn (r^2=29.70%), **Pb** (r^2=46.55%) and **Zn** (r^2=58.94%);
- oxidisable phase: **Cd** (r^2=40.82%), Mn (r^2=28.78%), **Pb** (r^2=26.08%), V (r^2=27.63%) and **Zn** (r^2=44.55%), and
- residual phase: Ag (r^2=26.35%), Ca (r^2=39.62%), **Cd** (r^2=33.15%), **Pb** (r^2=44.18%), and **Zn** (r^2=47.31%).

Apart from the exchangeable phase, where all elements have coefficients of determination (r^2%) of <20.08%, elements with comparatively high coefficients of determination, that are common to the other four sequential extraction steps, are Cd, Pb and Zn, the main contaminant elements. It can be concluded, therefore, that a large part of the base metal contaminated particles of garden soil occurring in house dust, retain their original form.

The sequential results on house dust samples have also given important information about the amount of the bioavailable fraction of the elements studied. It is here again stressed, the significance of the very low pH (1 to 3) of gastric fluids, which is due to the presence of *"concentrated"* hydrochloric acid, and the low pH of about 1 of a completely empty stomach. At such low pH values considerable amounts of the elements studied could be released, for even the oxidisable phase element concentrations could be leached out, and part of the residual phase contents. Consequently, it is not surprising that children, and adults alike, have high blood-Pb concentrations and urine-As excretions (Benetou-Marantidou et al., 1985; Nakos, 1985; Hatzakis et al., 1987; Maravelias et al., 1989; Eikmann et al., 1991; Makropoulos et al., 1991, 1992; Kafourou et al., 1997; see also Chapter 3 in this Volume).

In Chapter 11, the total direct ingestion of soil or dust was calculated, and is tabulated in Table 11.4. The amount varies from 69.36 to 272.27 mg soil/day depending on land use type. For the sake of this discussion, the average of 200 mg soil/day is taken, which is also the amount used in the environmental management scheme (refer to Volumes 4 & 5). Table 8.8 tabulates Pb, As and Cd concentrations in garden soil and house dust, the estimated amount in 200 mg of soil and house dust, and the level that could be made available for absorption into the human body, provided the assumed 200 mg of soil is totally digested by gastric fluids. The absorption factors were taken from Ferguson (1990). As is shown in Table 8.8 large amounts of Pb, Cd and As could be absorbed by the human body. For infants at 40% absorption, total Pb varies from 65 to 12,126 μg Pb/200 mg of soil or 39 to 1,489 μg Pb/200 mg of house dust. More realistic are the data provided by the sequential extraction steps, e.g., for step 1, 53 μg exchangeable Pb/200 mg of soil or 9 μg exchangeable Pb/200 mg of house dust, and for the extractable Pb (combined steps 1+2) 4,701 μg extractable Pb/200 mg of soil or 559 μg extractable Pb/200 mg of house dust, etc. However, for Pb

Table 8.8. Total and extractable Pb and Cd contents, and total As contents in garden soil and house dust samples, their levels in 200 mg of soil/house dust that could be ingested, and the amount that is available for absorption by the human body.
Πίνακας 8.8. Ολικές και εκχυλίσιμες συγκεντρώσεις Pb και Cd, και ολικές συγκεντρώσεις As στα δείγματα εδάφους και σκόνης σπιτιών, οι συγκεντρώσεις τους σε 200 mg εδάφους/σκόνης σπιτιών που μπορούν να εισέλθουν μέσω του στόματος και η αντίστοιχη διαθέσιμη συγκέντρωση αυτών για πρόσληψη από τον ανθρώπινο οργανισμό.

Total and sequential extraction phases	*mg Pb/kg*		*μg Pb/200 mg*		*Absorption μg Pb/200 mg*			
					40% infants		*10% adults*	
	Garden soil	*House dust*	*Garden soil*	*House dust*	*Garden soil*	*House dust*	*Garden soil*	*House dust*
Minimum total	810	488	162	98	65	39	16	10
Maximum total	151579	18617	30316	3723	12126	1489	3032	372
Step 1	662	108	132	22	53	9	13	2
Steps 1+2	58762	6988	11752	1398	4701	559	1175	140
Steps 1+2+3	88762	13018	17752	2604	7101	1041	1775	260
Steps 1+2+3+4	92112	14548	18422	2910	7369	1164	1842	291

Total only	*mg As/kg*		*μg As/200 mg*		*Absorption μg As/200 mg soil*			
					5% absorption		*25% absorption*	
	Garden soil	*House dust*	*Garden soil*	*House dust*	*Garden soil*	*House dust*	*Garden soil*	*House dust*
Minimum total	50	130	10	26	0.5	1.3	2.5	0.3
Maximum total	24000	3820	4800	764	240.0	38.2	1200.0	9.6

Total and sequential extraction phases	*mg Cd/kg*		*μg Cd/200 mg*		*Absorption μg Cd/200 mg*		
					6% (infants & adults)		
	Garden soil	*House dust*	*Garden soil*	*House dust*	*Garden soil*	*House dust*	*Note:*
Minimum total	2.0	1.0	0.40	0.20	0.02	0.01	
Maximum total	1189.0	136.1	237.80	27.22	14.27	1.63	Adults are considered to ingest less material than children, *i.e.*, 100 mg/day. In such a case, the levels quoted for adults should be halved.
Step 1	79.7	8.3	15.94	1.66	0.96	0.10	
Steps 1+2	300.7	43.5	60.14	8.70	3.61	0.52	
Steps 1+2+3	327.7	101.1	65.54	20.22	3.93	1.21	
Steps 1+2+3+4	828.7	110.5	165.74	22.10	9.94	1.33	

the absorption factor is influenced by diet and fasting; for Cd it depends on Ca^{2+} and Zn^{2+}, protein content and solubility of Cd compounds, and in the case of As, the absorption is high for anionic and soluble species, and low for insoluble species (Ferguson, 1990). Consequently, lower amounts enter the human body.

Parents in Lavrion must realise that they raise their children in a hazardous environment. Officers of the Municipality of Lavrion must inform them, therefore, about the dangers to their health through suitable education programmes. The guidelines given in the last page of the information leaflet, prepared by project scientists is a first step (refer to Volumes 4 and 5 of this report). The US EPA (1998) has published an excellent booklet entitled *"Lead in Your Home: A Parent's Reference Guide"*, which should be translated, and given to all parents in Lavrion. It is stressed, that by performing some simple, everyday tasks, parents can reduce their children's exposure to Pb, but also to other toxic elements, which are present at hazardous levels in the Lavrion surface environment. Apart from a clean home, which is the responsibility of the parents, the Municipality of Lavrion must encapsulate all contaminated land in such a way to be virtually impossible for children to reach the contaminants in overburden. This action will also reduce significantly the aerial transportation of contaminants from the major pollution sources.

Parents must provide their children with good nutrition. The US EPA (1998) recommends that the following guidelines must be followed every day:

- Children must eat at least three meals day, since the absorbed amounts of Pb and other toxic elements are greatly reduced, when children have food in their systems. This action does not allow the pH of gastric fluids to reach a value of 1, which is the pH of a completely empty stomach.
- Children must eat foods with high Fe and Ca, such as milk, cheese, fish, peanut butter, and raisins. When a child does not have enough Fe or Ca in his or her body, the body mistakes Pb (or the other toxic elements) for these nutrients. A diet lacking protein, vitamin C, and Zn may cause increased blood-Pb levels.
- Children should not be given fried and fatty foods, because they allow the body to absorb Pb, and the other toxic elements, faster.

Milk, as a source of calcium is, however, questioned by some researchers, for they state that it is associated with increased Pb levels (Trattler, 1986). Hence, medical practitioners should consider carefully the prescription of milk.

8.5.1. HEAVY METALS AND HEALTH

Ever since humans started to extract and use metals, they have destroyed the natural balance, by taking from the earth's crust toxic substances, which are normally present in only very small quantities, and concentrating and dispersing them throughout the environment. These toxic heavy metals (especially Pb, Cd, Hg and Al are now at concentrations above those that existed during our evolution. Hence, people living in heavy metal polluted areas have problems of excess, as is the case in the Lavrion urban environment. Even low environmental levels of these elements are detrimental to human health. Since, it is realised that resettlement of all the population of Lavrion and Lavreotiki peninsula (>10,000 people) or the immediate rehabilitation of only the Lavrion urban area is an impossibility, because of the large financial investment required (refer to Volumes 4 & 5 of this report), certain comparatively low cost actions must, however, be taken.

The officers of the Municipality of Lavreotiki should honour the actions voted during a two-day workshop ***entitled "Environmental Charter and Workshop for Sustainable Growth***" on the 6th and 7th May 1995, organised by the Municipality of Lavreotiki and the Ministry of Environment, Planning and Public Works organised (Lavrion, 1995a, 1995b). The "*Environmental Charter*" was a programme of DG-XI of the European Union. The methodology was based on the "Local Scenario Workshops", a Value II programme of DG-III of the European Union. The first two actions that were decided by the majority were (Lavrion, 1995b, p.44):

1. "Soil rehabilitation with priority for the pollution creating areas. Information for the inhabitants", and
2. "Organisation of environmental quality monitoring programs (soil, ground-water, seashores)."

Four years have passed and the Municipality officers have not yet fulfilled these actions. Since, the situation is indeed very grave, but not hopeless provided certain actions are taken in collaboration with the Lavrion Medical Centre physicians and assistance from the Ministries of Health and Education, Schools, Parents-Teachers Associations and local non-profit organisations. The first item is to encourage the encapsulation of all

major sources of contamination (metallurgical processing wastes), and the highly contaminated soil by the people themselves, by provision of State grants and technical assistance. Subsequently, a literature research study has shown that a programme of heavy metal detoxification of the local population, and children especially, must be carried out with possible financial help from the Ministry of Health. It is stressed that the Lavrion medical officers must carefully monitor the detoxification programme.

8.5.2. HEAVY METAL DETOXIFICATION

Excess lead (Pb), mercury (Hg) and cadmium (Cd) in the body can be detoxified with high doses of vitamin C (up to 3000 mg daily) plus supplementary essential trace elements (Mervyn, 1986). The subject of detoxification is, however, very complex so only a concise outline will be given below. The reader is referred to the many excellent health books that have been written in the last fifteen years (Mervyn, 1985, 1986, 1996; Trattler, 1986; Davies and Stewart, 1987). The detoxification guidelines have been abstracted from Trattler (1986, p.337-339).

Once heavy metal toxicity is diagnosed or suspect, the following regimen and nutritional supplements will help slowly reverse the process, ***provided the cause has been removed by rehabilitation.*** It is important that the elimination of toxic metals takes place in a controlled manner, since toxins will be released from body stores in muscles, organs, and bones, creating elevated blood levels for a short period. This can be extremely serious if the elimination process is too pronounced, causing exaggeration of the patient's symptoms, or even stimulating uncontrolled psychotic behaviour. Hence, the recommendation that this detoxification process must be carried out under strict medical supervision.

Trattler (1986) stresses that once heavy metal poisoning has reached the stage of severe confusion, seizures, and disorientation (all signs of encephalopathy), the condition is a medical emergency, and is best treated in hospital with chelating agents. Due to the chance of brain damage, these severe symptoms should not be treated at home.

8.5.2.1. Diet

Short periods of citrus fruit or apple mono diets are useful in the elimination process. Each case will determine the length of the initial mono diet. The more severe the toxicity, the shorter will be this first elimination. The usual period for the first mono diet is three to seven days. This fairly rapid detoxification is followed with a mostly raw food regimen with the exception of cooked beans as protein. A typical diet outline is as follows:

- On rising: Hot water and lemon juice;
- Breakfast: Fresh grapefruit or just-ripe green apples;
- Mid-morning: Carrot juice;
- Lunch: Raw green salad with cooked beans;
- Mid-afternoon: Carrot juice;
- Supper: As lunch, or cooked vegetarian meal with plenty of ultra-green vegetables, sea-weeds, and beans; and
- Evening: Raw apple or carrot juice.

One tablespoon of raw bran is to be taken with all meals. Spirulina should be added whenever possible. All water should be distilled. No alcohol or cigarettes are allowed, and all foods should be organically grown, if at all possible.

This diet may last one to two weeks and then alternated with the mono diets, previously mentioned. The second mono diet series may be much longer than the first, since it is now needed to extract deeper stores of heavy metals. Some cases may benefit from a prolonged citrus fruit juice fast at this time.

Another one to two weeks on the mostly raw foods diet with cooked beans is then followed by a further fast or mono diet. By this time all symptoms will have disappeared, and the patient must be educated on how to avoid all toxic heavy metals, and placed on a mostly vegetarian diet, allowing fish three times per week, if desired. No other meat is allowed for at least three months or longer. Periodic fast, mono diets, or mostly raw food diets should be undertaken for at least three days two times per month.

8.5.3. THERAPEUTIC DETOXIFYING SUPPLEMENTS

The following vitamin and mineral supplements may be taken under ***strict medical supervision***. The asterisks indicate the most frequently used therapeutic agents.

8.5.3.1. Vitamins

- Vitamin A: 25,000 IU two times per day for 1 month, then one time per day. Use any dose of vitamin A over 50,000 IU per day with medical supervision only.
- Vitamin C plus bioflavonoids: 1000 mg six times per day or more in acute toxicity, to bowel tolerance. High dose of vitamin C plus calcium. Vitamin C is a detoxifier and chelator (binding agent) of toxic metals. Given intravenously in high dose (30 g) for acute toxicity.*
- Vitamin D: 400 IU two times per day.
- Vitamin E: 400 IU two to three times per day.
- Vitamin B complex: 50 mg two times per day.*
- Vitamin B6: 50 to 100 mg per day. This helps protect against kidney stone formation on a high vitamin C supplement regimen.*

8.5.3.2. Minerals

- Calcium orotate, calcium lactate, or bone meal (600 to 1500 mg per day): two tablets three to four times per day. Calcium decreases gastrointestinal absorption of some heavy metals and aids in their elimination. Milk as a calcium source is associated with increased lead levels and is not advised.* [Milk is a dubious food nowadays, although it is recommended by US EPA (1998), the medical practitioners must discuss carefully its consumption].
- Zinc: 15 to 30 mg two to three times per day.*
- Magnesium orotate: 300 mg.*
- Potassium iodide: 1000 mcg per day for one to two months.*
- Selenium*

8.5.3.3. Others

- Bran: One tablespoon three times per day.*
- Citric acid*
- Chlorophyll as supplement and in deep green vegetables.*
- Distilled water*
- Garlic*
- Kelp: two tablets three times per day.*
- Lecithin: four 1200 mg capsules three times per day, or one to two tablespoons of granules.
- Pectin: Found in just-ripe apples and white inner lining of citrus peels. It absorbs heavy metals and prevents absorption from gastrointestinal tract. It is chelating (or binding) agent.*
- Sodium alginate: 250 mg four to eight times per day; helps chelate and eliminate toxic metals. Algin is found in sea vegetables such as kelp.*
- Sulfhydryl amino acids (L-lysine, L-cysteine, dimethionine): As found in legumes and as supplement in many detoxification tablets.*

Chapter 9

DISTRIBUTION OF ELEMENTS IN DIFFERENT GRAIN-SIZE FRACTIONS OF THE METALLURGICAL WASTES AND RESIDUAL SOIL

Alecos Demetriades and Katerina Vergou-Vichou
Institute of Geology and Mineral Exploration, 70 Messoghion Street, Gr-115 27, Athens, Greece

9.1. INTRODUCTION

Metals in soil from both natural and anthropogenic sources may be concentrated in different phases with contrasting grain-size distributions. Metal concentrations generally increase in the finer fractions of soil. Silt (0.0039-0.0625 mm) and clay (<0.0039 mm) fractions normally comprise the major carriers of both natural and anthropogenic metals, since these fractions contain a high proportion of organic matter, precipitates and clays, whereas coarser fragments contain a large amount of detrital minerals, especially quartz.

As is pointed out by Ferguson *et al.* (1998) the suspended particle pathway is concerned with pollutant release from overburden materials and their transport by wind. Influencing factors include

- wind velocity,
- soil structure and grain-size,
- moisture content, and
- vegetation cover.

Grain-size distribution of surficial materials available to air transfer is important, because only fine dust (<10 μm or <0.01 mm) can penetrate deep into the lung. Very small, gaseous like particles, <0.01 μm (<0.00001 mm), may penetrate even deeper, but many will also be removed from the lungs by exhalation (Ferguson, 1990). Particles in the grain-size range 0.1-2 μm (0.0001-0.002 mm) can move deep into the pulmonary and alveolar system, and eventually some will be absorbed into the blood stream. In general, larger particles, >2 μm (>0.002 mm), are trapped in the mucus of the upper respiratory system, and removed by ciliary activity either into the mouth or via the glottis into the stomach (Ferguson, 1990). Finally, larger silt- and clay-size particles may be ingested and digested in the stomach, thus releasing their toxic element contents for absorption into the walls of the gastrointestinal tract, and into the blood stream.

A large part of the Lavrion urban area overburden is not covered by vegetation, housing, etc, and is, therefore, exposed to deflation. The strong winds, blowing almost throughout the year, transport large quantities of fine-grained particulates. Since, two of the exposure routes are inhalation and ingestion of fine-grained dust particles, it is important to know something about the levels of contaminant elements in the finer fractions of overburden materials. Consequently, the objectives of this work were to study:

- the grain-size distribution in samples of metallurgical wastes and residual soil, and especially the proportion in the finer, silt-size, particles, and
- the levels of contaminant elements in the different grain-size fractions.

Representative samples of earthy material within slag (*slag earth*, n=4), flotation residues (n=3), pyritiferous sand (n=3) and residual soil (n=8) were collected (Map 2.11 in Volume 2). It is stressed that this study is by no means exhaustive, but gives, however, an indication of the grain-size distribution in the different overburden materials, and the levels of contaminant elements in each fraction. Sufficient information to show the hazards of airborne heavy metal particulates. House dust may be considered, to a large extent, as the fine-grained portion of overburden materials transported by wind. It has, already, been shown that toxic element concentrations in house dust are very high (Chapter 8). Suggesting, therefore, that metal concentrations tend to increase in the finer fractions of particulate materials.

Sample collection, preparation and analysis have already been discussed in Chapters 2A and 2B. Samples were sieved to six different grain-sizes according to the Wentford classification of clastic particles (Lahee, 1959), *i.e.*,

- Very coarse sand grain <2.000 +1.000 mm
- Coarse sand grain <1.000 +0.500 mm
- Medium sand grain <0.500 +0.250 mm
- Fine sand grain <0.250 +0.125 mm
- Very fine sand grain <0.125 +0.063 mm
- Silt particle <0.063.

The elements determined by ICP-AES, following a hot aqua regia extraction were: Ag, Al, As, B, Ba, Be, Bi, Ca, Cd, Ce, Co, Cr, Cu, Fe, Ga, Ge, Hg, In, K, La, Li, Mg, Mn, Mo, Na, Nb, Ni, P, Pb, Rb, S, Sb, Sc, Se, Sn, Sr, Ta, Te, Th, Ti, U, V, W, Y, Zn, and Zr. It is noted that the aqua regia leach is partial for Mn, Fe, Sr, Ca, P, La, Cr, Mg, Ba, Ti, B, W and limited for Na, K and Al (refer to Chapter 2B, Section 2B.2.7.1 p.42). For this study only the contaminant elements are going to be discussed, *i.e.*, As, Cd, Hg, Sb and Zn. Lead has already been discussed in Chapter 3 (Section 3.4, p.68).

9.2. DATA PROCESSING AND PRESENTATION

Particle-size distribution and the concentrations of elements in the different fractions of samples of metallurgical processing wastes and residual soil are presented as coloured six-bar plots for each of the 18 samples at their respective sampling sites on maps with the three major categories of metallurgical processing wastes (Maps 9.1, 9.3, 9.9, 9.14, 9.24 & 9.30 in Volume 2 of this report) . This method shows pictorially the actual levels of

(a) the percentage proportion of the grain-size distribution, and
(b) element concentrations in each of the six grain-size fractions for every sample, and the spatial variability; it is noted that the coloured bars in both cases are proportional across variables.

Hence, within and between samples comparisons can be made with ease, and related to the metallurgical processing wastes and contaminated residual soil. The total dry sample weight to facilitate estimation of the weight of each fraction for every sample is given on Map 9.1. On each map are also presented:

- a multiple box-and-whisker plot, depicting either the grain-size distribution of all samples, or their element concentrations in each fraction, and
- a table of statistical parameters of each of the six grain-size fractions for samples of slag earth material, flotation residues, pyritiferous sand and residual soil.

Hence, the reader has all the necessary information to study in detail the variation of element concentrations of each of the six grain-size fractions without referring to the following description and discussion of results.

9.3. DESCRIPTION AND DISCUSSION OF RESULTS

In the following description and discussion, the results of toxic element only will be briefly discussed, *e.g.*, As, Cd, Hg, Pb, Sb and Zn, since these present the greatest potential health hazards.

9.3.1. PARTICLE-SIZE DISTRIBUTION (Map 9.1)

Generally, the greatest weight percent proportion of each sample is in the >2 mm fraction (granules and pebbles). The exception being two samples of pyritiferous sand from Komobil-Kiprianos, which have the greatest weight percent proportion in the <0.25 +0.125 mm fraction (fine sand). As expected, the very fine sand (<0.125 +0.063 mm) and silt (<0.063 mm) fractions, make up the smallest percentage proportion of each sample.

9.3.2. DISTRIBUTION OF ARSENIC (As) IN DIFFERENT GRAIN-SIZE FRACTIONS (Map 9.3)

The finer grain-size fractions of all sample types have the greatest As concentrations, *i.e.*, the silt (<0.063 mm) and fine-sand (<0.125 +0.063 mm) fractions with As levels up to 26,358 and 25,097 ppm respectively. Lower As levels are found in the coarser grain-size fractions (>0.25 mm).

Arsenic levels in the <0.063 mm, silt-size, fraction of the different sample types is as follows:

- slag earth 1,198-26,358 ppm As (mean=10,705 ppm As)
- flotation residues 7,067-15,333 ppm As (mean=10,490 ppm As)
- pyritiferous sand 6,601-21,213 ppm As (mean=14,088 ppm As)
- residual soil 456- 2,865 ppm As (mean= 1,313 ppm As)

Although, residual soil has the lowest As concentrations in the silt-size fraction, the levels are still very high. The flotation residues have also very high As contents in their silt-size fraction.

9.3.3. DISTRIBUTION OF CADMIUM (Cd) IN DIFFERENT GRAIN-SIZE FRACTIONS (Map 9.9)

The finer grain-size fractions of all sample types have the greatest Cd concentrations, *i.e.*, the silt (<0.063 mm) and fine-sand (<0.125 +0.063 mm) fractions with Cd levels up to 309 and 283 ppm respectively; the coarse sand fraction (<1 +0.5 mm) although it has a greater range of values (up to 327 ppm Cd), it has a lower median. Lower Cd levels are found in the coarser grain-size fractions (>0.25 mm).

Cadmium levels in the <0.063 mm, silt-size, fraction of the different sample types is as follows:

- slag earth 66-309 ppm Cd (mean=181 ppm Cd)
- flotation residues 170-212 ppm Cd (mean=193 ppm Cd)
- pyritiferous sand 27-170 ppm Cd (mean= 82 ppm Cd)
- residual soil 5-58 ppm Cd (mean= 38 ppm Cd)

Although, residual soil has the lowest Cd concentrations in the silt-size fraction, the levels are still high. The flotation residues have also high Cd contents in their silt-size fraction.

9.3.4. DISTRIBUTION OF MERCURY (Hg) IN DIFFERENT GRAIN-SIZE FRACTIONS (Map 9.14)

The finer grain-size fractions of almost all sample types have the greatest Hg concentrations, *i.e.*, the silt (<0.063 mm) fraction with Hg levels up to 8 ppm. The three samples from the flotation residues and one from the pyritiferous sand have also high Hg contents in the coarse-grained fraction, *i.e.*, very coarse sand (<2 +1 mm). Comparatively low Hg levels are found in the fine sand (0.25 +0.125 mm) and coarse sand (<1 +0.5 mm) with values up to 3.7 and 4.3 respectively.

Mercury levels in the <0.063 mm, silt-size, fraction of the different sample types is as follows:

- slag earth 2.25-8.00 ppm Hg (mean= 4.12 ppm Hg)
- flotation residues 5.11-6.75 ppm Hg (mean= 6.08 ppm Hg)
- pyritiferous sand <1.00-2.95 ppm Hg (mean= 1.32 ppm Hg)
- residual soil <1.00 ppm Hg (mean=<1.00 ppm Hg)

Residual soil has values below the detection limit of the analytical method. The flotation residues have very high Hg contents in their silt-size fraction.

9.3.5. DISTRIBUTION OF LEAD (Pb) IN DIFFERENT GRAIN-SIZE FRACTIONS (see Chapter 3, p.68)

9.3.6. DISTRIBUTION OF ANTIMONY (Sb) IN DIFFERENT GRAIN-SIZE FRACTIONS (Map 9.24)

The finer grain-size fractions of all sample types have the greatest Sb concentrations, *i.e.*, the silt (<0.063 mm) and fine-sand (<0.125 +0.063 mm) fractions with Sb levels up to 816 and 577 ppm respectively. Similar to As, lower Sb levels are found in the coarser grain-size fractions (>0.25 mm).

Antimony levels in the <0.063 mm, silt-size, fraction of the different sample types is as follows:

- slag earth 75-630 ppm Sb (mean=376 ppm Sb)
- flotation residues 525-816 ppm Sb (mean=672 ppm Sb)
- pyritiferous sand 101-585 ppm Sb (mean=266 ppm Sb)
- residual soil 12-109 ppm Sb (mean= 42 ppm Sb)

Although, residual soil has the lowest Sb concentrations in the silt-size fraction, the levels are still high. The flotation residues have the highest Sb contents in their silt-size fraction.

9.3.7. DISTRIBUTION OF ZINC (Zn) IN DIFFERENT GRAIN-SIZE FRACTIONS (Map 9.30)

The finer grain-size fractions of all sample types have the greatest Zn concentrations, *i.e.*, the silt (<0.063 mm) and fine-sand (<0.125 +0.063 mm) fractions with Zn levels up to 82,000 and 70,000 ppm respectively. Lower Zn levels are found in the coarsest grain-size fraction, the very coarse sand (<2 +1 mm) with values up to 51,000 ppm Zn.

Zinc levels in the <0.063 mm, silt-size, fraction of the different sample types is as follows:

- slag earth 8,477-82,000 ppm Zn (mean=37,419 ppm Zn)
- flotation residues 30,000-38,800 ppm Zn (mean=33,467 ppm Zn)
- pyritiferous sand 10,208-29,600 ppm Zn (mean=17,961 ppm Zn)
- residual soil 537-10,576 ppm Zn (mean= 4,423 ppm Zn)

Although, residual soil has the lowest Zn concentrations in the silt-size fraction, the levels are still very high. Slag earth has the greatest range of values, and flotation residues have consistently very high Zn contents in their silt-size fraction.

9.4. CONCLUSIONS

The very fine-grain sand (<0.125 +0.063 mm) and silt size (<0.063 mm) fractions make up to 35% of the total sample weight. However, the strong winds blowing throughout the year, in a comparatively dry environment like Lavrion, can move even the fine and medium sand-size grains. In these cases, a large part of uncovered overburden is, therefore, available to deflation, and also to inhalation and ingestion by the local population, and children especially.

The highest levels of toxic elements (As, Cd, Hg, Pb, Sb, Zn) are found, as expected, in the finest silt-size particles of all sample types. High element contents also occur in the fine and medium sand-size fractions. Consequently, the greatest proportion of toxic element concentrations is in the finest grain-size fractions of metallurgical processing wastes and residual soil.

Blank back page
Λευκή οπίσθια σελίδα

Chapter 10

GEOCHEMISTRY OF GROUND WATER: A PRELIMINARY ASSESSMENT

Alecos Demetriades and Katerina Vergou-Vichou
Institute of Geology and Mineral Exploration, 70 Messoghion Street, Gr-115 27, Athens, Greece

10.1. INTRODUCTION

Clean ground water is an important natural resource, which must be safeguarded, for it may be required by future generations. Human activities, however, due to lack of understanding of the natural hydrological cycle, have seriously affected both the quantity and quality of the available ground water resources. It is emphasised that ground water pollution lasts far longer than surface water pollution, because the former is replenished slowly by water moving through the pores and fractures in soil and rock. Once ground water is polluted, it is normally difficult and impractical to reclaim it. Hence, the slogan *"prevention is better than cure"* applies more to ground water than any other natural resource. The effects of ground water pollution are threefold

- damage to our health,
- damage to agricultural produce, and
- new clean water supplies are difficult and costly to find.

Ground water chemistry varies depending on the soil and rock types it passes through. During its passage through the soil, loose overburden materials and rock formations, the water dissolves and deposits various substances, while other solutes are being transformed or degraded. Most of these physicochemical changes of ground water tend to be slow but long lasting. In Lavrion the dominant rock types are marble and schist. Marble is the normal aquifer, and since it is the predominant rock type the water is hard, and contains high levels of calcium, magnesium, bicarbonate and other constituents (Dounas 1967, 1973; Kounis, 1981). Hard water reacts with soap to form insoluble compounds. In layman terms, soap is wasted since it will not cleanse or lather until the offending ions are precipitated. Heating hard water results in precipitation of a coating of calcium and magnesium carbonates, calcium sulphate, and other dissolved compounds in kettles, pipe systems, boilers, *etc.*

The widespread mineralisation in the Lavreotiki peninsula imparts to the ground water other chemical properties, such as high levels of calcium fluoride (CaF_2) (Papadellis, 1980, quotes a mean value of 2.7 ppm for fluoride). Hard ground water with fluoride is not harmful, and in fact may be beneficial to health, and according to the elderly inhabitants it had a pleasant taste. One beneficial aspect is their strong teeth, but at the expense of yellow-brown staining in the enamel of teeth. However, at toxic levels symptoms of fluorosis appear (Papadellis, 1980).

Ground water resources in Lavrion were used until 1984 for the potable water supply of the town. Since, there is no central sewage system for household wastes, cesspits are used. Residential wastes from cesspits were also thrown into unused mine shafts, resulting in the bacterial pollution of the ground water (*e.g.*, at Stefani). Because of these problems, and the infiltration of seawater due to over pumping, Lavrion was

linked to the city of Athens water supply network on the 30th April 1984 (K. Pogkas, person. commun., 1999). Nowadays ground water is only used for agricultural purposes.

Since the metallurgical wastes and contaminated soil present a potential hazard to ground water, it was considered significant to make a preliminary assessment. For this purpose, thirteen wells and two boreholes were sampled, and three replicate ground water samples were collected for the purpose of evaluating sample variability (refer to Chapter 2A, Section 2A.2.6. & Map 2.2 in Volume 2).

10.1. LOCATION OF WELLS AND BOREHOLES

The wells and boreholes sampled cover almost the whole Lavrion urban area (Map 2.12). Overall depth to ground water varied from 3.6 to 12.5 m, with one borehole reaching a depth of 60 m. Essentially the wells and boreholes are shallow. This means they are very vulnerable to anthropogenic influences.

From the available information (Dounas, 1967, 1971), and our own field observations, the ground water reservoir is mainly karstic marble, which is the most dominant rock type of the area. It was, therefore, expected that the ground water will have a high total ion content; the dominant ions to be Ca^{2+}, Mg^{2+}, and HCO_3^-; pH to be between 7.0 and 8.2, and to have a low SiO_2 content (White *et al.*, 1963).

10.2. GEOCHEMISTRY OF GROUND WATER

Since ground water is a dynamic system, its geochemistry varies with time. In fact, chemical analyses of natural water are not as accurate as one would like, because of various sources of error. A major source of error lies in the sampling method. As with other types of surveys, results obtained are only good to the extent that the samples analysed are representative of the water mass being studied. Often the ground water mass is not homogeneous, and normally its composition changes fairly rapidly. Water samples are analysed in a laboratory long after collection and storage conditions before analysis may not be suitable. The longer the period of time between collection and analysis, the more likely it is that unreliable results will be obtained. Analytical errors, under optimum conditions, will be generally small, but large errors are always possible. The overall composition of a given water sample will affect the level of analytical error. The accuracy of an analytical value for a given constituent will in general depend on its abundance, with larger errors possible for trace constituents.

Taking into consideration the aforesaid drawbacks of ground water sampling and analysis, previous results are tabulated in Table 10.1 for the sake of completeness of this report (Dounas, 1967, 1971; Kounis, 1981), but will not be discussed further, for they do not display the physicochemical properties of present day ground water resources in Lavrion. It is also stressed that the results of this study are preliminary, and the aim is to assess the possible toxic element contamination of ground water, and to emphasise that the geochemistry of ground water must be monitored continuously.

In Tables 10.2a, b are tabulated the measured physicochemical variables of the fifteen ground water samples collected from thirteen wells and two boreholes in the Lavrion urban area (Map 2.12). Maps 10.1 to 10.4 show the geographical distribution of the geochemistry of ground water samples, *i.e.*,

Table 10.1. Ground water analytical data from different sources (values in mg/l or ppm).
Πίνακας 10.1. Αναλύσεις υπόγειου νερού από διαφορετικές πηγές (τιμές σε mg/l ή ppm).

Determinant		*Neraki (Noria)*		*EVO*		
		Dounas (1967)	*Dounas (1971)*	*Kounis (1981)*	*NTUA (1994)**	
pH		7.45	7.70	7.900	7.00-	7.98
Calcium	(Ca)	148.80	147.89	166.730	57.00-	180.00
Magnesium	(Mg)	79.91	81.59	86.620	16.70-	100.00
Chloride	(Cl)	1063.71	1034.28	1099.290		-
Sodium	(Na)		486.45	625.860		-
Potassium	(K)	(Na+K) 601.22	8.60	35.55		
Sulphate	(SO_4)	206.30	53.79	297.590	20.00-	640.00
Nitrate	(NO_3)	18.92	3.72	66.460		-
Silica	(SiO_2)	-	-	12.500		-
Aluminium	(Al)	-	-	0.016		-
Arsenic	(As)	-	-	-		<2.00
Barium	(Ba)	-	-	0.069		-
Cadmium	(Cd)	-	-	0.016		<0.05
Cobalt	(Co)	-	-	0.019		-
Chromium	(Cr)	-	-	0.002		-
Copper	(Cu)	-	-	0.060		<0.10
Iron	(Fe)	-	-	0.060		-
Lithium	(Li)	-	-	0.011		-
Manganese	(Mn)	-	-	0.005		-
Molybdenum	(Mo)	-	-	0.004		-
Nickel	(Ni)	-	-	0.019		-
Lead	(Pb)	-	-	0.094		<0.50
Antimony	(Sb)	-	-	-		<1.00
Tin	(Sn)	-	-	0.023		-
Strontium	(Sr)	-	-	1.100		-
Zinc	(Zn)	-	-	1.048	0.07-	3.70

* Note: Range of measurements at 7 locations.

- Map 10.1: distribution of cations Pb^{2+}, Zn^{2+}, Cd^{2+}, Cu^{2+};
- Map 10.2: distribution of cations Fe^{3+}, Mn^{2+}, Cr^{3+}, Ni^{+};
- Map 10.3: distribution of cations Ca^{2+}, Mg^{2+}, Na^{+}, K^{+}, NH_4^{+}
- Map 10.4: distribution of anions and radicals: $HClO_3^{-}$, Cl^{-}, SO_4^{2-}, NO_3^{-}, NO_2^{-}.

Each variable is displayed with a different colour bar, ***proportional to its own concentration range***. All analytical determinands of each water sample are presented in Figs. 5.1 to 5.15 in Appendix 5 of Volume 1B of this report.

Electrical conductivity varies from 1990 to 5820 μS/cm with a mean of 3138 μS/cm. Elevated conductivity values show that ground water has a large amount of dissolved electrolytes, which is a characteristic of carbonate environments and the measured pH range.

Calcium (41.7-298.2 ppm; mean 141.8 ppm) and magnesium (37.4-176.9 ppm; mean 78.5 ppm) exceed in most cases their respective maximum admissible limits of 100 and 50 ppm. The temporary, permanent and total hardness are, consequently, high. It is pointed out that the hardness values presented in Table 10.2a have no great geochemical significance. They are, however, useful as indicators of the way a given water will behave when used for domestic purposes.

Table 10.2a. Statistical parameters of physicochemical variables of ground water in the Lavrion urban area (n=15). Parameters exceeding maximum admissible limits are highlighted.
Πίνακας 10.2α. Στατιστικές παράμετροι των φυσικοχημικών μεταβλητών του υπόγειου νερού στην αστική περιοχή του Λαυρίου (n=15). Οι παράμετροι που υπερβαίνουν τα ανώτατα αποδεκτά όρια έχουν τονιστεί.

Statistical parameters	*Temp.*	*pH*	*Cond.*	*Ca^{2+}*	***Mg^{2+}***	***Na^{+}***	***K^{+}***	***Cl^{+}***	*HCO^{3-}*	*Hardness*		
	°C		*μS/cm*	*ppm*	*ppm*	*ppm*	*ppm*	*ppm*	*ppm*	*Temporary*	*Permanent*	*Total*
Detection limit	-	-	-	0.1	0.1	0.1	0.1	0.2	0.1	-	-	-
Max. admissible limit	*-*	*-*	*-*	*100*	*50.0*	*150.0*	*12.0*	*200.0*	*-*	*-*	*-*	*-*
Minimum	23.60	6.96	1990.0	41.7	37.4	110.0	6.0	131.2	286.7	23.5	0.5	31.0
Maximum	24.10	7.96	5820.0	**298.2**	**176.9**	**1300.0**	**44.0**	**1851.0**	542.9	44.5	121.2	147.2
Mean	23.78	7.32	3138.0	**141.8**	**78.5**	**444.0**	**17.5**	**704.9**	411.4	33.3	34.4	67.7
Median	23.80	7.24	2530.0	**127.5**	**73.9**	**340.0**	11.0	**453.9**	439.2	32.6	23.9	55.6
First quartile	23.70	7.18	2146.5	89.0	49.7	**245.0**	8.3	**397.2**	330.0	27.1	18.6	49.9
Third quartile	23.88	7.42	3530.0	**186.2**	**102.3**	**587.5**	**29.0**	**953.9**	462.7	37.8	40.1	83.6
Standard error of mean	0.04	0.07	337.7	18.8	9.7	77.9	3.3	128.2	22.1	1.8	8.0	7.9
95% conf. int. of mean	0.08	0.15	724.3	40.3	20.8	167.0	7.1	275.1	47.4	3.9	17.1	16.9
99% conf. int. of mean	0.11	0.22	1012.0	56.3	29.1	233.4	9.9	384.3	66.2	5.4	23.9	23.6
Average deviation	0.11	0.21	1014.9	56.0	28.2	224.0	11.0	391.0	71.0	5.7	22.4	23.1
Standard deviation	0.15	0.28	1307.8	72.7	37.6	301.6	12.8	496.7	85.6	7.0	30.9	30.5
Coef. of variation (%)	0.6	3.8	41.7	51.3	47.9	67.9	73.0	70.5	20.8	20.9	89.7	45.1

Note: Values in ppm or mg/l or μg/dl; or ppb or μg/l

Table 10.2b. Statistical parameters of physicochemical variables of ground water in the Lavrion urban area (n=15). Parameters exceeding maximum admissible limits are highlighted.
Πίνακας 10.2β. Στατιστικές παράμετροι των φυσικοχημικών μεταβλητών του υπόγειου νερού στην αστική περιοχή του Λαυρίου (n=15). Οι παράμετροι που υπερβαίνουν τα ανώτατα αποδεκτά όρια έχουν τονιστεί.

Statistical parameters	*Cd*	*Cr*	*Cu*	*Fe*	***Mn***	*Ni*	*Pb*	*Zn*	***SO_4^{2-}***	***NO_2^{-}***	***NO_3^{-}***	***NH_4^{+}***	*O_2*
	ppb	*ppb*	*ppb*	*ppb*	*ppb*	*ppb*	*ppb*	*ppb*	*ppm*	*ppm*	*ppm*	*ppm*	*ppm*
Detection limit	1	10	10	1	1	10	10	10	0.1	0.001	0.3	0.001	0.1
Max. admissible limit	*5.0*	*50.0*	*3000.0*	*200.0*	*50.0*	*50.0*	*50.0*	*5000.0*	*250.0*	*0.1*	*50.0*	*0.5*	*-*
Minimum	0.5	5.0	5.0	0.5	19.0	5.0	5.0	10.0	18.6	0.0	0.2	0.0	0.3
Maximum	4.0	10.0	110.0	36.0	**1970.0**	10.0	30.0	1000.0	**1405.0**	**14.0**	**137.7**	**0.8**	1.8
Mean	1.2	6.3	15.3	13.5	**176.7**	6.3	10.3	211.3	**377.2**	**0.9**	44.7	0.1	0.7
Median	1.0	5.0	5.0	9.0	32.0	5.0	5.0	60.0	**317.5**	0.0	37.4	0.1	0.6
First quartile	0.5	5.0	5.0	2.8	25.0	5.0	5.0	30.0	207.6	0.0	21.9	0.0	0.3
Third quartile	1.0	8.8	10.0	24.3	40.8	8.8	10.0	165.0	**423.8**	0.0	**52.4**	0.1	1.1
Standard error of mean	0.3	0.6	7.0	3.2	129.1	0.6	2.3	82.0	81.9	0.9	9.6	0.1	0.1
95% conf. int. of mean	0.7	1.3	14.9	7.0	277.0	1.3	5.0	175.8	175.7	2.0	20.6	0.1	0.3
99% conf. int. of mean	0.9	1.8	20.9	9.7	387.0	1.8	6.9	245.6	245.5	2.8	28.8	0.2	0.4
Average deviation	0.8	2.0	14.6	10.5	252.0	2.0	6.5	235.5	188.5	1.7	26.4	0.2	0.4
Standard deviation	1.2	2.3	27.0	12.6	500.1	2.3	9.0	317.4	317.2	3.6	37.2	0.2	0.5
Coef. of variation (%)	96.7	36.1	175.8	93.0	283.1	36.1	86.7	150.2	84.1	386.5	83.2	158.2	62.5

Note: Values in ppm or mg/l or μg/dl; or ppb or μg/l

Nitrate [NO_3^-] varies from 0.2 to 137.7 ppm with a mean of 44.7 ppm and a median of 37.4 ppm. Concentrations of nitrate are above the maximum admissible limit of 50 ppm in wells in the centre of the town, where there are many cesspits, and manure from sheep is the normal fertiliser used in house gardens in Lavrion, both for flower and vegetable growing (samples LN6-7; Map 10.4 in Volume 2; Figs. 5.6 & 5.7 in Volume 1B, Appendix 5).

Ammonium [NH_4^+] and nitrous oxide [NO_2^{2-}] levels are high in a farm at Thorikon (sample LN15; Fig. 5.15) in the northern part of the study area; the latter is abnormally high in sample LN8 (Fig. 5.8), which is again in a farm between Panormos and Koukos in the southern part (Map 10.3).

Sulphate (SO_4^{2-}) is comparatively high, and exceeds the maximum admissible limit of 250 ppm, in the agricultural areas of Thorikon in the north and Panormos in the south (Map 10.4). Well LN12 (Fig. 5.12) to the south of Fougara has 1405 ppm SO_4^{2-}. High sulphate values suggest seawater intrusion, due to overexploitation in the past, but also pollution from the weathering of metallurgical processing wastes. It is noted that sea water infiltration has been verified from information given by the local people, and the reports by Dounas (1967, 1971) and Kounis (1981).

Sodium (110-1300 ppm, mean 444 ppm) and chloride (131.2-1851 ppm, mean 704.9 ppm) concentrations are high in some wells, especially in the agricultural area of Thorikon and well LN12 to the south of Fougara, indicating again the effects of sea water intrusion.

Potassium (6-44 ppm, mean 17.5 ppm) is generally high in the agricultural area of Thorikon (Map 10.3), but also in well LN12 (Fig. 5.12) to the south of Fougara, possibly suggesting contamination from fertilisers and sea water intrusion too.

The overall high contents of calcium (41.7-298.2 ppm; mean 141.8 ppm) and magnesium (37.4-176.9 ppm; mean 78.5 ppm) are ascribed to the weathering of carbonate rocks and minerals.

Iron, manganese, nickel and sulphate have comparatively high concentrations in sample LN15 (Maps 10.2 & 10.4; Figs. 5.2 & 5.4) in the northern part of the study area, which is sited to the north of a pyritiferous waste heap, indicating possibly their leaching by acid drainage generated by this waste.

Chromium concentrations (5-10 ppm; mean 6.3 ppm) are below the maximum admissible limit of 50 ppm.

Lead, zinc, cadmium and copper contents are below the maximum admissible limit. If, however, the CEC (1980) guideline value is taken for copper (100 ppb) then one well has an elevated Cu content (110 ppb Cu), *i.e.*, well LN10 in Panormos (Fig. 5.10), which is in the southern part of the study area (Map 10.1). This particular well is shallow and in the garden are produced vegetables for home consumption. It was recorded, on the field observations sheet, that copper sulphate was sprayed over the plants suggesting, therefore, that this may be the source of the slightly elevated copper value.

10.4. DISCUSSION AND CONCLUSIONS

This preliminary assessment of ground water geochemistry has shown that human activities in the Lavrion urban area have polluted this valuable natural resource.

The occurrence of nitrate [NO_3^-] in ground water is a reliable indicator of pollution, because nitrate is produced by decomposition of human and farmyard wastes, by breakdown of plant materials and from fertilisers. Other substances indicating ground water pollution from anthropogenic activities are ammonia [NH_3], iron [Fe^{3+}], potassium [K^+], chloride [Cl^-], faecal bacteria and viruses. The latter two variables were not

determined in this preliminary study, since the objective was the toxic element contamination of ground water.

The United States of America's maximum admissible limit for nitrate is 10 ppm, compared to the guideline value of 50 ppm, set by Hellenic and European legislation. If this lower value is taken, then the majority of the Lavrion ground water samples exceed this limit. Such, high nitrate concentrations pose a danger of "blue baby" syndrome, *i.e.*, the inability to maintain healthy oxygen levels, for infants of 6 months and younger (Press and Siever, 1998).

Lead, zinc and cadmium, although their concentrations are below the maximum admissible concentrations, their contents are slightly elevated in the three wells/ boreholes (LN4, LN5, LN7) that are situated in the area covered by the beneficiation/flotation residues (Map 10.1 in Volume 2; Figs. 5.4, 5.5. & 5.7 in Volume 1B). This slight increase, above the general background value for all three elements, suggests that leaching of these elements from the metallurgical wastes by percolating water has started. Since, the leaching process of these toxic elements from the beneficiation residues has began, it is difficult to stop, unless these wastes are completely isolated by an impervious cover.

Fluoride, although not determined by this study, is known to have high concentrations in the Lavrion ground water (Papadellis, 1980). A fluoride mean value of 2.7 ppm is quoted in this work. According to WHO (1993) guidelines the maximum admissible limit is 1.5 ppm F. Fluoride has always been considered a highly toxic element similar to lead or arsenic (Trattler, 1987). At toxic level symptoms of fluorosis appear. Papadellis (1980) studied the endemic fluorosis in 236 children in Lavrion, aged 12 to 18, and found that 189 children had dental fluorosis, and 139 endemic fluorosis. It is indeed fortunate that Lavrion is linked to the Athens potable water supply network for apart from fluorosis, a number of studies link high fluoride concentrations to an increase in cancer incidences, Down's syndrome, heart disease, *etc.* (Trattler, 1985; Edmunds and Smedley, 1996).

A significant variable, which was not determined, is the dissolved organic matter. The presence of organic matter in solution binds with free metal ions to form soluble metal-organic ions (McLaughlin, 1998). This complexation reaction reduces significantly the concentration of free metal ions in water. It is stressed that the concentration of free metal ions is the predominant factor that determines toxicity. Consequently, in the presence of dissolved organic matter, higher concentrations of total metal can be tolerated in solution, before adverse health effects on organisms are observed.

McLaughlin (1998) emphasises that this complexation reaction is particularly strong for copper and lead, and decreases in importance for nickel, zinc and cadmium. This means that natural water containing appreciable quantities of dissolved organic matter, little of the copper and lead in solution is actually toxicologically "active". The concentration of free metal ions is, of course, affected by other factors, such as pH and hardness.

This preliminary assessment of Lavrion ground water has shown that subsurface water has been contaminated by human actions, *e.g.*, past overexploitation, cesspits and agricultural activities. Contamination from the large amount of metallurgical processing residues, that characterise the present day Lavrion topography, appears to have started with respect to cadmium, lead and zinc. Their concentrations have not yet

reached maximum admissible limits for potable water, but the elevated levels should serve as a warning. Future investigations should determine other toxic elements, such as arsenic, antimony, mercury and fluoride.

10.5. RECOMMENDATIONS

Ground water must be monitored continuously by analysing all possible inorganic and organic contaminants.

Ground water must not be used for drinking and cooking purposes.

Ground water used for irrigation purposes must comply with stipulated legislative guideline values.

It is strongly recommended that all agricultural activities in the Lavrion urban area stop immediately and, hence, the use of ground water for irrigation purposes, for preliminary studies have shown that olives (5.6 ppm Pb) and grapes (8.7 ppm Pb) have high toxic element concentrations (Xenidis *et al.*, 1997). European Union recommended maximum limits for olives and grapes are 0.1 ppm Pb for both cases.

Blank back page
Λευκή οπίσθια σελίδα

Chapter 11

SPATIALLY RESOLVED HAZARD AND EXPOSURE ASSESSMENTS

Emma Tristán, Michael H. Ramsey, Iain Thornton and George Kazantzis
Environmental Geochemistry Research Group, T.H. Huxley School of Environment, Earth Science & Engineering, Royal School of Mines, Imperial College of Science, Technology & Medicine, Prince Consort Road, London SW7 2BP, U.K.

Michael S. Rosenbaum
Faculty of Construction and the Environment, The Nottingham Trent University, Newton Building, Burton Street, Nottingham NG1 4BU, U.K.

Alecos Demetriades, Evripides Vassiliades and Katerina Vergou-Vichou
Division of Geochemistry, Institute of Geology and Mineral Exploration, 70 Messoghion Street, Gr-115 27, Athens, Greece

11.1. INTRODUCTION

The process of pollution control has been advanced, incorporating the principal of ***environmental risk assessment*** as pointed out by Douben (1998) from whom the major part of this introductory paragraph is abstracted. Environmental risk assessment has become an important tool in modern day decision-making both within and beyond the environmental pollution arena. Risk has become, however, a catch phrase to encompass many aspects of life and that under the banner of *"no risk"* many actions are justified. The former part is a truism, in that this has always been the case, but the increasing importance of **"risk"** as a concept has led to comparisons being made between **pollution** risk and **other types** of risk, which are accepted as a normal part of life, such as crossing the street, driving a car or travelling by an aircraft; by appealing to these analogies a particular course of action is justified. The Netherlands Health Council tackled this and attempted to clarify the matter in its report, ***"Not All Risks are Equal"*** (Gezondheidsraad, 1995). Common examples of this phenomenon are lotteries and smoking, where inverse perceived and actual risks apply.

Techniques for **environmental risk assessment** and **environmental risk management** have been developed rapidly over the last decade or so (Douben, 1998; Ferguson *et. al.*, 1998; 1999). The U.S. National Research Council (US NRC) has encouraged discussions and made considerable progress in this field. *Environmental risk management* as a separate activity from *environmental risk assessment* was firmly put on the agenda by this body (NAS, 1983). A decade later the Royal Society of London published and updated an advanced version of its 1983 study on environmental risk assessment, since it was considered timely *"to institute an upgraded study in which public perception of risk and related considerations would receive greater attention"* (Royal Society, 1992). Shortly thereafter the U.K. Government stated in its sustainable development strategy that *"decisions should be based on the best possible scientific information and analysis of risk"* (UK Government, 1994). The Royal Society of London report regards *environmental risk assessment* as the structured gathering of available information about risks and forming a judgement about them. One important aspect is the systematic approach and perhaps, therefore, a certain cleanliness with which this concept is handled. Such systematic dealings were, and remain, necessary to formalise the process and to ensure that the outcome is handled in a transparent

manner for management purposes. Developments have continued and a guide issued by the United Kingdom Department of the Environment (DoE, 1995) clarifies that "*the current approach is aimed at encouraging a continuing improvement in environmental quality through the careful balancing of risks and benefits and through the stringent* ***management*** *of activities which may have harmful effects on the environment* (DoE, 1995).

The following year the US NRC published a new approach to assess environmental and public-health risks. This body considered that handling of risk often breaks down at the **risk characterisation** stage. Hence, before proceeding further, the committee charged to look into this matter adopted a revised task by stipulating that: ***"risk characterisation*** *is a complex and often controversial activity that is both a product of analysis and dependent on the process of defining and conducting analysis".* It was concluded that scientists and the public should be allowed to become more involved in discussing risk before it is given a formal assessment (Stern and Fineberg, 1996). Risk characterisation is more than a summary or popular translation of the outcome of risk assessment. It has been described therein as a **decision-driven activity**, and is the outcome of **an analytical-deliberative process** directed towards informing choices and solving problems. Industrialists responded that this approach could swamp objective scientific risk assessment. Nevertheless, the Committee included amongst the criteria of success both *"getting the science right"* and *"getting the right science".* Essentially, it conceded that the sharp distinction between two functions, ***environmental risk assessment*** (understanding) and ***environmental risk management*** (action), remained useful for various purposes, such as insulating scientific activity from political pressure, and maintaining the analytical distinction between the magnitude of risk and the cost of coping with it. It considers *"improving decision-relevant understanding of risk and making that understanding more widely accepted"*, as an important aspect of the entire process to enhance understanding of risk (Stern and Fineberg, 1996). This facet of risk echoed the view of the Dutch Health Council, which advocated *"a dynamic process of risk assessment and management"* partly due to inevitable external influences (Gezondheidraad, 1996). In the U.K. the Royal Commission on Environmental Pollution announced in 1995 that it would carry out a study on environmental standards. It considers this issue from a strategic and policy angle and, therefore, covers the objectives of environmental standards, the ways of achieving protection, including non-scientific considerations, and addresses risk-related issues (RCEP, 1995).

The European Commission realising the significance of environmental risk assessment for contaminated sites approved a programme of "Concerted Action on Risk Assessment for Contaminated Sites in the European Union" with the acronym CARACAS (Ferguson *et. al.*, 1998, 1999). The published first part of the report summarises the practical state-of-the-art on risk assessment in Europe, and outlines clearly the necessary research needs in the context of current approaches for contaminated land risk assessment in European countries. One of the conclusions made is that *"risk assessment for contaminated sites is a rather loose assemblage of concepts and methods borrowed from various disciplines."* Further, risk assessment is not yet recognised as a coherent scientific discipline. It is also pointed out in this report, that *the valuation of risks and risk management options is a multidisciplinary field involving many areas of risk study, including remediation, economics, insurance, law, ethics and policy*. A significant task is to complement traditional cost-benefit and risk-benefit analyses with modern multi-criteria decision methods (Ferguson *et. al.*, 1998).

The second volume of the CARACAS project (Ferguson and Kasamas, 1999) places an unprecedented "stress factor" on the present project, for in the report about Greece it is stated that *"research on contaminated land in Lavrion is related to the development of a methodology for the environmental characterisation of the site …"* (Isaakidis *et. al.*, 1999, p. 81). The Lavrion project was indeed a challenge, and in the opinion of all participating scientists, the approach used for characterisation of contamination is innovative. It is hoped, that these techniques will be applied for the characterisation of other contaminated areas, and at some stage, in the not too distant future, they may be refined and incorporated in a standardised methodology for contaminated land assessment.

11.2. OBJECTIVES

The principal objective of this study is to describe and evaluate different methodologies for assessing personal hazard and exposure from environmental contaminants, incorporating spatial parameters.

The secondary, site-specific, objectives were:

1. to define the exposure and hazards to be assessed;
2. to compare exposure and hazard maps produced by two different approaches:
   - based on thresholds of contamination,
   - based on environmental indicators;
3. to assess the advantage of incorporating uncertainty in probabilistic hazard assessment;
4. to evaluate whether the hazard can also be assessed without utilising the Pb concentration in overburden samples, and
5. to test the validity of the assessment by comparing predicted exposure with biomedical measurements.

11.3. HAZARD ASSESSMENT AND EXPOSURE ASSESSMENT

Hazard Assessment (**HA**) and ***Exposure Assessment*** (**EA**) for environmental contaminants are two fundamental components of **Environmental Risk Assessment** (**ERA**) (DoE, 1995; Callow, 1998). **ERA** is the process by which hazards are identified, exposure quantified and dose-response relationships determined for risk characterisation (NAS, 1983). ERA has become an accepted basis for the assessment and management of contaminated sites in many countries (Ferguson and Denner, 1994; NEHF, 1996; Douben, 1998; Ferguson *et. al.*, 1998), particularly for environmental relationships between soil, water and air. However, on a site-specific basis, conventional (*i.e.,* traditional) ERA, and especially **Human Health Risk Assessment** (**HHRA**) approaches, have several spatial limitations that could be overcome by using a Geographical Information System (GIS).

Firstly, the ERA often provides only a single assessment in a context that can be highly variable, both temporally and spatially. The average measured concentration in the medium of concern (*e.g.,* air, water or soil) is used to quantify the hazard by comparing this value with some regulatory threshold (NEHF, 1996; ICRCL, 1987; MH, 1994). However, within any study area, sectors of high, medium and low hazards are identifiable by looking at the spatial distribution of contaminant levels. Similarly, ERA has both spatial and temporal variability. The exposure or dose that each individual

receives depends on the hazard present at the specific locations, where most time is spent. **Probabilistic Exposure** and **Risk Assessments** can allow for uncertainty in the input data and the predictions, but input measurements are still population based rather than specific to individual people. To the knowledge of the authors, there appear to be no published studies that have assessed exposure from environmental contaminants *on a person by person basis* in the general population.

Secondly, ERA should not be based, from the beginning of the process, on an exhaustive and often expensive sampling campaign. ERA can be considered as a process consisting of several tiers. To be efficient, data from each tier is used to evaluate whether there is sufficient information to make a qualified management decision. If so, the assessment is concluded at that point (DoE, 1995). Therefore, existing qualitative ("soft") information (*e.g.*, from geological, geographical, geomorphologic or sociological sources) can sometimes be very valuable in providing a sound and less expensive assessment than direct observation on specific parameters alone and considered in isolation. Quantitative assessments do not necessarily produce a result of better quality, especially if they are carried out in a very simplistic way (*e.g.*, by comparing the environmental measurement or prediction against a regulatory threshold). Statutory thresholds do not incorporate uncertainty by definition; measurements normally carry an appreciable amount of uncertainty, which is not necessarily stated (Burmaster and Harris, 1993; Finley and Paustenbach, 1993; Ferguson *et. al.*, 1998).

Thirdly, exposure estimates from exposure assessment models would depend on the circumstances in which the chemical occurs. An assessment based on total metal levels in the environment will generally be misleading, because different species of a given metal can have substantially different bioavailability (ICME, 1997). Similarly, the spatial variability of the bioavailability factor should be taken into account, even within a small area, because the metal could have been derived from different sources.

Determination of **exposure** requires an assessment of environmental pathways and investigations of the behaviour and fate of pollutants in the environment (Douben, 1998). In some circumstances, they do not exert any damage, because they do not reach levels sufficiently high to do so as a result of degradation. It can be argued that the substance has been rendered harmless, a concept that is crucial in policy objectives throughout the world. On the other hand, they may form substances that are more toxic or concentrate them to such an extent that harmful levels are reached at which they can exert their effect.

The **Human Health Exposure Assessment** addresses the relation between the concentration of a contaminant in an environmental medium (air, soil, water) and the amount available for human ingestion, inhalation or dermal absorption (McKone, 1989). The European Commission has recently published a technical guidance (EC, 1996) to undertake HHRA for the new notified and existing substances, which is a comprehensive document on methodologies and models for assessing the different types of human exposure.

The final problem with ERA is concerned with **"risk perception",** defined as the process by which people receive and process physical signals (such as witnessing an explosion), as well as information about possible outcomes of human actions or natural events (Durant, 1997; Renn, 1991). People tend to form an opinion or an attitude in response to the perceived signals or information about risks (Renn, 1998). Essentially,

experts and non-experts should be able to understand the results of the assessment, but usually the terminology and numerical outputs tend to confuse even the learned, and management guidelines cannot be drawn. The appropriate spatial visualisation, however, of hazardous problems and their assessment can facilitate improved communication of risk between parties.

11.3.1. DEFINITIONS OF HAZARD

"Hazard" has been widely defined by different authors as a possible source of danger, *i.e.*,

- hazard includes the innate properties of an agent (biological, chemical or physical) to cause harm without regard to the circumstances under which it exists (IETC,1996);
- hazard is a situation that can lead to harm or damage (Royal Society, 1983, 1992);
- hazard is the capacity to produce a particular type of adverse health effect, *e.g.*, one hazard of benzene is leukaemia (Paustenbach, 1989);
- a hazard, as applied to the assessment of contaminants in soil, exists provided there is a potential to cause harm or damage by virtue of the *properties* of a substance and the *circumstances* in which it occurs (Ferguson and Denner, 1994);
- hazard is a property … that in particular circumstances could lead to harm (Douben, 1998).

According to the latter two definitions, a toxic chemical is not necessarily hazardous if the circumstances in which it occurs prevent the potential for harm.

11.3.1.1. Hazards assessed at Lavrion

The first two, wider, definitions of hazard are used in this report to assess "**Pb concentration in surface overburden and dust**"; *i.e.*, the properties of Pb in surface overburden (or soil in the wider sense), particularly its concentration, are the only concern. Properties such as pH, organic content and texture of overburden are not used in this study, since the pathway of exposure to children from ingestion of *home-grown* vegetables has not been studied.

The concentration of Pb in soil is contrasted with an "accepted" threshold, in this case the ICRCL (1987) trigger concentration for domestic gardens and allotments, which is 500 μg Pb/g soil.

The latter two concepts of hazard, applied for assessment of contaminants in soil, involves a deeper understanding of the real situation to establish whether the circumstances in which Pb in soil occurs, make it "hazardous" or not, *i.e.*, whether the Pb in soil and in dust is accessible to children. The hazard in the case of Lavrion is "**Pb accessible to children from overburden materials, including soil, and dust**".

11.3.2. DEFINITIONS OF EXPOSURE

According to Tsuhi & Searl (1996) and (Lu, 1992) exposure can be quantified in terms of *external* and *internal exposure*, *i.e.*,

(a) *External exposure* estimates are based on the determination of the quantity of material that reaches the target, per day, per unit of body weight. This value should

always be referred as *intake*. *Uptake* is, by contrast, the quantity of material that is taken up in the blood stream, and is a modest equivalent of the quantity that reaches the target organ. This is obtained by multiplying the *intake* by a factor of absorption or *bioavailability.* These terms, however, are not always used according to their original definition. In general, the value of *uptake* obtained is called an ADI (Average Daily *Intake*) that can be compared, in case of non-carcinogen substances, with the TDI (Tolerable Daily *Intake*), based on criteria derived by the FAO/WHO (accepted daily *intakes*) in order to assess the risk of exposure.

(b) *Internal exposure* is quantified after the exposure has occurred, measuring internal body indicators (*biomarkers*) or chemical burdens. If the dose-response relationships are appropriately characterised, these measurements will be used to back-calculate dose (Lu, 1992). The biomarker can give either a value of recent exposure (*e.g.*, blood-Cd) or chronic exposure (*e.g.*, blood-Pb, urine-Cd).

Ferguson (1998, p.108) gives a more general definition of exposure: *exposure* is the intake of a contaminant via all relevant routes of entry into the human body (skin, respiratory tract, gastrointestinal tract).

11.3.2.1. Exposure assessed at Lavrion

The pathways of exposure studied to assess child exposure to Pb in Lavrion are:

- direct ingestion of soil and dust, and
- direct inhalation of particulate matter.

Other potential pathways of exposure (*i.e.*, consumption of garden produce, consumption of the rest of the diet, drinking water, consumption of local meat, milk, dairy and fish products) have not been studied, since key, site-specific information, is lacking.

Both an indicator and a quantitative approach are presented in this report. The quantitative approach is based on two Exposure Assessment Models, *i.e.*, *the Human Exposure from Soil Pollutants* model (HESP) (Shell, 1994) and *the Integrated Exposure Uptake BioKinetic* model for Lead Exposure (IEUBK) (US EPA, 1994).

The exposure predicted by the HESP model is an *"external exposure"*, or ADI (Average Daily Intake) in μg Pb/day/kg-BW (body weight), whereas the exposure obtained with the IEUBK model is a prediction of *"internal exposure"*. Both concepts are defined in the previous section (Section 11.3.2).

11.4. SITE INFORMATION AND GEOSTATISTICAL DATA ESTIMATES USED FOR HAZARD AND EXPOSURE ASSESSMENT

All site information used in this study is in digital form and is described in the report by Demetriades *et. al.* (1998). This information is tabulated below:

- total Pb concentrations in overburden samples (including soil) (Map 3.4 in Volume 2),
- total Pb concentrations in house dust samples (Map 3.5 in Volume 2),
- kriged estimates of total Pb in overburden samples on a grid of 50 x 50 m (Statistics in Table 11.1A at the end of this Chapter; see also Map 3.4 in Volume 2),

- kriged estimates of exchangeable Pb (Step 1) in overburden samples on a grid of 50 x 50 m (Statistics in Table 11.2A at the end of this Chapter; see also Map 3.8 in Volume 2),
- kriged estimates of carbonate Pb (Step 1) in overburden samples on a grid of 50 x 50 m (Statistics in Table 11.3A at the end of this Chapter; see also Map 3.9 in Volume 2),
- kriged estimates of combined exchangeable and carbonate Pb (*extractable* = Steps 1+2) in overburden samples on a grid of 50 x 50 m (Statistics in Table 11.4A at the end of this Chapter; see also Map 3.10 in Volume 2),
- kriged estimates of Pb in house dust samples on a grid of 50 x 50 m,
- blood-Pb concentrations in children (Map 3.6 in Volume 2),
- lithology (Quaternary deposits) (Map 2.2 in Volume 2),
- smelter wastes map (Map 2.3 in Volume 2),
- land use map (Map 2.4 in Volume 2),
- town plan (Map 2.1 in Volume 2), and
- stacks.

The semi-quantitative maps are based on a larger number of factors derived from various images, *i.e.*, land use, stacks, rivers, lithology, town plan, and smelter wastes.

The kriged total Pb concentration and kriged extractable concentration were plotted after an exhaustive geostatistical structural analysis on the two data sets (Demetriades *et. al.*, 1998; refer also to Chapter 3, this volume and Volume 2). The spatial relationships were examined by constructing variograms in different directions of raw and log (base 10) total and extractable Pb contents (Pennatier, 1996). Since, both data sets are positively skewed, the $\log_{10}$-transformed Pb concentrations gave more realistic variograms. The different geostatistical models were examined against the actual Pb values with cross-validation kriging techniques (Englund and Sparks, 1988). The model with the lowest mean kriging standard deviation and estimation error was selected for total and extractable Pb concentrations.

Kriged estimates of house dust were based on the geostatistical parameters of overburden (see Chapter 3 this volume).

11.5. GIS FOR HAZARD AND EXPOSURE ASSESSMENT

GIS is a tool that has the potential to overcome some of these limitations by combining spatial data from diverse sources. It allows description and analysis interactions, developing predictive models, and providing support for decision-making. GIS is widely applied for environmental modelling (Bonham-Carter, 1994; Goodchild *et. al.*, 1996), but very few applications in human health related studies have been published, most of which concern applications in epidemiology (Guthe *et. al.*, 1992; Kitron and Kasmierczak, 1997; Vine *et. al.*, 1997) rather than risk or exposure assessments (Valjus *et. al.*, 1995; Siniscalchi *et. al.*, 1996).

As it has already been mentioned, the principal aim of this study is to describe and evaluate different methodologies for assessing personal hazard and exposure from environmental contaminants incorporating spatial parameters. These methodologies have been named either "***Spatially Resolved Hazard Assessment***" (SRHA) or "***Spatially Resolved Exposure Assessment***" (SREA), with both quantitative and semi-quantitative elements.

The quantitative SRHA and SREA are more traditional in concept, and are based on a threshold approach. In order to account for measurement uncertainty in the SRHA (Ramsey and Argyraki, 1997), both a deterministic and a probabilistic approach are used. The semi-quantitative SRHA and SREA are based on modelling using "Weighted Factors in Linear Combination" (WLC), described in detail below, a method allowing for the impact of more influential parameters.

11.5.1. HAZARD AND EXPOSURE MAPPING AT LAVRION

The concentration of Pb in soil in the Lavrion urban area varies from 810 to 151,579 ppm (mg/kg or μg/g), with a mean value of 11,578 ppm and a standard deviation of 15,491 ppm (n=224). People in the town live on or are close to smelter wastes and some of them eat *home-grown* vegetables and fruits. Furthermore, health studies on children have indicated that there is some evidence for substantial exposure to Pb, with documented medical evidence for mental retardation, a slower response rate and increase in sickliness in school age children (Benetou-Marantidou *et. al.*, 1985; Nakos, 1985; Hatzakis *et. al.*, 1987; Maravelias *et. al.*, 1989; Eikmann *et. al.*, 1991; Makropoulos *et. al.*, 1991, 1992; Kafourou *et. al.*, 1997)..

The feasibility of the SERA approach was assessed for selected pathways of Pb exposure. The existing person-specific information included blood-Pb concentration of selected children, but it did not include details of their activity patterns (*e.g.*, time spent outside or inside the house, consumption of *home-grown* vegetables and fruits). Nevertheless, such an approach could easily be expanded to include these aspects in the future.

The exposure situation at Lavrion appears to be multiple-source and multiple-pathway (Fig. 11.1). However, there are several gaps and inconsistencies in the biomedical data, obtained from previous studies, which have thus limited the scope of the current assessment concerning Pb in soil.

11.5.1.1. Methods of quantitative hazard mapping

As mentioned in the previous section, the hazard defined in the Lavrion urban area is either

- Pb concentration in overburden, including soil, and dust, or
- Pb accessible to children from the fine-grained overburden materials, including soil and dust.

Following the first definition, seven hazard related maps (Maps 11.1 to 11.7 in Volume 2) were created using the *Idrisi*® GIS (Eastman *et. al.*, 1997). These were derived either from raw, site-specific, total Pb concentration data or kriged total Pb concentration data (see Fig. 11.2). The quantitative hazard assessment maps (both probabilistic and deterministic) are based on the threshold concept, whereby the land is contaminated if it exceeds the established statutory threshold value. In this case the threshold used, to create the categories for the different hazard maps, was the ICRCL (1987) trigger concentration for domestic gardens and allotments (500 ppm Pb in soil) has been selected to demonstrate the approach, although more appropriate lower, site specific, statutory threshold values could be considered, if required. Nevertheless, this is a simplistic approach, because the hazard is only related to total Pb concentration in

overburden materials, including soil, and the dust regardless of its availability to children.

The image used for the elaboration of the quantitative hazard maps is the total soil Pb concentration at each sample site. Total soil Pb concentration is classified on the basis of its position relative to the statutory threshold in order to create the categories for the different hazard maps.

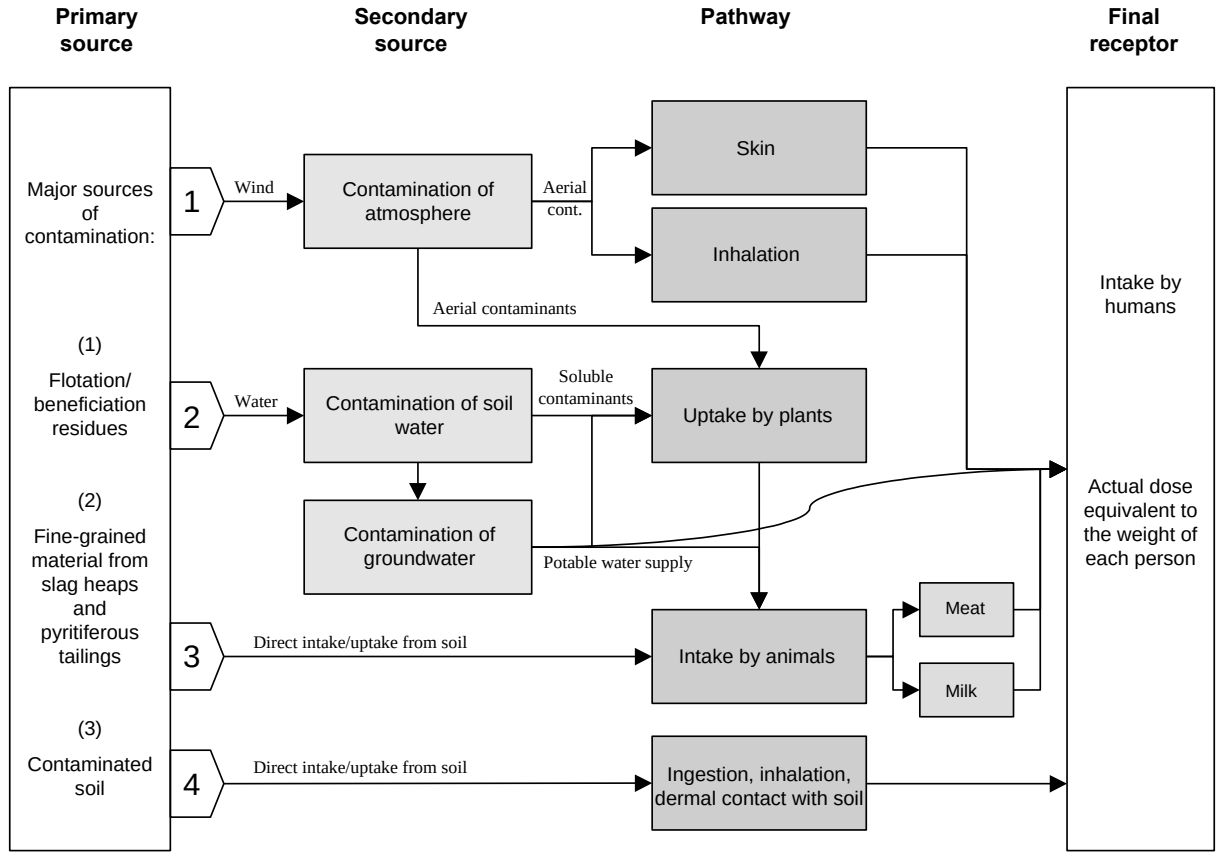

Compiled by A. Demetriades

Fig. 11.1. Conceptual contamination source-pathway-receptor model for the Lavrion urban area.
Σχ. 11.1. Σχηματικό μοντέλο πηγής ρύπανσης-διόδου-αποδέκτη για την αστική περιοχή του Λαυρίου.

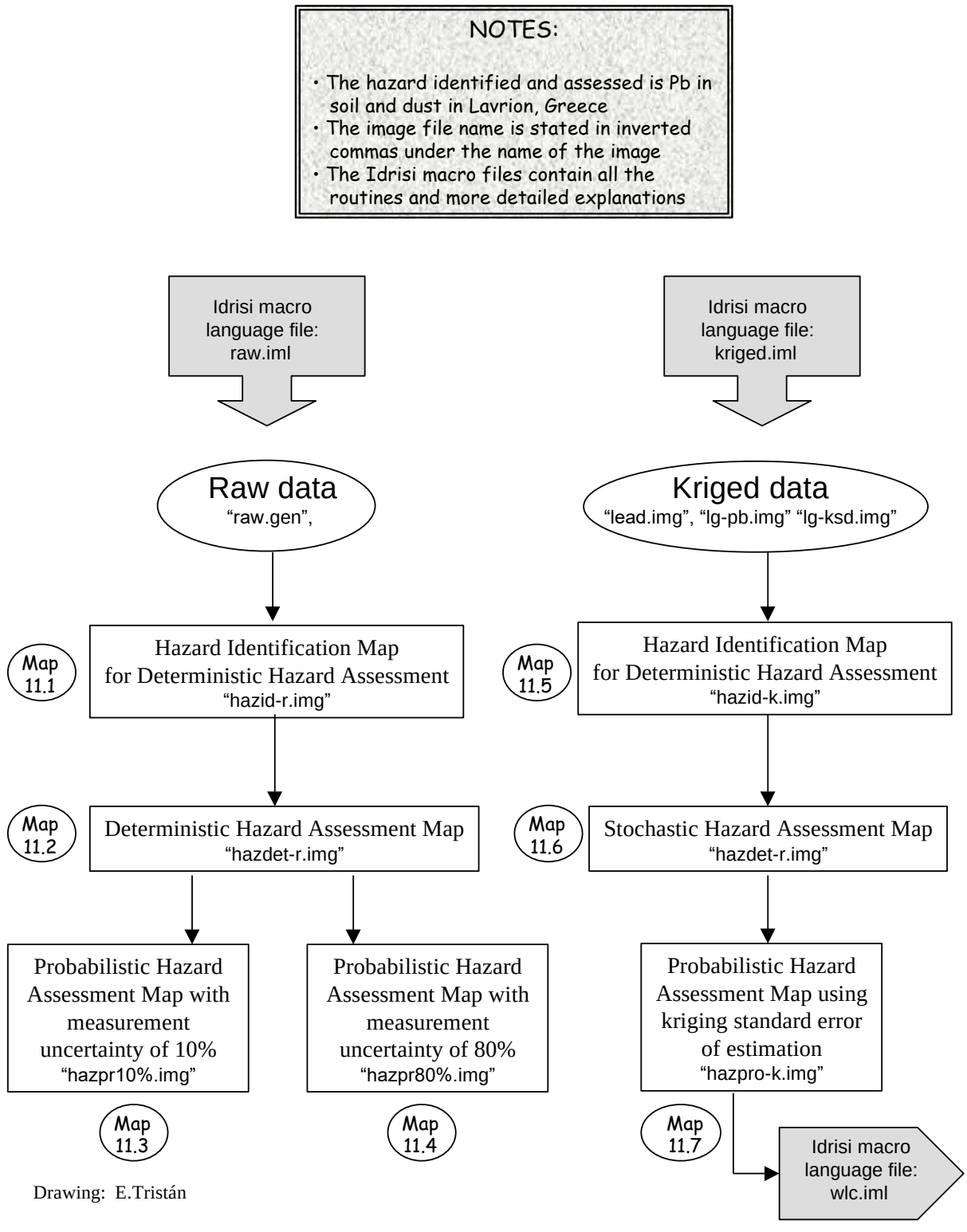

Fig. 11.2. Flow chart of the preparation of hazard maps in Lavrion
[for more details refer to Tristán *et. al.*, 1998].
Σχ. 11.2. Ροόγραμμα για τη σύνταξη των χαρτών επικινδυνότητας του Λαυρίου
[για περισσότερες λεπτομέρειες βλ. Tristán *et. al.*, 1998].

The **Hazard Identification Map** displays the distribution of concentration of the substance across the area (Map 11.1). The **Deterministic Hazard Map** (Map 11.2) defines two categories for the level of contamination in soil: (1) contaminated or (2) uncontaminated. Such a classification, however, does not consider the uncertainty in the measurement of concentration of the substance in soil, which can have profound effects on a realistic assessment of the degree and extent of contamination.

11.5.1.1.1. Effects of Uncertainty

In order to address the uncertainty of the measurements, a probabilistic classification of contaminated land (Ramsey and Argyraki, 1997) is used to produce the **Probabilistic Hazard Maps** (Maps 11.3 & 11.4). The probabilistic hazard maps address decision rule uncertainty by considering the uncertainty as being on the statutory threshold used to determine the decision rule. The classification defines four categories based on the extent of overlap of uncertainty with a single threshold value:

(1) contaminated,
(2) probably contaminated,
(3) possibly contaminated, and
(4) uncontaminated.

For the category “uncontaminated”, for example, the entire range of uncertainty is lower than the regulatory threshold value (T). The probability of this site being contaminated, because the element concentration lies over the statutory threshold is, therefore, <0.025 (*i.e.,* 2.5%). This computational device can be used to classify soil samples directly, without the need to calculate uncertainty values for each measurement.

The use of duplicate samples is one method that has been proposed for the estimation of sampling uncertainty (Ramsey and Argyraki, 1997). Unfortunately, such duplicates were not available at the time of this study. However, in order to illustrate the technique, uncertainties of 10% and 80% were taken as the most optimistic and pessimistic case scenarios respectively.

An alternative approach to Probabilistic Hazard Map was applied using the kriged estimates of total Pb concentration, described above (Map 16.5). Two times the logarithm to the base 10 of the kriging standard error of estimation (lg-ksd) is used as an estimate of uncertainty, “U”; this is different for each 50 x 50-m kriged cell in the region. The images of log-base 10 for the kriged concentration of Pb and of the log-base 10 for the kriging standard error of estimation are used. As explained earlier, the uncertainty is expressed on the threshold value, as a shortcut to define “contaminated” and “uncontaminated” land.

Ramsey and Argyraki (1997) also mention that there is evidence of uncertainty changes with the concentration. The upper limit of uncertainty for each single concentration measurement is given by:

$$C + U = C\,(1 + U\% / 100)$$

where:

C is the concentration of Pb in fine-grained overburden materials, including soil,
U is the extended measurement uncertainty and U% is the uncertainty relative to the mean concentration.

The lower limit is similarly given by: $C - U = C (1 - U\% / 100)$

A “short cut” can be used by classifying overburden samples directly, without calculating uncertainties for each measurement, *i.e.*, the uncertainty values for the particular measurements made are calculated for the concentration equal to the statutory threshold value (T). When the “short cut” method is used, with the uncertainty expressed on the threshold value, then the upper and lower limits are given by:

$$T + U = T (1 + U\% / 100)$$

$$T - U = T (1 - U\% / 100)$$

The probabilistic classification boundaries can then be calculated using these equations:

“uncontaminated”: $C = T - U$ or $C + U = T$

“contaminated” : $C = T + U$ or $C - U = T$

11.5.1.1.1.1. Sampling uncertainty 10% (Map 11.3)

The equations used for the estimation of 10% uncertainty on the ICRCL (1987) trigger concentration of 500 µg Pb/g soil for domestic gardens and allotments, and the classification of land into (i) uncontaminated, (ii) contaminated, (iii) possibly contaminated and (iv) probably contaminated are given below.

(i) Uncontaminated: $C + U = T$

$C + 0.1\ C = 500$

$C = 500/1.1 = 454.5$ µg Pb/g soil

(ii) Contaminated: $C - U = T$

$C - 0.1\ C = 500$

$0.9\ C = 500$

$C = 500/0.9 = 555.6$ µg Pb/g soil

(iii) Possibly contaminated: $454.5 < C < 500$ µg Pb/g soil

(iv) Probably contaminated: $500 < C < 555.6$ µg Pb/g soil

11.5.1.1.1.2. Sampling uncertainty 80% (Map 11.4)

The equations used for the estimation of 80% uncertainty on the ICRCL (1987) trigger concentration of 500 µg Pb/ g soil for domestic gardens and allotments, and the classification of land into uncontaminated, contaminated, possibly contaminated and probably contaminated are given below.

(i) Uncontaminated: C + U = T

C + 0.8 C = 500

1.8 C = 500

C = 500/1.8 = 277.7 µg Pb/g soil

(ii) Contaminated: C – U = T

C – 0.8 C = 500

0.2 C = 500

C = 500/0.2 = 2500 µg Pb/g soil

(iii) Possibly contaminated: 277.7 < C < 500 µg Pb/g soil

(iv) Probably contaminated: 500 < C < 2500 µg Pb/g soil

11.5.1.1.1.3. Kriging standard error of estimation as an estimate of uncertainty

The equations used for the kriging standard error of estimation as a measure of uncertainty on the ICRCL (1987) threshold (T) trigger concentration of 500 µg Pb/ g soil for domestic gardens and allotments, and the classification of land into uncontaminated and contaminated are given below and are used in Map 11.7.

"uncontaminated": log kriged C = T – (2 x lg-ksd), or

log kriged C + (2 x lg-ksd) = T

"contaminated": log kriged C = T + (2 x lg-ksd), or

log kriged C – (2 x lg-ksd) = T.

11.5.1.2. Methods of quantitative exposure mapping

The exposure mapping follows the same principle as in hazard mapping, *i.e.*, it either assesses exposure from Pb concentration in overburden materials (including soil) and dust or exposure from Pb accessible to children from overburden and dust.

The **exposure from Pb in overburden and dust** is assessed using a quantitative approach based on two Exposure Assessment Models, the *Human Exposure from Soil Pollutants* model (HESP) (Shell, 1994), and the *Integrated Exposure Uptake BioKinetic* Model for Lead Exposure model (IEUBK) (US EPA, 1994). In total, three different methodologies were developed, one based on the IEUBK model, and two based on the HESP model (Fig. 11.3; Maps 11.8, 11.9, 11.11 & 11.12).

The HESP (Shell, 1994) and IEUBK (US EPA, 1994) models have been chosen to predict exposure using the bioavailable fraction of Pb in overburden materials, including soil. The bioavailable fraction is obtained by multiplying the total Pb concentration measured at the site by a bioavailability factor that is assumed to be constant

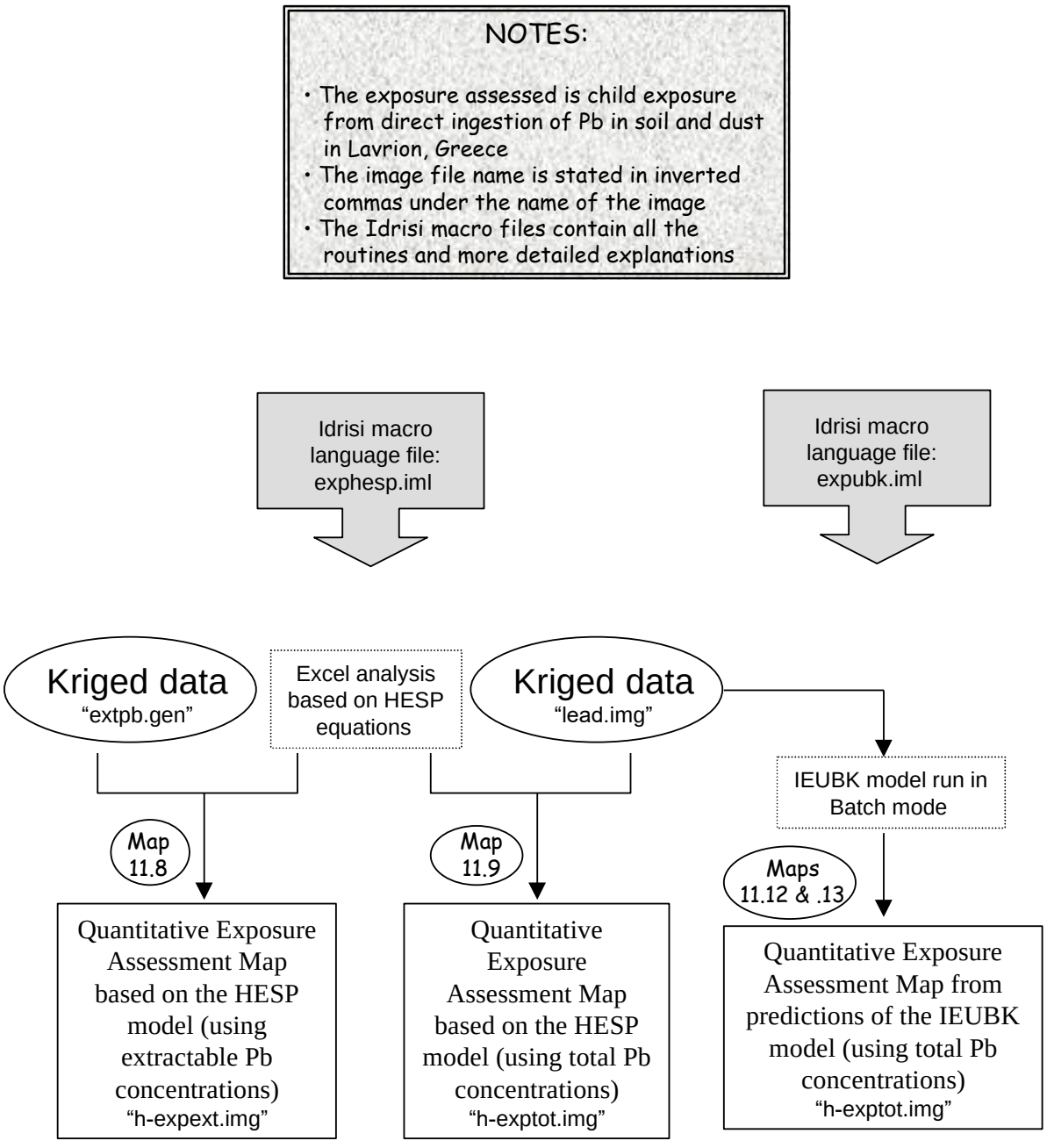

Drawing: E.Tristán

Fig. 11.3. Quantitative Exposure Assessment maps based on the HESP and IEUBK models [for more details refer to Tristán *et. al.*, 1998].
Σχ. 11.3. Χάρτες ποσοτικής εκτίμησης της έκθεσης βασισμένοι στα μοντέλα HESP και IEUBK [για περισσοτέρες λεπτομέρειες βλ. Tristán *et. al.*, 1998].

throughout the surveyed area. Either the user can specify the bioavailable fraction, or the default value provided by the model can be used.

In this study, exposure assessment mapping using the HESP model has been based first on total Pb concentration in soil, and employed the HESP model algorithm directly. The second approach predicts exposure by using the experimentally measured bioavailable fraction in each soil sample directly, and modifying the HESP algorithm slightly to allow for this difference. In this case, the personal exposure can be predicted from the known bioavailable Pb fraction at an individual's place of residence. For the development of the second methodology, the available sequential extraction data on Lavrion overburden materials for chemical fractionation of trace elements were used, as an approximation to the bioavailable fraction of Pb in soil (Demetriades *et. al.*, 1998). The first and second extractions (*i.e.*, exchangeable and bound onto carbonates, respectively) represent the most readily dissolved fraction of Pb in overburden (Li *et. al.*, 1995); these concentrations have been added together to represent a "bioavailable" fraction. There are several *in vitro* methods that have been developed to mimic bioavailability from ingested Pb in soil and dust that could be used in the future to derive a more refined assessment (*e.g.*, Ruby *et. al.*, 1995).

The Integrated Exposure Uptake BioKinetic model (IEUBK) is a computerised mathematical model that derives a deterministic estimate of blood-Pb in young children. It is based on environmental exposure to Pb from various sources, including soil. The main objective of this particular model is to predict blood-Pb levels for children from 1 to 84 months (7 years old).

11.5.1.2.1. Exposure assessment maps using the HESP model as a basis

The Human Exposure from Soil Pollutants model (HESP) (Shell, 1994) is a computer model, which derives a deterministic value of exposure to humans from contaminants in soil. It estimates exposure for two types of residents, an adult and a young child (Shell, 1994). Since, its aim is to give information on potential human exposure to soil contamination, it can be applied to carry out a preliminary exposure assessment in an early phase of the risk assessment process. In cases where it indicates the possibility of significant exposure, a site specific exposure assessment should then be undertaken.

The model works with fixed parameter sets concerning the characteristics of the scenario, *e.g.*, basement, bathroom, cattle, climate, crop and crop type, fish, poultry, recipient and water.

The user can set parameters related to:

- soil usage or "land use" (the pathways which are relevant according to the particular land use can be selected and defined);
- soil type, and
- specific chemical.

The calculated exposure represents the Average Daily Intake (ADI), where the average indicates the year's average, independent of seasonal changes.

A bioavailability factor can be used for the chemical studied. For ingested soil-Pb and inhaled soil-Pb, the bioavailability factors are respectively 0.3 and 0.5.

The HESP model was not used directly to derive the maps, but the algorithms mentioned in the reference manual (Shell, 1994b) were employed. These algorithms are listed below (*11.5.1.2.1.1*). Two different quantitative exposure maps were created:

1. Quantitative exposure assessment map using extractable (first and second extraction) soil-Pb and dust-Pb concentrations for each house where children live (Map 11.8).

2. Quantitative exposure assessment map using total soil-Pb and dust-Pb concentrations for each house where children live (Map 11.9).

Child exposure is calculated in those areas where most time is spent, *i.e.,* agricultural area, residential area, recreational area, or school. Therefore, the land use map (Map 2.4) is an essential to identify these geographical differences.

The methodology to create these maps includes two steps. To begin with, a spreadsheet, such as *Microsoft® Excel®*, is used to determine the uptake from direct ingestion of fine-grained overburden materials, including soil, or dust ($DU_{n,x}$), which is calculated for a child living in a house with a garden. Then, the *Idrisi® GIS* (Eastman, 1997) is utilised to assign the calculate $DU_{n,x}$ to every house of interest (*i.e.*, those with children who have permitted blood-Pb measurements), in order to create the quantitative exposure maps (Maps 11.8 & 11.9). Both maps use the value of either kriged extractable Pb (first and second extractions) or total soil-Pb concentration corresponding to each house where the assessed children live.

11.5.1.2.1.1. Algorithms and values used to develop the quantitative exposure assessment maps based on the HESP model

The HESP model estimates a deterministic value of exposure to humans, from contaminants in soil for two types of residents: an adult and a young child. The calculated exposure represents the Average Daily Exposure (ADE) in µg Pb/day/kg-BW (Body Weight). The average indicates the year's average, independent of seasonal changes.

*11.5.1.2.1.1.1. Uptake through direct ingestion of soil and dust (***DU***)*

In the following equations the underlying notation is used:

- the values given by the user are in **bold text**, and
- the calculated values are in *italics*.

The algorithm used in HESP to predict exposure through direct ingestion of soil and dust (DU) is:

$$DU = (\sum DU_{n,x}) * \mathbf{c_s} / \mathbf{w} \qquad \text{(equation 11.1)}$$

where:

$Du_{n,x}$ = *uptake from direct ingestion of soil or dust per unit body weight per season (mg soil/d)*
n = index indicating soil or dust
x = index indicating summer or winter
$\mathbf{c_s}$ **= c_t = concentration in the soil's top layer (0-0.25 m) (mg/kg – dry matter)**
w = receptor weight (kg).

The concentration of Pb in house dust is not required, since it is approximated by allocating a fraction of the outdoor soil to indoor dust. The model provides default

values for the rest of the input parameters, *e.g.*, child's weight, time activity patterns, bioavailability fraction.

$DU_{n,x}$, the uptake from direct ingestion of soil or dust per unit body weight per season (mg soil/d), is calculated by adding both the contribution of soil and of indoor dust ingestion during the summer and winter seasons:

$$DU_{x,dust} = \mathbf{AID} * f_{a,ing} * f_{rs,i} * f_i * N_i \qquad \text{(equation 11.2)}$$

$$DU_{x,soil} = \mathbf{AID} * f_{a,ing} * f_o * N_o \qquad \text{(equation 11.3)}$$

where:

AID **= amount of soil ingested daily (mg/d) based on the average amount on a yearly basis**
$f_{a,ing}$ **= fraction uptake/intake for ingestion (bioavailability)** [dimensionless]
$f_{rs,i}$ **= fraction of soil in dust (indoors)** [dimensionless]
f_y *= fraction of soil or indoor dust covering the skin indoors (i) or outdoors (o)* [dimensionless]
f_y $= [DAE_y/(DAE_i + DAE_o]$
DAE *= amount of soil or dust on the skin [kg/m²]*
N_y *= fraction of time spent annually indoors, outdoors, sleeping or away from the location* $(N_y = \sum N_x)$ *(always* ≤ 1*)* [dimensionless]
y = index indicating indoors (i), outdoors (o), sleeping or away from the location.

$$N_x = \sum \mathbf{t_x1_y}/24 * (\mathbf{t_x2_y}/7) * f_x \qquad \text{(equation 11.4)}$$

where:

t_x1_y = time spent indoors, outdoors, sleeping or away from the location in a season per day (hr/day)
t_x2_y = time spent indoors, outdoors, sleeping or away from the location in a season per week (d/week), and
f_x = fraction of the season.

Equation 11.1 is slightly modified in order to use c_e instead of c_s as follows:

$$DU = (\sum DU_{n,x}) * c_e / (w * f_{a,ing}) \qquad \text{(equation 11.5)}$$

where,

c_e = the extractable soil-Pb concentration, which in theory should correspond to "**c_s * $f_{a,ing}$**" (*i.e.*, the total soil-Pb concentration multiplied by the bioavailable fraction for soil and house dust ingestion) in equation 11.1.

A value of extractable soil-Pb concentration is given to each house using a kriged extractable soil-Pb concentration image. For both maps, the child's weight (w) is taken as constant (*i.e.*, 24.2 kg).

In Table 11.1 are given the values used in the equations described above.

Πίνακας 11.1. Τιμές που χρησιμοποιήθηκαν στους αλγόριθμους για την εκτίμηση της πρόσληψης διά απ' ευθείας κατάποσης του εδάφους και της σκόνης σπιτιών (Εξισώσεις 11.1 έως 11.4).

*Parameter**	*Value*	*Unit*
AID	1100	mg/day
$f_{a,ing}$ (for Pb)	0.3	dimensionless
$f_{rs,i}$ (for Pb)	0.5	dimensionless
f_I	0.09894	dimensionless
f_o	0.90106	dimensionless
DAE_I	0.00056	kg/m^2
DAE_o	0.00510	kg/m^2

*The terms have been defined in the text

11.5.1.2.1.1.2. Uptake through direct inhalation of particulate matter (IP)

In the following equations the following notation is used:

- the values given by the user are in **bold text**, and
- the calculated values are in *italics*.

$$IP = (\sum IP_{y,x}) * \mathbf{c_s} / \mathbf{w} \qquad \text{(equation 11.6)}$$

where:

$IP_{y,x}$ = *inhalation of particulate matter per unit body weight per season in soil equivalents (mg soil/d)*
x = index indicating summer or winter
y = index indicating indoor or outdoor (dust)
c_s = c_t = concentration in the soil's top layer (0-0.25 m) (mg/kg - DM)

$$IP_{y,x} = \mathbf{VA} \times \mathbf{TSP_y} * \boldsymbol{f}_{\mathbf{rs,y}} * \boldsymbol{f}_{\mathbf{r}} * \boldsymbol{f}_{\mathbf{a,inh}} * N_y \qquad \text{(equation 11.7)}$$

where:

VA = volume of air breathed (m^3/d)
TSP_o = total suspended particulate outdoors
TSP_i = *total suspended particulate indoors*
$\boldsymbol{f}_{\mathbf{a,inh}}$ **= fraction uptake/intake for inhalation (bioavailability)** [dimensionless]
$\boldsymbol{f}_{\mathbf{rs,y}}$ **= fraction of soil in dust (indoors or outdoors)** [dimensionless]
N_y = $N_{sleep} + N_{indoor}$
y = index indicating indoors (i), outdoors (o), sleeping or away from the location

$$TSP_i = \mathbf{TSP_o} * \mathbf{0.75} \qquad \text{(equation 11.8)}$$

In Table 11.2 the values of the parameters used in equations, 11.6 to 11.8 are tabulated.

Table 11.2. Values to be used in the algorithms for estimating uptake through inhalation of particulate matter (these values are described along with the equations above).
Πίνακας 11.2. Τιμές που χρησιμοποιήθηκαν στους αλγόριθμους για την εκτίμηση της πρόσληψης διά της εισπνοής σωματιδίων (αυτές οι τιμές περιγράφονται σε σχέση με τις παραπάνω εξισώσεις).

Parameter	*Value*	*Units*
f_r	0.75	dimensionless
VA	7.6	dimensionless
TSP_o	to be given	$\mu g/m^3$
TSP_I	to be calculated[1]	$\mu g/m^3$
$f_{a,inh}$ (for Pb)	0.5	dimensionless

[1] $TSP_i = 0.75 * TSPo$

11.5.1.2.1.1.3. Distribution of time for children in Lavrion

For this analysis factor N_y (fraction of time spent annually indoors, outdoors, sleeping or away from the location) is not calculated using the model defaults for The Netherlands, but using a more realistic child distribution of time in Lavrion (See Table 11.3 below). The Netherlands values are also given for comparison purposes.

Table 11.3. Time spent inside, outside or away of the contaminated site for each category of land use, in h/day, for children in Lavrion and in The Netherlands.
Πίνακας 11.3. Κατανομή του χρόνου εντός, εκτός και μακριά από τη ρυπασμένη περιοχή για κάθε κατηγορία χρήσης γης, σε ώρες/ημέρα, για τα παιδιά του Λαυρίου και της Ολλανδίας.

Child activities	*Child in Lavrion*								*Child in The Netherlands (land use No. 1.00, in HESP, 1994a)*					
	Summer				*Winter*				*Summer*			*Winter*		
	Rec	Res	Agr	Sch	Rec	Res	Agr	Sch	Rec	Res	Agr	Rec	Res	Agr
d, active	5	5	5	5	4	5	5	5	5	5	5	4	5	5
t, sleep	0	10	10	0	0	10	10	0	0	12	12	0	12	12
t, away, active	16	6	6	18	22	6	6	18	16	0	0	22	0	0
t, out, active	8	4	5	2	2	1	1	2	8	8	8	2	0	0
t, inside, active	0	4	3	4	0	7	7	4	0	4	4	0	12	12
t, away, passive	24	0	0	24	24	0	0	24	24	0	0	24	0	0
t, out, passive	0	6	8	0	0	2	2	0	0	0	0	0	0	0
t, inside, passive	0	8	6	0	0	12	12	0	0	12	12	0	12	12
t, swimming	0	0	0	0	0	0	0	0	2	0	0	0	0	0

Legend for abbreviations of Table 11.3:

Rec	Recreational area	t, sleep	Assumed to be the same for active and passive time
Res	Residential area	t, away, active	Time away from the contaminated site
Agr	Agricultural area	t, out, active	On site time spent outdoor
Sch	School	t, inside, active	On site time spent indoor
d, active	Days active, in this case taken as non-working days	t, away, passive	Time spent away from the contaminated site
		t, out, passive	On site time spent outdoors
t	Time apportioning (see below)	t, swimming	Time spent swimming in addition to being outdoors

Υπόμνημα των συντμήσεων του Πίνακα 11.3:

Rec	Χώρος αναψυχής	t, sleep	Θεωρείται ίδιος για τον ενεργητικό και τον παθητικό χρόνο
Res	Οικιστική περιοχή		
Agr	Αγροτική περιοχή	t, away, active	Χρόνος μακριά από τη ρυπασμένη περιοχή (ενεργητικός)
Sch	Σχολείο	t, out, active	Χρόνος εκτός σπιτιού (ενεργητικός)
d, active	Ενεργητικές ημέρες, στην περίπτωση αυτή θεωρούνται οι μη εργάσιμες ημέρες	t, inside, active	Χρόνος εντός σπιτιού (ενεργητικός)
		t, away, passive	Χρόνος μακριά από τη ρυπασμένη περιοχή (παθητικός)
t	Κατανομή του χρόνου (βλ. παρακάτω)	t, out, passive	Χρόνος εκτός σπιτιού (παθητικός)
		t, swimming	Χρόνος εκτός σπιτιού που αφιερώνεται στην κολύμβηση

11.5.1.2.1.1.4. Using Excel® to calculate the ingestion and inhalation rates of soil and dust

The total direct ingestion of soil or house dust (DU) is calculated for each land use category in Microsoft® Excel® worksheet (See Tables 11.4, 11.5, 11.6, 11.7).

Table 11.4. Total direct ingestion of soil or indoor dust (DU) by children, estimated for different land use categories with the HESP model algorithms [Values in mg soil/day].
Πίνακας 11.4. Εκτίμηση της συνολικής απ' ευθείας κατάποσης εδάφους ή σκόνης σπιτιών (DU) από παιδιά με τους αλγόριθμους του μοντέλου HESP για διαφορετικές κατηγορίες χρήσης γης [Τιμές σε mg εδάφους/ημέρα]

	Recreational area	*Residential area*	*Agricultural area*	*School*
DU[1]	141.5952	231.9083	272.2699	69.36312

[1]Note: $DU = (\sum DU_{n,x}) * \mathbf{c_s} / \mathbf{w}$ (refer to equation 11.1 above for notation, p.326)

The following Tables 11.5 to 11.7 show the values and calculations performed in the worksheet for obtaining the intake of Pb (in mg/day * kg-body weight) through ingestion of soil (DU) and inhalation of dust (IP), based on the algorithms of the HESP model, version 2.1 (Shell, 1994a,b). As already mentioned above, the distribution of time has been modified for the Lavrion situation (refer to Table 11.3, p.329).

Table 11.5. Estimated time spent inside, outside or away from the contaminated site for each land use category, in hours/day, for children in Lavrion [First input into the HESP model].
Πίνακας 11.5. Εκτίμηση του χρόνου εντός, εκτός ή μακριά από τη ρυπασμένη περιοχή για κάθε κατηγορία χρήσης γης, σε ώρες/ημέρα, για τα παιδιά του Λαυρίου [Αρχική εισαγωγή στο μοντέλο HESP].

Activity	*Summer*				*Winter*			
	Recreational	*Residential*	*Agricultural*	*School*	*Recreational*	*Residential*	*Agricultural*	*School*
D,act	5	5	5	5	4	5	5	5
t,sleep	0	10	10	0	0	10	10	0
t,away,active	16	6	6	18	22	6	6	18
t,out,active	8	4	5	2	2	1	1	2
t,ins,active	0	4	3	4	0	7	7	4
t,away,passive	24	0	0	24	24	0	0	24
t,out,passive	0	6	8	0	0	2	2	0
t,ins,passive	0	8	6	0	0	12	12	0

Note: For notation used refer to legend of Table 11.3, p.329.

Table 11.6. Fraction of time spent annually indoors, outdoors, sleeping away or away from Lavrion based on the HESP model equation 11.4 for a four year-old child and a body weight of 15 kg.
Πίνακας 11.6. Μέρος του χρόνου που αφιερώνεται ανά έτος εντός, εκτός, διανυκτέρευση εκτός ή μακριά από το Λαύριο, βασισμένο στην εξίσωση 11.4 του μοντέλου HESP για ένα παιδί ηλικίας τεσσάρων χρονών και βάρους 15 κιλών.

Activity	*Summer*[1]				*Winter*[1]				*Variables*	*Values*	*Units*
	Rec	*Res*	*Agr*	*School*	*Rec*	*Res*	*Agr*	*School*	AID	1100	mg/day
N,sleep	0.000	0.149	0.149	0.000	0.000	0.149	0.149	0.000	$f_{a,ing}$	0.300	Dimensionless
N,away,act	0.238	0.089	0.089	0.268	0.262	0.089	0.089	0.268	$f_{rs,i}$ (totals)	0.500	Dimensionless
N,out,act	0.119	0.060	0.074	0.030	0.024	0.015	0.015	0.030	f_i	0.099	Dimensionless
N,ins,act	0.000	0.060	0.045	0.060	0.000	0.104	0.104	0.060	f_o	0.901	Dimensionless
N,away,pas	0.357	0.000	0.000	0.357	0.286	0.000	0.000	0.357	DAE_i	0.001	Kg/m^2
N,out,pas	0.000	0.089	0.119	0.000	0.000	0.030	0.030	0.000	DAE_o	0.005	Kg/m^2
N,ins,pas	0.000	0.119	0.089	0.000	0.000	0.179	0.179	0.000	weight	15	kg
[1]Note: $N_x = \sum \mathbf{t_x1_y}/24 * (\mathbf{t_x2_y}/7) * \boldsymbol{f_x}$ (for legend refer to equation 11.4 on p.327)									age	4	Years

Note: For other notation used refer to legend of Table 11.3 on p.329, and equations 11.2 & 11.3 on p.327

AID	Amount of soil ingested daily (mg/day) based on the average amount on a yearly basis	Ημερήσια ποσότητα (mg/ημέρα) του εδάφους που προσλαμβάνεται μέσω κατάποσης βασισμένη στη μέση ετήσια ποσότητα
$f_{a,ing}$	Fraction intake/uptake for ingestion (bioavailability)	Κλάσμα πρόσληψης/απορρόφησης για κατάποση (βιοδιαθεσιμότητα)
$f_{rs,i}$	Fraction of soil in dust (indoors)	Κλάσμα του εδάφους στη σκόνη σπιτιών (εντός οικίας)
f_i	Fraction of indoor soil or dust covering the skin	Κλάσμα εδάφους ή σκόνης εντός της οικίας που καλύπτει την επιδερμίδα (kg/m^2)
f_o	Fraction of outdoor soil or dust covering the skin	Κλάσμα εδάφους ή σκόνης εκτός της οικίας που καλύπτει την επιδερμίδα (kg/m^2)
DAE_I	Amount of indoor soil or dust on the skin (kg/m^2)	Ποσότητα εδάφους ή σκόνης εντός της κατοικίας που βρίσκεται πάνω στην επιδερμίδα (kg/m^2)
DAE_o	Amount of outdoor soil or dust on the skin (kg/m^2)	Ποσότητα εδάφους ή σκόνης εκτός της κατοικίας που βρίσκεται πάνω στην επιδερμίδα (kg/m^2)

Table 11.7. Uptake from direct ingestion of soil or dust per unit body weight per season (mg soil/day) based on HESP model equations 11.2 and 11.3 (on p. 327 above).
Πίνακας 11.7. Πρόσληψη διά απ' ευθείας κατάποσης του εδάφους ή σκόνης ανά μονάδα βάρους του σώματος για κάθε εποχή (mg εδάφους/ημέρα) βασισμένη στις εξισώσεις 11.2 και 11.3 του μοντέλου HESP (βλ. ανωτέρω).

ActIvity	*Summer*				*Winter*			
	Recreational	*Residential*	*Agricultural*	*School*	*Recreational*	*Residential*	*Agricultural*	*School*
DU,away,act	-	-	-	-	-	-	-	-
DU,out,act	117.996	58.998	73.747	29.499	23.599	14.749	14.749	29.499
DU,ins,act	0.000	5.183	3.887	5.183	0.000	9.069	9.069	5.183
DU,away,pas	0.000	0.000	0.000	0.000	0.000	0.000	0.000	0.000
DU,out,pas	0.000	88.497	117.996	0.000	0.000	29.499	29.499	0.000
DU,ins,pas	0.000	10.365	7.774	0.000	0.000	15.548	15.548	0.000

Note: For notation refer to equations 11.2 and 11.3 on p.327 above.

11.5.1.2.1.1.5. Using Idrisi® GIS to combine the information

Two maps were created in *Idrisi® GIS* using the "image calculator", both combining data from the Microsoft® Excel® worksheet (see Section 11.5.1.2.1.1.4 above, and Tables 11.5 to 11.7) using the kriged soil-Pb concentrations maps (extractable and total Pb contents).

The first exposure map (Map 11.8) combines the rate of direct ingestion of soil and dust calculated in Excel® and the extractable kriged concentration of Pb (values of first and second extractions are added). The *Idrisi® GIS* image calculator is then used to divide the result by the child's body weight.

The second exposure map (Map 11.9) combines the rate of direct ingestion of soil calculated in Excel® and the total kriged concentration of Pb at each cell. The *Idrisi® GIS* image calculator is subsequently used to multiply the result by the bioavailability factor for ingested Pb, and the result is divided by the child's body weight. Since the body weight of each child at Lavrion was not available, an average for 6-7 year old children in the United Kingdom from the CLEA model (Ferguson, 1995) was used.

The methodology is explained in detail by Demetriades *et. al.* (1998).

11.5.1.2.2. Exposure assessment map using the IEUBK model as a basis

The Integrated Exposure Uptake-Biokinetic model (IEUBK) (US EPA, 1994) is a mathematical model that derives a deterministic estimate for blood-Pb concentration in young children based on environmental exposure to Pb from various sources including soil (Tsuhi and Searl, 1996). The main objective is to predict blood-Pb levels for children from 1 to 84 months old (7 years old). The IEUBK mode has two principal components:

1. uptake sub-model (includes intake and absorption of Pb from different sources), and
2. biokinetic sub-model (calculation of a blood-Pb value from uptake).

The user is able to specify uptake, but not biokinetic assumptions, which are included in the model by default.

The quantitative exposure map using the IEUBK model is based directly on the "batch mode" run, *i.e.,* the soil Pb concentration for a house is used to estimate an individual child's mean blood-Pb level, and percentage of risk of exceeding a given blood-Pb level (Doe, 1995). All default values of the model are used. These results were imported into the *Idrisi® GIS* for creating the **Quantitative Exposure Map based on the IEUBK model and the total soil-Pb concentration** (Maps 11.11 & 11.12). Map 11.11 includes children below the age of 7-years-old (n=75), and Map 11.12 children of all ages, and since there were children living in the same house or flat, the last child belonging to each house or flat was used in this analysis (n=184). For comparison purposes the actual measured blood-Pb concentrations of children below the age of 7-years-old are displayed on Map 11.10 (n=75).

11.5.2. METHOD OF SEMI-QUANTITATIVE HAZARD ASSESSMENT MAPPING

According to the definition of hazard (Callow, 1998) a toxic chemical is not necessarily hazardous if the circumstances in which it occurs prevent the potential for harm. The quantitative hazard mapping described above, however, provides a simplistic approach, since the hazard is only related to Pb concentration in overburden materials, including soil. Other environmental factors that can influence its accessibility to children are disregarded, so providing a single objective/single criterion decision rule. In order to classify the areas according to the level of *"Pb accessible to children from fine-grained overburden materials, including soil, and dust"*, a single objective/multi-criteria evaluation needs to be applied (Fig. 11.4). This can be achieved using the procedure called Multi-Criteria Evaluation (MCE) (Eastman, 1997), whereby the criteria are combined according to the objective of the decision. MCE is run using the weighted linear combination (WLC) procedure in *Idrisi®* GIS, for which continuous criteria (factors) and Boolean constraints are standardised to a common numeric range, and then

combined by means of a weighted average. A somewhat similar procedure has been applied to address mineral exploration issues (Bonham-Carter, 1994).

The methodology has been called semi-quantitative hazard mapping, because it is based on maps containing both qualitative information (*e.g.,* lithology and land use) and quantitative information (*e.g.,* Pb concentration in overburden, including soil). The analysis relies on a numerical categorisation of hazard, which is created partly using fuzzy logic. Fuzzy sets enable the classification of parameter groups, that are not delimited by sharp boundaries, *i.e.,* the transition between membership and non-membership of a fuzzy set is gradational (Eastman, 1997).

The methodology developed for computing the semi-quantitative hazard map based on MCE and WLC involves five basic steps:

(1) setting the objective,
(2) selecting,
(3) weighting and (4) standardising the criteria, and
(4) creating the maps.

11.5.2.1. Weighting the factors

The *Idrisi*® GIS module "Weight" is used to develop a set of relative weights for a group of factors in a multi-criteria evaluation. The weights are developed by providing a series of pairwise comparisons of the relative importance of factors to the suitability of pixels for the hazard being evaluated. These pairwise comparisons are then analysed to produce a set of weights that sum to 1. The factors, and their resulting weights, can be used as input to the Multi-Criteria Evaluation (MCE) module for Weighted Linear Combination (WLC) or ordered weighted average (or the "Scalar" and "Overlay" modules). The procedure by which the weights are produced follows the logic developed by Saaty (1977) under the Analytical Hierarchy Process (AHP) (Eastman, 1997).

The rating used to develop the pairwise comparisons is given in Table 11.8.

Table 11.8. Rating for developing the pairwise comparisons.
Πίνακας 11.8. Βαθμονόμηση για την ανάπτυξη των συγκρίσεων ανά ζεύγος.

Rating	*Rating description*
9	Extremely strongly more important
7	Very strongly more important
5	Strongly more important
3	Moderately more important
1	Equally important
1/3	Moderately less important
1/5	Strongly less important
1/7	Very strongly less important
1/9	Extremely strongly less important

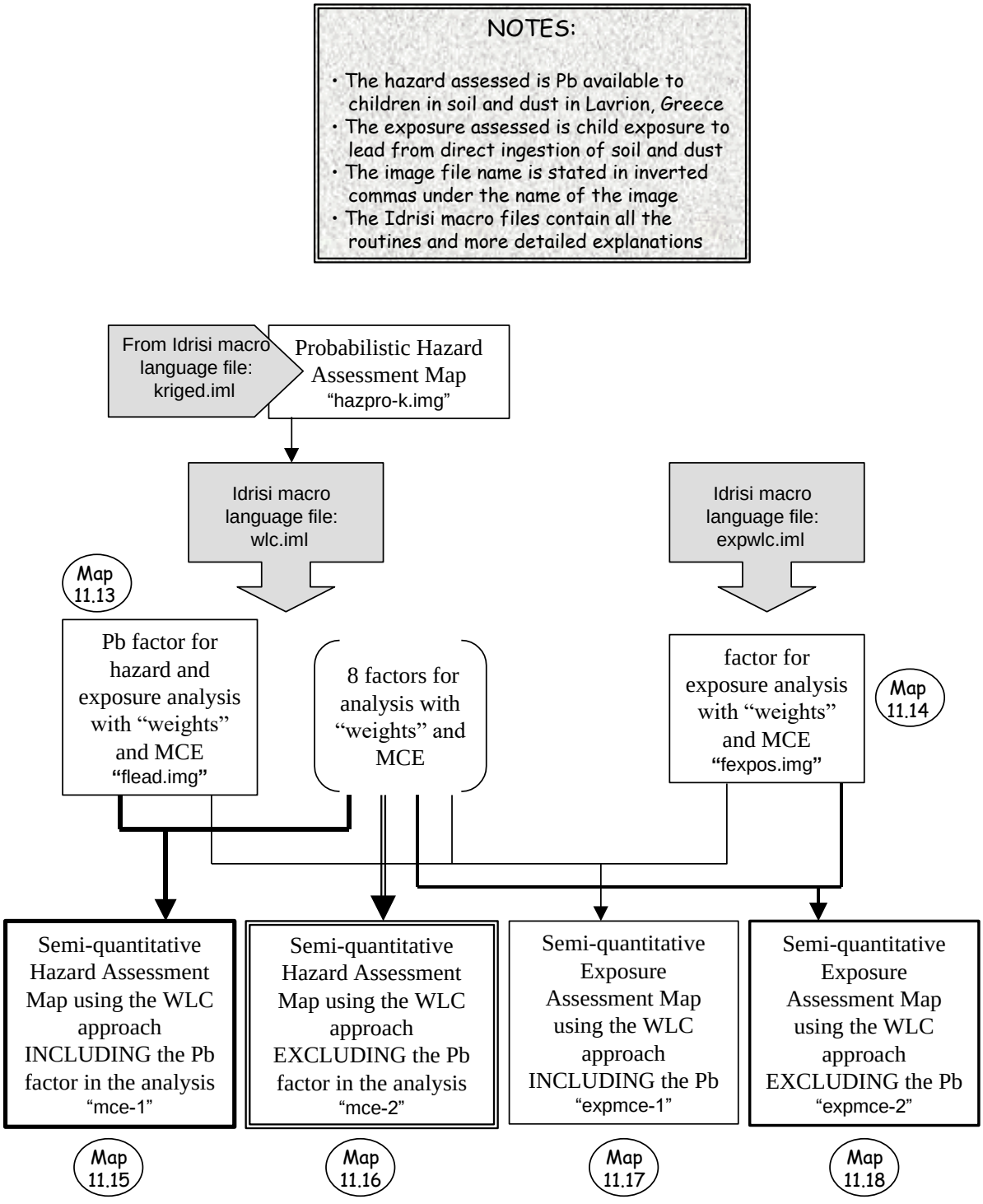

Fig. 11.4. Semi-quantitative Hazard and Exposure Assessment maps using Weighted Factors and Linear Combination (WLC) [for more details refer to Tristán *et. al.*, 1998].
Σχ. 11.4. Χάρτες ημιποσοτικής εκτίμησης της Επικινδυνότητας και Έκθεσης χρησιμοποιώντας τη μέθοδο του Βαρυ-γραμμικού συνδυασμού (WLC) [για περισσότερες λεπτομέρειες βλ. Tristán *et. al.*, 1998].

11.5.2.2. Fuzzy Set Membership functions

Fuzzy Sets are sets (or classes) without sharp boundaries; that is, the transition between membership and non-membership of a location in the set is gradual (Zadeh, 1965; Eastman, 1997). A Fuzzy Set is characterized by a fuzzy membership grade (also called a possibility) that ranges from 0 to 255, indicating a continuous increase from non-membership to complete membership. Four fuzzy set membership functions are provided in the *Idrisi®* GIS: Sigmoidal, J-Shaped, Linear and User-defined. Figure 11.5 shows the monotonically decreasing J-shaped function and the positions of the inflection points. It should be pointed out, that with the J-shaped function, the function approaches 0, but only reaches it at infinity. Thus, the inflection points (a) and (d) indicate the points at which the function reaches 0.5 rather than 0.

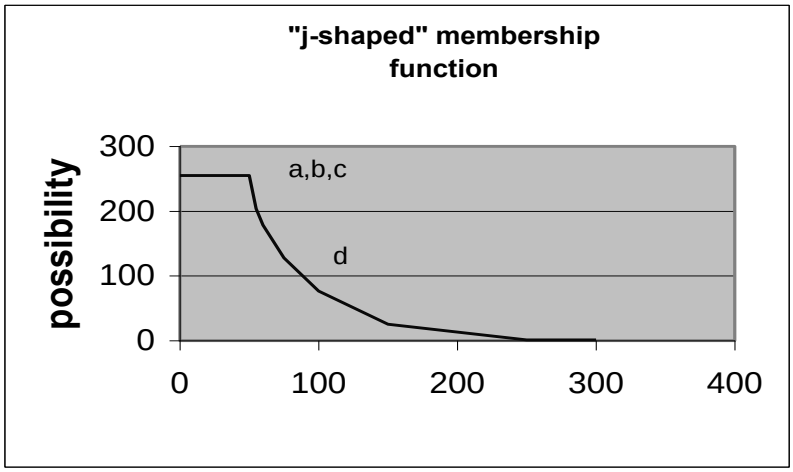

Fig. 11.5. It shows the monotonically decreasing J-shaped function and the positions of the inflection points of the fuzzy set curve.
Σχ. 11.5. Απεικόνιση της μονοτονικά φθίνουσας συνάρτησης μορφής-J και των θέσεων των σημείων καμπής της καμπύλης της ομάδας ασαφούς συνόλου.

11.5.2.3. Criteria for Weighted Linear Combination (WLC) and Multi-Criteria Evaluation (MCE)

Criteria may be of two types: *factors* and *constraints*. *Factors* are generally continuous in nature; they indicate the relative suitability of certain areas. *Constraints*, on the other hand, are always Boolean in character. They serve to exclude certain areas from consideration. *Factors* and *constraints* can be combined in the MCE module of *Idrisi®* GIS.

Criteria are further classified into two groups, *categorical* and *numerical*. *Categorical or qualitative* variables have values with no intrinsic meaning as numbers (Rasmussen, 1992); in effect the values cannot be interpreted as numbers, because of their qualitative nature. Categorical variables characterise or qualify explicitly the site, and may comprise either a range of numbers (*e.g.*, element concentration values), or may have two possible values, yes and no, which can be represented by numbers, such as 1 and 0.

Numerical or quantitative variables, on the other hand, have numerical values that are measurements or counts, and can be interpreted as such. Nine criteria were

selected for the WLC and MCE analysis among a larger number that could be influencing the hazard. These criteria are described below.

11.5.2.3.1. Categorical criteria

11.5.2.3.1.1. Pb concentration in soil (factor)

Pb concentration in soil is taken as a factor for multi-criteria evaluation only for the first Hazard Map (Map 11.13). The Probabilistic Hazard Assessment using kriging uncertainty (Map 11.7) is the basis of Map 11.13 (Lead factor for hazard and exposure assessment by WLC and MCE). The "contaminated" category is given a new value of 255 (the highest hazard) and the "probably contaminated" category is given a value of 200.

It is hereby noted that for the construction of the semi-quantitative hazard and exposure assessment maps, an arbitrary scale from 0 (minimum) to 255 (maximum) is used for the hazard and exposure values.

11.5.2.3.1.2. Degree of dustiness of the metallurgical processing wastes (factor)

Metallurgical processing or smelter wastes with a higher proportion in the fine grain-size fraction are more likely to generate dust. The categories present in the metallurgical wastes map (Map 2.3) are given a value of hazard, related to the assumed degree of dustiness of the waste, and transportation of fine-grained material by aeolian processes (Table 11.9). At the time that this study was carried out there were no data about the grain-size distribution of metallurgical processing wastes and contaminated soil. Nevertheless, the data presented in Table 11.9 are adequate for the present study.

Table 11.9. Hazard values of the degree of dustiness of the metallurgical processing wastes.
Πίνακας 11.9. Τιμές επικινδυνότητας του βαθμού κονιορτοποίησης των μεταλλουργικών απορριμμάτων.

Category No.	*Category*	*Hazard value*
2	Beneficiation/flotation residues	255
6	Sand-blast wastes	255
8	Pyritiferous flotation residues	255
7	Beneficiation/flotation sands with disseminated pyrite	200
4	Slag with sand-blast wastes	125
10	Beneficiation/flotation sands and coarse-grained flotation	125
11	Beneficiation/flotation residues with disseminated slag	125
5	Disseminated slag	75
3	Slag	75
9	Disseminated slag and coarse-grained flotation residues	75
1	Areas with no metallurgical residues (contaminated soil)	0

11.5.2.3.1.3. Area over metal-related industry (constraint)

Those industries that use metallic products are likely to increase the level of Pb available to children. All categories with metal-related industry present in the land use map (Map 2.4) are given a value of hazard (Table 11.10). The two categories of other "industries & storage sites" and the "cotton weaving industries" are assigned a low hazard value.

Table 11.10. Hazard value given to all industries and Municipal waste site.
Πίνακας 11.10. Τιμές επικινδυνότητας που δίδονται για όλες τις βιομηχανίες και τη χωματερή του Δήμου.

Category No.	*Category*	*Hazard value*
16	Ore treatment plants and storerooms	255
18	Lead-acid battery factory	255
17	Sandblasting units with slag	200
19	Factories: explosives, ammunition, artillery	200
20	Petrol stations, lorry garages and motor repairs	150
21	Iron converter industries	150
22	Aluminium converter industries	150
27	Municipal waste site	150
23	Other industries and storage sites	50
24	Cotton weaving industries	50

11.5.2.3.1.4. Over Quaternary deposits (constraint)

Quaternary deposits may contain a higher concentration of Pb, as they may comprise erosion products from the mineralised areas upstream and/or wastes from past mining and ore processing activities. The map of lithology displaying the geographical extent of Quaternary deposits is used (Map 2.2). If the area is over Quaternary deposits a value of 255 is given. All other areas are given a value of 0.

11.5.2.3.2. <u>Numerical criteria</u>

11.5.2.3.2.1. Proximity to metallurgical processing wastes (factor)

Areas close to the dustiest metallurgical processing wastes have a higher hazard. Wastes that are likely to create an impact at a distance by generating larger amounts of dust are selected from the map of metallurgical processing wastes (Map 2.3), and are tabulated in Table 11.11 together with the assigned category number.

Table 11.11. Metallurgical processing wastes considered as generating dust by aeolian processes.
Πίνακας 11.11. Οι κατηγορίες των μεταλλουργικών απορριμμάτων που θεωρούνται ότι δημιουργούν σκόνη μέσω των αιολικών διεργασιών.

Category No.	*Category of metallurgical processing wastes*
2	Beneficiation/flotation residues
6	Sandblast wastes
8	Pyritiferous flotation residues
7	Beneficiation/flotation sands with disseminated pyrite
4	Slag with sandblast wastes
10	Beneficiation/flotation sands and coarse-grained flotation residues
11	Beneficiation/flotation residues with disseminated slag

"Slag", "disseminated slag" and "disseminated slag & coarse-grained flotation residues" are the remaining categories than are not selected in this case, for they do not generate dust by natural means (wind-blown). Dust could, however, be generated if they are tampered with by humans, as for example when the slag was loaded and transported to the harbour, for use as hardcore of the new platform extending into the sea, or in other constructions. Hazardous actions created by human negligence!

The fuzzy set membership function for the proximity to metallurgical processing wastes is defined. It is a monotonically decreasing J-shaped function, with inflection points at c=50 and d=100.

11.5.2.3.2.2. Proximity to industry (factor)

The industries that could be generating dusts containing Pb are selected.

11.5.2.3.2.3. Proximity to current or previous stacks (factor)

Impact of emissions from the metallurgical processing and lead-acid battery plants is taken into account. The fuzzy set membership function for proximity to current or previous stacks is defined. It is a monotonically decreasing J-shaped function, with inflection points at c=100 and d=200.

11.5.2.3.2.4. Proximity to rivers (factor)

The process of fluvial deposition of erosion products from the mineralised areas upstream and/or the waste products from mining, described also for Quaternary deposits (see above, is likely to have occurred close to the river beds. The fuzzy set membership function for proximity to rivers is defined. It is a monotonically decreasing J-shaped function, with inflection points at c=50 and d=75.

11.5.2.3.2.5. Proximity to roads (factor)

At the time of the blood-Pb survey, most of the roads in Lavrion were not covered by asphalt. Hence, they could be an important source of dust. The fuzzy set membership function for proximity to non-asphalt roads is defined. It is a monotonically decreasing J-shaped function, with inflection points at c=50 and d=75.

11.5.2.4. Relative weights for the semi-quantitative hazard assessment mapping

The relative weights for the different semi-quantitative hazard assessment maps are tabulated in Tables 11.12 and 11.13.

Table 11.12. Relative weights for the semi-quantitative hazard assessment map ***including*** soil-Pb concentration as a factor (Map 11.15).
Πίνακας 11.12. Σχετικά βάρη του χάρτη ημιποσοτικής εκτίμησης επικινδυνότητας, που ***συμπεριλαμβάνει*** ως παράγοντα και τις συγκεντρώσεις μολύβδου (Pb) στο έδαφος (Χάρτης 11.15).

Factor and constraint	*Pb contents in overburden*	*Proximity to industry*	*Proximity to smelter wastes*	*Degree of dustiness of waste*	*Over Quaternary deposits*	*Proximity to stacks*	*Proximity to roads*	*Proximity to rivers*	*Over metal related industry*
Pb contents in overburden	1								
Proximity to industry	1/5	1							
Proximity to smelter wastes	1/5	1	1						
Degree of dustiness of smelter wastes	1	5	5	1					
Over Quaternary deposits	1/7	1/5	1/5	1/7	1				
Proximity to stacks	1/5	1	1	1/5	3	1			
Proximity to roads	1/5	1	1	1/5	3	1	1		
Proximity to rivers	1/9	1/7	1/7	1/9	1/5	1/7	1/5	1	
Over metal related industry	1/7	1/3	1/3	1/7	1	1/3	1/3	3	1/5

Note: The factors are rated according to the 9-point scale mentioned in Section 11.5.3.1 (Table 11.8)

Table 11.13. Relative weights for the semi-quantitative hazard assessment map *excluding* soil-lead (Pb) concentration (Map 11.16).
Πίνακας 11.13. Σχετικά βάρη του χάρτη ημιποσοτικής εκτίμησης της επικινδυνότητας, που *δεν συμπεριλαμβάνει* τις συγκεντρώσεις μολύβδου (Pb) στο έδαφος (Χάρτης 11.16).

Factor and constraint	*Proximity to industry*	*Proximity to smelter wastes*	*Degree of dustiness of waste*	*Over Quaternary deposits*	*Proximity to stacks*	*Proximity to roads*	*Proximity to rivers*	*Over metal related industry*
Proximity to industry	1							
Proximity to smelter wastes	1	1						
Degree of dustiness of smelter wastes	3	3	1					
Over Quaternary deposits	1/5	1/5	1/7	1				
Proximity to stacks	1/3	1/3	1/5	3	1			
Proximity to roads	1/3	1/3	1/5	3	1/3	1		
Proximity to rivers	1/7	1/7	1/9	1/3	1/7	1/5	1	
Over metal related industry	3	3	1/3	5	3	3	7	1

Note: The factors are rated according to the 9-point scale mentioned in Section 11.5.3.1 (Table 11.8)

11.5.2.5. Weights for the semi-quantitative hazard and exposure assessment maps

The weights of the different criteria used in the semi-quantitative hazard and exposure assessment maps are given in Table 11.14.

Table 11.14. Weights of the different criteria used in the semi-quantitative hazard and exposure assessment maps (Maps 11.15 to 11.18).
Πίνακας 11.14. Βάρη των διαφόρων κριτηρίων που χρησιμοποιήθηκαν στους χάρτες ημιποσοτικής εκτίμησης της επικινδυνότητας και έκθεσης (Χάρτες 11.15 έως 11.18).

Factor and constraint	*Weights for Hazard Map with soil-Pb factor[1] (Map 11.15)*	*Weights for Hazard Map without soil-Pb factor[2] (Map 11.16)*	*Weights for Exposure Map with soil-Pb factor[3] (Map 11.17)*	*Weights for Exposure Map without soil-Pb factor[4] (Map 11.18)*
(a) Likely to increase the Pb concentration in soil:				
• Soil Pb concentration	0.2881	N/A [a]	0.2157	N/A [a]
• Over metal-related industry	0.0520	0.2121	0.0404	0.1511
• Proximity to industry	0.0850	0.1337	0.0612	0.0997
• Proximity to stacks	0.0787	0.0816	0.0582	0.0603
• Proximity to rivers	0.0151	0.0182	0.0128	0.0151
• Over Quaternary deposits	0.0323	0.0320	0.0248	0.0246
(b) Likely to make Pb more accessible to children:				
• Proximity to roads	0.0757	0.0577	0.0560	0.0481
• Dustiness of wastes	0.2881	0.3308	0.1998	0.2468
• Proximity to wastes	0.0850	0.1337	0.0612	0.0997
• Time of exposure	N/A[a]	N/A[a]	0.2699	0.2544

Notes: [a] N/A - Not applicable
[1&3]Consistency ratio = 0.10; Consistency is acceptable
[2&4]Consistency ratio = 0.06; Consistency is acceptable.

11.5.3. METHOD OF SEMI-QUANTITATIVE EXPOSURE ASSESSMENT MAPPING

Similar logic has been applied to the exposure assessment, as described above, for the semi-quantitative hazard assessment mapping. The quantitative exposure assessment provides an *Average Daily Exposure* (ADE) that is compared with a *Tolerable Daily Intake* (TDI) in order to assess risk. It consists again of a single criterion decision rule. Exposure, however, is a function of both hazard and the *time of exposure*. Therefore, the same multi-criteria used to assess a hazard may also be employed to assess

exposure, adding a further criterion that is related to the time of exposure. This factor concerning *"time of exposure"* depends on the social characteristics of the population, the distribution of their time and their activity patterns.

11.5.3.1. Criteria used for the semi-quantitative exposure assessment maps

The semi-quantitative exposure assessment maps are based on the same nine or ten criteria, *factors and constraints*, used for the semi-quantitative hazard assessment mapping, but it includes an additional *factor of exposure*. This factor is related to the amount of time that a child might spend at the location. The land use map (Map 2.4) is the basis for the map of the exposure factor for hazard assessment by WLC and MCE (Map 11.14).

The schools, agricultural areas, residential areas and recreational areas are given a value of "exposure" on a scale from 0 to 255. It is assumed that the child will be spending only part of his day at school.

11.5.3.2. Relative weights for the semi-quantitative exposure assessment maps

The relative weights used for the different criteria of the two semi-quantitative exposure assessment maps, with or without Pb concentrations, are given in Tables 11.15 to 11.16. It is again noted that the criteria and weights are the same as for the semi-quantitative hazard assessment maps (Tables 11.13 to 11.14), but the semi-quantitative exposure assessment maps include an extra criterion, *exposure time*.

Table 11.15. Relative weights for the semi-quantitative exposure assessment map *including* soil-lead (Pb) concentrations as a factor (Map 11.17).
Πίνακας 11.15. Σχετικά βάρη για το χάρτη ημιποσοτικής εκτίμησης της έκθεσης, που *συμπεριλαμβάνει* ως παράγοντα τις συγκεντρώσεις μολύβδου (Pb) στο έδαφος (Χάρτης 11.17).

Factors and constraints	*Pb contents in over-burden*	*Proximity to industry*	*Proximity to smelter wastes*	*Degree of dustiness of waste*	*Over Quaternary deposits*	*Proximity to stacks*	*Proximity to roads*	*Proximity to rivers*	*Over metal related industry*	*Time of exposure*
Pb contents in overburden	1									
Proximity to industry	1/5	1								
Proximity to smelter wastes	1/5	1	1							
Degree of dustiness of smelter wastes	1	5	5	1						
Over Quaternary deposits	1/7	1/5	1/5	1/7	1					
Proximity to stacks	1/5	1	1	1/5	3	1				
Proximity to roads	1/5	1	1	1/5	3	1	1			
Proximity to rivers	1/9	1/7	1/7	1/9	1/5	1/7	1/5	1		
Over metal related industry	1/7	1/3	1/3	1/7	1	1/3	1/3	3	1/5	
Time of exposure	1	7	7	3	9	5	5	5	5	1

Note: The factors are rated according to the 9-point scale mentioned in Section 11.5.3.1 (Table 11.8, p.333)

Table 11.16. Relative weights for the semi-quantitative exposure assessment map *excluding* the soil-Pb concentration factor (Map 11.18).
Πίνακας 11.16. Σχετικά βάρη για το χάρτη ημιποσοτικής εκτίμησης της έκθεσης, που *δεν συμπεριλαμβάνει* ως παράγοντα τις συγκεντρώσεις μολύβδου (Pb) στο έδαφος (Χάρτης 11.18).

Factors and constraints	*Proximity to industry*	*Proximity to smelter wastes*	*Degree of dustiness of waste*	*Over Quaternary deposits*	*Proximity to stacks*	*Proximity to roads*	*Proximity to rivers*	*Over metal related industry*	*Time of exposure*
Proximity to industry	1								
Proximity to smelter wastes	1	1							
Degree of dustiness of smelter wastes	3	3	1						
Over Quaternary deposits	1/5	1/5	1/7	1					
Proximity to stacks	1/3	1/3	1/5	3	1				
Proximity to roads	1/3	1/3	1/5	3	1/3	1			
Proximity to rivers	1/7	1/7	1/9	1/3	1/7	1/5	1		
Over metal related industry	3	3	1/3	5	3	3	7	1	
Time of exposure	3	3	1	9	7	3	9	3	1

Note: The factors are rated according to the 9-point scale mentioned in Section 5.1.

11.6. COMPARISON BETWEEN OBSERVED BLOOD-LEAD AND MODEL PREDICTIONS

11.6.1. COMPARISON BETWEEN OBSERVED BLOOD-LEAD AND HESP PREDICTIONS

Figure 11.6 presents the correlation results between actual blood-Pb measurements in the "y" axis (Map 11.10) and the HESP model predictions in the "x" axis (Map 11.9) using total soil-Pb concentrations.

Figure 11.7 shows the correlation results between actual blood-Pb measurements in the "y" axis (Map 11.10) and the HESP model predictions in the "x" axis (Map 11.8) using the extractable Pb contents (addition of first and second step Pb extractions). Blood-Pb measurements are in μg Pb/dl of blood (multiplied by 10) and the HESP predictions are in (μg Pb/day/kg-BW).

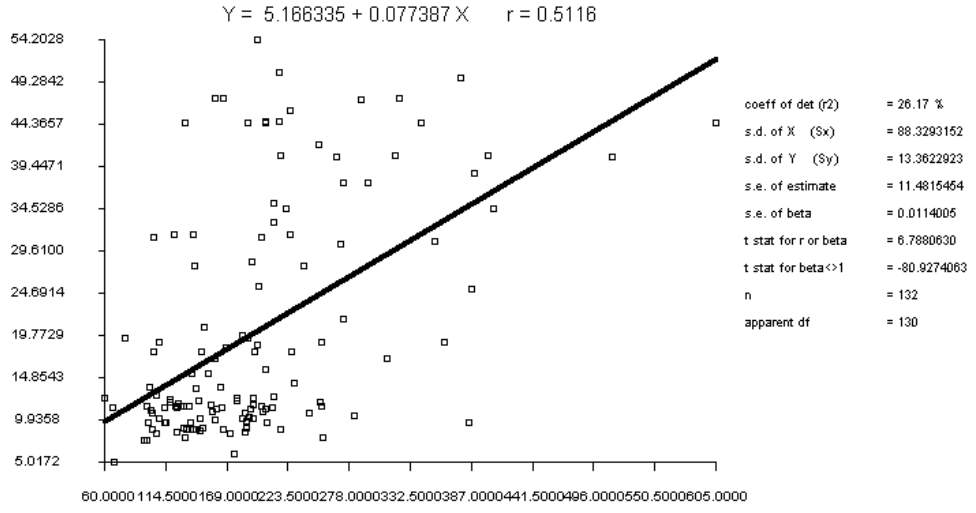

Fig. 11.6. Linear regression between actual blood-Pb measurements ("y" axis) and the HESP model predictions ("x" axis) using total soil-Pb concentrations.
Σχ. 11.6. Γραμμική συμμεταβολή μεταξύ των πραγματικών τιμών μολύβδου (Pb) στο αίμα (άξονας "y") και των προβλέψεων του μοντέλου HESP (άξονας "x") χρησιμοποιώντας τις ολικές συγκεντρώσεις του μολύβδου (Pb) στο έδαφος.

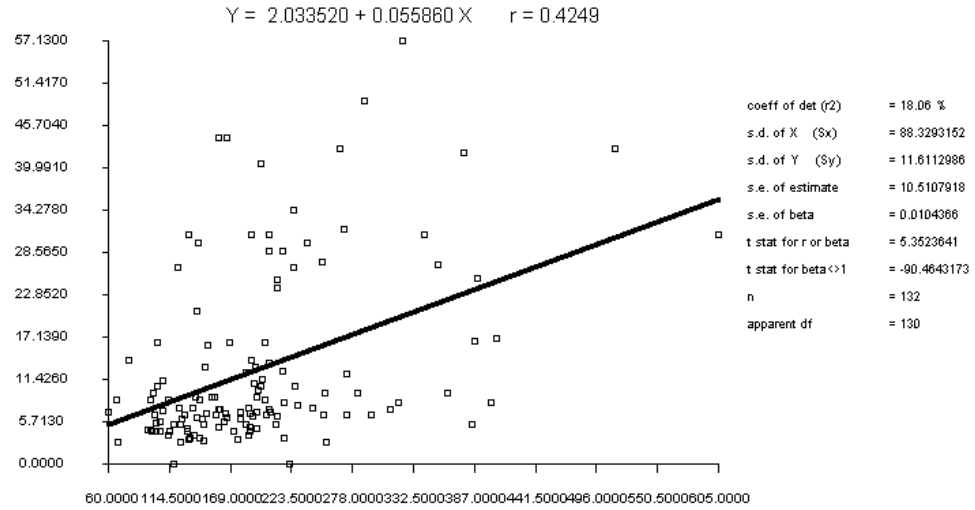

Fig. 11.7. Linear regression between actual blood-Pb measurements ("y" axis) and the HESP model predictions ("x" axis) using extractable soil-Pb concentrations (addition of first and second step Pb extractions).
Σχ. 11.7. Γραμμική συμμεταβολή μεταξύ των πραγματικών τιμών μολύβδου (Pb) στο αίμα (άξονας "y") και των προβλέψεων του μοντέλου HESP (άξονας "x") χρησιμοποιώντας τις εύκολα εκχυλίσιμες συγκεντρώσεις του μολύβδου (Pb) στο έδαφος (άθροισμα πρώτης και δεύτερης φάσης εκχύλισης του Pb).

11.6.2. Comparison Between Observed Blood-Lead and IEUBK Predictions

Figure 11.8 displays the correlation results between actual blood-Pb measurements in the "y" axis (Map 11.10) and the IEUBK model predictions using total soil-Pb concentrations in the "x" axis (Map 11.11). It is noted that not all the children are included. Only the last child belonging to each house is recorded. Both variables have the same units: μg Pb/dl of blood (multiplied by 10).

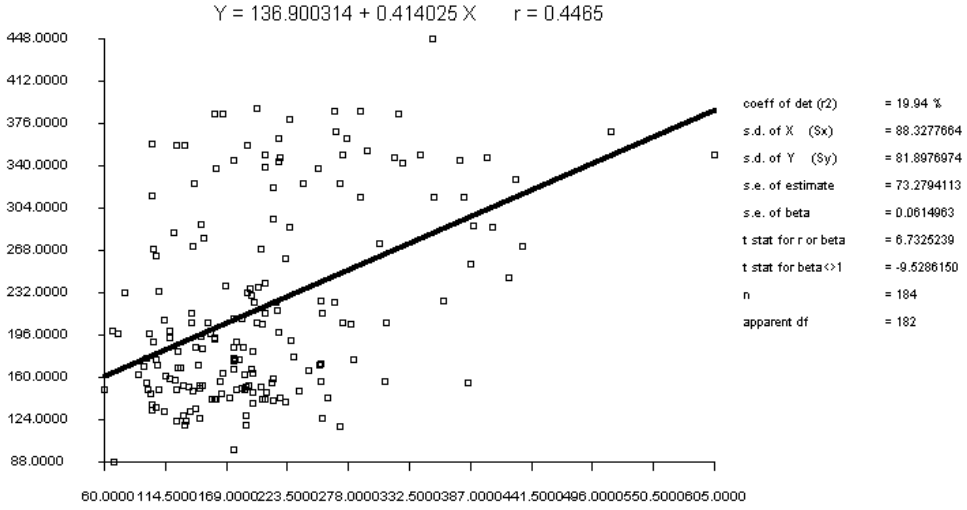

Fig. 11.8. Linear regression between actual blood-Pb measurements ("y" axis) and the IEUBK model predictions ("x" axis) using total soil-Pb concentrations.
Σχ. 11.8. Γραμμική συμμεταβολή μεταξύ των πραγματικών τιμών μολύβδου (Pb) στο αίμα (άξονας "y") και των προβλέψεων του μοντέλου IEUBK (άξονας "x") χρησιμοποιώντας τις ολικές συγκεντρώσεις του μολύβδου (Pb) στο έδαφος.

11.7. RESULTS AND DISCUSSION

11.7.1. QUANTITATIVE HAZARD MAPPING

The **Hazard Identification Map** (Map 11.1) displays the high level of total Pb concentrations in soil (overburden) across the area; these vary from 810 to 152,000 μg Pb/g soil (see also Map 3.4).

The regulatory threshold used for the **Deterministic Hazard Assessment Map** (Map 11.2) is the ICRCL (1987) trigger concentration for domestic gardens and allotments, 500 μg Pb/g soil. This statutory threshold has been selected to demonstrate the methodology at the highly contaminated urban area of Lavrion. Most of the samples are contaminated according to this classification, but this approach ignores the uncertainty in the measurements.

The Probabilistic Hazard Assessment Maps based on total soil Pb concentration at each sampling site are based on an assumed measurement uncertainty of

(a) 10% (Map 11.3), and
(b) 80%, taken as the worst-case scenario (Map 11.4).

A comparison of the deterministic and probabilistic hazard assessment maps shows, in both cases, that the major part of the soil cover is contaminated. The large measurement uncertainty of 80% has, nevertheless, a small effect in expressing a reduced probability of contamination, except at a small proportion of localities (mainly in the N, W and S of the area). This contrasts with the large effect of the probabilistic approach, when areas have concentrations close to the statutory threshold value (Ramsey and Argyraki, 1997). The “probably contaminated land” displayed in the **Probabilistic Hazard Assessment Map based on kriged soil Pb concentrations** (Map 11.7) is more frequent in those areas where the sampling density is lower (*i.e.*, kriging standard error of estimation is high), at the N, W and S of the study area.

11.7.2. QUANTITATIVE EXPOSURE MAP BASED ON THE IEUBK MODEL

From the 234 children that participated in the biomedical survey, only those with ages below 84 months (7-years-old) were selected, since it is the last category considered in the IEUBK model. The total number of children in this age group is 103 with an average age (AM) of 6.5-years-old. The number of children used in the analysis is further reduced to 75, as some of the children live in the same house, and only the first is recorded in the GIS database (Map 11.11). Another drawback is that it is not possible to predict, by using the IEUBK model in batch mode, the exposure from soil and dust only. Therefore, the predicted blood-Pb level is estimated from all other possible pathways (*i.e.*, water, air, food, *etc.*). Nevertheless, by checking the results in normal mode, the magnitude of the intake from soil and dust is much higher than that from all the other pathways of exposure.

The measured blood-Pb has an arithmetic mean (am) and standard deviation (sd) of 19.1 and 8.6 μg Pb/dl blood respectively; whereas the predicted blood-Pb has, correspondingly, values of 21.1 and 8.6 μg Pb/dl blood. The Pearson’s correlation coefficient between predicted (dependent variable) and measured (independent variable) blood-Pb levels is 0.41 which is statistically significant (p=0.05). The regression equation for the relationship is:

- predicted blood-Pb level = 12.8 + (0.43 * measured blood-Pb level); [n = 75]

Model predictions are, therefore, higher than the measured blood-Pb levels by up to 22.4 µg/dl. From this value upward, the situation is the inverse, the predictions are lower than the measured values. The degree of scatter could be related to all the other factors not accounted for in the analysis, *i.e.*, specific time activity patterns, nutritional factors, and personal variability.

The highest positive residuals from the regression are located towards the central part of the Lavrion urban area, where there are very high levels of Pb in soil, which do not result in very high blood-Pb levels in children. Similarly, relatively high measured blood-Pb levels (from 25-30 µg Pb/dl blood) were not predicted by the model, in parts of Lavrion with much lower soil Pb levels, perhaps indicating contributions to blood-Pb from some other exposure route, or biokinetic differences among the child population.

11.7.3. QUANTITATIVE EXPOSURE ASSESSMENT MAPS BASED ON THE HESP MODEL

The equations and values used are given in section 11.5.1.2.1. All values used are the ones given by the HESP model, except those related to the time activity pattern. For this analysis factor N_y (fraction of time spent annually indoors, outdoors, sleeping or away from the location) is calculated using a child distribution of time estimated for Lavrion children (Table 11.3).

The DU (total direct ingestion of soil or dust) calculated for a house with a garden is 231.9-mg soil/day. Most children sampled for blood-Pb were between the ages of 7- and 8-years-old. The average body weight for a male child of 7.5-years-old, used in the CLEA model (Ferguson, 1995), was employed instead of the value provided by HESP, which is for a 4-year-old child. The weight is assumed constant and has a value of 24.2 kg.

One method of checking, the broad validity of the predicted exposure of children to Pb by this method, is to quantify the relationship with measured internal exposure as blood-Pb. Pearson's regression coefficient (r) for the relationship between predicted ADE using (i) extractable soil Pb concentrations (Map 11.8) and (ii) total soil Pb contents (Map 11.9), and the measured blood-Pb levels (Map 11.10) were found to be 0.34 and 0.40 respectively ($p<0.001$). Predictions with respect to extractable soil Pb concentrations (Map 11.8) are low compared to the measured blood-Pb contents especially in the North part of the Lavrion urban area. The correlation coefficient, r, between the predictions by IEUBK (Map 11.11) and by HESP (Map 11.9) is 0.95 ($p<0.001$).

11.7.4. SEMI-QUANTITATIVE HAZARD AND EXPOSURE ASSESSMENT MAPPING

11.7.4.1. Setting the objective

The primary objective of the semi-quantitative hazard and exposure assessment maps is to assess hazard and exposure from *"Pb accessible to children"*. A secondary objective is to test the relevance of including Pb concentration in soil as a factor in hazard and exposure analysis. Four different maps are created: two hazard maps (Maps 11.15 & 11.16) and two exposure maps (Maps 11.17 & 11.18). The first map of each type (*i.e.*, hazard and exposure) includes Pb concentration in soil as a factor in the analysis (Maps 11.15 & 11.17), whereas the second does not (Maps 11.16 & 11.18).

11.7.4.2. Criteria selected

Ten criteria were selected for this analysis from among a larger number that could be influencing the hazard and exposure (*e.g.*, wind direction; position of the hill with respect to the wind direction). These criteria are divided in two categories related to whether they are likely to increase the Pb concentration in soil (*e.g.*, when the area is situated over the site of a former metal-related industry) or to make the Pb more accessible to children (*e.g.*, the degree of dustiness of the waste) (Table 11.9). The proximity to roads factor is included in the analysis, because at the time of the biomedical survey (N. Vlachoyiannis, personal com., 1997), most of the roads in Lavrion were not tarred, and significant amounts of dust could have been derived from them.

The exposure factor is exclusive to the exposure maps (Maps 11.17 & 11.18). The image used as a basis for estimating the *"time of exposure"* is the land use map. Four main categories of exposure can thus be established based on the areas where children spend most of their time. The categories are:

(a) residential area (with a garden),
(b) agricultural area,
(c) recreational area, and
(d) school.

The exposure in the rest of the area is taken as minimal.

11.7.4.3. Weighting the criteria

The technique used in this paper for assigning appropriate weights is that developed by Saaty (1977; Eastman, 1997) in the context of a decision-making procedure known as the Analytical Hierarchy Process (AHP). The weights are developed by providing a series of pairwise comparisons of the relative importance of factors to the suitability of pixels for the hazard being evaluated. These pair wise comparisons are then analysed to produce a set of weights that sum to 1 (Table 11.14).

11.7.4.4. Standardisation of criteria

All areas in the different criteria maps are allocated a value of hazard ranging from 0 to 255. However, the hazard values are not necessarily assigned in a similar manner. Some criteria have discrete categories (*e.g.*, degree of dustiness of the waste, or whether or not a site overlies Quaternary deposits), and others have continuous categories (*e.g.*, proximity to current or previous stacks or proximity to roads).

A value is given to the discrete categories of a hazard. Continuous categories of hazards are based on the application of fuzzy set membership functions.

11.7.4.5. Creating the maps

Once the criteria map (images) have been developed, the MCE module of the *Idrisi*® GIS is used following the logic of WLC. The module requires the specification of the number of factors, their names, and the weights to be applied to the factors. The exposure maps should be interpreted as the *potential child exposure expected at a specific location* (*e.g.*, if a child lives there, studies there, plays there); it is not the total exposure expected.

All regression coefficients (r) between Maps 11.15 to 11.18 and measured blood-Pb concentrations are statistically significant, having values of 0.47, 0.43, 0.36 and 0.34 respectively ($p<0.001$). This confirms that the MCE-WLC approach shows effectively the areas with highest exposure, ***even when soil Pb concentrations are not included in the model***.

11.7.5. HAZARD AND EXPOSURE CLASSIFICATION OF CONTAMINATION SOURCES & LAND USE

Hazard and exposure index values were estimated on the same grid of 50 x 50 m, used for the kriging of total, exchangeable (step 1), carbonate (step 2) and extractable (exchangeable + carbonate; steps 1+2) lead concentrations in overburden/soil samples (see Chapter 3; Demetriades *et. al.*, 1998). The original arbitrary hazard and exposure index scale of 0 to 255 was reduced to percent (0 to 100) for the purposes of the environmental management scheme (refer to Volumes 4 & 5 of this report). Statistical parameters of the kriged estimates of Pb, the hazard and exposure index values for the different metallurgical processing wastes and contaminated soil, and land use categories are tabulated in Tables 11.1A to 11.10A and displayed in Figures 11.1A to 11.8A (at the end of this Chapter). Lead results will not be discussed in this section. They are, however, presented, because Pb was one of the eight factors used in the hazard and exposure assessment mapping (Maps 11.15 & 11.17), *i.e.*,

(1) lead concentration in overburden/soil;
(2) degree of dustiness of the metallurgical waste;
(3) proximity to metallurgical wastes;
(4) proximity to current or previous stacks;
(5) proximity to roads;
(6) proximity to rivers;
(7) proximity to lead-industry, and
(8) degree of child exposure, and

two constraints:
(1) area with metal-related industry, and
(2) area over Quaternary deposits.

Hazard and exposure index values for the different metallurgical wastes and land use categories are compared by means of box-and-whisker plots, a powerful an Exploration Data analysis tool (Tukey, 1977; Kürzl, 1988; Reimann *et. al.*, 1998). The box-and-whisker plots (Figs. 11.1A to 11.8A) display the variation of hazard or exposure index for (a) the ten categories of metallurgical processing wastes and contaminated soil, and (b) the thirty land use categories. The rectangular part of the plot extends from the lower quartile (25%) to the upper quartile (75%) of the hazard or exposure index, covering the central half of the variation for each type of waste and contaminated soil or land use category. The centre line within each box shows the location of the median, and the plus (+) sign that of the mean. The whiskers extend from the box to the minimum and maximum hazard or exposure index values for each waste type and contaminated soil or land use category, except for any outside or far outside points, which are plotted separately. Outside points are points, which lie more than 1.5 times the interquartile range of the hazard or exposure index, above or below the box and are shown as small squares. Far outside points are points, which lie more than 3.0 times the interquartile range of the hazard or exposure index, above or below the box and are shown as small squares with a plus sign through them.

11.7.5.1. Hazard and exposure rating of contamination sources

The median value of the hazard and exposure index of each of the ten metallurgical processing waste categories and contaminated soil is used as a robust indicator to define the order from the most to the less hazardous waste (Table 11.17; Tables & Figs. 11.5A & Fig. 11.6A,). The time of exposure factor, incorporated in the estimation of child exposure, changes the order of hazard index. The exposure index is, therefore, used to rate classify the metallurgical processing waste categories and contaminate soil. It is clear from the box-and-whisker plot of exposure index (Fig. 11.6A) that the most hazardous metallurgical processing waste is the beneficiation/flotation residues (1) followed by the pyritiferous flotation tailings (7).

The greatest exposure variation is exhibited by the beneficiation/flotation residues and contaminated soil, indicating the heterogeneity of the two materials with respect to Pb concentration and the other criteria used in the estimation of hazard and exposure indices.

Table 11.17. Median values of hazard and exposure index of metallurgical processing wastes and contaminated soil, and of estimated kriged total and extractable Pb levels (see also Tables & Figs. 11.5A & 11.6A in Appendix 5A of Volume 1A, p.201-203).
Πίνακας 11.17. Διάμεσες τιμές του δείκτη επικινδυνότητας και έκθεσης για τα μεταλλουργικά απορρίμματα και το ρυπασμένο έδαφος, καθώς και των εκτιμηθεισών τιμών kriging του ολικού και εκχυλίσιμου Pb (βλ. επίσης Πίνακες & Σχ. 11.5A & 11.6A στο Παράρτημα 5A του Τόμου 1A, σελ. 201-203).

Metallurgical processing wastes category *(number in brackets refers to the figure codes)*	*Hazard Index (%)*	***Exposure Index (%)***	*Estimated kriged Pb values (ppm)*			
			Total	*Exchange-able*	*Carbonate*	*Exchang. + Carbonate*
(1) Beneficiation/flotation residues	80.8	**63.5**	15038	18.9	4965	4984
(7) Pyritiferous tailings	86.3	**63.3**	14124	21.8	1080	1102
(6) Beneficiation/flotation residues with disseminated pyrite	72.9	**53.3**	8608	7.3	1330	1337
(8) Disseminated slag and coarse-grained beneficiation/ flotation	66.3	**48.6**	10571	8.9	618	627
(9) Beneficiation/flotation sands and coarse-grained materials	66.5	**48.6**	12089	8.7	1299	1308
(3) Slag with sand-blast wastes	60.4	**44.3**	9201	4.1	1012	1016
(5) Sand-blast wastes	58.8	**43.9**	13449	11.7	1112	1124
(10) Beneficiation/flotation residues with disseminated slag	55.7	**41.0**	8447	6.2	2817	2823
(4) Disseminated slag	52.6	**39.8**	4497	4.4	451	455
(2) Slag	52.6	**38.8**	7224	3.6	427	431
(0) Contaminated soil	41.6	**33.7**	6083	6.8	910	917

11.7.5.2. Hazard and Exposure Rating of Land Use Categories

Although the ore treatment plant & storeroom category has the highest total and extractable Pb concentrations is at 11th position in the succession of median exposure index values, because is indirectly affecting child exposure (Table 11.18). The highest hazard and exposure indices are assigned to the football pitch & sports field category, for they are situated in highly hazardous and exposed areas. In the top ten highly exposed areas are included agricultural and residential areas. As expected houses with a garden have a higher exposure index than the ones with no garden.

Essentially, Table 11.18 gives the priority sequence for rehabilitation of contaminated land in Lavrion, in order to reduce child exposure to environmental contaminants.

Table 11.18. Median values of hazard and exposure index of land use categories, and of estimated kriged total and extractable Pb levels (see also Tables and Figs. 11.7A & 11.8A in Appendix 5A of Volume 1A, p.204-210).
Πίνακας 11.18. Διάμεσες τιμές του δείκτη επικινδυνότητας και έκθεσης για τις διάφορες κατηγορίες χρήσης γης, καθώς και των εκτιμηθεισών τιμών kriging του ολικού και εκχυλίσιμου Pb (βλ. επίσης Πίν. & Σχ. 11.7Α & 11.8Α στο Παράρτημα 5Α του Τόμου 1Α, σελ.204-210).

Land use category *(number in brackets refers to the figure codes)*	*Hazard Index (%)*	***Exposure Index (%)***	*Estimated kriged Pb values (ppm)*			
			Total	*Exchange-able*	*Carbonate*	*Exchang. + Carbonate*
(6) Football pitch & sports field	73.33	**68.04**	8980.20	9.89	2337.80	2347.7
(8) Vineyard	54.51	**67.06**	10173.50	15.06	3076.00	3091.1
(10) Wheat	41.57	**58.04**	7051.30	4.70	1449.55	1454.3
(7) Olive grove	41.57	**57.25**	6313.10	8.03	1101.45	1109.5
(3) School	68.04	**56.86**	10252.15	12.15	3200.15	3212.3
(4) Playground	65.69	**55.49**	11462.00	11.61	1983.50	1995.1
(2) House with a garden	41.57	**53.33**	4394.70	3.69	739.70	743.4
(9) Vegetables	35.10	**53.33**	3031.00	1.89	463.05	465.0
(1) House, shop & church	41.96	**52.94**	5115.20	3.52	818.90	822.4
(5) Park	49.41	**51.37**	6736.70	8.43	1492.60	1501.0
(16) Ore treatment plant & storeroom	67.84	**50.59**	36012.20	66.31	7142.70	7209.0
(26) Building materials wholesaler	66.27	**48.63**	15255.30	10.72	836.30	847.0
(19) Lead-acid battery factory	63.14	**47.06**	14586.85	30.00	4775.85	4805.9
(21) Petrol station, garage & motor repairs	62.55	**46.47**	20565.65	26.80	5361.05	5387.9
(24) Cotton-weaving industry	53.53	**40.00**	7849.05	6.4	1253.10	1259.5
(15) Cemetery	49.80	**37.25**	13447.80	30.31	3572.30	3602.6
(17) Smokeduct	48.24	**36.08**	14694.70	10.73	644.30	655.0
(22) Iron converter industry & trading	48.24	**36.08**	2195.30	2.73	396.10	398.8
(25) Other industries & storage sites	46.27	**34.51**	2675.65	4.07	486.85	490.9
(27) Port installations	46.67	**34.51**	7951.40	5.86	928.95	934.8
(12) Open space with trees	45.69	**34.31**	6804.55	11.51	1495.80	1507.3
(13) Open space	44.71	**33.73**	7092.30	7.02	881.30	888.3
(20) Factory (ammunition, weapons *etc.*)	43.53	**32.55**	7980.70	13.92	1450.60	1464.5
(14) Archaeological site	39.61	**29.80**	5930.90	7.18	947.00	954.2
(11) Pine forest	38.43	**28.63**	5692.60	7.67	650.30	658.0
(28) Marble quarry	36.86	**27.84**	8400.45	11.23	1753.20	1764.4
(18) Sand-blast unit with slag	-	**-**	-	-	-	-
(23) Aluminium converter industry	-	**-**	-	-	-	-
(29) Old mining works	-	**-**	-	-	-	-
(30) Municipal waste site	-	**-**	-	-	-	-

11.8. CONCLUSIONS

This study has illustrated the relevance of different spatially resolved hazard and exposure assessment techniques in assessing contaminated land. The following five conclusions summarise the most significant aspects of this study:

1. Different methodologies have been devised using GIS for spatially resolved hazard and exposure assessment, permitting spatial differences in the distribution of both hazard and target to be evaluated. The advantages of such maps are that they help to prioritise areas for action, such as remediation or identification of areas unsuitable for housing.

2. A partial validation of the methods has been achieved from significant correlation between Pb exposures predicted by the models and measured values of internal exposure from blood-Pb.

3. The semi-quantitative method, using the MCE-WLC technique, has been shown to integrate semi-quantitative information, such as dustiness of waste and presence of metal-related industry. This can improve upon traditional EA/RA procedures that rely solely on soil or dust Pb concentrations. Moreover, the robust nature of this approach was demonstrated by its correlation with measured blood-Pb levels, *even when data on soil Pb was excluded from the method*. The semi-quantitative hazard maps had a higher regression coefficient than the quantitative exposure maps, proving the strength of the semi-quantitative method.

4. The significant correlation between blood-Pb predictions using the IEUBK model and blood-Pb measurements provide a partial validation of the method, allowing for uncertainty in measurements (from both, sampling and analysis) and the lack of some site-specific measurements.

5. The successful application of these methodologies to the Lavrion urban area, although preliminary in nature, does nevertheless demonstrate the potential of the spatially resolved technique. Further refinement will include consideration of other exposure pathways to permit more accurate exposure assessments for Pb and more rigorous validation of the methodology. The principles of this approach should be generally applicable to other potentially contaminated areas, and other contaminants in the Lavrion urban area. Selection of suitable exposure routes and validation methods will clearly require site-specific adaptation of the methods.

Blank back page
Λευκή οπίσθια σελίδα

Chapter 12

ENVIRONMENTAL MANAGEMENT AND PLANNING

Editor's note
Institute of Geology and Mineral Exploration, 70 Messoghion Street, Gr-115 27 Athens, Greece

In Volume 2 of this report the following maps are presented:

- **Map 12.1: Demonstration scale application of rehabilitation techniques**. This map shows the location of the two areas where the National Technical University of Athens (NTUA) carried out the demonstration scale application of rehabilitation techniques studied in the laboratory. Details about the methods will be found in Volume 3 of this report, and with respect to the environmental management scheme in Volume 4 (Part 1: Greek text and Part 2: English text) (originally planned to be in separate Volumes, *i.e.*, 4 & 5).

- **Map 12.2: Distribution of Cost Index of the methods for the rehabilitation of the Lavrion urban area**. This map shows the cost in drachmas of the least cost and best available technologies for the rehabilitation of contaminated land in Lavrion. The dimensions of blocks are 50 x 50 metres. Details about this map will be found in Volume 4 of this report.

- **Map 12.3: Distribution of Benefit Index for the rehabilitation of contaminated land in Lavrion**. This map shows the benefit index for rehabilitating contaminated land. Details about this map will be found in Volumes 4 of this report.

- **Map 12.4: Distribution of Cost/Benefit of the methods for the rehabilitation of the Lavrion urban area**. In this map the ratio of the Cost (Map 12.2) to Benefit Index (Map 12.3) is presented. Hence, decision-makers can use this map to prioritise the investment for rehabilitation of contaminated land.

- **Map 12.5. Property characterisation map of the Lavrion urban area**. The map was compiled from information obtained from the Municipality of Lavreotiki, the Lavrion Forestry Office, the Hellenic Port Authority at Lavrion and the Hellenic State Mortgage Company. This is a very useful map for the first time the Municipality of Lavrion has in its hands a detail map about property ownership, private and State. Again it can be used for planning purposes.

- **Map 12.6. Map of urban control zones of the Lavrion urban area**. This map was compiled from information obtained from Map Sheet 6478/9 of Urban Control Zones of Lavreotiki, S.E. Attiki, which was published by the Hellenic Ministry of Environment, Planning & Public Works. The exact reference is Case Number Γ2087/97, Decree, which was published in the official Government Newspaper of the Hellenic Republic (Fourth Series, Issue no. 125, 27.2.1998). It is again a very useful map for it shows a glimpse into the future, as planned by the Hellenic State. The Officers of the Municipality of Lavreotiki must also take into account the land characterisation shown on this map, for the future planning of their town.

Blank back page
Λευκή οπίσθια σελίδα

REFERENCES

Ahrens, L.H., 1954a. Lognormal distribution of the elements. Geoch. Cosmochim. Acta, 5(2): 49-73.

Ahrens, L.H., 1954b. Lognormal distribution of the elements. Geoch. Cosmochim. Acta, 6(2/3): 121-131.

Alloway, B.J., 1990. Soil processes and the behaviour of metals. In: B.J. Alloway (Editor), Heavy metals in soils. Blackie, London: 122-151.

Appleton, J.D., 1995. Potentially harmful elements from natural sources and mining areas: characteristics, extent and relevance to planning and development in Great Britain. British Geological Survey, Keyworth, U.K., Technical Report WP/95/3, 63 pp.

Appleton, J.D., Fuge, R. and McCall, G.J.H., 1996. Environmental geochemistry and health with special reference to developing countries. The Geological Society of London, Spec. Publ., 113, 264 pp.

ATSDR (Agency for Toxic Substances and Disease Registry), 1988. The nature and extent of lead poisoning in children in the United States: A report to Congress. US Public Health Service, Atlanta.

Auboin, J. (1959) Contribution a l'etude geologique de la Grece septentrionale: Les confins de l'Epireet de la Thessalie. Ann. Geol. Pays Hellen., 10: 1-483.

Barnes, H.L., 1967. Geochemistry of hydrothermal ore deposits. Holt, Rinehart and Winston, Inc., N.Y., 670 pp.

Beckett, P.H.T., 1988. The use of extractants in studies on the trace metals in soils, sewage sludges and sludge-treated soils. Advances in Soil Science, 9: 144-175.

Belzile, N., Lecompte, P. and Tessier, A., 1989. Testing reabsorption of trace elements during partial chemical extractions of bottom sediments. Environ. Sci. Technol., 23: 1015-1020.

Benetou-Marantidou, A., Nalou, S. and Micheloyiannis, I., 1985. The use of a battery of tests for the estimation of neurological effects of lead in children. In: T.D. Lekkas (Editor), International Conference Heavy Metals in the Environment, New Orleans, September, Vol. 1, CEP Consultants, Edinburgh, pp. 204-209.

Bermond, A.P., 1992. Thermodynamics applied to the study of the limits of sequential extraction of trace elements in sediments and soils. Environ. Technol., 13: 1175-1179.

Bingham, E. and Lutkenhoff, S.D., 1990. Keynote Address: Regulating a trace. In: D.D. Hemphill (Editor), Trace substances in environmental health - XXII. Supplement to volume 12 of Environmental Geochemistry and Health, University of Missouri, Columbia: 1-19.

Björklund, A. and Gustavsson, N., 1987. Visualization of geochemical data on maps. J. Geochem. Explor., 29: 89-103.

Bølviken, B. and Sinding-Larsen, R., 1973. Total error and other criteria in the interpretation of stream-sediment data. In: M.J. Jones (Editor), Geochemical Exploration 1972. Inst. Min. Metall., London: 285-295.

Bølviken, B., Bergstrøm, A., Bjørklund, A., Kontio, M., Lehmuspelto, P., Lindholm, T., Magnusson, J., Ottesen, R.T., Steenfelt, A. and Volden, T., 1986. Geochemical Atlas of Northen Fennoscandia. Geological Survey of Sweden, Uppsala.

Bonham-Carter, G.F., 1994. "Geographic Information Systems for geoscientists: Modelling with GIS". Pergamon, Elsevier Science Ltd., U.K.

Boyle, R.W., 1974. Elemental associations in mineral deposits and indicator elements of interest in geochemical prospecting. Energy, Ines and Resources Canada, Geological Survey paper 74-75, 40 pp.

Brandvold, L.A. and McLemore, V.T., 1998. A study of the analytical variation of sampling and analysis of stream-sediments from areas contaminated by mining and milling. J. Geochem. Explor., 64: 185-196.

Breward, N., Williams, N. and Bradley, D., 1996. Comparison of alternative extraction methods for determining particulate metal fractionation in carbonate-rich Mediterranean soils. Applied Geochem., 11: 101-104.

Briskin, J. and Marcus, A., 1990. Goals and implications of EPA's new drinking water standard for lead. In: D.D. Hemphill (Editor), Trace substances in environmental health - XXII. Supplement to volume 12 of Environmental Geochemistry and Health, University of Missouri, Columbia: 33-50.

Brockhaus, A., Collet, W., Dolgner, R., Engelke, R., Ewers, U., Frier, I., Jermann, E., Krämer, U., Turfeld, N. and Winneke, G., 1988. Exposure ot lead and cadmium of children living in different areas of North-West Germany: results of biological monitoring studies, 1982-1986. Int. Arch. Occup. Environ. Health, 60: 211-222.

Brookins, D.G., 1988. Eh-pH diagrams for geochemistry. Springer-Verlag, Berlin.

Brunekreef, B., Veenstra, S.J., Bierksteker, K. and Boleij, J.S., 1981. The Arnhem lead study I. Lead uptake by 1- to 3-year-old children living in the vicinity of a secondary lead smelter in Arnhem, The Netherlands. Environ. Res., 25: 441-448.

Buckman, H.O. and Brady, N.C., 1970. The nature and properties of soil. The Macmillan Co., N.Y., 653 pp.
Burmaster, D.E. and Harris, R.H., 1993. The magnitude of compounding conservatisms in superfund risk assessments. Risk Analysis, 13**,** 131-134.
Calabrese, E.J., Stanek, E.J., James, R.C. and Roberts, S.M., 1997. Soil ingestion: A concern for acute toxicity in children. Environ. Health Perspect., 105: 1354-1358.
Callow, P. , 1998. Environmental Risk Assessment and Management: the Whats, Whys and Hows? In "Handbook of Environmental Risk Assessment and Management" (P. Callow, Ed.), pp. 1-6. Blackwell Science Ltd., U.K.
Carignan, J., 1979. Geochemistry and geostatistics applied to exploration for volcanogenic deposits at the Millenbach deposit. Unpubl. Ph.D. thesis, University of Montreal, Canada (in French).
Cattell, R.B., 1965. Factor analysis: an introduction to essentials. Parts 1 and 2. Biometrics, 21: 190-215; 405-435.
CDC, 1978. Preventing lead poisoning in young children. A statement by the Center for Disease Control, Atlanta. U.S. Dept. of HEW. J. Pediatr., 93: 709-720.
CEC (Commission of European Communities), 1977. Council Directive 77/312 on biological screening of the population for lead. Official Journal of the European Communities, L105.10.
CEC (Commission of European Communities), 1980. Directive relating to the quality of water intended for human consumption (80/778/EEC). CEC, Brussels.
CEC (Commission of European Communities), 1986. Directive (No. 86/278/EEC) of June 1986 on the protection of the environment and in particular of the soil when sewage sludge is used in agriculture. Official Journal of the European Communities, No. L181, 6-12, Brussels.
Chambers, J.M., Cleveland, W.S., Kleiner, B. and Tukey, P.A., 1983. Graphical methods for data analysis. Wadsworth International Group, Belmont, Calif., Duxbury Press, Boston, M.A., 395 pp.
Chao, T.T., 1984. Use of partial dissolution techniques in geochemical exploration. J. Geochem. Explor., 20: 101-135.
Chester, R. and Hughes, M.J., 1967. A chemical technique for the separation of ferro-manganese minerals, carbonate minerals and adsorbed trace elements from pelagic sediments. Chem. Geol., 2: 249-262.
Chronopoulos, J. and Chronopoulou-Sereli, C., 1986a. Scwermetalltoleranz von *Crocus sieberi*, *Arisarum vulgare* und *Cyclamen graecum* in Lavrion (Attika). Verhandlungen der Gesellschaft für Ökologie (Hohenheim 1984), XIV: 357-360 (text in German with a synopsis in English).
Chronopoulos, J. and Chronopoulou-Sereli, C., 1986b. Vegetational development of halophytes to heavy metals in industrial regions in Lavrion (Attika). Landschaft u. Stadt, 18 (1): 42-45 (text in German with a summary in English).
Chronopoulos, J. and Chronopoulou-Sereli, C., 1991. Effects of the mining-metallurgical activity on the natural vegetation of Lavreotiki. In: Abstracts of 1st Scientific Conference on Geosciences and the Environment. University of Patras, Dept. of Geology, Patras: 147.
Chronopoulou-Sereli, C. and Chronopoulos, J., 1991a. Untersuchungen über die Pb-belastung der vegetation in Lavreotiki (Attika). In: S. Riewenherm und H. Lieth (Editors), Verhandlungen der gesellschaft für Ökologie (Osnabrück 1989): XIX/III: 223-228 (text in German with a summary in English).
Chronopoulou-Sereli, C. and Chronopoulos, J., 1991b. Unweltbelastung der Stadt Lavrion (Attika) und Umgebung durch ein Bleinhüttenwerk. Natur und Landschaft, 66 (9): 442-443 (text in German with a summary in English).
Chuan, M.C., Shu, G.Y. and Liu, J.C., 1996. Solubility of heavy metals in a contaminated soil: effects of redox potential and pH. Water, Air, Soil Pollut., 51: 153-160.
Clark, I., 1979. Practical geostatistics. Applied Science Publishers Ltd., London, 129 pp.
Clevenger, T.E., Saiwan, C. and Koirtyoham, S.R., 1991. Lead speciation of particles on air filters collected in the vicinity of a lead smelter. Environ. Sci. Technol., 25: 1128-1133.
Cohen, D.R., Shen, X.C., Dunlop A.C. and Rutherford, N.F., 1998. A comparison of selective extraction soil geochemistry and biogeochemistry in the Cobar area, New South Wales. J. Geochem. Explor., 61: 173-189.
Conophagos, C., 1975. Fours de fusion et technique de la fusion des minerais de plomb argentifere du Laurium par les anciens Grecs. (Paper in Greek with an abstract in French). Annales Geologiques des pays Helleniques, 26: 338-366.
Conophagos, E.C., 1980. Le Laurium antique et la technique Grecque de la production deo l'argent. National Technical University, Athens, 458 pp. (in French).
Conophagos, C., 1985. L' evolution de la technique Grecque de la concentration des minerais au Laurium antique. (Paper in Greek with an abstract in French). Proceedings of the first seminar on the archaeometry of slags of ancient Greek metallurgy. Institute of Geology and Mineral Exploration, Athens: 21-40.

Cotter-Howells, J., 1991. Lead minerals in soils contaminated by mine-waste: implications for human health. Unpublished Ph.D. Thesis, University of London.
Cotter-Howells and Thornton, I., 1991. Sources and pathways of environmental lead to children in a Derbyshire mining village. Environ. Geochem. Health, 13: 127-135.
Croissant, A., 1977. Geostatistics as used in geochemical prospecting. Sci. Terre, Ser. Inform., no. 9: 129-144 (in French).
Culbard, E., Thornton, I., Watt, J., Moorcroft, S., Brooks, K. and Thompson, M., 1983. Metal contamination of dusts and soils in urban and rural households in the United Kingdom. In: D.D. Hemphill (Editor), Trace substances in environmental health – XVII. University of Missouri, Columbia: 236-241.
Daugherty, M.L., 1992. Toxicity summary for beryllium. Chemical Hazard Evaluation and Communication Group Biomedical and Environmental Information Analysis Section Health and Safety Research Division, Oak Ridge National Laboratory, Oak Ridge, Tennessee, 32 pp.
Daultrey, S., 1976. Principal component analysis. Geo Abstracts, University of East Anglia, Norwich, U.K., CATMOG 8, 50 pp.
Davies, B.E., 1980. Trace element pollution. In: B.E. Davies (Editor), Applied trace elements, Chapter 9. J. Wiley & Sons, Chichester, U.K.: 287-351.
Davies, B.E., 1987. Lead: The environment and man: Current issues. In: I. Thornton and E. Culbard (Editors), Lead in the Home Environment. Scientific Reviews Ltd., Northwood, U.K.: 3-13.
Davies, D.J., Thornton, I., Watt, J., Culbard, E., Harvey, P., Delves, H., Sherlock, J., Smart, G., Thomas, J.F. and Quinn, M., 1990. Lead intake and blood lead in 2 year old UK urban children. Sci. Total Environ., 90, 13-29.
Davies, D.J.A. and Watt, J., 1986. An assessment of the quantity and significance of lead on the hands of inner city children in the United Kingdom. In: Trace Substances in Environmental Health - XX, D.D. Hemphill, Ed, University of Missouri, Columbia: 333-344.
Davies, D.J.A., Watt, J.M. and Thornton, I., 1987. Lead levels in Birminham dusts and soils. Sci. Total Environ., 67: 177-185.
Davies, S. and Stewart, A., 1987. Nutritional medicine. The drug-free guide to better family health. Pan Books, London, U.K., 543 pp.
Davis, J.C., 1973. Statistics and data analysis in geology. J. Wiley & Sons, Inc., N.Y., 550 pp.
Demetriades, A., 1990. A comparison of overbank and stream sediment in a low sampling density geochemical survey, N.E. Greece. In: A. Demetriades, R.T. Ottesen and J. Locutura (Editors), Geochemical mapping of Western Europe towards the Year 2000. Pilot Project Report. Open File Report 90-105, Appendix Report 7.2. Geological Survey of Norway, Trondheim, 84 pp.
Demetriades, A., 1992. Development of integrated collaborative research programmes between the U.K. (BGS) and Greece (IGME). Environmental Geochemistry, Lavreotiki peninsula, and Multidisciplinary data interpretation, Eastern Macedonia and Thrace. Vol. 1: Text, 165 pp.; Vol. 2: Maps, diagrams and tables, 128 pp. Inst. Geol. Mineral Explor. (IGME), Athens, Open File Report E-6700 (in English).
Demetriades, A., 1997. Arsenic and antimony in the surface soil of Lavreotiki peninsula, Attiki Prefecture, Greece. Seminar hosted by Imperial College for the Royal Society of Chemistry, Environmental Chemistry Discussion Group, 3.12.1997, Abstract only.
Demetriades, A., 1998. Global geochemical baselines: A fundamental international project for environmental management. Bull. Geol. Soc. Greece, XXXII (1): 321-329.
Demetriades, A. and Vassiliades, E., 1998. Software, data bases, quality control, digital, statistical and geostatistical processing of data, Lavrion Attiki. In: A. Demetriades, E. Vassiliades, E. Tristán, M.S. Rosenbaum and M.H. Ramsey, Technical Report, Child blood lead content as a basis for risk assessment of the metallurgical processing residues and contaminated soil in Lavrion Attiki. Inst. Geol. Min. Expl., Athens, Open File Report 7977-E, 112 pp. (in Greek) + Appendix 1: Data bases and data treatment (in English), 33 pp.
Demetriades, A., Bφlviken, B., Hindel, R., Ottesen, R.T., Salminen, R. and Schermann, O., 1993. The geochemical implications of environmental pollution. In: HELECO'93, 1st International Exhibition and Conference on Environmental Technology. Technical Chamber of Greece, Athens, 1: 467-479.
Demetriades, A., Bφlviken, B., Bogen, J., Croke, J.C., Hindel, R., Locutura, J., Macklin, M.G., Ottesen, R.T., Salminen, R., Schermann, O. and Volden, T., 1994. The recording of environmental contamination by overbank sediment. In: S.P. Varnavas (Editor), Environmental Contamination, 6th International Conference, Delphi, Greece. CEP Consultants Ltd., Edinburgh, U.K.: 340-342.
Demetriades A., Stavrakis, P., Vergou-Vichou, K., 1994a. Maps of the environmental geochemistry study of Lavreotiki peninsula. Environmental Geochemistry Study - Lavreotiki Peninsula. Inst. Geol. Min. Expl., Athens, Greece. Open File Report E-7424, Vol. 2, 36 pp. (in Greek with an English summary).
Demetriades A., Stavrakis, P., Vergou-Vichou, K., 1994b. Environmental soil geochemical survey of Lavreotiki peninsula Attiki. Environmental Geochemistry Study - Lavreotiki Peninsula. Inst. Geol.

Min. Expl., Athens, Greece. Open File Report E-7424, Vol. 3, 147 pp. (in Greek with an English summary).
Demetriades, A., Vergou-Vichou, K. and Stavrakis, P., 1994c. Orientation soil geochemical survey in the Lavreotiki peninsula Attiki. Environmental Geochemistry Study - Lavreotiki Peninsula. Inst. Geol. Min. Expl., Athens, Greece. Open File Report E-7424, Vol. 6, 64 pp. (in Greek with an English summary).
Demetriades, A., Stavrakis, P. and Vergou-Vichou, K., 1996a. Contamination of surface soil of the Lavreotiki peninsula (Attiki, Greece) by mining and smelting activities. Mineral Wealth, 98: 7-15.
Demetriades, A., Stavrakis, P., Vergou-Vichou, K., Li, X. and Ramsey, M., 1996b. Distribution of lead and arsenic in the surface soil of Lavreotiki peninsula, Attiki Prefecture, Greece. 14th European Conference, Society of Environmental Geochemistry and Health, Centre for Environmental Technology, Imperial College of Science, Technology and Medicine, London, U.K., 1.-3.4.1996, Book of abstracts: 11.
Demetriades, A., Stavrakis, P., Vergou-Vichou, K., Makropoulos, V., Vlachoyiannis, N. and Fosse, G., 1996c. Lead in the surface soil of Lavreotiki peninsula (Attiki, Greece) and its effects on human health. In: Aug. Anagnostopoulos, Ph. Day and D. Nicholls (Editors), Proceedings Third International Conference on Environmental Pollution. Aristotelean University of Thessaloniki, Thessaloniki, Greece: 143-146.
Demetriades, A., Stavrakis, P. and Vergou-Vichou, K., 1997. Exploration geochemistry in environmental impact assessment: examples from Greece. In: P.G. Marinos, G.C. Koukis, G.C. Tsiambaos and G.C. Stournaras (Editors), Engineering Geology and the Environment, Balkema, Rotterdam, Vol. 2: 1757-1762.
Demetriades, A., Vassiliades, E., Tristán, E., Rosenbaum, M.S., and Ramsey, M.H., 1998. Child blood lead content as a basis for risk assessment of the metallurgical processing residues and contaminated soil in Lavrion Attiki. Inst. Geol. Min. Expl., Athens, Greece. Open File Report E7977 (text in Greek and English).
Dermatis, G.N., 1994. Landscape and monuments of Lavreotiki. Municipality of Lavreotiki, Lavrion, 298 pp. (text in Greek).
De Vos, W., Ebbing, J., Hindel, R., Schalich, J., Swennen, R. and Van Keer, I., 1996. Geochemical mapping based on overbank sediments in the heavily industrialised border area of Belgium, Germany and the Netherlands. J. Geochem. Explor., 56: 91-104.
Dijkstra, S., Van Den Hull, H.J. and Bill, E., 1979. Experiments on the usefulness of some selected chemical quantities in geochemical exploration in a former mining district. In: J.R. Watterson and P.K. Theobald (Editors), Geochemical Exploration 1978. Association of Exploration Geochemists, Rexdale, Ont.: 283-288.
DoE (Department of Environment), 1995. “A guide to Risk Assessment and Risk Management for environmental protection”. London, HSMO.
Douben, P.E.T., 1998. Perspectives on pollution risk. In: P.E.T. Douben, Pollution risk assessment and management. J. Wiley & Sons, Chichester, U.K.: 1-20.
Drossos, Ch., Papadopoulou-Ntafioti, Z., Mavroidis, K. Michalodimitriadis, D., Salamalikis, L. Gounaris, A. and Varonos, D., 1982. Environmental contamination by lead in Greece. Paediatrics, Athens, 45: 114-124 (in Greek).
Dudka, S. and Chlopecka, A., 1990. Effect of solid-phase speciation on metal mobility and phytoavailability in sludge-mended soil. Water, Air and Soil Pollut., 51: 153-160.
Duggan, M.J., 1983. Contribution of lead in dust to children’s blood lead level. Environ. Health Perspect., 50: 371-381.
Durant, J., 1997. Scientific truth and political reality: professional and public perceptions of risk. In: J. Ashworth (Editor), “Science, Policy and Risk”, Royal Society, London: 45-51.
Eastman, J.R., 1997. Idrisi for Windows (version 2.0) (1997). Clark University, Massachusetts.
EC (European Commission), 1996. Technical guidance document in support of commision directive 93/67/EEC on risk assessment for new notified substances and commission regulation (EC) No. 1488/94 on risk assessment for existing substances. Part I.
Edelgaard, I. and Dahlstrøm, K., 1999. Denmark. In: C. Ferguson and H. Kasamas (Editors), Risk assessment for contaminated sites in Europe, Vol. 2, Policy Frameworks. LQM Press, Nottingham, U.K.: 29-39.
Edmunds, W.M. and Smedley, P.L., 1996. Groundwater geochemistry and health: an overview. In: J.D. Appleton, R. Fuge and G.J.H. McCall (Editors), Environmental Geochemistry and Health. Geological Society of London, Special Publication No. 113: 91-105.
Eikmann, Th., Michels, S., Makropoulos, V., Krieger, Th., Einbrodt, H.J., Tsomi, K., 1991. Cross-sectional epidemiological study on arsenic excretion in urine of children and workers in Greece. Gordon and Breach Science Publ., Toxicological and Environmental Chemistry, Vols, 31-32: 461-466.

Englund, E. and Sparks, A., 1988. GEO-EAS (Geostatistical Environmental Assessment Software) User's Guide. EPA/600/4-88/033a. Environmental Monitoring Systems Laboratory, Office of Research and Development, U.S. Environmental Protection Agency, Las Vegas, Nevada.
Essington, M.E. and Mattigod, S.V., 1991. Trace element solid-phase associations in sewage sludge and sludge-amended soil. Soil Sci. Soc. Am. J., 55: 350-356.
Fairbridge, R.W. (Editor), 1972. The encyclopedia of geochemistry and environmental sciences. Van Nostrand Reinhold Co., N.Y., 1321 pp.
Fairbrother, A. and Kapustka, L.A., 1997. Hazard classification of metals in terrestrial systems. A discussion paper. Intern. Council on Metals and the Environment, Ottawa, Ontario, Canada, 30 pp.
Ferguson, C. and Denner, J., 1994. Developing guideline (trigger) values for contaminants in soil: underlying risk analysis and risk management concepts. Land Contamination & Reclamation, 2 (3): 117-123.
Ferguson, C. and Kasamas, H. (Editors), 1999. Risk assessment for contaminated sites in Europe, Vol. 2, Policy Frameworks. LQM Press, Nottingham, U.K., 223 pp.
Ferguson, C. and Marsh, J., 1993. Assessing human health risks from ingestion of contaminated soil. Land Contamination & Reclamation, 1: 177-185.
Ferguson, C., Darmendrail, D., Freier, K., Jensen, B.K., Jensen, J., Kasamas, H., Urzelai, A. and Vegter, J. (Editors), 1998. Risk assessment for contaminated sites in Europe, Vol. 1, Scientific Basis. LQM Press, Nottingham, U.K., 165 pp.
Ferguson, C.C., 1995a. "The Contaminated Land Exposure Assessment Model (CLEA). Technical basis and algorithms". Draft report prepared for Department of the Environment under Contracts PECD 7/10/305, PECD 7/10/337 and EPG 1/6/18.
Ferguson, C.C., 1995b. The Contaminated Land Exposure Assessment Model (CLEA). Technical basis and algorithms. Final report. Department of the Environment. U.K.
Ferguson, J.E., 1990. The heavy elements: Chemistry, Environmental Impact and Health Effects. Pergamon Press, Oxford, 614 pp.
Finley, B. and Paustenbach, D., 1994. The benefits of probabilistic exposure assessment: three case studies involving contaminated air, water and soil. Risk Analysis, 14 (1): 53-73.
Fletcher, W.K., 1981. Analytical methods in geochemical prospecting. In: G.J.S. Govett (Editor), Handbook of Exploration Geochemistry, Vol. 1. Elsevier Scient. Publ. Co., Amsterdam, 255 pp.
Földvári-Vogl, M., 1978. Theory and practice of regional geochemical exploration. Akadémiai Kiadó, Budapest, Hungary, 272 pp.
Fosse, G. and Wesenberg, G.B.R., 1981. Lead, cadmium, zinc and copper in deciduous teeth of Norwegian children in the pre-industrial age. Intern. J. Environmental Studies, 16: 163-170.
Förstner, U., 1985. Chemical forms and reactivities of metals in sediments. In: R. Leschber, R.D. Davis and L'Hermie (editors), Chemical methods for assessing bio-available metals in sludges and soils. Elsevier Applied Science Publishers, London: 1-31.
Foster, R.L. and Lott, P.F., 1980. X-ray diffractometry examination of air filters for compounds emitted by lead smelting operations. Environ. Sci. Technol., 14: 1240-1244.
Garrels, R.M. and Christ, C.L., 1965. Solutions, minerals and equilibria. Harper & Row, N.Y., 450 pp.
Garrett, R.G. and Goss, T.I., 1978. The statistical appraisal of survey effectiveness in regional geochemical surveys for Canada's uranium reconnaissance program. Math. Geol., 12 (5): 443-458.
Garrett, R.G., 1969. The determination of sampling and analytical errors in exploration geochemistry. Econ. Geol., 64: 568-574.
Garrett, R.G., 1973. The determination of sampling and analytical errors in exploration geochemistry - a reply. Econ. Geol., 68: 282-283.
Garrett, R.G., 1983. Sampling methodology. In: R.J. Howarth (Editor), Statistics and Data Analysis in Geochemical Prospecting, Vol. 2, Chapter 4. G.J.S. Govett (Editor), Handbook of Exploration Geochemistry. Elsevier, Amsterdam: 83-110.
Garrett, R.G., Kane, V.G. and Zeigler, R.K., 1980. The management and analysis of regional geochemical data. J. Geochem. Explor., 13: 115-152.
Gatehouse, S., Russell, D.W. and Van Moort, J.C., 1977. Sequential soil analysis in exploration geochemistry. J. Geochem. Explor., 8: 483-494.
Gee, C., Ramsey, M.H., Maskall, J. and Thornton, I., 1997. Weathering processes in historical smelting slags – factors controlling the release of heavy metals. J. Geochem. Explor., 58: 249-257.
Gelaude, P., Kalmthout, P.V. and Rewitzer, C., 1996. Laurion. The minerals in the ancient slags. Janssen Print, Nijmegen, The Netherlands, 195 pp.
Gezondheidsraad, 1996. Risk is more than a number. Reflections on the development of the enrironment risk management approach. Gezonheidsraad Publication 1996/03E, The Hague.
Goddard, J., 1968. Multivariate analysis of office location patterns in the city centre: a London example. Regional Studies, 2: 69-8é5.

Goddard, J. and Kirby, A., 1976. An introduction to factor analysis. University of East Anglia, U.K., CATMOG series No. 7, 39 pp.
Golden Software, 1995. Surfer® for Windows. Golden Software, Inc., Golden, CO.
Golden Software, 1997. MapViewer® user's guide. Golden Software, Inc., Golden, CO.
Goldschmidt, V.M., 1970. Geochemistry. Oxford University Press, Oxford, U.K., 730 pp.
Goodchild, M.F., Steyaert, L.T., Parks, B.O., Johnston, C., Maidment, D., Crane, M. and Glendinning, S. (Eds) (1996). "GIS and environmental modelling: progress and research issues". GIS World books. Colorado.
Gough, L.P., Shacklette, H.T. and Case, A.A., 1979. Element concentrations toxic to plants, animals and man. US Geol. Survey Bulletin 1466, 80 pp.
Govett, G.J.S., 1983. Rock geochemistry in mineral exploration. In: G.J.S. Govett, Handbook of Exploration Geochemistry, Vol. 3. Elsevier Scient. Publ. Co., Amsterdam, 461 pp.
Guthe, W., Tucker, R.K., Murphy, E.A., England, R., Stevenson, E., and Luckhardt, J.C., 1992. Reassessment of lead exposure in New Jersey using GIS technology. Environmental Research, 59, 318-325.
Hadjigeorgiou-Stavrakis, P. and Vergou-Vichou, K., 1992. Environmental geochemistry study of the Lavrion and Ayios Constantinos (Kamariza) area in Attica. Inst. Geol. Min. Expl., Athens, Greece, Open File Report E6778, 33 pp. (in Greek with an English summary).
Hadjigeorgiou-Stavrakis, Vergou-Vichou, K., Demetriades, A., 1993. The contribution of geochemical exploration in the study of interior and exterior quality of the Lavrion and Ayios Constantinos (Kamariza) urban areas Attiki. In: Proceedings Heleco'93, First International Exhibition and Conference of Environmental Technology for the Mediterranean Region. Technical Chamber of Greece, Athens, Greece. Vol. II: 301-313 (in Greek with an English abstract).
Hall, G.E.M., 1998. Analytical perspective on trace element species of interest in exploration. In: G.E.M. Hall and G.F. Bonham-Carter (Editors), Selective extractions. Special Issue, J. Geochem. Explor., 61: 1-19.
Hall, G.E.M. and Bonham-Carter, G.F. (Editors), 1998. Selective extractions. Special Issue, J. Geochem. Explor., 61, 232 pp.
Hall, G.E.M., Vaive, J.E. and Kaszycki, C., 1993. The diagnostic capabilities of selective leaching. Explore, 80: 3-9.
Hall, G.E.M., Vaive, J.E., Beer, R. and Hoashi, M., 1996. Selective leaches revisited, with emphasis on the amorphous Fe-oxyhydroxide phase extraction. J. Geochem. Explor., 56: 59-78.
Hamilton, R.S., Revitt, D.M. and Warren, R.S., 1984. Level and physicochemical associations of Cd, Cu, Pb and Zn in road sediment. Sci. Total Environ., 33: 59-74.
Hämman, M. and Gupta, S.K., 1998. Derivation of trigger and clean-up values for inorganic pollutants in soil. Environmental Documentation No. 83: Soil. Swiss Agency for the Environment, Forests and Landscape, Berne, 105 pp.
Hamssen, M. and Marsden, J., 1985. "E"for additives. The complete "E" number guide. Thorsons Publishing Group, Wellingborough, U.K., 223 pp.
Hansuld, J.A., 1966. Eh and pH in geochemical exploration. Canadian Min. Metall. Bull., March 1966: 315-322.
Harrison, R.M., Laxen, D.P.H. and Wilson, S.J., 1981. Chemical association of lead, cadmium, copper and zinc in street dust and roadsite soils. Environ. Sci. Technol., 15: 1378-1383.
Hatzakis, A., Kokkevi, A., Katsouyanni, K., Maravelias, C., Salaminios, F., Kalandidi, A., Koutselinis, A., Stefanis K. and Trichopoulos, D., 1987. Psychometric intelligence and attentional performance deficits in lead-exposed children. In: S.E. Lindberg and T.C. Hutchinson (Editors), International Conference Heavy Metals in the Environment, New Orleans, September. CEP Consultants, Edinburgh, Vol. 1: 204-209.
Hemphill, D. (Editor), 1990. Trace substances in environmental health – XXIII. University of Missouri. Science Reviews Ltd., Northwood, U.K., 386 pp.
Henderson, P., 1982. Inorganic chemistry. Pergamon Press, Oxford, 353 pp.
Hesp, W.R. and Rigby, D. Cluster analysis of rocks in the New England igneous complex, New South Wales, Australia. In: M.J. Jones (ed.) Geochemical Exploration 1972. London, Inst. Min. Metall.: 221-235.
Hilts, S.R., 1996. A co-operative approach to risk management in an active lead/zinc smelter community. Environmental Geochemistry and Health, 18: 17-24.
Hoffman, S.J., 1986. Soil sampling. In: W.K. Fletcher, S.J. Hoffman, M.B. Mehrtens, A.J. Sinclair and I. Thompson (Editors), Exploration geochemistry: Design and interpretation of soil surveys. Reviews in Economic Geology, Vol. 3. Society of Economic Geologists, Univ. of Texas, El Paso, Texas: 39-77.

Hoffman, S.J. and Fletcher, W.K., 1979. Selective sequential extraction of Cu, Zn, Fe, Mn, and Mo from soils and sediments. In: J.R. Watterson and P.K. Theobald (Editors), Geochemical Exploration 1978. Association of Exploration Geochemists, Rexdale, Ont.: 289-299.

Howarth, R.J. (Editor), 1983. Statistics and data analysis in geochemical prospecting. G.J.S. (Editor)), Handbook of Exploration Geochemistry. Elsevier, Amsterdam, 437 pp.

Howarth, R.J. and Lowestein, P.L., 1971. Sampling variability of stream sediments in broad-scale regional geochemical reconnaissance. Trans. Inst. Min. Metall., Section B, 80: B363-372.

Howarth, R.J. and Sinding-Larsen, R., 1973. Multivariate analysis. In: R.J. Howarth (Editor), Statistics and data analysis in geochemical prospecting, Vol. 2, Chapter 6. G.J.S. (Editor), Handbook of Exploration Geochemistry. Elsevier, Amsterdam: 207-289.

Howarth, R.J. and Thompson, M., 1976. Duplicate analysis in geochemical practice, Part II. Analyst, 101: 699-709.

ICME (International Council on Metals and the Environment), 1997. “Report of the International Workshop on Risk Assessment of Metals and Their Inorganic Compounds”. Angers, France, November 13-15, 1996.

ICRCL, 1987. Guidance on the assessment and redevelopment of contaminated land. Interdepartmental Committee on the Redevelopment of Contaminated Land, Guidance Note 59/83 (2nd Edition), Department of the Environment, London, U.K..

IETC (International Environmental Technology Centre), 1996. Environmental Risk Assessment for sustainable cities. Technical Publication Series (3).

IGME Working Group, 1987. Exploration results in Lavrion for the location of mixed sulphide mineralisation (geology-ore deposits-prefeasibility study). Inst. Geol. Min. Expl., Athens, Greece, Open File Report E6411, 124 pp. (in Greek).

Isaakidis, A., Boura, F. and Liakopoulos, A., 1999. Greece. In: C. Ferguson and H. Kasamas, H. (Editors), Risk assessment for contaminated sites in Europe, Vol. 2, Policy Frameworks. LQM Press, Nottingham, U.K.: 77-84.

Isaaks, E.H. and Srivastava, R.M., 1990. An introduction to applied geostatistics. Oxford University Press, Oxford, U.K., 561 pp.

Jackson, J.A. (Editor), 1997. Glossary of geology. American Geol. Inst., Alexandria, Va., 769 pp.

Jenne, E.A., 1977. Trace element sorption by sediments and soils – site and processes. In: W. Chappell and S.K. Peterson (Editors), Proc. Symp. Molybdenum in the Environment. Marcel Dekker, N.Y.: 425-552.

Jöreskog, K.G., Klovan, J.E. and Reyment, R.A., 1976. Geological factor analysis. Elsevier Scient. Publ. Co., 178 pp.

Jouanneau, J.M., Latouche, C. and Pautrizel, F., 1983. Critical analysis of sequential extractions through the study of several attack constituent residues. Environ. Technol. Lett., 4: 509-514.

Journel, A.G. and Huijbreghts, Ch.J., 1978. Mining geostatistics. Academic Press, London, 600 pp.

Kabata-Pendias, A. and Pendias, H., 1984. Trace elements in soils and plants. CRC Press, Inc., Boca Raton, Florida, 315 pp.

Kafourou, A., Touloumi, G., Makropoulos, V., Loutradi, A., Papanagiotou, A. and Hatzakis, A., 1997. Effects of lead on the somatic growth of children. Archives of Environmental Health, 52 (5): 377-383.

Katerinopoulos, A. and Zissimopoulou, E., 1994. Minerals of the Lavrion mines. The Greek Association of Mineral and Fossil Collectors, Athens, 304 pp.

Katzikatsos, G., Migiros, G., Triantaphyllis, M. and Mettos, A., 1986. Geological structure of internal Hellenides (E.Thessaly – SW. Macedonia, Euboea – Attica – Northern Cyclades Islands and Lesvos). Inst. Geol. Min. Expl., Athens, Special Issue, Geological and Geophysical Research: 191-212.

Kazantzis, G., 1973. Metal contaminants in the environment. Practitioner, 210: 482-489.

Kheboian, C. and Bauer, C., 1987. Accuracy of selective extraction procedures for metal speciation in model aquatic sediments. Anal. Chem., 59: 1417-1423.

Kim, N.D. and Ferguson, J.E., 1991. Effectiveness of a commonly used sequential extraction technique in determining the speciation of calcium in soils. Sci. Tot. Environ., 105: 191-209.

Kiratli, N. and Ergin, M., 1996. Partitioning of heavy metals in surface Black Sea sediments. Applied Geochem., 11: 775-788.

Kitron, U. and Kasmierczak, J.J., 1997. Spatial analysis of the distribution of Lyme disease in Winsconsin. American Journal of Epidemiology, 145 (6), 558-566.

Kloke, A., 1977. Orientierungsdaten fur tolerierbare Gesamtgehalte einiger Elemente in Kulturboden. Mittl. d. VDLUFA 2: 53-61.

Kloke, A., 1979. Content of arsenic, cadmium, chromium, fluorine, lead, mercury and nickel in plants grown on contaminated soil. Paper presented at United Nations-ECE Symp. on Effects of Air-borne Pollution on Vegetation. Warsaw, 20 August 1979: 192.

Klovan, J.E., 1975. R- and Q-mode factor analysis. In: R.B. McCammon (Editor), Concepts in geostatistics, Chapter 2. Springer-Verlag, Berlin: 21-69.
Kober, L., 1929. Beiträge zur geologie von Attika. Sitzber. Ak. Wiss. Math. Nat. Kl., Abt. I, Wien.
Koch, G.S. and Link, R.F., 1971. The coefficient of variation – A guide to the sampling of ore deposits. Econ. Geol., 66: 293-301.
Koljonen, T. (Editor), 1992. The geochemical atlas of Finland. Part 2: Till. Geological Survey of Finland, Espoo, 218 pp.
Kontopoulos, K., Komnitsas, A., Xenidis, A. and Papassiopi, N., 1995. Environmental characterisation of the sulphidic tailings in Lavrion. Minerals Engineering, 8 (10): 1209-1919.
Korre, A., 1997. A methodology for the statistical and spatial analysis of soil contamination in GIS. Unpublished Ph.D. thesis, University of London (Imperial College of Science, Technology and Medicine), 205 pp.
Korre, A. and Durucan, S., 1995a. The application of geographic information systems to the analysis and mapping of heavy metal contamination around Lavrio mine workings. APCOM XXV Conference, Brisbane: 579-585.
Korre, A. and Durucan, S., 1995b. Assessment of soil contamination. In: Environmental Management in the Minerals Industries (ENVIRO-MIN), Med-Campus C035: 5.1-5.19.
Krige, D.G., 1951. A statistical approach to some basic mine valuation problems on the Witwatersrand. J. Chem. Metall. Min. Soc. S. Afr., Dec. 52: 119-139.
Krige, D.G., 1952. A statistical analysis of some of the borehole values in the Orange Free State Goldfield. J. Chem. Metall. Min. Soc. S. Afr., Sept. 53: 47-70.
Krige, D.G., 1962. Statistical applications in mine valuation. J. Inst. Mine Survey. S. Afr., June 12, Sept. 12, 3, 82.
Krige, D.G., 1970. The role of mathematical statistics in improved ore valuation techniques in South African gold mines. In: M.A. Ranova et al. (editors), Topics in Mathematics. Consultants Bureau, New York.
Krige, D.G., 1976a. Some basic considerations in the application of geostatistics to the valuation of ore in South African gold mines. J. S. Afr. Inst. Min. Metall., 76: 383-391.
Krige, D.G., 1976b. A review of the development of geostatistics in South Africa. In: M. Guarascio, M. David and C. Huijbregts (editors), Advanced geostatistics in the mining industry. D. Reidel, Dordrecht, Holland: 279-293.
Kürzl, H., 1988. Exploratory data analysis: recent advances for the interpretation of geochemical data. J. Geochem. Expl., 30 (3): 309-322.
Labonté, M., 1989. Description of computer methods and computer programs for correspondence analysis and use of the dendograph analysis as means of coal data processing. In: Contributions to Canadian Coal Geoscience, Geological Survey of Canada, Paper 89-8: 156-162.
Labonté, M. and Goodarzi, F., 1987. The relationship between dendographs and Pearson product-moment correlation coefficients. In: Current Research, Part A, Geological Survey of Canada, Paper 87-1A: 353-356.
Labonté, M. and Goodarzi, F., 1990. Application of statistical analyses (dendograph and correspondence analysis) in the geological sciences. In: Current Research, Part A, Geological Survey of Canada, Paper 90-1A: 79-84.
Lahee, F.H., 1959. Field geology. McGraw-Hill Book Co., Inc., N.Y., 926 pp.
Lahermo, P., Ilmasti, M., Juntunen, R. and Taka, M., 1990. The Geochemical Atlas of Finland, Part 1: The hydrogeochemical mapping of Finnish groundwater. Geological Survey of Finland, Espoo, 66 pp.
Lake, D.L., Kirk, P.W.W. and Lester, J.N., 1984. Fractionation, characterization, and speciation of heavy metals in sewage sludge and sludge-amended soils: a review. J. Environ. Qual., 13: 175-183.
Landrigan, P.J., 1982. Epidemiology of lead and other metal poisonings in children. In: L. Finberg (Editor), Chemical and Radiation Hazards to Children. Ross Laboratories, Columbius, Ohio: 40-49.
Lapedes, 1978. McGraw-Hill dictionary of scientific and technical terms. McGraw-Hill Book Co., N.Y., 1771 pp. + A58 pp.
Lavrion, 1995a. Environment and development. Ministry of Environment, Planning and Public Works and Lavrion Municipality, Lavrion, 56 pp. (in Greek and English).
Lavrion, 1995b. Environmental Charter and Workshop for sustainable growth. Ministry of Environment, Planning and Public Works and Lavrion Municipality, Lavrion, 50 pp. (in Greek with a Preface in English).
Laxen, D.P.H., Lindsay, F., Raab, G.M., Hunter, R., Fell, G.S. and Fulton, M., 1988. The variability of lead in dusts within the homes of young children. Envir. Geochem. Health, 10 (1): 3-9.
Lepsius, R., 1893. Geologie von Attika. Berlin.
Leschber, R., Davis, R.D. and L'Hermite, P. (Editors), 1985. Chemical methods for assessing bio-available metals in sludges and soils. Elsevier Applied Science Publishers, London.

Levinson, A.A., 1974. Introduction to Exploration Geochemistry. Applied Publishing Ltd., Wilmette, Illinois, USA, 614 pp.
Levinson, A.A., 1980. Introduction to Exploration Geochemistry. 2nd Edition - The 1980 Supplement. Applied Publishing, Wilmette, Illinois, USA: 615-924.
Levinson, A.A., Bradshaw, P.M.D. and Thomson, I., 1987. Practical problems in exploration geochemistry. Applied Publishing, Wilmette, Illinois, USA, 269 pp.
Li, X., 1993. The study of multielement associations in the soil-plant system in some old metalliferous mining areas, England. Unpublished Ph.D. thesis. Environmental Geochemistry Research, Centre for Environmental Technology, Royal School of Mines, Imperial College of Science, Technology and Medicine, University of London, 386 pp.
Li, X., Coles, B.J., Ramsey, M.H. and Thornton, I., 1995. Sequential extraction of soils for multielement analysis by ICP-AES. Chem. Geol., 124: 109-123.
Lindholm, R., 1987. A practical approach to sedimentology. Allen and Unwin, London.
Lindsay, W.L., 1979. Chemical equilibria in soils. J. Wiley & Sons, New York.
Lu, F.C., 1992. Principes de toxicologie: données génerales, procédures d'évaluation, organes cibles, évaluation du risque. Edit. Masson.
Lux, W., 1993. Long-term heavy metal and As pollution of soils, Hamburg, Germany. In: B. Hitchon and R. Fuge (Editors), Environmental Geochemistry: Selected papers from the 2nd International Symposium, Uppsala, Sweden, 16-19 September 1991. Applied Geochem., Suppl. Issue No. 2: 135-143.
Makropoulos, V., Konteye, C., Eikmann, Th., Einbrodt, H.J., Hatzakis, A., Papanagiotou, G., 1991. Cross-sectional epidemiological study on the lead burden of children and workers in Greece. Gordon and Breach Science Publ., U.K., Toxicological and Environmental Chemistry, 31-32: 467-477.
Makropoupos, W., Stilianakis, N., Eikmann, Th., Einbrodt, H.J., Hatzakis, A. and Nikolau-Papanagiotou, A., 1992a. Cross-sectional epidemiological study of the effect of various pollutants on the health of children in Greece. Fresenius Envir. Bull 1: 117-122.
Makropoulos, W., Jakobi, K., Stilianakis, N., Vlachogiannis, N., Pesch, T. and Tambakis, S., 1992b. Blood and cadmium burden in pregnant women, newborns and schoolage children in Lavrion (Greece). Wissenschaft und Umweit 3: 221-224 (in German with an abstract in English).
Manousakis, G., 1992. Trace elements in human health. Kiriakidis Brothers, Thessaloniki, Greece, 204 pp. (in Greek).
Manthos, G.K., 1990. Mining and metallurgical Lavrion. Muncipality of Lavrion, Lavrion, 168 pp.
Manugistics, 1995. Statgraphics plus for Windows version 1: Multivariate methods. Manugistics, Rockville, Maryland, USA.
Manugistics, 1997. Statgraphics plus for Windows version 3 user manual. Manugistics, Rockville, Maryland, USA.
Maravelias, C., Hatzakis, A., Katsouyanni, K., Trichopoulos, D., Koutselinis, A., Ewers, U. and Brockhaus, A., 1989. Exposure to lead and cadmium of children living near a lead smelter at Lavrion, Greece. The Science of the Total Environment, 84: 61-70.
Marinos, G.P. and Petrascheck, W.E., 1956. Laurium. (In Greek with an extended abstract in English). Geological and Geophysical Research, IV, no. 1. Athens, Institute for Geology and Subsurface Research, 246 pp.
Marshall, N.J., 1972. Geostatistics in geochemical exploration – a review. United Nations: 314-340.
Martin, J.P., Nirel, P. and Thomas, A.J., 1987. Sequential extraction techniques: Promises and problems. Marine Chemistry, 22: 313-341.
Mason, B., 1966. Principles of geochemistry. J. Wiley & Sons, Inc., N.Y., 329 pp.
Matheron, G., 1963. Principles of geostatistics. Economic Geology, 58: 1246-1266.
Matheron, G., 1971. The theory of regionalised variables and its applications. Les Cahiers du Centre de Morphologie Mathématique de Fontainbleau, Ecole Nationale Supérieure des mines de Paris.
Mattigod, S.V. and Page, A.L. 1983. Assessment of Metall Pollution in Soils. In: I. Thornton (ed.) Applied Environmental Geochemistry. Academic Press, London: 357-394.
Mattigod, S.V., Page, A.L. and Thornton, I., 1986. Identification of some trace metal minerals in a mine-waste contaminated soil. Soil Sci. Soc. Am. J., 50: 254-258.
McCammon, R.B., 1968. The dendrograph: a new tool for correlation. Bull. geol. Soc. Am., 79: 1663-70.
McCammon, R.B., 1969. Multivariate methods in geology. In Fenner, P. (Editor) Models of geologic processes, Washington, D.C.. Am. Geol. Inst. (a 141 p. long article).
McCammon, R.B., 1974. The statistical treatment of geochemical data, Chapter 12. In: A.A. Levinson (author), Introduction to Exploration Geochemistry. Applied Publishing Ltd., Wilmette, Illinois, USA: 469-508.

McClendon, J.H., 1976. Elemental abundance as a factor in the origins of mineral nutrient requirements. J. Mol. Evol., 8: 175-195.
McGrath, S.P. and Loveland, P.J., 1992a. The soil geochemical atlas of England and Wales. Blackie, Glasgow.
McGrath, S.P. and Loveland, P.J., 1992b. The geochemical survey of topsoils in England and Wales. In: B.D. Beck (Editor), Trace Substances in Environmental Health, XXV: 39-51.
McGrath, S.P., Sanders, J.R., Tancock, N.P. and Laurie, S.H., 1984. A comparison of experimental methods and computer programs for determining metal ion concentrations. In: Proc. Int. Conf. Environmental Contamination (London, 1984). CEC Consultants, Edinburgh: 707-712.
McGrath, S.P., Sanders, J.R., Laurie, S.H. and Tancock, N.P., 1986. Experimental determinations and computer predictions of trace metal ion concentration in dilute complex solutions. Analyst, 111: 459-465.
McKone, T.E., 1989. Household exposure models. Toxicology Letters. 49: 321-339.
McLaughlin, M., 1998. Bioavailability of metals: complexation. International Council on Metals and the Environment, Newsletter, 6 (4): 4.
Mervyn, L., 1980. Minerals and your health. Unwin Paperbacks, London, U.K., 129 pp.
Mervyn, L., 1985. The dictionary of minerals. The complete guide to minerals and mineral therapy. Thorsons Publishing Group, Wellingborough, U.K., 224 pp.
Mervyn, L., 1986. Thorsons complete guide to vitamins and minerals. Thorsons Publishing Group, Wellingborough, U.K., 336 pp.
Mervyn, L., 1989. Thorsons complete guide to vitamins and minerals. Thorsons Publishing Group, Wellingborough, U.K.
Mervyn, L., 1996. Ο πλήρης οδηγός για βιταμίνες και μεταλλικές ουσίες. Β. Βασδέκης, Αθήνα, 472 σελ.
MH (Ministry of Housing, Spatial Planning and the Environment), 1994. "Environmental Quality Objectives in The Netherlands – a review of environmental quality objectives and their policy framework in The Netherlands". Risk Assessment and Environmental Quality Division, Directorate for Chemicals, External Safety and Radiation Protection, Ministry of Housing, Spatial Planning and the Environment. The Netherlands.
Miesch, A.T, 1964. Effects of sampling and analytical error in geochemical prospecting. In: G.A. Parks (Editor), Computers in the Mineral Industry, Part 1. Stanford University Publ. Geol. Sci., 9 (1): 156-170.
Miesch, A.T., 1967. Theory of error in geochemical data. U.S. Geol. Surv., Prof. Paper, 574-A: 17 pp.
Miesch, A.T., 1973. The determination of sampling and analytical errors in exploration geochemistry - a reply. Econ. Geol., 68: 281-282.
Miesch, A.T., 1975. Variograms and variance components in geochemistry and ore evaluation. In: E.H.T. Whitten (Editor), Quantitative studies in Earth Sciences. Geol. Soc. Am. Mem., 142: 333-340.
Miesch, A.T., 1976. Geochemical survey of Missouri: methods of sampling, laboratory analysis and statistical reduction of data. U.S. Geol. Surv., Prof. Paper 954-A: 39 pp.
Miesch, A.T., 1977. Log transformations in geochemistry. Math. Geol., 9 (2): 191-194.
Miesch, A.T., 1990. G-RFAC User's Manual. Grand Junction, Colorado, Miesch Programs, 72 pp.
Nakos, G., 1979a. Environmental contamination by lead: The fate of lead lead in soil and its effects on *Pinus halepensis*. Ministry of Agriculture, Hellenic Forestry Research Institute, Report No. 105, Athens, 34 pp. (in Greek with an English summary).
Nakos, G., 1979b. Lead pollution: Fate of lead in the soil and its effects on *Pinus halepensis*. Plant and Soil, 53: 427-443.
Nakos, S., 1985. Blood lead levels and renal tubular function in children living in an area polluted with lead. University of Ioannina, Greece. Unpublished Ph.D. thesis. 97 pp. (in Greek with English summary).
NAS (National Academy of Sciences), 1983. "Risk Assessment in the Federal Government: Managing the Process". National Academy Press, Washington, D.C.
National Research Council, 1983. Risk assessment in the Federal Government: Managing the process. National Academy Press, Washington, DC.
NEHF (National Environmental Health Forum), 1996. "Health-Based Soil Investigation Levels". National Environmental Health Forum Monographs. Soil Series No.1. South Australian Health Commission.
Nichol, I., Garrett, R.G. and Webb, J.S., 1969. The role of some statistical and mathematical methods in the interpretation of regional geochemical data. Econ. Geol. 64: 204-20.
O'Connor, P.J., Reimann, C. and Kürzl, H., 1988. A geochemical survey of Inishowen, Co. Donegal. Geological Survey of Ireland, Dublin.
Obial, R.C., 1970. Cluster analysis as an aid in the interpretation of multi-element geochemical data. Trans. Inst. Min. Metall., Sect. B., Appl. earth sci., 79: B175-180.
Obial, R.C. and James, C.H., 1973. Use of cluster analysis in geochemical prospecting, with particular reference to southern Derbyshire, England. In: M.J. Jones (ed.) Geochemical Exploration 1972. London, Inst. Min. Metall.: 237-257.

Olade, M. and Fletcher, W.K., 1974. Potassium chlorate-hydrochloric acid; a sulfide selective leach for bedrock geochemistry. J. Geochem. Explor., 3: 337-344.
OME (Ontario Ministry of the Environment), 1991. Soil clean up guidelines for decommissioning of industrial lands: background and rationale for development. OME, Queen's Printer for Ontario, Toronto, ON, 33 pp.
Papadeas, G.D., 1991. Recent considerations for the geological-tectonic evolution of the metamorphic rocks in Attiki and Variskia mineralization. Proceedings Academy of Athens, 66: 331-370.
Papadellis, F., 1980. Endemic fluorosis in children from Lavrion Attiki and Kolchikon Langada. Unpublished Ph.D. thesis, University of Athens A' Paediatric Clinic, 49 pp. (in Greek).
Papanikolaou, D.I. (1986) Geology of Greece. Athens, Eptalofos Publications, 240 pp.
Park, C.F. and MacDiarmid, R.A., 1970. Ore deposits. W.H. Freeman & Co., San Francisco, 522 pp.
Parkes, G.D., 1967. Mellor's modern inorganic chemistry. Longmans, London, 1025 pp.
Pennatier, Y., 1996. Variowin: Software for spatial data analysis in 2D. Springer-Verlag, N.Y., 91 pp.
Perel'man, A.I., 1977. Geochemistry of elements in the supergene zone. Israel Program for Scientific Translations, Jerusalem, 266 pp.
Pickering, W.F., 1986. Metal ion speciation - soils and sediments (A review). Ore Geology Reviews, 1: 83-146.
Plant, J.A. and Raiswell, R., 1983. Principles of Environmental Geochemistry. In: I. Thornton (Editor), Applied Environmental Geochemistry. Academic Press, London: 1-39.
Plant, J.A., Jeffery, K. Gill, E. and Fage, C., 1975. The systematic determination of accuracy and precision in geochemical exploration data. J. Geochem. Explor., 4: 467-486.
Pöppelbaum, M. and Van den Boom, G., 1980a. Prospecting for hidden ore deposits. A method for determining mercury (Hg) concentrations in hard rock. In: W. Ernst, J.H. Hohnholz, H.R. Lang, K.H. Jacob and S.V. Wahl (Editors), Natural Resources and Development, a Biannual Collection of Recent German Contributions Concerning the Exploration and Exploitation of Natural Resources. Inst. Scient. Co-operation, Tübingen, Germany, 11: 68-77.
Pöppelbaum, M. and Van den Boom, G., 1980b. Eine Methode zur Bestimmung der Quecksilbergehalter in Festgesteinen. Geol. Jb., Hannover, D 37: 5-14.
Potts, P.J., Tindle, A.G. and Webb, P.C., 1992. Geochemical Reference Material Compositions. Whittes Publishing, Caithness, U.K., 313 pp.
Press, F. and Siever, R., 1998. Understanding Earth. W.H. Freeman & Co., N.Y., 682 pp.
Quarrie, J. (Editor), Earth Summit 1992. The United Nations Conference on Environment and Development, Rio de Janeiro 1992. The Regency Press Corporation, London, 237 pp.
Ramsey, M.H., 1993. Sampling and analytical quality control (SAX) for improved error estimation in the measurement of Pb in the environment using robust analysis of variance. Appl. Geochem., Suppl. Issue 2: 149-153.
Ramsey, M.H. and Argyraki, A., 1997. Estimation of measurement uncertainty from field sampling: implications for the classification of contaminated land. The Science of the Total Environment, 198: 243-257.
Ramsey, M.H. and Thompson, M., 1987. High-accuracy analysis by inductively coupled plasma atomic emission spectrometry using the parameter-related internal standard method. J. Anal.At.Spectrosc., 2: 497-502.
Ramsey, M.H., Thompson, M. and Banerjee, E.K., 1987. Realistic assessment of analytical data quality from Inductively Coupled Plasma Atomic Emission Spectrometry. Analytical Proceedings, 24: 260-265.
Ramsey, M.H., Thompson, M. and Hale, M., 1992. Objective evaluation of precision requirements for geochemical analysis using robust analysis of variance. J. Geochem. Explor., 44: 23-36.
Rankama, K. and Sahama, Th. G., 1952. Geochemistry. The University of Chicago Press, Chicago, Illinois, U.S.A., 912 pp.
Rasmussen, S., 1992. An introduction to statistics and data analysis. Brooks/Cole Publ. Co., Pacific Grove, Ca, 707 pp.
Rendu, J.M., 1978. An introduction to geostatistical methods of mineral evaluation. South Afr. Inst. Min. Metall., Johannesburg, 84 pp.
RCEP (Royal Commission on Environmental Pollution), 1995. Royal Commission seeks views on basis for environmental standards. HMSO, London.
Reagan, P.L. and Silbergeld, E.K., 1990. Establishing a health based standard for lead in residential soils. In: D.D. Hemphill (Editor), Trace substances in environmental health - XXII. Supplement to volume 12 of Environmental Geochemistry and Health, University of Missouri, Columbia: 199-238.
Reimann, C., 1989. Reliability of geochemical analyses: recent experiences. Trans. Instn. Min. Metall., Sect. B: Appl. Earth Sci., 98: B123-129.
Reimann, C., Äyräs, M., Chekushin, V., Bogatyrev, I., Boyd, R., Caritat, P. de, Dutter, R., Finne, T.E., Halleraker, J.H., Jæger, Ø., Kashulina, G., Lehto, O., Niskavaara, H., Pavlov, V., Räisänen, M.L.,

Strand, T. and Volden, T., 1998. Environmental geochemical atlas of the Central Barents Region. Geological Survey of Norway, Trondheim, 745 pp.
Rendall, P.S., Batley, G.E. and Cameron, A.J., 1980. Adsorption as a control of metal concentration in sediment extracts. Environ. Sci. Technol., 14: 314.
Renn, O., 1991. Risk communication and the social amplification of risk. In: R.E. Kasperson and P.J. Stallen (Editors), Communicating risk to the public. Kluwer, Dordrecht: 287-324.
Renn, O., 1998. The role of risk perception for risk management. In: P.E.T. Douben, Pollution risk assessment and management. J. Wiley & Sons, Chichester, U.K.: 429-450.
Ribo, J.M., Zaruk, B.M., Hunter, H. and Kaiser, K., 1985. Microtox toxicity test results for water samples from Detroit River. J. Great Lake Research, 11: 297-304.
Robbins, J.C., 1973. Zeeman spectrometer for measurement of atmospheric mercury vapour. In: M.J. Jones (Editor), Geochemical Exploration 1972. Inst. Min. Metall., London: 315-323.
Roels, H.A., Buchet, J.P., Lauwerys, R.R., Bruaux, P., Claeys-Thoreau, F., Lafontaine, A. and Verduyn, G., 1980. Exposure to lead by the oral and the pulmonary routes of children living in the vicinity of a primary lead smelter. Environ. Res., 22: 81-99.
Rose, A.W., Hawkes, H.E. and Webb, J.S., 1979. Geochemistry in Mineral Exploration. 2nd edition. Academic Press, London, 657 pp.
Royal Society, 1992. Risk: Analysis, perception and management. The Royal Society, London.
Ruby, M.V., Schoof, R., and Eberle, S., 1995. “Development of a physiologically based test to estimate arsenic bioavailability”. Internal report. PTI Environmental Services. San Diego, California.
Russell, E.J., 1970. The world of the soil. Collins, The Fontana New Naturalist, London, 285 pp.
Saaty, T.L., 1977. A scaling method for priorities in hierarchical structures. J. Math. Psychology, 15: 234-281.
Sainsbury, C.L., Hudson, T., Kachadoorian, R. and Richards, D., 1970. Geology, mineral deposits, and geochemical and radiometric anomalies, Serpentine Hot Springs Area, Seward Peninsula, Alaska. U.S. Geol. Surv. Bull., 1312-H: H1-H19.
Schmitt, N., Philion, J.J., Larsen, A.A., Harnadek, M. and Lynch, A.J., 1979. Surface soil as a potential source of lead exposure for young children. Can. Med. J., 121: 1474-1478.
Sharp, W.E., 1987. Two basic rules for valid contouring. Geobyte, Nov. ’87: 11-15.
Shell, 1994a. Human exposure to soil pollutants, version 2.10a (HESP). Shell Internationale Petroleum Maatschappij B.V. The Hague, The Netherlands.
Shell, 1994b. “Human exposure to soil pollutants, version 2.10a (HESP). The concepts of HESP-Reference manual”. Shell Internationale Petroleum Maatschappij B.V. The Hague, The Netherlands.
Sheppard, S.C., Gaudet, C., Sheppard, M.I., Cureton, P.M. and Wong, M.P., 1992. The development of assessment and remediation guidelines for contaminated soils, a review of the science. Can. J. Soil Sci., 72: 359-394.
Shuman, L.M., 1985. Fractionation method for soil microelements. Soil Sci., 140: 11-22.
Sichel, H.S., 1952. New methods in the statistical evaluation of mine sampling. Trans. Inst. Min. Metall., 61: 261-288.
Sichel, H.S., 1966. The estimation of means and associated confidence limits for small samples from lognormal populations. In: Symposium on mathematical statistics and computer applications in ore valuation. S. Afr. Inst. Min. Metall., Johannesburg: 106-122.
Sichel, H.S., 1973. Statistical valuation of diamondiferous deposits. In: M.D.G. Salamon et al. (editors), Applications of computer methods in the mineral industry. S. Afr. Inst. Min. Metall., Johannesburg: 17-25.
Siegel, F.R., 1974. Applied Geochemistry. J. Wiley & Sons, N.Y., 353 pp.
Simpson, P., 1996. BGS Meeting Report. AEG-BGS Workshop on Environmental and Legislative Uses of Regional Geochemical Baseline Data for Sustainable Development. Explore (Newsletter of the Association of Exploration Geochemists) No. 92: 10-13.
Sinclair, A.J., 1976. Applications of probability graphs. Association of Exploration Geochemists, Nepean, Ontario, 95 pp.
Sinclair, A.J., 1983. Univaritate analysis. In: R.J. Howarth (Editor), Statistics and data analysis in geochemical prospecting, Vol. 2, Chapter 3. G.J.S. (Editor), Handbook of Exploration Geochemistry. Elsevier, Amsterdam: 59-81.
Siniscalchi, A., Tibbetts, S.J., Beakes, R.C. and Soto, X.,1996. A Health Risk Assessment model for home owners with multiple pathway radon exposure. Environment International, 22 (suppl. 1): s739-s747.
Smirnov, V.I., 1976. Geology of mineral deposits. MIR Publishers, Moscow, 520 pp.
Song, Y., Wilson, M.J., Moon, H.-S., Bacon, J.R. and Bain, D.C., 1999. Chemical and mineralogical forms of lead, zinc and cadmium in particle size fractions of some wastes, sediments and soils in Korea. Applied Geochem., 14: 621-633.

SPC, 1993. Harvard Graphics for Windows 2.0. Software Publishing Corp., Braknell, Berks, U.K.
Sposito, G. and Coves, J., 1988. SOILCHEM: A computer program for the calculation of chemical speciation in soils. Kearney Foundation of Soil Science, University of California, Riverside and Berkeley, U.S.A.
Stanek, E.J., III and Calabrese, E.J., 1995. Daily estimates of soil ingestion in children. Environ. Health Perspect., 103: 276-285.
Stanners, D. and Bourdeau, P. (Editors), 1995. Europe's Environment. The Dobříš Assessment. European Environmental Agency, Copenhagen, 676 pp.
Stanton, R.L., 1972. Ore petrology. McGraw-Hill Book Co., N.Y., 713 pp.
Stanway, A., 1983. Trace elements - A new chapter in nutrition. Van Dyke Books Ltd., Redhill, Surrey, U.K., 80 pp.
Stavrakis, P., Demetriades, A. and Vergou-Vichou, K., 1994a. Environmental impact assessment in the Lavreotiki peninsula Attiki. Inst. Geol. Min. Expl., Athens, Greece. Open File Report E7424, Vol. 1, 44 pp. (in Greek with an English summary).
Stavrakis, P., Vergou-Vichou, K., Fosse, G., Makropoulos, V., Demetriades, A., Vlachoyiannis, N., 1994b. A multidisciplinary study on the effects of environmental contamination on the human population of the Lavrion urban area, Hellas. In: S.P. Varnavas (Editor), Environmental Contamination. 6th International Conference, Delphi, Greece, CEP Consultants, Edinburgh: 20-22.
Stern, P.C. and Fineberg, H.V., 1996. Understanding risk: informing decisions in a democratic society. National Academy Press, Washington, DC.
Taylor, R. and Langley, A., 1996. Exposure scenarios and exposure settings. National Environmental Health Forum Monographs, Soil Series No. 2. South Australian Health Commission, 25 pp.
Tennant, C.B. and White, M.L., 1959. Study of the distribution of some geochemical data. Econ. Geol., 54: 1281-1290.
Tessier, A. and Campbell, P.G.C., 1988. Partitioning of trace metals in sediments. In: J.R. Kramer and H.E. Allen (Editors), Metal speciation: Theory, analysis and application. Lewis Publisher, Inc., M.I., U.S.A.: 183-199.
Tessier A., Campbell P.G.C. and Bisson M., 1979. Sequential extraction procedure for speciation of particulate trace metals. Analyt. Chem., 51: 844-851.
Thompson, M. and Howarth, R.J., 1976. Duplicate analysis in geochemical practice. Part 1. Theoretical approach and estimation of analytical reproducibility. Analyst, 101: 690-698.
Thompson, M. and Howarth, R.J., 1978. A new approach to the estimation of analytical precision. J. Geochem. Explor., 9: 23-30.
Thompson, M. and Howarth, R.J., 1980. The frequency distribution of analytical error. Analyst, 105: 1188-1195.
Thompson, M. and Maguire, M., 1993. Estimating and using sampling precision in surveys of trace constituents of soils. Analyst, 118: 1107-1110.
Thompson, M. and Walsh, J.J., 1989. Handbook of inductively coupled plasma spectrophotometry. Blackie, Glasgow, 273 pp.
Thornton, I. (Editor), 1988. Geochemistry and health: Proceedings of the Second International Symposium. Science Reviews Ltd., Northwood, U.K., 272 pp.
Thornton, I. and Culbard, E. (Editors), 1987. Lead in the home environment. Science Reviews Ltd., Northwood, U.K., 224 pp.
Thornton, I., Culbard, E., Moorcroft, S., Watt, J., Wheatley, M., Thompson, M. and Thomas, J.F.A., 1985. Metals in urban dusts and soils. Envir. Technol. Letters, 6: 137-144.
Thornton, I., Davies, D.J.A., Watt, J.M. and Quinn, M.J., 1990. Lead exposure in young children from dust and soil in the United Kingdom. Environ. Health Perspect., 89: 55-60.
Tidball, R.R., 1984. Geochemical Survey of Missouri. Geography of Soil Geochemistry of Missouri Agricultural Soils. USGS Professional Paper 954-H,I: H1-H54.
Till, R., 1974. Statistical methods for the earth scientist – An introduction. Macmillan, London, 154 pp.
Tipping, E., Hethering, N.B., Hilton, J., Thompson, D.W., Bowels, E. and Hamilton-Taylor, J., 1985. Artifacts in the use of selective extraction to determine the distribution of metals between oxides of manganese and iron. Anal. Chem., 57: 1944.
Tipping, E., Thompson, D.W., Ohnstad, M. and Hetherington, N.B., 1986. Effects of pH on the release of metals from naturally-occurring oxides of Mn and Fe. Environ. Technol. Lett., 7: 109-114.
Trattler, R., 1987. Better health through natural healing. Thorsons Publishing Group, Wellingborough, Northamptonsire, U.K., 624 pp.
Tristán, E., Rosenbaum, M.S. and Ramsey, M.H., 1998. Evaluation of child exposure to lead in Lavrion as a basis for risk assessment, Part II. In: A. Demetriades, E. Vassiliades, E. Tristán, M.S. Rosenbaum and M.H. Ramsey, Technical Report, Child blood lead contents as a basis for risk assessment of the metallurgical processing residues and contaminated soil in Lavrion Attiki. Inst. Geol. Min. Expl., Athens, Open File Report 7977-E, 69 pp.

Tsuhi, J.E. and K.M. Searl., 1996. Current uses of EPA lead model to assess health risk and action levels for soil. Environmental Geochemistry and Health, 18: 25-33.

Tukey, J.W., 1977. Exploration data analysis. Addison-Wesly, Reading, MA., 506 pp.

Tzoulis, H. and Kaminari, M., 1999. Determination of the physicochemical forms of metals in soil with the methodology of sequential extraction. Inst. Geol. Min. Expl., Athens, Open File Report 8131-E, 23 pp.

UK Governmnet, 1994. Sustainable development, The UK strategy. Cmnd 2425, HMSO, London.

Ullrich, S.M., Ramsey, M.H. and Helios-Rybicka, E., 1999. Total and exchangeable concentrations of heavy metals in soils near Bytom, an area of Pb/Zn mining and smelting in Upper Silesia, Poland. Applied Geochem., 14: 187-196.

Uniska, R., 1985. Evaluation of levels of selected heavy metals in Polish soils - A contribution to environmental exposure. In: Proceedings of the 1st International Symposium on Geochemistry and Health. Northwood, Middlesex, U.K.: 68-71.

US CT, 1994. Proposal for the Connecticut clean-up standard regulations. State of Connecticut, Dept. of Environmental Protection.

US CT, 1997. Remediation standard. State of Connecticut, Dept. of Environmental Protection, Section 22a-133k-1, 66 pp.

US EPA (United States Environmental Protection Agency), 1986. Carcinogen risk assessment guidelines. 51 FR 33992.

US EPA (United States Environmental Protection Agency), 1991. Beryllium. Integrated Risk Information System (IRIS). Environmental Criteria and Assessment Office, Office of Health and Environmental Assessment, Cincinnati, OH.

US EPA (United States Environmental Protection Agency), 1994. Integrated Exposure Uptake Biokinetic Model for lead in children (version 0.99d). Environmental Protection Agency. Washington D.C. USA.

US EPA (United States Environmental Protection Agency), 1996. Exposure factors handbook. Environmental Protection Agency, Washington, D.C.

US EPA (United States Environmental Protection Agency), 1998. Lead in your home: A parent's reference guide. EPA 747-B-98-002, 70 pp.

Valin, R.V. and Morse, J.M., 1982. An investigation of methods commonly used for the selective removal and characterization of trace metals in sediments. Marine Chemistry, 11: 535-564.

Valjus, J., N, Hongisto, M., Verkasalo, P., Järvinen, P., Heikkilä, K. and Koskenvuo, M., 1995. Residential exposure to magnetic fields generated by 110-400 kV power lines in Finland. Bioelectromagnetics, 16, 365-376.

Van den Berg, R., Denneman, C.A.J. and Roels, J.M., 1993. Risk assessment of contaminated soil: Proposals for adjusted, toxicologically based Dutch soil clean-up criteria. In: F. Arendt, G.J. Annokkıe, R. Bosman and W.J. Van den Brink (Editors), Contaminated soil '93 (Volume 1): Fourth International KfK/TNO Conference on Contaminated Soil. Kluwer Academic Press, Dordrecht, The Netherlands: 1-21.

Van der Sluys, J., Brusselmans, A., De Vos, W. and Swennen, R., 1997. Regional geochemical mapping of overbank and stream sediments in Belgium and Luxembourg. Vol. III – Geochemical maps of Belgium and Luxembourg based on overbank and active stream sediments. Service Geologique de Belgique, Brussel, Professional Paper 1997/1-N.283, 93 pp.

Vanloon, J.C. and Barefoot, R.R., 1989. Analytical methods for geochemical exploration. Academic Press Inc., San Diego.

Vassiliades, E., 1994. Drilltools. A PC based software package for the treatment and presentation of core-drillholes and sections. Inst. Geol. Mineral. Explor., Athens. IGME Open file report (in Greek).

Vassiliades, E., in preparation. DEPRECIS – A computer programme for estimating the analytical variance, detection limit and precision of geochemical surveys. Inst. Geology & Mineral Explor., Athens, Greece, Open File Report.

Vine, M.F., Degnan, D. and Hanchette, C., 1997. Geographic Information Systems: Their use in environmental epidemiologic research. Environmental Health Perspectives, 1 (6): 598-605.

Vourlakos, N., 1992. The minerals of Lavreotiki and the mineral components of its rocks. Library of the Society of Lavreotiki Studies, Lavrion, Publ. 5, 31 pp. (text in Greek)

VROM, 1983. Soil protection guideline. Staatsuitgeverij, The Hague.

Walton, N.R.G. and Higgins, A., 1998. The legacy of contaminated land in Portsmouth: its identification and remediation within a socio-political context. In: D.N. Lerner and N.R.G. Walton (Editors), Contaminated land and groundwater: Future directions. Geological Society of London, Engineering Geology Special Publ., 14: 29-36.

Wang, W.H., Wong, M.H., Leharne, S. and Fisher, B., 1998. Fractionation and biotoxicity of heavy metals in urban dusts collected from Hong and London. Envir. Geochem. Health, 20: 185-198.

Watt, J.M., 1990. Automated feature analysis in the scanning electron microscope. Microsc. Anal., 15: 25-28.

Watt, J., 1996. Individual particle analysis of contaminated waste, soils and household dusts form the town of Lavrion, Greece. Environmental Geochemistry Research Group, Imperial College of Science, Technology and Medicine, University of London, U.K.

Watt, J.M. and Thornton, I., 1990. The role of particulate material in the transfer of lead from the environment to young children. Proc. Conf. "Environmental Contamination" Barcelona, CEP Consultants, Edinburgh: 493-495.

Watt, J.M., Thornton, I. and Cotter-Howells, J., 1993. Physical evidence suggesting the transfer of soil Pb into young children via hand to mouth activity. Applied Geochem., Suppl. Issue 2: 269-272.

Wedepohl, K.H., 1995. The composition of the continental crust. Geochemica et Cosmochimica Acta, 59: 1217-1232.

White, D.E., Hem, J.D. and Waring, G.A., 1963. Chemical composition of subsurface waters. U.S. Geol. Survey Profess. Paper 440-F, 67 pp.

WHO (World Health Organisation), 1993. Guidelines for drinking water quality. Geneva.

Wixson, B.G. and Davies, B.E., 1994. Lead in soil – Recommended guidelines. Science and Technology Letters, Northwood, Middlesex, U.K., 132 pp.

Xenidis, A., Komnitsas, K., Papassiopi, N. and Kontopoulos, A., 1997. Environmental implications of mining activities in Lavrion. In: P.G. Marinos, G.C. Koukis, G.C. Tsiambaos and G.C. Stournaras (Editors), Engineering Geology and the Environment. A.A. Balkema, Rotterdam, Vol. 3: 2575-2580.

Xian, X., 1989. Response of Kidrney Bean to concentration and chemical form of cadmium, zinc and lead in polluted soils. Environ. Pollut., 57: 127-137.

Yankel, A.J., Von Linden, I.H. and Walter, S.D., 1977. The Silver Valley study: the relationship between childhood blood levels and environmental exposure. J. Air Pollut. Control Assoc., 27: 763-767.

Zadeh, L.A., 1965. Fuzzy sets. Information and Control, 8: 338-353.